Coventry University

Coventry University

DOCTOR OF PHILOSOPHY

The influence of suspension and tyre modelling on vehicle handling simulation

Blundell, Mike

Award date:
1997

Awarding institution:
Coventry University

[Link to publication](#)

THE INFLUENCE OF SUSPENSION AND TYRE MODELLING ON VEHICLE HANDLING SIMULATION

M. V. Blundell

A thesis submitted in partial fulfilment

of the University's requirements

for the Degree of Doctor of Philosophy

November 1997

Coventry University in collaboration

with Rover Group and SP Tyres UK Ltd

THE INFLUENCE OF SUSPENSION AND TYRE MODELLING ON VEHICLE HANDLING SIMULATION

ABSTRACT

A study has been carried out in order to investigate the influence of suspension and tyre modelling on the outputs predicted by vehicle handling simulations. The computer models have been generated using data for a Rover vehicle, for which instrumented track test measurements were also available. The results obtained from a high speed lane change manoeuvre have been used as a benchmark for comparison of the various computer modelling strategies. This investigation addresses two main areas. The first of these is the influence of suspension modelling on calculated outputs. The second and more complex area investigates the influence of models representing the effects of the tyres. In each case a primary aim has been to assess the accuracy of models which use a simplified approach, reduce the number of model parameters and may hence be more amenable to vehicle and tyre design studies. Comparison of the results from this study indicate that for quite an extreme manoeuvre a relatively simple vehicle and tyre model can be used to carry out a simulation with a good level of accuracy. A sensitivity study has also been carried out to illustrate how the models respond to design changes for both vehicle and tyre parameters.

The multibody systems analysis program ADAMS (*Automatic Dynamic Analysis of Mechanical Systems*) has been used to generate the models, formulate and solve the equations of motion, and postprocess the results. An initial literature survey has been carried out investigating this analysis discipline and its usage in vehicle dynamics. Previous work in the areas of vehicle handling simulation, tyre theory, and computer modelling of both vehicles and tyres has also been studied.

Initial investigations have been carried out looking at the modelling of the suspension systems and the steering system. Information from this phase has been used to provide inputs for a set of four full vehicle models ranging in complexity from a model where the suspensions are treated as lumped masses, a model where the suspensions are treated as swing arms, a model based on roll stiffness and a final detailed model which represents the suspension

linkages as fitted on the vehicle. Of the three simple models it will be shown that the roll stiffness model is most suitable for further comparisons with the detailed linkage model, where aspects of tyre modelling are considered.

Tyre testing has been carried out at SP Tyres UK Ltd. and at Coventry University. A set of FORTRAN subroutines, which interface with ADAMS, has been developed in association with a computer model of a tyre test rig to represent and validate the various tyre models. The provision of these tools forms part of a new system developed during this study and is referred to as the *CUTyre* System due to its origins at Coventry University. The tyre models compared include a well known and accurate model which requires up to fifty model parameters and a more simple model requiring only ten parameters. An interpolation method is also used as a benchmark for the comparisons.

To the author's knowledge the work described in this thesis can be considered to make an original contribution to the body of knowledge involving the application of multibody systems analysis in vehicle dynamics by:

(i) Providing a detailed comparison of vehicle suspension modelling strategies with the ADAMS program.

(ii) Developing a tyre modelling and validation tool which can interface directly with the ADAMS software.

(iii) Providing a comparison between a sophisticated and a simple tyre model in ADAMS. Of particular significance is the assessment of the influence of the tyre models on simulation outputs and not just the shape of the tyre force and moment curves.

ACKNOWLEDGEMENTS

This thesis is dedicated to the memory of Beatrice Alice Blundell

CONTENTS

List of Figures

List of Tables

Nomenclature

CONTENTS (Continued)

CONTENTS (Continued)

CONTENTS (Continued)

CONTENTS (Continued)

List of Figures

List of Tables

Nomenclature

ADAMS Modelling and Theory

GRF	Ground Reference Frame
WBid	Wheel Base Marker
WCid	Wheel Centre Marker
DX(I,J)	Displacement in X-direction of I marker relative to J marker parallel to GRF
DY(I,J)	Displacement in Y-direction of I marker relative to J marker parallel to GRF
DZ(I,J)	Displacement in Z-direction of I marker relative to J marker parallel to GRF
TKid	Top Kingpin Marker
BKid	Bottom Kingpin Marker
WFid	Wheel Front Marker
FGid	Fixed Ground Marker
ICY	Y Coordinate of Instant Centre
ICZ	Z Coordinate of Instant Centre
LPRF	Local Part Reference Frame
QP	Position vector of a marker relative to the LPRF
QG	Position vector of a marker relative to the GRF
ψ	1st Euler Angle Rotation
θ	2nd Euler Angle Rotation
ϕ	3rd Euler Angle Rotation
ZP	Position vector of a point on a marker z-axis
XP	Position vector of a point on a marker x-axis
Kt	Roll Stiffness
K	Spring Stiffness
DM(I,J)	Magnitude of displacement of I marker relative to J marker
L	Free length of spring
VR(I,J)	Radial line of sight velocity of I marker relative to J marker
$\{R_n\}_1$	Position vector for part n resolved parallel to frame 1 (GRF)
$\{V_n\}_1$	Velocity vector for part n resolved parallel to frame 1 (GRF)
$\{\omega_n\}_1$	Angular velocity vector for part n resolved parallel to frame 1 (GRF)

$\{\omega_n\}_1$	Angular velocity vector for part n resolved parallel to frame e
$[A_{1n}]$	Euler matrix for part n
O_1	Frame 1 (GRF)
O_n	Frame for part n
O_e	Euler axis frame
$[B]$	Transformation matrix from frame O_e to O_n
$\{\gamma_n\}_e$	Set of Euler angles for part n
q_j	Set of part generalised coordinates
T	Kinetic energy for a part
$[I_n]$	Inertia tensor for a part
$\{A_n\}_1$	Acceleration vector for part n resolved parallel to frame 1 (GRF)
$\{P_{nt}\}_1$	Translational momenta vector for part n resolved parallel to frame 1 (GRF)
M	Mass of a part
$\{F_{nA}\}_1$	Applied force vector on part n resolved parallel to frame 1 (GRF)
$\{F_{nC}\}_1$	Constraint force vector on part n resolved parallel to frame 1 (GRF)
$\{P_{nr}\}_1$	Rotational momenta vector for part n resolved parallel to frame 1 (GRF)
$\{M_{nA}\}_e$	Applied moment vector on part n resolved parallel to frame e
$\{M_{nC}\}_e$	Constraint moment vector on part n resolved parallel to frame e
$\{F_A\}_1 \{F_B\}_1...$	Applied force vectors at points A, B, ... resolved parallel to frame 1(GRF)
$\{T_A\}_1 \{T_B\}_1...$	Applied torque vectors at points A, B, ... resolved parallel to frame 1 (GRF)
$m\{g\}_1$	Weight force vector for a part resolved parallel to frame 1 (GRF)
$\{R_{AG}\}_n$	Position vector of point A relative to mass centre G resolved parallel to frame n
$\{R_{BG}\}_n$	Position vector of point B relative to mass centre G resolved parallel to frame n
$\{R_i\}_1$	Position vector of frame i on part i resolved parallel to frame 1 (GRF)
$\{R_j\}_1$	Position vector of frame j on part j resolved parallel to frame 1 (GRF)
Oi	Reference frame for part i
Oj	Reference frame for part j
$\{r_I\}_1$	Position vector of marker I relative to frame i resolved parallel to frame 1(GRF)
$\{r_J\}_1$	Position vector of marker J relative to frame j resolved parallel to frame 1(GRF)
$\{\Phi_a\}_1$	Vector constraint equation resolved parallel to frame 1 (GRF)
$\{d_{IJ}\}_1$	Position vector of marker I relative to J resolved parallel to frame 1 (GRF)
$\{\lambda\}_1$	Reaction force vector resolved parallel to frame 1 (GRF)

$\{a_J\}_1$	Unit vector at marker J resolved parallel to frame 1 (GRF)
$\{a_I\}_1$	Unit vector at marker I resolved parallel to frame 1 (GRF)
Φ_d	Scalar constraint expression for constraint d
λ_d	Magnitude of reaction force for constraint d
Φ_p	Scalar constraint expression for constraint p
λ_p	Magnitude of reaction force for constraint p
Φ_α	Scalar constraint expression for constraint α
λ_α	Magnitude of reaction force for constraint α
$\{x_I\}_1$	Unit vector along x-axis of marker I resolved parallel to frame 1 (GRF)
$\{y_I\}_1$	Unit vector along y-axis of marker I resolved parallel to frame 1 (GRF)
$\{z_I\}_1$	Unit vector along z-axis of marker I resolved parallel to frame 1 (GRF)
$\{x_J\}_1$	Unit vector along x-axis of marker J resolved parallel to frame 1 (GRF)
$\{y_J\}_1$	Unit vector along y-axis of marker J resolved parallel to frame 1 (GRF)
$\{z_J\}_1$	Unit vector along z-axis of marker J resolved parallel to frame 1 (GRF)

Pacjeka Tyre Model

F_x	Longitudinal tractive or braking tyre force
F_y	Lateral tyre force
F_z	Vertical tyre force
M_z	Tyre self aligning moment
α	Tyre slip angle
κ	Longitudinal slip (Pacjeka)
Sh	Horizontal shift
Sv	Vertical shift
D	Peak value
C	Shape factor
B	Stiffness factor
E	Curvature factor
y_s	Asymptotic value at large slip
γ	Camber angle

Fiala Tyre Model

R_1	Unloaded tyre radius
R_2	Tyre carcass radius
K_z	Tyre radial stiffness
C_S	Tyre longitudinal stiffness
C_α	Tyre lateral stiffness due to slip angle
C_γ	Tyre lateral stiffness due to camber angle
C_r	Rolling resistance moment coefficient
ζ	Radial damping ratio
μ_o	Tyre to road coefficient of static friction
μ_1	Tyre to road coefficient of sliding friction
$\{U_s\}$	Unit vector acting along spin axis of tyre
$\{U_r\}$	Unit vector normal to road surface at tyre contact point
$\{X_{sae}\}_1$	Unit vector acting at tyre contact point in X_{sae} direction referenced to frame 1
$\{Y_{sae}\}_1$	Unit vector acting at tyre contact point in Y_{sae} direction referenced to frame 1
$\{Z_{sae}\}_1$	Unit vector acting at tyre contact point in Z_{sae} direction referenced to frame 1
$\{R_w\}_1$	Position vector of wheel centre relative to frame 1, referenced to frame 1
$\{R_p\}_1$	Position vector of tyre contact point relative to frame 1, referenced to frame 1
$\{V_p\}_1$	Velocity vector of tyre contact point referenced to frame 1
V_{xc}	Longitudinal slip velocity of tyre contact point
V_y	Lateral slip velocity of tyre contact point
V_z	Vertical velocity of tyre contact point
S_L	Longitudinal slip ratio
S_α	Lateral slip ratio
$S_{L\alpha}$	Comprehensive slip ratio
F_z	Vertical tyre force
F_{zc}	Vertical tyre force due to damping
F_{zk}	Vertical tyre force due to stiffness
m_t	Mass of tyre
S_L^*	Critical value of longitudinal slip
S_α^*	Critical slip angle

1.0 INTRODUCTION

1.1 Background

For a modern commercial road vehicle the handling and road holding are aspects of vehicle performance which not only contribute to the customers' perception of the vehicle quality but are also significant in terms of road transport safety. There is often confusion over the use of terminology when referring to vehicle handling. The road holding or stability of a vehicle can be considered to be the performance for extreme manoeuvres such as cornering at speed for which measured outputs such as the lateral acceleration, roll angle and yaw rate can be used to indicate performance. The handling quality of a vehicle is thought to be more subtle and to indicate the feeling and confidence the driver has in the vehicle due to its responsiveness and feedback through the steering system. In any case the series of tests carried out on the track or simulated on the computer are often collectively referred to as falling into the general area of vehicle handling.

Deciding whether a vehicle has good or bad handling characteristics is often a matter of human judgement based on the response or feel of the vehicle, or how easy the vehicle is to drive through certain manoeuvres. To a large extent automotive manufacturers still rely on track measurements and the instincts of experienced test engineers as to whether the design has produced a vehicle with the required handling qualities. It is however possible with certain tests such as steady state cornering to make quantitative measurements which will identify the basic under or oversteering characteristics of the vehicle and hence provide an indication of it's handling response and stability. Without computer simulation or rough analysis this information would not usually be available until the design has progressed to the build of a prototype and expensive track testing takes place.

Although modern computer programs (1) can be used to model and simulate the handling performance of a vehicle the complicated forces and moments acting at the tyre road interface need to be represented in some way. Before a computer simulation can be performed the design of the tyre is required and the tyre force and moment data must be found either by experimental test or mathematical modelling. The design of the tyre is one of the most

1

significant elements of the total vehicle design when considering handling and stability performance. In the design of a new vehicle the prediction of handling performance is of paramount importance. In modern road vehicles the critical control forces which determine how a vehicle turns, brakes and accelerates are generated at the tyre-road contact patch. Apart from aerodynamic forces the motion of the vehicle is developed by forces in four contact patches each about the size of a man's hand (2). Considering also the tread pattern and the road texture it is clear that the actual contact area is reduced even more significantly.

The design of the tyre is one of the most important elements if the overall vehicle design is to result in good and safe handling qualities. One of the key factors in the vehicle modelling process is the method chosen to represent the complex combination of forces generated between the tyre and the surface of the road. There are two basic methods by which these forces can be represented in a full vehicle model:

(i) Test the tyre using a tyre test machine and measure the resulting force and moment components for various camber angles, slip angles and values of vertical force. The measured data is set up in tabular form which is interpolated during the computer simulation in order to transfer the forces to the full vehicle model.

(ii) Mathematical functions are used to fit equations to the measured test data. These equations provide a mathematical tyre model which can be incorporated into the full vehicle model. This method requires the generation of a number of parameters which must be derived from the measured data before the simulation can proceed.

Both of these methods require that the tyre actually exists and has been tested before any computer modelling can take place, although in theory a model based on parameters could be adapted and used to represent a new tyre for a similar vehicle.

At this stage it is worth outlining the general sequence of events usually followed by a tyre company when developing a new tyre:

(i) The automotive manufacturer will submit a requirement to the tyre company for a tyre to fit a new vehicle design. The requirement is likely to be quite basic specifying the tyre geometry in terms of radius and aspect ratio.

(ii) Based on this requirement the tyre company will commence work on the new tyre design. Tyres are not designed from scratch. The new design will be a development of an existing similar tyre which has previously been used.

(iii) The tyre company will then obtain a vehicle from the manufacturer and embark on a series of track tests. The tests may be carried out with up to four variations on a tyre design with the final selection based on the comments of the test driver.

(iv) The new tyre design is then forwarded to the car manufacturer who then carry out their own program of tests using tyres submitted from a range of tyre companies. Based on the feedback from their own test drivers the car companies will then decide which tyres to fit on the new vehicle, which tyres to recommend for future use, and which tyres will not be recommended.

There appears to be a fundamental problem with this whole approach in that the design and testing of the tyre is not addressed until the vehicle design has progressed to the stage where an actual vehicle has been built. Clearly the use of simplified computer models will benefit studies involving the tyre earlier in the design process.

The use of industry standard software to carry out dynamic studies involving vehicle suspensions is well established (3,4) and has been extended to the use of full vehicle models for ride and handling studies (5,6). There is however some debate over the level of modelling refinement required when preparing full vehicle models for a handling simulation. Analysts in industry will often generate very complex models which attempt to recreate exactly all suspension linkage geometry and also to include the nonlinear characteristics of all the

3

suspension bushes. Experienced academic researchers reinforce the view (7), that typical full vehicle models used in industry are over complex and inefficient as design tools. In terms of developing the sort of full vehicle models described in this paper it is worth quoting Sharp in reference (7):-

"Models do not possess intrinsic value. They are for solving problems. They should be thought of in relation to the problem or range of problems which they are intended to solve. The ideal model is that with minimum complexity which is capable of solving the problems of concern with an acceptable risk of the solution being "wrong". This acceptable risk is not quantifiable and it must remain a matter of judgement. However, it is clear that diminishing returns are obtained for model elaboration."

The concept of refining a model for a particular analysis is well established in finite element modelling and can be considered as a two stage process. The first stage is to define an idealisation for the model. This involves making experienced judgements such as how to constrain a model, apply loads, exploit symmetry or select element types. The result is an idealisation or in other words a model which is 'ideal'. The second phase is more straightforward and involves deciding on the size and distribution of elements throughout the model. This is referred to as the discretisation. Typically an analyst would refine the distribution of elements until the calculated stresses converged on a realistic value. Many finite element programs can now automate this process.

For the multibody systems analyst involved in setting up a vehicle model for a handling simulation the process is not so straightforward. There is no discretisation as such. All decisions are in fact in the area of setting up an idealisation. The modelling issues will be fundamental and may include how to represent the suspension, roll bars, whether to include body flexibility, to model bushes as linear, nonlinear or not at all. The selection of a tyre model is a major issue and forms a significant part of the investigation described in this thesis.

1.2 Project aim and objectives

This programme of work was initiated through contact with SP Tyres UK Ltd. and can be considered to have the following overall aim:

This thesis aims to demonstrate the influence of vehicle and tyre models on the accuracy of predicted outputs for a typical handling simulation. The manoeuvre chosen is a lane change at 100 kph. By comparing detailed models with simpler models using reduced numbers of parameters, it is intended to indicate the levels of accuracy that can be expected by tyre and vehicle designers using the simplified approach.

In attempting to meet this broad aim this project can be considered to have four fundamental objectives. These are listed in the chronological order which they have been addressed during this study and not necessarily in terms of importance.

(i) The first objective of the work described in this thesis was to establish a level of suspension modelling suitable for vehicle handling simulation. The ability to show that relatively simple representations of a suspension could be incorporated into a full vehicle model and produce accurate handling simulation outputs is of particular significance to the vehicle and tyre designers who want to make more use of computer simulation at an earlier stage in the design process when suspension geometry has not been fixed.

(ii) The second objective was to compare methods used to model the forces and moments occurring at the tyre to road surface contact patch. By comparing a simple and sophisticated tyre model with an established interpolation model using test data, it was intended to demonstrate the influence of the tyre model on the calculated vehicle response.

(iii) Having investigated the influence of suspension and tyre model refinement, the third objective was to demonstrate the outcomes when changing from one tyre to a tyre of another design and to also consider the sensitivity of the models when making parametric variations in tyre and vehicle design characteristics.

(iv) The final objective was to develop a working design and analysis system tool based around a set of data files and routines. These files could be considered to be a set of deliverables which would allow tyre designers to rapidly assemble a vehicle model and investigate the influence of tyre design changes on handling and stability. These files and routines would work with the ADAMS software and can be summarised as:

(a) A basic ADAMS data file defining the vehicle and using a simplified modelling approach for which broad vehicle design parameters such as roll stiffness can be easily identified and changed.

(b) A command file which runs a typical handling simulation such as the lane change but can be readily modified to recreate other manoeuvres. The commands which control the steering inputs, simulation time and number of output steps would be contained in these files.

(c) A postprocessing command file to automatically animate the manoeuvre and plot all the relevant vehicle response time histories.

(d) A set of FORTRAN subroutines which can be used to represent a simple tyre model, a sophisticated tyre model and an interpolation tyre model. These subroutines would interface with the ADAMS program.

(e) An ADAMS model of a tyre test machine and a command file to run simulations which automatically read and plot the tyre force and moment curves. This is essentially a modelling tool which allows the analyst to validate a tyre model and the associated data before integrating it into a full vehicle model.

1.3 Programme of work

In order to meet the aim and objectives of this work the following programme of work has been followed:

(i) An initial literature survey has been carried out with emphasis in the following areas:

(a) Research into vehicle dynamics has been carried out in order to establish the sorts of manoeuvres carried out on the proving ground when developing a new vehicle. Information has been obtained through published papers, text books, international standards and direct contacts with automotive manufacturers. Background reading was carried out in order to become more familiar with vehicle dynamics terminology and to establish the measured outputs from handling testing.

(b) A review of multibody systems analysis software systems has been carried out. Different analytical approaches have been studied and available commercial packages identified. Particular emphasis has been placed on obtaining papers describing the theory and application of the ADAMS program which was the simulation tool adopted for this study.

(c) The complex area of tyre testing and computer modelling has been researched by accessing published papers and text books. Initial work focused on the underlying theory describing the tyre force and moment characteristics as applied to vehicle handling. This was followed by a study of the mathematical methods used to model these characteristics for multibody systems simulation.

(ii) The data required to model a vehicle needed to be obtained and collated. This data included the vehicle and suspension geometry, spring and damper data, roll bar and steering data, nonlinear bush properties and the mass and inertial properties of all relevant parts. This information needed to be organised carefully. In order to administer this task successfully many system and subsystem schematics were prepared.

7

(iii) An initial study was carried out to model the front and rear suspension systems and to simulate these moving vertically relative to the vehicle body. These models were used to obtain information such as roll centres, instant centres and suspension rates which were later used for simplified full vehicle modelling studies. A direct comparison of the modelling of connections with rigid joints, linear bushes or full nonlinear bushes was also carried out in order to determine a suitable bush modelling strategy for a full vehicle model including linkages.

(iv) A separate computer analysis was carried out of the steering system and front suspension in order to establish a linear ratio between the rotation at the steering column and the steer change at the road wheels. The influence of suspension movement on this ratio was also investigated. The information obtained from this study was then used later for simplified full vehicle modelling studies.

(v) A roll analysis of the vehicle was also carried out using ADAMS in order to establish the front and rear roll stiffnesses of the vehicle for use later with a simplified full vehicle model based on roll stiffness. This work involved building detailed models of the vehicle and suspensions and then carrying out roll simulations for the front and rear suspensions in isolation. Calculations were also carried out in order to check the results at this stage.

(vi) A range of full vehicle models has been developed and compared in order to establish the influence of suspension modelling on the measured outputs for a typical vehicle handling simulations. A variety of manoeuvres were considered but in order to keep the information in this thesis to a manageable size the results for a lane change at 100 kph have been used for the basis of comparison. At this stage the tyre model was fixed using an interpolation approach together with the data for the tyre fitted on the vehicle during track testing. The suspension modelling approaches which have been generated and are presented here are:

(a) A model where the suspension linkages and compliant bush connections have been modelled in great detail in order to recreate as closely as possible the actual assemblies on the vehicle. This is referred to as the *Linkage Model.*

(b) A model where the suspensions have been simplified to act as single lumped masses which can only slide in the vertical direction with respect to the vehicle body. This is referred to as the *Lumped Mass Model.*

(c) A model where the suspensions are treated as single swing arms which rotate about a pivot point located at the instant centres for each suspension. This is referred to as the *Swing Arm Model.*

(d) A final model where the body rotates about a single roll axis which is fixed and aligned through the front and rear roll centres. This is referred to as the *Roll Stiffness Model.*

(vii) A separate tyre modelling tool known as the *CUTyre* System has been developed. This includes an ADAMS model of a tyre test rig which will automatically read the data for a tyre model and then plot the relevant curves which illustrate the tyre force and moment characteristics. This allows the tyre model and data to be studied and presented graphically before integration into a full vehicle handling simulation. In addition FORTRAN subroutines have been developed which can model tyre test data in three ways. One approach utilises a sophisticated model based on work by Pacejka (8-10) which is known to be accurate but can require up to fifty parameters. Another approach has been to use the relatively simple Fiala model (11,12) requiring less than ten parameters to represent the tyre. In addition tyre models based on interpolation of the test data have been used and provide a benchmark for comparison of the other two models. The *CUTyre* System was a valuable development during this study and would be useful to any organisation engaged in handling simulations using ADAMS.

(viii) Tyre testing has been carried out both at SP Tyres UK Ltd. and using the tyre test rig within the School of Engineering at Coventry University. The tyre force and moment data obtained has been used as the basis for the various tyre models compared in this study. In addition the handling results obtained using this tyre were compared with those obtained using model data supplied by Rover for the actual tyre used during the vehicle testing on the proving ground. Of the three simple models it will be shown later that the Roll Stiffness model was the most suitable for further comparison with the Linkage model. Various comparisons have been

carried out, using the lane change as the basic manoeuvre. The range of simulations can be summarised as:

(a) A detailed suspension model, *Linkage Model*, running with an *Interpolation* tyre model.

(b) A detailed suspension model, *Linkage Model*, running with the *Pacejka* tyre model.

(c) A detailed suspension model, *Linkage Model*, running with the *Fiala* tyre model.

(d) A simple suspension model,*Roll Stiffness Model*, running with an *Interpolation* tyre model.

(e) A simple suspension model, *Roll Stiffness Model*, running with the *Pacejka* tyre model.

(f) A simple suspension model, *Roll Stiffness Model*, running with the *Fiala* tyre model.

The above modelling strategies were investigated with data for the tyre supplied by Rover and data for the tyre tested at SP Tyres UK Ltd. This range of tests was intended to compare the influence of suspension and tyre modelling on simulation accuracy when comparing data for different tyres.

(ix) The final objective in this project was to demonstrate how the system of models and routines developed could be used to carry out sensitivity studies by making parametric variations in tyre and vehicle design parameters and establishing the influence of these changes on the calculated vehicle response for the lane change manoeuvre. Using the results for the tyre tested at SP Tyres UK Ltd., the Roll Stiffness Model has been used together with the Fiala tyre model to investigate the influence on simulation outputs for variations in:

(a) Tyre cornering stiffness

(b) Tyre to road friction coefficient

(c) Tyre radial stiffness

(d) Vehicle centre of mass height

(e) Vehicle roll centre height

(f) Rear wheel toe angle

2.0 LITERATURE REVIEW

2.1 Introduction

There are a number of distinct areas of expertise which are integrated into this research study and have formed the basis of a supporting literature survey. In broad terms the subject matter can be considered to fall into areas covering vehicle dynamics and handling, computer modelling and simulation, the ADAMS program, and the modelling of tyre force and moment characteristics. Some of the papers and material which have been reviewed focus specifically in one of these areas but generally authors researching in this field will discuss several if not all the above areas when publishing. In documenting this literature survey an attempt has been made to categorise material into these main subject areas but given the integrated nature of the material there is inevitably a cross over when discussing any one particular reference. The approach therefore has been to attempt a review of a particular publication as a whole whether it addresses one or more of the above subject areas and to locate it in the section of the survey which is most applicable.

Wherever possible the relevance of the published work to the research described in this thesis is also discussed. It should also be noted that the work of some authors such as Pacejka (8-10) is so relevant to this project as to require a very detailed analysis of the published material. For that reason publications such as these are mentioned briefly in this section of the report but are discussed in more detail in later sections of the report such as those specifically dealing with the theory of tyre models.

In the general field of vehicle dynamics references have been identified going as far back as the 1950's in order to chart the development of vehicle handling theory, modelling and simulation. Many of these texts are general covering most areas of interest in this survey. In many cases the ADAMS program is referenced as an established program for vehicle handling but is often criticised for encouraging inefficient modelling practices. Papers describing the models, simulation tools and practices of analysts from both academia and industry have been obtained and are reviewed here, in order to set the scene for the programme of research described in this thesis.

11

Material has also been obtained to identify the work carried out by researchers and vehicle engineers describing the tests and measurements carried out during instrumented testing on the proving ground. The relevant British and International standards associated with the testing of handling performance have also been obtained. Information has also been obtained directly from Rover documenting the series of tests carried out on the vehicle.

A review has been carried out of published literature describing the computer dynamic analysis software available in this field. Particular emphasis has been placed on studying the application of multibody systems analysis software to problems in ground vehicle dynamics. The formulation of software based on numerical or symbolic solutions is also reviewed. A review has been carried out of literature describing applications of ADAMS with the main emphasis again in the area of vehicle dynamics and suspension design. The general capabilities and some of the specialist modules within the system are also described. The way in which the program is used to model vehicle systems is dealt with in a separate section of this report. For completeness references have been obtained which describe the theoretical basis of ADAMS and the associated solution processes. Information from this literature has been collated and used to prepare a description of ADAMS theory describing the equations using three dimensional vector algebra. This is also dealt with in a separate section of this report.

The modelling of the forces and moments occurring at the tyre to road surface contact patch required detailed consideration. The literature describing the sophisticated 'Magic Formula' tyre model developed by Pacejka (8-10) has been obtained and the theoretical content summarised here. The theoretical basis of the more simple Fiala tyre model (11,12) which has been used in this project has also been obtained and documented.

2.2 Road vehicle dynamics

A suitable starting point for any researcher about to embark on a programme of study in the area of road vehicle dynamics is the paper by Crolla (13). As suggested by the title, "Vehicle dynamics - theory into practice", this paper provides a contemporary review of vehicle dynamics theory and the contribution to practical vehicle design, with a particular focus on advanced simulation of actively controlled components such as four wheel steering and active suspensions. In addition the author identifies the main types of computer based tools which can be used for vehicle dynamic simulation and categorises these as:

(i) Purpose designed simulation codes

(ii) Multibody simulation packages which are numerical such as ADAMS

(iii) Multibody simulation packages which are algebraic

(iv) Toolkits such as MATLAB

For each of these methods strengths and weaknesses are identified. In the case of programs such as ADAMS weaknesses such as having limited use in design and excessive computer time are highlighted. In the case of ADAMS it could be argued that the library of elements and features encourages analysts to 'over model' a vehicle leading to the weaknesses that Crolla has identified. For the work described in this thesis it will be shown that with sensible modelling computer times are not excessive and that an efficient model based on relevant parameters can be useful in design.

One of the major conclusions that Crolla draws is that it is still generally the case that the ride and handling performance of a vehicle will be developed and refined mainly through subjective assessments. Most importantly he suggests that in concentrating on sophistication and precision in modelling, practising vehicle dynamicists may have got the balance wrong. This is an important issue which reinforces the main approach in this thesis which is to establish the suitability of simple models for a particular application.

Crolla's paper also provides an interesting historical review which highlights an important meeting at IMechE headquarters in 1956, "Research in automobile stability and

control and tyre performance". The author states that in the field of vehicle dynamics the papers presented at this meeting are now regarded as seminal and are referred to in the USA as simply "The IME Papers".

One of the authors at that meeting Segel, can be considered to be a pioneer in the field of vehicle dynamics. His paper (14) is one of the first examples where classical mechanics has been applied to an automobile in the study of lateral rigid body motion resulting from steering, inputs. The paper describes work carried out on a Buick vehicle for General Motors and is based on transferable experience of aircraft stability gained at the Flight Research Department, Cornell Aeronautical Laboratory (CAL). The main thrust of the project was the development of a mathematical vehicle model which included the formulation of lateral tyre forces and the experimental verification using instrumented vehicle tests.

In 1993 almost forty years after embarking on this early work in vehicle dynamics Segel again visited the IMechE to present a comprehensive review paper (15), "An overview of developments in road vehicle dynamics: past, present and future".

This paper provides a historical review which considers the development of vehicle handling theory in three distinct phases:

Period 1 - Invention of the car to early 1930's.
Period 2 - Early 1930's to 1953
Period 3 - 1953 to present

In describing the start of Period 3 Segel references his early " IME paper" (14). In terms of preparing a review of work in the area of vehicle dynamics there is an important point made in the paper regarding the rapid expansion in literature which makes any comprehensive summary and critique difficult. This is highlighted by the example of the 1992 FISITA Congress where a total of seventy papers were presented under the general title of "Total Vehicle Dynamics".

In the present world of vehicle dynamics there is no fixed legislation that requires manufacturers to meet a certain standard of handling performance. A number of tests are recommended in British Standards (16-18) and computer simulation is often used to recreate these tests. The procedure for the lane change manoeuvre which forms the basis of this study is described in (19). Vehicle manufacturers will often have there own set of tests which broadly follow the recommended standards but may be modified to meet their own particular requirements for the particular marque of vehicle under development. For the vehicle analysed in this study the Rover document (20) summarises the full range of tests carried out with the vehicle.

2.3 Computer modelling and simulation

In industry vehicle manufacturers make use of commercial computer software packages such as ADAMS to study suspension designs and vehicle ride and handling. These programs have a general capability and can be used to perform large displacement static, kinematic or dynamic analysis of systems of interconnected rigid bodies. In the past this discipline has been referred to by various labels amongst which are dynamics, kinematics, mechanism or linkage analysis. In fact none of these completely describe the methodology and in recent years the term Multibody Systems Analysis (MBS) has gained favour as collectively describing the above. ADAMS is not the only program which has this general capability and a review of the most widely used packages which perform Multibody Systems Analysis is given in (21).

A general description of how MBS is used in vehicle design is given in (22). This paper identifies applications of MBS within the automotive industry such as:

(i) Calculation of suspension characteristics such as camber angle, steer angle and caster angle as a function of vertical suspension movement.

(ii) Prediction of joint and bush reaction forces for various loadcases at the tyre to road surface contact patch.

(iii) Full vehicle ride and handling simulations.

(iv) Advanced simulation of features such as Antilock Braking Systems (ABS).

A similar approach based on industrial experiences is given in (5) where it is suggested that the development of a full vehicle model with a program such as ADAMS can be described by the following stages of activity:

(i)　Stage 1

Initial studies can involve the development of kinematic models of both the front and rear suspension units (quarter models). At this stage it is not necessary to include the road springs dampers, tyres or bushings. The simulations investigate movements between full bump to full rebound and steering rack displacement inputs.

(ii)　Stage 2

During this stage the quarter models can be developed to introduce the compliances and the full bump to full rebound simulations from Stage 1 are repeated. In addition the effects of longitudinal braking and driving forces can be examined for both front and rear suspensions. At this stage the simulations can be run quasi-statically.

(iii)　Stage 3

In this phase dynamic analyses may be run on separate front and rear half models of the vehicle. The simulations can involve the input of vertical displacements to a moving ground patch below the tyres in order to represent the effects of a high speed kerb impact.

(iv)　Stage 4

The final stage will require the assembly of the full-vehicle model and can consist of a series of handling simulations. The full-vehicle model can be driven using torques input at the differential and transferred via the driveline to the wheels. Typical handling simulations can involve:-

(a) A fixed steering input of 90 degrees with a constant torque input at the differential

(b) Steady state cornering at various speeds using a speed controller to maintain constant velocity

(c) Lane change manoeuvres around fixed obstacles with again a constant torque input at the differential.

The authors in (23) give further insights into how computer models and simulation programs are used by industry in the field of road vehicle dynamics. In this case the company is Lotus. Additional information about the work at Lotus in the field of vehicle dynamics and simulation is also given in (24). In (23) the paper describes how simulation tools can be used at various stages in the design process. This includes the manner in which ADAMS is used to 'tune' a suspension design during development to produce for example very low but accurately controlled levels of steer change during suspension stroke. This sort of modelling of suspension systems with ADAMS was also a necessary component of this project and is described in Section 4 of this thesis.

The authors in (23) continue to describe how for vehicle handling they use their own Simulation and Analysis Model (SAM). This is a functional model which requires a minimum of design information and uses input parameters which can be obtained by measurement of suspension characteristics using a static test rig. The SAM model has 17 rigid body degrees of freedom (DOF). The paper identifies that the vehicle body contributes 6 of these DOF and that each corner suspension unit has 2 DOF, one of which will be the rotation of the road wheel and the other will allow vertical movement relative to the vehicle body. In fact the suspensions are modelled to pivot about an instant centre which is the same approach used with the Swing Arm Model described in this thesis. The model also has 3 DOF associated with steering which suggests steering torque inputs and the modelling of compliance in the steering system. The SAM model uses the early tyre model proposed by Pacejka in (8).

The use of ADAMS by Lotus for handling simulations is also described in this paper (23). In this case an example output shows good correlation between ADAMS and test measurements when comparing yaw rate for an 80 kph lane change manoeuvre. It is also stated however that this model has over 200 DOF and uses the Pacejka model which requires up to 50 parameters. This is an example of the practice often carried out in industry which is referred to by Sharp in (7) and can be considered to be over elaboration in modelling. This is certainly relevant to the work described in this thesis where a Roll Stiffness Model which only has 12 DOF and a Fiala tyre model which only uses 10 parameters is later shown to give good agreement between ADAMS and test data when comparing yaw rate for a 100 kph lane change manoeuvre.

At Leeds University a vehicle specific system has been developed and is described by Crolla (25). In this case all the commonly required vehicle dynamics studies have been embodied in their own set of programs known as VDAS (Vehicle Dynamics Analysis Software). Examples of the applications incorporated in this system include, ride/handling, suspensions, natural frequencies, mode shapes, frequency response and steady state handling diagrams. The system includes a range of models and further new models can be added using a preprocessor. This paper also discusses software in general. Purpose designed simulation codes are described as those where the equations of motion have been developed and programmed for a specific model. Model parameters can be changed but the model is fixed unless the program is changed and recompiled.

For MBS programs ADAMS is identified as the most widely used but is suggested to encourage building complex models which are as close as possible to the real vehicle. This is again relevant to the work in this thesis which demonstrates that although programs such as ADAMS may have the capability for detailed modelling there is no reason the software can not be also used for efficient simple models. The authors also define two fundamental types of MBS program, the first of which are those such as ADAMS where the equations are generated in numerical format, can not be inspected and are solved directly using numerical integration routines embedded in the package. The second and more recent type of MBS program identified formulates the equations in symbolic form and often uses an independent solver. With these systems the equations of motion can be inspected if so desired.

The authors in (25) also describe toolkits as collections of routines which generate models, formulate and solve equations, and present results. Their own VDAS system is identified as falling into this category of computer software used for vehicle dynamics.

Other examples of more recently developed codes formulate the equations algebraically and use a symbolic approach (26-28) during solution. A comparison of the differences between a numeric and symbolic code is again given in (29). As stated MBS programs will usually automatically formulate and solve the equations of motion although in some cases such as with the work described in (30-33) a program SDFAST has been used to formulate the

equations of motion in symbolic form and another program ACSL (Automatic Continuous Simulation Language) has been used to generate a solution.

For any institution planning to obtain a MBS program the following criteria are identified in (22) as typical of those which would be involved in the decision making process.

(i) General: The establishment of the software as an industry standard tool may be of primary importance. A company providing components to a major manufacturer, for example, will be heavily influenced to use the same software. Other aspects will include the size of the software vendor company, their location and reputation for support. Some programs may also be targeted at a specific area such as the rail or road industries. The cost of the software and the availability of experienced staff to recruit will also have a bearing.

(ii) Modelling Capability: The choice of software may also be influenced by a specialist need such as modelling of a rolling contact or incorporating elastic bodies. For the automotive industry the most obvious requirement would be the availability of tyre models which can be integrated with the package.

(iii) Analysis Modes: Most programs will be able to perform static, kinematic and dynamic analysis. Additional capabilities such as quasi-static or modal analysis may also influence the choice.

(iv) Pre- and Post-processing: The capability to prepare models using an interactive pre-processor is desirable but not so essential as in the case of finite element modelling. Of more importance is the capability to post-process using graphics, animation and XY plotting of time histories. Interfaces to other programs, finite element packages or CAD systems may also be significant.

A detailed comparison between the various codes is beyond the capability of most companies when selecting a MBS program. For the automotive industry additional information is available in (34,35) where the authors have undertaken a comprehensive benchmarking exercise of all the main codes with the emphasis on vehicle system dynamics.

This exercise was organised by the International Association for Vehicle System Dynamics (IAVSD). In this study the various commercially available MBS programs have been used to benchmark two problems. The first is to model the Iltis military vehicle and the second is a five link suspension system. This is discussed further in (36) where some of the difficulties involved with such a wide ranging study are discussed. An example of the problems involved would be the comparison of results. With different investigators using the various programs at wide spread locations a simple problem occurred when the results were sent in plotted form using different size plots and inconsistent axes making direct comparisons between the codes extremely difficult. It was also very difficult to ensure that a consistent modelling approach was used by the various investigators so that the comparison was based strictly on the differences between the programs and not the models used. An example of this with the Iltis vehicle would be modelling a leaf spring for which in many, if not all programs such as ADAMS, there is no standard element within the main code.

The authors in (37) have carried out an interesting study where they have used two vehicles to make a comparison of three different vehicle simulation methodologies. They have also made use of the Iltis, a vehicle of German design, which at that time was the current small utility vehicle used by the Canadian military. The Iltis was a vehicle which was considered to have performed well and had very different characteristics to the M-151 jeep which was the other vehicle in this study. The authors state that the M-151 vehicle, also used by the Canadian military, had been declared unsafe due to a propensity for rolling over. In this study the authors have compared three simulation methods. The authors describe how they have made use of the Highway-Vehicle-Object Simulation Model (HVOSM) which is based on direct derivation of the equations of motion for a four-wheeled vehicle by Segal (15). Although this work (37) addresses using different simulation tools it does not provide a detailed description of the models or simulations. There is also no inclusion of plotted time history outputs by which a comparison in accuracy could be made by the reader. The authors do state that the ADAMS model resulted in over 500 equations for what they consider an analyst would regard as a 10 degrees-of-freedom model. They also state that using the ADAMS package was time consuming and required an input file in excess of 1000 lines, and that computer simulation time with ADAMS was an "order of magnitude" greater than the other two methods. On this

evidence it would appear that they have adopted the modelling approach with ADAMS which is common; that is to model everything that is there whether it is significant for the simulation in hand or not. These are some of the issues which this thesis attempts to address.

Special purpose programs are designed and developed with the objective of solving only a specific set of problems. As such they are aimed at a specific group of problems. A typical example of this sort of program would be AUTOSIM (26,38,39,40) which is intended for vehicle handling and has been developed as a symbolic code in order to produce very fast simulations. Programs such as this can be considered to be special purpose as they are specifically developed for a given type of simulation but do however allow flexibility as to the choice and complexity of the model. An extension of this is where the equations of motion for a fixed vehicle modelling approach are programmed and cannot be changed by the user such as the HVOSM (Highway-Vehicle-Object Simulation Model) developed at the University of Michigan Transport Research Institute (UMTRI) (39). The program includes tyre and suspension models and can be used for impact studies in addition to the normal ride and handling simulations. The authors in (29) indicate that the University of Missouri has also developed a light vehicle dynamics simulation (LVDS) program which runs on a PC and can produce animated outputs. In the mid 1980's Systems Technology Inc. developed a program for vehicle dynamics analysis non-linear (VDANL) simulation. This program is based on a 13 degree of freedom, lumped parameter model (41) and has been used by researchers at Ohio State University for sensitivity analysis studies (42).

To conclude the review of vehicle models for simulation, work has been carried out at the University of Bath (43) which is relevant to the work in this thesis. In this case the authors have compared ADAMS with their own hydraulic and simulation package. The results for both programs are compared with measured vehicle test data provided in this case by Ford. The Bath model is similar to the Roll Stiffness Model described in this thesis but in is based on a force roll centre as described by Dixon in (44). This requires the vehicle to actually exist so that the model can use measured inputs obtained through static rig measurements, using equipment of the type described in (45) and (46). The work in this current thesis is based on a kinematic roll centre which is based on suspension geometry as described in Section 4 of this report. This form of model can be used during design before the vehicle exists.

21

As a guide to the complexity of the models discussed in (43), the Bath model required 91 pieces of information and the ADAMS model although not described in detail needed 380 pieces of information. It is also stated in this paper that the ADAMS model used 150 sets of nonlinear data pairs which suggests detailed modelling of all the nonlinear properties of individual bushes throughout the vehicle. This again reflects the apparently common conception that to develop a model with ADAMS requires the very detailed modelling which this thesis will investigate.

2.4 The ADAMS program

General purpose programs such as ADAMS have been developed with a view to commercial gain and as such are able to address a much larger set of problems across a wide range of engineering industries. In addition to the automotive industry ADAMS is a well established tool within the aerospace, large construction, electro-mechanical and the general mechanical engineering industries. The general nature of the program means that within any one industry the class of applications may develop and extend over a broad range. A comprehensive overview of ADAMS is provided by the author in (1) although since the date of that publication the development of the software has moved on considerably, particularly in the area of graphical pre and post-processing. The typical range of applications for a program such as ADAMS throughout industry is outlined in (47) and is discussed further in Section 3 of this thesis.

Before the evolution of MBS programs such as ADAMS engineers analysed the behaviour of mechanisms such as cam-followers and four bar linkages on the basis of pure kinematic behaviour. Graphical methods were often used to obtain solutions. In (48) the author summarises the early programs which lead to the development of the ADAMS program. One of the first programs was KAM (Kinematic Analysis Method) (49) which performed displacement, velocity and acceleration analysis and determined reaction forces for a limited set of linkages and suspension models. Another early program was COMMEND (50) (Computer-Orientated Mechanical Engineering Design) which was used for planar problems.

The origin of ADAMS can be traced back to a program of research initiated by Chace at the University of Michigan in 1967. By 1969 Chace and Korybalski had completed the original version of DAMN (Dynamic Analysis of Mechanical Networks) (51-53). This was historically the first general program to solve time histories for systems undergoing large displacement dynamic motion. This work lead in 1971 to a new program DRAM (Dynamic Response of Articulated Machinery) which was further enhanced by Angel (54).

The first program known as ADAMS was completed by Orlandea in 1973 (55-56). This was a development of the earlier two-dimensional programs to a three-dimensional code but without some of the impact capability which was in DRAM at that time. In 1980 the company Mechanical Dynamics Incorporated (MDI) was formed and the ADAMS program became commercially available

In (5) the author describes how the ADAMS software is used to study the behaviour of systems consisting of rigid or flexible parts connected by joints and undergoing large displacement motion and in particular the application of ADAMS in vehicle dynamics. The paper also discusses a number of other systems based on ADAMS which have been developed specifically for automotive vehicle modelling applications. Several of the larger vehicle manufacturers have at some time integrated ADAMS into their own in-house vehicle design systems. Examples of these are the AMIGO system at Audi (57), and MOGESSA at Volkswagen (58). The WOODS system based on user defined worksheets has also been developed by German consultants for FORD in the UK (59).

The ADAMS/View pre- and postprocessor is provided with the ADAMS software and allows users to define models and evaluate results using the same graphical environment, with the capability to build a model, submit the analysis, and evaluate the results. The postprocessor will output results in tabular format, x-y plots and graphic animation. Before the introduction of ADAMS/View many users of ADAMS simply prepared the input deck for ADAMS using a text editor and a logical numbering system for the parts, markers and other system elements. That is the approach used for the work described in this thesis and also by some other users of ADAMS within industry (60). Another past approach to pre-processing made use of a macro programming language to prepare a model and generate an ADAMS input deck. This macro

language, known as the Data Modification Program (DMP) was originally developed by MDI as a pre-processor to ADAMS and gained favour with many automotive companies particularly in Europe. To a large extent the program has become outdated with the arrival of graphical interfaces although there is evidence that it still forms the basis of some customised applications used by the automotive industry (61). In this paper the authors describe how programs such as ADAMS and DMP have been integrated into a system known as SARAH (Suspension Analyses Reduced ADAMS Handling). This is another in house system for the automotive industry which has in this case been developed by the Fiat Research Centre Handling Group and uses a suspension modelling technique which ignores suspension layout but focuses on the final effects of wheel centre trajectory and orientation.

As a pre-processor the DMP program was most useful to more experienced ADAMS users with good programming skills. It was essentially a data management tool which allowed users to assemble large and sophisticated models in a structured manner. Although it had no graphical interface it allowed users to build up a library or 'tool kit' of macros for vehicle applications. The input to DMP was prepared in a language known as the Data Modification Language (DML) which allowed users to define macro descriptions of major full-vehicle subsystems. The macros which would be used to generate a full vehicle model are described in (5,62).

Many of these macros were developed by Fischer (62) who during the late 1980's and early 1990's was involved in consulting and research activities with several European Automotive manufacturer's (59) and was widely regarded as the most experienced ADAMS user outside of the USA. Fischer also went on to become one of the first users to implement Pacejka's "Magic Tyre" model (8-10) in ADAMS (63).

The DMP program was also used to generate a very large and complex full vehicle model with in excess of 160 degrees of freedom (64). This model was produced through consulting work with Rolls Royce Motor Cars Ltd. and was intended to include as much detail as possible and to be suitable for a wide range of applications including ride, handling and durability studies. The model was not efficient for any one analysis and contrasts with the modelling approach which this thesis attempts to present.

The model was however an early example of a parameter based model in ADAMS due to the way DMP macros could utilise program variables and was intended at that time to be a model database which could be used for a wide range of simulations while not being efficient for any particular one.

With the decline of DMP as a pre-processor there was another development of a customised ADAMS vehicle based pre-processor. ADAMS/Vehicle was originally developed by the consulting group of Mechanical Dynamics Inc. in the USA and became a commercially available product (65) which has been used by engineers from the Newman/Hass Indy Car racing team (66). The program allows a suspension model to be created, carry out an analysis and post-process the results without specialist knowledge of ADAMS. The program could also be used to automatically generate a full vehicle model, hence the title. The pre-processor included a number of established suspension configurations where the data was input via screen templates using familiar suspension terminology.

2.5 Tyre models

The modelling of the tyre forces and moments at the tyre to road contact patch is one of the most complex issues in vehicle handling simulation. The models used are not predictive but are used to represent the tyre force and moment curves. For the work described in this thesis it was necessary to become familiar with the theory of tyres before studying the more difficult aspects of integrating the theory into tyre models which can interface with a vehicle model during a handling simulation. The tyre models which have been investigated in this programme of study include:

(i) A sophisticated tyre model known as the "Magic Formula". This tyre model has been developed by Pacejka and his associates (8-10) and is known to give an accurate representation of measured tyre characteristics. The model uses modified trigonometric functions to represent the shape of curves which plot tyre forces and moments as functions of longitudinal slip or slip angle. It would have been impossible to carry out a research program in this field without considering this model as in recent years the work of Pacejka has become widely known throughout the vehicle dynamics community. The result of this is a tyre model

which is now widely used both by industry and institutions and is undergoing continual improvement and development. The complexity of the model does however mean that up to 50 parameters may be needed to define a tyre model and that software must be obtained or developed to derive the parameters from measured test data. It should also be noted that although known to be accurate the physical significance of many of the parameters is not always obvious.

(ii) The second model considered is known as the Fiala tyre model (11,12) and is provided as the default tyre model in ADAMS. This is a much simpler model which also uses mathematical equations to represent the tyre force and moment characteristics. Although not so widely recognised as Pacejka's model the fact that this model is the default in ADAMS and is simpler to use lead to its inclusion in this study. The advantage of this model is that it only requires 10 parameters and that the physical significance of each of these is easy to comprehend. The parameters can also be quickly and easily derived from measured test data without recourse to special software. It should also be noted however that this model unlike Pacejka's is not suitable for combined braking and cornering and can only be used under pure slip conditions as with the lane change described in this thesis.

(iii) The third modelling approach was to use a straightforward interpolation model. This was the original tyre modelling method used in ADAMS and is referred to in (1). This methodology has to a large extent been superseded by more recent parameter based models but has been included as a useful benchmark for the other two tyre models being compared. It should also be noted that interpolation tyre models are often described as using excessive computer simulation time although as will be shown later this was not found to be the case in this thesis.

The modelling of tyres is discussed at length in Section 6 of this thesis and for that reason a far more detailed review of the literature associated with tyre modelling is included in that Section. This is particularly necessary for the work of Pacejka. In order to develop FORTRAN models for this model a detailed study of the mathematical formulations given in (8-10) was necessary and is therefore documented in Section 6 of this thesis.

26

2.6 Summary

The literature survey presented here has established that there is a wide range of approaches in adapting vehicle dynamics theory to model and simulate handling performance. The main areas covered include:

(i) The type and complexity of vehicle model which is to be used.

(ii) The method of modelling the tyre force and moment characteristics.

(iii) The choice of simulation program/tools to be used.

Throughout the literature there appears to be a consistent view point, particularly from academia, that programs such as ADAMS encourage detailed modelling, are therefore inefficient and require excessive computer solution times. Authors also observe that these models have little value as a design tools due to the large number of model parameters. These conceptions are validated in several cases by publications from industry which indicate in some cases the use of full vehicle models having in excess of 200 degrees of freedom. Despite this the evidence from the literature is that ADAMS is recognised as the program most often used by automotive companies and vehicle manufacturers. ADAMS is also used at Rover Group and at SP Tyres UK Ltd, the two institutions which have supported this project.

A disappointing aspect of many of the references is the lack of information regarding the vehicle models used. In many cases there is no detail at all and certainly no schematics which would be useful in interpreting the modelling approach. In some cases different simulation tools or methodologies are compared but do not use the same model.

It is interesting to note from the literature that the inefficient modelling of vehicle systems is often discussed but little mention is given regarding the use of efficient tyre models. The Pacejka tyre model is very widely used despite having a complicated mathematical basis and requiring a large number of parameters. Papers which discuss or compare tyre modelling focus on showing the correlation of the tyre model with measured test data. This does not

always appear to be extended to the issue of demonstrating how well the tyre model performs when used to simulate the performance of a vehicle.

Having considered the issues raised by this literature survey the work in this thesis attempts to make a contribution in the field of vehicle dynamics by addressing the following:

(i) Although it has been shown that the ADAMS program encourages the use of over complex models it will be shown here that the program need not necessarily be used in this manner. As an industry standard tool it is useful to demonstrate that ADAMS can be readily used to generate simple and efficient models which are accurate for a chosen application.

(ii) The literature survey has indicated a lack of detail in describing models in published material and comparisons of different models using different simulation tools from which conclusions are difficult to draw. The work described here presents four vehicle modelling approaches and compares the outcomes for a particular application using a fixed solution method.

(iii) From the evidence provided in this literature survey the comparison of a simple model such as the Fiala model with a complex model such as the Pacejka model will provide new insights into the use of tyre models in handling simulations. If models are to be efficient for a particular application this should extend from the vehicle to include the tyre model.

(iv) Integration of a tyre model into a multibody systems program requires developing separate routines or software modules. During this programme of work a system referred to as the *CUTyre* System has been developed to include a set of FORTRAN tyre models which interface with the main ADAMS code.

The next section of this report provides an overview of ADAMS and its underlying theory. Readers already familiar with this material may prefer to move on to Section 4, where an account of the main body of work in this study commences.

3.0 SIMULATION SOFTWARE

3.1 Multibody systems analysis

In industry vehicle manufacturers make use of commercial computer software packages such as ADAMS to study suspension designs and vehicle ride and handling. These programs have a general capability and can be used to perform large displacement static, kinematic or dynamic analysis of systems of interconnected rigid bodies. The computer based analysis methodology known as multibody systems analysis (MBS) became established as a tool for engineering designers and analysts during the 1980's in a similar manner to the growth in finite element analysis (FEA) during the previous decade. The accompanying advances in computer technology at this time resulted in a growth in hardware capability and reduction in costs. The general thrust to exploit these developments contributed to the growth of computer aided engineering (CAE) programs and led to increased usage of MBS in many fields of engineering. As with other areas of computer modelling and simulation, the dynamic analysis capabilities of these programs can enhance the development of new products by reducing the time taken to bring them to the market place and getting them almost 'right first time'.

Multibody systems analysis is applicable to mechanical systems which may be built up from an assembly of rigid bodies. Applications arise across a wide range of industries and the scale of problems can vary form those involved in spacecraft dynamics to the mechanisms in a compact disc player. In some cases, although rarely, a finite element representation may be incorporated to account for the flexibility of a body. The most common example of this is the modelling of flexible solar panel deployment during a satellite orbit simulation. The relative motion between the bodies is constrained using constraint elements, or joints which represent real mechanical connectors such as universal joints. It is also possible to model flexible connectors such as the rubber bushes so commonly used to isolate vibration in vehicle suspensions. System elements such as springs and dampers can also be included. The non-linear force characteristics can also be modelled. This is particularly required for dampers which are not only nonlinear but also asymmetric having different properties during compression in bump or extension in rebound. Multibody systems analysis programs are mainly intended to analyse systems which move through large displacement motion. The most general

programs will have a graphical user interface which can be used to develop or pre-process a model and also during postprocessing for the animated and plotted presentation of results.

Computer programs which carry out MBS are used by engineers and designers to study the behaviour of systems subject to dynamic motion. The range of applications which can be solved using MBS is vast and will often encompass problems which can also be solved using the nonlinear analysis capabilities of FEA programs. The main difference between the two methods is that MBS programs consider systems consisting of rigid bodies connected by joints, rather than representing geometric shapes with discrete elements as in FEA. Consequently the output from MBS programs is generally confined to displacements, velocities, accelerations and forces and not stresses and strains.

The main users of MBS software have always been the automotive industry followed by aerospace, general machinery, electro-mechanical and heavy construction or agricultural equipment industries. During concept or feasibility studies engineers may conduct sensitivity studies, investigating certain trends due to successive variations in a design parameter, and the effects on the predicted motion of the system. At this stage the model may be quite simplistic gaining sophistication as the design progresses and more hard data becomes available. The initial prediction of loads acting on components may be used as inputs to finite element models and then the MBS process repeated after more detailed design of individual components.

At a later stage MBS may be used to evaluate the performance of existing designs or in parallel with the development and testing of full prototypes. In some cases the software may be used to investigate extreme operating conditions which could lead to a dangerous or expensive failure if attempted with a prototype. The software may also be used to reconstruct or investigate the behaviour of an existing system which is not operating correctly or is experiencing repeated failures. In some cases this may involve determining the reasons for an accident involving a vehicle or the operation of a mechanical system.

Within the automotive industry the main usage by manufacturers is by design groups in the area of chassis engineering involved with the design and analysis of the vehicle suspension systems and the prediction of the ride and handling performance of the total vehicle. Apart

from this applications of ADAMS within the automotive industry have also been known to include engine design, transmission systems, wiper mechanisms or door and tailgate latching simulation.

A more detailed description of the ADAMS program follows. It should be noted that commercial software such as ADAMS is undergoing continual development. The description provided here is limited to software features relevant to this study.

3.2 The ADAMS program

3.2.1 Overview

General purpose programs such as ADAMS are able to address a large set of problems across a wide range of engineering industries. The general nature of the program means that within any one industry the class of applications may develop and extend over a broad range.

The main use of ADAMS within the automotive industry is to simulate the performance of suspension systems and full vehicle models. The analyst will often wish to validate the performance of a suspension model over a range of displacements between full bump to rebound before the assembly of a full vehicle model. The final model may be used for ride and handling, durability or crash studies. A detailed model may include representations of the body, subframes, suspension arms, struts, roll bars, steering system, engine, drivetrain and tyres.

The main analysis code consists of a number of integrated programs that perform three-dimensional kinematic, static, quasi-static or dynamic analysis of mechanical systems. In addition there are a number of auxiliary programs which can be supplied to link with ADAMS. These programs can be used to perform modal analysis, model vehicle tyre characteristics, pre-process using a library of macros, automatically generate vehicle suspensions and full vehicle models, or model the human body. Once a model has been defined ADAMS will assemble the equations of motion and solve them automatically. It is also possible to include differential equations directly in the solution which allows the modelling of active suspensions or steering, braking and speed controllers.

31

The output from ADAMS will be calculated at selected points in time during the simulation. Results include displacements, velocities, accelerations and forces. These results can be resolved globally or relative to any other part in the system. Users can also formulate their own customised output using any mathematical combination of the normal request output. The output can be presented as tabular data or as X-Y plots where results can be displayed in the time or frequency domain. It is also possible to visualise the results of a simulation either as still frames or continuous graphic animation.

3.2.2 Modelling features

The first step in any simulation is to prepare the ADAMS data set which will define the vehicle being modelled. This will include a description of the rigid parts, connecting joints, motion generators, forces and compliances. The ADAMS data set is user friendly in that the data statements are easily understood with few restrictions on format. It is also possible to formulate complicated force and motion equations directly within the data deck. For advanced applications users can also prepare their own user-written subroutines in FORTRAN-77 which can be linked with the main ADAMS code.

For each rigid body in the system it is necessary to include a part statement defining the mass, centre of mass location, and mass moments of inertia. Each part will possess a set of markers which can be defined in global or local coordinate systems and are considered to move with the part during the simulation. Markers are used to define centre of mass locations, joint locations and orientations, force locations and directions. In every ADAMS model it is also necessary to include one non-moving part which is referred to as the ground part.

The relative motion between different parts in the system can be constrained using joints, joint primitives, couplers, gears and user defined constraints. The most direct method of connecting any two parts is to use standard joints provided with the software. Examples of eight of the most commonly used are described in (5) and shown here in Figure 3.1.

32
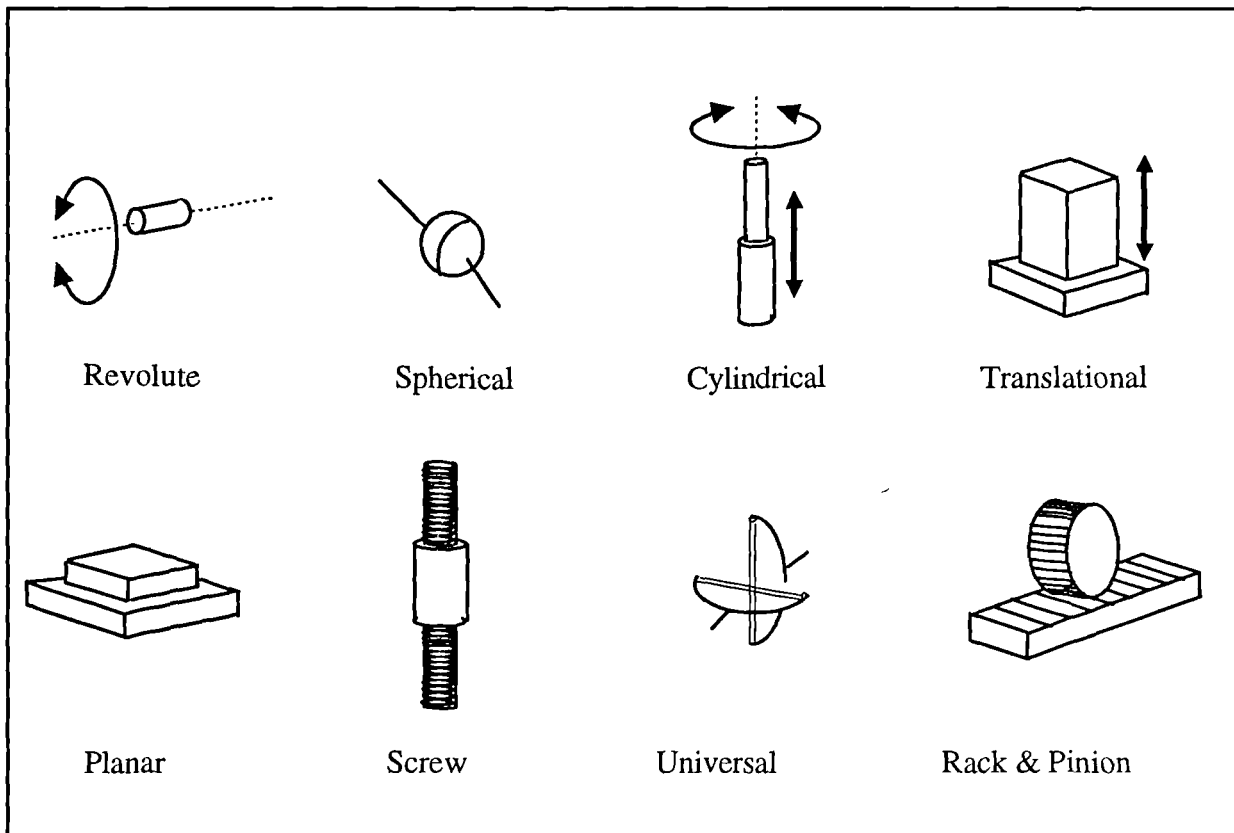
Figure 3.1 Typical joints provided with ADAMS

Where the type of connection between two parts can not be represented by a joint it is possible to access a set of six joint primitives. The joint primitives can be used to directly couple selected translational or rotational degrees of freedom between two parts. It is also possible to set up models for differentials, gear pairs and steering boxes using gear and coupler elements. The next step in building the model would typically be the definition of external forces and internal force elements. External forces can be constant, time histories or functionally dependent on any state variable. These forces can also be defined to be translational or torsional. They can act in the global system or can act in the local system of the part so that they effectively 'follow' the part during the simulation. In ADAMS terminology external forces are referred to as Action-Only forces.

Users can also set up internal force elements acting between two parts to represent springs, dampers, cables or rubber mounts. Internal force elements will always act along the line of sight between the points the force element connects on the two parts. These force

elements are referred to as Action-Reaction forces as they always produce equal and opposite forces on the two parts connected by the force element. The element can be defined to act in only tension, compression or both and may be linear or nonlinear. The user may define complicated mathematical equations for force within the input deck using the ADAMS 'FUNCTION' capability. This enables the user to formulate an expression involving user-defined constants, system constants, system variables, arithmetic IF's, FORTRAN-77 library functions, standard mathematical functions or 'off-the-shelf' ADAMS-supplied functions. The access to system variables can be a powerful modelling tool. The user can effectively access any displacement, velocity, acceleration or other force in the system when defining the force equation. Forces can also be defined as a function of time to vary or switch on and off as the simulation progresses.

Enforced displacement input can be defined at certain joints to be either constant or time dependent. When a motion is defined at a joint it may be translational or rotational. The motion effectively provides another constraint so that the degree of freedom at that joint is lost to the motion. Motion inputs can only be defined at translational, revolute or cylindrical joints. It is however fairly easy to build a simple jack element which can provide a displacement input anywhere in the system. Users in the automotive industry often do this to input vertical displacements at the base of a road wheel in order to study suspension characteristics. Motion expressions can be defined using all the functions available as for force definitions except that the only system variable which can be accessed is time. Users can also write there own user-written subroutines for motion inputs. ADAMS provides a number of elements which provide the capability to model flexibility of bodies and elastic connections between parts. Statements are available for modelling beam elements, rubber bushings or mounts, plus a general stiffness and damping field element. At various positions in a model rigid parts can be elastically connected together in preference to using a rigid constraint element such as a joint or joint primitive. Vehicle suspension bushes can be represented by a set of six action-reaction forces which will hold the two parts together. The equations of force are linear and uncoupled. The user is only required to provide the six diagonal coefficients of stiffness and damping. For more complicated cases the general purpose field statement can be used to provide a linear or nonlinear representation of a flexible body. In some cases the flexible body structure can be

modelled using a finite element program which has superelement or substructuring facilities in order to determine the terms required by ADAMS.

For full vehicle applications it is important to obtain an accurate model for the tyres and the associated forces generated at the tyre-road surface contact patch. For each tyre on the vehicle model the program will calculate the three orthogonal forces and three orthogonal torques acting at the wheel centre as a result of the conditions at the tyre-road surface contact patch. In order to perform these calculations it is necessary to continuously update the tyre model regarding the position, velocity and orientation of the wheel centre marker and any changes in the topography of the road surface. Once this information has been received the tyre model must then calculate the set of forces acting at the contact patch. Once these forces have been calculated they can be resolved back to the wheel centre. ADAMS will then integrate through time to find the new position and orientation of the vehicle and then the process can be repeated. A more detailed treatment of tyre modelling with ADAMS is given in Section 6 of this thesis.

3.2.3 Analysis capabilities

Once the model has been assembled the main ADAMS code may be used to carry out kinematic, static, quasi-static or dynamic analyses. Kinematic analysis is applicable to systems possessing zero rigid body degrees of freedom. Any movement in this type of system will be due to prescribed motions at joints. ADAMS uncouples the equations of motion and force and then solves separately and algebraically for displacements, velocities accelerations, and forces.

For static analysis ADAMS sets the velocities and accelerations to zero and the applied loads are balanced against the reaction forces until an equilibrium position is found. This may involve the system moving through large displacements between the initial definition and the equilibrium position and therefore ADAMS will perform a number of iterations until it converges on the solution closest to the initial configuration. Static analysis is often performed as a preliminary to a dynamic analysis. An example would be to perform a static analysis on a full vehicle model before a dynamic handling simulation. This establishes the configuration of the vehicle at 'kerb height' before the vehicle moves forward during the dynamic phase of the

simulation. Quasi-static analysis is a series of static equilibrium solutions at selected time steps. Although the system can be considered to be moving the dynamic response is not required. An example would be to perform a quasi-static analysis on a vehicle mounted on a tilting surface. As the surface rotates to different angles with time the static equilibrium of the vehicle can be calculated at selected angles.

Dynamic analysis is performed on systems with one or more degrees of freedom. The differential equations representing the system are automatically formulated and then numerically integrated to provide the position, velocities, accelerations and forces at successively later times. Although the user will select output at various points in time the program will often compute solutions at many intermediate points in time. The interval between each of these solution points is known as an integration time step. In ADAMS the size of the integration time step is constantly adjusted using internal logic although the user may override the system defaults if so desired. More experienced users can also use sensors to alter the integration parameters just before the introduction of some highly nonlinear event such as an impact. It is also possible to extract the linearised state-space plant model in a format suitable for input to a control system design package such as MATRIXx. The application of these methods is described in more detail in Reference (67).

3.2.4 Pre- and postprocessing

The ADAMS program is undergoing a continual process of development and improvement particularly in the area of graphical pre- and postprocessing. As such the information in this section does not cover all the latest capabilities of the ADAMS program in this area, but can be considered relevant for the activities described in this thesis.

For any full vehicle study involving ADAMS the pre and post-processing stages can represent a considerable part of the work. Most of the major CAD packages have interfaces to and from ADAMS. This allows the user to assemble components created in a geometry modeller and output an ADAMS input deck. The analysis is then run using ADAMS and the results passed back to the CAD package for postprocessing. In finite element analysis this is a

method often used but does not appear to be so common in the case of ADAMS, where the program's own pre- and postprocessing package is usually used.

The ADAMS/View pre- and postprocessor which is provided with the ADAMS software and allows users to define models and evaluate results using the same graphical environment. The postprocessor has been used to prepare the results presented in this thesis and has the capability to output results in tabular format, x-y plots and continuous graphic animation. An example of the animated output from ADAMS is included here in Figure 3.2.
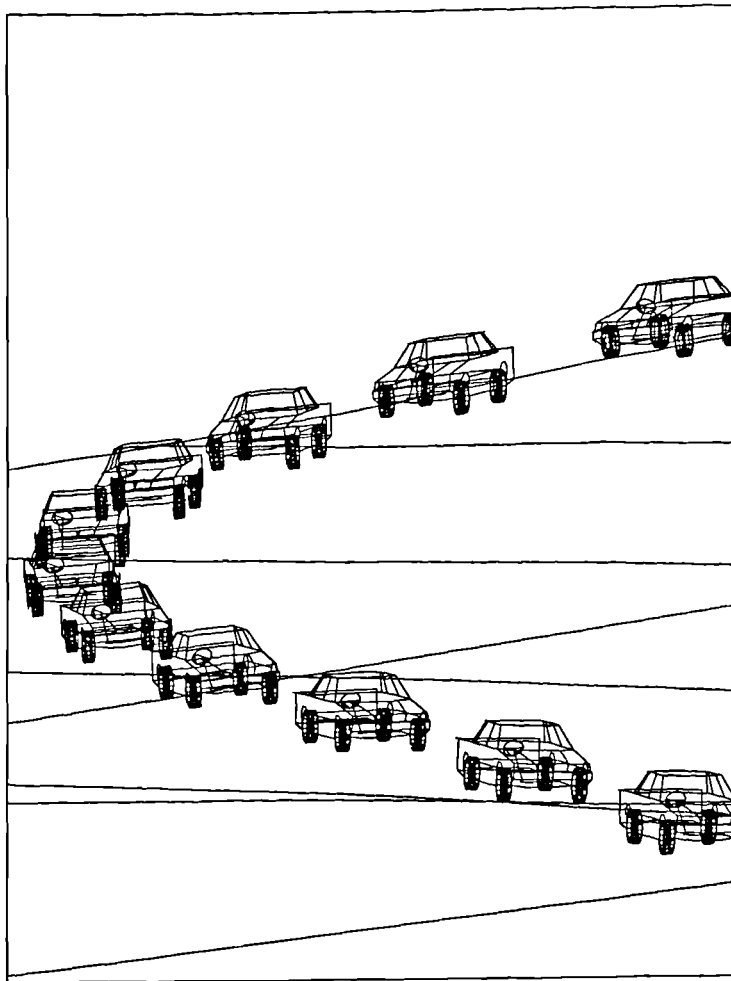
Figure 3.2 Graphical output of vehicle handling manoeuvres

3.3 ADAMS theory

3.3.1 Background

The ADAMS user manuals do not give a comprehensive description of the theory behind the software and there are no text books which provide this information specifically for the ADAMS program. Numerically based programs such as ADAMS have been criticised in the past (7) as, unlike symbolic codes, the equations of motion are embedded in the program and are not available for inspection by the user. It was considered necessary therefore to include the following sections which outline the formulation in ADAMS, for any rigid body, of the equations of motion, the representation of forces and moments and the constraint equations. The following sections of theory owe much to the text prepared by Wielenga (68). The vector terminology has been modified from Wielenga's notation to a system which is used for teaching automotive engineering students at Coventry University. Where possible figures have been added to aid in the comprehension.

3.3.2 Equations of motion for a part

In ADAMS kinematic variables are required to represent the location and orientation of a part with respect to the ground reference frame (GRF) as shown in Figure 3.3.
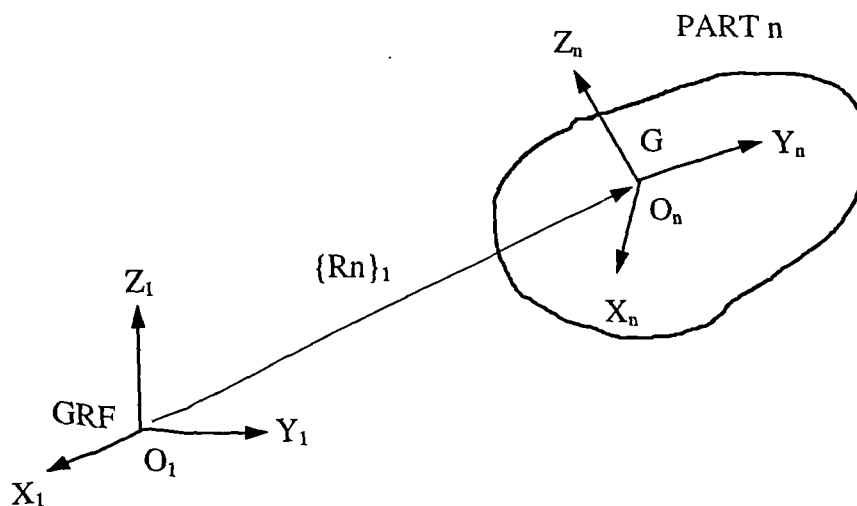
Figure 3.3 The location and orientation of a part

The location of any part is specified by a vector $\{Rn\}_1$ from the GRF to the centre of mass, G, of the part. In this case the part is labelled as the nth part in the system and the GRF is taken to be the first frame O_1. The components of the vector $\{Rn\}_1$ are resolved parallel to the axes of the GRF as indicated by the subscript 1. The velocity is obtained using:

$$\{Vn\}_1 = {}^d/_{dt}\{Rn\}_1 \tag{3.1}$$

The orientation of the part reference frame is specified by the set of Euler angles (ψ, ϕ, θ). The Euler angles are stored within ADAMS in an order that differs from the sequence used to change the orientation of a reference frame. In order to define the orientation of the part frame a series of successive rotations are applied, starting with a rotation ψ about the z axis (Z) of the GRF. The sequence is shown in Figure 3.4. The second rotation θ is about the new x axis (X_1) of the rotated frame. The final rotation ϕ is about the z axis (Z_1) of the part frame.
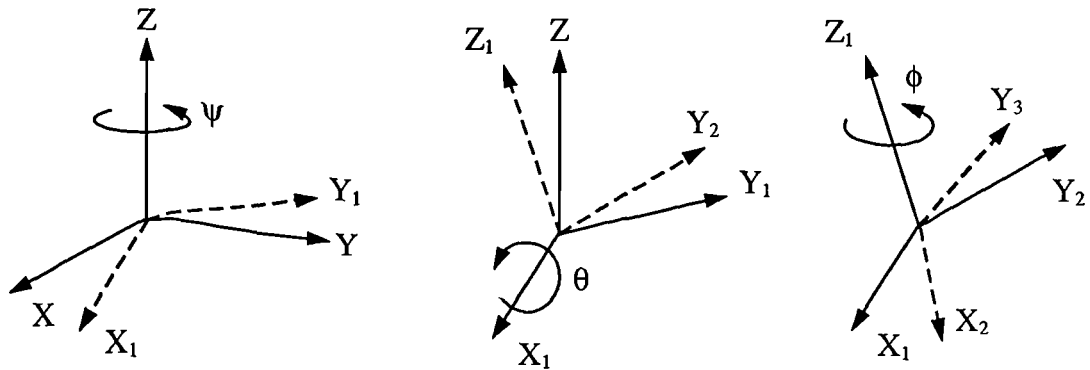
Figure 3.4 Orientation of the part frame by Euler angles

There are three frames of interest during the transformation. The first is the GRF (X,Y,Z) which is also frame O_1. The second is a frame made up of the axes about which each of the rotations take place. This is known as the Euler-axis frame (Z,X_1,Z_1) and will be referred to as frame O_e. Note that this is not a reference frame in the true sense as the three axes are not perpendicular to one another. The third frame is the resulting part frame (X_2,Y_3,Z_1). For the nth

part in a system this would be the part frame O_n. The matrix $[A_{1n}]$ is the Euler matrix for part n and performs the transformation from the part frame O_n to the GRF O_1.

$$[A_{1n}] = \begin{bmatrix} \cos\psi.\cos\phi - \sin\psi.\cos\theta.\sin\phi & -\cos\psi.\sin\phi - \sin\psi.\cos\theta.\cos\phi & \sin\psi.\sin\theta \\ \sin\psi.\cos\phi + \cos\psi.\cos\theta.\sin\phi & -\sin\psi.\sin\phi + \cos\psi.\cos\theta.\cos\phi & -\cos\psi.\sin\theta \\ \sin\theta.\sin\phi & \sin\theta.\cos\phi & \cos\theta \end{bmatrix} \quad (3.2)$$

Note that the inverse of this matrix $[A_{n1}]$ is simply the transpose and performs the transformation from the GRF to the part frame. Another matrix $[B]$ performs the transformation from the Euler-axis frame O_e (Z,X_1,Z_1) to the part frame O_n (X_2,Y_3,Z_1).

$$[B] = \begin{bmatrix} \sin\theta.\sin\phi & 0 & \cos\phi \\ \sin\theta.\cos\phi & 0 & -\sin\phi \\ \cos\theta & 1 & 0 \end{bmatrix} \quad (3.3)$$

Note that this matrix becomes singular when $\sin\theta = 0$. This corresponds to the situation where Z and Z_1 are parallel and point in the same direction ($\theta = 0$), or parallel and point in the opposite direction ($\theta = 180$ degrees). When this occurs ADAMS makes an internal adjustment to set up a new part frame where the Z_1 axis is rotated through 90 degrees. Note also that the $[B]$ matrix corresponds with an internal reordering of the Euler angles in ADAMS to (Z,Z_1,X_1).

For large rotations the set of Euler angles for the nth part $\{\gamma n\}_e = [\psi n \quad \phi n \quad \theta n]^T$ cannot actually be represented by a vector as indicated here although they can be considered to make up a set of kinematic orientation variables for the nth part. An infinitesimal change in orientation in the part frame O_n can, however, be represented by a vector which will be denoted $\{\delta\gamma n\}_n$. In a similar manner an infinitesimal change in the Euler angles can be represented by a vector $\{\delta\gamma n\}_e$ .The angular velocity vector for the part in the local part frame can also be specified by $\{\omega n\}_n$. ADAMS also requires the components of these vectors in the Euler-axis frame O_e. The angular velocity in the Euler-axis frame is simply the time derivative of the Euler angles.

$$\{\omega n\}_e = {}^d/_{dt} \{\gamma n\}_e \quad (3.4)$$

The transformation between the part frame and the Euler-axis frame is established using the [B] matrix.

$$\{\delta\gamma n\}_n = [B] \{\delta\gamma n\}_e \qquad (3.5)$$

$$\{\omega n\}_n = [B] \{\omega n\}_e \qquad (3.6)$$

In summary there are now a set of kinematic position and velocity variables for the nth part with components measured in the GRF and also a set of orientation and angular velocity variables measured about the Euler-axis frame.

$$\{Rn\}_1 = [\, Rnx \quad Rny \quad Rnz \,]^T \qquad (3.7)$$

$$\{Vn\}_1 = [\, Vnx \quad Vny \quad Vnz \,]^T \qquad (3.8)$$

$$\{\gamma n\}_e = [\, \psi n \quad \phi n \quad \theta n \,]^T \qquad (3.9)$$

$$\{\omega n\}_e = [\, \omega n \quad \omega n \quad \omega n \,]^T \qquad (3.10)$$

There is also a set of kinematic equations associated with the part which may be simply stated as:

$$\{Vn\}_1 = {}^d/_{dt}\{Rn\}_1 \qquad (3.11)$$

$$\{\omega n\}_e = {}^d/_{dt} \{\gamma n\}_e \qquad (3.12)$$

The remaining part variables and equations are those obtained by considering the equations of motion for a rigid body. Each part can be considered to have a set of six generalised coordinates given by:

$$q_j = [Rnx, \ Rny, \ Rnz, \ \psi n, \ \theta n, \ \phi n] \qquad (3.13)$$

The translational coordinates are the translation of the centre of mass measured parallel to the axes of the ground reference frame while the rotational coordinates are provided by the Euler angles for that part. For any part the translational forces are therefore summed in the X Y and Z directions of the GRF while the summation of moments takes place at the centre of

mass and about each of the axes of the Euler-axis frame. Using a form of the Lagrange equations this can be shown as:

$$\frac{d}{dt}(\partial T/\partial \dot{q}_j) - \partial T/\partial q_j - Q_j + \sum_{i=1}^{n} \partial \Phi_i/\partial q_j \, \lambda_i = 0 \qquad (3.14)$$

The kinetic energy T is expressed in terms of the generalised coordinates q_j and is given by:

$$T = 1/2\{Vn\}_1 \, m\{Vn\}_1 + 1/2\{\omega n\}_e [B]^T [I_n] [B]\{\omega n\}_e \qquad (3.15)$$

The mass properties are specified by m which is the mass of the part and $[I_n]$ which is the mass moment of inertia tensor for the part and given by:

$$[I_n] = \begin{bmatrix} I_{xx} & I_{xy} & I_{xz} \\ I_{yx} & I_{yy} & I_{yz} \\ I_{zx} & I_{zy} & I_{zz} \end{bmatrix} \qquad (3.16)$$

In most cases the user will specify a part frame which corresponds with the principal axes of the body and makes all off diagonal terms zero in the above tensor. The terms Φ and λ represent the reaction force components acting in the direction of the generalised coordinate q_j. The terms Q_j represents the sum of the applied force components acting on the part and in the direction of the generalised coordinate q_j. The equation can be simplified by introducing a term for the momenta P_j associated with motion in the q_j direction, and a term C_j to represent the constraints:

$$P_j = \partial T/\partial \dot{q}_j \qquad (3.17)$$

$$C_j = \sum_{i=1}^{n} \partial \Phi_i/\partial q_j \, \lambda_i \qquad (3.18)$$

This results in the equation:

$$\dot{P}_j - \partial T/\partial q_j - Q_j + C_j = 0 \qquad (3.19)$$

By way of example consider first the equations associated with the translational coordinates. The generalised translational momenta $\{Pn_t\}_1$ for the part can be obtained from:

$$\{An\}_1 = {}^{d}\!/\!_{dt}\{Vn\}_1 \tag{3.20}$$

$$\{Pn_t\}_1 = \partial T/\partial \{Vn\}_1 = M\{Vn\}_1 \tag{3.21}$$

$${}^{d}\!/\!_{dt}\{Pn_t\}_1 = m\{An\}_1 \tag{3.22}$$

where $\{An\}_1$ is the acceleration of the centre of mass for that part. It should also be noted that the kinetic energy is dependent on the velocity but not the position of the centre of mass, $\partial T/\partial \{Rn\}_1$ is equal to zero. We can now write the equation associated with translational motion in the familiar form:

$$m\{An\}_1 - \sum\{Fn_A\}_1 + \sum\{Fnc\}_1 = 0 \tag{3.23}$$

where $\{Fn_A\}_1$ and $\{Fnc\}_1$ are the individual applied and constraint reaction forces acting on the body. The rotational momenta $\{Pn_r\}_e$ for the part can be obtained from:

$$\{Pn_r\}_e = \partial T/\partial \{\omega n\}_e = [B]^T [I_n] [B]\{\omega n\}_e \tag{3.24}$$

We can now write the equations associated with rotational motion in the form:

$$\{Pn_r\}_e - \partial T/\partial \{\gamma n\}_e - \sum\{Mn_A\}_e + \sum\{Mnc\}_e = 0 \tag{3.25}$$

$$\{Pn_r\}_e = [B]^T [I_n] [B]\{\omega n\}_e \tag{3.26}$$

In this case $\{Mn_A\}_e$ and $\{Mnc\}_e$ are the individual applied and constraint reaction moments acting about the Euler-axis frame at the centre of mass of the body. Introducing the equation above for the rotational momenta introduces an extra three variables and equations for each part.

The fifteen variables for each part are:

$$\{Rn\}_1 = [\ Rnx \quad Rny \quad Rnz\ ]^T \qquad (3.27)$$

$$\{Vn\}_1 = [\ Vnx \quad Vny \quad Vnz\ ]^T \qquad (3.28)$$

$$\{\gamma n\}_e = [\ \psi n \quad \phi n \quad \theta n\ ]^T \qquad (3.29)$$

$$\{\omega n\}_e = [\ \omega n \quad \omega n \quad \omega n\ ]^T \qquad (3.30)$$

$$\{Pn_r\}_e = [\ P\psi n \quad P\phi n \quad P\theta n\ ]^T \qquad (3.31)$$

The fifteen equations for each part are:

$$\{Vn\}_1 = {}^d/_{dt}\{Rn\}_1 \qquad (3.32)$$

$$\{\omega n\}_e = {}^d/_{dt}\{\gamma n\}_e \qquad (3.33)$$

$$\{Pn_r\}_e = [B]^T [I_n] [B]\{\omega n\}_e \qquad (3.34)$$

$$m\{An\}_1 - \sum\{Fn_A\}_1 + \sum\{Fn_C\}_1 = 0 \qquad (3.35)$$

$$\{Pn_r\}_e - \partial T/\partial\{\gamma n\}_e - \sum\{Mn_A\}_e + \sum\{Mn_C\}_e = 0 \qquad (3.36)$$

3.3.3 Force and moment definition

An applied force or moment can be defined using an equation to specify the magnitude, which may be functionally dependent on displacements, velocities, other applied forces and time. Using the example in Figure 3.5 there is an applied force $\{F_A\}_1$ acting at point A, the weight of the body $m\{g\}_1$ acting at the centre of mass G, a force $\{F_B\}_1$ and a torque $\{T_B\}_1$ due to a field element such as a bush or beam connection to another part. In addition there is an applied torque $\{T_C\}_1$ acting at point C. Note that at this stage all the force and torque vectors are assumed to be resolved parallel to the GRF and that $\{g\}_1$ is the vector of acceleration due to gravity and is again measured in the GRF.
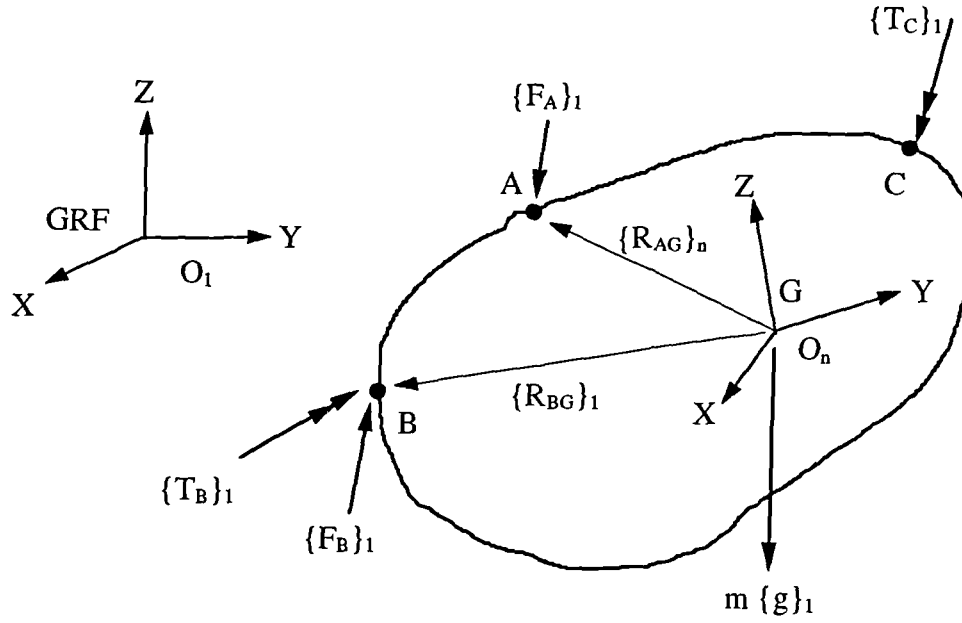
Figure 3.5 Applied forces and torques on a body

The summation of applied forces resolved in the GRF as required in equation (3.35) is obtained in this example by:

$$\sum \{Fn_A\}_1 = \{F_A\}_1 + \{F_B\}_1 + m\{g\}_1 \qquad (3.37)$$

The summation of moments about G is not so straight forward. ADAMS performs the moment calculations about the axes of the Euler-axis frame. It is therefore necessary to use the transformation matrix $[A_{n1}]$ to transform forces and torques to the part frame O_n and to use $[B_n]^T$ to transform from the part frame to the Euler-axis frame.

$$\{F_A\}_n = [A_{n1}] \{F_A\}_1 \qquad (3.38)$$

$$\{F_B\}_n = [A_{n1}] \{F_B\}_1 \qquad (3.39)$$

$$\{T_B\}_n = [A_{n1}] \{T_B\}_1 \qquad (3.40)$$

$$\{T_C\}_n = [A_{n1}] \{T_C\}_1 \qquad (3.41)$$

It is now possible to calculate the moments at G due to the forces at A and B working in the part frame.

$$\{M_A\}_n = \{R_{AG}\}_n \times \{F_A\}_n \qquad (3.42)$$

$$\{M_B\}_n = \{R_{BG}\}_n \times \{F_B\}_n \qquad (3.43)$$

The next step is to transform the moments and torques to the Euler-axis frame and to summate as required in equation (3.36).

$$\sum \{Mn_A\}_e = [B_n]^T\{M_A\}_n + [B_n]^T\{M_B\}_n + [B_n]^T\{T_B\}_n + [B_n]^T\{T_C\}_n \qquad (3.44)$$

3.3.4 Formulation of constraints

The relative motion between two parts can be constrained using standard joints, joint primitives, motion inputs, gears and couplers. Each of these introduces equations and reaction forces associated with the relative motion which is prevented between any two parts. The reaction forces and moments produced by a constraint do not develop any work in the system since the corresponding displacements are zero. The various joints and joint primitives can be developed using combinations of four basic constraint elements. For each constraint the resulting forces and moments need to be added into the force and moment balance for a part working in generalised coordinates in a similar manner as that described for applied forces in Section 3.3.3.

Consider first the basic *atpoint* constraint element shown in Figure 3.6 which constrains a point I on one part to remain at the same location in space as a point J on another part, but does not prevent any relative rotation between the two points.
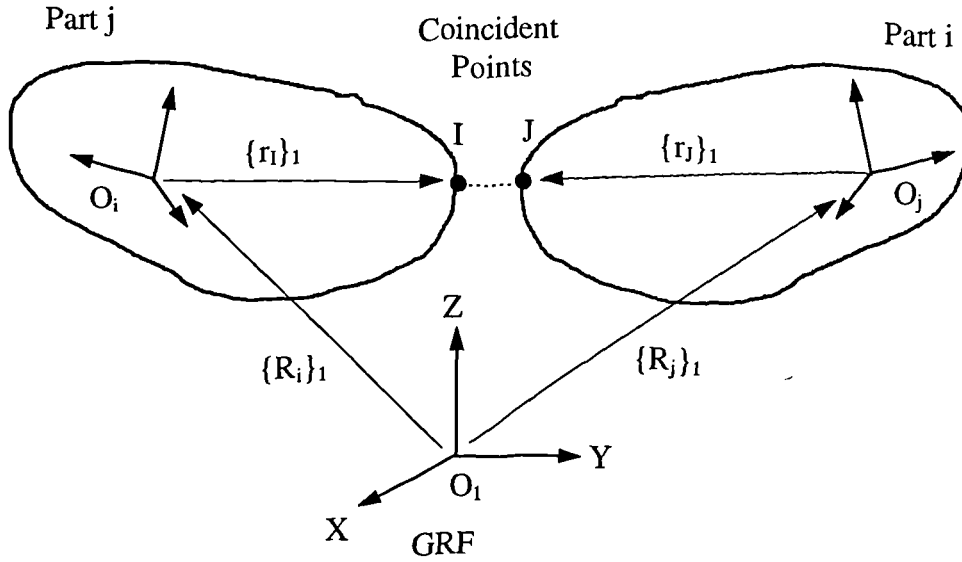
Figure 3.6 Atpoint constraint element

This constraint can be represented by a vector constraint equation working in the generalised coordinates parallel to the axes of the GRF.

$$\{\Phi_a\}_1 = (\{R_i\}_1 + \{r_I\}_1) - (\{R_j\}_1 + \{r_J\}_1) = \{0\} \qquad (3.45)$$

This expression may be simplified by introducing a vector term $\{d_U\}_1$ to represent the constrained displacement between the I and the J marker.

$$\{d_U\}_1 = (\{R_i\}_1 + \{r_I\}_1) - (\{R_j\}_1 + \{r_J\}_1) \qquad (3.46)$$

The reaction force on part i can be represented by the vector $\{\lambda\}_1$ with a moment given by $\{r_I\}_1 \times \{\lambda\}_1$. Applying Newton's third law the reaction force on part j can be represented by the vector $-\{\lambda\}_1$ with a moment given by $-\{\lambda\}_1 \times \{r_J\}_1$. In order to complete the calculation the contribution to the term $\sum \{M_{nc}\}_e$ in equation (3.36) must be obtained by transforming the moments into the generalised coordinates of the part Euler-axis frame. For part i this would be achieved using $[B_i]^T \{r_I\}_i \times [A_{i1}] \{\lambda\}_1$. For part j this would be achieved using $-[B_j]^T \{r_J\}_i \times [A_{j1}] \{\lambda\}_1$.

47

The second basic constraint element constrains a point on one part to remain fixed within a plane on another part and is known as the *inplane* constraint. As such it removes one degree of freedom, out of the plane as shown in Figure 3.7.
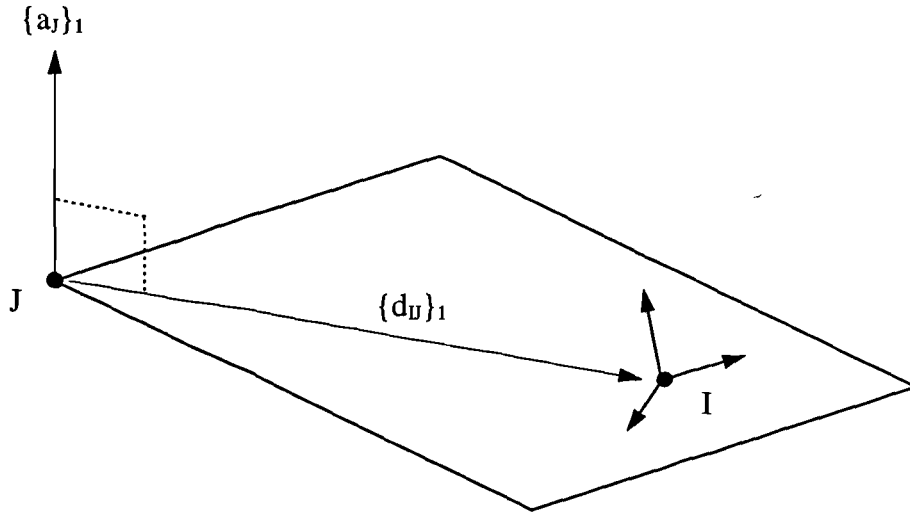
Figure 3.7 Inplane constraint element

The plane is defined by a unit vector $\{a_J\}_1$ fixed in part j and perpendicular to the plane. The I marker belonging to part i is constrained to remain in the plane using the vector dot (scalar) product to enforce perpendicularity:

$$\{d_U\}_1 \cdot \{a_J\}_1 = 0 \tag{3.47}$$

Expanding this using the definition given for $\{d_U\}_1$ in equation (3.46) gives the full expression for the constraint Φ_d:

$$\Phi_d = [(\{R_i\}_1 + \{r_i\}_1) - (\{R_j\}_1 + \{r_j\}_1)] \cdot \{a_J\}_1 = 0 \tag{3.48}$$

48

This constraint can be represented by a vector constraint equation working in the generalised coordinates parallel to the axes of the GRF. The magnitude of the reaction force corresponding to this constraint can be represented by a scalar term λ_d. The reaction force on Part i can be represented by the vector $\{a_J\}_1\lambda_d$ with a moment given by $\{r_I\}_1 \times \{a_J\}_1\lambda_d$. Applying Newton's third law again the reaction force on Part j can be represented by the vector $- \{a_J\}_1 \lambda_d$.

The moment contribution to part j is given by $- (\{r_J\}_1 + \{d_{IJ}\}_1) \times \{a_J\}_1\lambda_d$.

Expanding this again using the definition given for $\{d_{IJ}\}_1$ in equation (3.46)

gives $- (\{R_i\}_1 + \{r_I\}_1 - \{R_j\}_1) \times \{a_J\}_1 \lambda_d$. In order to complete the calculation the contribution to the term $\sum \{M_{nc}\}_e$ in equation (3.36) must be obtained by transforming the moments into the generalised coordinates of the part Euler-axis frame.

For part i this would be achieved using $[B_i]^T \{r_I\}_i \times [A_{ij}] \{a_J\}_1\lambda_d$.

For part j this would be achieved using $[B_j]^T\{a_J\}_j \times [A_{j1}] (\{R_i\}_1 + [A_{1i}]\{r_I\}_i - \{R_j\}_1) \lambda_d$.

The third basic constraint element constrains a unit vector fixed in one part to remain perpendicular to a unit vector located in another part and is known as the *perpendicular* constraint. The constraint shown in Figure 3.8 is defined using a unit vector $\{a_J\}_1$ located at the J marker in part j and a unit vector $\{a_I\}_1$ located at the I marker belonging to part I.
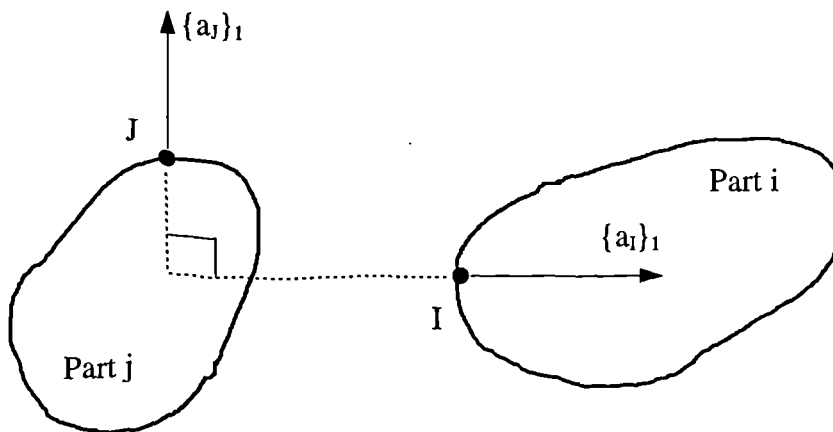
Figure 3.8 Perpendicular constraint element

The vector dot (scalar) product is used to enforce perpendicularity as shown in equation (3.49).

$$\Phi_p = \{a_i\}_1 \cdot \{a_J\}_1 = 0 \qquad (3.49)$$

The constraint can be considered to be enforced by equal and opposite moments acting on part i and part j. The constraint does not contribute any forces to the part equations but does include the scalar term λ_p in the formulation of the moments. The moment acting on part i is given by $\{a_i\}_1 \times \{a_J\}_1 \lambda_p$. Applying Newton's third law the moment acting on part j is given by $-\{a_i\}_1 \times \{a_J\}_1 \lambda_p$. The moments must be transformed into the generalised coordinates of the part Euler-axis frame. For part i this would be achieved using $[B_i]^T \{a_i\}_i \times [A_{ij}]\{a_J\}_j \lambda_p$. For part j this would be achieved using $[B_j]^T \{a_J\}_j \times [A_{ji}]\{a_i\}_i \lambda_p$.

The fourth and final basic constraint element is the *angular* constraint which prevents the relative rotation of two parts about a common axis. The constraint equation is:

$$\Phi_\alpha = \tan\text{-}1 \left(\{x_i\}_1 \cdot \{y_j\}_1 \,/\, \{x_i\}_1 \cdot \{x_j\}_1 \right) = 0 \qquad (3.50)$$

In applying this constraint it is assumed that other system constraints will maintain the z axes of the two parts to remain parallel as shown Figure 3.9.
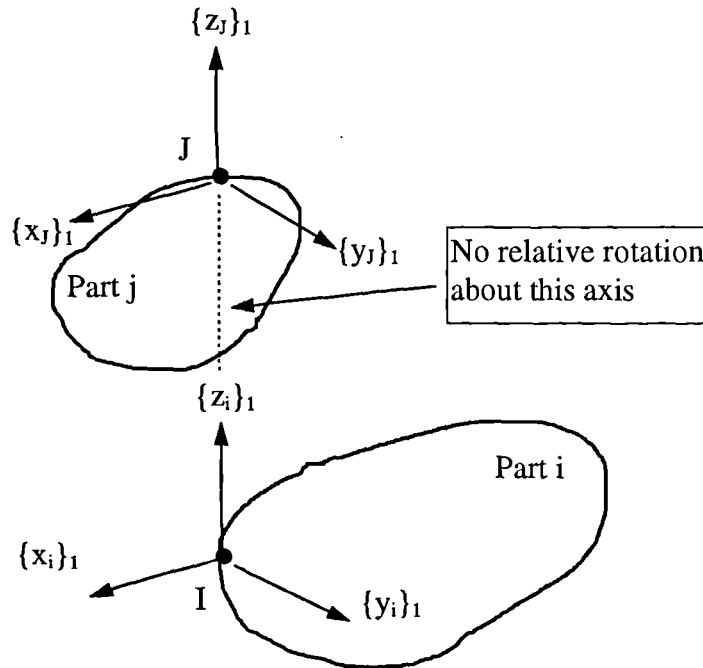
Figure 3.9 Angular constraint element

The moment acting on part i is given by $\{z_i\}_1\lambda_\alpha$ and on part j by $-\{z_j\}\lambda_\alpha$.

Transforming into the Euler axis system for each part gives a moment in the generalised coordinate system for part i equal to $[B_i]^T\{z_i\}_i$ λ_α and on part j by $-[B_j]^T\{z_j\}_j$ λ_α.

The equations associated with each of the four basic constraint elements are summarised in Table 3.1.

Table 3.1 Basic constraint element equations

Constraint	Full Equation	Abbreviated Form
Atpoint	$\{\Phi_a\}_1 = (\{R_i\}_1 + \{r_I\}_1) - (\{R_j\}_1 + \{r_J\}_1)$	$\{d_U\}_1$
Inplane	$\Phi_d = [(\{R_i\}_1 + \{r_I\}_1) - (\{R_j\}_1 + \{r_J\}_1)] \cdot \{a_J\}_1$	$\{d_U\}_1 \cdot \{a_J\}_1$
Perpendicular	$\Phi_p = \{a_I\}_1 \cdot \{a_J\}_1$	$\{a_I\}_1 \cdot \{a_J\}_1$
Angular	$\Phi_\alpha = \tan\text{-}1 (\{x_i\}_1 \cdot \{y_j\}_1 / \{x_i\}_1 \cdot \{x_j\}_1)$	α_U

The force and moment contributions to each part in the generalised coordinates is summarised in Table 3.2 and Table 3.3.

Table 3.2 Force contributions for basic constraint elements

Constraint	Part I Force	Part J Force
Atpoint	$\{\lambda\}$	$-\{\lambda\}$
Inplane	$[A_{1j}]\{a_J\}_j \lambda_d$	$-[A_{1j}]\{a_J\}_j \lambda_d$
Perpendicular	0	0
Angular	0	0

51

Table 3.3 Moment contributions for basic constraint elements

Constraint	Part I Moment	Part J Moment
Atpoint	$[B_i]^T\{r_I\}_i X[A_{i1}]\lambda$	$[B_j]^T\{r_J\}_i X[A_{j1}]\lambda$
Inplane	$[B_i]^T\{r_I\}_i X[A_{ij}]\{a_J\}_j\lambda_d$	$[B_j]^T\{a_J\}_j X[A_{j1}](\{R_i\}_1+[A_{1i}]\{r_I\}_i-\{R_j\}_1)\lambda_d$
Perpendicular	$[B_i]^T\{a_I\}_i X[A_{ij}]\{a_J\}_j\lambda_p$	$[B_j]^T\{a_J\}_j X[A_{ji}]\{a_I\}_i\lambda_p$
Angular	$[B_i]^T\{z_i\}_i\lambda_\alpha$	$-[B_j]^T\{z_j\}_j\lambda_\alpha$

The main constraint elements in ADAMS are selected from a set of joints, joint primitives, motion inputs, gears and couplers. While it is not intended to describe all of these some of the most commonly used joints are tabulated in Table 3.4 by way of example.

Table 3.4 Joint constraints in ADAMS

Joint Type	Constraints Trans'	Rot'	Total	Abbreviated Equation
Spherical	3	0	3	$\{d_U\}_1 = 0$
Planar	1	2	3	$\{z_I\}_i{\cdot}\{x_J\}_j = 0$ $\{z_I\}_i{\cdot}\{y_J\}_j = 0$ $\{d_U\}_I{\cdot}\{z_J\}_j = 0$
Universal	3	1	4	$\{d_U\}_1 = 0$ $\{z_I\}_i{\cdot}\{z_J\}_j = 0$
Cylindrical	2	2	4	$\{z_I\}_i{\cdot}\{x_J\}_j = 0$ $\{z_I\}_i{\cdot}\{y_J\}_j = 0$ $\{d_U\}_I{\cdot}\{x_J\}_j = 0$ $\{d_U\}_I{\cdot}\{y_J\}_j = 0$
Revolute	3	2	5	$\{d_U\}_1 = 0$ $\{z_I\}_i{\cdot}\{x_J\}_j = 0$ $\{z_I\}_i{\cdot}\{y_J\}_j = 0$

4.0 MODELLING AND ANALYSIS OF SUSPENSION SYSTEMS

4.1 General

The front and rear suspensions for the vehicle were initially modelled as separate units (quarter models) and then simulated moving through the full range of vertical movement between the bump and the rebound positions. The output from these analyses is mainly geometric and allows results such as camber angle or roll centre position to be plotted graphically against vertical wheel movement. The front suspension is a variation on a double wishbone design although the bushes connecting the links to the body are not colinear on the lower arm as would be normal in this type of design. The rear suspension is a combination of a McPherson strut and a trailing arm. The front suspension system is a development of a suspension system the rationale for which is discussed in (69). This paper outlines the constraints due to packaging a suspension system in a given space due to styling requirements and the front wheel drive transmission, whilst attempting to meet specified performance goals.

The primary role of the bushes in a suspension system is to isolate the vehicle and driver from small amplitude high frequency road inputs, or in other words to improve the ride quality of the vehicle. The effects of the bushes on vehicle handling will depend on whether the bushes have any influence on geometric changes in the suspension and road wheel as the wheel moves vertically relative to the vehicle body. In the more modern multilink suspensions such as the rear suspension on the Mercedes Model W201 (70) this would appear to be the case. For this type of arrangement it would appear impossible to build an ADAMS model without including the compliance in the bushes. For the vehicle considered in this thesis both the front and rear suspensions are assembled in such a way that suggested a dependence on the bushes for the way in which they move.

Obtaining data for bushes and modelling them in ADAMS can add considerably to the amount of time and effort required to prepare a model for a vehicle handling simulation. This study had a main objective of investigating the influence of modelling the bushes on the calculated suspension outputs that are likely to influence vehicle handling behaviour.

For both the front and rear suspension systems three types of model have been considered:

(i) Modelling bushes as non-linear

(ii) Modelling bushes as linear

(iii) Modelling with rigid joints (kinematic analysis)

A secondary objective from this phase of work was to establish for both front and rear suspensions the instant centre and the roll centre positions. The positions of the instant centre are used later as pivot points for a full vehicle handling model where the suspensions are represented by single swing arms. The roll centres are used for a full vehicle handling model based on roll stiffness.

4.2 Modelling approach

One of the earliest applications of ADAMS by the automotive industry (3) was the use of the software to analyse suspension geometry. The suspension linkages are modelled as rigid parts connected using either joints or bushes and the suspension is moved between the full bump and full rebound positions. As the suspension moves the position and orientation of the wheel is calculated and used to plot results such as camber angle or track change against vertical wheel movement. At this stage of the analysis work supporting a vehicle design it is desirable if possible to produce a zero degree of freedom model, connected by rigid joints and to perform a kinematic analysis. If the design of the suspension is such that it relies significantly on the compliance in the bushes as it moves it will not be possible to perform a kinematic analysis and it will be necessary to obtain the stiffness of the bushes before an analysis is performed.

This modelling issue is best explained by an example using the established double wishbone suspension system, also referred to as a short-long arm (SLA) suspension system in the USA. The modelling of the suspension using bushes to connect the upper and lower arms to the vehicle body is shown in Figure 4.1. Vertical motion is imparted to the suspension using a jack part connected to the ground part by a translational joint. A translational motion is applied at this joint to move the jack over a range of vertical movement equivalent to moving

54

between the full bump and full rebound positions. Although the jack is shown below the wheel in Figure 4.1 the jack is connected to the wheel using an inplane joint primitive acting at the wheel centre. The joint primitive constrains the wheel centre to remain in the plane at the top of the jack but does not constrain the wheel to change orientation or to move in the lateral or longitudinal directions A zero motion input is applied at the revolute joint connecting the wheel to the wheel knuckle in order to constrain the spin freedom of the wheel.
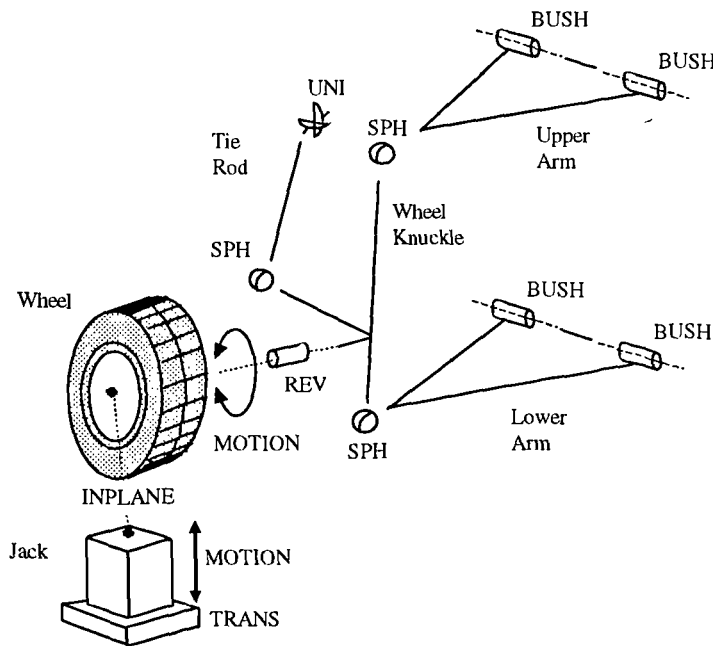
Figure 4.1 Double wishbone suspension modelled with bushes

For the suspension modelled in this manner it is possible to calculate the degrees of freedom for the system as follows:

Parts	6 x 6	= 36
Trans	1 x -5	= -5
Rev	1 x -5	= -5
Uni	1 x -4	= -4
Sphs	3 x -3	= -9
Inplane	1 x -1	= -1
Motion	2 x -1	= -2
Σ DOF		= 10

55

The double wishbone suspension shown in Figure 4.1 can be simplified to represent the bushes connecting the upper arm and the lower arm to the vehicle body by revolute joints as shown in Figure 4.2 .
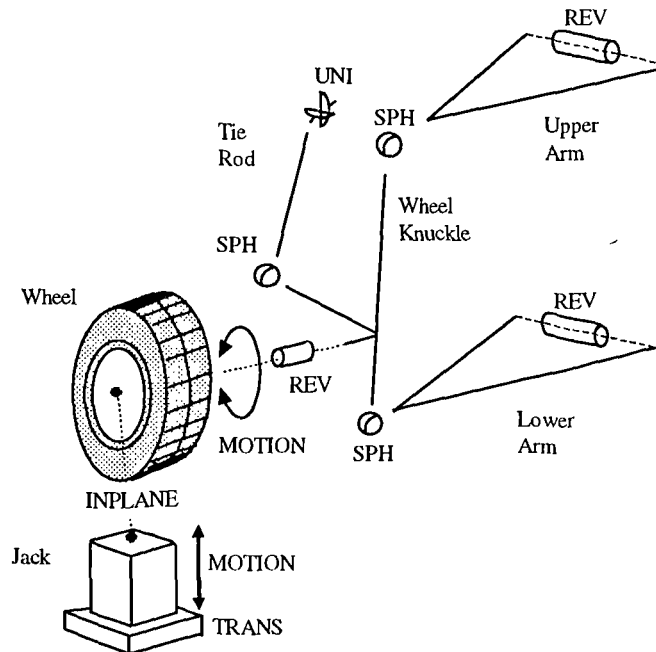
Figure 4.2 Double wishbone suspension modelled with joints

For the suspension modelled in this manner it is possible to calculate the degrees of freedom for the system as follows:

$$
\begin{array}{llll}
\text{Parts} & 6 \times 6 & = 36 \\
\text{Trans} & 1 \times -5 & = -5 \\
\text{Rev} & 3 \times -5 & = -15 \\
\text{Uni} & 1 \times -4 & = -4 \\
\text{Sphs} & 3 \times -3 & = -9 \\
\text{Inplane} & 1 \times -1 & = -1 \\
\underline{\text{Motion} & 2 \times -1 & = -2} \\
\Sigma_{DOF} & & = 0
\end{array}
$$

This generates a model which has zero degrees of freedom and allows a kinematic analysis to be performed in ADAMS. For this suspension changing from bushes to revolute

joints has little effect on the calculated changes in suspension geometry due to vertical movement. There is therefore, little merit in modelling the bushes in this suspension if the model is to be included in a full vehicle model intended for handling simulation and not for ride studies or durability investigations.

4.3 Modelling the front suspension system

The assembly of parts used to make up the front suspension system is shown schematically in Figure 4.3.

Figure 4.3 Assembly of parts in the front suspension system

The modelling of the suspension system using bushes is shown in Figure 4.4. The upper link is attached to the body using a connection which is rigid enough to be modelled as a revolute joint. Bushes were used to model the connection of the lower arm and the tie bar to the vehicle body. Bushes were also used to model the connections at the top and bottom of the damper unit. Where the tie bar is bolted to the lower arm a fix joint has been used to rigidly connect the two parts together. This joint removes all six relative degrees of freedom between the two parts creating in effect a single lower wishbone.

Figure 4.4 Modelling the front suspension using bushes

The modelling issue raised here is that rotation will take place about an axis through these two bushes but that the bushes are not aligned with this axis. As rotation takes place the bushes must distort in order to accommodate this. This can be seen quite clearly form the graphics obtained from ADAMS at full bump position shown in Figure 4.6. The modelling of these connections as non-linear, linear or as a rigid joint was therefore investigated to establish the effects on suspension geometry changes during vertical movement.

For the suspension modelled in this manner it is possible to calculate the degrees of freedom for the system as follows:

Parts	9 x 6	= 54
Fix	1 x -6	= -6
Trans	1 x -5	= -5
Rev	2 x -5	= -10
Uni	1 x -4	= -4
Cyl	1 x -4	= -4
Sphs	3 x -3	= -9
Inplane	1 x -1	= -1
Motion	2 x -1	= -2
Σ_{DOF}		= 13

58

In order to produce a zero degree of freedom model for this suspension the bushes at the top and bottom of the strut have been replaced by a universal and a spherical joint. The bushes connecting the lower arm and the tie rod to the vehicle body have been replaced by a single revolute joint with an axis aligned between the two bushes as shown in Figure 4.5.

Figure 4.5 Modelling the front suspension using rigid joints

For the suspension modelled in this manner using rigid joints it is possible to calculate the degrees of freedom for the system as follows:

Parts	9 x 6	= 54
Fix	1 x -6	= -6
Trans	2 x -5	= -10
Rev	3 x -5	= -15
Uni	2 x -4	= -8
Sphs	4 x -3	= -12
Inplane	1 x -1	= -1
Motion	2 x -1	= -2

$$\Sigma_{DOF} = 0$$

At this stage the question of whether the use of a rigid revolute joint on the lower arm is suitable is foremost, given the level of distortion in the bushes at full bump as shown in Figure 4.6. In this case the deformed plot of the bushes has been obtained using the model with non-linear characteristics.
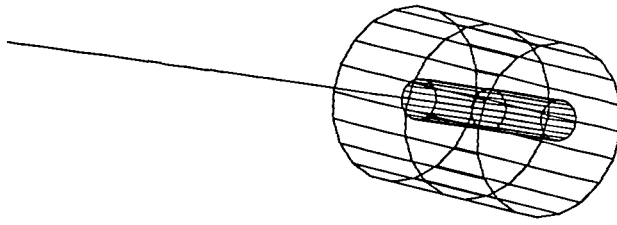
Figure 4.6 Distortion in front bushes at full bump

4.4 Modelling the rear suspension system

The assembly of parts used to make up the rear suspension system is shown schematically in Figure 4.7.
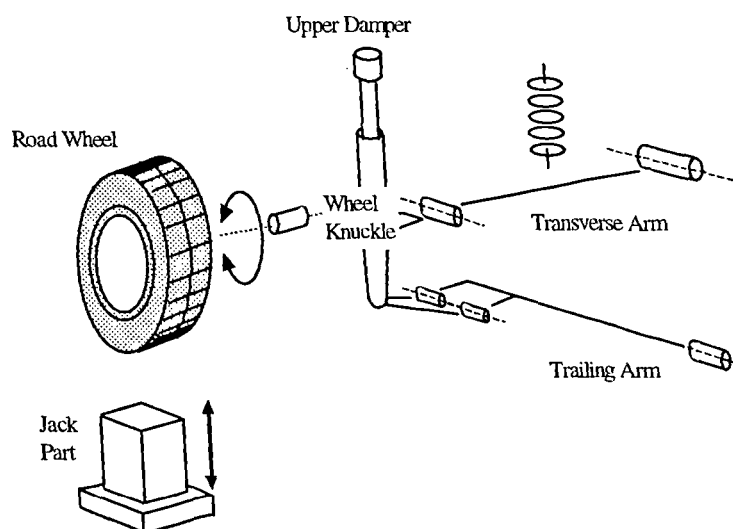
Figure 4.7 Assembly of parts in the rear suspension system

The modelling of the suspension system using bushes is shown in Figure 4.8. The trailing arm and the transverse arm connect not only to the vehicle body but also to the wheel knuckle using bushes. The upper damper is also connected to the vehicle body using a bush.
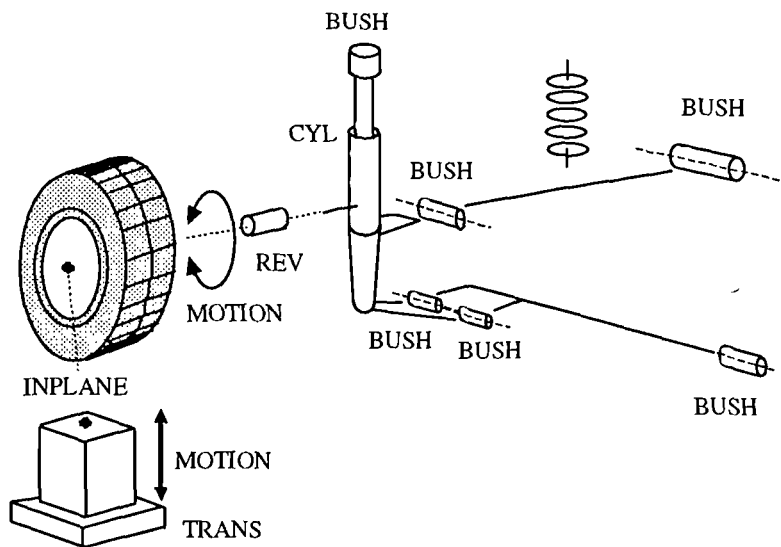
Figure 4.8 Modelling the rear suspension using bushes

For the suspension modelled in this manner it is possible to calculate the degrees of freedom for the system as follows:

```
Parts     6 x 6  = 36
Trans     1 x -5 = -5
Rev       1 x -5 = -5
Cyl       1 x -4 = -4
Inplane   1 x -1 = -1
Motion    2 x -1 = -2
          Σ DOF  = 19
```

Producing a model of this suspension system which uses rigid joints and has zero degrees of freedom is less straightforward than for the front suspension system. The system used is shown in Figure 4.9.

61
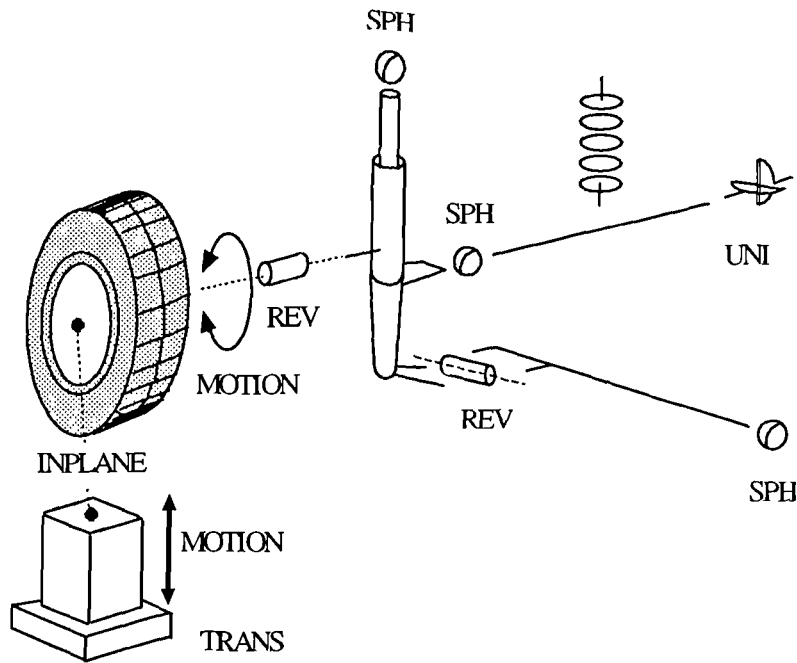
Figure 4.9 Modelling the rear suspension using rigid joints

For the suspension modelled in this manner using rigid joints it is possible to calculate the degrees of freedom for the system as follows:

Parts   6 x 6   = 36

Trans   2 x -5 = -10

Rev   2 x -5 = -10

Uni   1 x -4 = -4

Sph   3 x -3 = -9

Inplane 1 x -1   = -1

Motion 2 x -1   = -2

Σ DOF   = 0

For this arrangement the zero degree of freedom model allows a kinematic analysis to be performed in ADAMS.

4.5 Suspension calculations

For both the front and rear suspension systems it was necessary to program calculations related to the changes in suspension geometry and to relate these to the vertical movement of the suspension. The calculated outputs are presented as XY plots and are summarised as follows:

(i)   Camber angle (deg) with Bump Movement (mm)

(ii) Caster angle (deg) with Bump Movement (mm)

(iii) Steer angle (deg) with Bump Movement (mm)

(iv) Track Change (mm) with Bump Movement (mm)

(v)   Roll Centre Height (mm) with Bump Movement (mm)

(vi) Vertical Force (N) with Bump Movement (mm)

In each case the plots are presented with the bump movement on the x-axis. The calculation of these outputs was programmed using the VARIABLE statement to create a variable which was a function of displacement system variables within the suspension. The calculation of each of these is explained in more detail.

4.5.1 Camber angle

Camber angle is defined as the angle measured in the front elevation between the wheel plane and the vertical. Camber angle is measured in degrees and taken as positive if the top of the wheel leans outwards as shown in Figure 4.10.

The calculation of camber angle is converted from radians to degrees by the factor $(180/\pi)$ and is based on the following system variables:

DY(WCid,WBid) - the Y component of the displacement of the wheel centre marker relative to the wheel base marker referenced to the Ground Reference Frame (GRF).

DZ(WCid,WBid) - the Z component of the displacement of the wheel centre marker relative to the wheel base marker referenced to the Ground Reference Frame (GRF).

$$\theta = (180/\pi) \cdot \text{ATAN (DY (WCid,WBid)/DZ(WCid,WBid))}$$
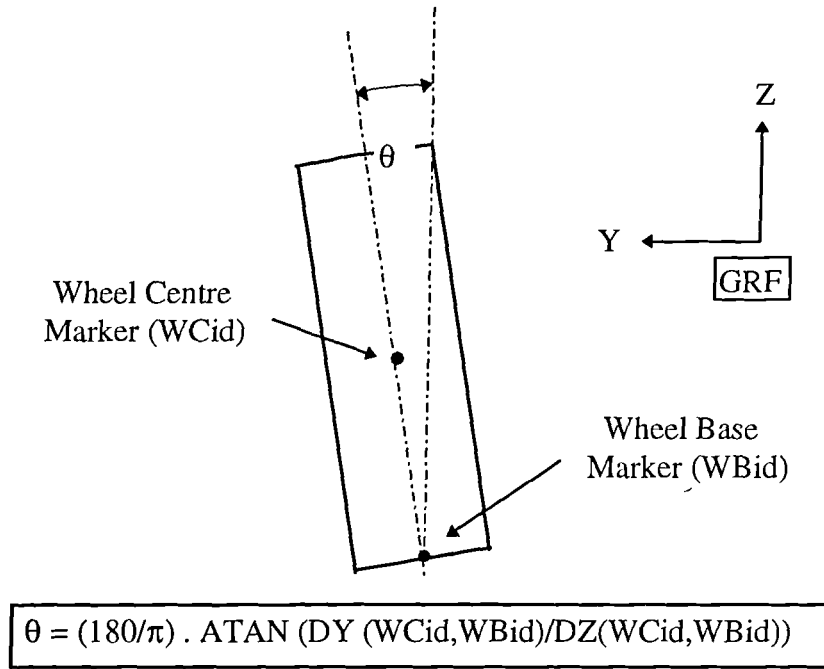
Figure 4.10 Calculation of camber angle

4.5.2 Caster angle

Caster angle is defined as the angle measured in the side elevation between the kingpin axis and the vertical. Caster angle is measured in degrees and taken as positive if the top of the kingpin leans towards the rear as shown in Figure 4.11.

$$\phi = (180/\pi) \cdot \text{ATAN (DX (TKid,BKid)/DZ(TKid,BKid))}$$
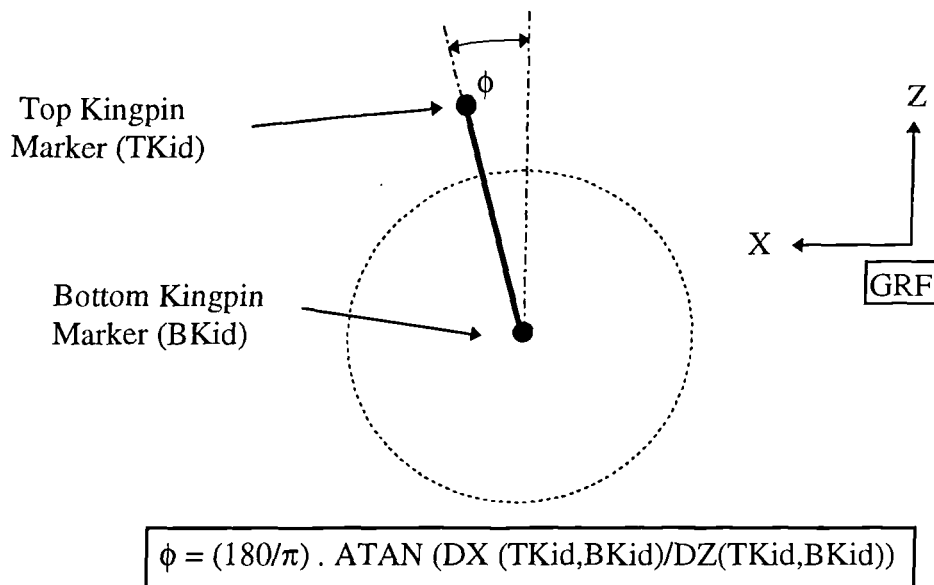
Figure 4.11 Calculation of caster angle

The calculation of caster angle is converted from radians to degrees by the factor $(180/\pi)$ and is based on the following system variables:

DX(TKid,BKid) - the X component of the displacement of the top kingpin marker relative to the bottom kingpin marker referenced to the Ground Reference Frame (GRF).

DZ(TKid,BKid) - the Z component of the displacement of the top kingpin marker relative to the bottom kingpin marker referenced to the Ground Reference Frame (GRF).

4.5.3 Steer angle

The steer or toe angle, α, is defined as the angle measured in the top elevation between the longitudinal axis of the vehicle and the line of intersection of wheel plane and road surface. Steer angle is measured in degrees and taken as positive if the front of the wheel points inwards as shown in Figure 4.12.
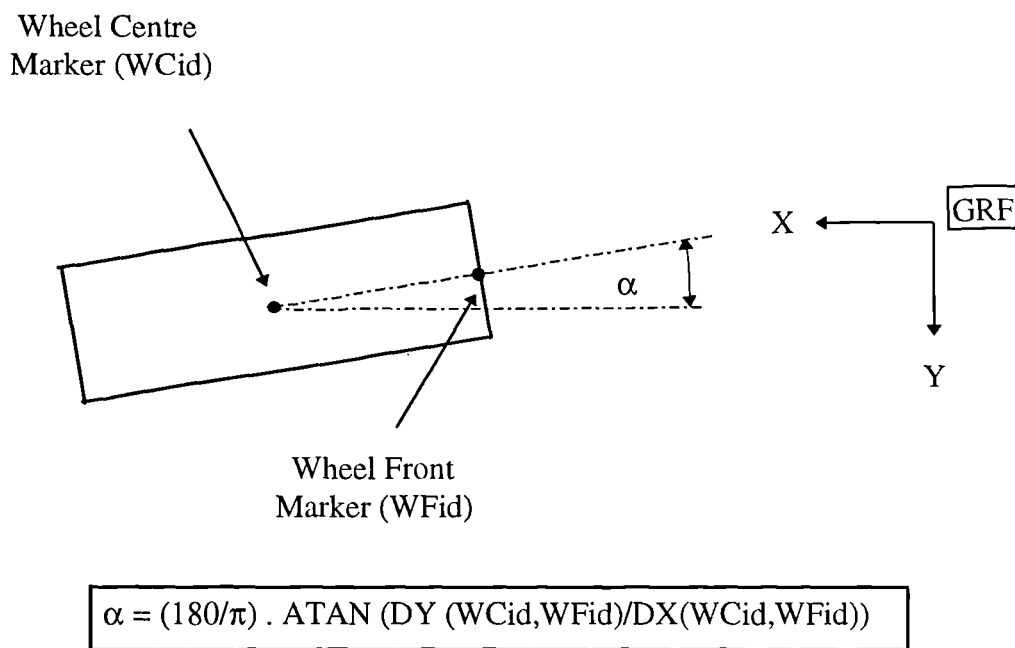
Figure 4.12 Calculation of steer angle

The calculation of steer angle is converted from radians to degrees by the factor $(180/\pi)$ and is based on the following system variables:

DX(WCid,WFid) - the X component of the displacement of the wheel centre marker relative to the wheel front marker referenced to the Ground Reference Frame (GRF).

DY(WCid,WBid) - the Y component of the displacement of the wheel centre marker relative to the wheel front marker referenced to the Ground Reference Frame (GRF).

4.5.4 Track change

Track change is taken as the lateral movement of the wheel base from a fixed point on the ground. Track change is measured in millimetres and taken as positive if the wheel base moves outwards relative to the vehicle as shown in Figure 4.13.
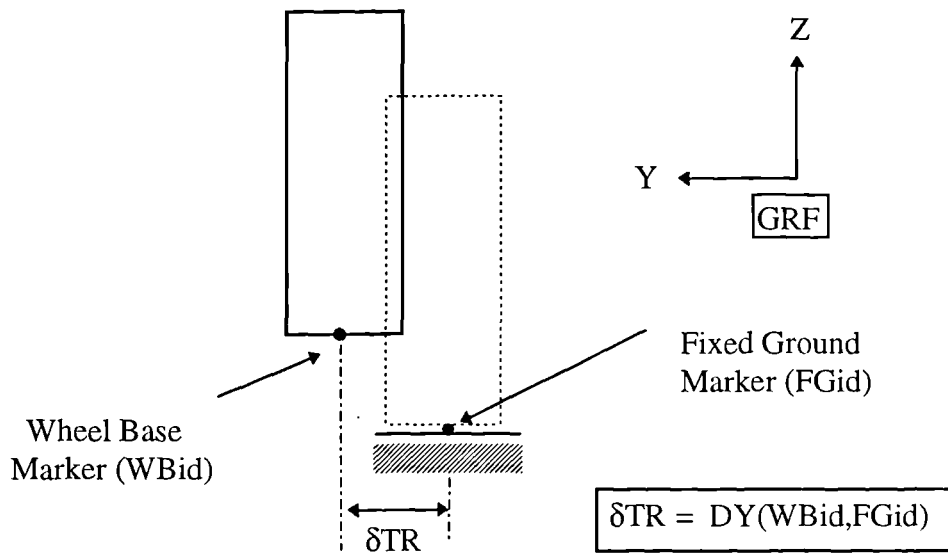
Figure 4.13 Calculation of track change

The calculation of track change is based on the following system variable:

DY(WBid,FGid) - the Y component of the displacement of the wheel base marker relative to the fixed ground marker referenced to the Ground Reference Frame (GRF).

66

4.5.5 Calculation of wheel rate

The calculation of wheel rate for the suspension system can be determined from the plot of vertical force (N) with bump movement (mm). The vertical force is obtained by requesting the force acting between the two markers which make up the translational joint connecting the jack part to the ground. The bump movement is obtained by requesting the displacement between the two markers which make up the translational joint connecting the jack part to the ground. The gradient of this curve will give the wheel rate for the suspension (N/mm).

4.6 Calculation of instant centre and roll centre height

The determination of the instant centre and the roll centre position is more complicated than any of the previous calculations. The methods used are based on the traditional graphical construction described in (2). There are two approaches which can be adopted to perform these calculations in ADAMS:

(i) Programming in the input deck using the VARIABLE statement.
(ii) Preparing a user-written FORTRAN subroutine and linking with ADAMS.

4.6.1 Front suspension

The methods used to determine the instant centre and roll centre position for the front suspension are based on the construction shown in Figure 4.14.
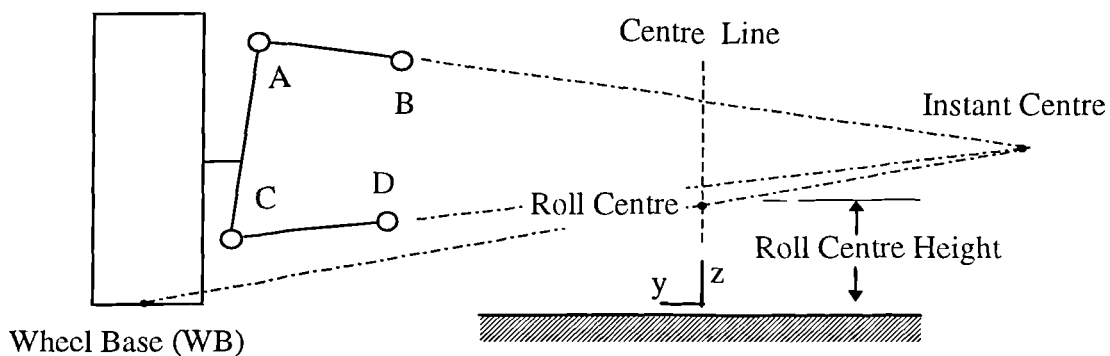
Figure 4.14 Construction of the instant centre and roll centre for the front suspension

67

The instant centre is found by intersecting lines projected along the upper and lower arms and determining the y and z coordinates. The roll centre is found by projecting a line between the wheel base and the instant centre. The point at which this line intersects the centre line of the vehicle is taken to be the Roll Centre. All calculations are assumed to take place in the same YZ plane as the wheel centre. In order to program this method into ADAMS the construction must be set up algebraically. The first step is to set up expressions for the gradients GR1 and GR2, of the upper and lower arms:

$$GR1 = (BZ-AZ) / (BY-AY)$$
$$GR2 = (DZ-CZ) / (DY-CY)$$

where AY, AZ, BY, ... DZ are the y and z coordinates of points A, B, C and D.

The coordinates of the instant centre ICY and ICZ, can be established from two simultaneous equations based on the upper and lower arms:

$$ICZ = AZ + GR1 * (ICY - AY)$$
$$ICZ = CZ + GR2 * (ICY - CY)$$

Rearranging these two equations gives:

$$AZ + GR1 * ICY - GR1 * AY = CZ + GR2 * ICY - GR2 * CY$$
$$ICY * (GR1 - GR2) = GR1 * AY - GR2 * CY + CZ - AZ$$

which allows the instant centre to be located using:

$$ICY = (GR1 * AY - GR2 * CY + CZ - AZ) / (GR1 - GR2)$$
$$ICZ = AZ + GR1 * (ICY - AY)$$

The gradient of the line joining the wheel base to the instant centre GR3, can be expressed as:

$$GR3 = (ICZ-WBZ) / (ICY-WBY)$$

where WBY and WBZ are the y and z coordinates of the wheel base.

which allows the roll centre to be located using:

RCY = 0.0

RCZ = WBZ + GR3 * (RCY - WBY)

The roll centre height RCH, can be defined by:

RCH = RCZ - RZ

where RZ is the z coordinate of the road .

4.6.2 Rear suspension

The methods used to determine the instant centre and roll centre position for the rear suspension are based on the construction shown in Figure 4.15.
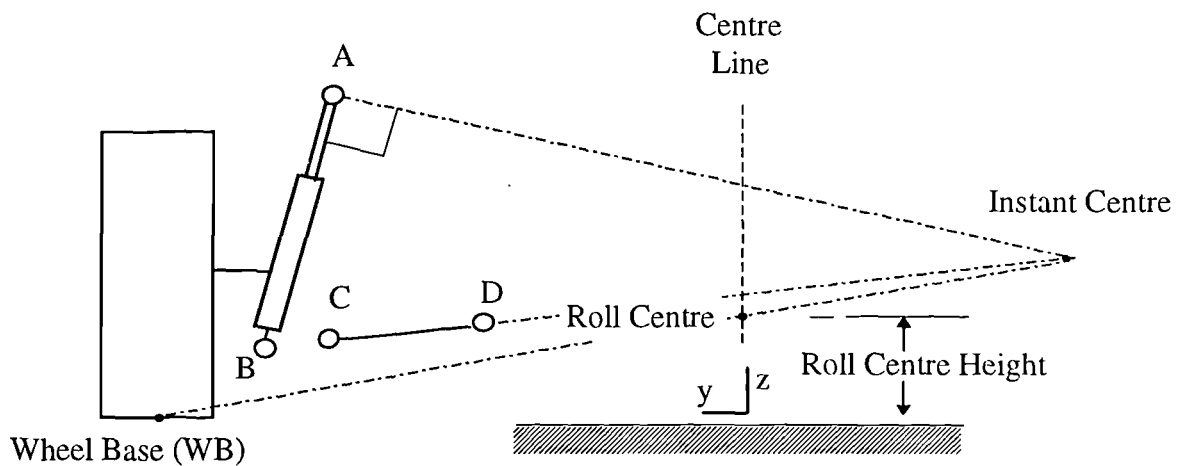
Figure 4.15 Construction of the instant centre and roll centre for the rear suspension

The instant centre is found by intersecting lines projected along the transverse arm and perpendicular to the axis of the strut. The roll centre is found by projecting a line between the

69

wheel base and the instant centre. The point at which this line intersects the centre line of the vehicle is taken to be the Roll Centre. All calculations are assumed to take place in the same YZ plane as the wheel centre. In order to program this method into ADAMS the construction must be set up algebraically. The first step is to set up expressions for the gradients GR1 for the line perpendicular to the strut and GR2 for the line projected along the transverse arm:

$$GR1 = (BY\text{-}AY) / (AZ\text{-}BZ)$$
$$GR2 = (DZ\text{-}CZ) / (DY\text{-}CY)$$

where AY, AZ, BY, ... DZ are the y and z coordinates of points A, B, C and D.

The coordinates of the instant centre ICY and ICZ, can be established from two simultaneous equations based on the upper and lower arms:

$$ICZ = AZ + GR1 * (ICY - AY)$$
$$ICZ = CZ + GR2 * (ICY - CY)$$

Rearranging these two equations gives:

$$AZ + GR1 * ICY - GR1 * AY = CZ + GR2 * ICY - GR2 * CY$$
$$ICY * (GR1 - GR2) = GR1 * AY - GR2 * CY + CZ - AZ$$

which allows the instant centre to be located using:

$$ICY = (GR1 * AY - GR2 * CY + CZ - AZ) / (GR1 - GR2)$$
$$ICZ = AZ + GR1 * (ICY - AY)$$

The gradient of the line joining the wheel base to the instant centre GR3, can be expressed as:

$$GR3 = (ICZ\text{-}WBZ) / (ICY\text{-}WBY)$$

where WBY and WBZ are the y and z coordinates of the wheel base.

70

which allows the roll centre to be located using:

RCY = 0.0

RCZ = WBZ + GR3 * (RCY - WBY)

The roll centre height RCH, can be defined by:

RCH = RCZ - RZ

where RZ is the z coordinate of the road .

4.6.3 Implementation in ADAMS

As stated earlier the calculation of instant centre and roll centre position can be implemented either by programming in the input deck with the VARIABLE statement or by preparing a user-written FORTRAN subroutine. By way of example these methods are demonstrated for the front suspension system only. Using the VARIABLE statement it is possible to program the equations laid out in Section 4.6.1 as shown in Table 4.1.

Table 4.1 Calculation of roll centre height using the VARIABLE statement

VAR/14,IC=1,FU=DZ(1414,1411)/(DY(1414,1411)+1E-6)	! GR1
VAR/15,IC=1,FU=DZ(1216,1213)/(DY(1216,1213)+1E-6)	! GR2
VAR/16,IC=1,FU=((VARVAL(14)*DY(1411))	! ICY
,-(VARVAL(15)*DY(1213))+DZ(1213)	
,-DZ(1411))/(VARVAL(14)-VARVAL(15)+1E-6)	
VAR/17,FU=DZ(1411)+VARVAL(14)*(VARVAL(16)-DY(1411))	! ICZ
VAR/18,FU=(VARVAL(17)-DZ(1029))/(VARVAL(16)-DY(1029)+1E-6)	! GR3
VAR/19,FU=DZ(1029)+VARVAL(18)*(0.0-DY(1029))	! RCZ
VAR/20,FU=VARVAL(19)+152.6	! RCH
REQ/1,F2=VARVAL(16)\F3=VARVAL(17)\F4=VARVAL(20)\	
,TITLE=NULL:ICY:ICZ:RCH:NULL:NULL:NULL:NULL	

The variables such as BZ-AZ are defined using ADAMS system variables which measure components of displacements between markers such as DZ(1414,1411). The REQUEST statement REQ/1 shows how to access the information calculated by the VARIABLE statements.

The alternative method of writing a FORTRAN subroutine is demonstrated in Table 4.2 by the listing of a user written REQSUB developed specifically for the front suspension of the ROVER. The subroutine would be called from the ADAMS input deck as follows:

REQUEST/id,FUNCTION=USER(1,par1,par2,par3,par4,par5,par6,par7,par8,par9)

Where the parameters par1,par2,...par9 are the various items of data outlined in the subroutine. The FORTRAN method was used with an earlier version of ADAMS and replaced with the VARIABLE method at a later date. The VARIABLE method has been used for the plots in this report.

4.7 Results

The system schematics used to generate the models for this study are provided in Appendix A. For both the front and rear suspensions the results are plotted graphically and are included in Appendix B. In each plot the vertical displacement (Bump movement) is plotted on the X-axis. The front suspension has been moved from 90 mm displacement in rebound to 110 mm displacement in bump. The rear suspension has been moved from 85 mm displacement in rebound to 100 mm in bump.

For the front suspension it was possible to compare the ADAMS results with measured test data provided by Rover which shows the variation of:

(i) Camber angle (deg) with Bump Movement (mm)

(ii) Steer angle (deg) with Bump Movement (mm)

(iii) Vertical Force (N) with Bump Movement (mm)

Table 4.2 FORTRAN subroutine to calculate roll centre height

```
      SUBROUTINE REQSUB(ID,TIME,PAR,NPAR,
     , IFLAG,RESULT)
C
C   M Blundell   Coventry University   Nov 1994
C
C   Calculation of Roll Centre Height and Instant
C   Centre Position -ROVER  front suspension.
C
C   Definition of Parameters:
C
C   PAR(1)   Subroutine id. Must be 1
C   PAR(2)   WC marker
C   PAR(3)   WB marker
C   PAR(4)   Marker at point A
C   PAR(5)   Marker at point B
C   PAR(6)   Marker at point C
C   PAR(7)   Marker at point D
C   PAR(8)   Radius of wheel
C   PAR(9)   RZ Height of Road in global Z
C
C   Results passed back to ADAMS are as follows:
C   Note that the AView does not use
C   RESULT(1) or RESULT(5)
C
C   RESULT(2) Roll Centre Height above ground
C   RESULT(3) Roll Centre Z coordinate
C   RESULT(6) ICY coordinate
C   RESULT(7) ICZ coordinate
C
      IMPLICIT DOUBLE PRECISION (A-H,O-Z)
      DIMENSION PAR(*), RESULT(8)
      LOGICAL IFLAG
      DIMENSION DATA(6)
      LOGICAL ERRFLG
C
      IDWC=PAR(2)
      IDWB=PAR(3)
      IDA=PAR(4)
      IDB=PAR(5)
      IDC=PAR(6)
      IDD=PAR(7)
      RADIUS=PAR(7)
      RZ =PAR(8)
      CALL INFO ('DISP',IDWC,0,0,DATA,ERRFLG)
      CALL ERRMES(ERRFLG,'WC ID',ID,'STOP')
      WCX=DATA(1)
      WCY=DATA(2)
      WCZ=DATA(3)
      CALL INFO('DISP',IDWB,0,0,DATA,ERRFLG)
      CALL ERRMES(ERRFLG,'WB ID',ID,'STOP')
      WBY=DATA(2)
      WBZ=DATA(3)
      CALL INFO ('DISP',IDA,0,0,DATA,ERRFLG)
      CALL ERRMES(ERRFLG,'IDA',ID,'STOP')
      AY=DATA(2)
      AZ=DATA(3)
      CALL INFO ('DISP',IDB,0,0,DATA,ERRFLG)
      CALL ERRMES(ERRFLG,' IDB',ID,'STOP')
      BY=DATA(2)
      BZ=DATA(3)
      CALL INFO ('DISP',IDC,0,0,DATA,ERRFLG)
      CALL ERRMES(ERRFLG,'IDC',ID,'STOP')
      CY=DATA(2)
      CZ=DATA(3)
      CALL INFO ('DISP',IDD,0,0,DATA,ERRFLG)
      CALL ERRMES(ERRFLG,'IDD',ID,'STOP')
      DY=DATA(2)
      DZ=DATA(3)
C
      GR1=(BZ-AZ)/(BY-AY)
      GR2=(DZ-CZ)/(DY-CY)
      RICY=((GR1*AY)-(GR2*CY)+CZ-AZ))
     ,/(GR1-GR2)
      RICZ=AZ+GR1*(RICY-AY)
      RCY=0.0
      GR3=(RICZ-WBZ)/(RICY-WBY)
      RCZ=WBZ+GR3*(RCY-WBY)
      RCH=RCZ-RZ
C
      RESULT(2)=RCH
      RESULT(3)=RCZ
      RESULT(6)=RICY
      RESULT(7)=RICZ
      RETURN
      END
```

73

4.8 Summary

Examination of the results given in Appendix B for both the front and rear suspension models indicates that, except for the steer change in the rear suspension, models using rigid joints, linear bushes or non-linear bushes could be used. It is noticeable with the front suspension that the plots begin to deviate when approaching the full bump or full rebound positions. This is due to the forces building up in the bump stop or rebound stop which are reacted through the suspension to the bushes. The reaction forces at the bushes lead to distortion which results in the changes in suspension geometry as shown in the plots. This effect is not present in the models using rigid joints which have zero degrees of freedom. Geometry changes are entirely dependent on the position and orientation of the joints.

On the rear suspension the range of vertical movement is such that the effects of the bump and rebound stops are clearly not as evident as for the front suspension. When considering the merits of each modelling approach it appears from the curves plotted that for the range of vertical movement expected of a handling model there is little difference between models using rigid joints, linear bushes or non-linear bushes, except for the plots which show the steer change of the wheel as a function of vertical movement. This is particularly noticeable with the rear suspension as shown in Figure B.9.

The steer angle curve for the rigid joint model diverges from the curves for the linear bush and non-linear bush model. This is due to the design of this suspension which does not easily allow kinematic modelling with the same level of accuracy as a double wishbone suspension as described earlier.

The results of this study indicate that for a handling model of this vehicle based on modelling the suspension linkages either the linear bush or non-linear bush models could be incorporated but that the rigid joint model may not be suitable due to the bump-steer characteristics, particularly in the rear suspension. The use of the non-linear model will significantly increase the effort required to model the vehicle. This is evident from Table 4.3 which compares the ADAMS data inputs required to model the connection of the front suspension lower arm to the vehicle body. As can be seen there is a significant amount of data

74

required to model a non-linear bush. The modelling of a linear bush requires only a reasonable amount of extra data input when compared with the rigid joint model.

From Table 4.3 it is clear that the modelling of non-linear bushes has a significant impact on the preparation of the ADAMS input deck. There is however a great deal of extra effort which needs to be documented. For the non-linear bushes in these models the characteristics were entered in the form of X-Y pairs making up a non-linear spline. It is important to check that the spline that ADAMS fits through the data is consistent with the test figures. For each of the non-linear splines used here the data has been and checked. In some cases the spline fit is poor leading to an oscillatory characteristic in the spline. In these cases it is necessary to fit additional points in the test data to ensure a smooth curve fit. It is also very easy to make an error when entering such large amounts of non-linear data in the ADAMS input deck. The plotting of non-linear data is therefore a necessary activity in terms of the quality assurance of the model but very time consuming.

The testing of the bushes is also an activity which will impact on the timescales of a simulation project. Research project work carried out in parallel to this project within the School of Engineering has required physical testing of the bushes on a similar vehicle. Based on the physical testing of the bushes for that vehicle and the plotting and checking of data an estimate of the effort, in man-days, required to prepare the bush data for a typical suspension is given in Table 4.4.

Table 4.3 ADAMS data input for a joint, linear bush and nonlinear bush

JOINT

JO/16,REV,I=1216,J=0116

LINEAR BUSH

BUSH/16,I=1216,J=0116
,K=7825,7825,944
,KT=2.5E6,2.5E6,500
,C=35,35,480
,CT=61000,61000,40

NON-LINEAR BUSH

BUSH/16,I=1216,J=0116
,K=0,0,0
,KT=0,0,500
,C=35,35,480
,CT=61000,61000,40

GFORCE/16,I=1216,JFLOAT=011600,RM=1216
,FX=CUBSPL(DX(1216,0116,1216),0,161)\
,FY=CUBSPL(DY(1216,0116,1216),0,161)\
,FZ=CUBSPL(DZ(1216,0116,1216),0,162)\
,TX=CUBSPL(AX(1216,0116),0,163)\
,TY=CUBSPL(AY(1216,0116),0,163)\
,TZ=0.0\

SPLINE/161
,X=-1.8,-1.5,-1.4,-1.22,-1.123,-1.0,-0.75,-0.5,-.25,0,0.25,0.5,0.75,1.0,1.123,1.22,1.4,1.5,1.8
,Y=15350,10850,9840,6716,5910,5059,3761,2507,1253,0,-1253,-2507,-3761,-5059,-5910,
,-6716,-9840,-10850,-15350
SPLINE/162,
,X=-5,-4,-3,-2.91,-2.75,-2.5,-2,-1.5,-1,-0.5,0,0.5,1,1.5,2,2.5,2.75,2.91,3,4,5
,Y=7925,3925,1925,1790,1626,1450,1136,830,552,276,0,-276,-552,-830
,-1136,-1450,-1626,-1790,-1925,-3925,-7925
SPLINE/163,
,X=-0.22682,-0.20939,-0.19196,-0.17453,-0.1571,-0.13963,-0.10472,-0.06981
,-.03491,0,0.03491,0.06981,0.10472,0.13963,0.1571,0.17453,0.19196,0.20939,0.22682
,Y=241940,198364,160018,125158,93387,75415,52951,35702,18453,0,-18453,-35702
,-52951,-75415,-93387,-125158,-160018,-198364,-241940

Table 4.4 The impact of modelling nonlinear bushes on project timescales

Obtaining bushes and planning tests	2 day
Design of brackets to support bushes in test rig	5 day
Manufacture of brackets	5 days
Static Testing of bushes	1 day
Dynamic testing of bushes	2 days
Checking test data	2 days
Preparing ADAMS spline data	2 days
Plotting and checking of spline data	2 days
Total	21 man-days

For the Linkage model which is described in the next section of this thesis it has been decided to model the suspensions using the linear bush approach. As discussed earlier the rigid joint model may work for the front suspension but for the rear suspension the bump steer characteristics are not accurate. The nonlinear bush model does not appear to be any more accurate than the linear bush model so the suspensions will be modelled using linear bushes.

5.0 MODELLING OF VEHICLE SYSTEMS

5.1 Introduction

One of the main objectives of this thesis has been to investigate the influence of modelling on handling simulations. With regard to this the modelling issues can be considered to divide into two main areas:

(i) The modelling of the forces and moments occurring at the tyre to road surface contact patch.

(ii) The modelling of the rest of the vehicle systems, namely the suspension systems, roll bars, vehicle body, steering system, steering inputs, and drive inputs to the road wheels. Although not considered here more advanced systems such as traction control or anti-lock braking systems may also be considered.

This section of the report will address the modelling of vehicle systems. The modelling of tyre characteristics is a large and complex subject and is therefore addressed separately in Section 6 of this report. Detailed schematics for all the models described here are included in Appendix A.

5.2 Vehicle body, coordinate frames and rigid part definitions

For each rigid body in the system it is necessary to include a statement defining the mass, centre of mass location, and mass moments of inertia. These statements are referred to as Part statements. The mass moments of inertia are defined with respect to an inertial reference frame. Throughout this project each part has utilised a reference frame which is located at the mass centre and aligned with the principal axes of the body. This means that it was only necessary to define the principal mass moments of inertia (Ixx, Iyy, Izz) and not include product moments of inertia (Ixy, Iyz, Izx). The use of coordinate systems is now explained in more detail but for the vehicle body it will be seen later that Ixx is associated with roll, Iyy with pitch and Izz with yaw.

It is also possible to model the flexibility of bodies using different methods depending on the geometry of the part. For example, a component such as a tie bar or roll bar could be modelled using a beam element with the usual stiffness matrix formulation as used in finite element analysis. Such an element is available as a standard modelling feature in ADAMS.

A more complex modelling approach for flexible bodies is used where the geometry is more detailed such as for a suspension arm or the vehicle body itself. In these cases the component or body may be modelled in a finite element program ensuring that nodes exist in coincident positions to those required for joint or force attachments in the multibody systems program. The stiffness matrix is condensed in the finite element program to a matrix which references these locations. The resulting stiffness matrix, which is sometimes referred to as a superelement can then be included in the multibody systems program. An example of this is given in (71) which describes work carried out by the Ford Light Truck division in the USA. In this case suspension arms have been modelled in a finite element program and included in an ADAMS model used for handling simulations. For an open top sports vehicle the torsional stiffness of the body may also be of concern when trying to predict handling performance. In this case a finite element approach may again be used. Alternatively a more simplistic representation of the torsional stiffness of the body may be used as in (64). In that case the vehicle body was modelled as two rigid masses connected by a revolute joint aligned along the longitudinal axis of the vehicle and located at the mass centre. The relative rotation of the two body masses about the axis of the revolute joint was resisted by a torsional spring with a stiffness corresponding to the torsional stiffness of the whole body.

Each rigid part possesses a set of markers which can be defined in global or local coordinate systems and are considered to move with the part during the simulation. Markers are used to define centre of mass locations, joint locations and orientations, force locations and directions. It is also necessary to include one non moving part which is referred to as the ground part.

For the modelling work carried out here there are three types of right-handed Cartesian coordinate systems which may be used:

(i) The ground reference frame (GRF) is fixed and is the datum from which all other reference frames are defined.

(ii) The local part reference frame (LPRF) can be defined as a local system belonging to and moving with any part in the model. The LPRF is defined relative to the ground reference frame.

(iii) Markers are the essential reference frame used to define physical data such as mass centres, spring attachment points or joint positions and orientation. The markers belong to, move with and change orientation with a given part. As such they are defined relative to the LPRF for that part. If an LPRF has not been defined for that part then the initial position of the marker is defined with respect to the GRF.

The positioning of the reference frames described above is illustrated in Figure 5.1. The position of the LPRF is defined by the vector QG which has components measured parallel to the GRF. The position of a marker is defined by the vector QP which has components measured parallel the LPRF or as shown, parallel to the GRF in the absence of an LPRF for that part.
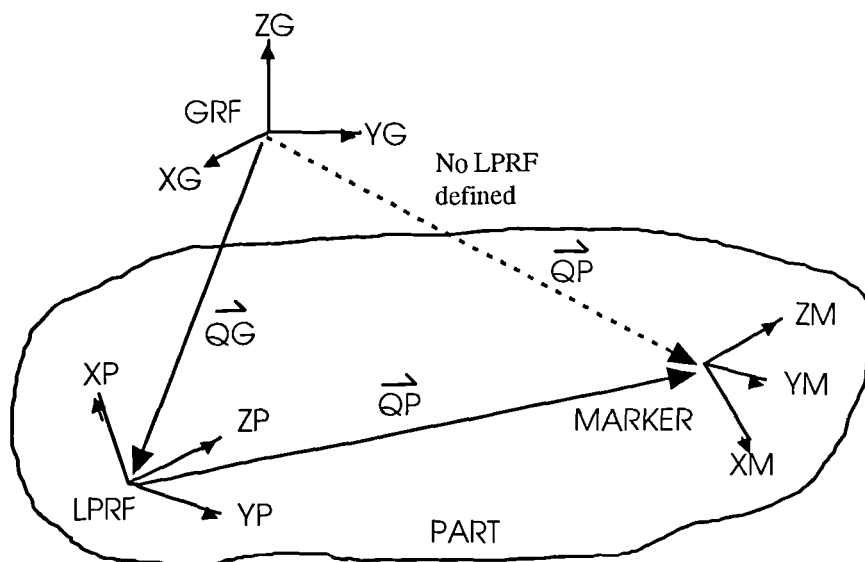
Figure 5.1 Co-ordinate systems

For the vehicle models described in this thesis there was no use made of LPRFs and all markers were defined relative to a single GRF as shown in Figure 5.2. The GRF is located near the centre of the vehicle and is orientated with the x-axis pointing aft, the z-axis upwards and the y-axis towards the left of the vehicle. This means that for most manoeuvres the vehicle is defined with initial negative x-components of velocity.
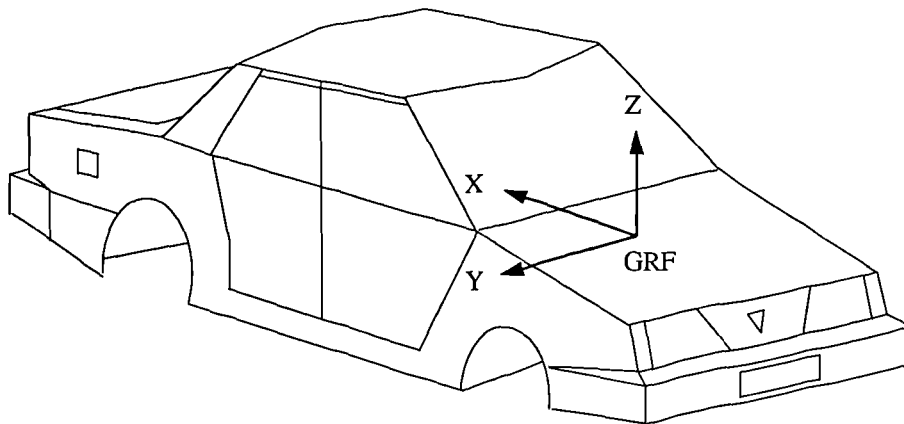
Figure 5.2 Vehicle ground reference frame (GRF)

In addition to defining the position of a marker relative to the GRF using the QP vector it is also necessary to define any required change in orientation. The first method shown in Figure 5.3 makes use of successive Euler angle rotations, psi, theta and phi. Note that for this work no LPRFs were defined so that the rotations are relative to the GRF.

In some instances it is more convenient to define the orientation of a marker by defining a point ZP at any position along the z-axis of the new marker reference frame. This is often all that is required as for example in the case where the z-axis of the marker is used to define the axis of a revolute joint. If the orientation of the x and y-axes are also required this can be achieved by defining any point XP on the new zx plane. ADAMS can then manipulate the vectors to cross the new z-axis with the XP coordinate in the marker frame to obtain the y-axis.
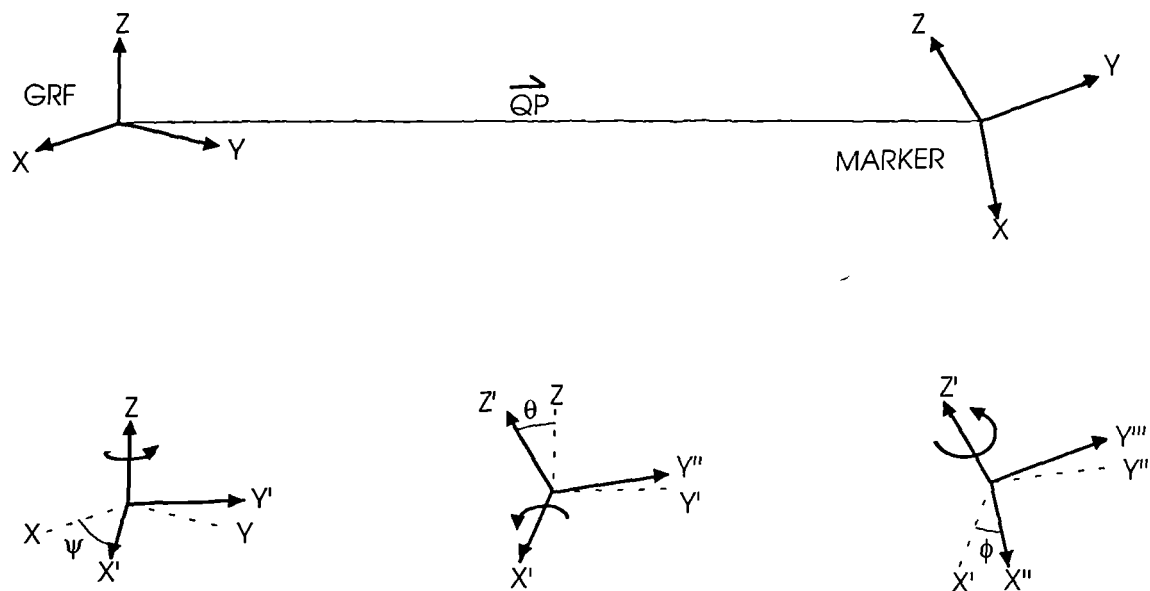
Figure 5.3 Euler angle approach

The new y and z-axes can then be used in a similar manner to obtain the x-axis. This method is shown in Figure 5.4. Note that for the vehicle work described here LPRFs were not used so that the XP and ZP vectors when used were defined relative to the GRF.
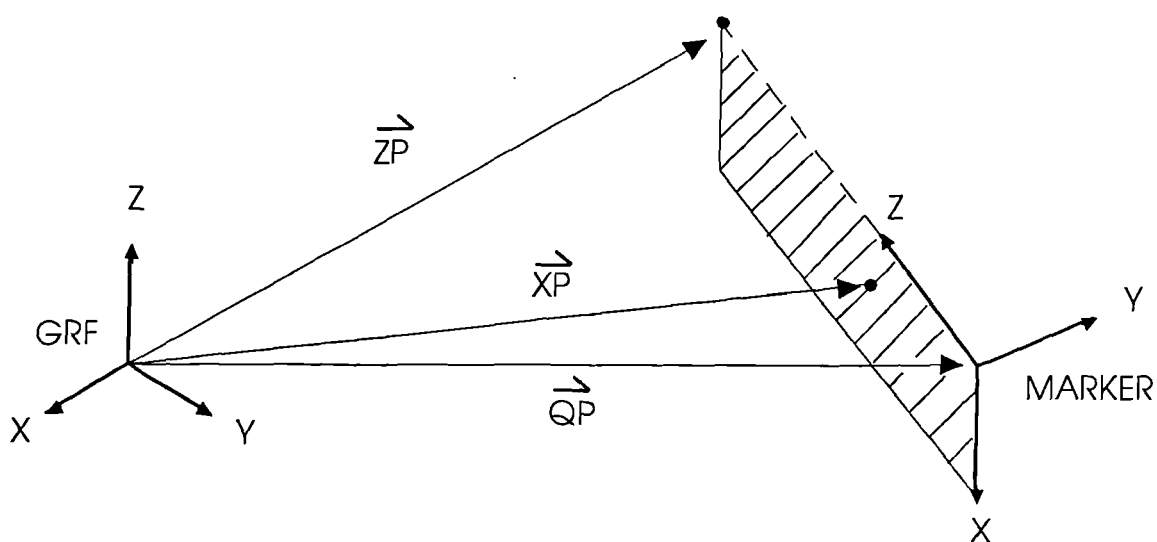
Figure 5.4 The XP-ZP method for marker orientation

5.3 Modelling of suspension systems

5.3.1 Overview

The study described in Section 4 of this report has laid the ground work for the further investigation described here. As described earlier the four suspension modelling approaches which have been compared are:

(i) The *Linkage Model* where the suspension linkages and compliant bush connections have been modelled in detail in order to recreate as closely as possible the actual assemblies on the vehicle.

(ii) The *Lumped Mass Model* where the suspensions have been simplified to act as single lumped masses which can only slide in the vertical direction with respect to the vehicle body.

(iii) The *Swing Arm Model* where the suspensions are treated as single swing arms which rotate about a pivot point located at the instant centres for each suspension.

(iv) The *Roll Stiffness Model* where the body rotates about a single roll axis which is fixed and aligned through the front and rear roll centres.

The four suspension arrangements are shown schematically in Figure 5.5 and described in more detail in the following sections.

LINKAGE MODEL

LUMPED MASS MODEL

SWING ARM MODEL

ROLL STIFFNESS MODEL
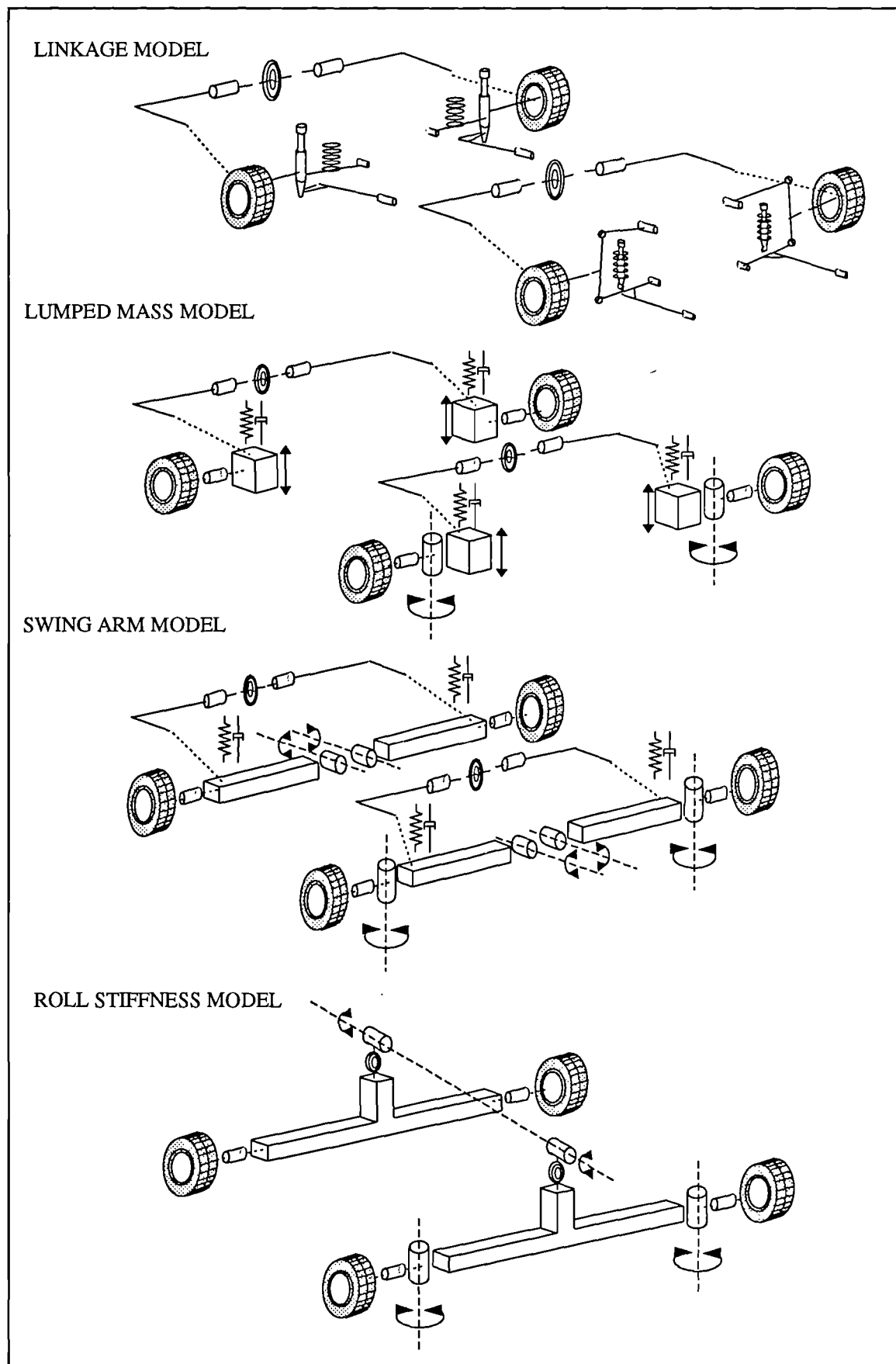
Figure 5.5 Modelling of suspension systems

5.3.2 Linkage model

The model based on linkages as shown in Figure 5.6 is the model which most closely represents the actual vehicle. The work discussed in Section 4 lead to the decision to model the bushes as linear. This sort of vehicle model is the most common approach adopted by ADAMS users in the automotive industry even extending the model definition to include full nonlinear bush characteristics as with the work in (64).
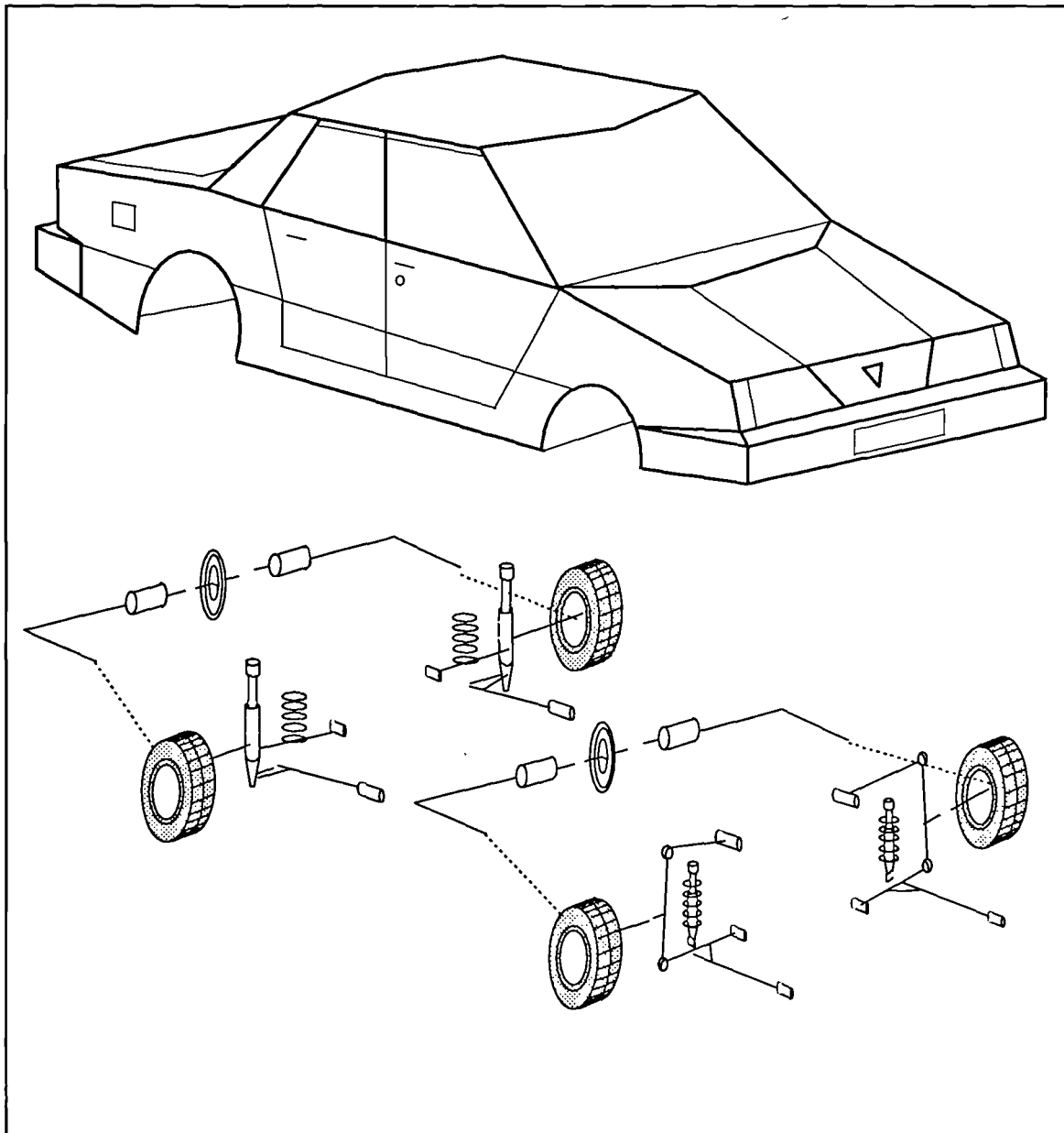
Figure 5.6 The Linkage model

A simplification of a model based on linkages is to treat the joints as rigid and generate a kinematic representation of the suspension system. As described in Section 4 a double wishbone arrangement is typical of a suspension system that can be modelled in this way and used for handling simulations. This has been confirmed in (24) where a kinematic modelling approach was discussed for vehicles with double wishbone suspensions. Note that although for completeness the schematic in Figure 5.6 also shows the front and rear roll bars the modelling of these is discussed in more detail in Section 5.6 of this report.

5.3.3 Lumped Mass model

For the Lumped Mass model the suspension components are considered to be lumped together to form a single mass. The mass is connected to the vehicle body at the wheel centre by a translational joint which only allow vertical sliding motion. This means that there is no change in the relative camber angle between the road wheels and the body. The camber angle between the road wheels and the road will therefore be directly related to the roll angle of the vehicle. Spring and damper forces act between the suspensions and the body.

The front wheel knuckles were modelled as separate parts connected to the lumped suspension parts by revolute joints. The steering motion required for each manoeuvre was achieved by applying time dependent rotational motion inputs about these joints. Each road wheel was modelled as a part connected to the suspension by a revolute joint. The Lumped Mass model is shown schematically in Figure 5.7.
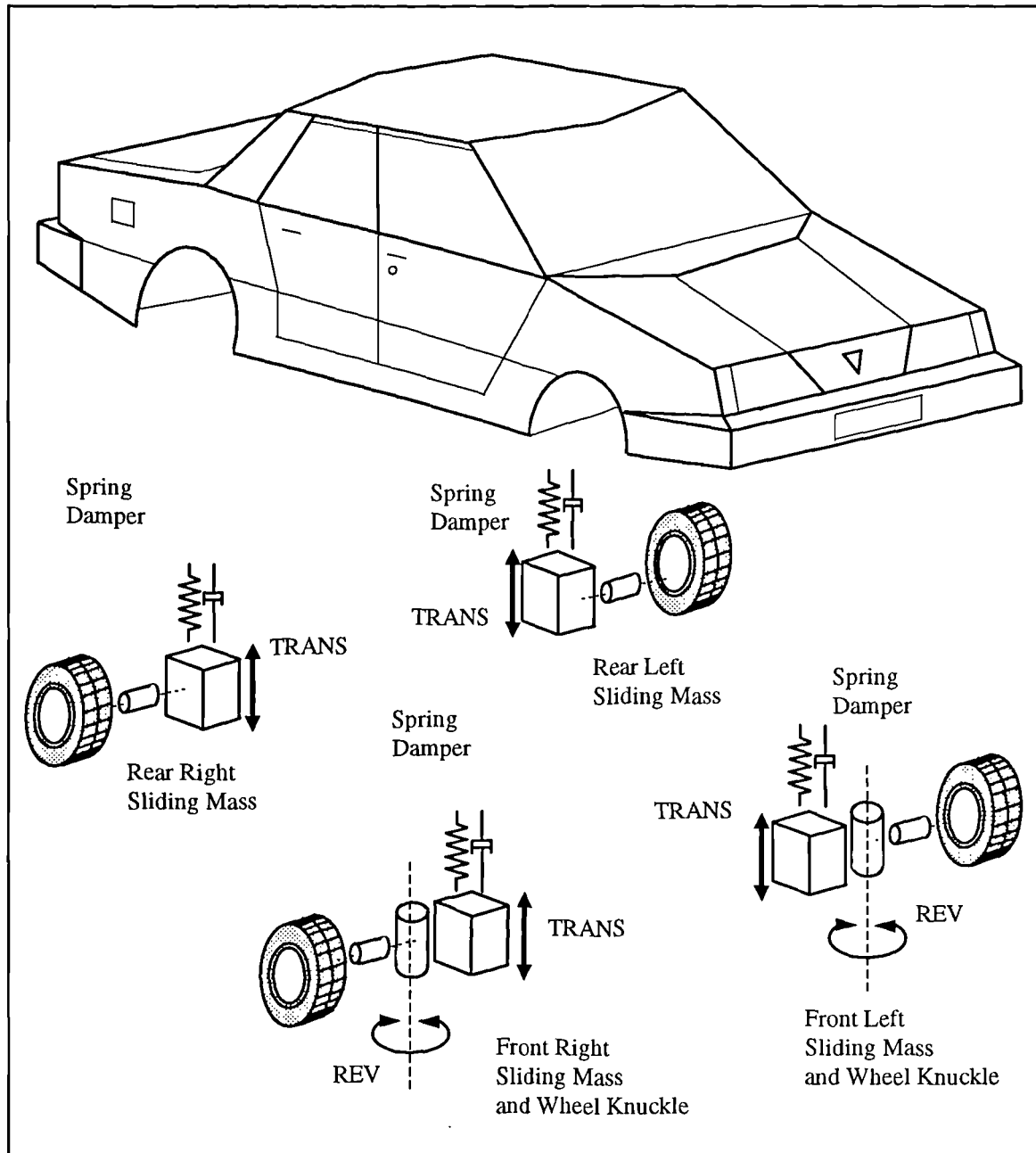
Figure 5.7 The Lumped Mass model

5.3.4 Swing Arm model

This model was developed from the lumped mass model by using revolute joints to allow the suspensions to 'swing' relative to the vehicle body rather than using translational joints which only allow sliding motion to take place. The revolute joints were located at the instant centres of the actual suspension linkage assembly. These positions were found by modelling the

suspensions separately as described in Section 4. The swing arm model has an advantage over the lumped mass model in that it allows the wheels to change camber angle relative to the vehicle body. The Swing Arm model is shown schematically in Figure 5.8.
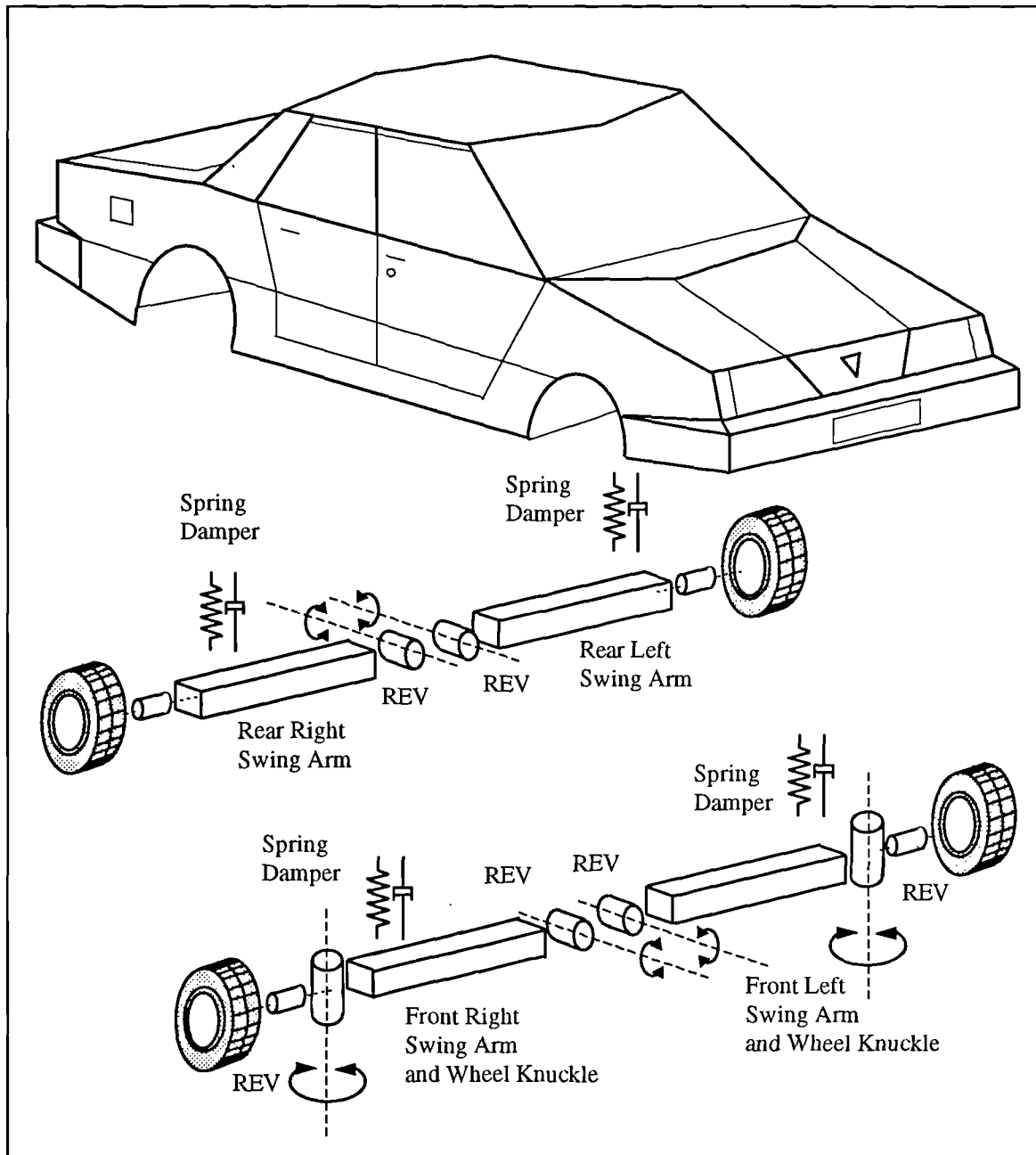
Figure 5.8 The Swing Arm model

5.3.5 Roll Stiffness model

This model was a further simplification treating the front and rear suspensions as rigid axles connected to the body by revolute joints at the roll centres. The roll centre positions were obtained from the study described in Section 4. A torsional spring was located at the front and rear roll centres to represent the roll stiffness of the vehicle. The determination of the roll stiffness of the front and rear suspensions required a detailed investigation which is described in the following section. The Roll Stiffness model is shown schematically in Figure 5.9.
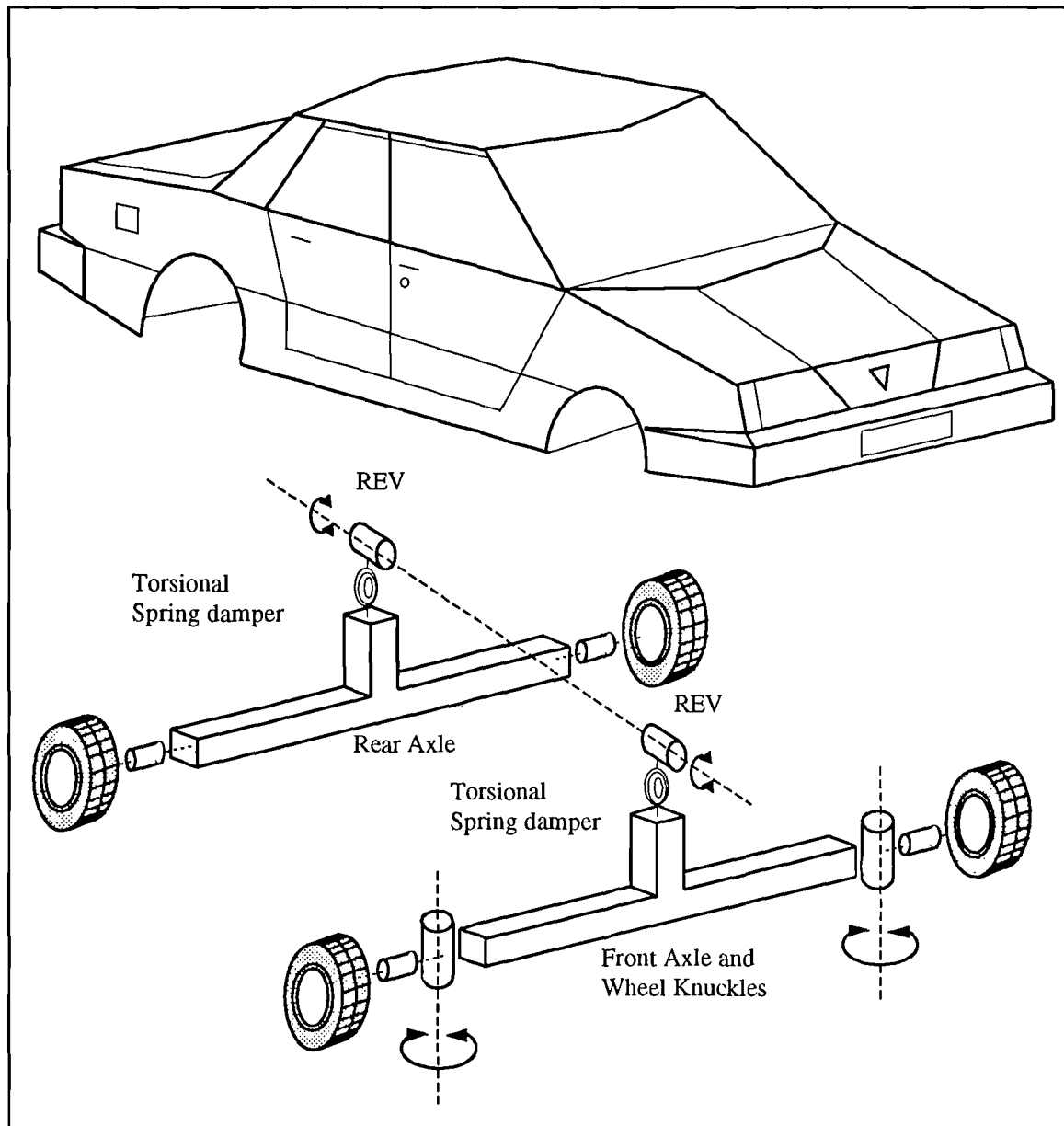
Figure 5.9 The Roll Stiffness model

5.3.6 Model size

For each of the vehicle models described here it is possible to estimate the model size in terms of the degrees of freedom in the model and the number of equations which ADAMS is using to formulate a solution. The calculation of the number of degrees of freedom (DOF) in a system is based on the Greubler equation:

DOF = 6 x (No. of Parts) - (Constraints from Joints and Motions)

Note that each Part has six rigid body degrees of freedom. The ground part is not included in the calculation as it does not move. An example, for some of the joints used in this study, of the degrees of freedom removed by constraints is given in Table 5.1.

Table 5.1 Degrees of freedom constrained by joints

ADAMS Joint	Translational Constraints	Rotational Constraints	Total Constraints
Cylindrical	2	2	4
Fixed	3	3	6
Planar	1	2	3
Revolute	3	2	5
Spherical	3	0	3
Translational	2	3	5
Universal	3	1	4

It is therefore possible for any of the vehicle models to calculate the degrees of freedom in the model. An example is provided here for the Roll Stiffness model where the degrees of freedom can be calculated as follows:

Parts   9 x 6   = 54
Rev   8 x -5   = -40
Motion 2 x -1   = -2
Σ_{DOF} = 12

In physical terms it is more meaningful to describe these degrees of freedom in relative terms as follows. The body part has 6 degrees of freedom. The two axle parts each have 1 rotational degree of freedom relative to the body. Each of the four wheel parts has 1 spin degree of freedom relative to the axles making a total of 12 degrees of freedom for the model.

When a simulation is run in ADAMS the program will also report the number of equations in the model. As discussed in Section 3 ADAMS will formulate 15 equations for each part in the model and additional equations corresponding to all the constraint and applied forces in the model. On this basis the size of all the models is summarised in Table 5.2.

Table 5.2 Vehicle model sizes

Model	Degrees of freedom	Number of Equations
Linkage	78	961
Lumped Mass	14	429
Swing Arm	14	429
Roll Stiffness	12	265

The size of the model and the number of equations is not the only consideration when describing efficiency in vehicle modelling. Of perhaps more importance is the engineering significance of the model parameters. The Roll Stiffness model, for example, may be preferable to the Lumped Mass model. It is not only a smaller model but is also based on parameters such as roll stiffness which will have relevance to a vehicle engineer. The roll stiffness can be measured on an actual vehicle or estimated during vehicle design.

5.4 Determination of roll stiffness and damping

5.4.1 Modelling approach

In order to develop the full vehicle model based on roll stiffness it was necessary to determine the roll stiffness and damping of the front and rear suspension elements separately. The estimation of roll damping was obtained by assuming an equivalent linear damping and using the positions of the dampers relative to the roll centres to calculate the required coefficients. The positions of the front and rear roll centres were already established using the quarter suspension models and the methods set out in Section 4. The procedure used to find the roll stiffness for the front suspension elements involved the development of a model as shown in Figure 5.10. This model included the vehicle body which was constrained to rotate about an axis aligned through the front and rear roll centres. The vehicle body was attached to the ground part by a cylindrical joint located at the front roll centre and aligned with the rear roll centre. The rear roll centre was attached to the ground by a spherical joint in order to prevent the vehicle sliding along the roll axis. A motion input was applied at the cylindrical joint to rotate the body through a given angle. By requesting the resulting torque acting about the axis of the joint it was possible to calculate the roll stiffness associated with the front end of the vehicle. The front suspensions were modelled using the suspension model where bushing characteristics were treated as linear. The springs were also included as was the complete front roll bar model. The road wheel parts were not included nor were the tyre properties. The wheel centres on either side were constrained to remain in a horizontal plane using inplane joint primitives. Although the damper force elements were retained in the suspension models they have no contribution as the roll stiffness was determined using static analysis. The steering system, although not shown in Figure 5.10, was also included in the model. A motion input was used to lock the steering in the straight ahead position during the roll simulation.

For the rear end of the vehicle the approach was essentially the same as for the front end, with in this case a cylindrical joint located at the rear roll centre and a spherical joint located at the front roll centre. The model used for the rear roll analysis is shown in Figure 5.11.
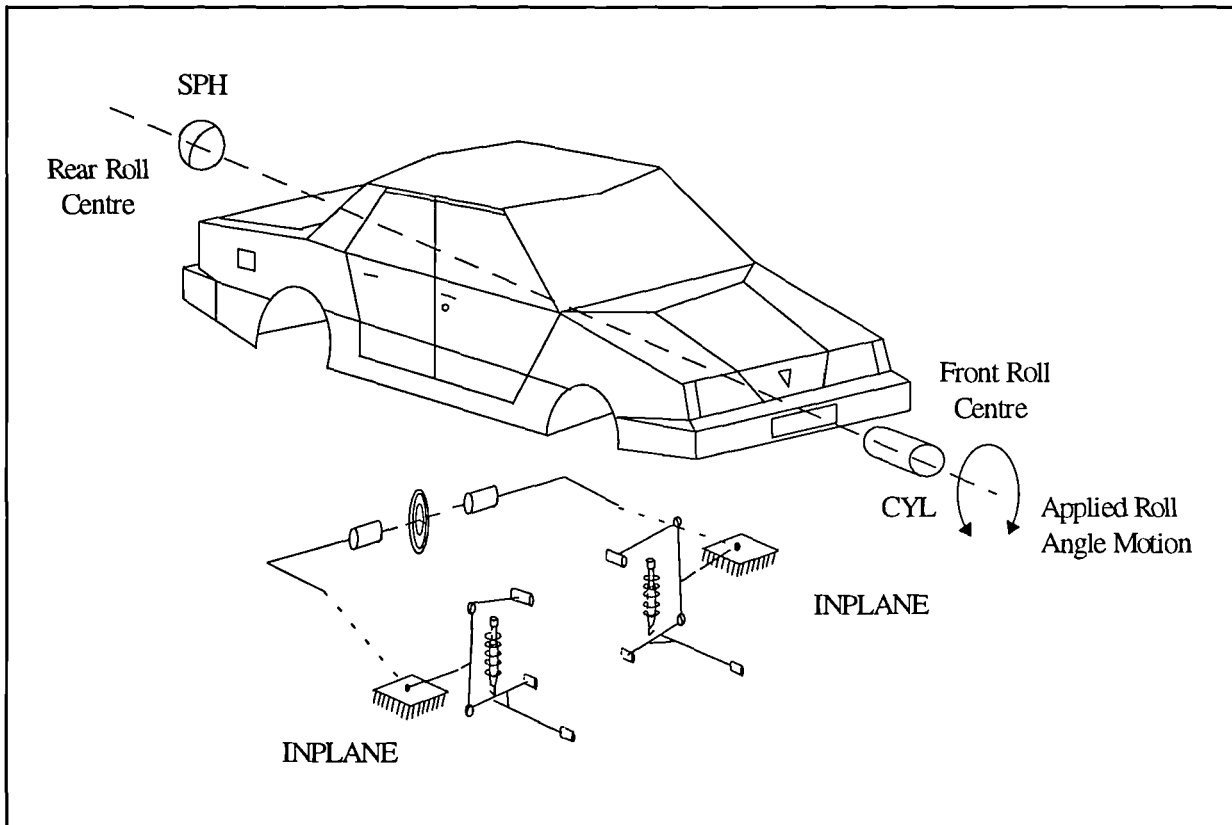
Figure 5.10 Determination of front end roll stiffness
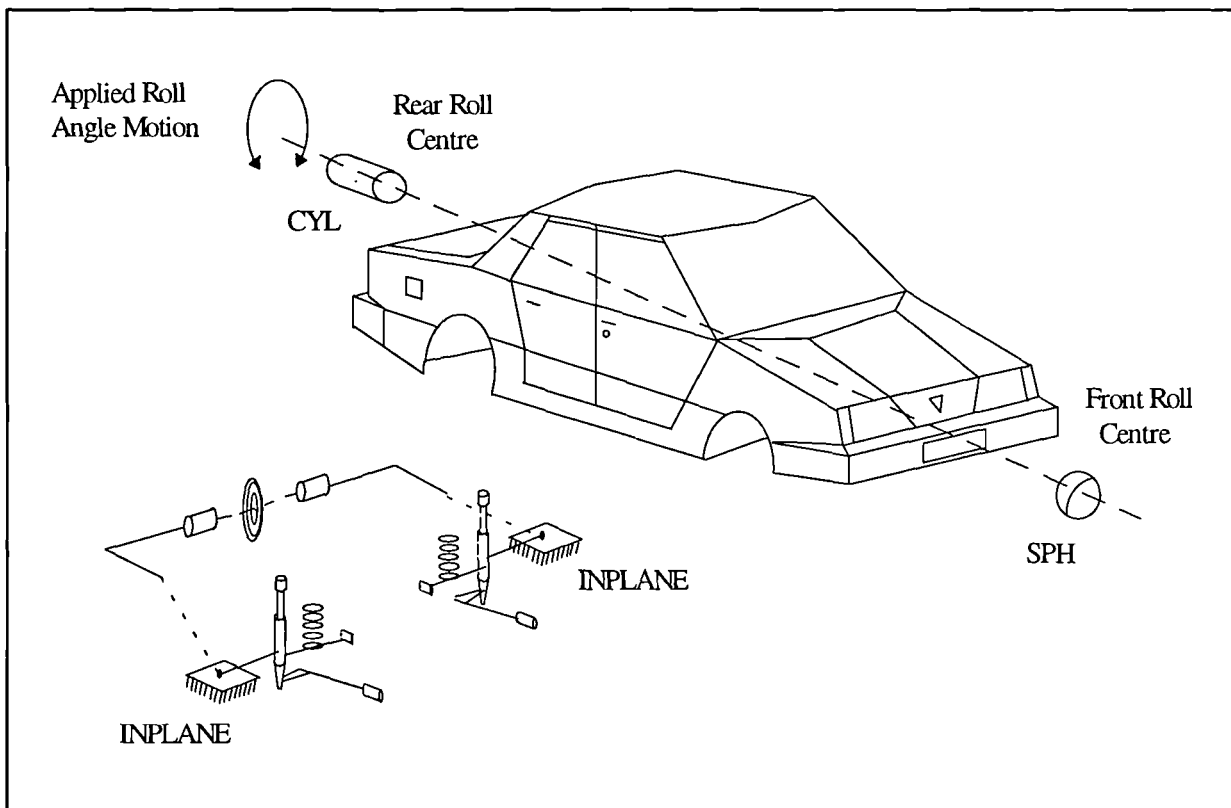
Figure 5.11 Determination of rear end roll stiffness

For both the front and rear models the vehicle body was rotated through an angle of ten degrees either side of the vertical. In each case a quasi-static analysis was performed over three seconds with thirty output steps. The roll motion was defined as a function of time to roll the model at a rate of ten degree per second. During the first second the model rotates ten degrees to the left and then back to the upright position between one and two seconds. Over the third second the model rotates ten degrees to the right.

The results for the front and rear end models are plotted in Figure 5.12 and Figure 5.13 and are linear to within 2% for the front and 4% for the rear. The data from these curves has been used to obtain the values of torsional stiffness used in the roll stiffness model.

Front End

Rear End

$Kt = 608.459 \ 10^3$ Nmm/deg

$Kt = 496.459 \ 10^3$ Nmm/deg

$Kt = 34.862 \ 10^6$ N mm/rad

$Kt = 28.445 \ 10^6$ Nmm/rad

Roll Moment (Nmm)

Roll Angle (deg)
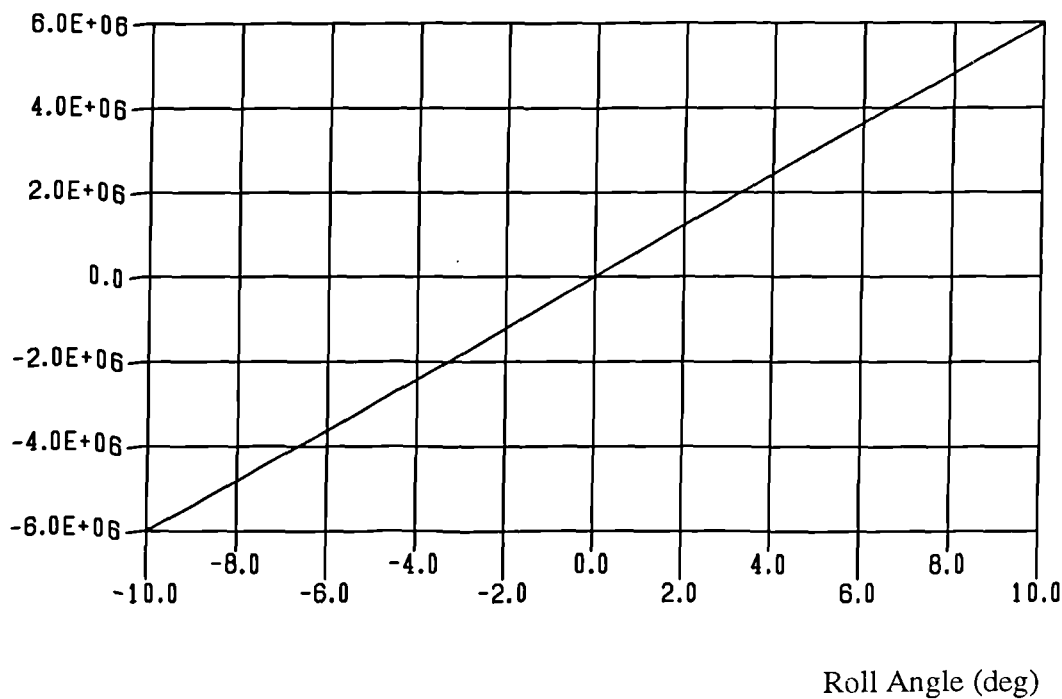
Figure 5.12 Front end roll test

94

Roll Moment (Nmm)
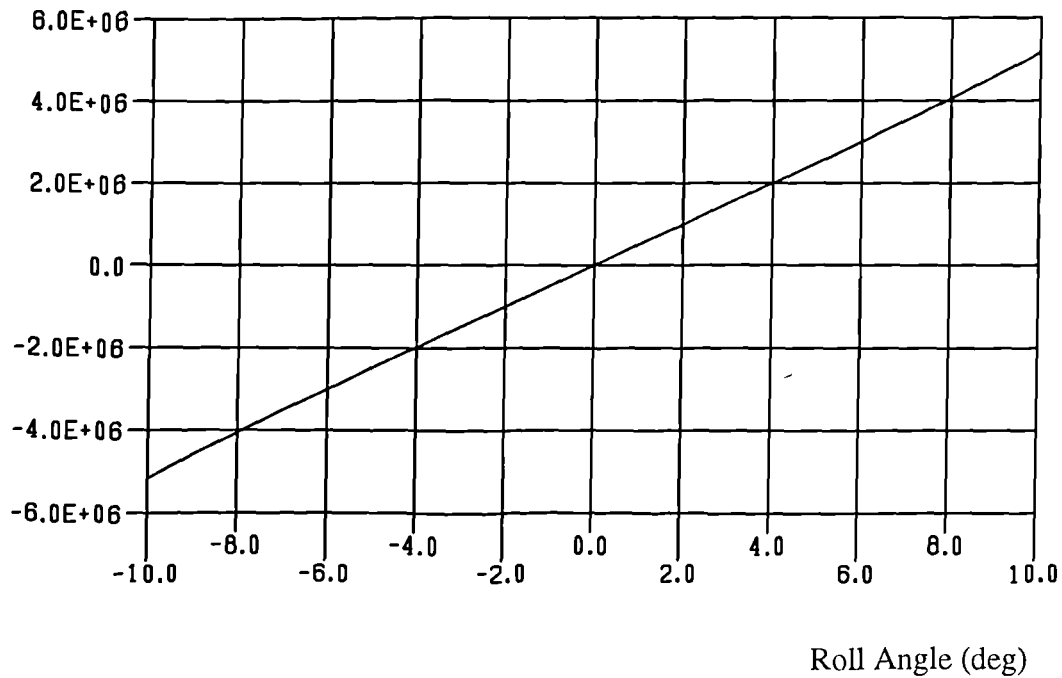
Figure 5.13 Rear end roll test

5.4.2 Calculation check

As a check on the values for roll stiffness obtained from the ADAMS simulations a hand calculation has been performed for the roll stiffness at the front end of the vehicle. The deformed geometry used for the calculation has been obtained by producing a scaled drawing of the rolled vehicle. The maximum roll angle of ten degrees has been used to facilitate the drawing and measuring of the dimensions used in the hand calculation. The value obtained from the hand calculation is compared with the value computed by ADAMS. The roll stiffness due to the road springs and the roll stiffness due to the roll bar have been calculated separately and then added to get a total roll stiffness. The calculation of the contribution due to the springs is based on the forces due to spring deformation and the moment of these forces about the roll centre. The deformation of the springs and the moment arms were measured from the scaled drawing based on a roll angle θ, of ten degrees. This is illustrated in Figure 5.14 which is not to scale.

95
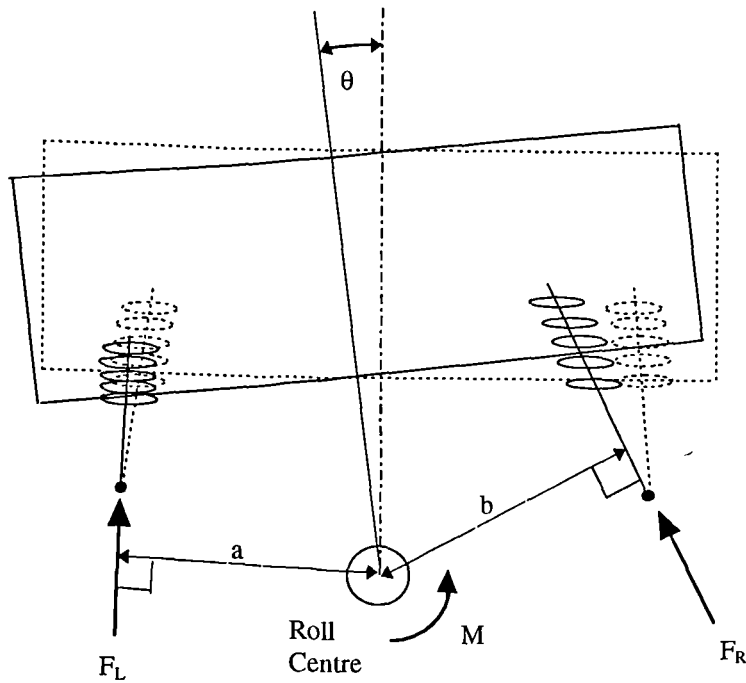
Figure 5.14 Calculation of roll stiffness due to road springs

The spring stiffness is given as:

k = 31.96 N/mm

The deformation in the left spring and extension in the right spring are equal and were found to be:

δL = 110 mm

The forces F_L and F_R can be calculated as:

F_L = k . δL = 3516 N

F_R = k . δL = 3516 N

The moment arms a and b were found to be:

a = 630 mm   b = 600 mm

This gives a moment M_S due to the springs acting at the roll centre:

M_S = F_L . a + F_R . b = 4324.7 10^3 Nmm

The roll bars have been modelled in ADAMS as two rigid parts connected at the vehicle centre line by a torsional spring. In order to calculate the moment acting at the roll centre due to the roll bar it is first necessary to calculate the relative angle of twist between the two parts representing the roll bar. This is shown below in Figure 5.15.
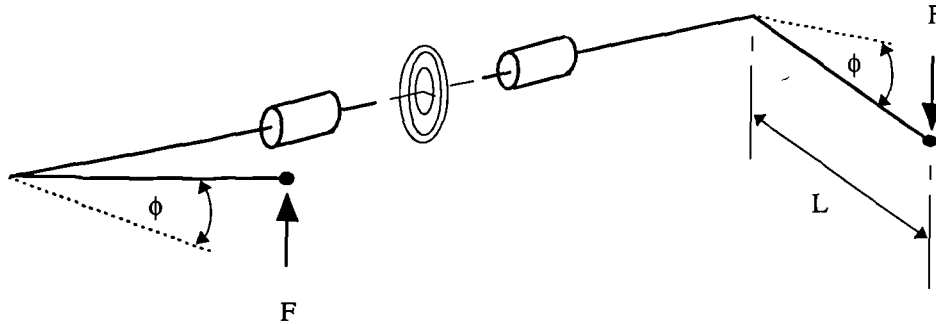
Figure 5.15 Calculation of roll stiffness due to the roll bar

The angle ϕ was found to be :

$\phi = 25^\circ$

The torsional stiffness of the roll bar Kt is given as:

$Kt = 490.0 \ 10^3 \ Nmm/rad$

The torque T required to produce an angle of twist of ϕ on each side of the roll bar is given by:

$T = Kt . \phi . (\pi/180) = 213.8 \ 10^3 \ Nmm$

The lever arm L from the roll bar to the wheel centre is given as:

$L = 298 \ mm$

The force F required to produce the torque is given by:

$F = T/L = 717.5 \ N$

The moment M_R due to the roll bar acting at the roll centre is given by multiplying the force F by the track Tr:

Tr = 1488 mm

$M_R = F \cdot Tr = 1067.5 \ 10^3$ Nmm

The total moment M acting at the roll centre is found by adding the contribution due to the springs M_S and the contribution due to the roll bar M_R:

$M = M_S + M_R = 5392.2 \ 10^3$ Nmm

The roll stiffness K_{TF} of the front end of the vehicle can be found from:

$K_{TF} = M / \theta = $ Nmm/deg $= 539.2 \ 10^3$ Nmm/deg

$K_{TF} = M / [\theta \cdot (\pi/180)] = 30895.0 \ 10^3$ Nmm/rad

Comparing this value with the roll stiffness computed by the ADAMS model gives a difference of 9.8%. On this basis the hand calculation appears to validate the modelling approach and analyses used in ADAMS to determine roll stiffness for the front and rear end of the vehicle.

5.5 Road Springs and dampers

5.5.1 Modelling of springs and dampers in the linkage model

The treatment of road springs in a vehicle where the suspensions have been modelled using linkages and the suspension geometry is usually straightforward and allows a linear formulation to be used. The spring is defined as connecting two points, referred to as an I marker and a J marker. For the front suspension shown schematically in Figure 5.16 the spring force acts between an I marker which is taken as belonging to the body representing the upper part of the damper and a J marker which is taken as belonging to the body representing the lower part of the damper. For the rear suspension the spring force is taken as acting between an I marker

which belongs to the vehicle body and a J marker which belongs to the suspension arm. For both the front and rear suspension the damper forces act between the upper and lower parts used to model the damper body.

Front Suspension   Rear Suspension
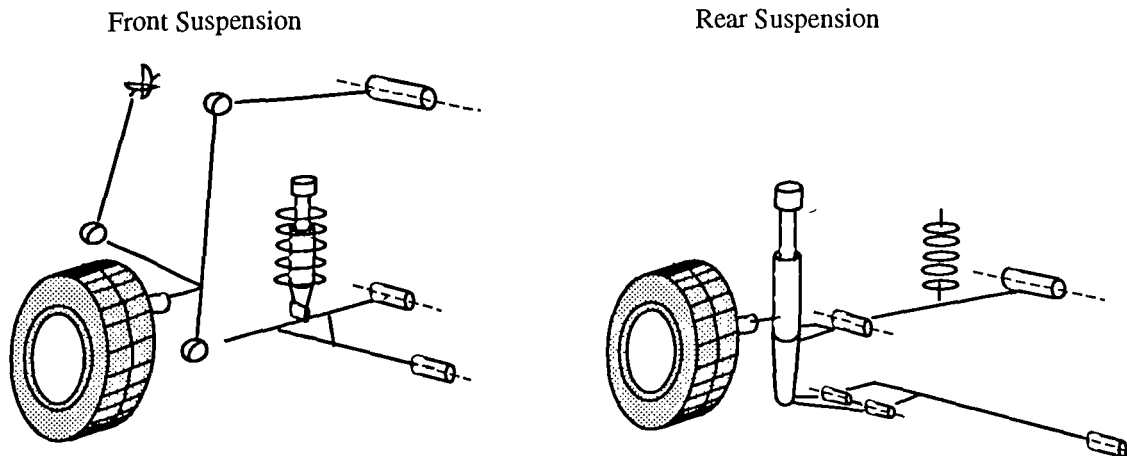
Figure 5.16 Location of spring and damper elements in the linkage model

The force in the springs when treated as linear is given by:

$$F = K * (DM (I,J)-L)$$

where:

L = Free Length of Spring (at zero force)

DM(I,J) = Magnitude of Displacement between I and J Marker

K = Spring Stiffness

In this case K and L are model parameters and DM(I,J) is a system variable which is continually calculated and updated by ADAMS during an analysis. The sign convention used is that the equation for the spring will return a value which is positive when the spring is in compression and negative in tension.

The damper forces were modelled as nonlinear and dependent on the relative velocity between the I marker and J marker used to define the damper force. The system variable used

to represent the velocity is VR(I,J) also known as the *radial line of sight velocity*. The sign convention used is that during bump when a positive force is needed VR(I,J) is negative and that during rebound when I and J are separating the sign convention is reversed.

The nonlinear damper forces are defined in ADAMS using xy data sets where the x values represent velocity and the y values are the force. During the analysis the force values are extracted using a cubic spline fit. The curves for the front and rear dampers are shown in Figure 5.17.

FRONT DAMPER - SOLID, REAR DAMPER - DASH
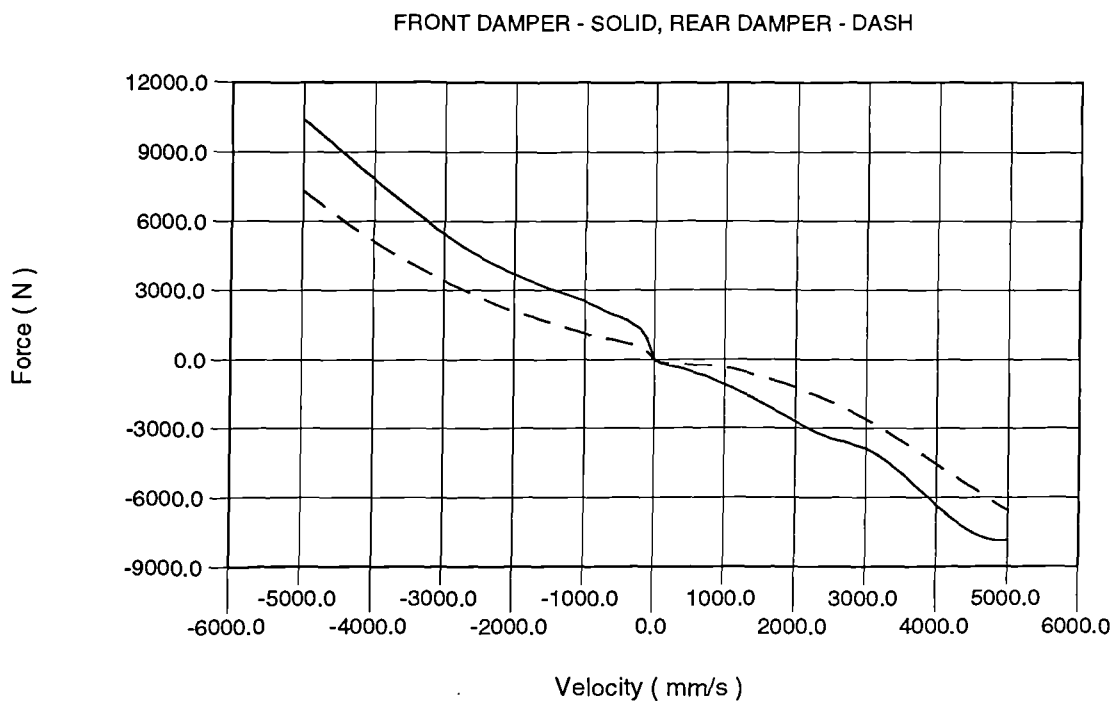
Figure 5.17 Nonlinear force characteristics for the front and rear dampers

5.5.2 Modelling of springs in the Lumped Mass and Swing Arm models

For the simplified modelling approach used in the Lumped Mass and Swing Arm models it was discovered that the road springs could not be directly installed in the vehicle model as with the linkage model. Consider the Lumped Mass model when compared with the Linkage model as shown in Figure 5.18.

100

$$\delta s \doteq (ls/lw)\delta w \qquad\qquad \delta s = \delta w$$
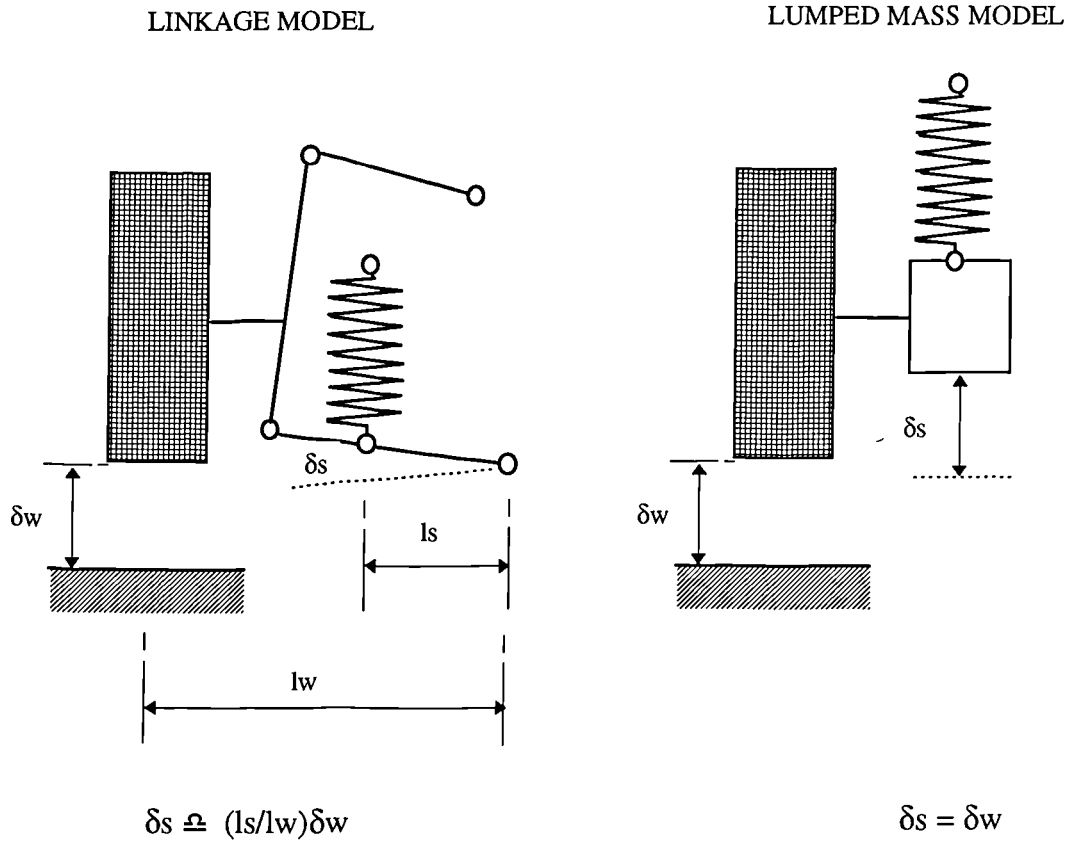
Figure 5.18 Road spring in the Linkage and Lumped Mass models

Clearly there is a mechanical advantage effect in the Linkage model which is not present in the Lumped Mass vehicle model. At a given roll angle for the Lumped Mass model the displacement and hence the force in the spring will be too large when compared with the corresponding situation in the Linkage model.

For the Swing Arm model as shown in Figure 5.19 the instant centre about which the suspension pivots is actually on the other side of the vehicle. In this case the displacement in the spring is approximately the same as at the wheel and a similar problem occurs as with the Lumped Mass model.

101
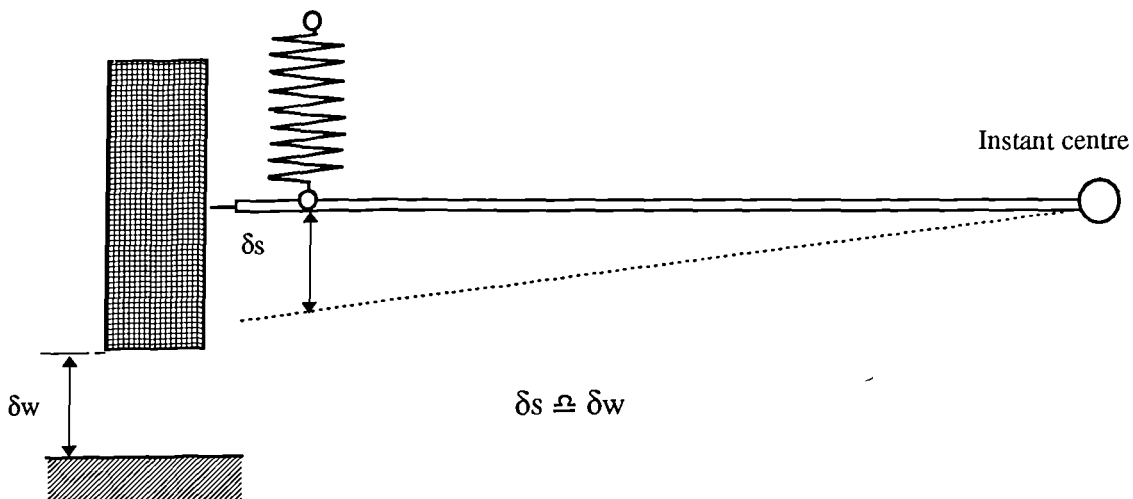
Figure 5.19 Installation of the road spring in the Swing Arm model

For the Lumped Mass and Swing Arm models this problem has been overcome as shown in Figure 5.20 by using an 'equivalent' spring which acts at the wheel centre. From the work with the quarter suspension model described in Section 4 it was possible to measure the force and displacement at the wheel centre and plot this as shown in Figure B.6 for the front suspension and Figure B.12 for the rear suspension.
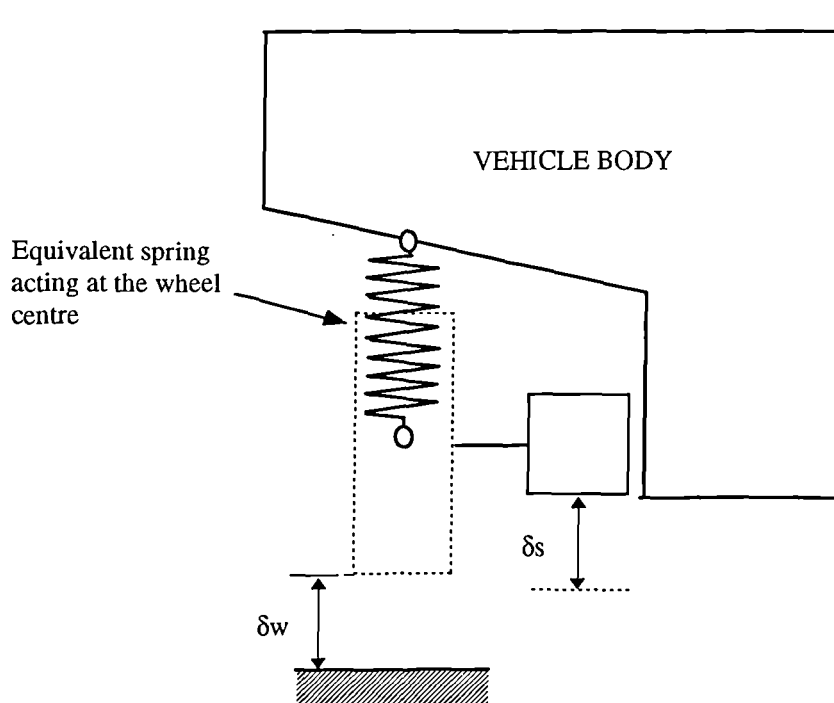
Figure 5.20 Equivalent spring acting at the wheel centre

102

Although not used in the work described here a similar approach could be used in concept design when detailed geometry is not available and a wheel rate curve can not be obtained using the methods described in Section 4 of this report. This would involve scaling the initial estimates of a linear spring out to the wheel centre and is illustrated in Figure 5.21.
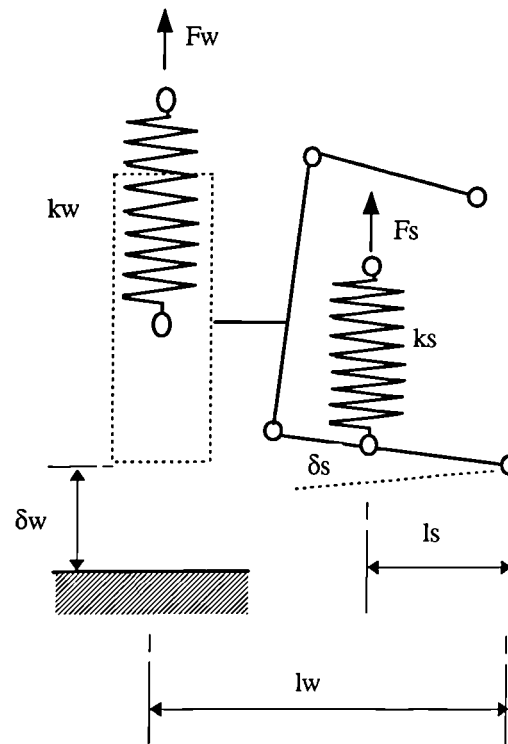
Figure 5.21 Scaling a linear spring to the wheel centre position

For the standard road spring the basic force displacement relationship gives:

$$Fs = ks.\delta s$$

For the equivalent spring we also have:

$$Fw = kw.\delta w$$

Mechanical advantage gives:

$$Fw = (Ls/Lw) \, Fs$$

Geometry gives:

$$\delta s = (Ls/Lw) \, \delta w$$

Therfore:

$$kw = Fw/\delta w = (Ls/Lw) \, Fs \, / \, (Lw/Ls) \, \delta s = (Ls/Lw)^2 \, ks$$

The introduction of a square function in the ratio can be considered a combination of two effects:

(i) The extra mechanical advantage in moving the road spring to the wheel centre.

(ii) The extra spring compression at the wheel centre.

5.6 Roll bars

As shown in Figure 5.22 the roll bars were modelled using two parts connected to the vehicle body by revolute joints and connected to each other by a torsional spring located on the centre line of the vehicle. The roll bars were not modelled in detail, rather each roll bar part was connected to the suspension using an inplane joint primitive which allowed the vertical motion of the suspension to be transferred to the roll bars and hence produce a relative twisting motion between the two sides.
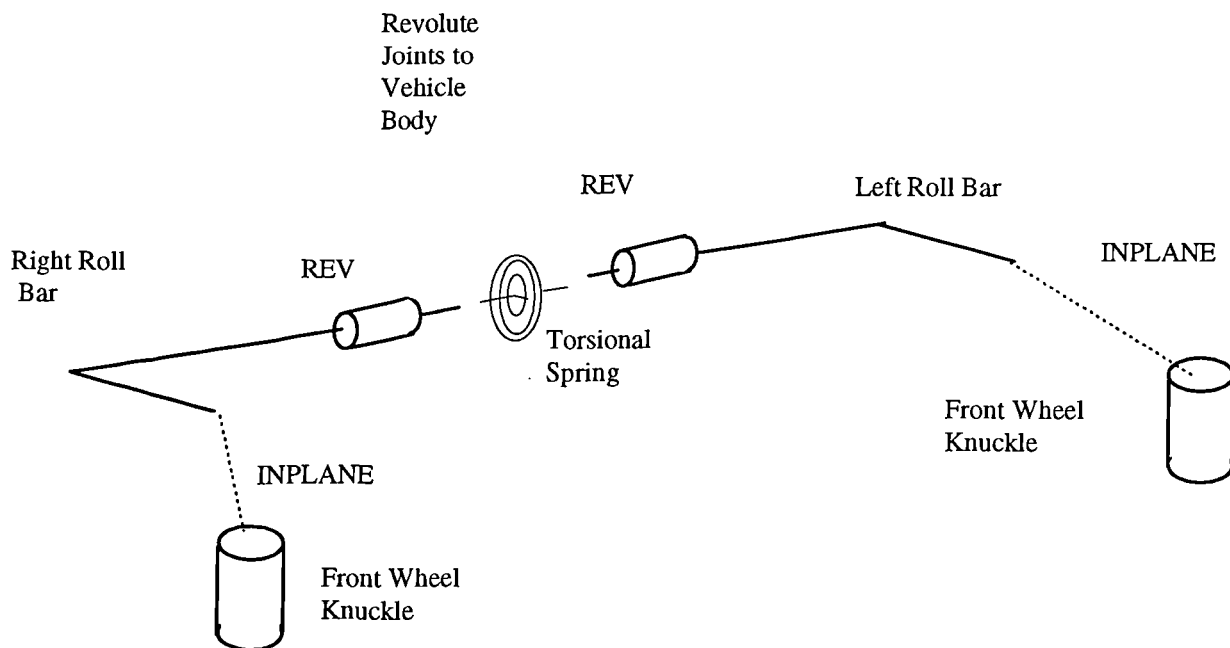
Figure 5.22 Modelling the roll bars

5.7 Steering system

5.7.1 Modelling with the linkage model

It was discovered that for the simple full vehicle models such as that modelled with lumped mass suspensions there were problems when trying to incorporate the steering system. Consider first the arrangement of the steering system on the actual vehicle and the way this has been modelled on the detailed Linkage model as shown in Figure 5.23. In this case only the suspension on the right hand side is shown for clarity.
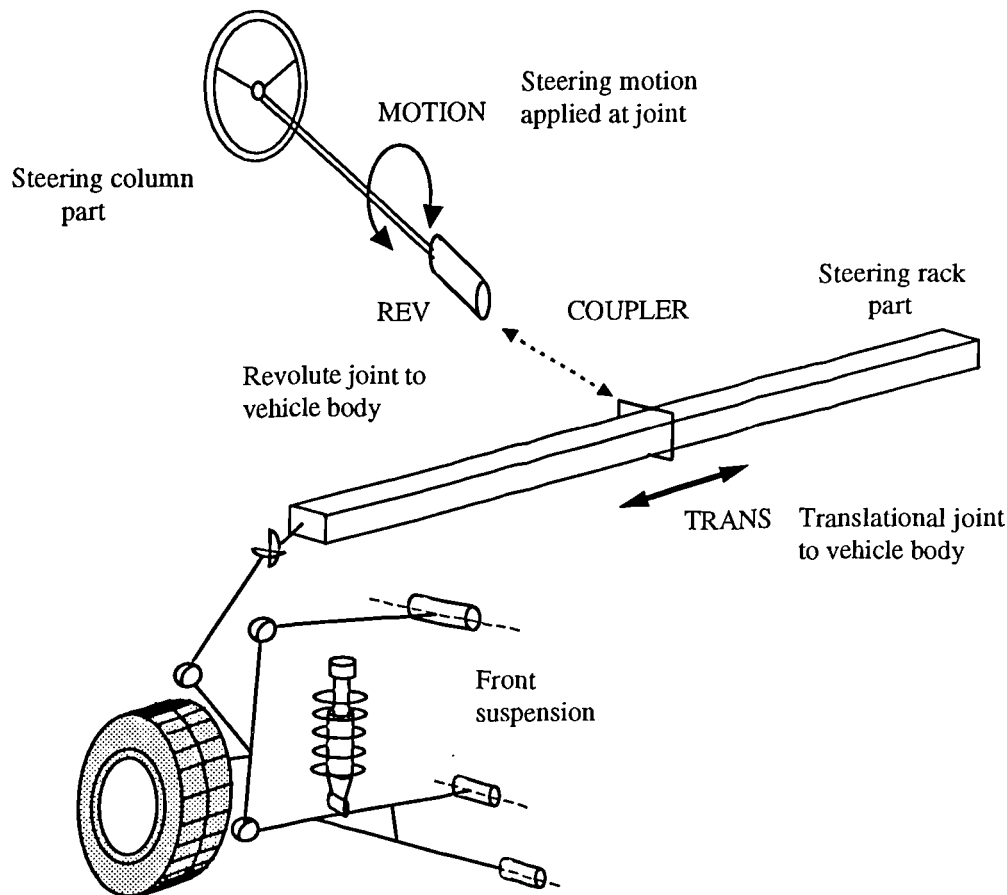
Figure 5.23 Modelling the steering system

The steering column was represented as a part connected to the vehicle body by a revolute joint with its axis aligned along the line of the column. The steering inputs required to manoeuvre the vehicle were applied as motion inputs at this joint and are described in Section 7. The steering rack part was connected to the vehicle body by a translational joint and

connected to the tie rod by a universal joint. The translation of the rack was related to the rotation of the steering column by a coupler statement which defines the ratio as follows:

COUPLER/510502,JOINTS=501,502,TYPE=T:R,SCALES=8.44898D,1.0

In this case joint 501 is the translational joint and 502 is the revolute joint. the coupler statement ensures that for every 8.44898 degrees of column rotation there will be 1 mm of steering rack travel.

5.7.2 Steering ratio test

Initial attempts to incorporate the steering system into the simple models using lumped masses, swing arms and roll stiffness met with a problem when connecting the steering rack to the actual suspension part. This is best explained by considering the situation shown in Figure 5.24.

Motion on the steering system is 'locked' during the initial static analysis

Downward motion of vehicle body and steering rack relative to suspension during static equilibrium

Connection of tie rod causes the front wheels to toe out
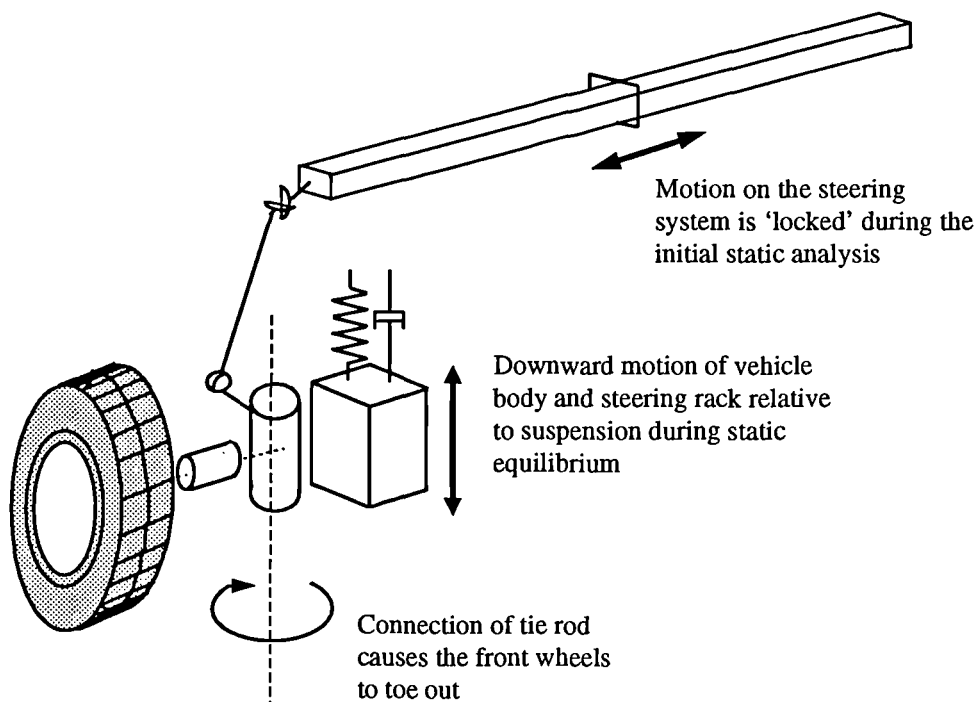
Figure 5.24 Toe change in front wheels at static equilibrium for simple models

The geometry of the tie rod has been established for the suspension and works well for the linkage model. Physically connecting the tie rod to the simple suspensions does not work. During the initial static analysis the rack moves down with the vehicle body relative to the suspension system. This has a pulling effect on the tie rod which actually causes the front wheels to toe out during the initial static analysis. This is similar to a bump steer effect. The solution to this was to establish the relationship between the steering column rotation and the steer change in the front wheels and to model this as a direct ratio using two coupler statements to link the rotation between the steering column and each of the front wheel joints as shown in Figure 5.25.
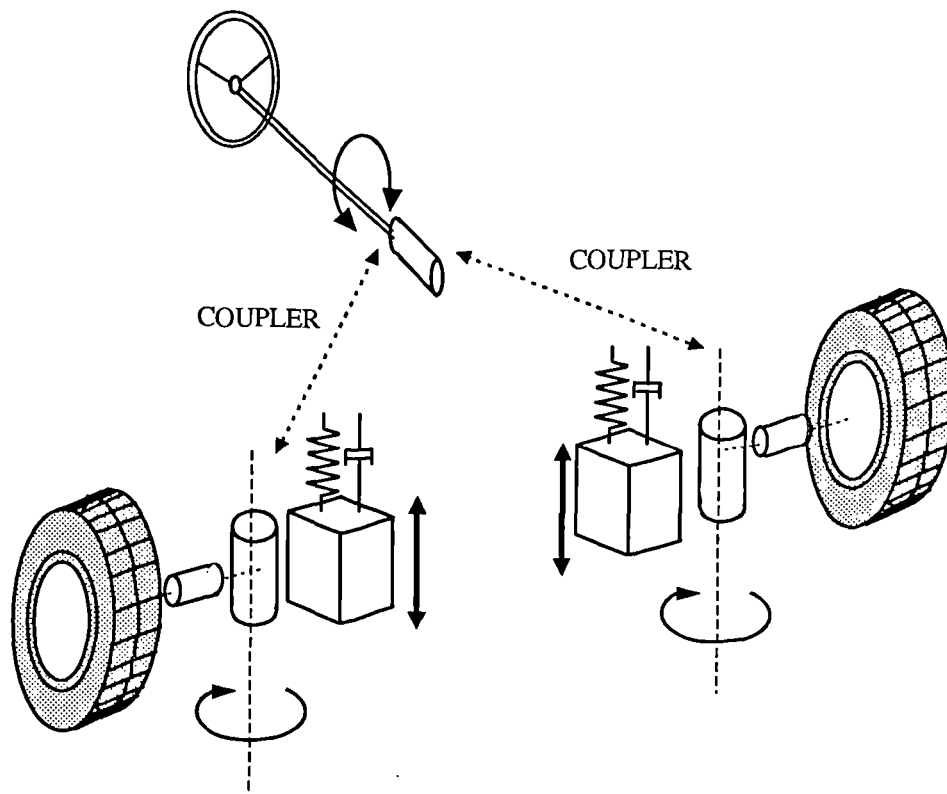
Figure 5.25 Coupled steering system model

During the track testing of the actual vehicle described in (20), a steering test was carried out to measure the ratio between the steering wheel rotation and the road wheel steer angle. This ratio was found to be 20:1. In order to check this with the ADAMS models a separate study was carried out using the front right suspension system modelled with linear bushes and connected to the ground part instead of the vehicle body. The modelling of these two subsystems is shown in Figure 5.26.

107
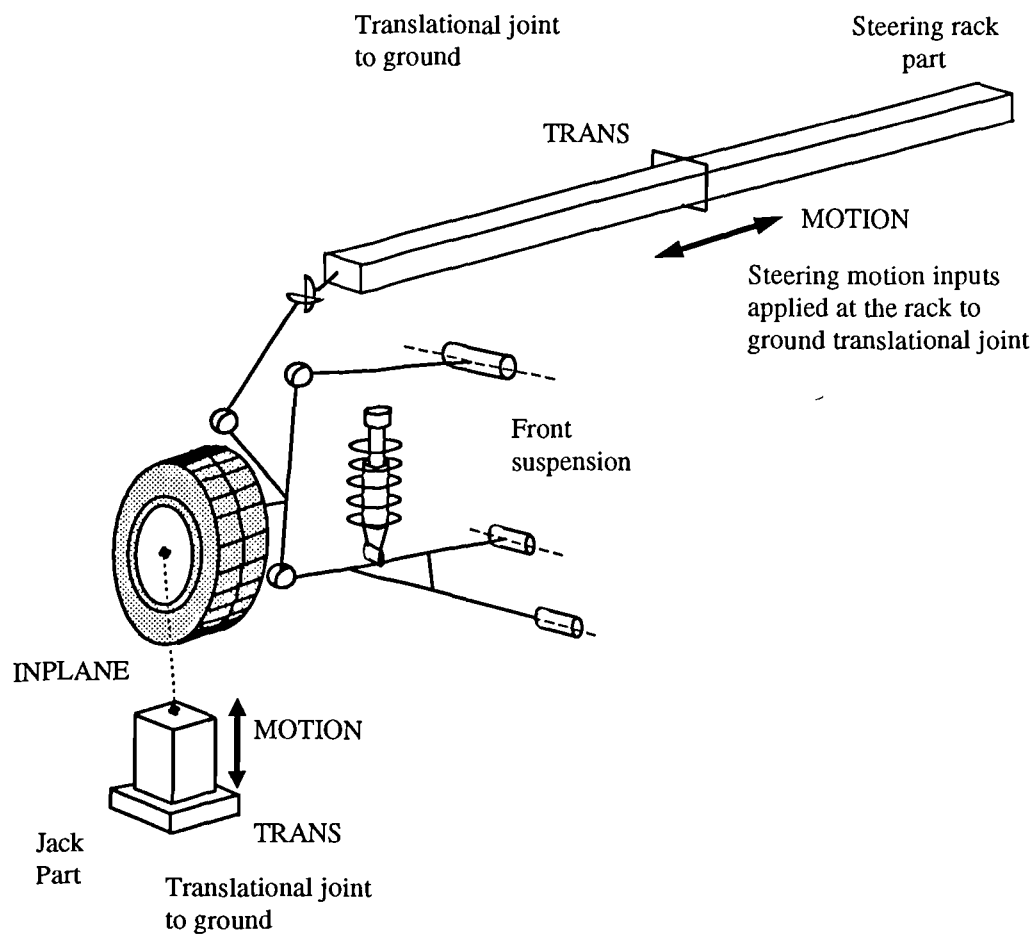
Figure 5.26 Front suspension steering ratio test model

The approach of using a direct ratio to couple the rotation between the steering column and the steer angle of the road wheels was considered to have two main limitations which should be investigated before continuing with the development of the simplified full vehicle models:

(i) In the real vehicle and the Linkage model the ratio between the column rotation and the steer angle at the road wheels would vary as the vehicle rolls due to the bump steer effects generated by the suspension geometry.

(ii) For either wheel the ratio of toe out or toe in as a ratio of left or right steering wheel angle rotation would not be exactly symmetric.

Although both of these effects could be included the relationships would be very difficult to model and to a certain extent would defeat the object of not modelling linkages and using more simple suspension models.

The geometric ratio between the rotation of the steering column and the travel of the rack was already known and so it was possible to apply a motion input at the rack to ground joint which was equivalent to a steering wheel rotation 180 degrees either side of the straight ahead position. In order to check the relevance of this the jack part shown in Figure 5.31 was used to raise or lower the suspension during the steering test. The results of these simulations are shown in the graph in Figure 5.27 where the steering wheel angle is plotted on the x-axis and the road wheel angle is plotted on the y-axis. The three lines plotted represent the steering ratio test when simulated in the following positions:

FRONT RIGHT SUSPENSION - STEERING RATIO TEST
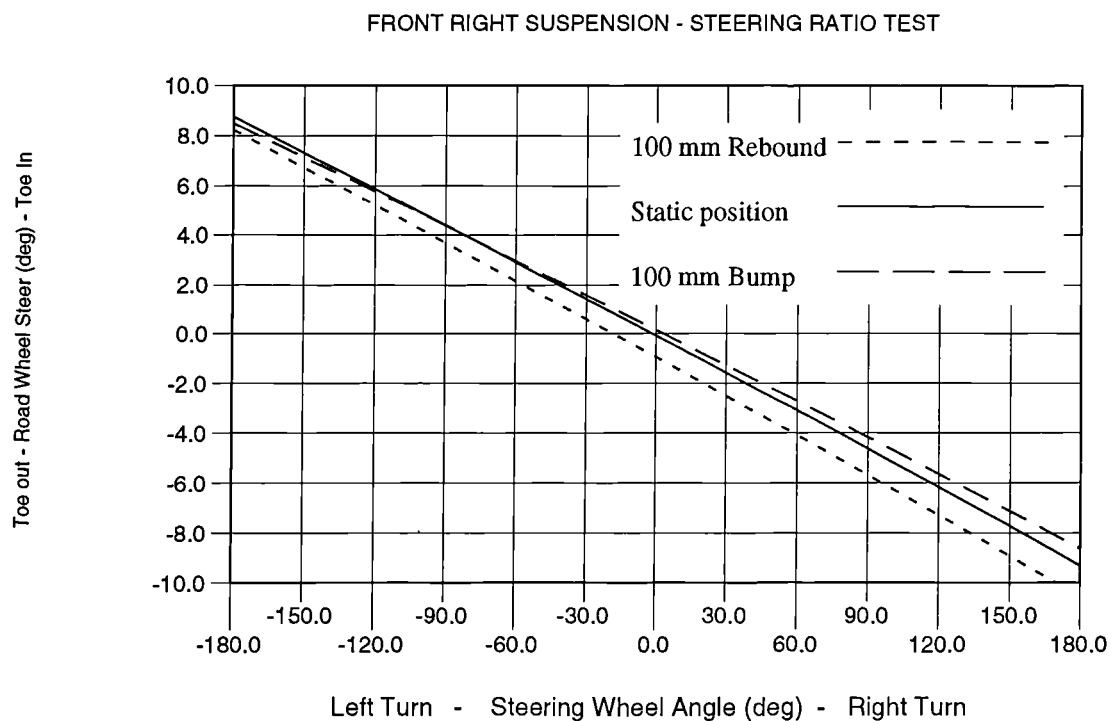
Figure 5.27 Results of steering ratio test for ADAMS front right suspension model

The lines plotted are reasonably linear but the bump and rebound results indicate an offset from the normal static position due to the bump steer effect. A more detailed analysis of the results is available in Table 5.3 where for each increment in steer angle the road wheel angle has been computed and the ratio between the two calculated.

Table 5.3 Relationship between steering column rotation and road wheel angle

Steering Wheel Angle (Degrees)	Normal Static		100 mm Bump		100 mm Rebound	
	Toe Angle (Degrees)	Ratio	Toe Angle (Degrees)	Ratio	Toe Angle (Degrees)	Ratio
-180	8.76855	20.5279	8.50155	21.1726	8.23804	21.8499
-160	7.79887	20.5158	7.58745	21.0875	7.23006	22.1298
-140	6.82707	20.5066	6.67076	20.9871	6.22003	22.5079
-120	5.85285	20.5028	5.75122	20.8651	5.20761	23.0432
-100	4.87588	20.5091	4.82854	20.7102	4.19242	23.8525
-80	3.89582	20.5348	3.90240	20.5002	3.17410	25.2040
-60	2.91233	20.6021	2.97249	20.1851	2.15224	27.8779
-40	1.92502	20.7790	2.03848	19.6224	1.12642	35.5108
-20	0.93351	21.4245	1.10001	18.1816	0.09618	207.940
20	-1.06382	18.8002	-0.79181	25.2586	-1.97946	10.1038
40	-2.07054	19.3186	-1.74598	22.9098	-3.02591	13.2192
60	-3.08329	19.4597	-2.70623	22.1711	-4.07887	14.7100
80	-4.10260	19.4999	-3.67305	21.7803	-5.13896	15.5673
100	-5.12903	19.4969	-4.64693	21.5196	-6.20686	16.1112
120	-6.16321	19.4704	-5.62843	21.3203	-7.28327	16.4761
140	-7.20578	19.4289	-6.61812	21.1541	-8.36897	16.7285
160	-8.25746	19.3764	-7.61662	21.0067	-9.46483	16.9047
180	-9.31901	19.3154	-8.62462	20.8705	-10.5718	17.0265

The results in Table 5.5 show that for this vehicle the ratio between the steering column rotation and the toe angle change at the wheels does vary as the wheel moves between bump and rebound positions and is not symmetric for left or right lock. This is particularly noticeable in rebound at about -20 degrees of steering lock when the influence of the suspension geometry results in an angle at the road wheel of close to zero degrees and distorts the calculation of the ratio value. On the basis of the above and the measured test data a ratio of 20:1 has been used.

6.0 TYRE MODELLING

6.1 Introduction

The modelling of the forces acting at the contact patch between the tyre and the surface of the road can be considered to be one of the most complicated aspects of a multibody systems computer model which is developed for vehicle handling simulation. As mentioned earlier, it has been stated (2) that with the exception of aerodynamic effects the forces which dictate the motion of a typical vehicle are developed over the four tyre contact patches each of which has an area about the size of a man's hand. In fact if the tread pattern on the tyre and the texture of the road surface is taken into account then these small areas are reduced significantly further.

The modelling of the forces and moments at the tyre contact patch has been the subject of extensive research in recent years. A review of some of the most common models is given by Pacejka and Sharp in (72) where the authors stated that it is necessary to compromise between the accuracy and complexity of the model. This reflects one of the objectives undertaken in this thesis to compare a complex and relatively simple tyre model. The authors in (72) also state that the need for accuracy must be considered with reference to various factors including the manufacturing tolerances in tyre production and the effect of wear on the properties of the tyre. This would appear to be a very valid point not only from the consideration of computer modelling and simulation but also in terms of track testing where new tyres are used to establish levels of vehicle performance. A more realistic measurement of how a vehicle is going to perform in service may be to consider track testing with different levels of wear or incorrect pressure settings.

One of the methods discussed in (72) focuses on a multi-spoke model developed by Sharp where the tyre is considered to be a series of radial spokes fixed in a single plane and attached to the wheel hub. The spokes can deflect radially and bend both circumferentially and laterally. Sharp provides more details on the radial spoke model approach in (73-75). The other method of tyre modelling reviewed is based on the 'Magic Formula' (8-10) which will be discussed in more detail later in this section. Another review of tyre models is given by Pacejka

in (76) where the role of the tyre is discussed with regard to 'active' control of vehicle motion and the radial-spoke and 'Magic Formula' models are again discussed.

Before considering tyre models in more detail it should be stated that tyre models are generally developed according to the type of application the vehicle simulation will address. For ride and vibration studies the tyre model is often required to transmit the effects from a road surface where the inputs are small but of high frequency. In the most simple form for this work the tyre may be represented as a simple spring and damper acting between the wheel centre and the surface of the road. The simulation may in fact recreate the physical testing using a four poster test rig with varying vertical inputs at each wheel. A concept of the tyre model for this type of simulation is provided in Figure 6.1. where for clarity only the right side of the vehicle is shown.

Translational motion inputs to represent road surface irregularities

Simple spring damper tyre model
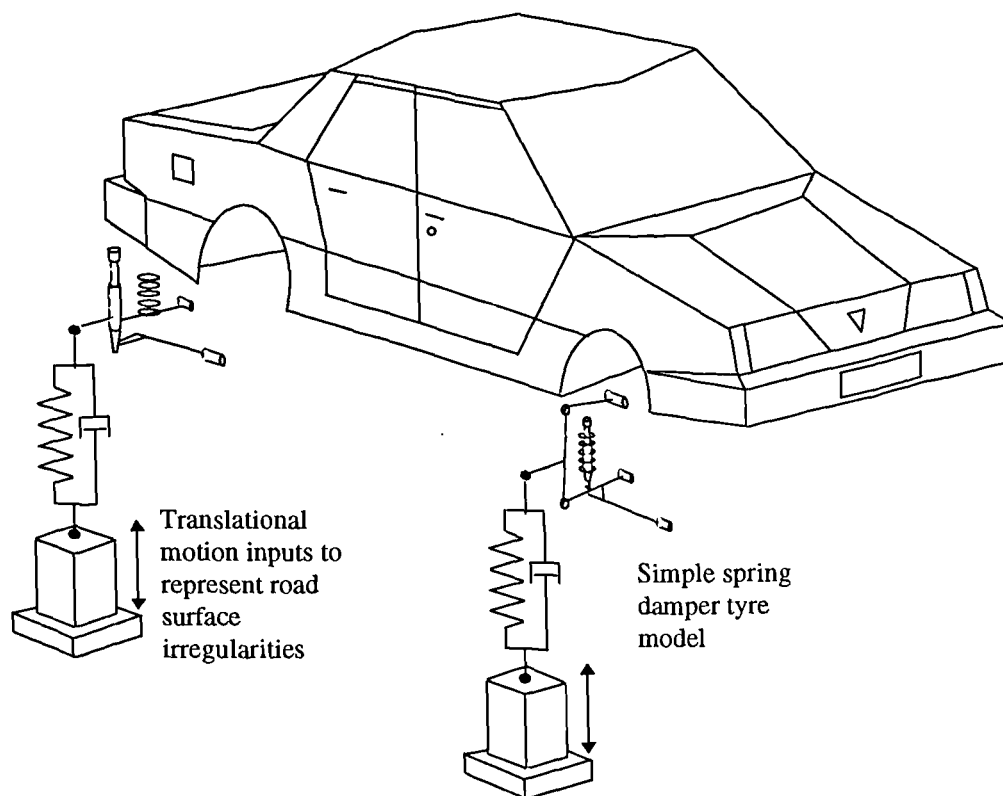
Figure 6.1 A simple tyre model for ride and vibration studies

In suspension loading or durability studies the tyre model must accurately represent the contact forces generated when the tyre strikes obstacles such as potholes and road bumps. In these applications the deformation of the tyre as it contacts the obstacle is of importance and is a factor in developing the model. These sort of tyre models are often developed for agricultural or construction type vehicles used in an off road environment and dependent on the tyre to a larger extent in isolating the driver from the terrain surface inputs. An example of this sort of tyre model is described in (77) where a radial spring model was developed to envelop irregular features of a rigid terrain. The tyre is considered to be a set of equally spaced radial springs which when in contact with the ground will provide a deformed profile of the tyre as it envelops the obstacle. The deformed shape is used to redefine the rigid terrain with an "equivalent ground plane". The concept of an equivalent ground plane model was used in the early ADAMS/Tire model (78) for the durability application but has the main limitation that the model is not suitable for very small obstacles which the tyre might completely envelop. This is clarified in (77) where it is stated that the wave length of surface variations in the path of the tire should be at least three times the length of the tyre to ground contact patch. The other and most basic limitation of this type of model is that the simulation is restricted to straight line motion and would only consider the vertical and longitudinal forces being generated by the terrain profile. An example of a radial spring tyre model is shown in Figure 6.2.
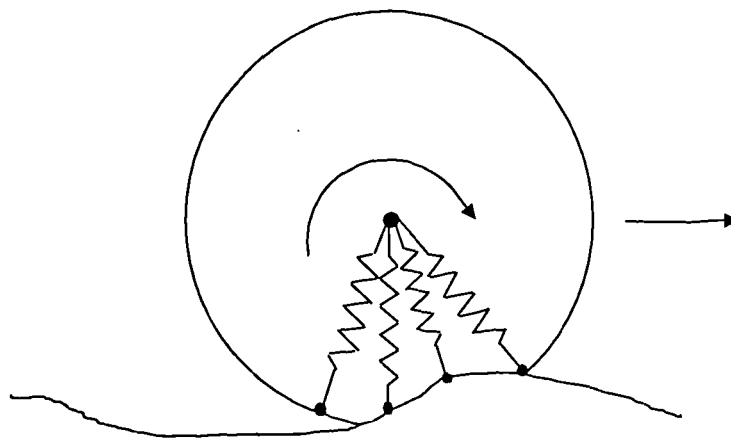
Figure 6.2 A radial spring terrain enveloping tyre model

The work carried out in (79) describes how two different programs have been interfaced to carry out a vehicle simulation where the interaction between the tyre and the road surface has been calculated using an advanced non-linear finite element analysis program. The technology used to model the tyre with finite elements is similar to that used to carry out a finite element analysis for a crash study involving an air bag.

For vehicle handling studies of the type studied here we are considering the manoeuvring of the vehicle on a flat road surface. The function of the tyre model is to establish the forces and moments occurring at the tyre to road contact patch and resolve these to the wheel centre and hence into the vehicle as indicated in Figure 6.3.
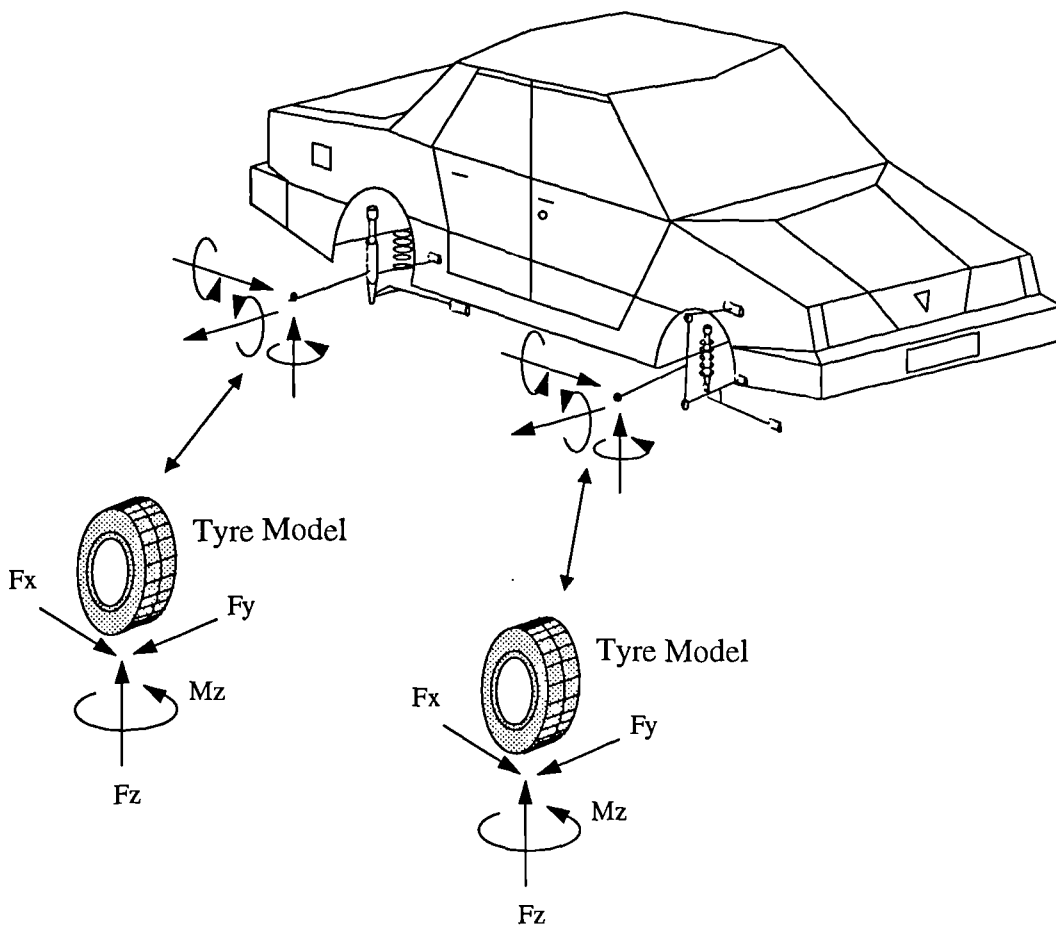
Figure 6.3 Interaction between vehicle model and tyre model

For each tyre the tyre model will calculate the three orthogonal forces and the three orthogonal moments which result from the conditions arising at the tyre to road surface contact patch. These forces and moments are applied at each wheel centre and control the motion of the vehicle. In terms of modelling the vehicle is actually 'floating' along under the action of these forces at each corner. For a handling model the forces and moment at the tyre to road contact patch which are usually calculated by the tyre model are:

(a) F_x - longitudinal tractive or braking force

(b) F_y - lateral cornering force

(c) F_z - vertical normal force

(d) M_z - aligning moment

The other two moments which occur at the patch, M_x the overturning moment and M_y the rolling resistance moment are generally not significant for a handling tyre model. The calculation of the these forces and moments at the contact patch is the essence of a tyre model and will be discussed in more detail later.

As a simulation progresses and the equations for the vehicle and tyre are solved at each solution point in time there is a flow of information between the vehicle model and the tyre model. The tyre model must continually receive information about the position, orientation and velocity at each wheel centre and also the topography of the road surface in order to calculate the forces and moment at the contact patch. The road surface is usually flat but may well have changing frictional characteristics to represent varying surface textures or changes between dry, wet or ice conditions. The information from the wheel centre such as the height, camber angle, slip angle, spin velocity and so on are the inputs to the tyre model at each point in time and will dictate the calculation of the new set of forces at the contact patch.

These newly computed tyre conditions are then fed back the vehicle model at each wheel centre. This will produce a change in the vehicle position at the next solution point in time. The conditions at each wheel centre will change and will be relayed back to the tyre model again. A new set of tyre forces and moment will then be calculated and so the process will continue.

6.2 Interpolation models

Early tyre models such as the initial ADAMS/Tire model (78) used the results of laboratory rig testing directly to generate 'look up' tables of data which were used directly by the tyre model to interpolate the lateral force and aligning moment at the contact patch. Figure 6.4. illustrates a sample of some results which might typically be obtained from a tyre rig test where for variations in vertical load F_z the lateral forces F_y are plotted as a function of changes in positive slip angle and the camber angle is zero.

Lateral Force Measurements

Fy (N)

Camber Angle = 0

Fz = 8 kN
Fz = 6 kN
Fz = 4 kN
Fz = 2 kN

Slip Angle (degrees)
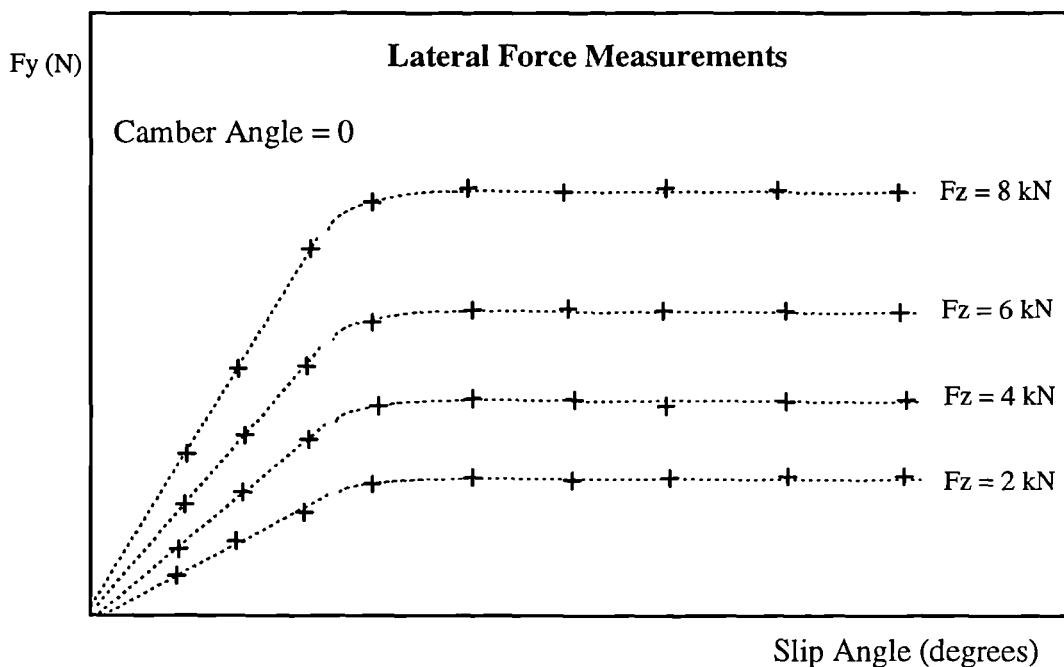
Figure 6.4 Interpolation of measured tyre test data

For this set of data the independent variables which are set during the test are the camber angle, the vertical force, and the slip angle. The measured dependent variable is the lateral force. Using this measured data the tyre model uses the curve fit to obtain a value for the lateral force for the value of Fz and slip angle determined by the wheel centre position and orientation. If the instantaneous camber angle lies between two sets of measured data at different camber angles set during the test then the tyre model can use linear interpolation

between the two camber angles. If the instantaneous camber angle is for example 2.4 degrees and measured data is available at 2 and 3 degrees, then the curve fitting as a function of Fz and slip angle is carried out at the two bounding camber angles and the linear interpolation is carried out between these two points. The approach described here for lateral force is applied in exactly the same manner when determining by interpolation a value for the aligning moment. The data for an interpolation model is contained in a separate tyre data file. There are some disadvantages in using an interpolation tyre model:

(i) The process of interpolating large quantities of data at every integration step in time may not be an efficient simulation approach and is often considered to result in increases in computer solution times for the analysis of any given manoeuvre.

(ii) This sort of model does not lend itself to any design modification or optimisation involving the tyre. The tyre must already exist and have been tested. In order to investigate the influence of tyre design changes on vehicle handling and stability then the tyre model must be reduced to parameters which can be related to the tyre force and moment characteristics. This has lead to the development of tyre models represented by formulae which will now be discussed.

6.3 The "Magic Formula" tyre model

The tyre model which is now most well established and has generally gained favour is based on the work by Pacejka and is often referred to as the "Magic Formula" (8-10). The "Magic Formula" is not a predictive tyre model but is used to represent the tyre force and moment curves and is undergoing continual development. The early version (8,9) is sometimes referred to as the "Monte Carlo version" due to the conference location (9) at which this model was presented. The tyre models discussed here are based on the formulations described in (9) and that in (10) which was referred to as Version 3 of the "Magic Formula". Other authors have developed systems based around the "Magic Formula". The BNPS model (80) is a particular version of the "Magic Formula" that automates the development of the coefficients working from measured test data. The model name BNPS is in honour of Messrs. Baker, Nyborg and Pacejka who originated the "Magic Formula" and the S indicates the particular implementation

developed by Smithers Scientific Services Inc. This particular tyre model was also introduced in ADAMS Version 8.0 where it was simply referred to as the "Smithers" model.

In the original "Magic Formula" paper the authors in (8) discuss the use of formulae to represent the force and moment curves using established techniques based on polynomials or Fourier series. The main disadvantage with this approach is that the coefficients used have no engineering significance in terms of the tyre properties and as with interpolation methods the model would not lend itself to design activities. This is also reflected in (81) where the author describes a representation based on polynomials where the curves are divided into five regions but this still has the problem of using coefficients which do not typify the tyre force and moment characteristics.

The general acceptance of the "Magic Formula" is reinforced by the work carried out at Michelin and described in (82). In this paper the authors describe how the 'Magic Formula' has been tested at Michelin and 'industrialised' as a self-contained package for the pure lateral model which is the level of modelling investigated in this thesis. The authors in (82) also considered modifications to the "Magic Formula" to deal with the complicated situation of combined slip.

The "Magic Formula" model is undergoing continual development which is reflected in a recent publication (83) where the model is not restricted to small values of slip and the wheel may also run backwards. The authors also discuss a relatively simple model for longitudinal and lateral transient responses restricted to relatively low time and path frequencies. The tyre model in this paper has also acquired a new name and is referred to as the 'Delft Tyre 97' version.

The "Magic Formula" has been developed using mathematical functions which relate:

(i) The lateral force F_y as a function of slip angle α.

(ii) The aligning moment M_z as a function of slip angle α.

(iii) The longitudinal force F_x as a function of longitudinal slip κ.

When these curves are obtained from steady state tyre testing and plotted the general shape of the curves is similar to that indicated in Figure 6.5. It is important to note that the data used to generate the tyre model is obtained from steady state testing. The lateral force F_y and the aligning moment M_z are measured during pure cornering, i.e. cornering without braking, and the longitudinal braking force during pure braking, i.e. braking without cornering.
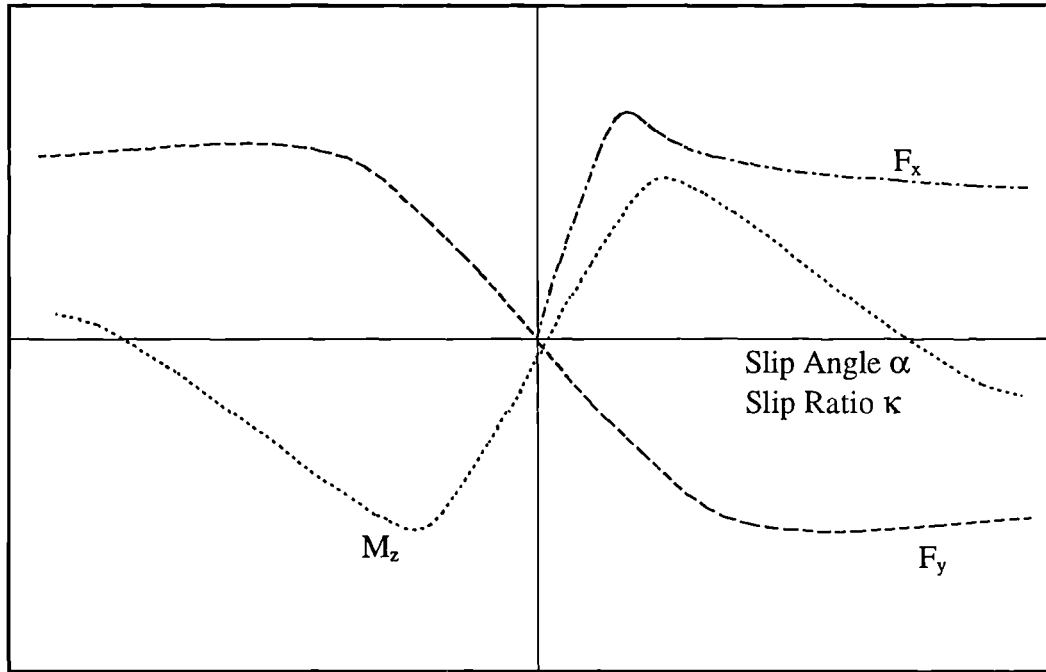
Figure 6.5 Typical form of tyre force and moment curves from steady state testing

The basis of this model is that tyre force and moment curves obtained under pure slip conditions and shown in Figure 6.5 look like sine functions which have been modified by introducing an arctangent function to "stretch" the slip values on the x-axis.

The general form of the model as presented in (10) is:

$$y(x) = D \sin [\, C \arctan\{ \, Bx - E \, (\, Bx - \arctan (\, Bx \,)) \}]$$

where

$$Y(X) = y(x) + S_v$$

$$x = X + S_h$$

$$S_h = \text{horizontal shift}$$

$$S_v = \text{vertical shift}$$

120

In this case Y is either the side force F_y, the aligning moment M_Z or the longitudinal force F_X and X is either the slip angle α or the longitudinal slip κ. The physical significance of the coefficients in the formula become more meaningful when considering Figure 6.6.
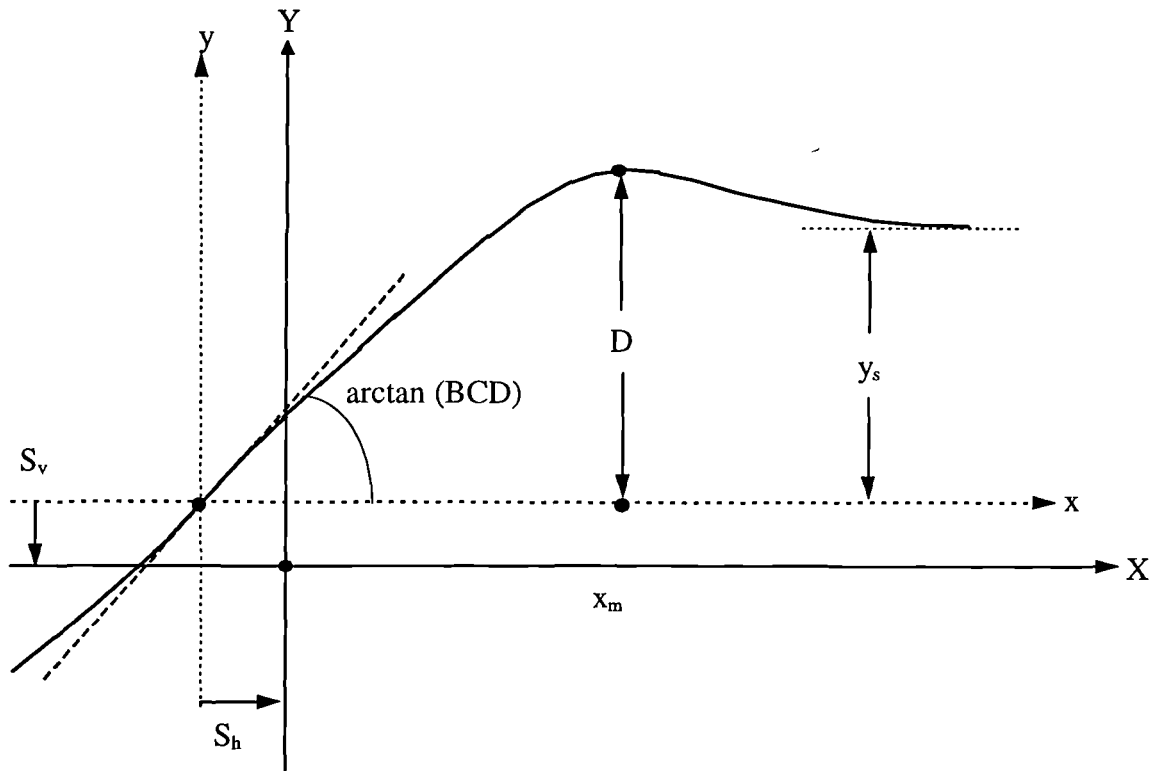
Figure 6.6 Coefficients used in the "Magic Formula" tyre

For lateral force or aligning moment the offsets S_v and S_h arise due to adding camber or physical features in the tyre such as conicity and ply steer. For the longitudinal braking force this is due to rolling resistance.

Working from the offset xy axis system the main coefficients are:

D - is the peak value.

C - is a shape factor that controls the "stretching" in the x direction. The value is determined by whether the curve represents lateral force, aligning moment, or longitudinal braking force. These values can be taken as the constants given in (10):

1.30 - lateral force curve.

1.65 - longitudinal braking force curve.

2.40 - aligning moment curve.

B - is referred to as a "stiffness" factor. From Figure 6.6 it can be seen that BCD is the slope at the origin, i.e. the cornering stiffness when plotting lateral force. Obtaining values for D and C leads to a value for B.

E - is a "curvature" factor which effects the transition in the curve and the position x_m at which the peak value if present occurs. E is calculated using:

$$E = \frac{Bx_m - \tan(\pi/2C)}{Bx_m - \arctan(Bx_m)}$$

y_s - is the asymptotic value at large slip values and is found using:

$$y_s = D \sin(\pi C / 2)$$

The curvature factor E can be made dependent on the sign of the slip value plotted on the x-axis.

$$E = E_0 + \Delta E \, \text{sgn}(x)$$

This will allow for the lack of symmetry between the right and left side of the diagram when comparing tractive and braking forces or to introduce the effects of camber angle γ. This effect is illustrated in (10) by the generation of an asymmetric curve using coefficients C = 1.6, E_O = 0.5 and ΔE = 0.5. This is recreated here using the curve shape illustrated in Figure 6.7. Note that the plots have been made non-dimensional by plotting y/D on the y-axis and BCx on the x-axis.
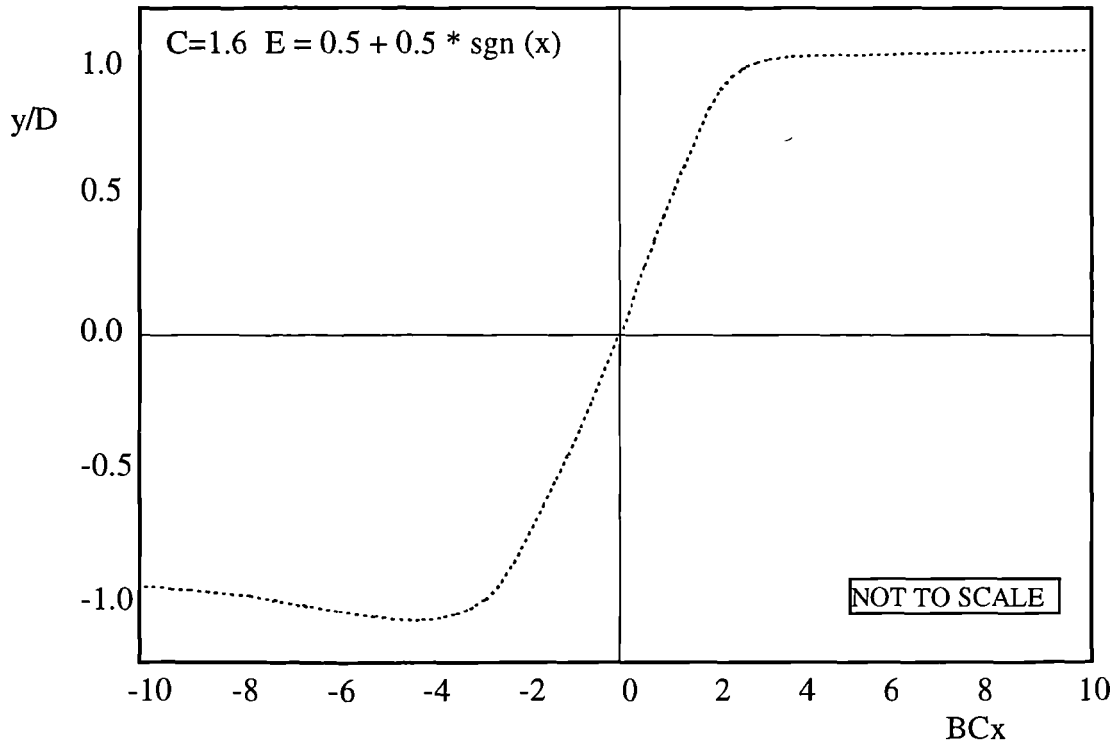
Figure 6.7 Generation of an asymmetric curve

At zero camber the cornering stiffness BCD_y reaches a maximum value defined by the coefficient a_3 at a given value of vertical load F_z which equates to the coefficient a_4. This relationship is illustrated in Figure 6.8 where the slope at zero vertical load is taken as $2a_3/a_4$. This model has been extended to deal with the combined slip situation where braking and cornering occur simultaneously. This complex situation is not covered here where the modelling is concerned only with the pure slip situation. A detailed account of the combined slip model is given in (10). The equations for pure slip only and as developed for the Monte Carlo model (9) are summarised in Table 6.1 and similarly for Version 3 (10) in Table 6.2. As can be seen a large number of parameters are involved and great care is needed to avoid confusion between each version.
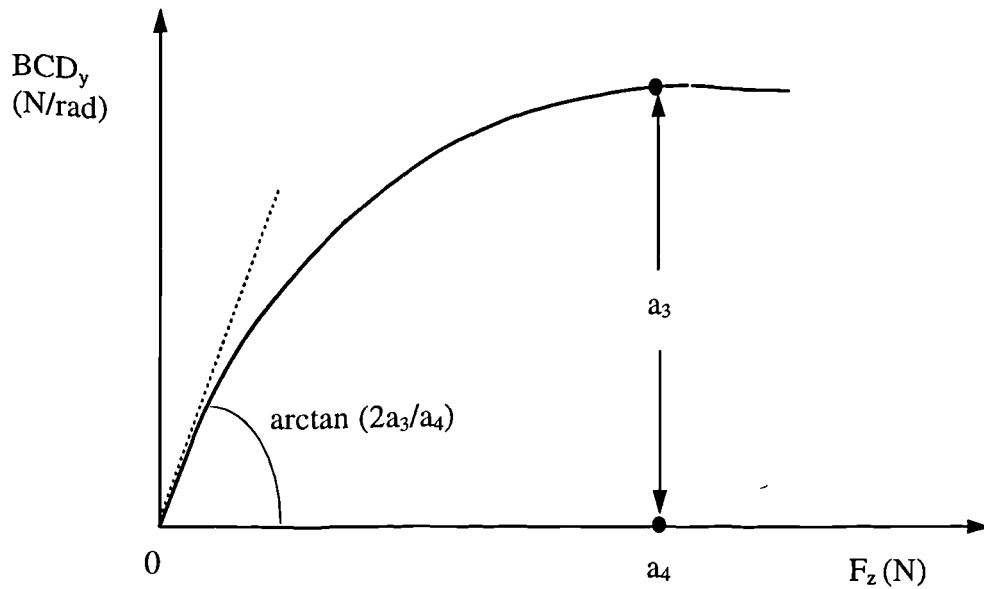
Figure 6.8 Cornering stiffness as a function of vertical load at zero camber angle

Apart from implementing the model into a multibody systems analysis program for vehicle simulation some method is needed to obtain the coefficients from raw test data. In (84) a suggested approach is to use an appreciation of the properties of the "Magic Formula" is to fix C based on the values suggested in (10) for lateral force, longitudinal force and aligning moment. For each set of load data it is then possible to obtain the peak value D and the position at which this occurs x_m. Using the slope at the origin and the values for C and D it is now possible to determine the stiffness factor B and hence obtain a value for E. Having obtained these terms at each load the various coefficients are determined using curve fitting techniques to express B, C, D and E as functions of load. An issue which occurs when deriving the coefficients for this model is whether those which have physical significance should be fixed to match the tyre or set to values which give the best curve fit.

The authors in (85) describe their work using measured data and software developed at the TNO Road-Vehicles Research Institute to apply a regression method and obtain the coefficients. The authors in (80) have also automated the process for the BNPS version of the model. Comparisons of output from the "Magic Formula" with measured test data (8-10) indicate good correlation. A study in (86) comparing the results of this model with those obtained from vehicle testing under pure slip conditions also indicates the high degree of accuracy which can be obtained using this tyre model.

Table 6.1 Pure slip equations for the "Magic Formula" tyre model (Monte Carlo Version)

General Formula

$y(x)=D\sin[C\arctan\{Bx-E(Bx-\arctan(Bx))\}]$

$Y(X) = y(x) + S_v$

$x = X + S_h$

B = stiffness factor

C = shape factor

D = peak factor

S_h = horizontal shift

S_h = vertical shift

$B = dy/dx_{(x=0)} / CD$

$C = (2/\pi) \arcsin (y_s/D)$

$D = ymax$

$E = (Bx_m-\tan(\pi/2C))/(Bx_m - \arctan (Bx_m))$

Longitudinal Force

$X_x = \kappa$

$Y_x = F_x$

$D_x = \mu_x F_z$

$\mu_x = b_1F_z + b_2$

$BCD_x = (b_3 F_z^2 + b_4F_z) \exp(-b_5F_z)$

$C_x = b_0$

$E_x = b_6F_z^2 + b_7F_z + b_8$

$B_x = BCD_x / C_xD_x$

$S_{hx} = b_9F_z + b_{10}$

$S_{vy} = 0$

Lateral Force

$X_y = \alpha$

$Y_y = F_y$

$D_y = \mu_y F_z$

$\mu_y = a_1F_z + a_2$

$BCD_y = a_3 \sin(2 \arctan(F_z/a_4)) (1 - a_5|\gamma|)$

$C_y = a_0$

$E_y = a_6F_z+a_7$

$B_y = BCD_y / C_yD_y$

$S_{hy} = a_8 \gamma + a_9 F_z + a_{10}$

$S_{vy} = a_{11}F_z \gamma + a_{12} F_z + a_{13}$

Aligning Moment

$X_z = \alpha$

$Y_z = M_z$

$D_z = c_1F_z^2 + c_2F_z$

$BCD_z = (c_3F_z^2+c_4F_z)(1-c_6|\gamma|) \exp (-c_5F_z)$

$C_z = c_0$

$E_z = (c_7F_z^2 + c_8F_z + c_9) (1 - c_{10}|\gamma|)$

$B_z = BCD_z / C_zD_z$

$S_{hz} = c_{11} \gamma + c_{12} F_z + c_{13}$

$S_{vz} = (c_{14}F_z^2 + c_{15}F_z)\gamma + c_{16}F_z + c_{17}$

Table 6.2 Pure slip equations for the "Magic Formula" tyre model (Version 3)

General Formula

$y(x)=D\sin[C\arctan\{Bx-E(Bx-\arctan(Bx))\}]$

$Y(X) = y(x) + S_v$

$x = X + S_h$

B = stiffness factor

C = shape factor

D = peak factor

S_h = horizontal shift

S_h = vertical shift

$B = dy/dx_{(x=0)} / CD$

$C = (2/\pi) \arcsin (y_s/D)$

$D = y_{max}$

$E = (Bx_m - \tan(\pi/2C))/(Bx_m - \arctan (Bx_m))$

Longitudinal Force

$X_x = \kappa$

$Y_x = F_x$

$D_x = \mu_x F_z$

$\mu_x = b_1 F_z + b_2$

$BCD_x = (b_3 F_z^2 + b_4 F_z) \exp(-b_5 F_z)$

$C_x = b_0$

$E_x = (b_6 F_z^2 + b_7 F_z + b_8)(1-b_{13}\text{sgn}(\kappa + S_{hx}))$

$B_x = BCD_x / C_x D_x$

$S_{hx} = b_9 F_z + b_{10}$

$S_{vy} = b_{11} F_z + b_{12}$

Brake force only ($b_{11} = b_{12} = b_{13} = 0$)

Lateral Force

$X_y = \alpha$

$Y_y = F_y$

$D_y = \mu_y F_z$

$\mu_y = (a_1 F_z + a_2) (1 - a_{15} \gamma^2)$

$BCD_y = a_3 \sin(2 \arctan(F_z/a_4)) (1 - a_5| \gamma |)$

$C_y = a_0$

$E_y = (a_6 F_z + a_7)(1 - (a_{16}\gamma + a_{17})\text{sgn}(\alpha + S_{hy}))$

$B_y = BCD_y / C_y D_y$

$S_{hy} = a_8 F_z + a_9 + a_{10}\gamma$

$S_{vy} = a_{11} F_z + a_{12} + (a_{13} F_z^2 + a_{14} F_z)\gamma$

Aligning Moment

$X_z = \alpha$

$Y_z = M_z$

$D_z = (c_1 F_z^2 + c_2 F_z) (1 - c_{18}\gamma^2)$

$BCD_z = (c_3 F_z^2 + c_4 F_z)(1-c_6| \gamma |) \exp (-c_5 F_z)$

$C_z = c_0$

$E_z = (c_7 F_z^2 + c_8 F_z + c_9) (1 - (c_{19}\gamma + c_{20})*$

$\quad\quad *\text{sgn}(\alpha + S_{hz})) / (1 - c_{10}| \gamma |)$

$B_z = BCD_z / C_z D_z$

$S_{hz} = c_{11} F_z + c_{12} + c_{13}\gamma$

$S_{vz} = c_{14} F_z + c_{15} + (c_{16} F_z^2 + c_{17} F_z)\gamma$

6.4 The Fiala tyre model

6.4.1 Input parameters

The Fiala tyre model was developed in (11) and has been adapted as a standard tyre model supplied with the ADAMS program (12). This model has the advantage that it only requires ten input parameters and that these are directly related to the physical properties of the tyre. The input parameters are shown in Table 6.3

Table 6.3 Fiala tyre model input parameters

R_1 - The unloaded tyre radius (units - length)

R_2 - The tyre carcass radius (units - length)

k_z - The tyre radial stiffness (units - force/length)

C_s - The longitudinal tyre stiffness. This is the slope at the origin of the braking force F_x when plotted against slip ratio (units - force)

C_α - Lateral tyre stiffness due to slip angle. This is the cornering stiffness or the slope at the origin of the lateral force F_y when plotted against slip angle α (units - force / radians)

C_γ - Lateral tyre stiffness due to camber angle. This is the cornering stiffness or the slope at the origin of the lateral force F_y when plotted against camber angle γ (units - force / radians)

C_r - The rolling resistant moment coefficient which when multiplied by the vertical force F_z produces the rolling resistance moment M_y (units - length)

ζ - The radial damping ratio. The ratio of the tyre damping to critical damping. A value of zero indicates no damping and a value of one indicates critical damping (dimensionless)

μ_0 - The tyre to road coefficient of "static" friction. This is the y intercept on the friction coefficient versus slip graph

μ_1 - The tyre to road coefficient of "sliding" friction occurring at 100% slip with pure sliding

127

In fact the parameters R_1, R_2, k_z, ζ, are all used to formulate the vertical load in the tyre and are required for all tyre models that are used, including the Pacejka and Interpolation models. The Fiala model also ignores camber so the coefficient which defines lateral stiffness due to camber angle, C_γ, is not used. In this study the rolling resistance has also been ignored so the C_r coefficient is set to zero. This means that the generation of longitudinal forces, lateral forces and aligning moments with the Fiala model can be controlled using just 4 parameters (C_s, C_α, μ_0 and μ_1).

6.4.2 Tyre geometry and kinematics

The tyre is modelled using the input radii R_1 and R_2 as shown in Figure 6.9.
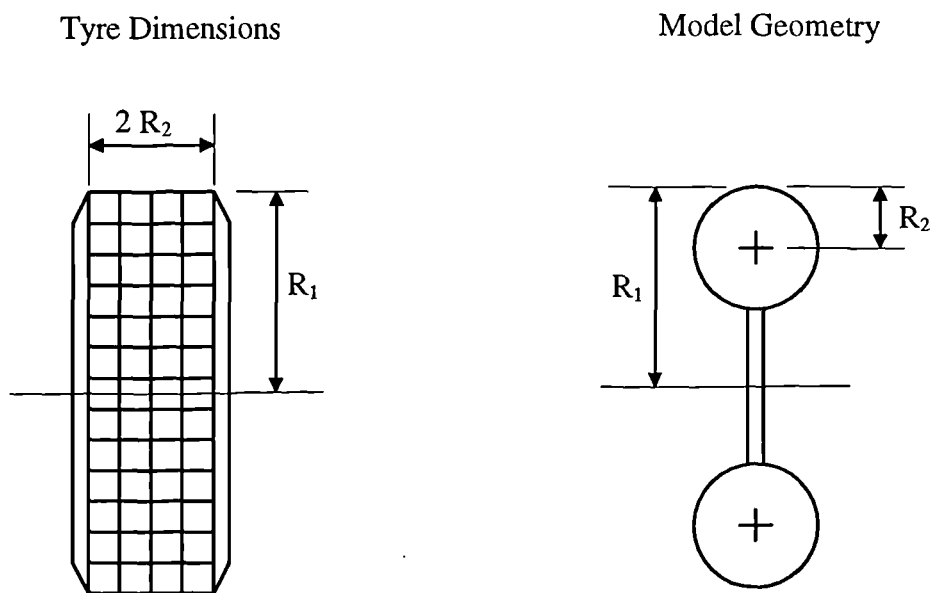
Figure 6.9 ADAMS/Tire model geometry

Using the tyre model geometry based on a torus it is possible to determine the geometric outputs which are used in the subsequent force and moment calculations. Consider first the view in Figure 6.10 looking along the wheel plane at the tyre inclined on a flat road surface.
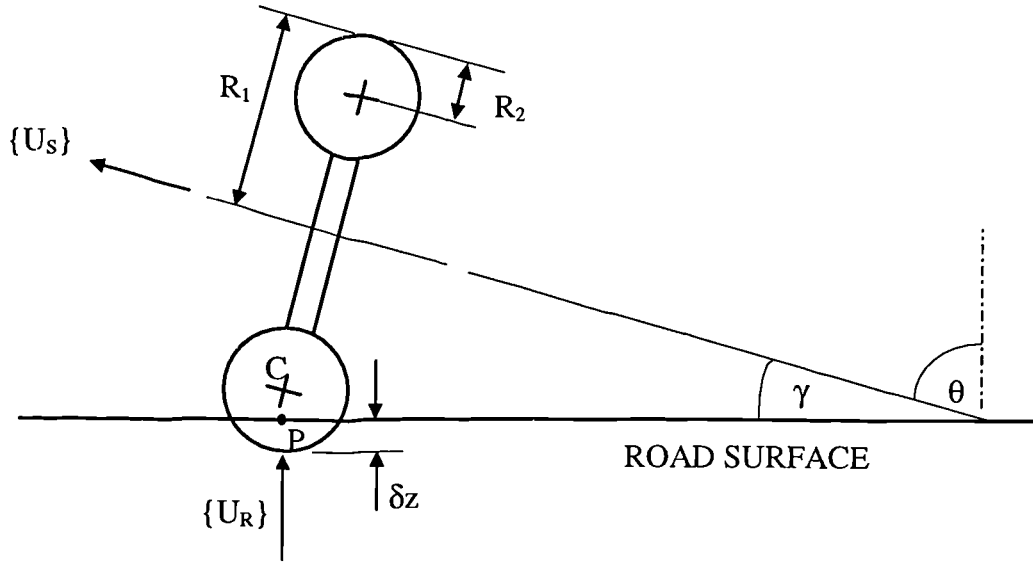
Figure 6.10 Definition of geometric terms in ADAMS/Tire

The vector $\{U_s\}$ is a unit vector acting along the spin axis of the tyre. The vector $\{U_r\}$ is a unit vector which is normal to the road surface and points towards the centre of the tyre carcass at C. The contact point P between the tire and the surface of the road is determined as the point at which the vector $\{U_r\}$ intersects the road surface. For the purposes of this document it is assumed the road is flat and only one point of contact occurs.

The camber angle γ between the wheel plane and the surface of the road is calculated using:

$$\gamma = \pi/2 - \theta$$

where

$$\theta = \cos^{-1}(\{U_r\} \bullet \{U_s\})$$

The vertical penetration of the tyre δz at point P is given by:

$$\delta z = R_2 - |CP|$$

In order to calculate the tyre forces and moment it is also necessary to determine the velocities occurring in the tyre. In Figure 6.11 the SAE coordinate system (87) is introduced at the contact point P. This is established by the three unit vectors $\{X_{sae}\}_1$, $\{Y_{sae}\}_1$ and $\{Z_{sae}\}_1$.

129

Note that the subscript 1 indicates that the components of a vector are resolved parallel to reference frame 1 which in this case is the Ground Reference Frame (GRF).
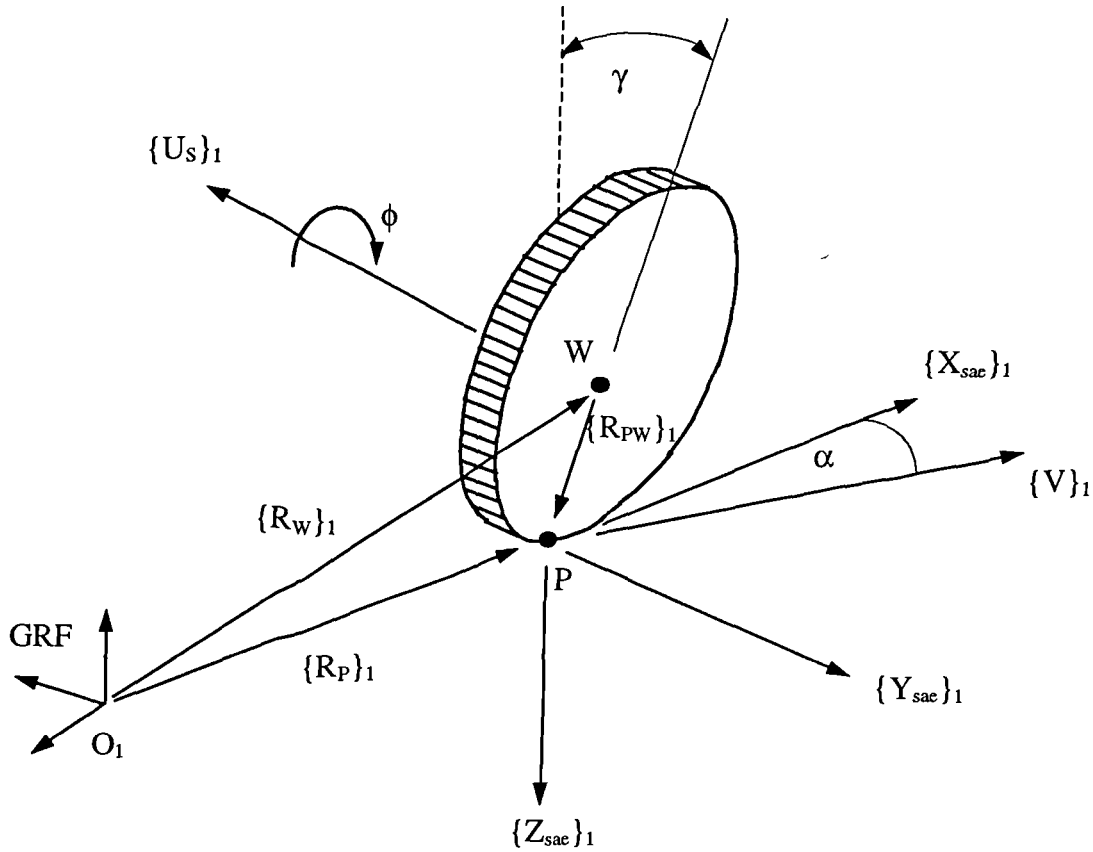
Figure 6.11 Tyre geometry and kinematics

Using the triangle law of vector addition it is possible to locate the contact point P relative to the fixed Ground Reference Frame O_1 :

$$\{R_P\}_1 = \{R_W\}_1 + \{R_{PW}\}_1$$

If the angular velocity vector of the wheel is denoted by $\{\omega\}_1$ then the velocity $\{V_P\}_1$ of point P is given by:

$$\{V_P\}_1 = \{V_W\}_1 + \{V_{PW}\}_1$$

130

where

$$\{V_{PW}\}_1 \ = \ \{\omega\}_1 \times \{R_{PW}\}_1$$

It is now possible to determine the components of $\{V_P\}_1$ which act parallel to the SAE coordinate system superimposed at P. The longitudinal slip velocity V_{XC} of point P is given by:

$$V_{XC} = \ \{V_P\}_1 \bullet \{X_{sae}\}_1$$

The lateral slip velocity V_Y of point P is given by:

$$V_Y = \ \{V_P\}_1 \bullet \{Y_{sae}\}_1$$

The vertical velocity V_Z at point P which will be used to calculate the damping force in the tyre is given by:

$$V_Z = \ \{V_P\}_1 \bullet \{Z_{sae}\}_1$$

Considering the angular velocity vector of the wheel $\{\omega\}_1$ in more detail we can consider it to be developed as follows. The wheel develops a slip angle α which is measured about $\{Z_{sae}\}_1$, a camber angle γ which is measured about $\{X_{sae}\}_1$ and a spin angle ϕ which is measured about $\{U_S\}_1$. The total angular velocity vector of the wheel is the summation of all three motions and is given by:

$$\{\omega\}_1 = \ \dot{\alpha}\{Z_{sae}\}_1 + \ \dot{\gamma}\{X_{sae}\}_1 + \dot{\phi}\{U_S\}_1$$

It is possible to consider an angular velocity vector $\{\omega_S\}_1$ which only considers the spinning motion of the wheel and does not contain the contributions due to α and γ. This vector for angular velocity which only considers spin is given by:

$$\{\omega_S\}_1 = \ \dot{\phi}\{U_S\}_1$$

The Fiala tyre model considers the lateral slip of the contact patch relative to the road due to the slip angle α. The slip angle α is defined as:

$$\alpha = \tan{-1} \{V_Y/V_X\}$$

A lateral slip ratio S_α is computed as:

$$S_\alpha = |\tan \alpha| = |V_Y/V_X|$$

During cornering S_α will have a value of zero when V_Y is zero and can have a maximum value of 1.0 which equates to a slip angle α of 45 degrees.

6.4.3 Force calculations

The calculation of the vertical force F_z acting at point P in the tyre contact patch has a contribution due to stiffness F_{zk} and a contribution due to damping F_{zc}. These forces act in the direction of the $\{Z_{SAE}\}_1$ vector shown in Figure 6.11 and are hence specified as negative to indicate that the forces actually act upwards.

$$F_z = F_{zk} + F_{zc}$$
$$F_{zk} = -k_z \, \delta z$$
$$F_{zc} = -c_z \, V_Z$$

where

$$c_z = 2.0 \, \zeta \sqrt{m_t \, k_z}$$

m_t = mass of tyre

k_z = radial tyre stiffness

ζ = radial damping ratio

The instantaneous value of the tyre to road friction coefficient μ is obtained by linear interpolation:

$$\mu = \mu_0 - S_\alpha (\mu_0 - \mu_1)$$
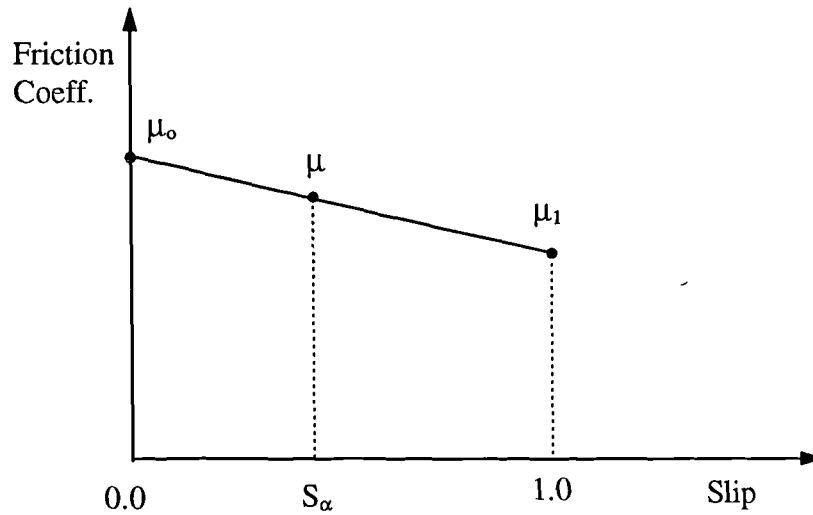
Figure 6.12 Linear tyre to road friction model

For the lateral force a critical slip angle α^* is calculated using:

$$\alpha^* = \tan^{-1} | 3 \mu F_z / C_\alpha |$$

If $| \alpha |$ is less than α^* then the tyre is considered to be in a state of elastic deformation and:

$$H = 1 - C_\alpha | \tan \alpha | / 3 \mu | F_z |$$

$$F_y = - \mu | F_z | (1 - H^3) \, sgn \, (\alpha)$$

If $| \alpha |$ is greater than α^* then the tyre is considered to be sliding and:

$$F_y = - \mu | F_z | \, sgn \, (\alpha)$$

The rolling resistance moment M_y is given by:

$$M_y = -C_r F_z \quad \text{(forward motion)}$$

$$M_y = C_r F_z \quad \text{(backward motion)}$$

For the work here C_r has been set to zero.

133

For the aligning moment M_z if $|\alpha|$ is less than α^* (Elastic deformation state) then:

$$H = 1 - C_\alpha \mid \tan \alpha \mid / \, 3 \mid \mu \mid F_z \mid$$

$$M_z = 2 \mid \mu \mid F_z \mid R_2 \, (\, 1 - H \,) \, H^3 \, \text{sgn} \, (\alpha)$$

If $\mid \alpha \mid$ is greater than α^* (Complete sliding state) then:

$$M_z = 0.0$$

6.4.4 Road surface/terrain definition

The geometry and frictional characteristics of the road surface are defined in a separate file using a finite element approach as shown in Figure 6.13.
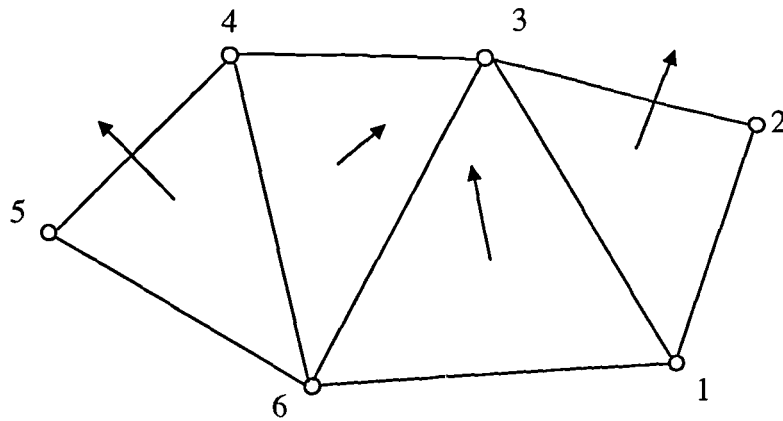
Figure 6.13 Definition of road surface for the Fiala tyre model

The road surface is defined as a system of triangular patches. As with finite elements the outward normal or road surface is defined by numbering the nodes for each element using a sequence which is positive when considering a rotation about the outward normal. For each element it is possible to define frictional constants μ_0 and μ_1 which are factored with the μ_0 and μ_1 parameters in the tyre property file. This would allow simulations when the vehicle encounters changing road conditions as with driving from dry to wet conditions.

6.5 Experimental tyre testing

6.5.1 Introduction

For the studies described in this report two tyres were used to provide the data for the comparisons. These are referred to as TYRE A and TYRE B.

TYRE A was the tyre fitted to the vehicle during the actual track testing, the results of which are used to correlate the models and simulations here. Rover were able to provide test data and parameters for the Monte Carlo version of the Pacejka model.

TYRE B was the DUNLOP D8 195/65 R15 provided by SP TYRES UK and tested as described in the following sections. The results of the tyre testing were used to extract the parameters for the Fiala tyre model and to generate the arrays for an Interpolation model. The parameters for the Pacejka model were provided by SP Tyres UK but did not include terms representing camber effects. A summary is given in Table 6.4 for both tyres indicating the source of information for the three separate modelling approaches.

Table 6.4 Source of tyre model data for TYRE A and TYRE B

MODEL/TYRE	TYRE A	TYRE B
Fiala	Extracted from test data	Extracted from test data
Pacejka	Provided by Rover	Provided by SP Tyres UK
Interpolation	Extracted from test data	Extracted from test data

6.5.2 Tyre testing at SP TYRES

In order to obtain the data needed for the tyre modelling investigations carried out in this thesis a series of tests were carried out with TYRE B using tyre testing facilities within the dynamics laboratory at SP Tyres UK Ltd. The tyre was tested using the High Speed Dynamics Machine which is illustrated in Figure 6.14. This machine is capable of generating speeds of up to 230 kph with a 2.39m diameter test drum and sophisticated hydraulic controls to measure the handling properties of tyres. The tyre testing was carried out at a speed of 20 kph and with an internal pressure of 2.0 bar.

Courtesy of SP TYRES UK Ltd.
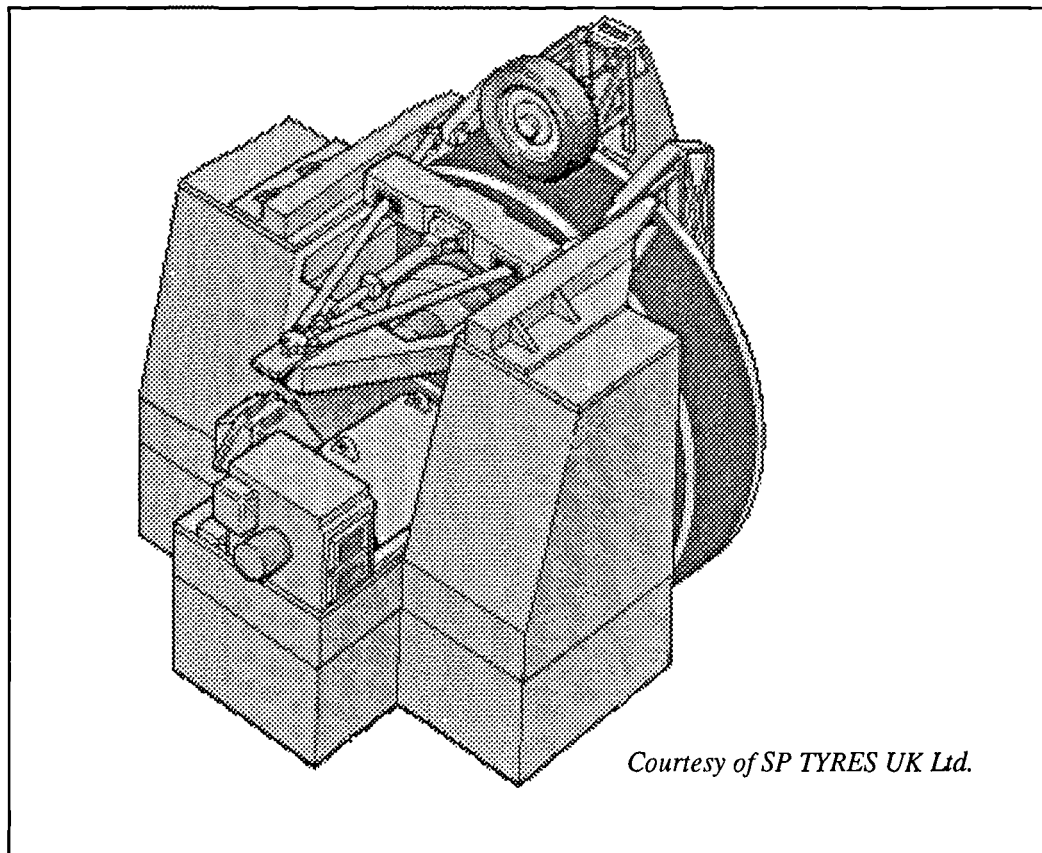
Figure 6.14 High Speed Dynamics Machine for tyre testing at SP TYRES UK Ltd.

The following tests were carried out and measurements of forces and moments were taken using the SAE coordinate system (87).

(i) Varying the vertical load in the tyre 200, 400, 600, 800 kg

(ii) For each increment of vertical load the camber angle was varied from -10 to 10 degrees with measurements taken at 2 degree intervals. During this test the slip angle was fixed at 0 degrees.

(iii) For each increment of vertical load the slip angle was varied from -10 to 10 degrees with measurements taken at 2 degree intervals. During this test the camber angle was fixed at 0 degrees. The results of the test have been plotted and are included in Appendix C. In summary the plots provided show:

(i) Lateral force Fy with slip angle α

(ii) Aligning moment Mz with slip angle α

(iii) Lateral force Fy with aligning moment Mz (Gough Plot)

(iv) Cornering stiffness with load

(v) Aligning stiffness with load

(vi) Lateral force Fy with camber angle γ

(vii) Aligning moment Mz with camber angle γ

(viii) Camber stiffness with load

(ix) Aligning camber stiffness with load

6.5.3 Tyre testing at Coventry University

Additional testing was carried out with TYRE B at Coventry University using the Flat Bed tyre test machine shown in Figure 6.15. The testing was carried out in order to measure the variation of braking force with slip ratio for vertical loads of 1, 2, 3, and 4kN. The measured data has been plotted and is shown in Figure C10.
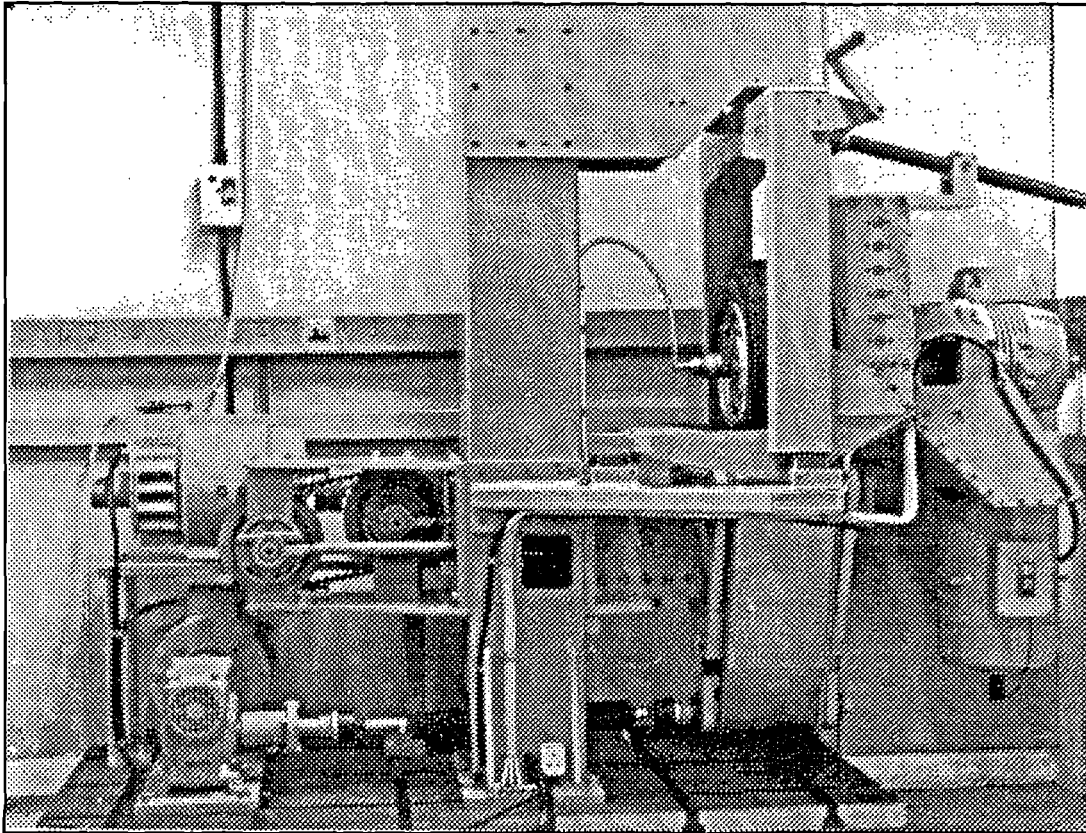
Figure 6.15 Flat Bed Tyre Test machine at Coventry University

The following tests were also carried out as a check against the tests carried out on the drum machine at SP Tyres UK Ltd.

(i) Varying the vertical load in the tyre 1kN, 2kN, 3kN, 4kN, 5kN, 6kN.

(ii) For each increment of vertical load the camber angle was varied from -6 to 6 degrees with measurements taken at 1 degree intervals. During this test the slip angle was fixed at 0 degrees.

(iii) For each increment of vertical load the slip angle was varied from -6 to 6 degrees with measurements taken at 1 degree intervals. During this test the camber angle was fixed at 0 degrees. The results of the test have been plotted using an interpolation tyre model and are included in Appendix E.

6.6 Tyre model data

6.6.1 Data for TYRE A

The data for TYRE A was supplied by Rover in the form of test data and parameters for the Pacejka tyre model. The data from the tests carried out on TYRE A has been used to extract the necessary lateral force and aligning moment values and to set these up in interpolation arrays. This has been achieved using the ADAMS spline statements as shown in Table 6.5. for the lateral force data and Table 6.6 for the aligning moment data. The numerical values set up in the spline statements have been reformatted from the tabular printed values which were written to computer files during the tyre testing. In each spline the X values correspond to either the slip or camber angle and are measured in degrees. The first value in each Y array corresponds to the vertical load measured in kg. The following values in the Y arrays are the measured lateral forces (N) or the aligning moments (Nm) which correspond with the matching slip angles in the X arrays. All the required conversions to the vehicle model units are carried out in the FORTRAN subroutine for the tyre models listed in Appendix D.

Table 6.5 Lateral force interpolation arrays for TYRE A

```
LATERAL FORCE (N) WITH SLIP ANGLE (DEG) AT CAMBER = -5 DEG
SPLINE/1
,X=-9,-6,-4,-2,-1,0,1,2,4,6,9
,Y=185,1988,1929,1706,1050,567,-80,-741,-1210,-1861,-2055,-2059
,Y=370,3438,3323,2866,1685,843,-188,-1257,-2186,-3562,-3899,-3749
,Y=491,4222,4079,3353,1858,895,-230,-1381,-2471,-4251,-4875,-4697
,Y=615,5043,4709,3597,1858,817,-293,-1393,-2522,-4533,-5640,-5543
,Y=800,6147,5051,3410,1582,603,-377,-1408,-2393,-4364,-6097,-6673
LATERAL FORCE (N) WITH SLIP ANGLE (DEG) AT CAMBER = 0 DEG
SPLINE/2
,X=-9,-6,-4,-2,-1,0,1,2,4,6,9
,Y=185,2044,2016,1843,1223,761,127,-590,-1096,-1824,-2050,-2121
,Y=370,3684,3615,3277,2159,1282,205,-955,-1905,-3229,-3678,-3703
,Y=491,4553,4477,3928,2392,1345,171,-1048,-2148,-3826,-4491,-4664
,Y=615,5341,5184,4244,2382,1287,146,-1023,-2143,-4078,-5145,-5408
,Y=800,6431,5797,4105,2156,1145,78,-940,-1971,-3954,-5618,-6527
LATERAL FORCE (N) WITH SLIP ANGLE (DEG) AT CAMBER = 5 DEG
SPLINE/3
,X=-9,-6,-4,-2,-1,0,1,2,4,6,9
,Y=185,2058,2045,1871,1323,888,280,-400,-942,-1698,-1926,-1968
,Y=370,3642,3817,3571,2445,1539,492,-574,-1508,-2828,-3338,-3424
,Y=491,4721,4782,4340,2744,1690,529,-610,-1642,-3278,-4055,-4289
,Y=615,5520,5626,4708,2767,1686,552,-578,-1662,-3490,-4629,-5058
,Y=800,6775,6316,4573,2608,1574,582,-430,-1431,-3311,-4915,-611
```

Table 6.6 Aligning moment interpolation arrays for TYRE A

```
ALIGNING MOMENT (NM) WITH SLIP ANGLE (DEG) AT CAMBER = -5 DEG
SPLINE/4
,X=-9,-6,-4,-2,-1,0,1,2,4,6,9
,Y=185,2.4,-10.7,-17.5,-18,-19.4,-9.2,0,1.9,6.8,0,-2.4
,Y=370,-3.4,-31.1,-66.6,-62.7,-51,-17,16,36.9,49.1,26.3,4.4
,Y=491,-15.6,-64.2,-116.2,-101.1,-71.9,-21.4,30.6,71.5,98.2,50.6,14.6
,Y=615,-48.1,-115.7,-169.2,-133.7,-88.5,-22.8,45.7,103.5,158.5,101.6,34
,Y=800,-126.4,-260.6,-274.7,-188.6,-113.3,-26.3,63.7,143.9,245,211.5,93.8
ALIGNING MOMENT (NM) WITH SLIP ANGLE (DEG) AT CAMBER = 0 DEG
SPLINE/5
,X=-9,-6,-4,-2,-1,0,1,2,4,6,9
,Y=185,4.9,-4.4,-9.3,-15.1,-11.2,-2.9,7.8,11.7,14.2,5.9,0
,Y=370,8.8,-20,-50.8,-55.6,-41,-9.3,28.3,51.2,55.6,29.8,7.8
,Y=491,1,-46.4,-98.1,-95.6,-65.4,-13.7,42.5,84.9,105.9,62.5,16.1
,Y=615,-26.4,-84.9,-162.5,-134.2,-84.9,-18.5,54.7,109.3,161.5,103.5,35.6
,Y=800,-81,-217.6,-264.5,-181.5,-110.3,-18.5,68.8,148.4,243,237.2,104.9
ALIGNING MOMENT (NM) WITH SLIP ANGLE (DEG) AT CAMBER = 5 DEG
SPLINE/6
,X=-9,-6,-4,-2,-1,0,1,2,4,6,9
,Y=185,12.2,1.9,-2.4,-7.3,-3.9,8.3,15.6,17.5,21.4,12.6,-1.5
,Y=370,17,-10.7,-37.9,-47.6,-28.7,1.5,36,58.8,68.1,39.4,13.1
,Y=491,4.4,-31.1,-89,-86.5,-56.4,-4.4,48.1,89,114,71,25.3
,Y=615,-13.6,-76.8,-159.5,-126.4,-79.2,-9.2,59.3,113.8,165.3,119.6,54.4
,Y=800,-62.2,-192.5,-260.6,-177,-103.1,-18.5,77.3,155.1,256.7,270.3,131.3
```

The parameters for the Fiala tyre model, as described in Section 6.4.1, have been derived from the test data and are given in Table 6.7 using data derived at the average of the front and rear wheel loads. Data at front and rear wheel loads as used with the simulation models is given in Tables 6.8 and 6.9. The parameters supplied for TYRE A using the Monte Carlo version of the Pacejka tyre model are shown in Table 6.10.

Table 6.7 Fiala tyre model parameters for TYRE A (Average wheel load)

$R_1 = 318.5$ mm	$R_2 = 97.5$ mm
$k_z = 160$ N/mm	$C_s = 30000$ N
$C_\alpha = 59885$ N/rad	$C_\gamma = 3240$ N/rad
$C_r = 0.0$ mm	$\xi = 0.05$
$\mu_0 = 1.15$	$\mu_1 = 0.9$

Table 6.8 Fiala tyre model parameters for TYRE A (Front wheel load)

R_1 = 318.5 mm	R_2 = 97.5 mm
k_z = 160 N/mm	C_s = 30000 N
C_α = 63210 N/rad	C_γ = 4095 N/rad
C_r = 0.0 mm	ξ = 0.05
μ_0 = 1.15	μ_1 = 0.9

Table 6.9 Fiala tyre model parameters for TYRE A (Rear wheel load)

R_1 = 318.5 mm	R_2 = 97.5 mm
k_z = 160 N/mm	C_s = 30000 N
C_α = 56555 N/rad	C_γ = 2385 N/rad
C_r = 0.0 mm	ξ = 0.05
μ_0 = 1.15	μ_1 = 0.9

Table 6.10 Pacejka tyre model parameters (Monte Carlo version) for TYRE A

Lateral Force	Aligning Moment
A0=1.3	C0=2.4
A1=-46.8451	C1=-3.98725
A2=1185.46	C2=-2.70372
A3=1146.06	C3=0.552334
A4=4.92921	C4=-6.22588
A5=0.00547748	C5=-0.225629
A6=-0.655688	C6=0.00142515
A7=1.86868	C7=-0.0175979
A8=-0.0280612	C8=-0.143857
A9=0.0147439	C9=-0.822518
A10=-0.212575	C10=0.0174298
A111=-13.4328	C11=-0.0244277
A112=0.428945	C12=0.0116074
A12=-3.71929	C13=-0.322245
A13=33.6686	C14=0.0210605
	C15=-0.565934
	C16=0.376785
	C17=-2.3039

6.6.2 Data for TYRE B

The data from the tests carried out on TYRE B has been used to extract the necessary lateral force and aligning moment values and to set these up in interpolation arrays. This has been achieved using the ADAMS spline statements as shown in Table 6.11. The numerical values set up in the spline statements have been reformatted from the tabular printed values which were written to computer files during the tyre testing at SP Tyres UK Ltd.

Table 6.11 Interpolation arrays for TYRE B

```
LATERAL FORCE (N) WITH SLIP ANGLE (DEG) AND LOAD (KG)
SPLINE/100
,X=-10,-8,-6,-4,-2,0,2,4,6,8,10
,Y=200,2148,2050,1806,1427,867,16,-912,-1508,-1881,-2067,-2151
,Y=400,3967,3760,3409,2727,1620,75,-1587,-2776,-3482,-3759,-3918
,Y=600,5447,5099,4436,3385,1962,94,-1893,-3397,-4557,-5049,-5269
,Y=800,6738,5969,4859,3533,2030,66,-1971,-3662,-5122,-6041,-6500
ALIGNING MOMENT (NM) WITH SLIP ANGLE (DEG) AND LOAD (KG)
SPLINE/200
,X=-10,-8,-6,-4,-2,0,2,4,6,8,10
,Y=200,4.6,-0.1,-6,-11.1,-10.9,-1.3,10.6,11.2,7.9,3.2,-0.3
,Y=400,-4.8,-19.6,-39,-52.1,-41.9,-6.7,35.8,49.1,38.6,23.4,10.1
,Y=600,-36.5,-73.1,-102.6,-107.9,-78.7,-14.2,60.6,96.2,93.4,65.8,40.7
,Y=800,-105.1,-181.1,-206.1,-172.4,-116.0,-23.6,79.9,143.3,172.2,141.5,98.5
LATERAL FORCE (N) WITH CAMBER ANGLE (DEG) AND LOAD (KG)
SPLINE/300
,X=-10,-8,-6,-4,-2,0,2,4,6,8,10
,Y=100,-123.3,-96.3,-64.6,-39.3,-3,19,46,80.6,108.3,146,173.3
,Y=200,-142.6,-106.6,-57.3,-14.6,28,78,127,169.6,212.3,255,285.6
,Y=300,-173.6,-106.6,-44,20.6,87.6,159,223.6,291.3,344.3,393.3,443.6
,Y=400,-194,-115.6,-31.3,53,141.6,237,319.6,396.3,468.6,526.3,579
,Y=500,-219.6,-121.6,-17.3,91,199,304,403.3,487,572.6,651.3,717
,Y=600,-247.6,-128.3,-9.3,109.3,234,351,453.3,557.3,651.6,734.6,829.6
,Y=700,-278,-138.6,-3.6,126.3,254,381,499.3,616,723,827,922.6
,Y=800,-318.6,-165,-21,128,261.3,404.0,524.3,656,780,895,1012
ALIGNING MOMENT (NM) WITH CAMBER ANGLE (DEG) AND LOAD (KG)
SPLINE/400
,X=-10,-8,-6,-4,-2,0,2,4,6,8,10
,Y=100,-5,-5,-4.3,-2.2,-0.9,1.2,2.6,4.2,5.8,7,6.4
,Y=200,-14.6,-13.7,-12,-9.2,-4.9,-0.9,3.6,6.7,9.6,11,11.7
,Y=300,-24.1,-22.6,-19.6,-16.7,-11.1,-4.2,2.8,8.1,11.9,15.2,17
,Y=400,-34.2,-31.8,-28.5,-22.9,-15.8,-8.2,-0.3,6.5,12.2,15.6,17.7
,Y=500,-41.5,-38,-32.7,-26.5,-18.8,-10.8,-2.5,3.9,10.7,16.5,19.6
,Y=600,-48.7,-43.6,-38,-31.6,-23.9,-15.9,-8.1,-0.4,6.4,12.1,16.8
,Y=700,-52.5,-47.5,-40.9,-34.4,-26.6,-19.5,-11.9,-4.7,1.3,7.2,12.6
,Y=800,-56.9,-51.3,-44.2,-37.9,-30.7,-23.9,-16.7,-10.1,-4,2.4,8.3
```

In each spline the X values correspond to either the slip or camber angle and are measured in degrees. The first value in each Y array corresponds to the vertical load measured in kg. The following values in the Y arrays are the measured lateral forces (N) or the aligning moments (Nm) which correspond with the matching slip or camber angles in the X arrays. All the required conversions to the vehicle model units are carried out in the FORTRAN subroutine for the interpolation tyre model listed in Appendix D.

The parameters for the Fiala tyre model have been derived from the test data and are given in Table 6.12 using data derived at the average of the front and rear wheel loads. Data at front and rear wheel loads as used with the simulation models is given in Tables 6.13 and 6.14.

Table 6.12 Fiala tyre model parameters for TYRE B (Average wheel load)

$R_1 = 318.5$ mm	$R_2 = 97.5$ mm
$k_z = 150$ N/mm	$C_s = 110000$ N
$C_\alpha = 51560$ N/rad	$C_\gamma = 2580$ N/rad
$C_r = 0.0$ mm	$\xi = 0.05$
$\mu_0 = 1.05$	$\mu_1 = 1.05$

Table 6.13 Fiala tyre model parameters for TYRE B (Front wheel load)

$R_1 = 318.5$ mm	$R_2 = 97.5$ mm
$k_z = 150$ N/mm	$C_s = 110000$ N
$C_\alpha = 54430$ N/rad	$C_\gamma = 2750$ N/rad
$C_r = 0.0$ mm	$\xi = 0.05$
$\mu_0 = 1.05$	$\mu_1 = 1.05$

Table 6.14 Fiala tyre model parameters for TYRE B (Rear wheel load)

$R_1 = 318.5$ mm	$R_2 = 97.5$ mm
$k_z = 150$ N/mm	$C_s = 110000$ N
$C_\alpha = 46980$ N/rad	$C_\gamma = 2350$ N/rad
$C_r = 0.0$ mm	$\xi = 0.05$
$\mu_0 = 1.05$	$\mu_1 = 1.05$

The Pacejka tyre model parameters (Version 3) were derived from the test data for TYRE B by SP Tyres UK Ltd. and are shown in Table 6.15. It should be noted that the parameters due to camber effects were not available from this set of tests.

Table 6.15 Pacejka tyre model parameters (Version 3) for TYRE B

Lateral Force	Aligning Moment
A0=.103370E+01	C0=.235000E+01
A1=-.224482E-05	C1=.266333E-05
A2=.132185E+01	C2=.249270E-02
A3=.604035E+05	C3=-.159794E-03
A4=.877727E+04	C4=-.254777E-01
A5=0.0	C5=.142145E-03
A6=.458114E-04	C6=0.00
A7=.468222	C7=.197277E-07
A8=.381896E-06	C8=-.359537E-03
A9=.516209E-02	C9=.630223
A10=0.00	C10=0.00
A11=-.366375E-01	C11=.120220E-06
A12=-.568859E+02	C12=.275062E-02
A13=0.00	C13=0.00
A14=0.00	C14=-.172742E-02
A15=0.00	C15=.544249E+01
A16=0.00	C16=0.00
A17=.379913	C17=0.00
	C18=0.00
	C19=0.00
	C20=0.00

6.7 The *CUTyre* System

6.7.1 Implementation of tyre models in ADAMS

The Fiala tyre model is the default in ADAMS and can be implemented directly without any special programs. Implementation of the Pacejeka tyre model and the Interpolation model requires writing a FORTRAN program and linking this in with ADAMS to provide a customised user executable of ADAMS. These subroutines together with the ADAMS tyre rig model described in the following section form the basis of a tyre modelling, checking and plotting facility which has been developed as part of this study at Coventry University and is hence referred to as the *CUTyre* System.

The interface between ADAMS and a user programmed FORTRAN tyre model is through a user-written TIRSUB subroutine (88). The subroutine defines a set of three forces and three torques acting at the tyre to road surface contact patch and formulated in the SAE coordinate system (87). The equations used to formulate these forces and moments have been programmed into the subroutines to represent the various tyre models. The transformation of the forces and moments from the contact patch to the wheel centre is performed internally by the ADAMS program. The TIRSUB subroutine is called from within the ADAMS input deck by a TIRE statement for each tyre on the vehicle. Tyre data can be passed from the TIRE statement, from SPLINE and ARRAY statements within the input deck, or programmed into the subroutine. In addition ADAMS passes a number of variables which describe the current set of contact properties and may be used in any model formulation. These variables, which are computed in the SAE coordinate system, are listed below:

(i) Longitudinal Slip Ratio

(ii) Lateral slip angle (radians)

(iii) Camber angle (radians)

(iv) Normal deflection of tyre into road surface

(v) Normal velocity of penetration of tyre into road surface

(vi) Longitudinal sliding velocity of contact patch

(vii) Distance from wheel centre to contact point (loaded radius)

(viii) Angular velocity about the spin axis of the tyre

(ix) Longitudinal velocity of tyre tread base

(x) Lateral velocity of tyre tread base

The FORTRAN TIRSUB subroutines which have been developed to support this project are included in Appendix D. Although the Fiala tyre model is coded in ADAMS as a default an example subroutine which programs the Fiala model equations is also included. In summary the following subroutines are included in Appendix D. The Interpolation routines are referred to as "full" or "limited". The full version uses results where a full range of slip angle variation tests have been carried out at different camber angles. The limited version uses results from a slip angle variation test at zero camber angle and a camber angle variation test at zero slip angle. These subroutines have also been adapted to run without camber effects to allow comparison with the Fiala model.

(i)   D.1 Fiala tyre model subroutine

(ii) D.2 Full Interpolation tyre model subroutine

(iii) D.3 Full Interpolation tyre model subroutine (No Camber)

(iii) D.4 Pacejka tyre model subroutine (Monte Carlo Version)

(iv) D.5 Limited Interpolation tyre model subroutine

(v)   D.6 Limited Interpolation tyre model subroutine (No Camber)

(vi) D.7 Pacejka tyre model subroutine (Version 3)

6.7.2 ADAMS tyre rig model

A functional model of the Flat Bed Tyre Test machine has been developed in ADAMS and forms part of the *CUTyre* System described here. The ADAMS model is in fact conceptually the same as the tyre test machine within the School of Engineering at Coventry University, where running at low speed it is possible to measure lateral force F_y and aligning moment M_z for variations in vertical load F_z, s lip angle α and camber angle γ.

The rig model has been developed in order to address the situation where a tyre data file has been supplied for a particular model but the test data is not available either in tabular

146

format or graphically as plotted curves. It is clearly desirable to use the tyre data parameters or coefficients to generate the sort of plots produced from a tyre test programme and to inspect these plots before using the data files with an actual full vehicle model. The tyre rig model is also useful where test data has been used to extract mathematical model parameters. The plots obtained from the mathematical model can be compared with test data to ensure the mathematical parameters are accurate and represent the actual tyre. The tyre test rig model performs a useful function for any vehicle simulation system activities developed around ADAMS. The process which this involves is shown conceptually in Figure 6.16. The system has been developed so that it can currently read the Fiala, Pacejka and Interpolation models described in this report.
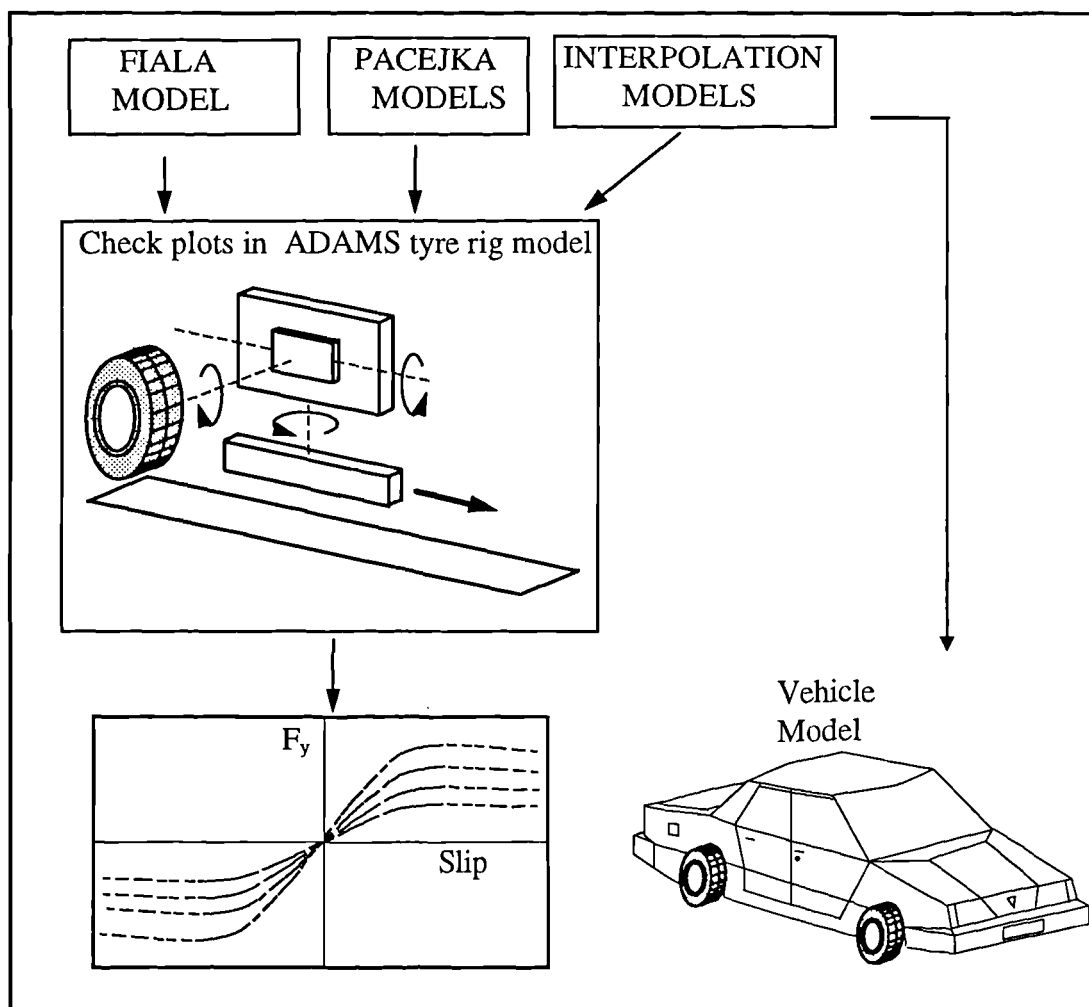

Figure 6.16 Overview of the *CUTyre* System

The orientation of the global axis system and the local axis system for the tyre has been set up using the same methodology as that required when generating a full vehicle model in

ADAMS as shown in Figure 6.17. The usual approach with full vehicle modelling is to set up a global coordinate system or Ground Reference Frame (GRF) where the x-axis points back along the vehicle, the y-axis points to the right of the vehicle and the z-axis is up. The local z-axis of each tyre part is orientated to point towards the left side of the vehicle so that the wheel spin vector is positive when the vehicle moves forward during normal motion. Note that this is the coordinate system as set up at the wheel centre and should not be confused with the SAE coordinate system (87) which is used at the tyre contact patch in order to describe the forces and moments occurring there.
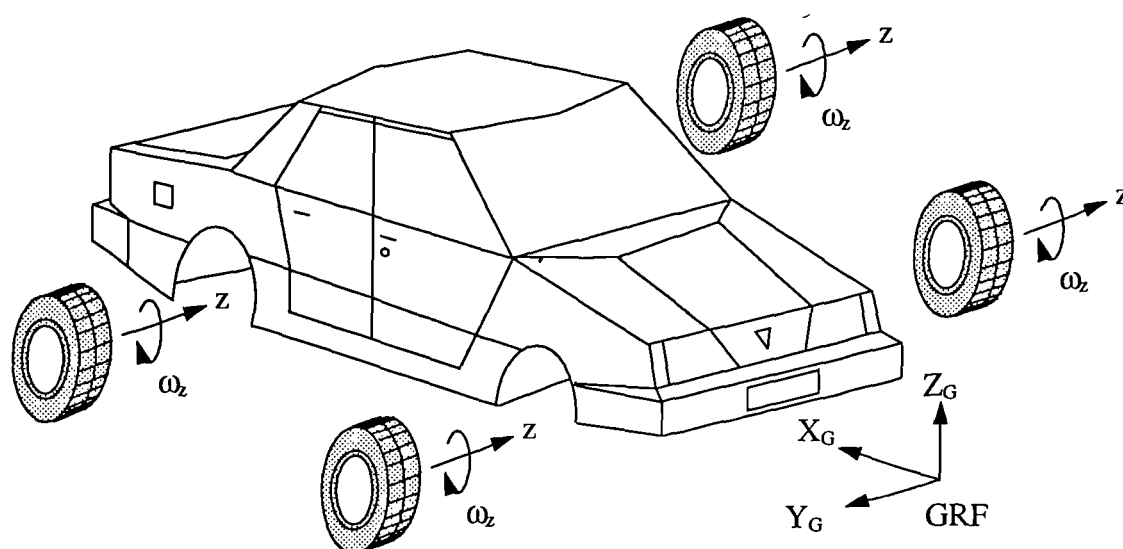

Figure 6.17 Orientation of tyre coordinate systems on the full vehicle model

The model of the tyre test machine which has been developed in ADAMS contains a tyre part which rolls forward on a flat uniform road surface in the same way that the tyre interacts with a moving belt in the actual machine. In the ADAMS model the road is considered fixed as opposed to the machine where the belt represents a moving road surface and the tyre is stationary. Considering the system schematic of this model shown in Figure 6.18 the tyre part 02 is connected to a carrier part 03 by a revolute joint aligned with the spin axis of the wheel. The carrier part 03 is connected to another carrier part 04 by a revolute joint which is aligned with the direction of travel of the vehicle. A motion input applied at this joint is used to set the required camber angle during the simulation of the test process. The carrier part 04 is connected to a sliding carrier part 05 by a cylindrical joint which is aligned in a vertical direction. A rotational motion is applied at this joint which will set the slip angle of the tyre

during the tyre test simulation. The cylindrical joint allows the carrier part 04 to slide up or down relative to 05 which is important as a vertical force is applied downwards on the carrier part 04 at this joint and effectively forces the tyre down on to the surface of the road. The model has been set up to ignore gravitational forces so that this load can be varied and set equal to the required wheel vertical load which would be set during the tyre test process. The sliding carrier part 05 is connected to the ground part 01 by a translational joint aligned with the direction of travel of the wheel. A motion input applied at this joint will control the forward velocity of the tyre during the test.
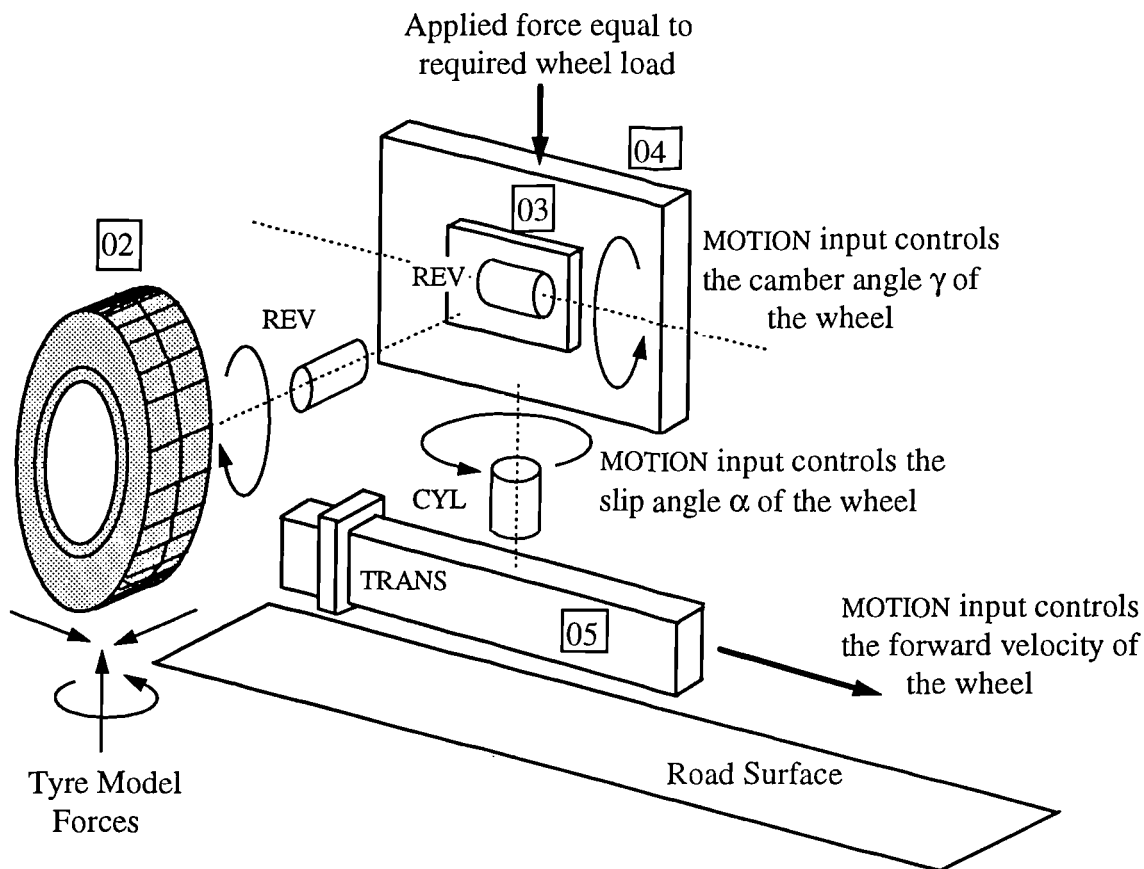

Figure 6.18 ADAMS model of a flat bed tyre test machine

The ADAMS model of the tyre test machine has two rigid body degrees of freedom as demonstrated by the calculation of the degree of freedom balance in Table 6.16.

Table 6.16 Degree of freedom balance equation for the tyre rig model

Model Component	DOF	Number	Total DOF
Parts	6	4	24
Revolutes	-5	2	-10
Translational	-5	1	-5
Cylindrical	-4	1	-4
Motions	-1	3	-3
		Σ_{DOF} =	2

One degree of freedom is associated with the spin motion of the tyre which is dependent on the longitudinal forces generated and the slip ratio. The other degree of freedom is the height of the wheel centre above the road which is controlled by the applied force representing the wheel load. The tyre test rig model has been used to read the tyre model data files used in this study and to plot tyre force and moment graphs. The ADAMS graphics of the tyre rig model are shown in Figure 6.19.
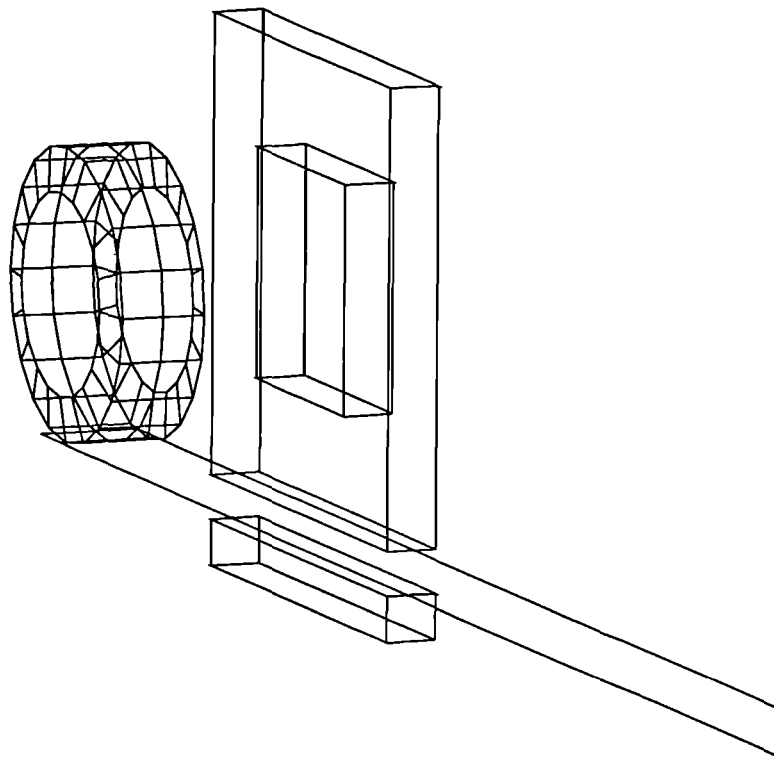

Figure 6.19 ADAMS graphics of the *CUTyre* rig model

7.0 VEHICLE HANDLING SIMULATIONS

7.1 Introduction

Vehicle handling simulations are intended to recreate the manoeuvres and tests which vehicle engineers carry out using prototype vehicles on the test track or proving ground. Standards exists (16-19) which outlines a series of recommended tests in order to substantiate the handling performance of a new vehicle. Manufacturers will generally follow these procedures but may modify the procedures in line with their own experience and the class of vehicles they produce. The goal of excellence in handling performance will be driven not by the need to meet fixed legislation but rather the ever increasing demands of a competitive marketplace.

The use of instrumented vehicles to investigate handling performance can be traced back to the work of Segal in the early 1950's which as mentioned earlier was the subject of one of the well known "IME Papers" (15). Testing was carried out using a 1953 Buick Super, four-door Sedan, to investigate steady state behaviour with a fixed steering input at various speeds and also transient response to sudden pulse inputs at the steering wheel. The instrumentation used at that time allowed the measurement of the following:

(i) Left front wheel steer

(ii) Right front wheel steer

(iii) Steering wheel rotation

(iv) Lateral acceleration

(v) Roll angle

(vi) Pitch angle

(vii) Yaw rate

(viii) Roll rate

(ix) Forward velocity

Computer based full vehicle handling simulations generally aim to reproduce the manoeuvres performed on the test track. There are a wide range of possible tests in any

handling study many of which may be vehicle dependent. For the work carried out in (64) a very large ADAMS model with approximately 160 degrees of freedom was used to carry out handling simulations. Working with the vehicle manufacturers the following set of manoeuvres were chosen for computer simulation.

(i) Straight line running.

(ii) Fixed steering input.

(iii) Steady state cornering.

(iv) Lane change manoeuvre.

(v) Sinusoidal steering input.

(vi) Braking in a turn

For the work described in this thesis a set of track tests had been performed by Rover (20) and are summarised in the following section. The results of these tests provided a valuable input to this project for the following:

(i) To provide guidance on a full range of tests and the associated measured outputs for a modern road vehicle.

(ii) To provide time history measurements of steering wheel angles obtained on the test track during a manoeuvre such as the I.S.O. Lane Change test (19). These measurements could then be included in the computer models as measured XY pairs and interpolated using a cubic spline fit to get the steering inputs.

(iii) To provide time history measurements of vehicle responses such as roll angle, yaw rate and lateral acceleration from which comparative assessments could be made of any computer modelling assumptions.

7.2 Handling test data

The documentation in (20) provides a full description of the series of tests carried out for which a summary is given here. Before the main handling tests were performed a steering ratio test was carried out in order to establish the steering wheel to road wheel turning ratio which was found to be 20:1. As described in Section 5 of this thesis this information was used when checking the ADAMS modelling of the steering system. During track testing the following range of manoeuvres were investigated:

(i) Steady State Cornering - where the vehicle was driven around a 33 metre radius circle at constant velocity. The speed was increased slowly maintaining steady state conditions until the vehicle became unstable. The test was carried out for both right and left steering lock.

(ii) Steady State with Braking - as above but with the brakes applied at a specified deceleration rate (in steps from 0.3g to 0.7g) when the vehicle has stabilised at 50 kph.

(iii) Steady State with Power On/Off - as steady state but with the power on (wide open throttle) when the vehicle has stabilised at 50 kph. As steady state but with the power off when the vehicle has stabilised at 50 kph.

(iv) On Centre - application of a sine wave steering wheel input (+ / - 25 deg.) during straight line running at 100 kph.

(v) Control Response - with the vehicle travelling at 100 kph, a steering wheel step input was applied (in steps from 20 to 90 deg.) for 4.5 seconds and then returned to the straight ahead position. This test was repeated for left and right steering locks.

(vi) I.S.O. Lane Change (ISO 3888) - The ISO lane change manoeuvre was carried out at a range of speeds. The test carried out at 100 kph has been used for the study described here.

(vii) Straight line braking - a vehicle braking test from 100 kph using maximum pedal pressure (ABS) and moderate pressure (no ABS).

For each handling manoeuvre it is necessary for vehicle engineers to decide what physical outputs are to be measured during the testing process. Many of these outputs will be common to more than one manoeuvre and may have more or less significance for any particular test. For example, the measurement of pitch angle may be useful for a braking test but of less interest for a lane change manoeuvre. During discussions and correspondence with staff at Rover a series of outputs for a range of tests were identified (89), where for each test the more important outputs could be classified as recommended and those of less significance as optional. Outputs which have no relevance to a given manoeuvre are classified as not applicable. This information is summarised in Table 7.1.

Table 7.1 Measured vehicle outputs for instrumented testing

Manoeuvre/Measurement	1	2	3	4	5	6	7	8	9	10	11	12
Steady State Cornering	R	R	R	R	O	R	R	R	N	R	N	N
Braking in a turn	R	O	R	R	R	R	O	R	O	O	N	R
Power on/off in a turn	R	O	R	R	R	R	O	R	O	O	R	N
On Centre	R	O	R	R	N	R	R	R	N	R	N	N
Control Response	R	O	R	R	O	R	R	R	N	R	N	N
Lane Change	R	R	R	R	R	R	R	R	N	R	N	N
Straight Line Braking	O	O	O	O	R	R	N	R	R	O	O	R

R - Recommended   O - Optional   N - Not applicable

1 - Steering wheel angle   7 - Roll angle

2- Steering wheel torque   8 - Yaw rate

3- Road wheel angle   9 - Pitch angle

4 - Lateral acceleration   10 - Sideslip angle (lat. & long. vel.)

5 - Longitudinal acceleration/ deceleration 11 - Throttle monitoring

6 - Longitudinal velocity   12 - Brake monitoring

7.3 Computer simulations

Following the guidelines in Table 7.1 performing all the simulations with a given ADAMS vehicle model, a set of results based on recommended and optional outputs would produce 67 time history plots. Given that several of the manoeuvres such as the control response are repeated for a range of steering inputs and that the lane change manoeuvre is repeated for a range of speeds the set of output plots would escalate into the hundreds.

This is an established problem in many areas of engineering analysis where the choice of a large number of tests and measured outputs combined with possible design variation studies can factor the amount of output up to a chaotic level for human interpretation. Table 7.3 shows an example of this as suggested in (22), to demonstrate how for any particular vehicle the range of handling simulations could become unmanageable.

Table 7.2 Possible handling simulations

MANOEUVRES - Steady State Cornering, Braking in a Turn, Lane Change, Straight Line Braking, Sinusoidal Steering Input, Step Steering Input,

DESIGN VARIATIONS - Wheelbase, Track, Suspension, ...

ROAD SURFACE - Texture, Dry, Wet, Ice, μ-Split

VEHICLE PAYLOAD - Driver Only, Fully Loaded, ...

AERODYNAMIC EFFECTS - Side Gusts, ...

RANGE OF VEHICLE SPEEDS - Steady State Cornering, ...

TYRE FORCES - Range of Designs, New, Worn, Pressure Variations, ...

ADVANCED OPTIONS - Active Suspension, ABS, Traction Control, Active Roll, Four Wheel Steer, ...

The simulation work described in this thesis can be summarised as :

(i) Comparing four methods of modelling the main vehicle using a linkage model, lumped mass model, swing arm model and a roll stiffness model.

(ii) Comparing three methods of modelling the tyre using the Fiala model, the Pacejka model and an interpolation model.

(iii) Using data for two sets of tyres, TYRE A and TYRE B

In addition to this investigations have been carried out comparing tyre models with and without camber effects, and sensitivity studies involving variations in tyre parameters such as cornering stiffness, radial stiffness and coefficients of friction. Sensitivity studies were also performed varying vehicle parameters such as mass centre position, roll centre heights and the toe in angle of the rear wheels.

In order to keep this study manageable it was clearly necessary to focus on a set of simulations and measured outputs which could provide the most relevant information. As this project was primarily concerned with transient lateral response and did not involve combined slip situations resulting from simultaneous braking it was decided to use the lane change manoeuvre at 100 kph.

For each simulation it was also decide to limit the amount of measured and plotted output. In some cases the investigation has required additional plotted output concerning tyre forces and geometry but in general the plotted outputs for each simulation are:

(i) Lateral acceleration
(ii) Roll angle
(iii) Yaw rate

The actual trajectory followed by the vehicle was not available from the test data provided. This is in fact difficult to obtain using instrumentation but can be obtained quite

practically by laying a trail of dye on the track during the test and taking measurements before the next run. Obtaining the trajectory of the vehicle from the ADAMS simulation is straightforward and has been used when comparing the roll stiffness and linkage models in association with the various tyre models.

For the lane change manoeuvre the measured steering wheel angles from the test vehicle have been extracted and put into ADAMS as a set of XY pairs which can be interpolated using a cubic spline fit. The time history plot for the steering inputs is shown in Figure 7.1.

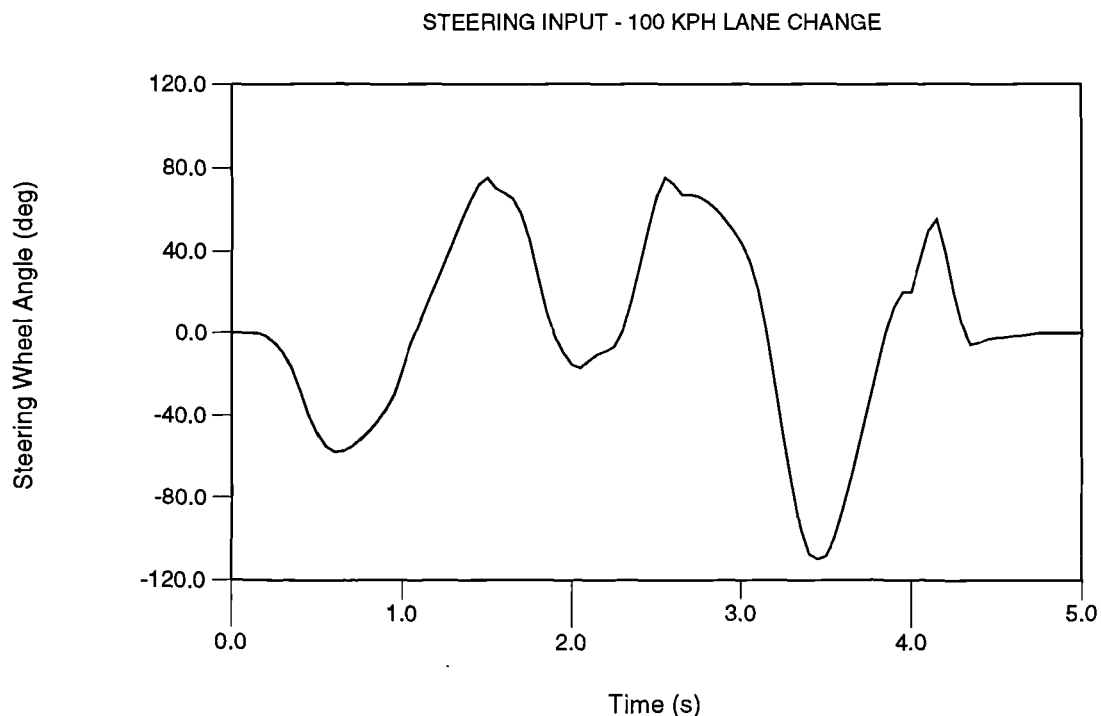STEERING INPUT - 100 KPH LANE CHANGE

Figure 7.1 Steering input for the lane change manoeuvre

The test procedure for the lane change manoeuvre is outlined in the international standard (19) and is summarised in Figure 7.2. By way of example the ADAMS statements which apply the steering motion to the steering column to body revolute joint and the spline data are shown in Table 7.3. The x values are points in time and the y values are the steering inputs in degrees. Examples of the animated graphical outputs from ADAMS are given in Figures 7.3.

157

A - 1.3 times vehicle width + 0.25m

B - 1.2 times vehicle width + 0.25m

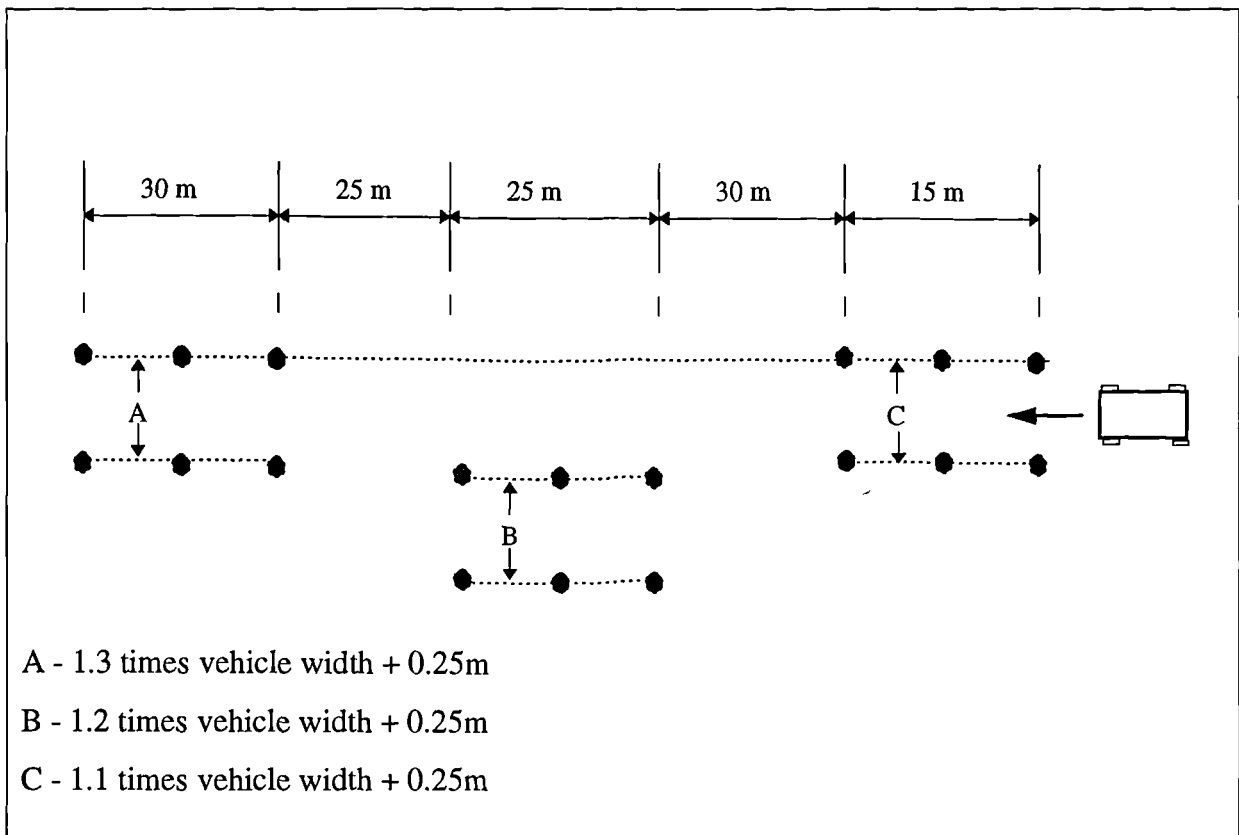C - 1.1 times vehicle width + 0.25m

Figure 7.2 ISO 3888 Lane change manoeuvre

Table 7.3 ADAMS statements for lane change steering inputs

```
MOTION/502,JOINT=502,ROT
,FUNC=(PI/180)*CUBSPL(TIME,0,1000)

SPLINE/1000
,X=0,1,2,3,4,5,6,7,8,9
,9.1,9.2,9.3,9.4,9.5,9.6,9.7
,9.8,9.9,10,10.1,10.2,10.3,10.4,10.5,10.6,10.7,10.8,10.9,11
,11.1,11.2,11.25,11.3,11.4,11.5,11.6,11.7,11.8,11.9,12,12.1
,12.2,12.3,12.4,12.5,12.6,12.7,12.8,12.9,13,13.1,13.2,13.3
,13.4,13.5,13.6,13.7,13.75,13.8,13.9,14,14.1,14.2,14.3,14.4,14.5
,14.6,14.7,14.8,14.9,15
,Y=0,0,0,0,0,0,0,0,0,0
,0,0,0,0,0,0,0
,0,0,-5,-17,-40,-55,-57,-52,-43,-30,-5,15,35,55,72,75,70,65,45,10
,-10,-17,-11,-7,15,50,75,67,66,60,50,35,0,-50,-95,-110,-100,-70,-35,0
,20,20,35,55,20,-6,-3,-2,-1,0,0,0,0,0,0
```
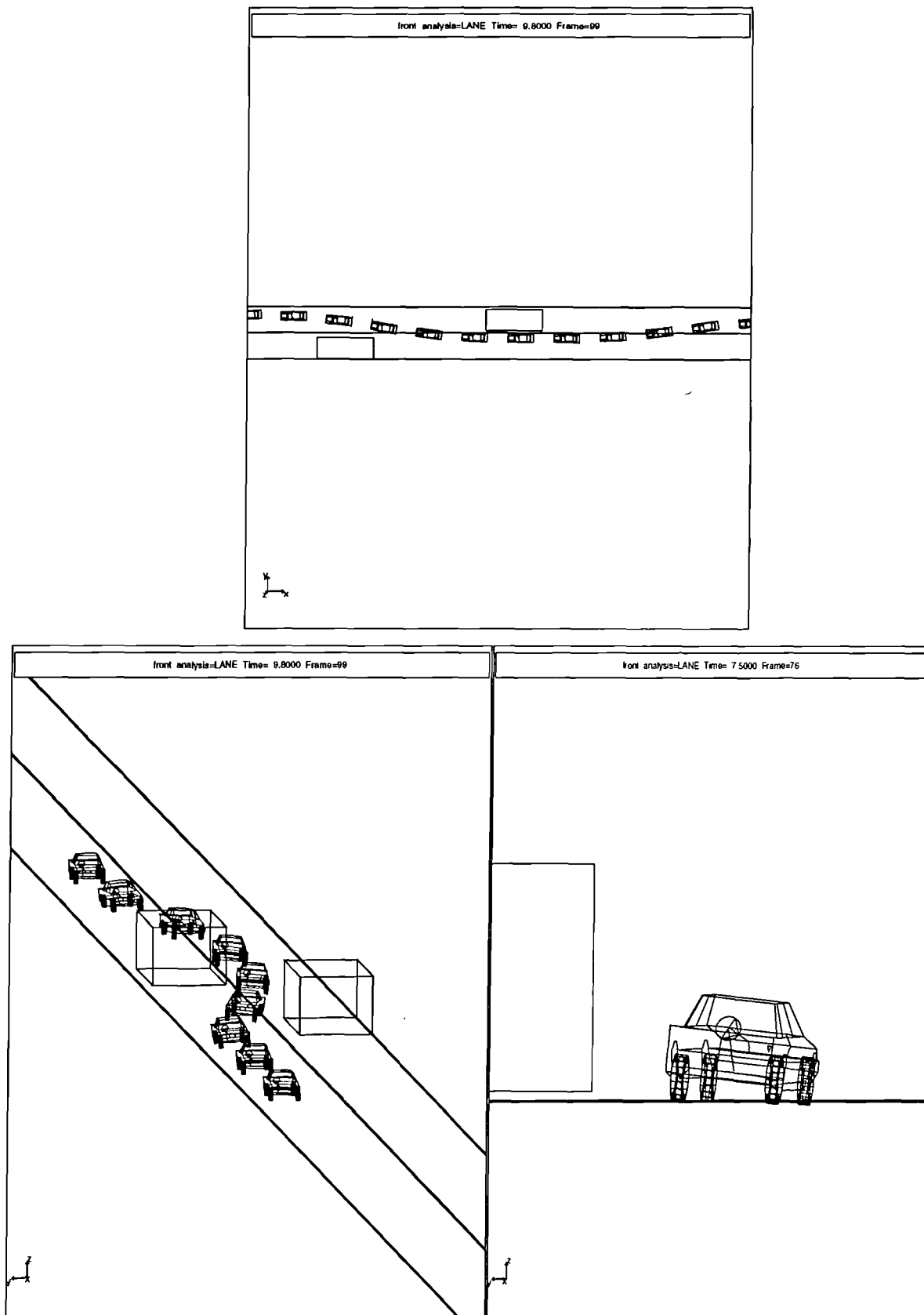
158

Figure 7.3 Graphical animation of the lane change manoeuvre

To conclude this section of the report the full range of comparisons and simulations which have been carried out are summarised. A study of this kind generates large amounts of plotted outputs which have been collated in the following appendices:

(i) Appendix G - This contains results from comparisons of each of the four vehicle modelling approaches (lumped mass, swing arm, roll stiffness and linkage models). As this phase of the study was concerned with comparing vehicle models an interpolation tyre model was used together with data for TYRE A which was fitted to the vehicle during the actual test. The results are discussed in more detail in the next section where it is explained why the roll stiffness model was selected to progress, with the linkage model, to the tyre model study phase.

(ii) Appendix H - This contains results where the linkage model has been used with the full range of tyre models (Interpolation, Pacejka and Fiala) using data for each model from TYRE A and TYRE B. The effects of omitting camber from each model are also included to investigate the significance of the shortcoming in the Fiala model where the lateral force and aligning moment due to camber are not computed.

(iii) Appendix I - This contains results repeating the tyre model comparisons carried out in Appendix H but this time using the roll stiffness rather than the linkage model. The objective of this phase of work being to ascertain whether a simple model such as the roll stiffness model could be as sensitive as the linkage model to changes in tyre model and tyre data.

(iv) Appendix J - The plots in this appendix summarise the results from all the simulations plotted in Appendix H and Appendix I. For both the linkage and roll stiffness models the results obtained using the three tyre models are plotted on the same graphs to help interpret the comparison.

(v) Appendix K - This final section uses the roll stiffness vehicle model and the Fiala tyre model together with data for TYRE B. Results are provided to demonstrate how the models could be used for vehicle and tyre parameter variation studies.

8.0 DISCUSSION

8.1 Introduction

The plotted outputs from the various studies undertaken here have been organised in appendices at the rear of this report. The results in each appendix are based on separate sets of investigations into modelling the vehicle and modelling the tyres. A final section investigates the use of the Roll Stiffness model combined with the Fiala tyre model to make systematic changes to vehicle and tyre design parameters.

The work involving the *CUTyre* System rig model and the three tyre modelling approaches is discussed next. The plots obtained help to provide insights into the effectiveness of the three modelling approaches. The plots also provide a graphical comparison of the force and moment characteristics of TYRE A and TYRE B.

8.2 Tyre model validation

8.2.1 Tyre A

The results obtained using the *CUTyre* System to investigate tyre model performance using data for TYRE A are presented in Appendix E of this report. Figures E.1 to E.5 show the results obtained using an Interpolation tyre model together with the test data provided for this tyre. Test data was available for slip angles ranging from -9 to +9 degrees of slip angle measured at three camber angles of -5, 0 and +5 degrees. This allowed use of the "full" interpolation tyre subroutine. In Figure E.1 the lateral force is plotted as a function of slip angle and it is interesting to note that the lateral force curves for this tyre appear to flatten out at high slip angles. Figure E.2 provides a zoom on the origin of the lateral force versus slip angle graph and clearly shows the offsets due to ply steer and conicity. The variation in cornering stiffness is also evident as is the fact that cornering stiffness is increasing with vertical load. In Figure E.3 the aligning moment is plotted as a function of slip angle and it can be seen that apart from a slight negative value at -9 degrees slip angle and 200 kg load the aligning moments remain positive at high slip angles. In Figure E.5 the lateral force is plotted

161

as a function of camber angle. The curves are approximately linear and the presence of offsets at zero camber angle is more obvious due to the lower lateral forces generated with camber angle variation than those obtained with slip angle variation. The increase in camber stiffness with vertical load is also evident from this plot. It should be noted that these curves have been plotted using the zero slip angle values from slip angle variation tests at fixed camber angles of -5, 0 and 5 degrees thus providing only three points for each curve. An alternative method of testing, as performed with TYRE B, is to fix the slip angle at zero and vary the camber angle over a greater range and provide more measurements to plot.

The Fiala model has been used with data derived from TYRE A using the cornering stiffness measured at the vehicle front wheel load, rear wheel load and the average of these. From Figure E.6 it can be seen that using the Fiala model all the curves of lateral force with slip angle are symmetric for positive or negative values of slip. For the curves at 200 kg of vertical load the lateral force levels out or saturates at about 3 degrees of slip angle while at the higher loads it can be seen that the lateral force is still increasing at 10 degrees of slip angle. The plot shown in Figure E.7 is a zoom on the origin of the lateral force with slip angle plot and confirms that the Fiala model ignores offsets due to conicity or ply steer and that there is no apparent variation in cornering stiffness with load. Figure E.8 plots aligning moment as a function of slip angle and confirms that at very high slip angles the Fiala moment does not consider the possibility for the aligning moment to change sign and simply sets the aligning moment to zero once the critical slip angle has been reached. For a vertical load of 200 kg this point is reached at about 5 degrees and for 400 kg the limit is 10 degrees. For the higher loads the limit is not reached but the aligning moment is reducing after 6 degrees.

Considering the plots obtained using the Pacejka terms for TYRE A it can be seen that in many ways these are quite different than those for the Fiala model. In Figure E.18 it is evident that after the peak values of lateral force are attained the curves show significant signs of flattening out and even decrease slightly at high values of slip angle. Figure E.19 is a zoom on the origin for this set of data and shows clearly that the Pacejka model accounts for vertical and horizontal offsets and that the cornering stiffness is varying with the vertical loads. In this respect the model is clearly more realistic than the Fiala model. In Figure E.20 the aligning

moment is plotted as a function of slip angle for the Pacejka model. It can be seen that these curves are quite different from those obtained using the Fiala model.

Comparing the Pacejka model with the Interpolation model it can be seen from Figures E.1 and E.18 that the Pacejka model develops lateral force more rapidly at lower slip angles. This can be seen at 4 degrees of slip angle where for higher vertical loads the Pacejka model clearly produces higher lateral force than the Interpolation model. It can also be seen from the Pacejka model in Figure E.20 that the aligning moment changes sign at higher slip angles although the Interpolation model shows in Figure E.23 that this does not actually happen with this tyre. Close inspection also reveals that the aligning stiffness varies with vertical load and that peak values are obtained at much lower slip angles than with the Interpolation model. The curves also indicate that the Pacejka model is including vertical and horizontal offsets.

8.2.2 Tyre B

The results obtained using the *CUTyre* System to investigate tyre model performance using data for TYRE B are presented in Appendix F of this report. Figures F.1 to F.5 show the results obtained using an Interpolation tyre model together with the data obtained from testing on the machine at SP Tyres UK Ltd. In Figure F.5 it can be seen that the lateral force offsets at zero camber angle are larger than would be expected reaching 400 N for a vertical load of 800 kg. The same tyre was tested using the flat bed machine at Coventry University for which the results are shown in Figures F.6 to F.9. The smaller machine at Coventry was limited to a range of -6 to +6 degrees of slip or camber angle and a maximum of 600 kg of vertical load. Using this machine much smaller offsets in lateral force were obtained at zero camber angle but using such a large tyre on a small machine it was not possible to produce such smooth curves as those obtained on the SP Tyres machine. In Figure F.9 the danger of using an interpolation routine outside the range of measured data is clearly illustrated. In this case the interpolation has been carried out up to 10 degrees using data only up to 6 degrees. Between 6 and 10 degrees the extrapolation is clearly unstable. This is an example of how useful the *CUTyre* System can be in validating a tyre model before use in a vehicle handling simulation.

163

The plots obtained using the interpolation model for TYRE B have been checked against the plots from the actual rig tests which are shown in Appendix C. Figure F.1 which shows the lateral force curves varying with slip angle provides good agreement for the Fiala model curves which are shown in Figure F.10. The zoom on the origin shown in Figure F.2 indicates a low cornering stiffness at 200 kg and confirms typical tyre characteristics as the cornering stiffness becomes more constant at higher values of vertical load.

The Fiala model has been used with data from TYRE B using the cornering stiffness measured at the vehicle front wheel load, rear wheel load and the average of these. Figure F.10 shows the variation of lateral force with slip angle. The Fiala model seems to be particularly suited to the characteristics of TYRE B where the lateral force continues to increase gradually at higher loads and slip angles. Figure F.11 which shows a zoom on the origin again confirms that the Fiala model does not vary cornering stiffness with load or consider offsets. The curves confirm that the cornering stiffness for TYRE B is lower than that used for the model of TYRE A. Figure F.12 shows the aligning moment curves as a function of slip angle. The agreement with the Interpolation model is reasonable although the peak values tend to be larger and occur at lower slip angles. It is also interesting that the aligning moment does not appear to change sign at higher slip angles for TYRE B.

Considering the Pacejka model for TYRE B the lateral force curves shown in Figures F.22 and F.23 show good agreement with the interpolation model. The aligning moment curves shown in Figure F.24 do not correspond as well as the lateral force curves but appear to be a better representation than the Fiala model in that the maximum values are about the same as the Interpolation model but still occur at lower slip angles. It is again evident that the Pacejka model also changes sign at higher slip angles which does not appear to happen in the test data or with the interpolation model.

8.3 Lane change manoeuvre (Interpolation model - TYRE A)

Appendix G contains plots produced for the lane change manoeuvre. At this stage the four vehicle models were being compared using results from the actual track test to assess the effectiveness of the models. The Interpolation tyre model was used as this was considered to

164

be the closest to using actual measured data. This phase of the study focused therefore on comparing the vehicle modelling without any influence from a tyre model. The data from TYRE A, which was the tyre used during track testing, was used throughout this phase of the investigation.

With the exception of the roll angle predicted by the Lumped Mass model, all three of the simple models appear to perform well when compared with the test data and the Linkage model. Of all the simple models inspection of the results indicates that the Roll Stiffness model consistently provides good agreement. This is particularly evident when comparing the yaw rate time history plots for both the Roll Stiffness and Linkage models shown in Figures G.11 and G.12.

In assessing the accuracy of the models a visual inspection of the graphs gives an initial indication of model performance when comparing the curves from ADAMS with those from the track test. In order to obtain some numerical measure of model accuracy the results were compared at the point in time when the first set of peak values arise. During the simulation the first peak values occur after 0.95 seconds. The results at this point in time were therefore extracted in order to calculate the percentage error when comparing the simulation results with measured test data. These results are shown in Table 8.1.

Table 8.1 Comparison of vehicle model results with track test (Interpolation model - TYRE A)

	Lateral Acceleration		Roll Angle		Yaw Rate	
	(g)	Error (%)	(deg.)	Error (%)	(deg/s)	Error (%)
Track Test	0.600	——	4.50	——	13.00	——
Lumped Mass Model	0.560	-6.7	5.49	22.0	11.92	-8.3
Swing Arm Model	0.549	-8.5	4.46	-0.9	11.92	-8.3
Roll Stiffness Model	0.568	-5.3	4.34	-3.6	12.61	-3.0
Linkage Model	0.585	-2.5	4.65	3.3	13.24	1.8

On the basis of this comparison the Roll Stiffness model compares very favourably with the Linkage model for the results extracted. The Lumped Mass model appears to have a problem in over estimation of roll angle which would also favour selecting the Roll Stiffness model for further studies. Discussions with SP Tyres also indicated the Roll Stiffness model to be favourable due to the capability to use laboratory test facilities to measure parameters for this vehicle model.

8.4 Sensitivity of lane change manoeuvre to tyre data and model

The Linkage model has been used to compare the accurate modelling of a tyre using the Pacejka approach with the more simple formulation of the Fiala model and the benchmark Interpolation model. The results of this investigation are presented in Appendix H. All three tyre modelling methods have been used with data for TYRE A and TYRE B. As usual the ADAMS results are plotted with the track test results for comparison. It should be noted that with TYRE B this is not a true comparison as this was not the tyre fitted during the test but the plots are useful in any case when comparing the different tyre models used with TYRE B. The track test results are plotted with TYRE B to provide a measure for comparing TYRE A and TYRE B and the different tyre models, rather than to correlate TYRE B results with track test results.

The Fiala model does not consider camber angle and the Pacejka parameters provided for TYRE B also did not account for camber. To aid the comparison and judge the influence of camber the interpolation tyre models were run with and without camber. The Pacejka model for TYRE A was also run with and without camber. The effect of omitting camber angle from the model can be discerned by close inspection of the curves but does not appear to be a significant factor in obtaining correlation. Clearly the camber effects are dominated by the forces and moments produced by slip angle when performing this type of manoeuvre and to a certain extent this justifies the use of the simple Fiala model which ignores camber angle.

An important consideration of this study was to establish whether the Roll Stiffness model would provide similar sensitivity to changes in tyre model and tyre data as the Linkage model. Appendix I therefore contains, for the Roll Stiffness model, a repeat of the plots

provided in Appendix H for the Linkage model. To assist with this comparison the results are summarised in Appendix J where results for all three tyre models are plotted on the same graphs. On each page the results for the Linkage model are followed immediately by the results for the Roll Stiffness model to aid the comparison. The results shown in Appendix J indicate that the Roll Stiffness model despite a lack of sophistication performs surprisingly well when compared with the detailed Linkage model. The results in Appendix J again indicate that the effects of including camber thrust in the tyre model appear to be marginal.

In order to assist the various comparisons the results corresponding to the first set of peak values occurring after 0.95 seconds of simulation time have been extracted. Using the results for TYRE A the track test results have again been used as a measure for comparison. With TYRE B the Interpolation tyre model results are used as the benchmark. The results are tabulated in Tables 8.2 to 8.5.

Table 8.2 Comparison of tyre model results with track test (Linkage model - TYRE A)

	Lateral Acceleration		Roll Angle		Yaw Rate	
	(g)	Error (%)	(deg.)	Error (%)	(deg/s)	Error (%)
Track Test	0.600	——	4.50	——	13.00	——
Interpolation Model	0.585	-2.5	4.65	3.3	13.24	1.8
Interpolation Model (No Camber)	0.597	-0.5	4.84	7.6	12.89	-0.9
Fiala Model	0.611	1.8	4.77	6.0	15.13	16.4
Pacejka Model	0.660	10.0	5.48	21.8	14.21	9.3
Pacejka Model (No Camber)	0.663	10.5	5.53	22.9	14.04	8.0

Table 8.3 Comparison of tyre models results with track test (Roll Stiffness model - TYRE A)

	Lateral Acceleration		Roll Angle		Yaw Rate	
	(g)	Error (%)	(deg.)	Error (%)	(deg/s)	Error (%)
Track Test	0.600	——	4.50	——	13.00	——
Interpolation Model	0.568	-5.3	4.34	-3.6	12.61	-3.0
Interpolation Model (No Camber)	0.577	-3.8	4.42	-1.8	12.72	-2.2
Fiala Model	0.591	-1.5	4.46	-0.89	14.73	12.4
Pacejka Model	0.643	7.2	4.84	7.6	13.52	4.0
Pacejka Model (No Camber)	0.642	7.0	4.87	8.2	13.58	4.5

Table 8.4 Comparison of tyre models results (Linkage model - TYRE B)

	Lateral Acceleration		Roll Angle		Yaw Rate	
	(g)	Error (%)	(deg.)	Error (%)	(deg/s)	Error (%)
Interpolation Model	0.554	——	4.41	——	14.84	——
Interpolation Model (No Camber)	0.567	2.3	4.55	3.2	14.67	-1.1
Fiala Model	0.566	2.2	4.40	-0.2	15.47	4.2
Pacejka Model (No Camber)	0.581	4.9	4.68	6.1	15.64	5.4

Table 8.5 Comparison of tyre models results (Roll Stiffness model - TYRE B)

	Lateral Acceleration		Roll Angle		Yaw Rate	
	(g)	Error (%)	(deg.)	Error (%)	(deg/s)	Error (%)
Interpolation Model	0.543	———	4.14	———	14.15	———
Interpolation Model (No Camber)	0.549	1.1	4.20	1.5	14.27	0.8
Fiala Model	0.551	1.5	4.17	0.7	15.07	7.2
Pacejka Model (No Camber)	0.561	3.3	4.27	3.1	15.07	7.2

The numerical comparisons presented when studied in conjunction with the time history plots provided in the Appendices lead to the following:

The Roll Stiffness model is a good model given the level of simplicity when compared with the Linkage model. The Roll Stiffness model is based on 12 rigid body degrees of freedom whereas the Linkage model for this vehicle requires 78. Given also the great reduction in data and modelling effort the Roll Stiffness model appears to be very good value.

When comparing tyre models it is clear that the results for TYRE B show better agreement than those for TYRE A. This is not so much a function of the tyre models but more the tyre characteristics and model parameters. The model based on Pacejka parameters for TYRE A appears to overestimate peak values. This is not due to a flaw in the Pacejka model but rather the lack of accuracy in this set of parameters in fitting the model. Some understanding of this can be obtained by referring again to the tyre curves for this data produced by the CUTyre System and shown in Figure E.18. At higher loads the lateral force reaches a peak value and saturates at lower slip angles, than is evident with the Interpolation

model curves shown in Figure E.1. In order to improve the agreement it would be necessary to iterate on the derivation of the Pacejka coefficients until a more realistic set were obtained for TYRE A and then repeat the simulations.

The Interpolation tyre models used here have as expected given good results. Although these models are no longer fashionable and have little use in design studies they have proven useful for benchmark comparisons and validations of other tyre models. As such they are a useful component within the *CUTyre* System.

The Interpolation models have also proven useful in determining the influence of omitting camber angle effects from a tyre model. On the evidence of this study the effect seems small and certainly appears to be dominated by the quality of the model and parameters used to fit the tyre lateral force characteristics as a function of slip angle.

The results for TYRE B provide very good agreement due to the following. The Pacejka coefficients provided give a much better fit for this model than those given for TYRE A. This can be seen by comparing the plots produced by the *CUTyre* System in Appendix F. In this case the Pacejka model curves for lateral force shown in Figure F.22 show good agreement with the Interpolation model shown in Figure F.1. Corresponding with this the results for the lane change also show good agreement despite the fact that camber is again not represented in this tyre model.

The characteristics of TYRE B also seem to suit the simple Fiala tyre model as can be seen by the good agreement shown in Figure F.10. This tyre has the characteristic that the lateral force curves do not flatten out at higher loads which appears to assist when getting a good fit with the Fiala model. For this sort of tyre and others with similar characteristics produced by SPTYRES UK the implication at this stage would appear to be that the Roll Stiffness model and the Fiala tyre model would provide, in association with the *CUTyre* System, a useful set of tools to investigate the influence of tyre design changes on handling simulation outputs.

170

As a final step at this stage of the investigation it was decided to examine results for the tyres and to compare the Roll Stiffness model and the Linkage model. An important aspect of using a simplified vehicle model such as the Roll Stiffness model is the accuracy obtained in the prediction of the vertical load, slip angle and camber angle for each road wheel. These outputs from the vehicle model become inputs to whatever tyre model is chosen and are hence highly significant in terms of the overall simulation model. Using results obtained with an Interpolation model of TYRE B a direct comparison of the Linkage and Roll Stiffness models can now be made. In Figure 8.1 it can be seen that the Roll Stiffness model with a maximum value of about 1.5 degrees underestimates the amount of camber angle produced during the simulation when compared with the Linkage model where the camber angle approaches 5 degrees. Clearly the Roll Stiffness model does not have a camber degree of freedom relative to the rigid axle parts and the camber angle produced here is purely due to tyre deflection.

More importantly though the slip angle comparison shown in Figure 8.2 shows good agreement. It is worth remembering that the slip angle at the front wheels is determined by the transfer of the steering inputs through the suspension to the road wheel. The Linkage model accounts for changes in steering ratio as the vehicle rolls whereas the Roll Stiffness model assumes a constant ratio. Future studies may require more detailed investigations in this area as an accurate prediction of slip angle is clearly a critical factor in the model. The inaccuracy in the Roll Stiffness model with regard to camber angle will have no effect here with the Fiala model as the current formulations here ignore the influence of camber angle. Future studies may however focus on extending the Roll Stiffness model to refine this area of prediction.

The comparison of tyre load for all four tyres shown in Figures 8.3 to 8.6 also show good agreement. This shows that the weight transfer in the Roll Stiffness model agrees well with the Linkage model. A consideration which could be noted at this stage is that the Roll Stiffness model does not include the pitch of the body relative to the wheels as would be present in the Linkage model. For this simulation involving pure lateral slip that modelling decision appears to be justified. An extension of this work to braking or combined slip situations would need to investigate if this was still justified. Figures 8.3 to 8.6 also confirm that there is at no time any loss in tyre contact at any wheel during this aggressive manoeuvre.

FRONT RIGHT TYRE - 100 KPH LANE CHANGE
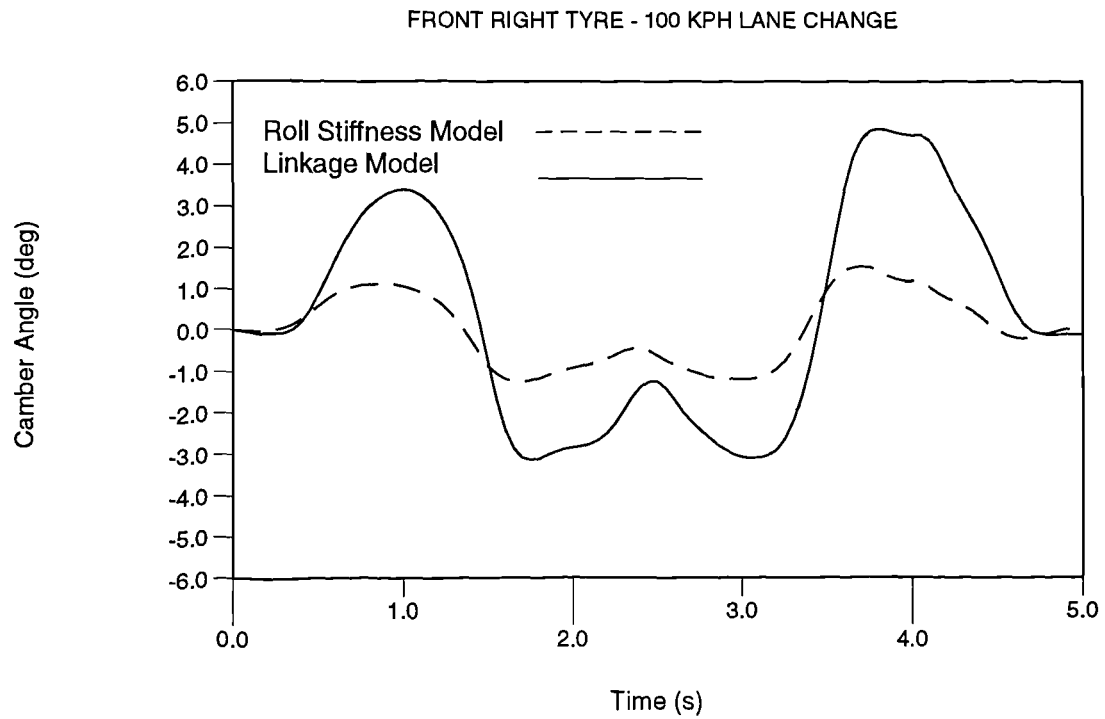
Figure 8.1 Camber angle comparison - linkage and roll stiffness models

FRONT RIGHT TYRE - 100 KPH LANE CHANGE
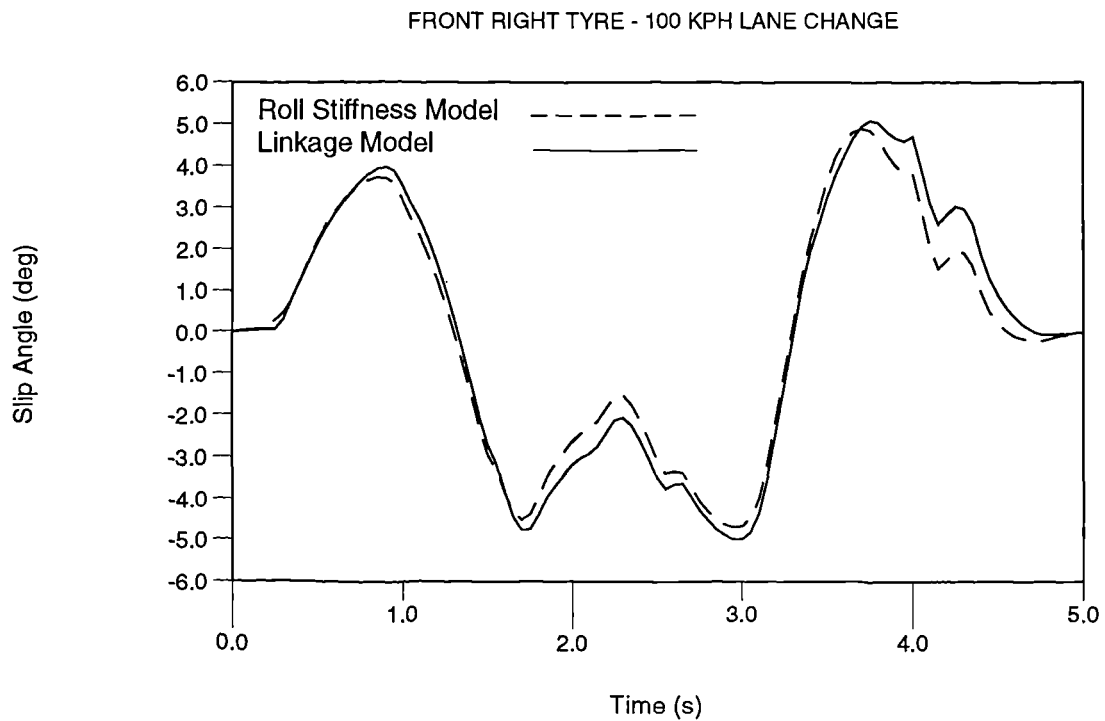
Figure 8.2 Slip angle comparison - linkage and roll stiffness models

172

FRONT RIGHT TYRE - 100 KPH LANE CHANGE
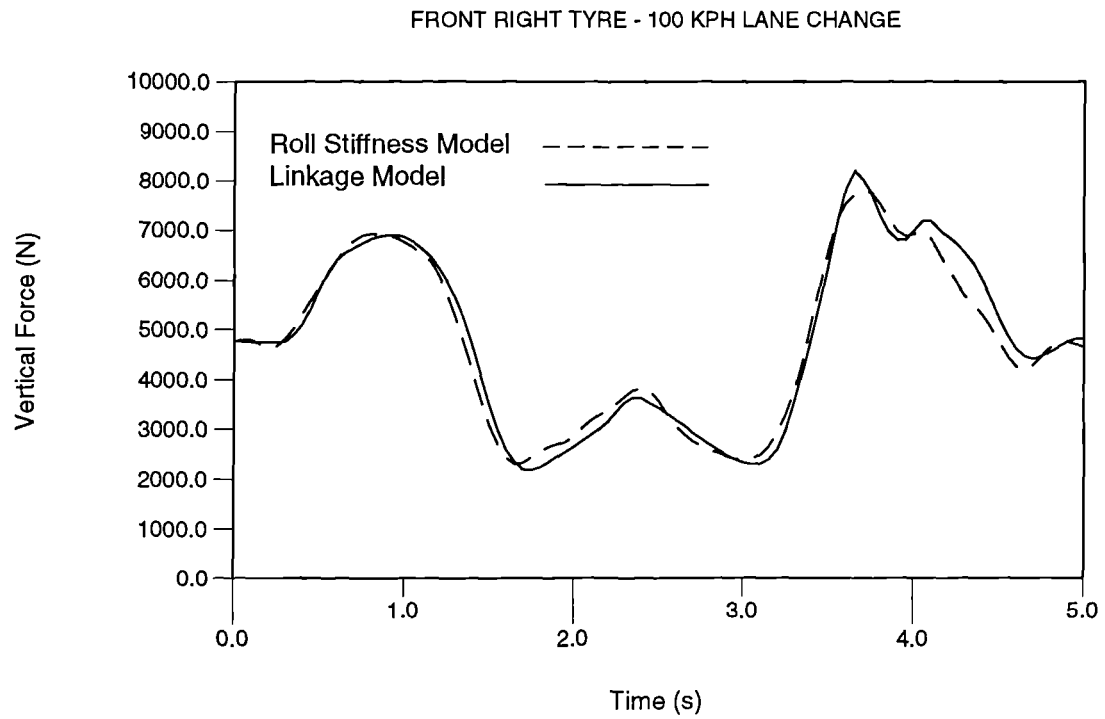
Figure 8.3 Vertical tyre force comparison - linkage and roll stiffness models

FRONT LEFT TYRE - 100 KPH LANE CHANGE
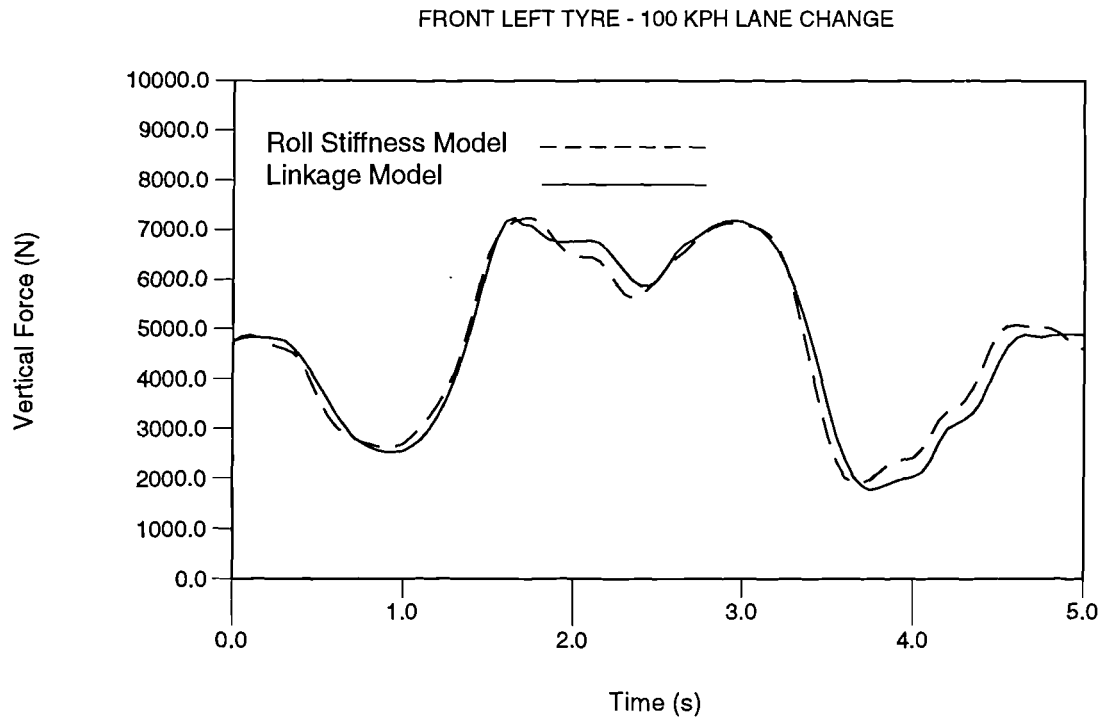
Figure 8.4 Vertical tyre force comparison - linkage and roll stiffness models

REAR RIGHT TYRE - 100 KPH LANE CHANGE
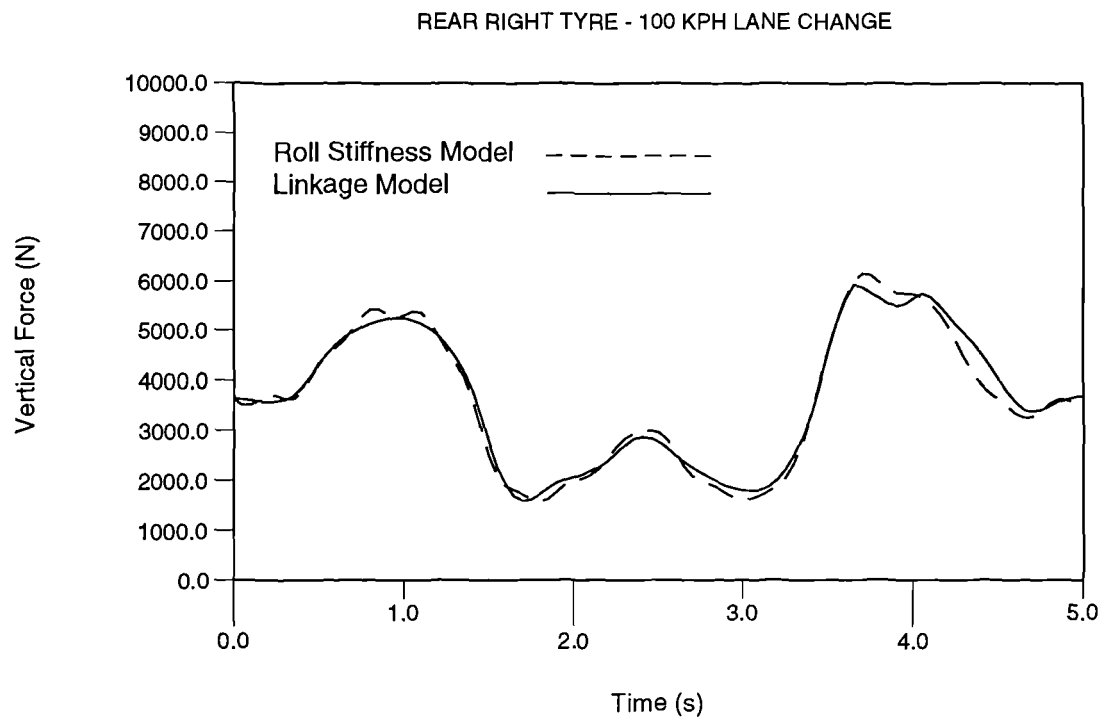
Figure 8.5 Vertical tyre force comparison - linkage and roll stiffness models

REAR LEFT TYRE - 100 KPH LANE CHANGE
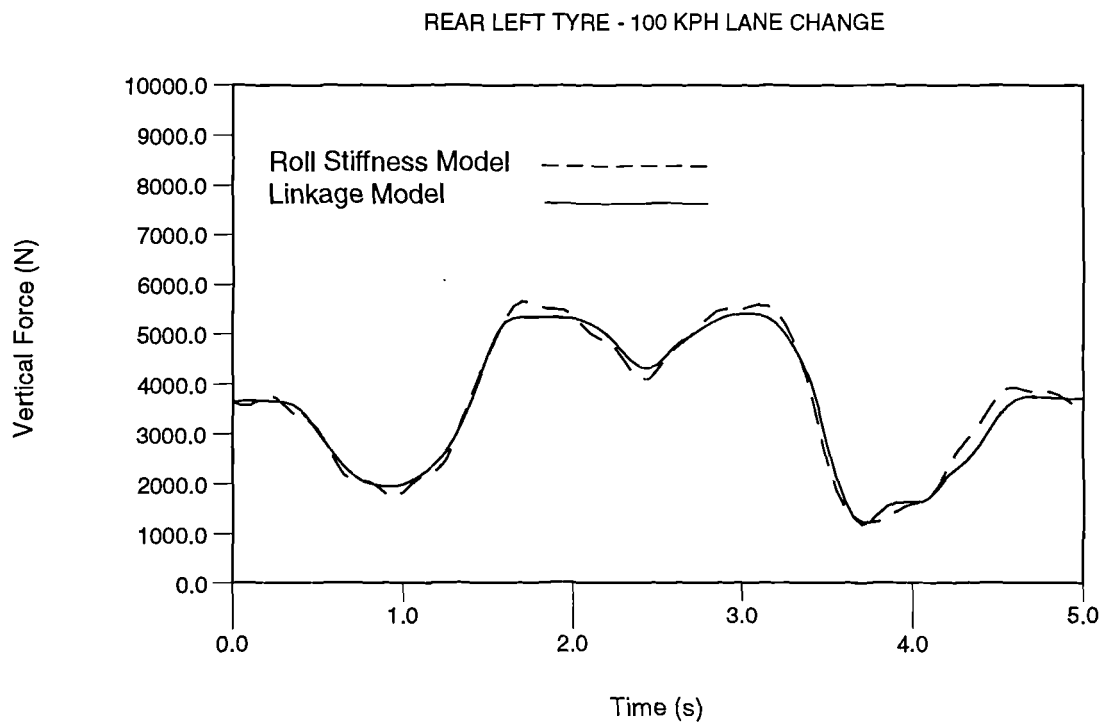
Figure 8.6 Vertical tyre force comparison - linkage and roll stiffness models

174

A general observation from the study was that the comparison of vehicle and tyre models was less accurate towards the end of the manoeuvre. In the simulation, this period is between 4 and 5 seconds as the vehicle pulls out of the last turn having reached a lateral acceleration of about 0.8g. This is particularly noticeable when comparing the results provided in Appendix J where different tyre models have been used with data for TYRE B. A further examination of the steering inputs measured during the track test and used as inputs to the simulation models shows that these are quite extreme in order to control the vehicle as it approaches the limit of stability. The severity of these steering inputs can be seen by comparing the steering inputs measured for the same lane change manoeuvre but at a reduced speed. This is illustrated in Figure 8.7 where the steering inputs at 70 kph are compared with those used in this study at 100 kph.

STEERING INPUT - LANE CHANGE MANOEUVRE
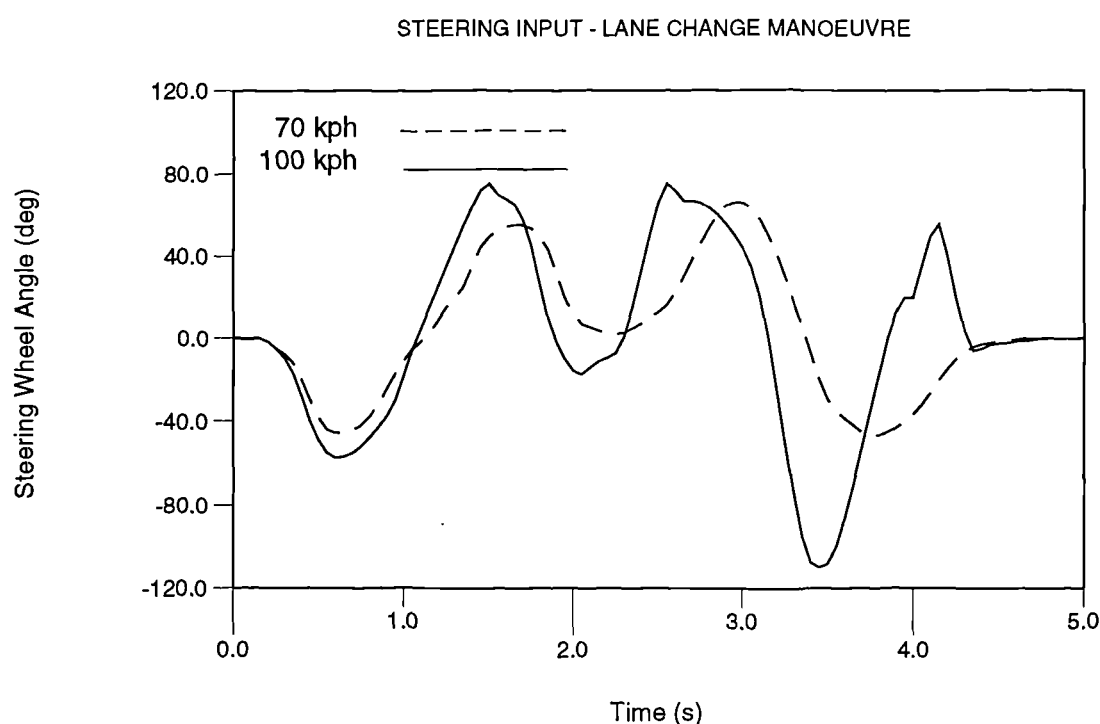
Figure 8.7 Comparison of steering inputs at different speeds

As can be seen the steering inputs at the reduced speed are much smoother. It can also be seen that in order to control the vehicle at 100 kph there is an additional "overshoot" in the steering input after 4 seconds. Future studies could extend the investigation in two ways. The first of these would investigate the accuracy of the models using less extreme manoeuvres such

175

as the 70 kph lane change shown here. The second extension of the work could move in the other direction comparing models for manoeuvres approaching the limit of stability and possibly involving the spin out or roll over of vehicles.

8.5 Final sensitivity studies

The final set of studies carried out in this project involved demonstrating how the combination of the simple roll stiffness vehicle model and the simple Fiala tyre model could be used to carry out handling sensitivity studies at potentially very early stages in the design of the tyre and the vehicle. The results of this investigation are included in Appendix K and involve parametric design variations to both vehicle data parameters and tyre data parameters. All the comparisons have been carried out using the SP Tyres data for TYRE B.

The first set of variations concentrate on looking at a range of values for individual parameters in the Fiala data file. In Figure K.1 the yaw rate has been plotted to indicate the change in vehicle response for systematic changes in cornering stiffness. The plots indicate that going from low to high cornering stiffness leads to increased rates of change in yaw rate and could indicate the sort of design variations investigated in establishing how responsive a vehicle is.

In Figure K.2 the yaw rate has again been plotted where in this case the coefficient of tyre to road surface friction has been varied. The plots indicate that at lower coefficients of friction which could be those associated with water or ice contamination of road surfaces there is a loss of stability which will lead to the vehicle "spinning out" at very low values.

In Figure K.3 the roll angle has been plotted to show the effects of reducing the radial stiffness of the tyres. This could perhaps be considered also as investigating a reduction in tyre pressures. The resulting increase in roll angle can be seen when the radial stiffness is reduced from the standard value to one which is one half of that.

In Figure K.4 the first in the series of vehicle parameter changes is demonstrated where the effects on the roll angle have been established for the situation where the mass centre of the

vehicle is raised by 100 mm. This sort of situation could be considered to represent a case for a particular vehicle where loads are carried by a roof rack altering the mass centre position.

In Figure K.5 the effects of moving the roll axis of the vehicle have been demonstrated. The roll angle is plotted for the roll axis in the original position and then in a situation where the roll axis is at ground level. This is a situation which theoretically corresponds to a parallel link suspension. It should be noted that this change in model parameter was easy with the Roll Stiffness model but would require quite a bit of effort to modify the ADAMS data set for a Linkage model which includes all the suspension geometry.

The final demonstration of a vehicle design parameter change was influenced by another current research programme within the School of Engineering at Coventry University and involves track testing with a Rover vehicle (90). Early indications from that programme of work and based on subjective assessments are that a small amount of toe in at the rear wheels can lead to an improved handling feel or response of the vehicle. By way of example this has also been considered in Figure K.6 where the effects of one degree of toe in or toe out are compared with the zero toe angle case. The plot indicates that with one degree of toe in the vehicle develops yaw rate more rapidly which may be indicative of a more responsive vehicle.

8.6 The effect of model size on computer simulation time

This final section has been instigated by consistent reference in many publications to the effects of inefficient modelling practices on computer simulation time. The information summarised in Table 8.6 was presented in (91). These times are based on some initial work during this study where a control response manoeuvre was simulated at 60 kph. The times are for simulations running on a Viglen 4DX266 personal computer. The Fiala tyre model was used with data for TYRE A.

Table 8.6 Computer simulation times for a 60 kph control response manoeuvre

Model	Degrees of freedom	Number of Equations	CPU Time (s)
Linkage	78	961	146.0
Lumped Mass	14	429	108.0
Swing Arm	14	429	93.0
Roll Stiffness	12	265	68.0

The comparison shown in Table 8.7 is for the lane change carried out in this study. These times are based on the simulations presented in Appendix G where the four vehicle models have been run with an Interpolation model of TYRE A.

Table 8.7 Computer simulation times for a 100 kph lane change manoeuvre

Model	Degrees of freedom	Number of Equations	CPU Time (s)
Linkage	78	961	301.0
Lumped Mass	14	429	160.0
Swing Arm	14	429	188.0
Roll Stiffness	12	265	90.0

As can be seen from these comparisons the computer simulation time can not be scaled directly from the model size and does not scale directly from one sort of simulation to another. It is encouraging to note however, that the best performance is by the Roll Stiffness model which for the lane change runs more than three times faster than the Linkage model. This is clearly beneficial where a model is to be used in design studies involving parametric variations and repeated simulation runs.

Another comparison made in Table 8.8 shows the effect of the chosen tyre model when running this lane change simulation with both the Linkage and Roll Stiffness models. The data is again based on the study involving TYRE A.

Table 8.8 Computer simulation times for varying tyre models - 100 kph lane change

Tyre Model	Linkage model	Roll Stiffness model
Fiala	255.0 s	88.0 s
Pacejka	270.0 s	91.0 s
Interpolation	301.0 s	90.0 s

It is again interesting to note that the times for the different tyre models do not scale directly between the two vehicle models. The times for the Linkage model are as expected with the simple Fiala model running fastest and the Interpolation model taking the longest time. For the Roll Stiffness model the effect of changing tyre model appear to have negligible effect. A possible explanation for this is that the efficiency of the Roll Stiffness model means that simulation times are dominated by overheads, such as file handling or calling the tyre model subroutine, which are less significant for longer runs with more complex models.

9.0 CONCLUSIONS AND RECOMMENDATIONS

9.1 Conclusions

Based on the investigations and studies which have been carried out and are described in this thesis the following conclusions are offered:

(i)   From the literature review it is apparent that the use of relatively new computer based methods such as multibody systems analysis is still evolving as a working tool in the solution of problems in vehicle dynamics. Experiences in industry, and the literature reviewed indicate that the practice of modelling suspensions in very fine detail has often been followed when a simpler and more efficient modelling strategy may have been possible. It is likely that the issue of accurate vehicle modelling will be debated for some time with two possible streams of thought.

(a) The first of these will be that any model should be the most efficient for any given type of simulation and therefore likely to be the most useful for making rapid design decisions.

(b) The second approach is that a single detailed model could act as a database and be used for the full range of simulations needed to support vehicle design, but will be inefficient and less likely to assist with positive design decisions in any one application.

Vehicle engineers who use sophisticated analysis tools such as ADAMS will be encouraged by the capability of these programs to build complicated models. The main thrust of this thesis has been to follow the first approach and demonstrate the use of models which are as simple and efficient as possible in order to achieve the desired accuracy for the simulation under consideration.

(ii) On the issue of model simplification for vehicle handling, the focus from the literature appears to be on the actual vehicle and mainly the suspension systems. The effects of model simplification in the tyre does not seem to have received the same level of discussion. In addition to this, research in the field of tyre modelling has led to the development of complex and accurate tyre models which are widely accepted. The publications associated with this type of work appear in the main to concentrate on comparing the fit of tyre model data with tyre test data rather than demonstrating the accuracy of the tyre model when used for a given vehicle handling simulation. This has been one of the main areas this thesis has attempted to address.

(iii) An initial investigation of suspension modelling procedures has been carried out here with the particular emphasis on the influence of modelling the compliance in the bushes and the effect on suspension kinematics during movement between bump and rebound positions. It has been noted that for a full vehicle model based on linkages, the kinematic method of modelling suspensions is not always possible and that has proven to be the case here with the rear suspension on this vehicle. The modelling of suspensions using a rigid joint representation may became more difficult as modern multi-link suspensions gain popularity. The development of suspensions such as these has lead to the situation that they depend on the compliance in the bushes to control the way they move and will therefore create a greater need to obtain detailed bush information to support computer simulations.

(iv) It has been shown here that there is a large increase in modelling effort and also a greatly increased chance of modelling or data errors when moving from a simple rigid joint representation through to models using linear and non-linear bushes. For the Linkage model considered here a rigid joint representation would not work due to the geometry steer characteristics of the rear suspension.

(v)   It has been shown here that the modelling of the steering system needs careful consideration if the suspension linkages are not modelled. Attaching the rack to a simplified suspension model via a tie rod is not effective due to the introduction of steer changes during the initial static equilibrium analysis. It has been shown that it is necessary to use a mathematical coupling ratio in the steering model to overcome this. This method does not account for geometry steer and will require further study with other vehicle models.

(vi)   A method to obtain both the front and rear roll stiffness from a detailed ADAMS model has been demonstrated. In practice vehicle engineers should be able to make an estimate of the roll stiffness during initial design studies or take measurements off an actual vehicle at a later stage. The method used here will hold good however, should a detailed ADAMS model be available during the vehicle design process.

(vii)   For vehicle handling simulations it has been shown here that simple models such as the Roll Stiffness model can provide good levels of accuracy. It is known however, that roll centres will "migrate" as the vehicle rolls, particularly as the vehicle approaches limit conditions. The plots in Appendix B show the vertical movement of the roll centre along the centre line of the vehicle as the suspension moves between bump and rebound. On the complete vehicle the roll centre will also move laterally off the centre line as the vehicle rolls. For the simulations carried out here the fixed roll centre model appears to have worked well despite approaching the lateral accelerations of 0.8g and roll angles of 6 degrees or more.

(viii) A new computer system has been developed as part of this project to handle tyre models and is referred to as the *CUTyre* System. The system includes a range of FORTRAN subroutines which can be used to model tyre characteristics and then interface with the main ADAMS program. The *CUTyre* rig model has been developed and has proven to be useful during this study by providing a graphical check on tyre models and tyre data before integrating these into a full vehicle handling simulation.

(ix)   The Interpolation models generated here were used to show that ignoring camber does not appear to have a significant effect on the accuracy of the simulation. This was a useful discovery since the Fiala model does not include camber effects and it has also been shown here that the Roll Stiffness model does not give a good prediction of road wheel camber compared with the Linkage model. The results for TYRE B give a good correlation between all three models and would indicate that for this sort of simulation the Fiala model is highly suitable in terms of accuracy and the limited number of parameters required. One of the main outcomes of this project has been to show that the Roll Stiffness model combined with the Fiala tyre model compares well with the Linkage model combined with the Pacejka tyre model, although caution should be exercised as further investigation is needed before assuming these modelling strategies can be used with other vehicles and manoeuvres.

(x)   An interesting discovery during this study has been the effect of the modelling approach on computer simulation times. Criticisms in the literature surveyed, of complicated models running in programs such as ADAMS consistently identify excessive computation time as one of the drawbacks. From this study the computer times on a personal computer do not appear excessive given the complexity of the problem being solved. The Roll Stiffness model produces the lowest times which should prove useful for design applications.

(xi)   In summary this study has attempted to make an original contribution in the field of vehicle dynamics by:

(a) Comparing suspension models for a full vehicle handling simulation and establishing using ADAMS the influence of model simplifications on predicted outputs.

(b) Developing the *CUTyre* System to provide institutions and companies such as SP Tyres UK with tools which will validate tyre models and model parameters and interface these with an ADAMS full vehicle model.

(c) Comparing Interpolation tyre models, the Pacejka model and the Fiala model and establishing using ADAMS the influence of tyre model selection on the results of a handling simulation.

9.2 Recommendations

Following on from the work described in this thesis there are a number of avenues of further research and development which could be followed:

(i)   For the simulations carried out here the fixed roll centre model appears to have worked well despite approaching lateral accelerations of 0.8g and roll angles of 6 degrees or more. Future studies could investigate how well this modelling approach transfers to other designs of vehicle and also to consider the modelling issues involved with considering a moving roll centre during a simulation. An extension of the model to include camber change of the road wheel could also be considered with a view to more detailed study of the influence of camber angle for different vehicles and manoeuvres.

(ii)   For handling simulations a suspension modelling approach which has not been considered here but may form the basis of future studies is a method sometimes referred to as using suspension derivatives. This approach is conceptually more accurate than the three simple modelling approaches used here and involves modelling the road wheel and suspension as a single rigid body. The movement and change in orientation of this body relative to the vehicle body is controlled in the same way as it would be if the full suspension linkages were modelled. From an individual quarter suspension model it is possible to establish the path in space that the wheel centre follows and also to establish the change in angles such as camber and steer as the wheel moves along this path. These measurements could also be obtained by laboratory testing. The rates at which these angles change with vertical movement can be thought of as the suspension derivatives. The derivatives could be obtained for example, by considering the gradients at the origin of plots from individual suspension studies such as those shown in Appendix B. The advantage of a modelling approach such as this is that as with the roll stiffness model it involves parameters that vehicle engineers could estimate early in a design before the detailed suspension geometry is established, or otherwise could be measured in the laboratory at a later stage when the vehicle exists. Future studies could focus on investigating the derivation of these models and establishing for what sort of manoeuvres there could be an advantage over the roll stiffness model used here.

(iii)   It has been shown in this project that detailed modelling of suspension linkages and bushes can be avoided by using a simplified model for the lane change simulation. Future studies can extend this to consider if the assumptions are valid for simulations including features such as ABS with braking and cornering on uneven ground. If other simulations do prove to have dependence on the properties of bushes to produce accurate outputs this raises some questions which could be the subject of future studies such as:

(a)   It may be necessary to establish for extreme variations between hot and cold temperature, the effects on the characteristics of a bush, and the subsequent vehicle performance.

(b)   During the life of a vehicle bushes will be subject to ageing and general wear which will alter their properties. Future maintenance may also involve using non original replacement bushes. Investigations could be carried out in order to establish whether this would have an effect on suspension and vehicle performance.

(iv)   It should also be noted that the work carried out here is for quite extreme manoeuvres which could be said to be more associated with handling stability rather than handling "feel". Future work needs to consider manoeuvres where the perturbations to vehicle motion may only be slight, and establish the level of modelling complexity required to obtain useful feedback. It is likely that this would involve some monitoring of steering reaction torques together with vehicle responses such as yaw rate. The challenge with these sort of studies will be to correlate the objective outputs from a computer simulation with the subjective assessments of good vehicle handling feel.

(v)   The *CUTyre* System could be developed further and enhanced so as to provide a tool for engineers at companies such as Rover Group and SP Tyres UK Ltd. Some of the developments which could be considered are:

(a) The set of subroutines could be combined into one *CUTyre* subroutine which holds all the tyre models. The appropriate model could be selected based on a parameter inside the ADAMS data set that identifies which tyre model the subroutine should use.

(b) A FORTRAN program could be developed which can read the tyre test data files produced by SP Tyres UK Ltd. The program could automatically derive the Fiala model terms and generate a Fiala tyre property file. In a similar manner the program could be used to generate the ADAMS spline data which is needed for an interpolation model. Developments such as this could augment the existing routines at SP Tyres UK Ltd. which can generate the terms for Version 3 of the Pacejka tyre model.

(c) This project has demonstrated how tyre design parameters could be varied in order to investigate the influence of tyre design changes on vehicle performance. A potential extension of this capability could be developed around the current *CUTyre* System. At the moment it is possible to develop a set of tyre plots from a starting point of all three models discussed here, where the interpolation model can be considered to represent the raw test data. An advanced development of this would allow the tyre designer to distort the shape of the curves on the computer screen using point, click and drag type mouse operations. The plotting program developed could also provide numerical updates on the screen of how curve distortions change relevant tyre design parameters such as cornering stiffness in the Fiala model data. This would allow an experienced tyre designer to modify the curves until the desired appearance was obtained and then submit the tyre model and automatically perform the vehicle simulation. Given the rapid increases in computer hardware the turn around time for such interactive procedures is constantly reducing making the proposed system a feasible extension of the work described here.

186

(vi)   From the work carried out here it can be seen that the Fiala model does not consider the change in sign of aligning moment at high slip angles. For any future work where advanced simulations attempt to assess the 'feel' of a vehicle this may be important. The transition in aligning moment may produce a steering feeling which appears to lose stiffness or is suddenly 'free'. More work is needed in this difficult area and the Pacejka model would have an advantage here. Additional studies could also consider modifying the Fiala subroutine provided in Appendix D to improve the aligning moment formulation.

(vii)   As this work has been restricted to pure slip conditions a natural extension would appear to be the case of combined slip during simultaneous cornering and braking. Although the Pacejka model can deal with this the Fiala model can not. Future work could focus on identifying the most efficient combination of vehicle and tyre model for this situation and could possibly even involve enhancing the Fiala model to cater for this.

(viii) There is substantially more data associated with the Linkage model than with the Roll Stiffness model. Future work could focus on even further simplification using a parameter based Roll Stiffness model which requires the very minimum of input information such as track and wheelbase to generate the model.

(ix)   It has been demonstrated that using the simple combination of the Roll Stiffness model and the Fiala tyre model design sensitivity studies can be carried out. Of particular interest may be the study carried out where the rear toe in angle of the wheels was varied. As mentioned in Section 8 this study was prompted by a parallel research project (90) within the School of Engineering at Coventry University. This project involves track testing with a Rover vehicle and making subjective assessments and objective measurements of as to how changes such as the toe in angle effect handling quality. Future work could include using the Roll Stiffness model and the Fiala tyre model to represent this vehicle, and to recreate the track manoeuvres in ADAMS. Using manoeuvres such as the lane change described here it should be possible to compare ADAMS outputs such as yaw rate or yaw acceleration with measured data and the subjective test assessments.

REFERENCES

1. **Ryan, R.** ADAMS - Multibody Systems Analysis Software. *Multibody Systems Handbook/W. Schielen (Editor), Springer-Verlag, Berlin, 1990.*

2. **Gillespie, T. D.** Fundamentals of Vehicle Dynamics. *SAE Publications, Society of Automotive Engineers, 400 Commonwealth Drive, Warrendale, PA 15096, USA.*

3. **Orlandea, N. and Chase, M.** Simulation of a Vehicle Suspension with the ADAMS computer program. *SAE paper 770053, Society of Automotive Engineers, 400 Commonwealth Drive, Warrendale, PA 15096, USA, 1977.*

4. **Rai, N.S. and Soloman, A.R.** Computer simulation of suspension abuse tests using ADAMS. *SAE paper 820079, Society of Automotive Engineers, 400 Commonwealth Drive, Warrendale, PA 15096, USA, 1982.*

5. **Blundell M.V.** Full vehicle modelling and simulation using the ADAMS software system. *IMechE Paper C427/16/170, Autotech '91, Birmingham, November 1991.*

6. **Antoun, R. J., Hackert, P. B., O'Leary, M.C., Sitchen, A.** Vehicle dynamic handling computer simulation - Model development, correlation, and application using ADAMS. *SAE paper 860574, Society of Automotive Engineers, 400 Commonwealth Drive, Warrendale, PA 15096, USA, 1986.*

7. **Sharp, R.S.** Computer codes for road vehicle dynamic models. *IMechE Paper 427/16/064, Autotech '91, Birmingham, November 1991.*

8. **Bakker E., Nyborg L. & Pacejka, H.B.** Tyre modelling for use in vehicle dynamics studies, *SAE paper 870421, Society of Automotive Engineers, 400 Commonwealth Drive, Warrendale, PA 15096, USA, 1986.*

9. **Bakker E., Pacejka H.B. & Linder L.** A new tyre model with application in vehicle dynamics studies, *SAE paper 800087, 4th Auto Technologies Conference, Monte Carlo, 1989.*

10. **Pacejka H.B. & Bakker E.** The magic formula tyre model, Tyre models for vehicle dynamic analysis: *Proc. 1st international colloquium on tyre models for vehicle dynamic analysis, ed. H. B. Pacejka, Swets & Zeitlinger, Lisse, 1993, pp. 1-18.*

11. **Fiala, E.** Seitenkrafte am rollenden Luftreifen, *VDI-Zeitschrift 96, 973, 1954.*

12. **Mechanical Dynamics Inc.** ADAMS/Tire (6.1) User's Manual, *Mechanical Dynamics Inc., 2301 Commonwealth Blvd., Ann Arbor, Michigan, USA, October 1992.*

13. **Crolla, D.A.** Vehicle dynamics - theory into practice, *Automobile Division Chairman's Address, IMechE, 1995.*

14. **Segel, L.** Theoretical prediction and experimental substantiation of the response of the automobile to steering control, *Proc. of Automobile Division, IMechE, 1956-57, pp310-330.*

15. **Segel, L.** An overview of developments in road vehicle dynamics: past, present and future, *Proc. IMechE Conference on "Vehicle Ride and Handling", London, 1993, pp 1-12.*

16. **British Standards Institution,** BS AU 189: Steady state cornering behaviour for road vehicles, *British Standards Institution, 2 Park Street, London, W1A 2BS.*

17. **British Standards Institution,** BS AU 205: Effect of braking on steady state cornering behaviour of road vehicles, *British Standards Institution, 2 Park Street, London, W1A 2BS.*

18. **British Standards Institution,** BS AU 230: Methods of test for lateral transient response behaviour of passenger cars, *British Standards Institution, 2 Park Street, London, W1A 2BS.*

19. **International Organization for Standardization,** Road vehicles - Test procedure for a severe lane-change manoeuvre, ISO/TR 3888 - 1975 (E), *International Organization for Standardization, 1975.*

20. **Rover Group.** Internal Rover Report No: MBK 90488, Rover Handling Tests Supplementary Data, *23 April 1990.*

21. **Schielen, W.** (Editor) Multibody Systems Handbook. *Springer-Verlag, Berlin, 1990.*

22. **Blundell M.V., Phillips B.D.A. and Mackie A.** The role of multibody systems analysis in vehicle design. *Journal of Engineering Design, Vol. 7, No. 4, pp. 377-396, December 1996.*

23. **Hogg S.S., Dickison J.G., Maddison S.J., Yardley A.J.** Design and prediction of vehicle handling and stability, *IMechE paper C389/122, FISITA92, 1992.*

24. **Pilling, M.** Tyres from the car's point of view, *Institute of Materials, Wolverhampton, February 1995.*

25. **Crolla D.A., Horton, D.N.L., Brooks, P.C., Firth, G.R., Shuttleworth, D.W., Yip, C.N.** A systematic approach to vehicle design using VDAS (Vehicle Dynamics Analysis Software), *SAE paper 940230, Society of Automotive Engineers, 400 Commonwealth Drive, Warrendale, PA 15096, USA.*

26. **Sayers, M.W.** Automated formulation of efficient vehicle simulation codes by symbolic computation (AUTOSIM), *Proceedings 11th IAVSD Symposium of Vehicles on Roads and Tracks, Kingston, Ontario, Swets and Zeitlinger, Lisse, 1990.*

27. **Wittenburg, J. and Wolz, U.** MESA VERDE: a symbolic program for non-linear articulated rigid body dynamics. *Proceedings of Tenth ASME Design Engineering Division Conference on Mechanical vibration and noise, Cincinnati, 1985 (ASME).*

28. **Austin, A. and Hollars, M.G.** Concurrent design and analysis of mechanisms. *Kinematics and Dynamics of Multi-body Systems Seminar (S057), I.Mech.E., November 1992.*

29. **Crolla, D.A., Horton, D. & Firth, G.** Applications of multibody systems software to vehicle dynamics problems, *Kinematics and Dynamics of Multi-body Systems Seminar (S057), I.Mech.E., 1992.*

30. **Costa, A.N.** Application of multibody systems techniques to vehicle modelling. *Colloquium Model Building Aids for Dynamic Simulation, IEE Digest No. 1991/196, 1991.*

31. **Holt, M.J. and Cornish, R.H.** Simulation tools for vehicle handling dynamics, *Kinematics and Dynamics of Multi-body Systems Seminar (S057), I.Mech.E., November 1992.*

32. **Holt, M.J.** Simulation tools for vehicle handling dynamics, *Multi-body System dynamics Codes for Vehicle Dynamics Applications Seminar (S275), I.Mech.E., 1994.*

33. **Cherry, A.** Vehicle Modelling for Automotive control studies using SD/FAST, ACSL and MATLAB, *Multi-body System Dynamics Codes for Vehicle Dynamics Applications Seminar (S275), I.Mech.E., 1994.*

34. **Kortum, W., Sharp, R.S. & de Pater, A.D.** Application of multibody computer codes to vehicle system dynamics, *Progress Report to the 12th IAVSD Symposium on a Workshop and Resulting Activities, Lyon, 1991.*

35. **Kortum, W., Sharp, R.S.** (Editors), Multibody computer codes in vehicle system dynamics, *Supplement to Vehicle System Dynamics, Volume 22, 1993.*

36. **Sharp, R.S.** Review of Currently Available Codes - Benchmarking Attempt, *Multi-body System Dynamics Codes for Vehicle Dynamics Applications Seminar (S275), I.Mech.E., 1994.*

37. **Anderson, R. J. and Hanna, D.M** Comparison of three vehicle simulation methodologies. *Proceedings 11th IAVSD symposium 1989.*

38. **Sharp, R.S.** Use of the symbolic modelling code AUTOSIM for vehicle dynamics, *School of Mechanical Engineering, Cranfield University, 1997.*

39. **Sayers, M.W.** Computer modelling and simulation of vehicle dynamics, *UMTRI Research Review, Volume 23, Number 1, July 1992.*

40. **Mousseau, C.W., Sayers, M.W. and Fagan** D.J. Symbolic quasi-static and dynamic analyses of complex automobile models. *In The dynamics of vehicles on roads and on tracks (Ed. G. Sauvage), Proceedings of the Twelth IAVSD Symposium, 1992, pp. 446-459 (Swets and Zeitlinger, Lisse).*

41. **Allen, R.W., Rosenthal, T.J. and Szostak, H.T.** Steady State and Transient Analysis of Ground Vehicle Handling, *SAE Paper 870495, Society of Automotive Engineers, 400 Commonwealth Drive, Warrendale, PA 15096, USA, 1987.*

42. **Tandy, K., Heydinger, G.T., Christos, J.P. and Guenther, D.A.** Improving vehicle handling simulation via sensitivity analysis, *IMechE paper C389/396, FISITA92, 1992.*

43. **Ross-Martin, T.J., Darling, J. and Woolgar, R.** The simulation of vehicle dynamics using the roll centre concept, *IMechE paper C389/047, FISITA92, 1992.*

44. **Dixon J.C.** The roll-centre concept in vehicle handling dynamics, *Proc. IMechE, Vol. 210 No. D1, pp 69-78, 1987.*

45. **Coovert, D.A., Chen, H.F. and Guenther, D.A.** Design and operation of a new-type suspension parameter measurement device, *SAE paper 920048.*

46. **Whitehead, J.** Rig measurement to aid suspension design and development, *MIRA report MIRA-9524-KC3-02, MIRA, June 1995.*

47. **Blundell M.V.** Automatic dynamic analysis of mechanical systems. *Proc. Computer Vision UK Users Group - Summer Conference, Birmingham, June 1990.*

48. **Chace, M.A.** Modeling of Dynamic Mechanical Systems, *CAD/CAM Robotics and Automation Institute, Tucson, Arizona, February 1985.*

49. **Cooper, D.W., Bitonti, F., Frayne, D.N. and Hansen, H.H.** Kinematic Analysis Method (KAM), *Society of Automotive Engineers, Paper No. SP-272, May 1965.*

50. **Knappe, L.F.** A Computer-Orientated Mechanical System, Mechanical Engineering, *ASME vol.87, no. 5, May 1965.*

51. **Chace, M.A.** A Network-Variational Basis for Generalised Computer Representation of Multifreedom, Constrained, Mechanical Systems, *Design Automation Conference, Miami, Florida, 1969.*

52. **Chace, M.A.** DAMN-A Prototype Program for the Design Analysis of Mechanical Networks, *7th Annual Share design Automation Workshop, San Francisco, California, June 1970.*

53. **Chace, M.A. and Korybalski, K.E.** Computer Graphics in the Schematic Representation of Nonlinear, Constrained, Multifreedom Mechanical Systems, *Computer Graphics 70 Conference, Brunel University, April 1970.*

54. **Chace, M.A. and Angel, J.C.** Interactive Simulation of Machinery with Friction and Impact Using DRAM, *SAE paper No. 770050, February 1977.*

55. **Orlandea, N., Chace, M.A. and Calahan, D.A.** A Sparsity-Orientated Approach to the Dynamic Analysis and Design of Mechanical Systems - Part I , *Paper No. 76-DET-19, ASME Mechanisms Conference, Montreal, October 1976. (also Trans. ASME Journal of Engineering for Industry, 1977.)*

56. **Orlandea, N., Chace, M.A. and Calahan, D.A.** A Sparsity-Orientated Approach to the Dynamic Analysis and Design of Mechanical Systems - Part II , *Paper No. 76-DET-20, ASME Mechanisms Conference, Montreal, October 1976. (also Trans. ASME Journal of Engineering for Industry, 1977.)*

57. **Hudi, J.** AMIGO - A Modular System for Generating ADAMS Models. *Proceedings of the 5th European ADAMS News Conference, Tedas GmbH, Marburg, FR Germany, Oct. 1988.*

58. **Terlinden, M.W., Langer, W., and Hache, M.** MOGESSA - A Modular Full Vehicle Simulation System Based on ADAMS. *Proceedings of the 4th European ADAMS News Conference, Tedas GmbH, Marburg, FR Germany, Sept. 1987.*

59. **Kaminski, S.** WOODS - A Worksheet Orientated Design System. *Proceedings of the 6th European ADAMS News Conference, Kurhaus Wiesbaden, FR Germany, April 1990.*

60. **Dorey, A.** A Range Rover handling model in ADAMS, *Multi-body System Dynamics Codes for Vehicle Dynamics Applications Seminar (S275), I.Mech.E., 1994.*

61. **Scapaticci, D., Coeli, P., Minen, D.** ADAMS implementation of synthetic trajectories of the wheels with respect to the car body for handling manoeuvres simulations. *Proceedings of the 8th European ADAMS News Conference, Munich, October, 1992.*

62. **Fischer E.** Full Vehicle Modelling Seminar - Course Notes, *Tedas GmbH, Marburg, Germany, 1989.*

63. **Fischer E.** TINA Users Manual, *Tedas GmbH, Marburg, Germany, 1989.*

64. **Blundell M.V.** Full Vehicle Modelling and Simulation of a Rolls Royce, *Internal consulting report to Rolls Royce Motor Cars Ltd., Tedas Ltd., Coventry, 1990.*

65. **Mechanical Dynamics Inc.** ADAMS/Vehicle User's Manual, *Mechanical Dynamics Inc., 2301 Commonwealth Blvd., Ann Arbor, Michigan, USA, December 1990.*

66. **Trungle, C.V.** Engineering a winner at Newman/Hass Racing, *Dynamic Dimensions, Volume 2 Number 3, Mechanical Dynamics Inc., 1991.*

67. **Heath,R., Olszewski,W.** Control System Design Using ADAMS and MATRIXx, *Proceedings of the 6th European ADAMS News Conference, Kurhaus Wiesbaden, FR Germany, April 1990.*

68. **Wielenga, T.** Analysis methods and model representation in ADAMS, MDI Technical Paper No. 41, *Mechanical Dynamics Inc., 2301 Commonwealth Blvd., Ann Arbor, Michigan, USA, October 1987.*

69. **Kami, Y. and Minikawa, M.** Double-Wishbone Suspension for Honda Prelude, *SAE Paper No. 841186, 1984.*

70. **von der Ohe M.** Front and Rear Suspension of the New Mercedes Model W201, *SAE Paper No. 831045, 1983.*

71. **Pintar S. & McGuan S.** ADAMS/FEA gives Ford engineers new insight into product performance, *Dynamic Dimensions, Volume 3 Number 1, Mechanical Dynamics Inc., 1992.*

72. **Pacejka, H.B. & Sharp, R.S.** Shear force generation by pneumatic tyres in steady state conditions: A review of modelling aspects, *Vehicle System Dynamics, 20 1991, pp. 121-176.*

73. **Sharp, R. S. & El-Nashar, M. A.** A generally acceptable digital computer based model for the generation of shear forces by pneumatic tyres, *Vehicle System Dynamics, 15, 1986, pp. 187-209.*

74. **Sharp, R. S.** On the accurate representation of tyre shear forces by a multi-radial-spoke model, *Proc. 11th IAVSD symposium on the dynamics of vehicles on roads and tracks, ed. R. J. Anderson, Swets & Zeitlinger, Lisse, 1990, pp. 528-541.*

75. **Sharp, R. S.** Tyre structural mechanics influencing shear force generation: Ideas from a multi-radial-spoke model, *Tyre models for vehicle dynamic analysis: Proc.1st international colloquium on tyre models for vehicle dynamic analysis, ed. H. B. Pacejka, Swets & Zeitlinger, Lisse, 1993, pp. 145-155.*

76. **Pacejka, H.B.** The role of tyre dynamic properties, *Seminar on Smart Vehicles, delft, February 1995. Proccedings: Vehicle System Dynamics, Special Issue.*

77. **Davis,D.C.** A radial-spring terrain-enveloping tire model, *Vehicle System Dynamics 3 (1974), pp. 55-69.*

78. **Mechanical Dynamics Inc.** ADAMS/Tire (5.2.1) User's Manual, *Mechanical Dynamics Inc., 2301 Commonwealth Blvd., Ann Arbor, Michigan, USA, November 1989.*

79. **Kisielewicz, L.T., and Ando, K.** Accurate simulation of road tire vehicle interactions using PAM_CRASH^{TM}/ADAMS^{TM} coupled solution, *'92 ISID ADAMS Users Conference - Tokyo, November 1992.*

80. **Schuring, D.J., Pelz, W. & Pottinger, M.G.** The BNPS Model - An automated implementation of the "Magic Formula" concept, *IPC-7 Conference and Exposition, Phoenix, 1993.*

81. **Sitchen, A.,** Acquisition of transient tire force and moment data for dynamic vehicle handling simulations, *SAE paper 831790,Society of Automotive Engineers, 400 Commonwealth Drive, Warrendale, PA 15096, USA, 1983.*

82. **Bayle, P., Forissier, J.F. and Lafon, S.** A new tyre model for vehicle dynamic simulations, *Automotive Technology International, 1993, pp 193-198.*

83. **Pacejka, H.B. and Besselink, I.J.M.** Magic formula tyre model with transient properties, *Proc. Berlin Tyre Colloquium, Vehicle System Dynamics Supplement 27, Swets & Zeitlinger, Lisse, 1997, pp. 145-155.*

84. **Sharp, R.S.** Magic formula method for representation of tyre forces and moments, *Course notes, Cranfield Institute of Technology, 1992.*

85. **J. J. M. van Oosten & Bakker, E.** Determination of magic tyre model parameters, *Tyre models for vehicle dynamic analysis: Proc. 1st international colloquium on tyre models for vehicle dynamic analysis, ed. H. B. Pacejka, Swets & Zeitlinger, Lisse, 1993, pp. 19-29.*

86. **Makita, M. & Torii, S.** An analysis of tire cornering characteristics using a magic formula tire model, *JSAE paper 923063, Proc. Int. Symp. Advanced Vehicle Control 1992 (AVEC 92), Yokohama, Sept. 92.*

87. **SAE Publication,** Vehicle Dynamics Terminology, Handbook Supplement, *SAE J670e, Society of Automotive Engineers, 400 Commonwealth Drive, Warrendale, PA 15096, USA.*

88. **Mechanical Dynamics Inc.** ADAMS/Solver Subroutine Reference Manual, *Mechanical Dynamics Inc., 2301 Commonwealth Blvd., Ann Arbor, Michigan, November, 1994.*

89. **Forbes J.** Description of suggested measured outputs during track testing, *Private communiction, 1992.*

90. **Griffiths, P.J.** The quality engineering of concept design, *Cooperative research proposal between Rover Group and Coventry University, September 1995.*

91. **Blundell M.V.** Full vehicle modelling and the requirements for accurate handling simulations, *IMechE book publication "Automotive Refinement" (1 86058 021 1), C498/7/005/95, pp. 77-91, July 1996.*

APPENDIX A

VEHICLE MODEL SYSTEM SCHEMATICS
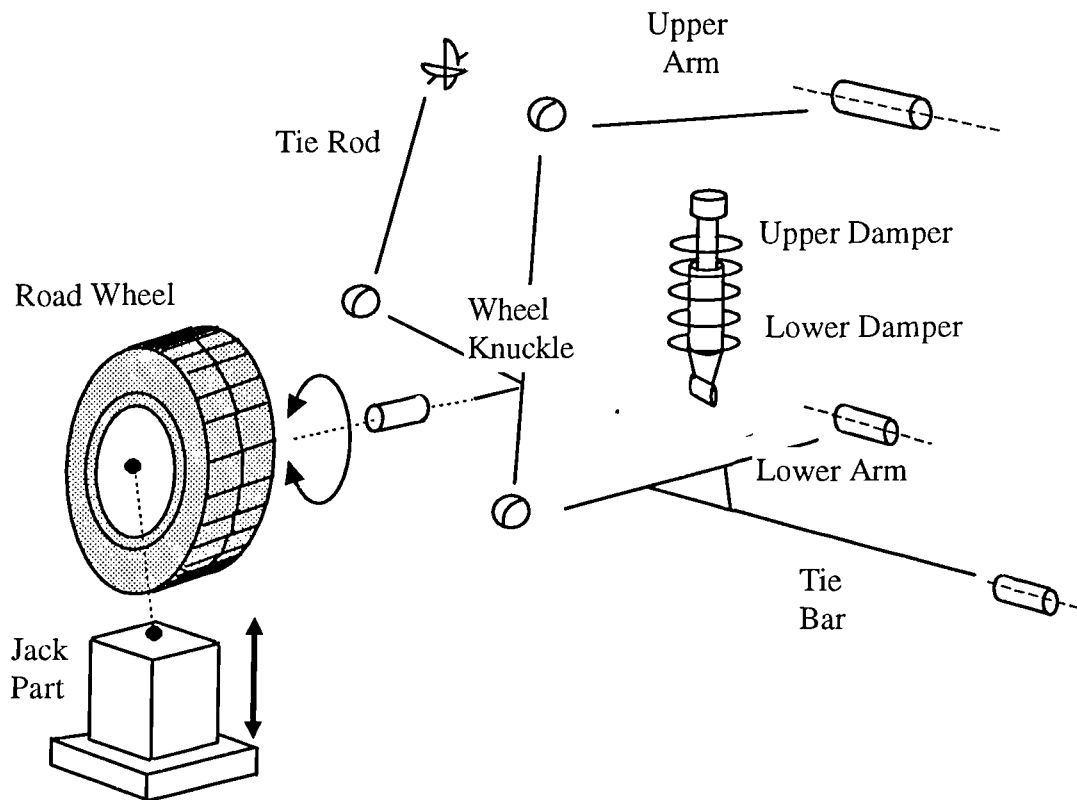
Figure A.1 Front suspension components
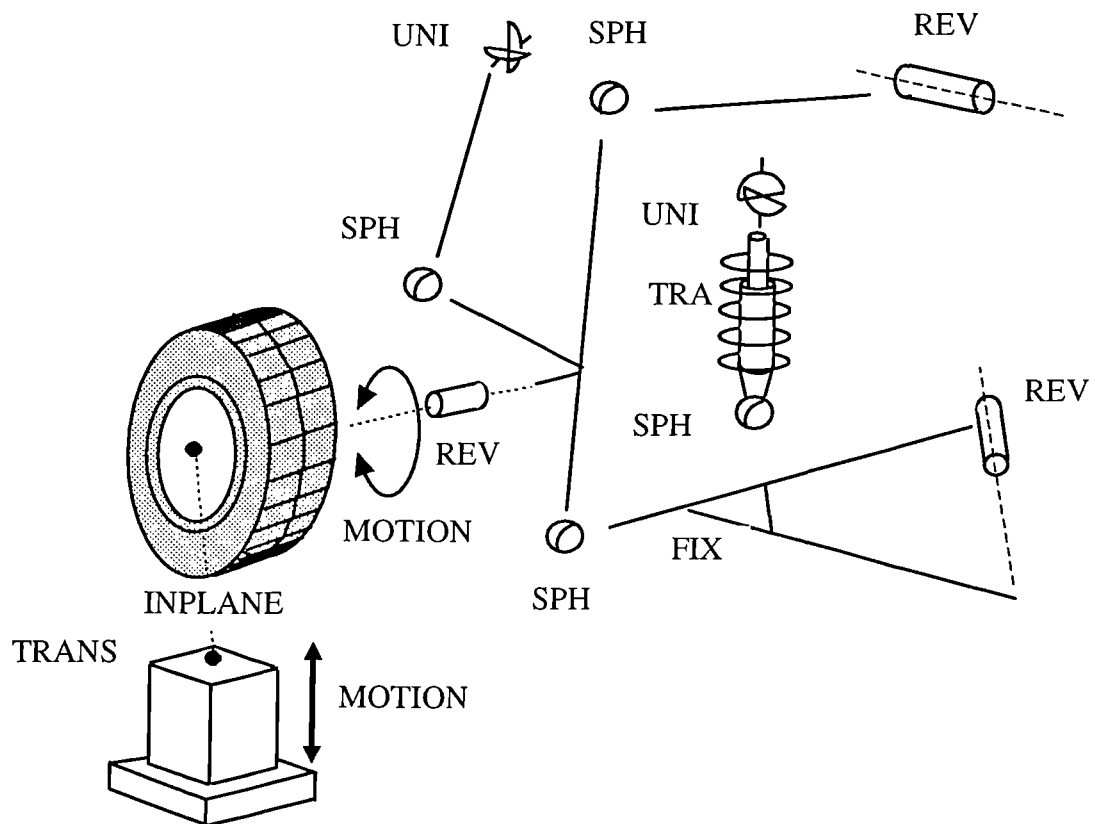
Figure A.2 Front suspension with joints

UNI

SPH

REV

BUSH

CYL

SPH

BUSH

SPH

BUSH

REV

BUSH

MOTION

FIX

SPH

INPLANE

TRANS

MOTION
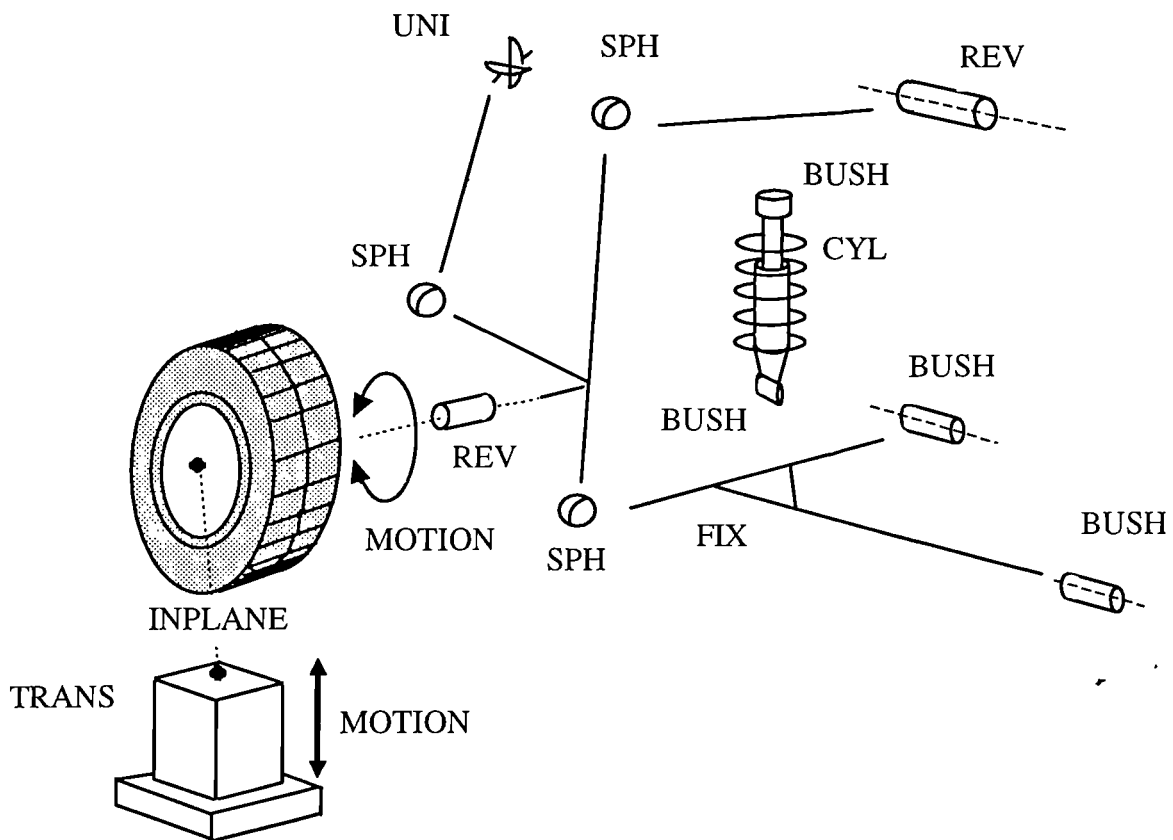
Figure A.3 Front suspension with bushes

Parts ☐

Points ◯

BODY/GROUND

01
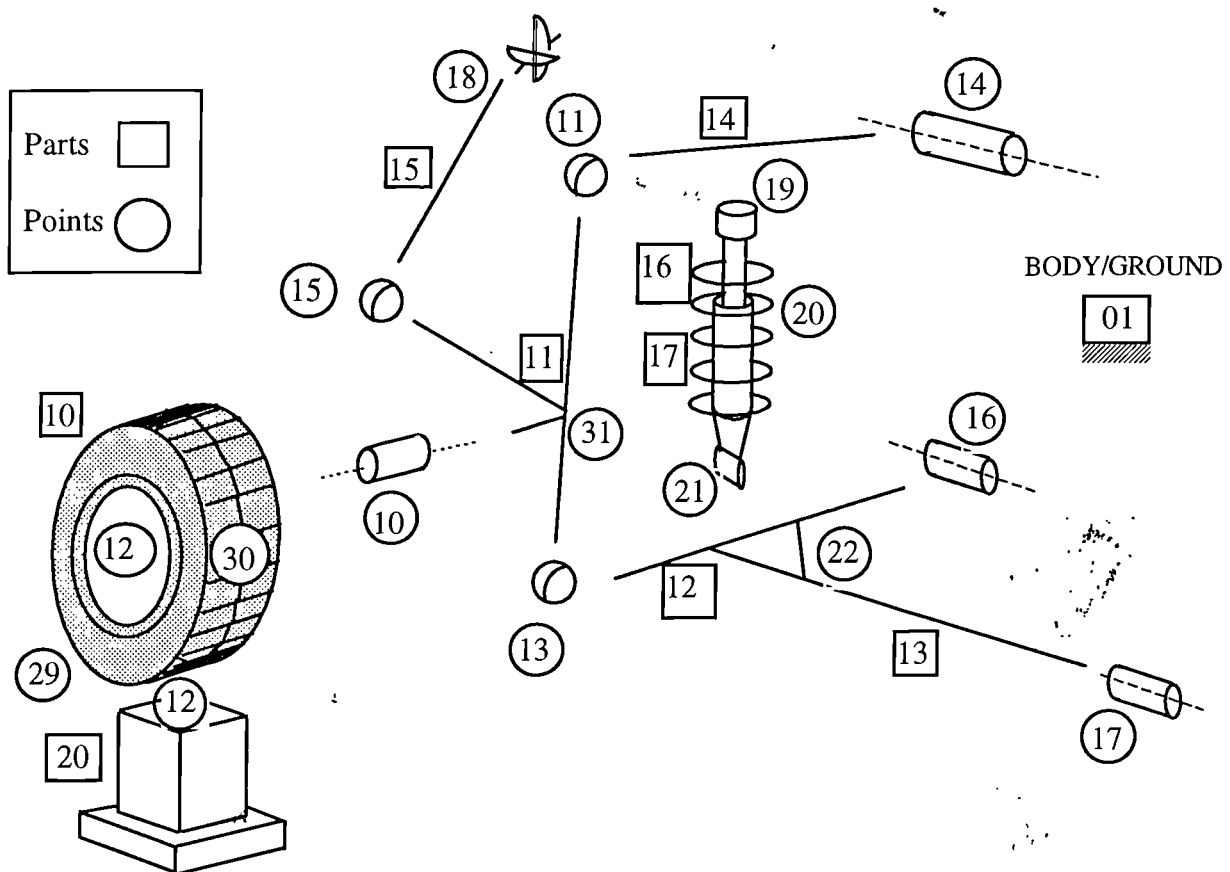
Figure A.4 Front suspension numbering convention
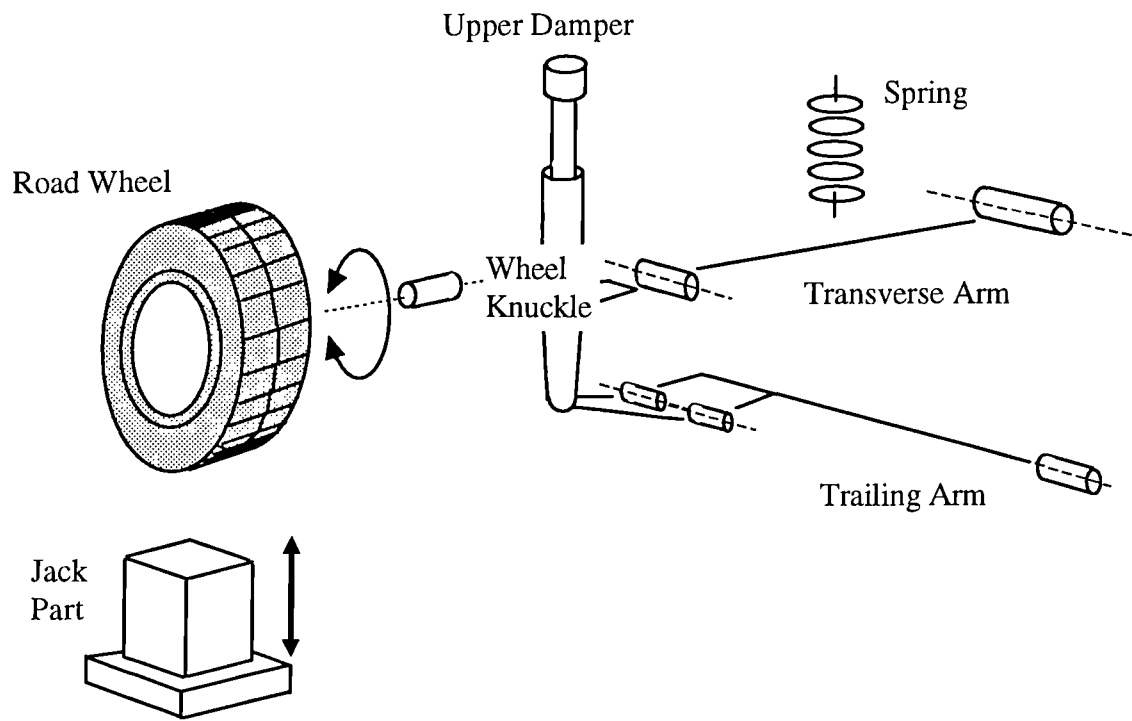
Figure A.5 Rear suspension components
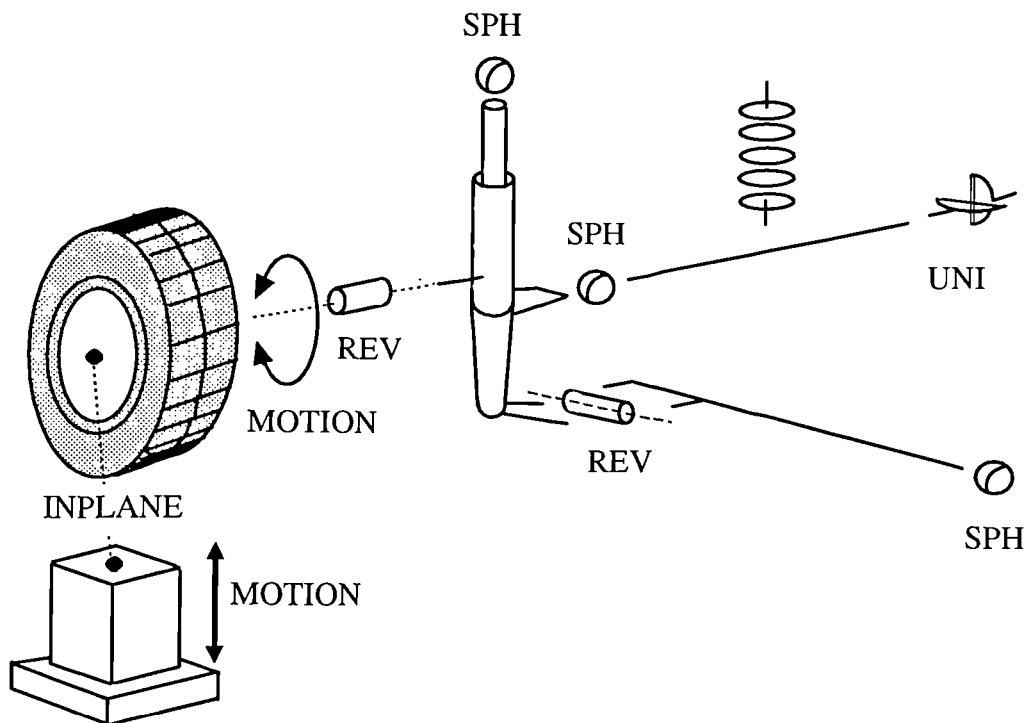
Figure A.6 Rear suspension with joints
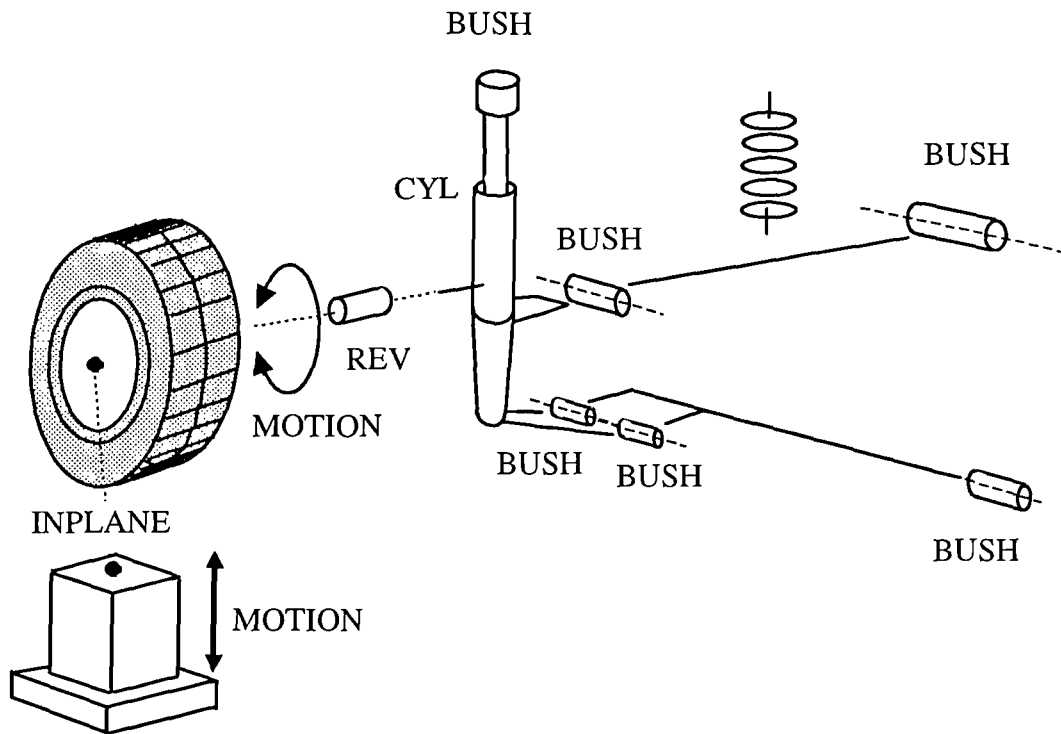
Figure A.7 Rear suspension with bushes
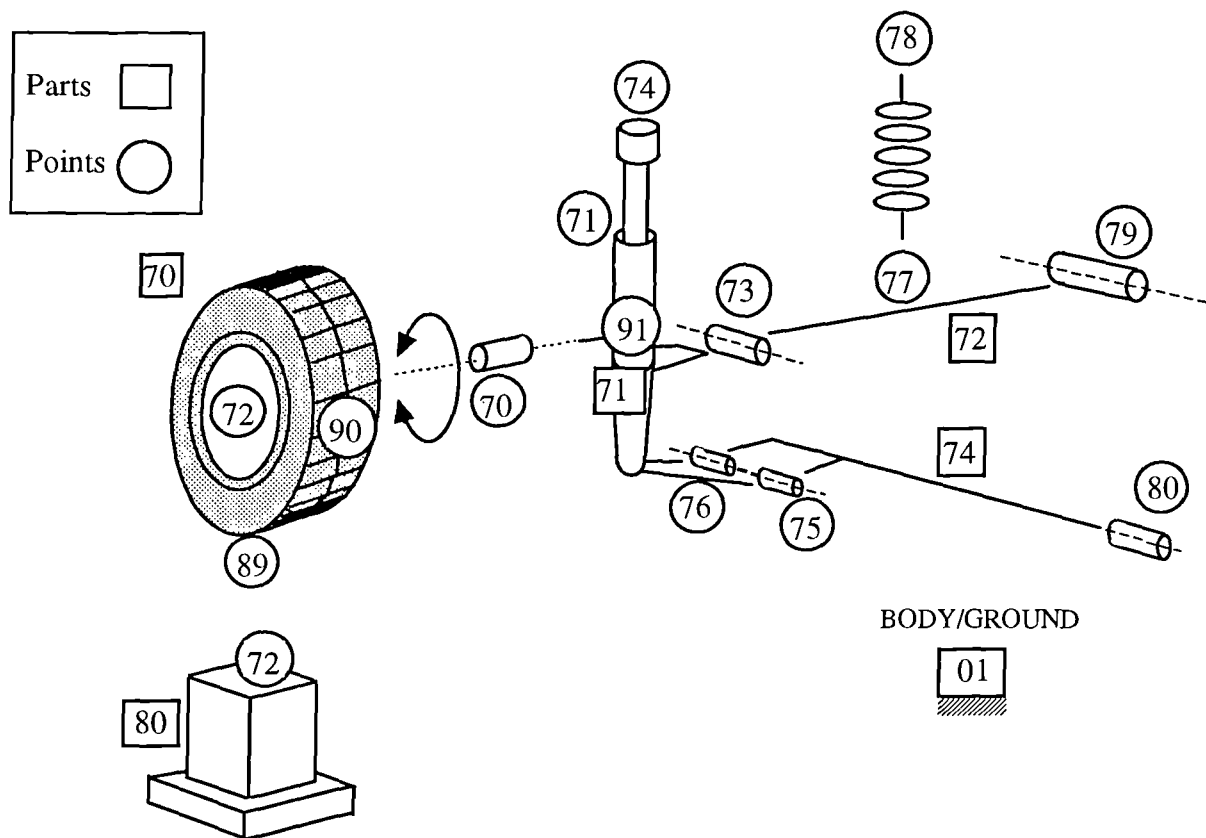
Figure A.8 Rear suspension numbering convention
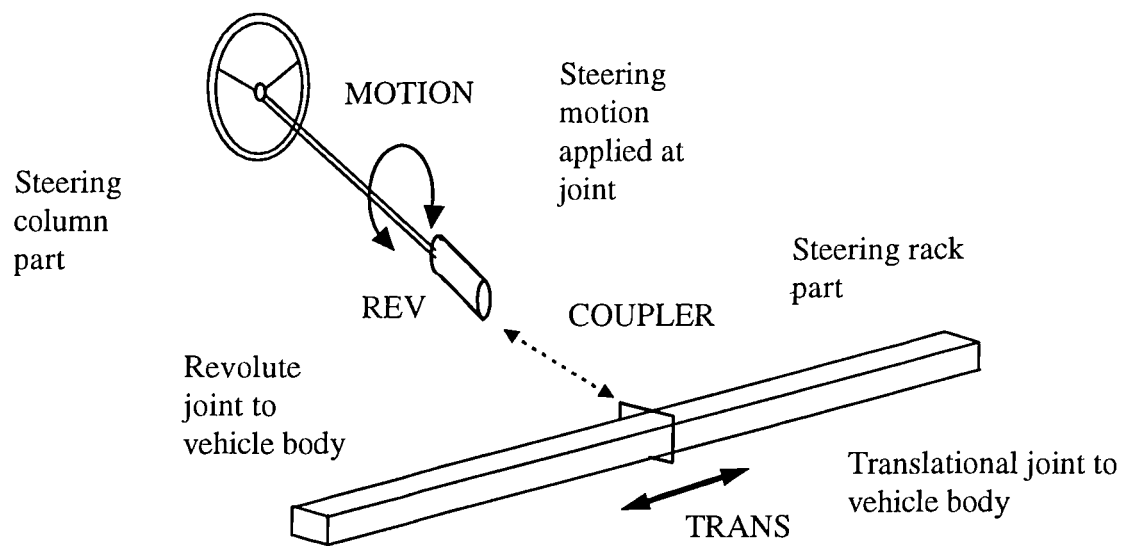
Figure A.9 Steering system components and joints
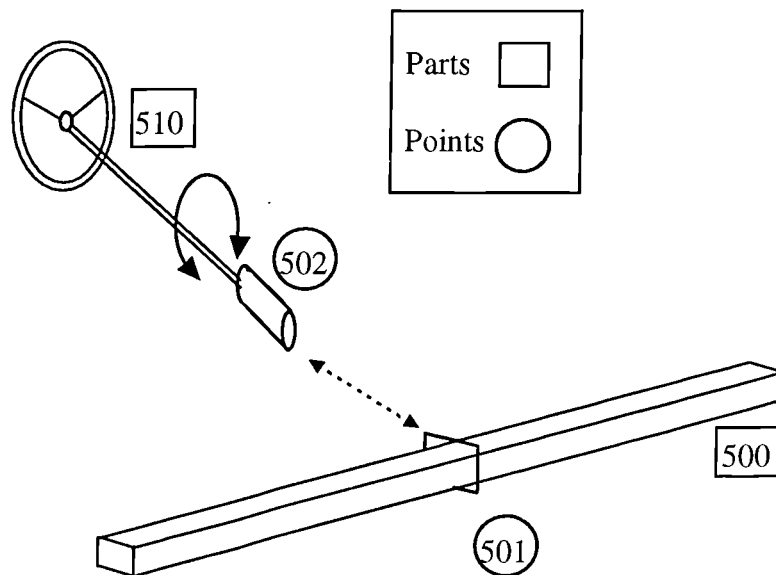
Figure A.10 Steering system numbering convention

Revolute
Joints to
Vehicle
Body

REV   Left Roll Bar

Right Roll   REV   INPLANE
Bar

                                   Torsional
                                   Spring   Front Wheel
                                                      Knuckle

                   INPLANE

                   Front Wheel
                   Knuckle
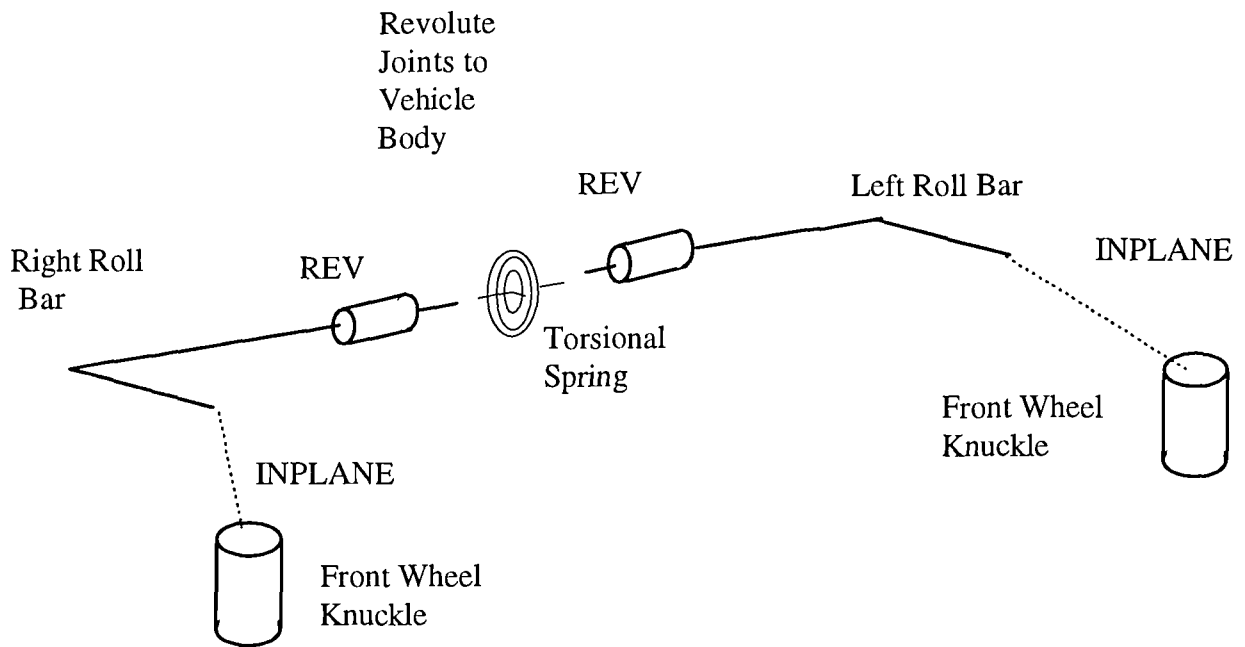
Figure A.11 Front roll bar system components and joints

Parts ☐
Points ○

          201   (203)   (202)   202

                  (201)   (205)

   201   41

             (204)

          11
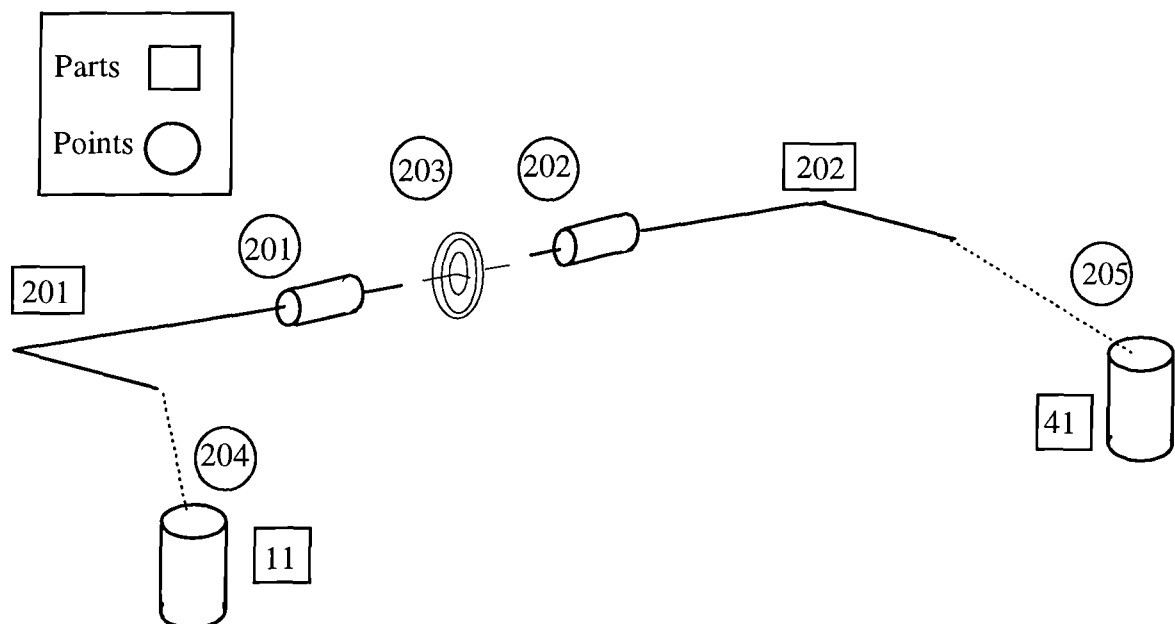
Figure A.12 Front roll bar system numbering convention

Revolute
Joints to
Vehicle
Body

REV   Left Roll Bar

Right Roll   REV   INPLANE
Bar

Torsional
Spring

INPLANE

Rear Wheel
Knuckle

Rear Wheel
Knuckle
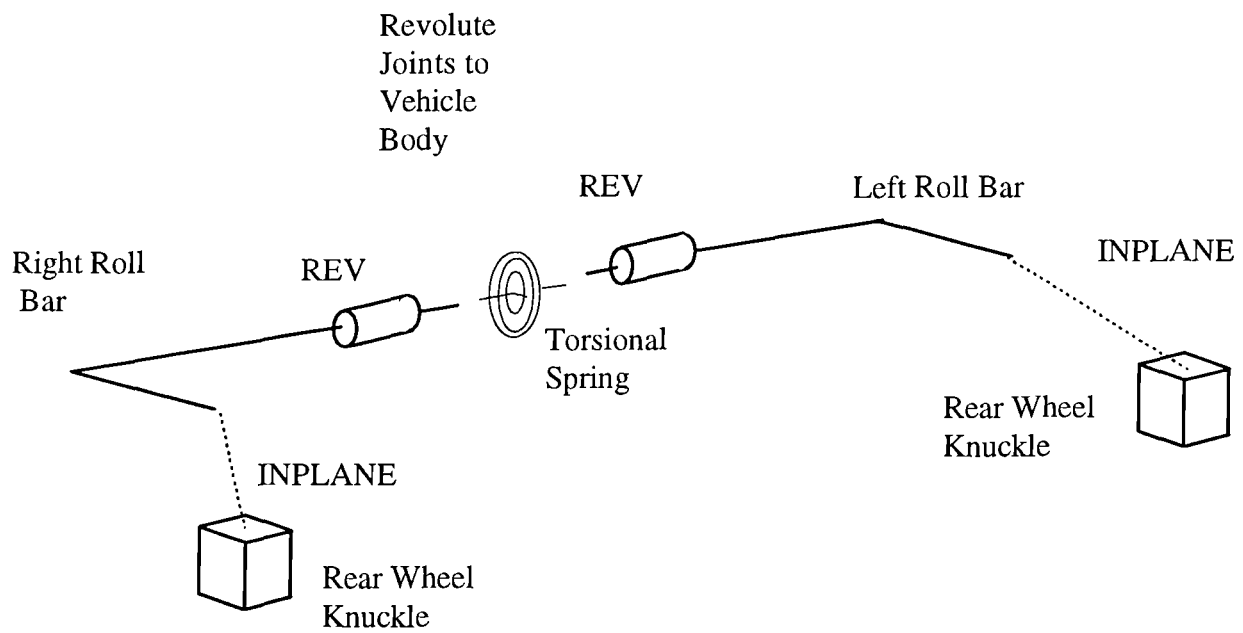
Figure A.13 Rear roll bar system components and joints

Parts □
Points ○

208   207   204

206   210

203

101

209

71
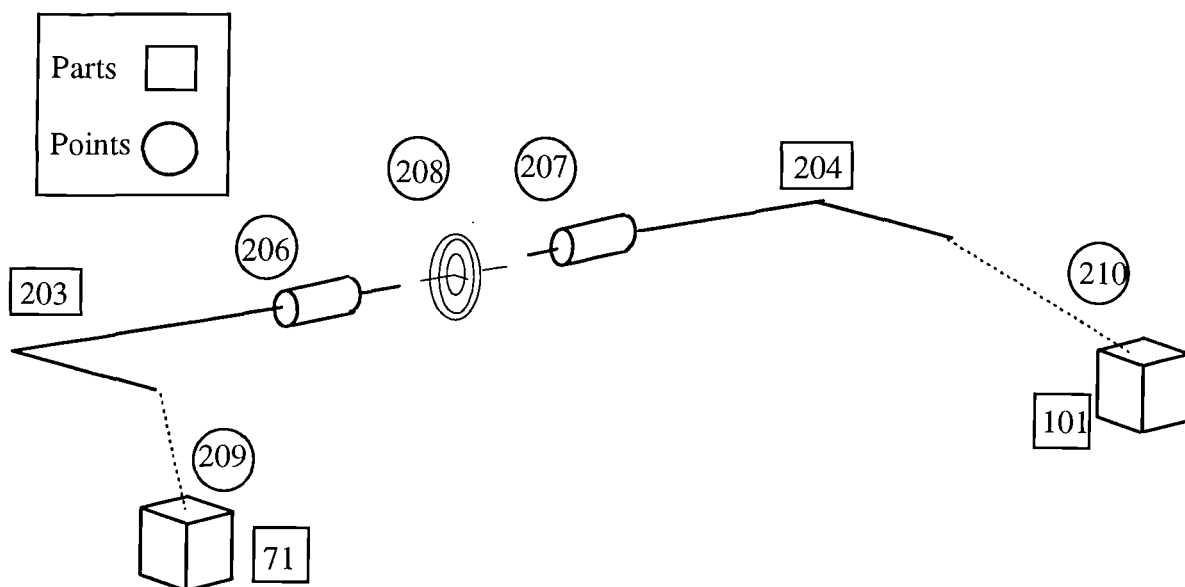
Figure A.14 Rear roll bar system numbering convention

Spring
Damper

Spring
Damper

TRANS

Rear Right
Sliding Mass

Rear Left
Sliding Mass

TRANS

Spring
Damper

Spring
Damper

TRANS

REV

TRANS

REV

Front Right
Sliding Mass
and Wheel Knuckle

Front Left
Sliding Mass
and Wheel Knuckle
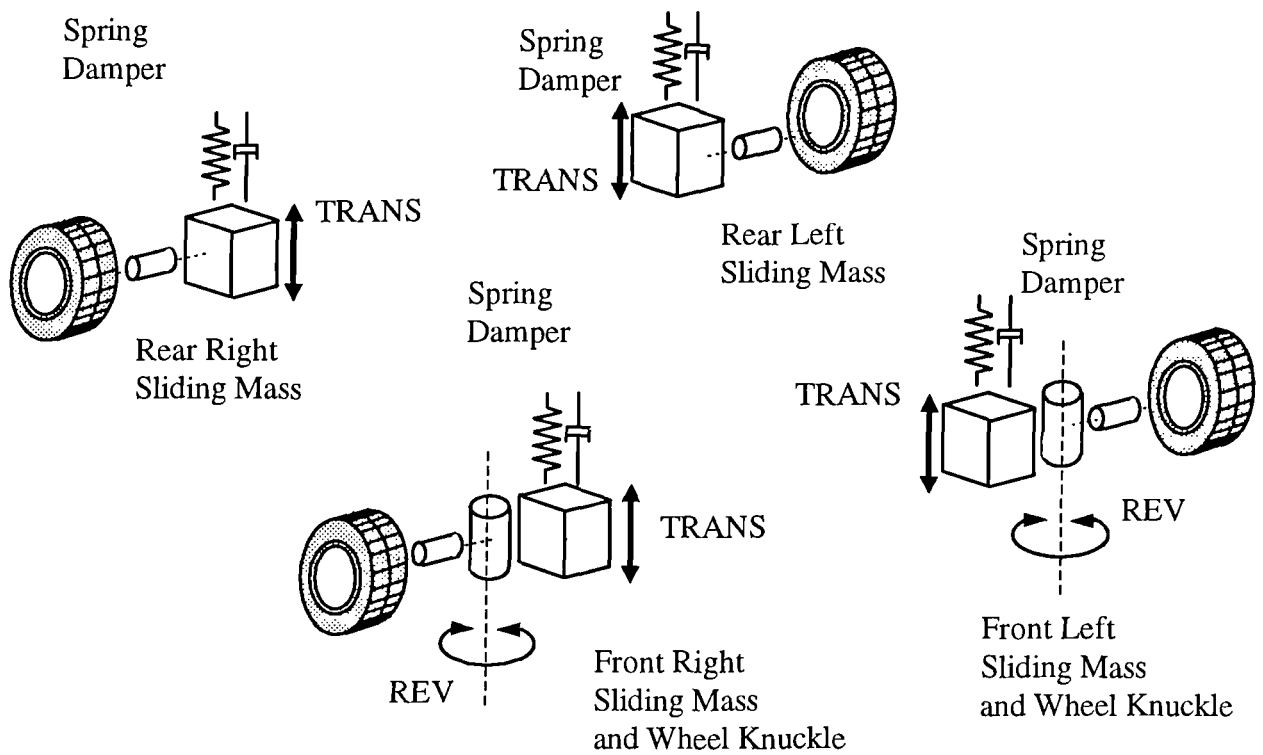
Figure A.15 Lumped mass model suspension components and joints

Parts ☐
Points ◯
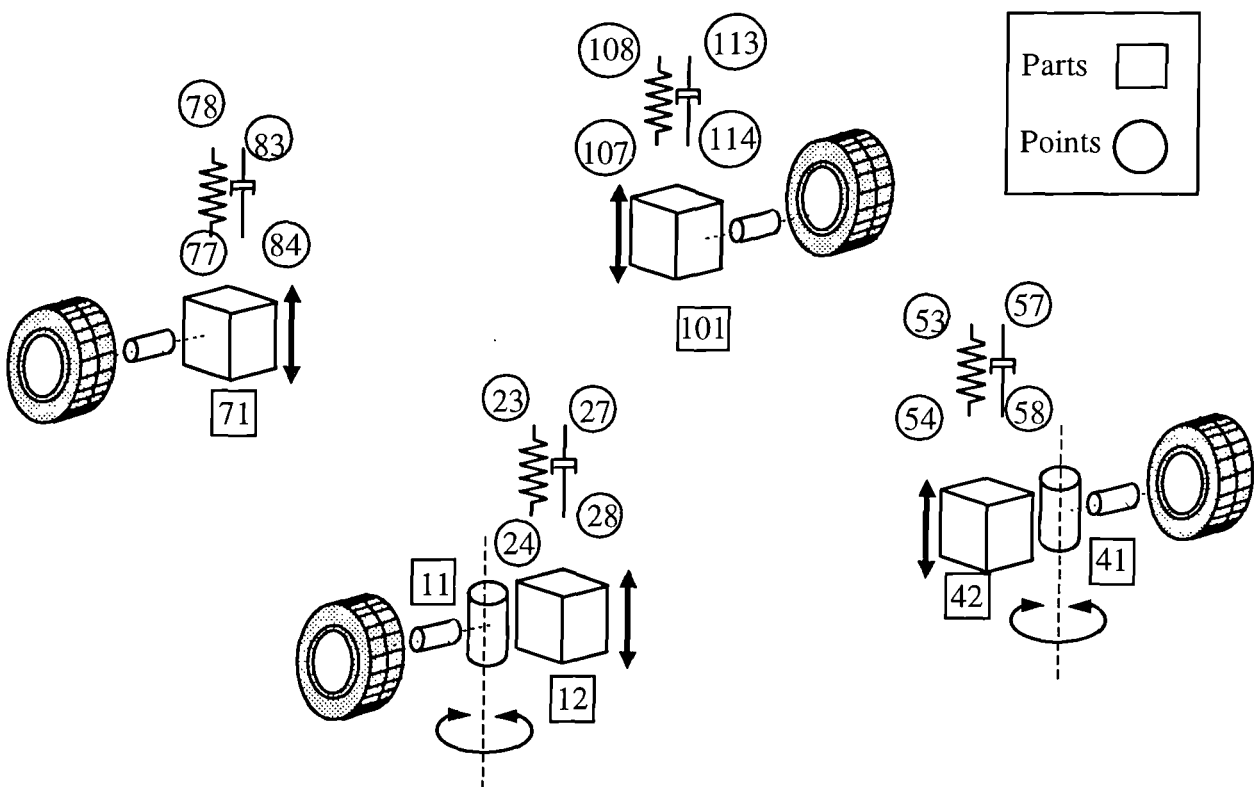
Figure A.16 Lumped mass model suspension numbering convention
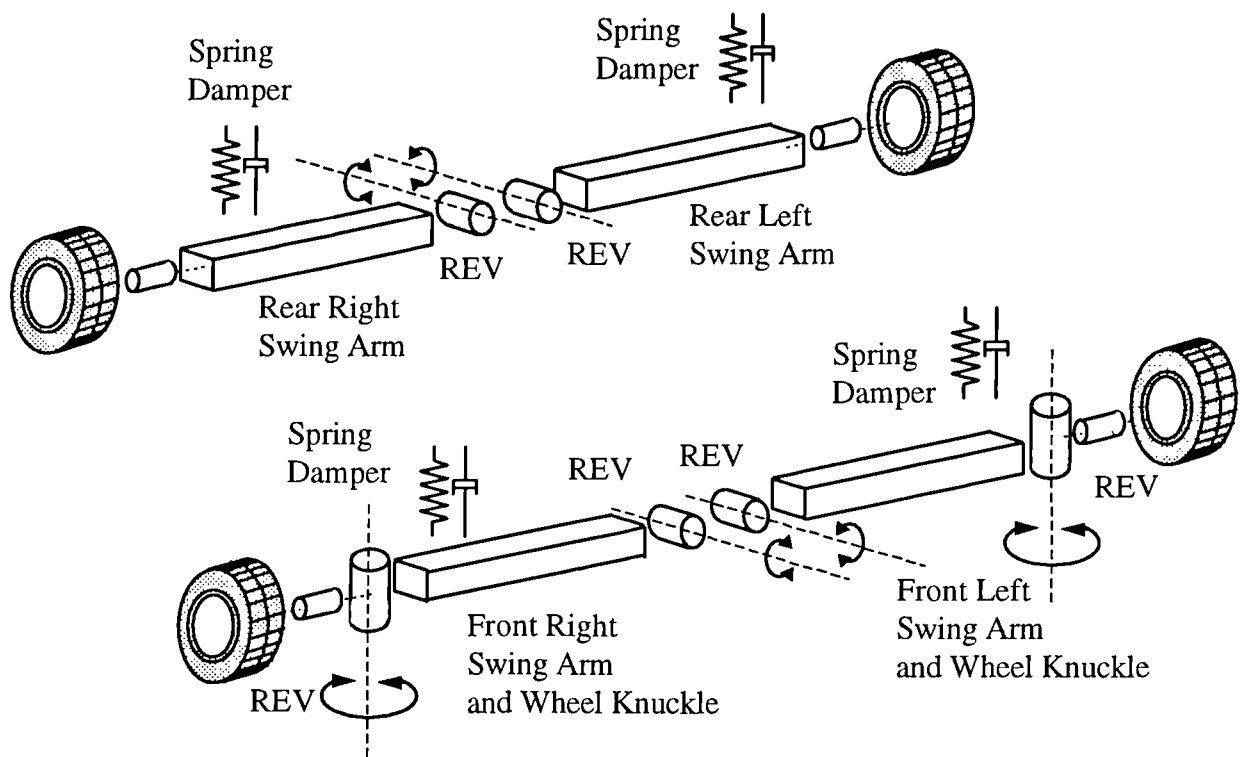
Figure A.17 Swing arm model suspension components and joints
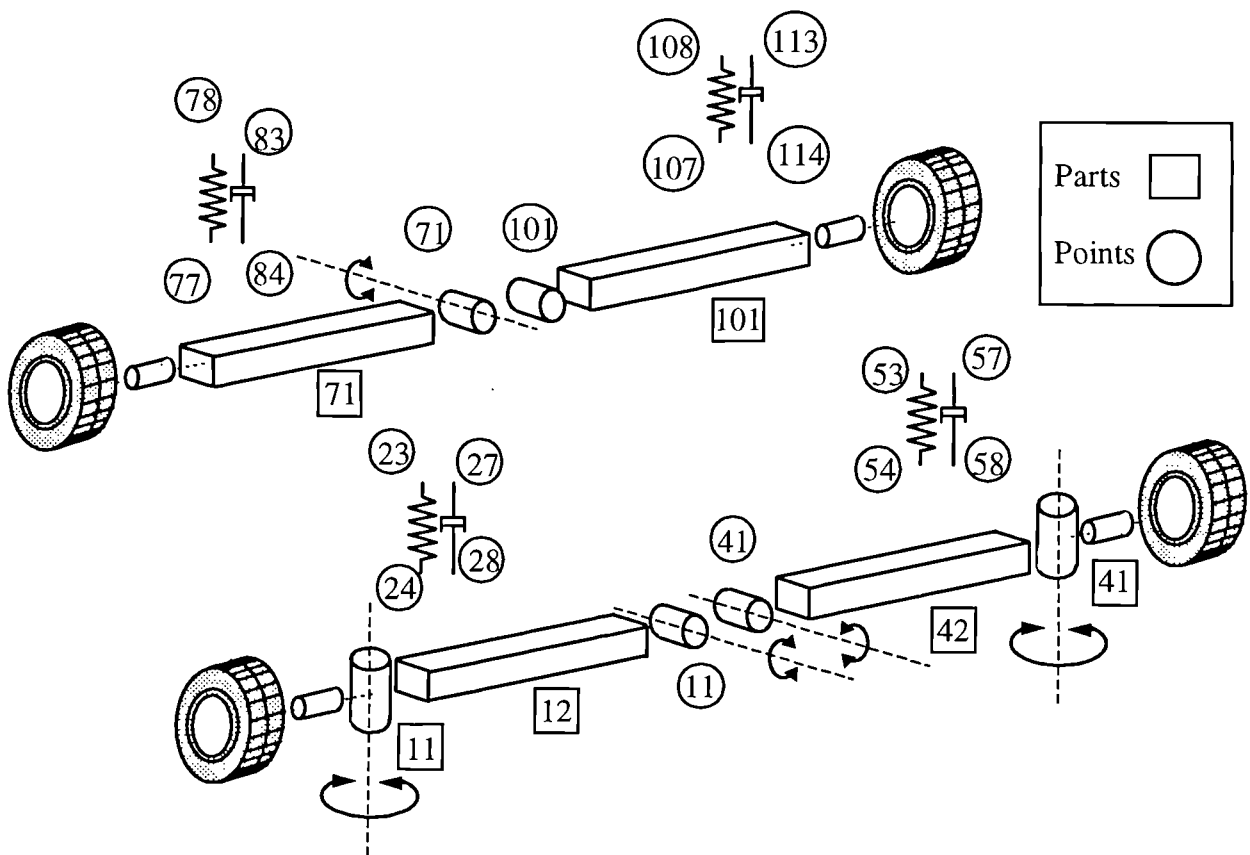
Figure A.18 Swing arm model suspension numbering convention
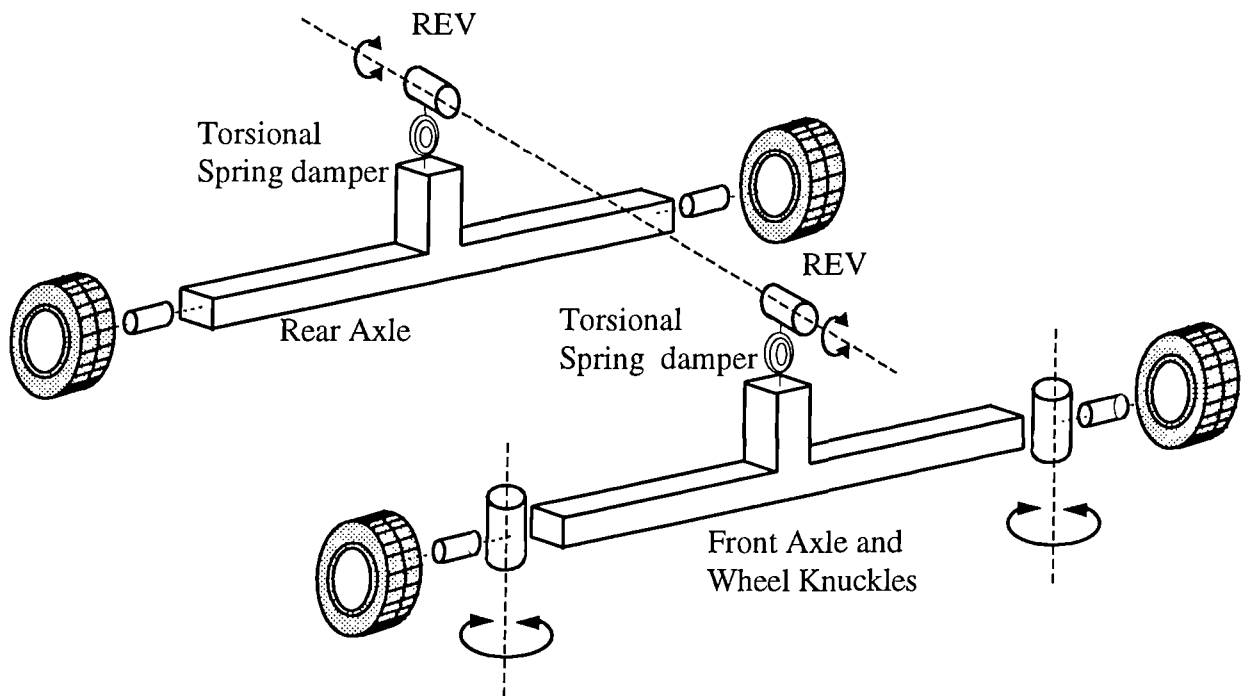
Figure A.19 Roll stiffness model suspension components and joints
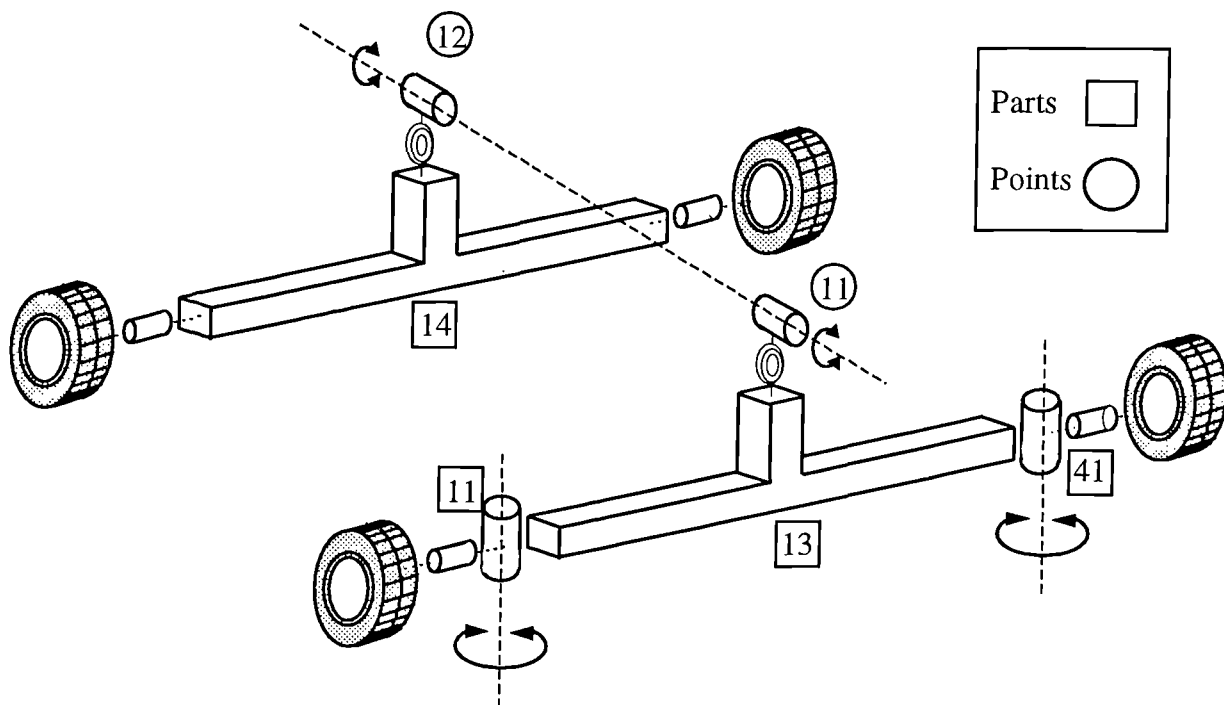
Figure A.20 Roll stiffness model suspension numbering convention

APPENDIX B

SUSPENSION ANALYSES OUTPUT PLOTS
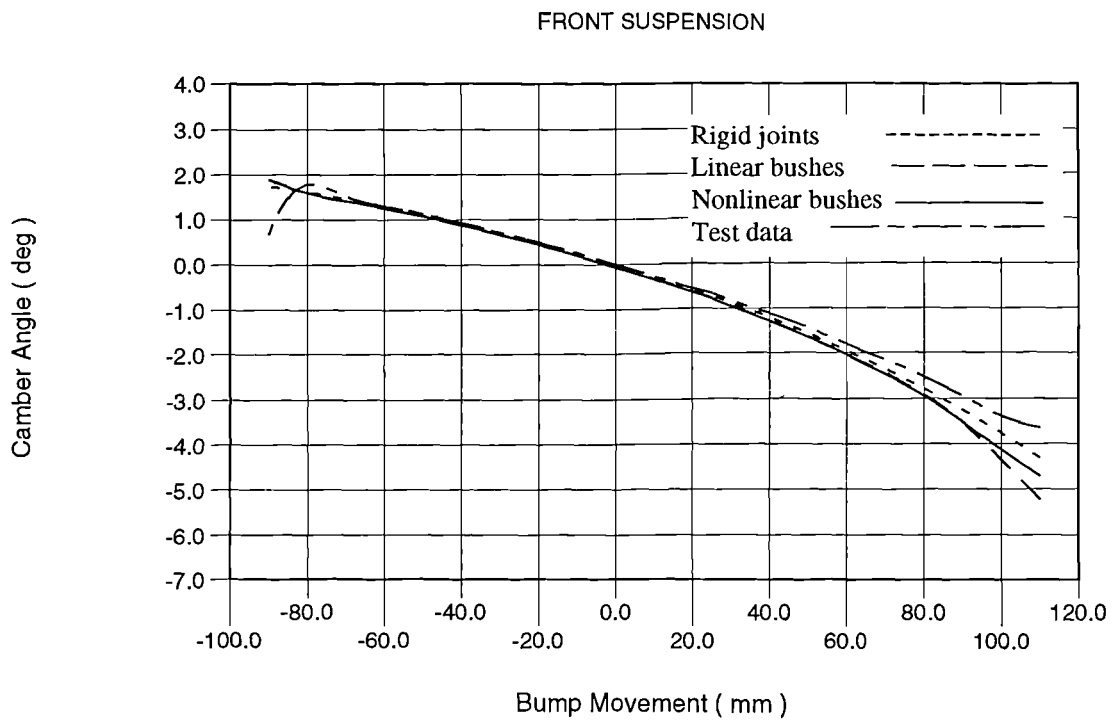
FRONT SUSPENSION

Figure B.1 Front suspension - camber angle with bump movement
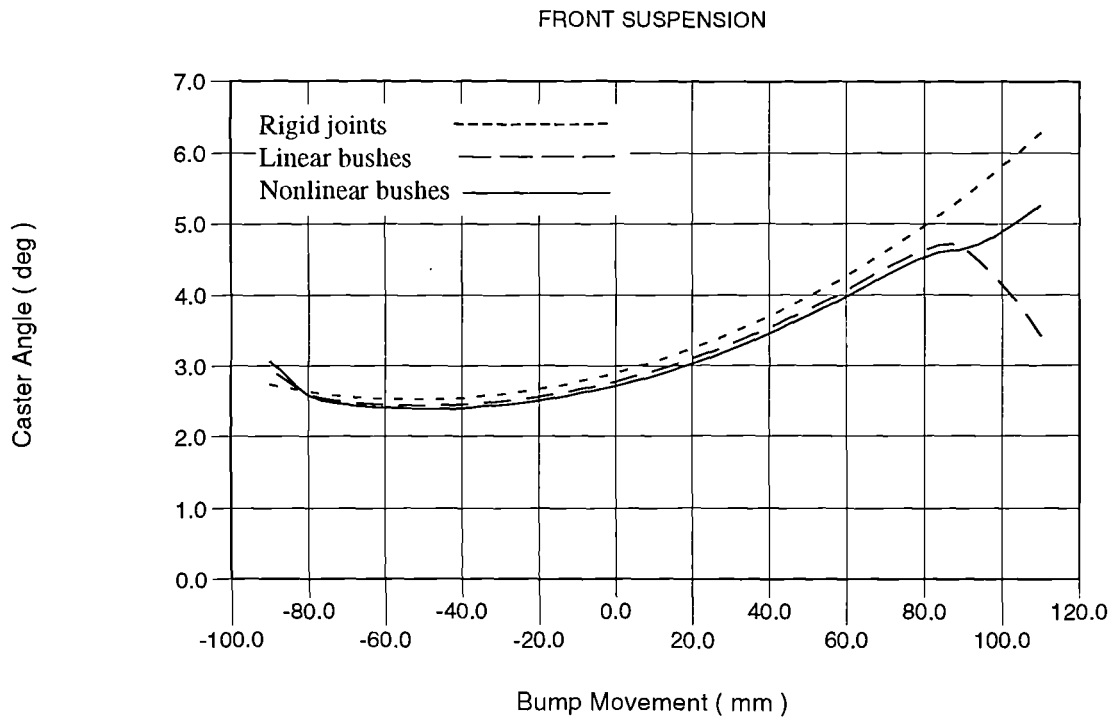
FRONT SUSPENSION

Figure B.2 Front suspension - caster angle with bump movement
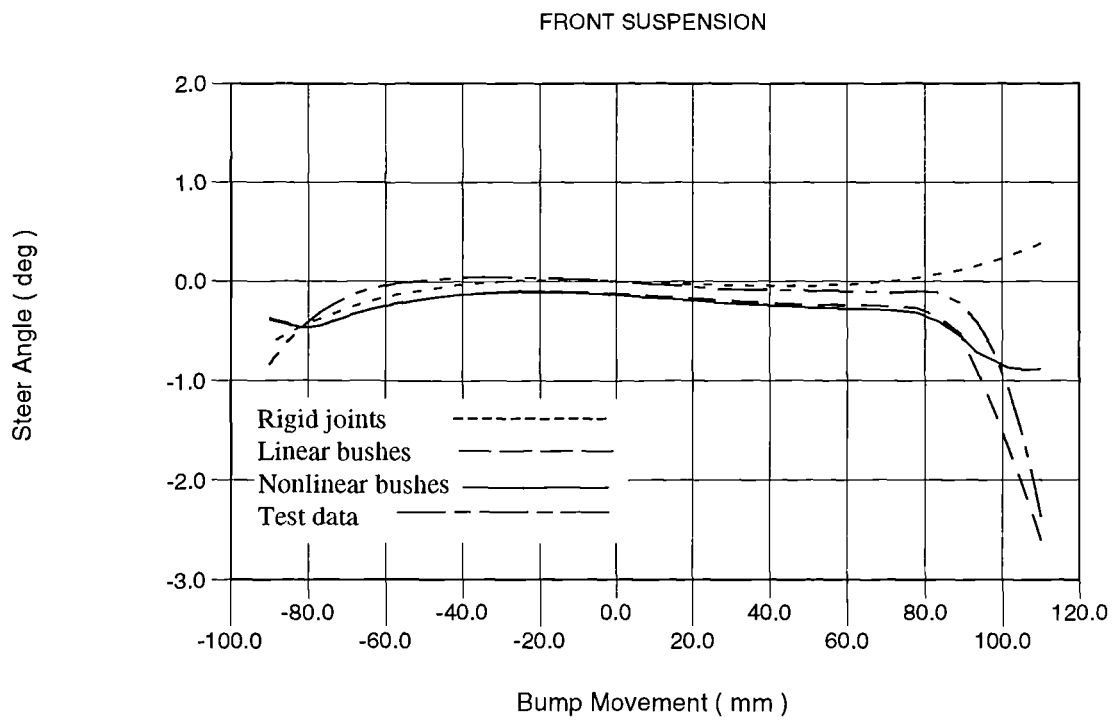
FRONT SUSPENSION

Figure B.3 Front suspension - steer angle with bump movement
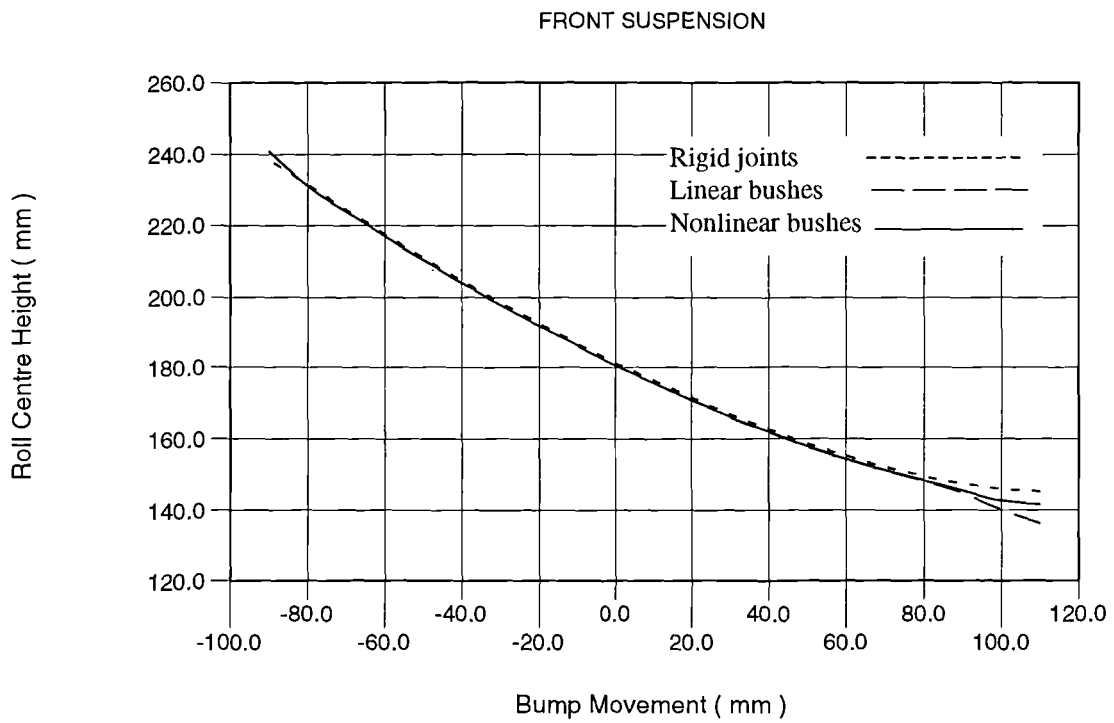
FRONT SUSPENSION

Figure B.4 Front suspension - roll centre height with bump movement
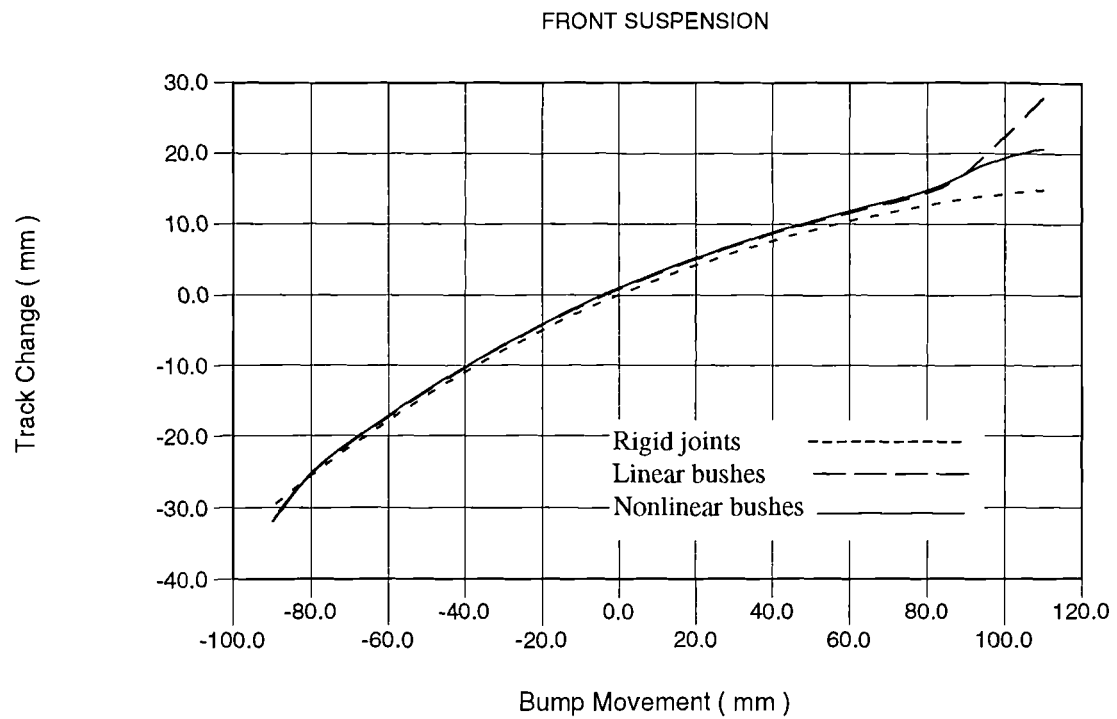
FRONT SUSPENSION

Figure B.5 Front suspension - track change with bump movement
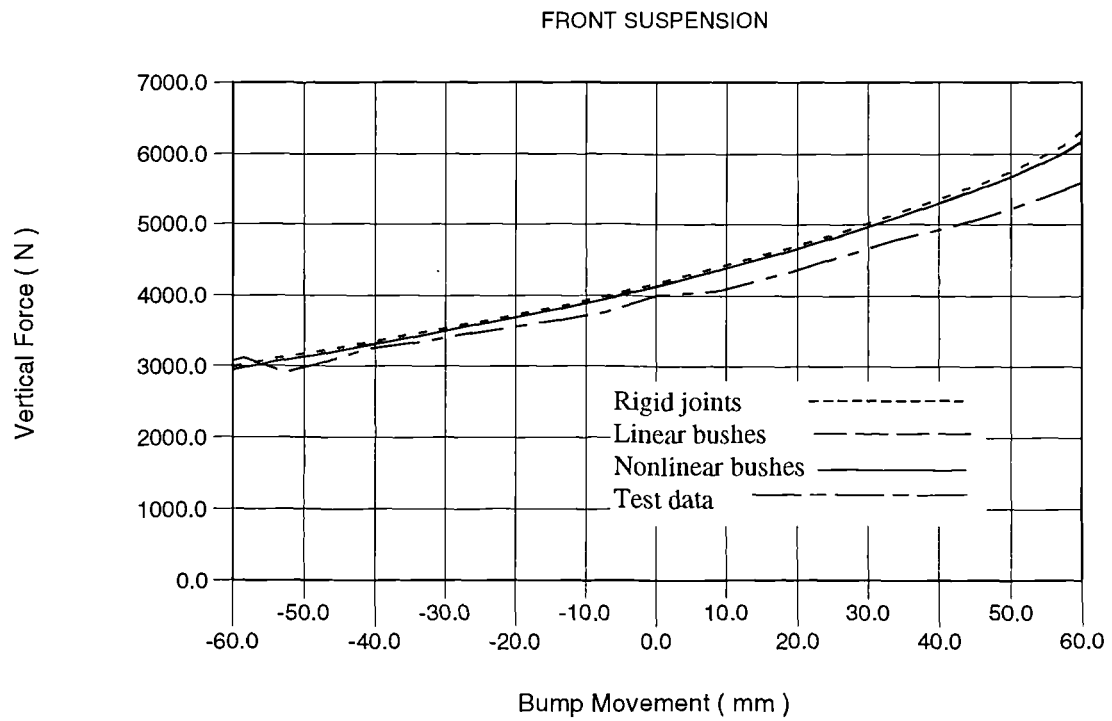
FRONT SUSPENSION

Figure B.6 Front suspension - vertical force with bump movement
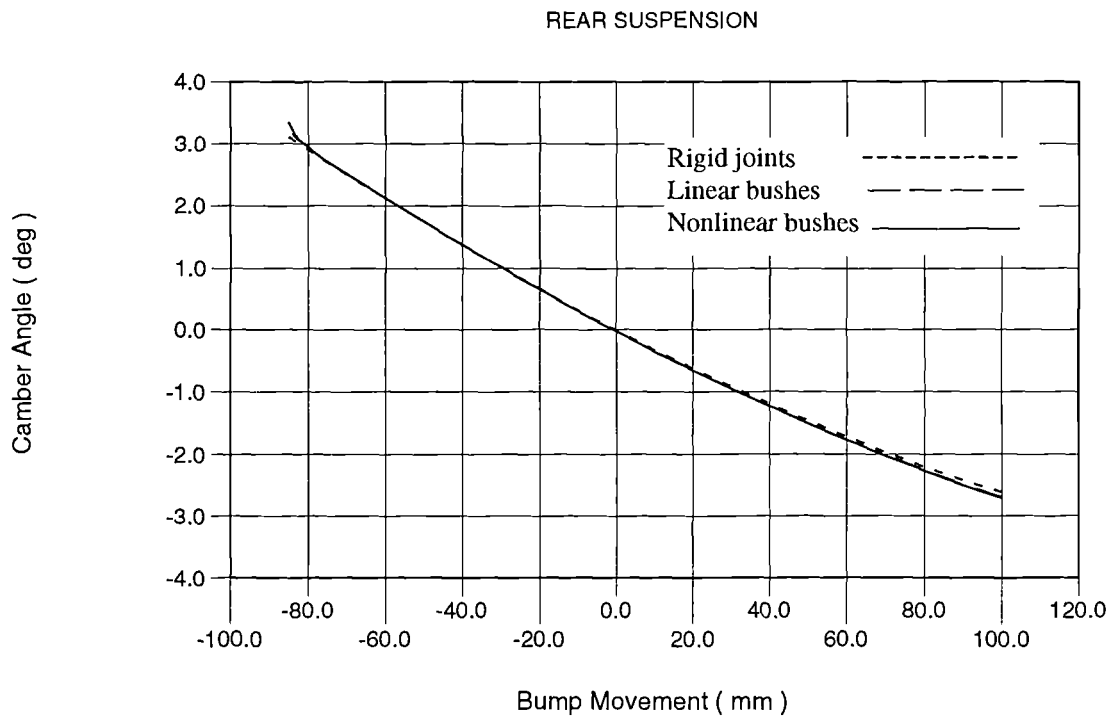
REAR SUSPENSION

Figure B.7 Rear suspension - camber angle with bump movement
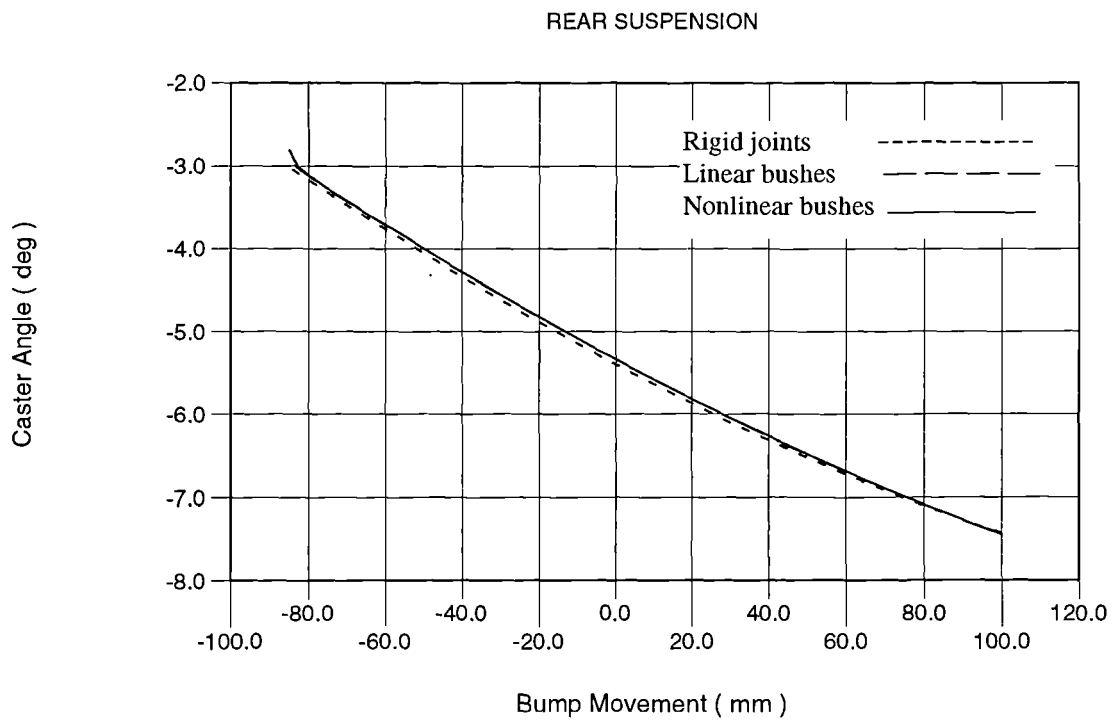
REAR SUSPENSION

Figure B.8 Rear suspension - caster angle with bump movement
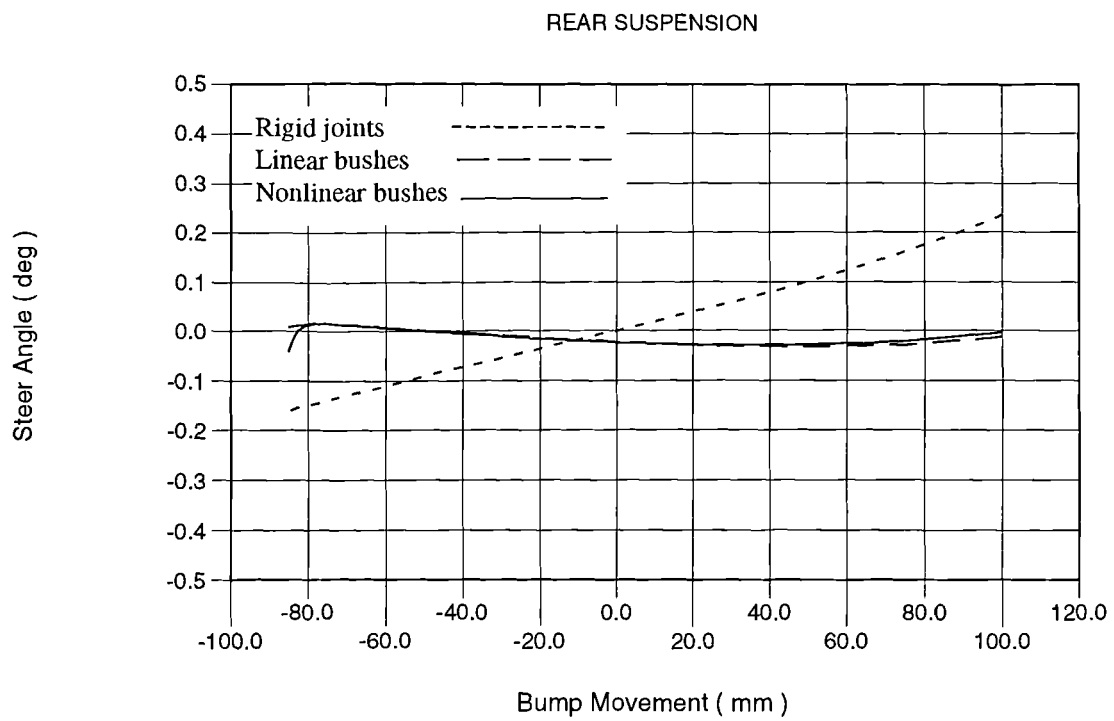
Figure B.9 Rear suspension - steer angle with bump movement
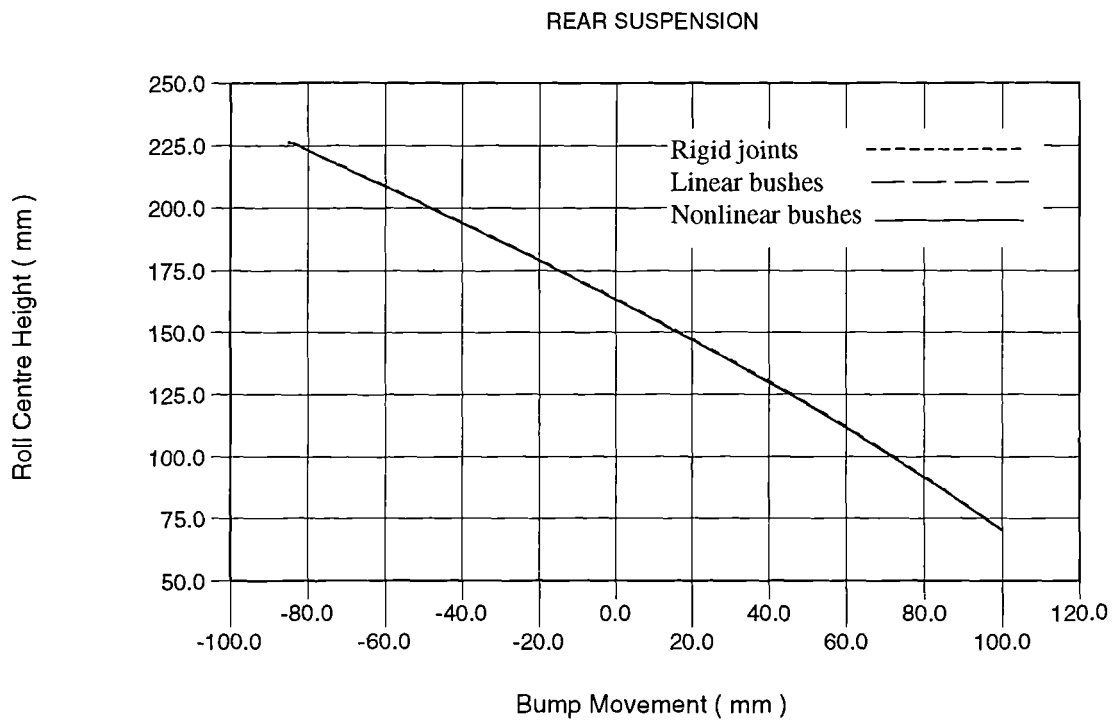
Figure B.10 Rear suspension - roll centre height with bump movement
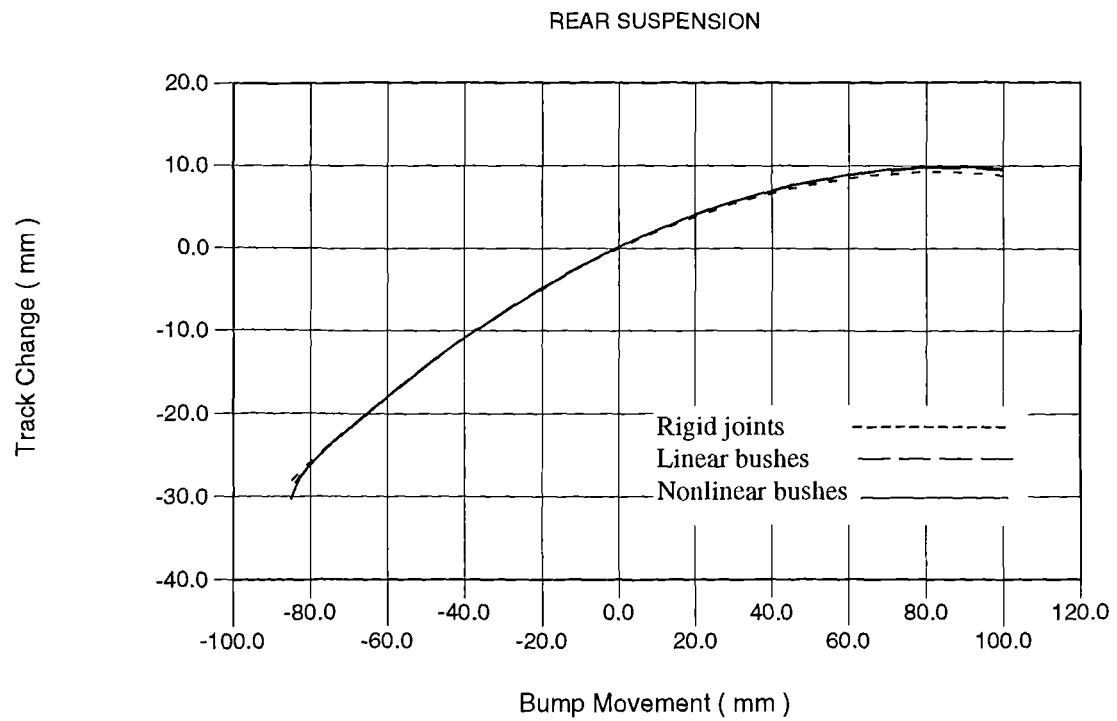
REAR SUSPENSION

Figure B.11 Rear suspension - track change with bump movement
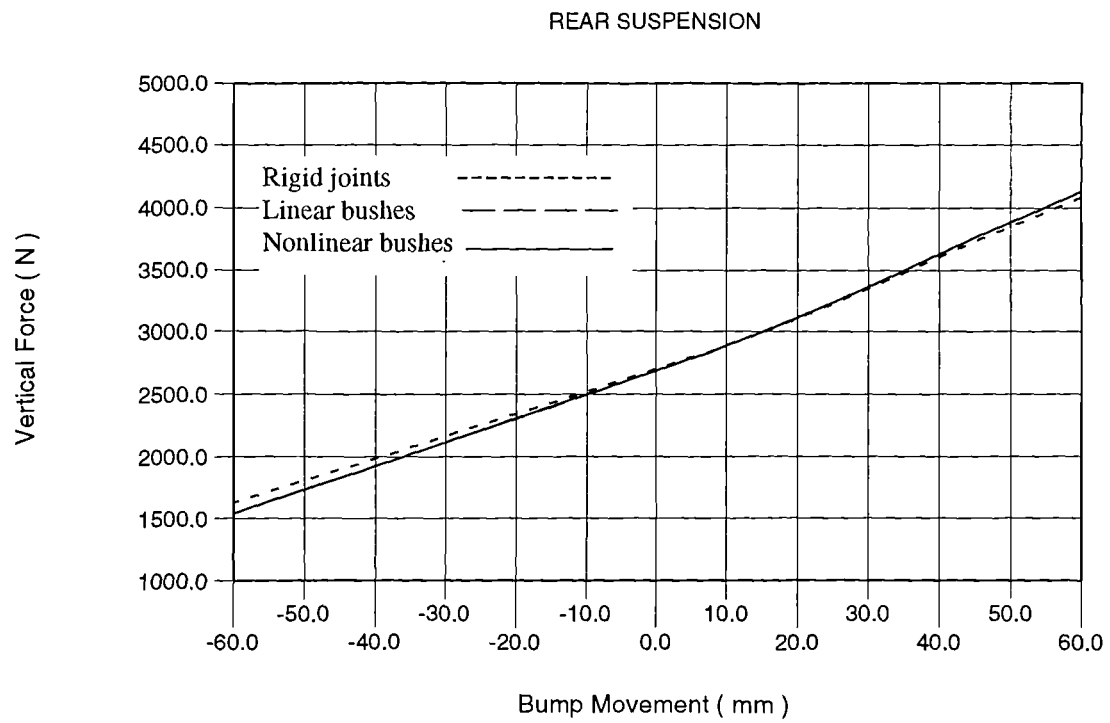
REAR SUSPENSION

Figure B.12 Rear suspension - vertical force with bump movement

APPENDIX C

RESULTS OF EXPERIMENTAL TYRE TESTING
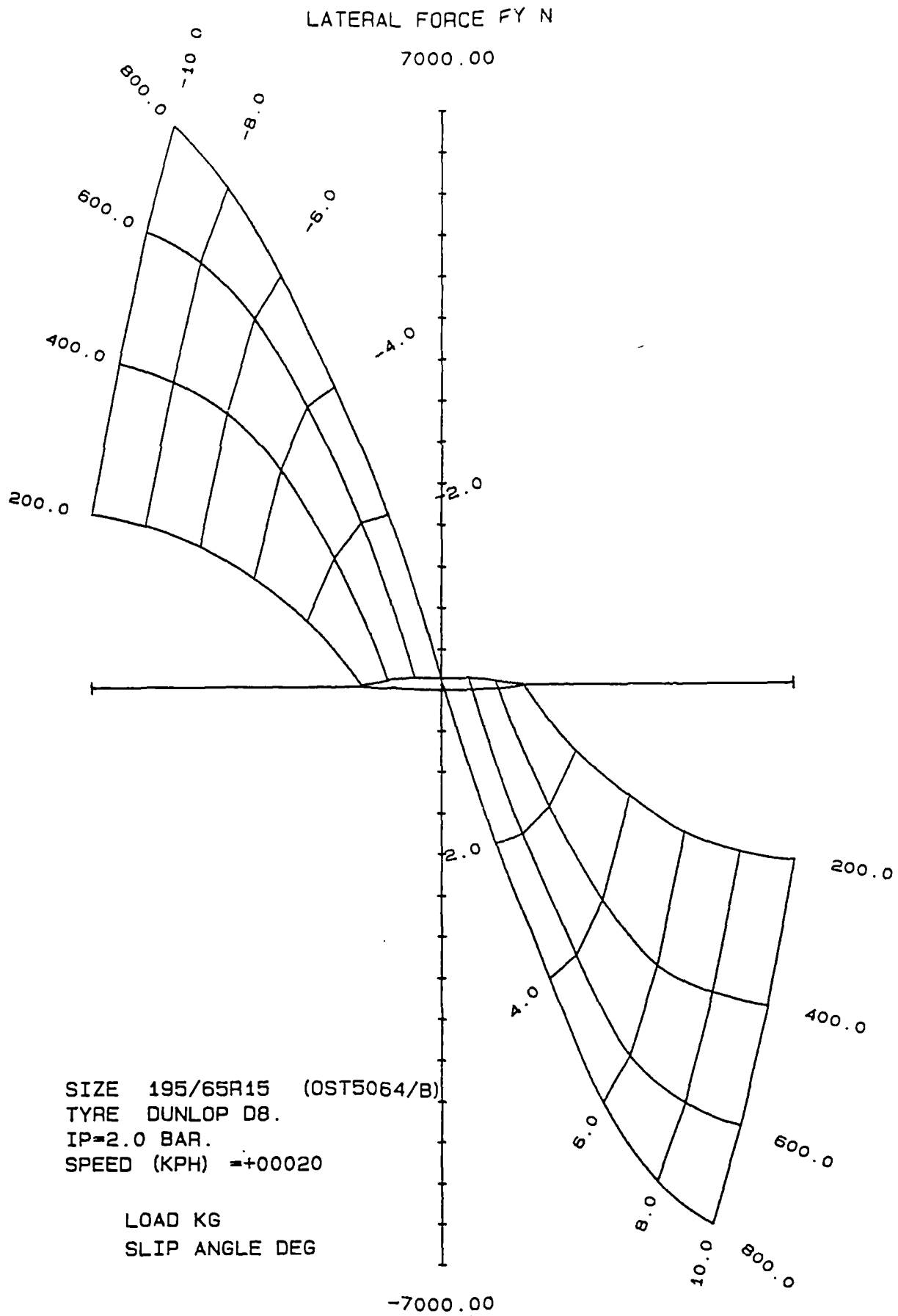
Figure C.1 Lateral force Fy with slip angle α

ALIGNING TORQUE MZ NM.

200.00

SIZE   195/65R15   (OST5064/B)
TYRE   DUNLOP D8.
IP=2.0 BAR.
SPEED (KPH) =+00020

6.0

4.0   8.0

10.0

2.0   800.0

800.0

-10.0

-2.0

800.
600.
400.
200.

-8.0
0.0   -4.0   LOAD KG
                 0.0
                                   SLIP ANGLE DEG
-6.0   -200.00
0.0
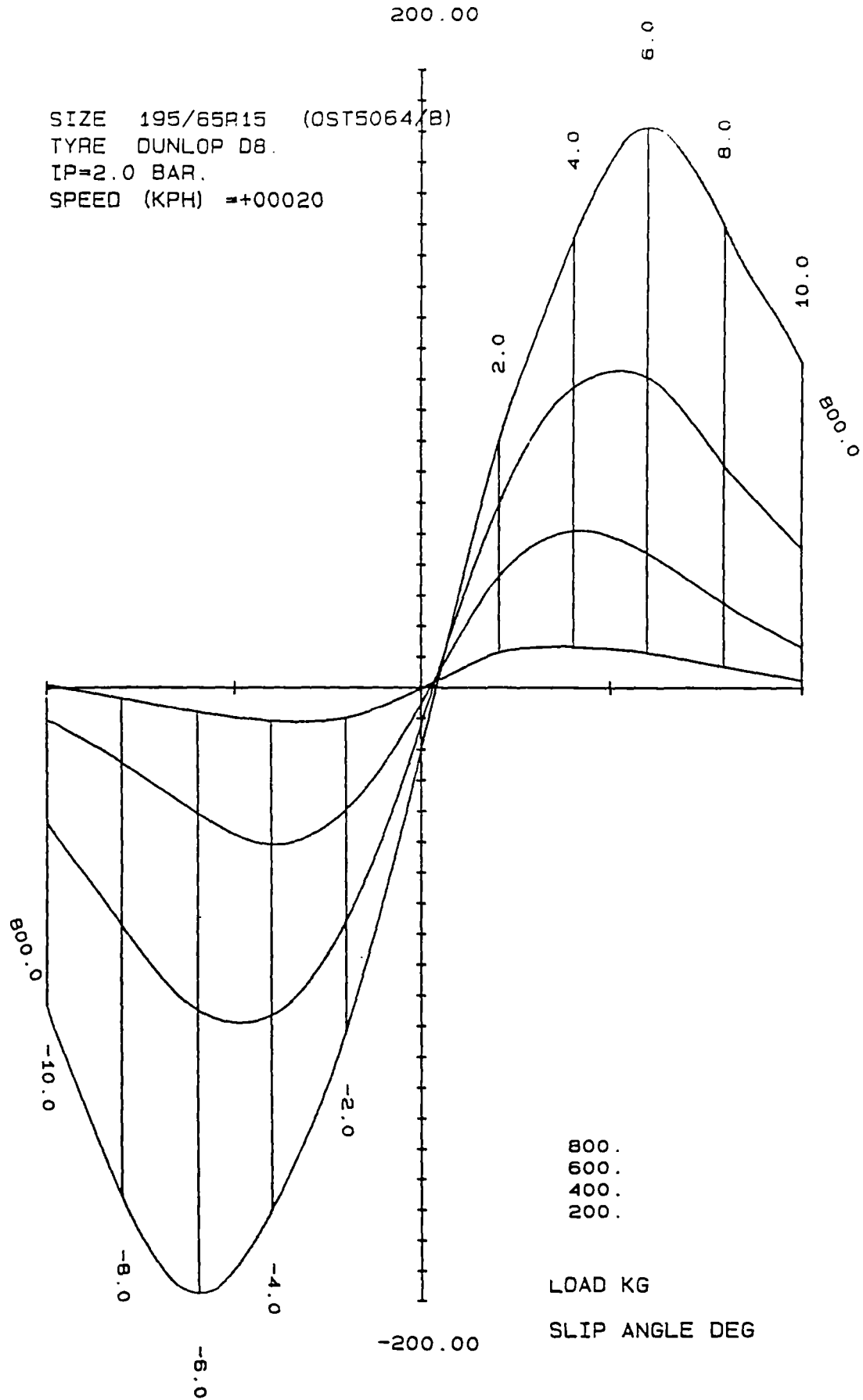
Figure C.2 Aligning moment Mz with slip angle α

LATERAL FORCE FY N

7000.00

SIZE   195/65R15   (OST5064/B)
TYRE   DUNLOP D8.
IP=2.0 BAR.
SPEED (KPH) =+00020

ALIGNING TORQUE MZ NM

-200.00

200.00

800.
600.
400.
200.

LOAD KG

SLIP ANGLE DEG

-7000.00
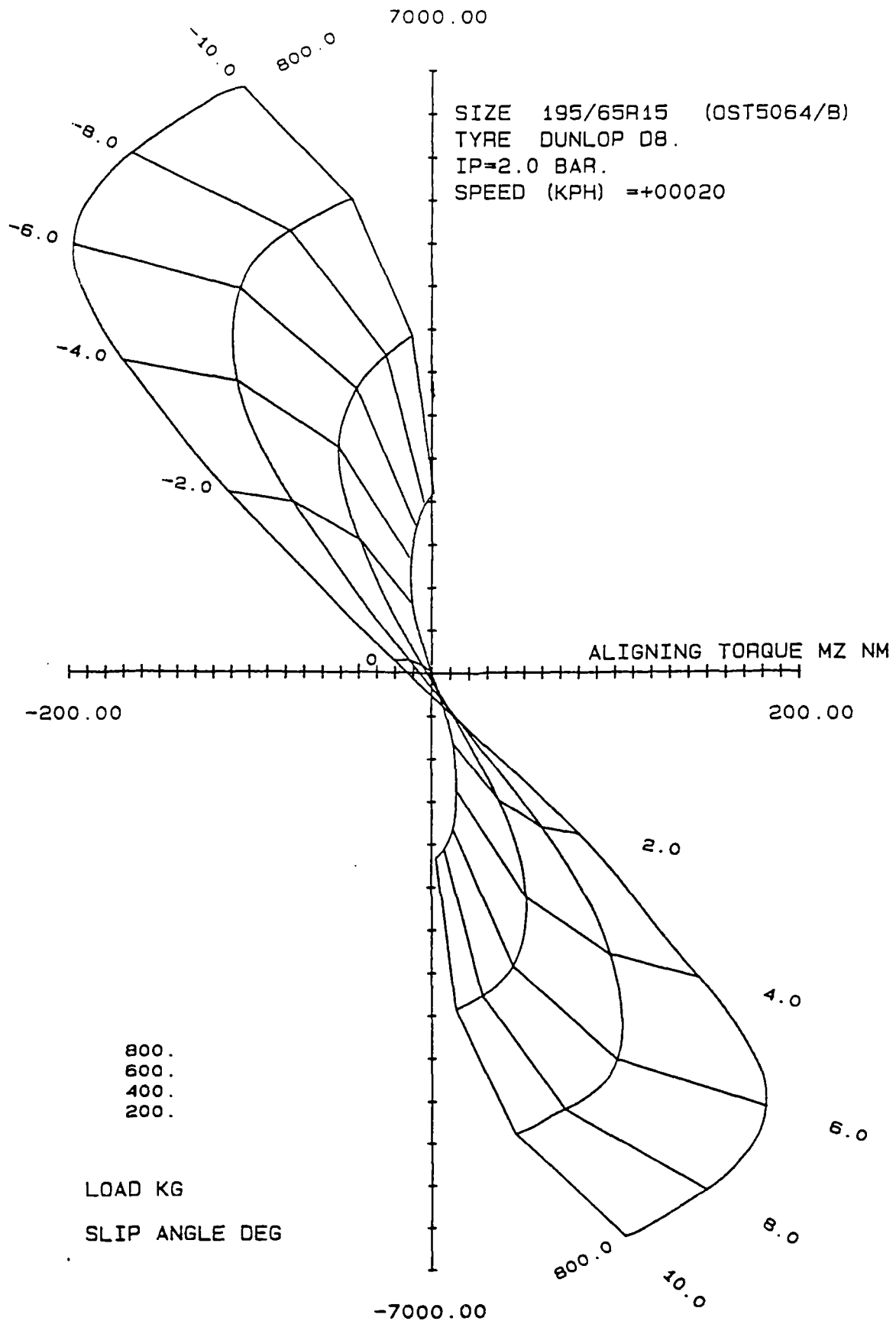
Figure C.3 Lateral force Fy with aligning moment Mz (Gough Plot)

CORNERING STIFFNESS N/DEG.   (AT ZERO SLIP ANGLE)

1000.00

SIZE   195/65R15   (OST5064/A)
TYRE   DUNLOP D8.
IP=2.0 BAR.
SPEED (KPH) =+00020

.00

.00   800.00
                                         LOAD KG
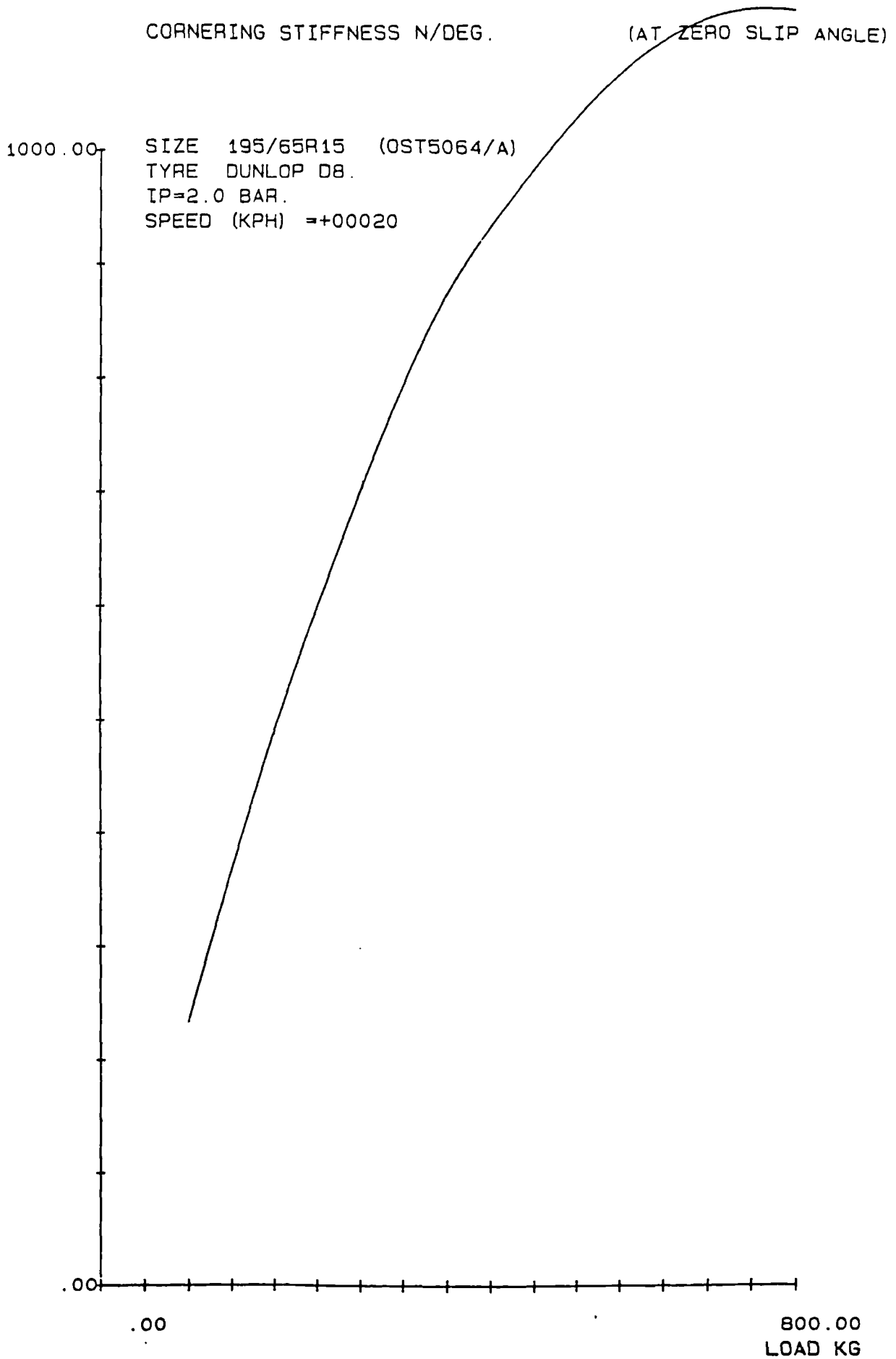
Figure C.4 Cornering stiffness with load
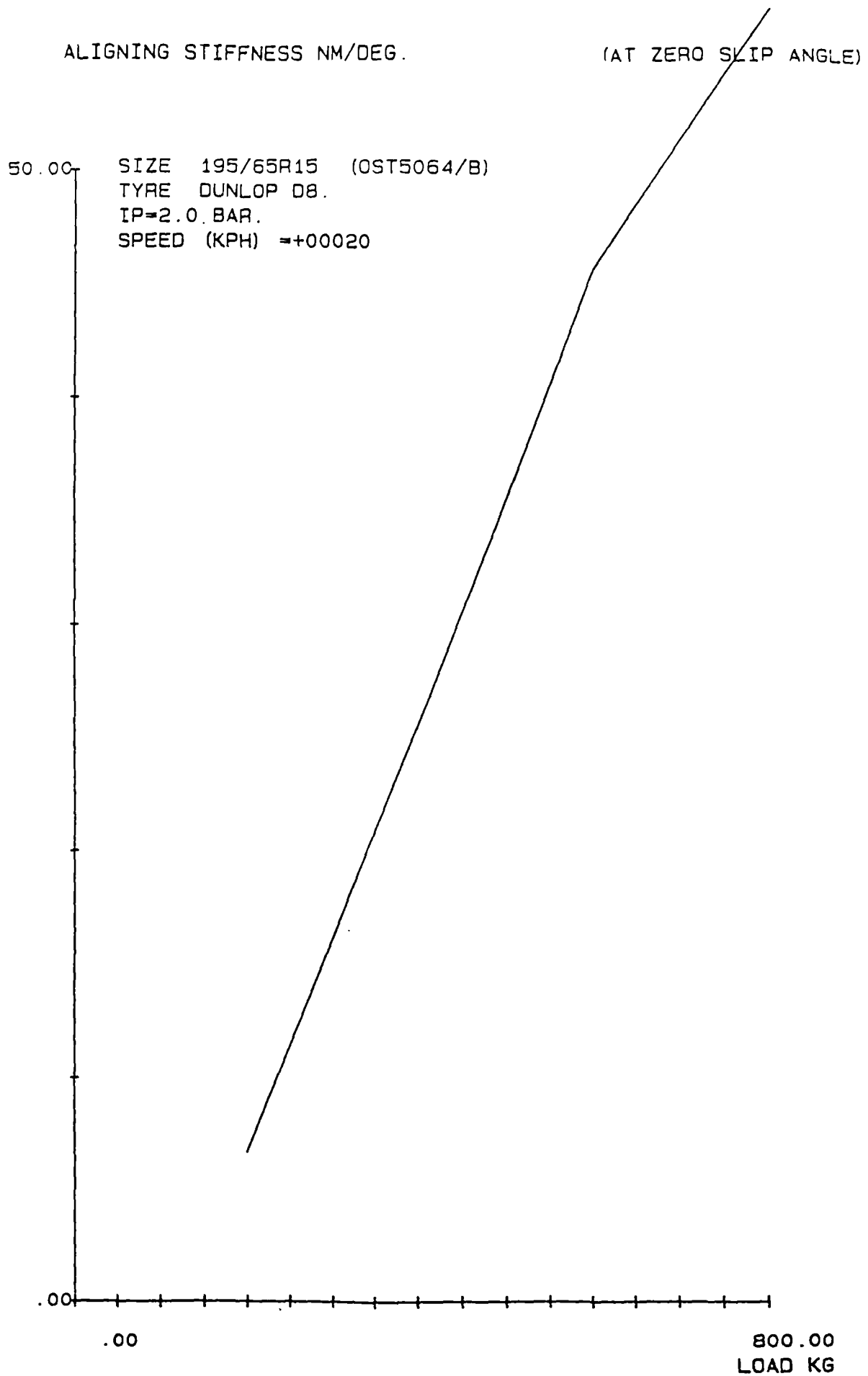
Figure C.5 Aligning stiffness with load

LATERAL FORCE FY N

1000.00

10.0
8.0
6.0
4.0
2.0
0.0
-2.0
-4.0
-6.0
-8.0
-10.0

800.0
700.0
600.0
500.0
400.0
300.0
200.0
100.0

SIZE   195/65R15   (OST5064/A)
TYRE   DUNLOP D8.
IP=2.0 BAR.
SPEED (KPH) =+00020

LOAD KG
CAMBER ANGLE DEG

-1000.00
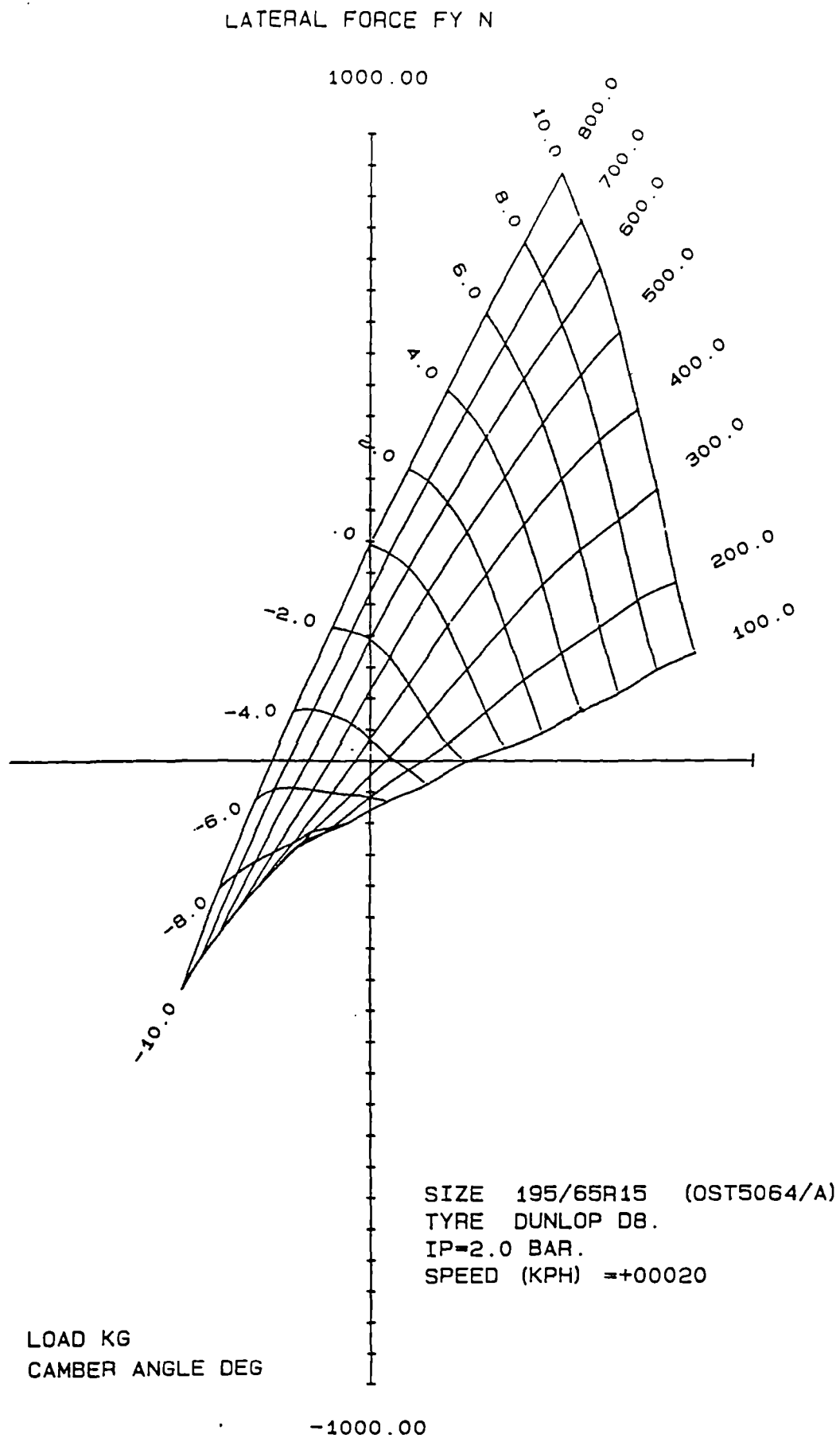
Figure C.6 Lateral force Fy with camber angle γ

ALIGNING TORQUE MZ NM.

50.00

SIZE   195/65R15   (OST5064/A)
TYRE   DUNLOP D8.
IP=2.0 BAR.
SPEED (KPH) =+00020

800.0

10.0

8.0

6.0

4.0

2.0

-2.0

-4.0

-6.0

-8.0

800.
700.
600.
500.
400.
300.
200.
100.

LOAD KG

CAMBER ANGLE DEG

-50.00

800.0

-10.0
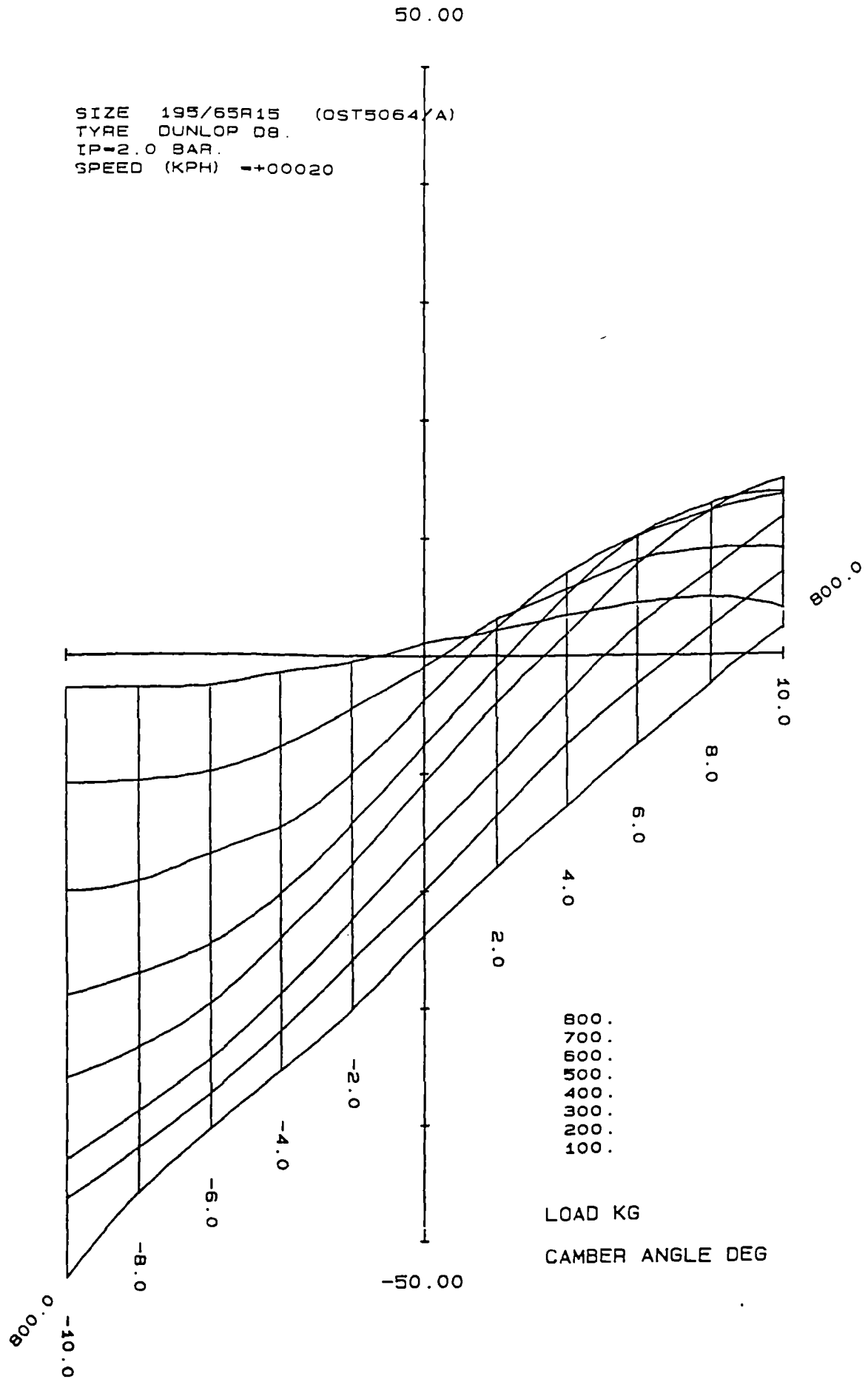
Figure C.7 Aligning moment Mz with camber angle γ

CAMBER STIFFNESS N/DEG.   (AT ZERO CAMBER ANGLE)

100.00

SIZE   195/65R15   (OST5064/A)
TYRE   DUNLOP D8.
IP=2.0 BAR.
SPEED (KPH) =+00020

.00

.00   800.00
                                           LOAD KG
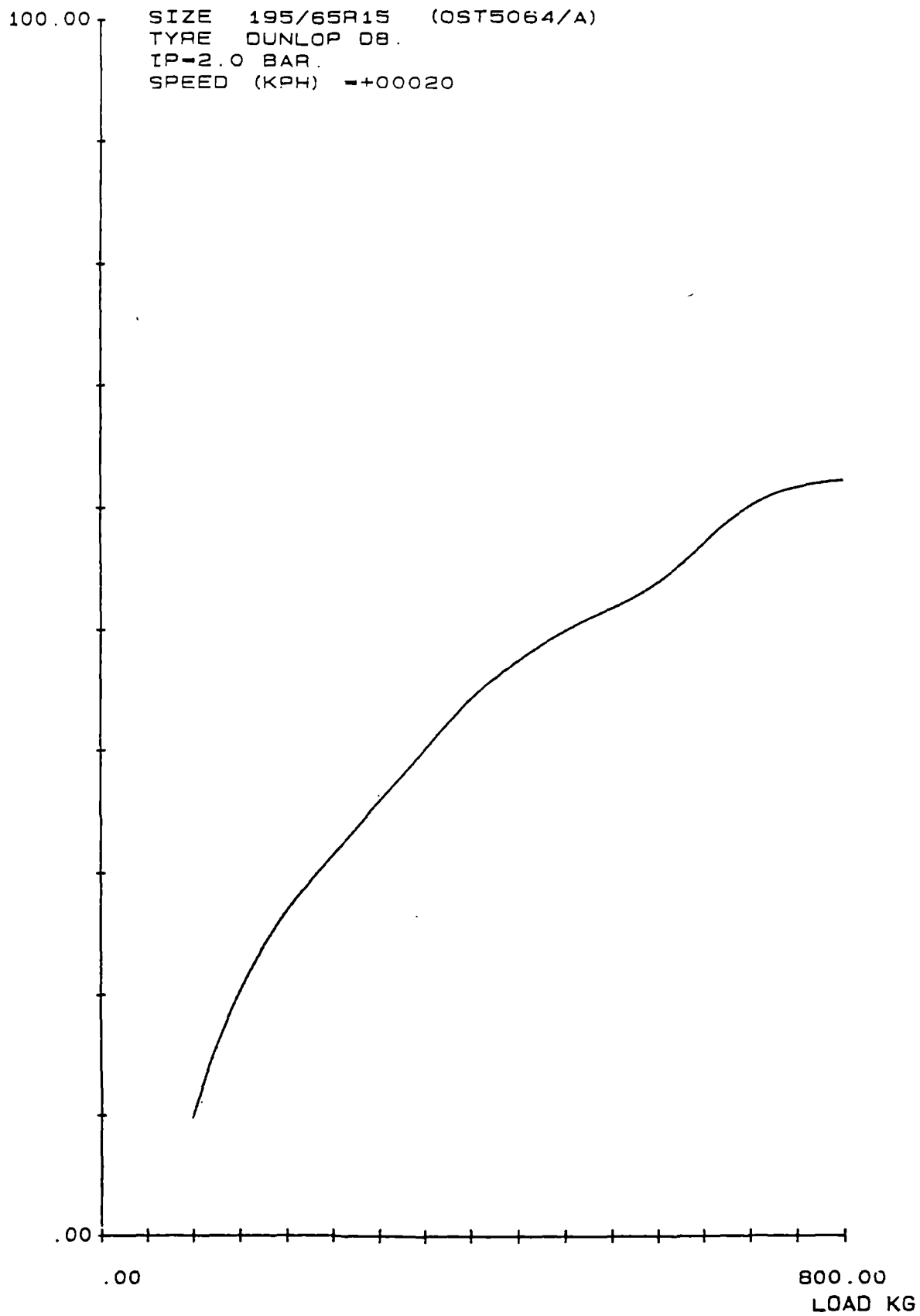
Figure C.8 Camber stiffness with load

ALIGNING CAMBER STIFFNESS NM/0   (AT ZERO CAMBER ANGLE)

10.00

SIZE   195/65R15   (OST5064/A)
TYRE   DUNLOP D8.
IP=2.0 BAR.
SPEED (KPH) =+00020

.00

.00   800.00
                                                          LOAD KG
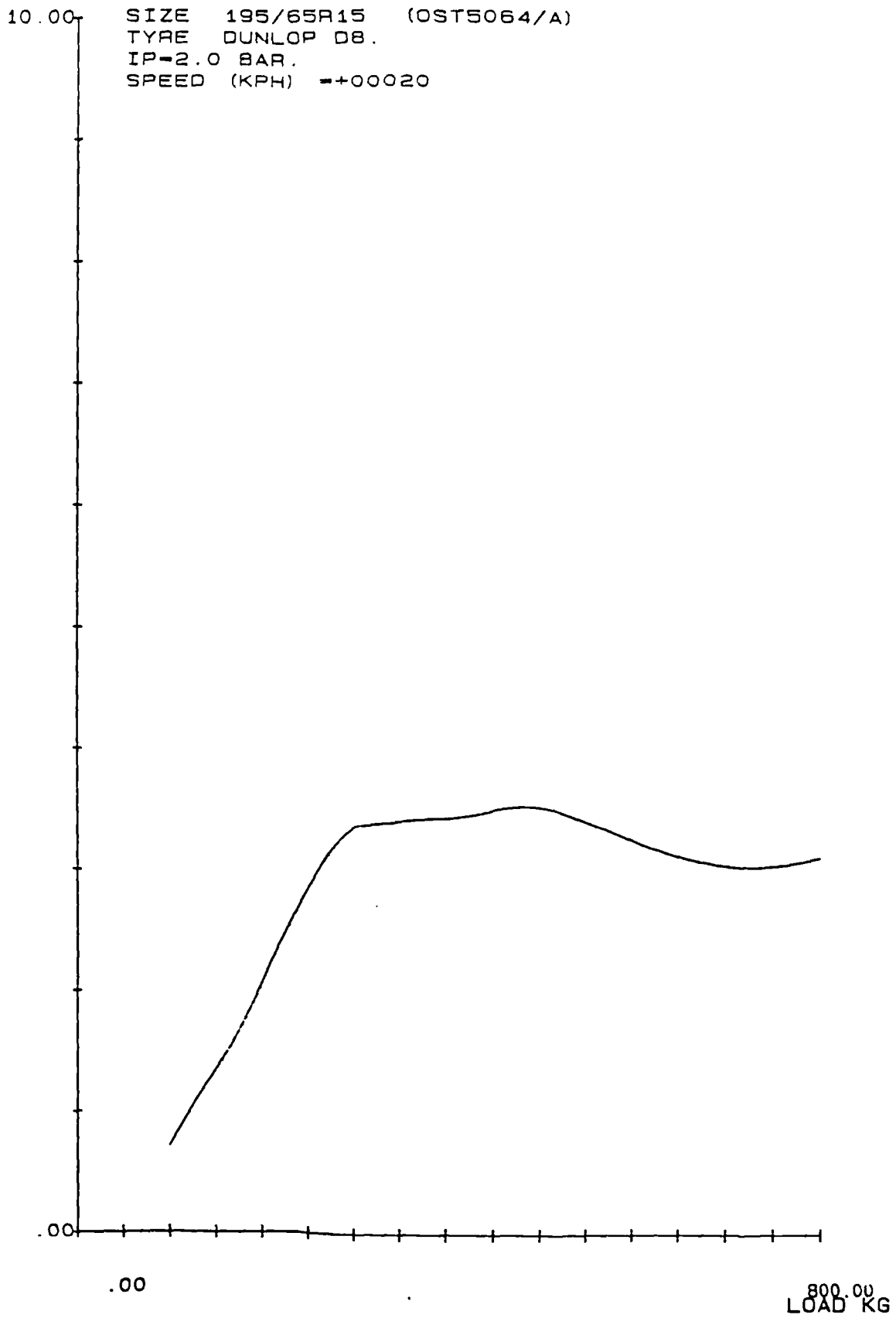
Figure C.9 Aligning camber stiffness with load

TYRE BRAKING FORCE TEST - TYRE B 195/65 R15

Vertical Load Increments - 1kN 2kN 3kN 4kN
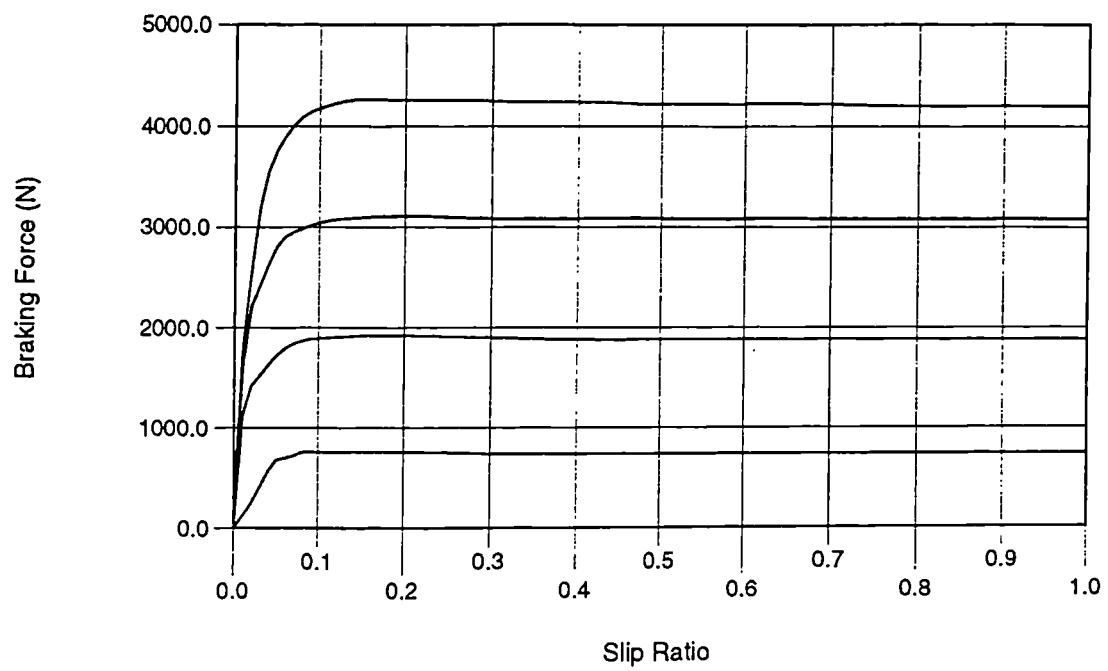
Figure C.10 Braking force with slip ratio

APPENDIX D

FORTRAN TYRE MODEL SUBROUTINES

.

D.1 Fiala Tyre Model Subroutine

```
SUBROUTINE TIRSUB ( ID, TIME, T0, CPROP, TPROP, MPROP,
     &            PAR, NPAR, STR, NSTR, DFLAG,
     &            IFLAG, FSAE, TSAE, FPROP )
C
C  This program is part of the CUTyre system - M Blundell, Feb 1997
C  This source code defines the Fiala tyre model as provided with the main ADAMS program.
C  Modifications have been included to introduce new variables for any future work to extend
C  the model to account for camber effects.
C
C  Inputs:
C
      INTEGER      ID, NPAR, NSTR
      DOUBLE PRECISION TIME, T0
      DOUBLE PRECISION CPROP(*), TPROP(*), MPROP(*), PAR(*)
      CHARACTER*80    STR(*)
      LOGICAL      DFLAG, IFLAG
C
C Outputs:
C
      DOUBLE PRECISION FSAE(*), TSAE(*), FPROP(*)
C
C Local Variables:
C
      DOUBLE PRECISION  SLIP, ALPHA, DEFL, DEFLD
      DOUBLE PRECISION  R2, CZ, CS, CA, CR, DZ, AMASS, WSPIN
C
C    Camber variables
C
      DOUBLE PRECISION  GAMMA, CG, HA, HG, FYA, FYG, TZA, TZG
C
      INTEGER         IORD
      DOUBLE PRECISION  ZERO, ONE, SCFACT, DELMAX
      DOUBLE PRECISION  FX, FY, FZ, FX1, FX2, TY, TZ, H, ASTAR, SSTAR
      DOUBLE PRECISION  U, FZDAMP, FZDEFL, WSPNMX
      LOGICAL         ERFLG
C
      PARAMETER       (ZERO=0.0)
      PARAMETER       (ONE=1.0)
      PARAMETER       (IORD=0)
      PARAMETER       (WSPNMX=5.0D-1)
C
C EXECUTABLE CODE
C
C   Extract data from input arrays
C
      SLIP  = CPROP(1)
      ALPHA = CPROP(2)
      DEFL  = CPROP(4)
      DEFLD = CPROP(5)
      WSPIN = CPROP(8)
C
      AMASS = MPROP(1)
C
      R2   = TPROP(2)
      CZ   = TPROP(3)
      CS   = TPROP(4)
```

```fortran
      CA    = TPROP(5)
      CR    = TPROP(7)
      DZ    = TPROP(8)
      U     = TPROP(11)
C
C    Camber
C
      GAMMA = CPROP (3)
      CG = TPROP (6)
C
C    Initialize force values
C
      FX = 0.D0
      FY = 0.D0
      FZ = 0.D0
      TY = 0.D0
      TZ = 0.D0
C
      IF(DEFL .LE. 0.D0) THEN
        GOTO 1000
      ENDIF
C
C    Calculate normal loads due to stiffness (always .LE. zero)
C
      FZDEFL = -DEFL*CZ
C
C    Calculate normal loads due to damping
C
      FZDAMP = - 2.D0*SQRT(AMASS*CZ)*DZ*(DEFLD)
C
C    Calculate total normal force (fz)
C
      FZ    = MIN (0.0D0, (FZDEFL + FZDAMP) )
C
C    Calculate critical longitudinal slip value
C
      SSTAR = ABS(U*FZ/(2.D0*CS))
C
C    Compute longitudinal force (fx)
C
      IF(ABS(SLIP) .LE. ABS(SSTAR)) THEN
        FX = -CS*SLIP
      ELSE
        FX1 = U*ABS(FZ)
        FX2 = (U*FZ)**2/(4.D0*ABS(SLIP)*CS)
        FX = -(FX1-FX2)*SIGN(1.0D0,SLIP)
      ENDIF
C
C    Calculate critical value of slip angle
C
      ASTAR = ATAN(ABS(3.D0*U*FZ/CA))
C
C    Compute lateral force and aligning torque (FYA & TZA) due to slip
C
      IF(ABS(ALPHA) .LE. 1.D-10) THEN
        FYA = 0.D0
        TZA = 0.D0
      ELSE IF( ABS(ALPHA) .LE. ASTAR ) THEN
```

```fortran
      HA = 1.D0 - CA*ABS(TAN(ALPHA))/(3.D0*U*ABS(FZ))
      FYA = -U*ABS(FZ)*(1.D0-HA**3)*SIGN(1.0D0,ALPHA)
      TZA = U*ABS(FZ)*2.D0*R2*(1.D0-HA)*(HA**3)*SIGN(1.0D0,ALPHA)
      ELSE
      FYA = -U*ABS(FZ)*SIGN(1.0D0,ALPHA)
      TZA = 0.D0
      ENDIF
C
C     Compute lateral force and aligning torque (FYG & TZG) due to camber
C     Currently set to zero, example of futire modifications -  FYG =CG*GAMMA
C
      FYG = 0.0
      TZG =0.D0
C
C     Compute total lateral force and aligning torque (FY & TZ)
C
      FY = FYA + FYG
      TZ = TZA + TZG
C
C     Copy the calculated values for FX, FY, FZ, TY & TZ to FSAE
C      and TSAE arrays
C
 1000 FSAE(1) = FX
      FSAE(2) = FY
      FSAE(3) = FZ
      TSAE(1) = 0.0
      TSAE(2) = TY
      TSAE(3) = TZ
      FPROP(1) = 0.0
      FPROP(2) = 0.0
      RETURN
      END
```

D.2 Full Interpolation Tyre Model Subroutine

```fortran
      SUBROUTINE TIRSUB ( ID, TIME, T0, CPROP, TPROP, MPROP,
     &          PAR, NPAR, STR, NSTR, DFLAG,
     &          IFLAG, FSAE, TSAE, FPROP )
C
C   This program is part of the CUTyre system - M Blundell, Feb 1997
C   This version is based on an interpolation approach using measured
C   tyre test data which is include in SPLINE statements. It is referred to as the Full model
C   as it accounts for a larger range of tests varying slip at given camber angles
C   Cubic interpolation is used for varying slip with linear interpolation between camber angles
C   Fx based on Fiala model
C   This model is used for full interpolation and is tested on TYRE A
C   Camber inputs are at -5, 0 and 5 degrees
C
C   The coefficients in the model asume the following units:
C   slip angle: degrees
C   camber angle: degrees
C   Fz (load): kg
C   Fy and Fx: N
C   Tz : Nm
C
C Inputs:
C
      INTEGER       ID, NPAR, NSTR
      DOUBLE PRECISION TIME, T0
      DOUBLE PRECISION CPROP(*), TPROP(*), MPROP(*), PAR(*)
      CHARACTER*80    STR(*)
      LOGICAL        DFLAG, IFLAG, ERRFLG
C
C Outputs:
C
      DOUBLE PRECISION FSAE(*), TSAE(*), FPROP(*), ARRAY(3)
C
C Local Variables:
C
      DOUBLE PRECISION  SLIP, ALPHA, DEFL, DEFLD
      DOUBLE PRECISION  R2, CZ, CS, CA, CR, DZ, AMASS, WSPIN
C
      DOUBLE PRECISION  GAMMA,CG,RALPHA,RGAMMA,FZL,TZL,TZLA,TZLG
      DOUBLE PRECISION CFY,DFY,EFY,SHFY,SVFY,PHIFY,TZL1,TZL2,TZL3
      DOUBLE PRECISION CTZ,DTZ,ETZ,BTZ,SHTZ,SVTZ,PHITZ
      DOUBLE PRECISION CFX,DFX,EFX,BFX,SHFX,SVFX,PHIFX
C
      INTEGER        IORD
      DOUBLE PRECISION  ZERO, ONE, SCFACT, DELMAX,FY1,FY2,FY3
      DOUBLE PRECISION  FX, FY, FZ, FX1, FX2, TY, TZ, H, ASTAR, SSTAR
      DOUBLE PRECISION  U, FZDAMP, FZDEFL, WSPNMX, DTOR, RTOD
      LOGICAL        ERFLG
C
      PARAMETER     (ZERO=0.0)
      PARAMETER     (ONE=1.0)
      PARAMETER     (IORD=0)
      PARAMETER     (WSPNMX=5.0D-1)
      PARAMETER     (DTOR=0.017453292)
      PARAMETER     (RTOD=57.29577951)
C
C   EXECUTABLE CODE
```

```
C   Extract data from input arrays
C
    SLIP  = CPROP(1)
    DEFL  = CPROP(4)
    DEFLD = CPROP(5)
    WSPIN = CPROP(8)
C
    AMASS = MPROP(1)
C
    R2    = TPROP(2)
    CZ    = TPROP(3)
    CS    = TPROP(4)
    CA    = TPROP(5)
    CR    = TPROP(7)
    DZ    = TPROP(8)
    U     = TPROP(11)
C
    RALPHA  = CPROP(2)
    RGAMMA = CPROP (3)
    CG = TPROP (6)
    ALPHA=RALPHA*RTOD
    GAMMA=RGAMMA*RTOD
C
C   Initialize force values
C
     FX = 0.D0
     FY = 0.D0
     FZ = 0.D0
     TY = 0.D0
     TZ = 0.D0
C
    IF(DEFL .LE. 0.D0) THEN
       GOTO 1000
    ENDIF
C
C   Calculate normal loads due to stiffness (always .LE. zero)
C
    FZDEFL = -DEFL*CZ
C
C   Calculate normal loads due to damping
C
    FZDAMP = - 2.D0*SQRT(AMASS*CZ)*DZ*(DEFLD)
C
C   Calculate total normal force (fz)
C
    FZ    =   MIN (0.0D0, (FZDEFL + FZDAMP) )
C
C   Convert to kg and change sign
C
    FZL = -FZ/9.81
C
C   Calculate critical longitudinal slip value
C
    SSTAR = ABS(U*FZ/(2.D0*CS))
C
C   Compute longitudinal force
C
    IF(ABS(SLIP) .LE. ABS(SSTAR)) THEN
```

```fortran
      FX = -CS*SLIP
      ELSE
      FX1 = U*ABS(FZ)
      FX2 = (U*FZ)**2/(4.D0*ABS(SLIP)*CS)
      FX = -(FX1-FX2)*SIGN(1.0D0,SLIP)
      ENDIF
C
C     Compute lateral force at gamma = -5, 0 and 5 degrees
C
      CALL CUBSPL (ALPHA,FZL,101,0,ARRAY,ERRFLG)
      FY1=ARRAY(1)
      CALL CUBSPL (ALPHA,FZL,102,0,ARRAY,ERRFLG)
      FY2=ARRAY(1)
      CALL CUBSPL (ALPHA,FZL,103,0,ARRAY,ERRFLG)
      FY3=ARRAY(1)
C
C     Use linear interpolation to get FY for actual Gamma
C
      IF (GAMMA.GE.-5.and.GAMMA.LT.0) THEN
      FY=FY1+((FY2-FY1)*((GAMMA+5)/5))
      ELSE
      FY=FY2+((FY3-FY2)*((GAMMA-0)/5))
      ENDIF
C
C     Compute self aligning moment
C
      CALL CUBSPL (ALPHA,FZL,104,0,ARRAY,ERRFLG)
      TZL1=ARRAY(1)
      CALL CUBSPL (ALPHA,FZL,105,0,ARRAY,ERRFLG)
      TZL2=ARRAY(1)
      CALL CUBSPL (ALPHA,FZL,106,0,ARRAY,ERRFLG)
      TZL3=ARRAY(1)
C
C     Use linear interpolation to get TZL for actual Gamma
C
      IF (GAMMA.GE.-5.and.GAMMA.LT.0) THEN
      TZL=TZL1+((TZL2-TZL1)*((GAMMA+5)/5))
      ELSE
      TZL=TZL2+((TZL3-TZL2)*((GAMMA-0)/5))
      ENDIF
C
C     Convert to Nmm
C
      TZ = TZL*1000.0
C
C     Copy the calculated values for FX, FY, FZ, TY & TZ to FSAE
C     and TSAE arrays
C
1000  FSAE(1) = FX
      FSAE(2) = FY
      FSAE(3) = FZ
      TSAE(1) = 0.0
      TSAE(2) = 0.0
      TSAE(3) = TZ
      FPROP(1) = 0.0
      FPROP(2) = 0.0
      RETURN
      END
```

D.3 Full Interpolation Tyre Model Subroutine (No Camber)

```fortran
      SUBROUTINE TIRSUB ( ID, TIME, T0, CPROP, TPROP, MPROP,
     &             PAR, NPAR, STR, NSTR, DFLAG,
     &             IFLAG, FSAE, TSAE, FPROP )
C
C    This program is part of the CUTyre system - M Blundell, Feb 1997
C    tyre test data which is include in SPLINE statements. It is referred to as the Full model
C    as it accounts for a larger range of tests varying slip at given camber angles
C   Cubic interpolation is used for varying slip with linear interpolation between camber angles
C    Fx based on Fiala model
C    This model is used for full interpolation and is tested on TYRE A
C    Camber inputs are not included here - results only used at camber = 0
C    The coefficients in the model asume the following units:
C    slip angle: degrees
C    camber angle: degrees
C    Fz (load): kg
C    Fy and Fx: N
C    Tz : Nm
C
C Inputs:
C
      INTEGER       ID, NPAR, NSTR
      DOUBLE PRECISION TIME, T0
      DOUBLE PRECISION CPROP(*), TPROP(*), MPROP(*), PAR(*)
      CHARACTER*80   STR(*)
      LOGICAL        DFLAG, IFLAG, ERRFLG
C
C Outputs:
C
      DOUBLE PRECISION FSAE(*), TSAE(*), FPROP(*), ARRAY(3)
C
C Local Variables:
C
      DOUBLE PRECISION  SLIP, ALPHA, DEFL, DEFLD
      DOUBLE PRECISION  R2, CZ, CS, CA, CR, DZ, AMASS, WSPIN
C
      DOUBLE PRECISION  GAMMA,CG,RALPHA,RGAMMA,FZL,TZL,TZLA,TZLG
      DOUBLE PRECISION CFY,DFY,EFY,SHFY,SVFY,PHIFY,TZL1,TZL2,TZL3
      DOUBLE PRECISION CTZ,DTZ,ETZ,BTZ,SHTZ,SVTZ,PHITZ
      DOUBLE PRECISION CFX,DFX,EFX,BFX,SHFX,SVFX,PHIFX
C
      INTEGER        IORD
      DOUBLE PRECISION  ZERO, ONE, SCFACT, DELMAX,FY1,FY2,FY3
      DOUBLE PRECISION  FX, FY, FZ, FX1, FX2, TY, TZ, H, ASTAR, SSTAR
      DOUBLE PRECISION  U, FZDAMP, FZDEFL, WSPNMX, DTOR, RTOD
      LOGICAL        ERFLG
C
      PARAMETER      (ZERO=0.0)
      PARAMETER      (ONE=1.0)
      PARAMETER      (IORD=0)
      PARAMETER      (WSPNMX=5.0D-1)
      PARAMETER      (DTOR=0.017453292)
      PARAMETER      (RTOD=57.29577951)
C
C   EXECUTABLE CODE
C    Extract data from input arrays
C
```

```fortran
      SLIP  = CPROP(1)
      DEFL  = CPROP(4)
      DEFLD = CPROP(5)
      WSPIN = CPROP(8)
C
      AMASS = MPROP(1)
C
      R2    = TPROP(2)
      CZ    = TPROP(3)
      CS    = TPROP(4)
      CA    = TPROP(5)
      CR    = TPROP(7)
      DZ    = TPROP(8)
      U     = TPROP(11)
C
      RALPHA = CPROP(2)
      RGAMMA = CPROP (3)
      CG = TPROP (6)
      ALPHA=RALPHA*RTOD
      GAMMA=RGAMMA*RTOD
C
C   Initialize force values
C
      FX = 0.D0
      FY = 0.D0
      FZ = 0.D0
      TY = 0.D0
      TZ = 0.D0
C
      IF(DEFL .LE. 0.D0) THEN
        GOTO 1000
      ENDIF
C
C   Calculate normal loads due to stiffness (always .LE. zero)
C
      FZDEFL = -DEFL*CZ
C
C   Calculate normal loads due to damping
C
      FZDAMP = - 2.D0*SQRT(AMASS*CZ)*DZ*(DEFLD)
C
C   Calculate total normal force (fz)
C
      FZ   =  MIN (0.0D0, (FZDEFL + FZDAMP) )
C
C   Convert to kg and change sign
C
      FZL = -FZ/9.81
C
C   Calculate critical longitudinal slip value
C
      SSTAR = ABS(U*FZ/(2.D0*CS))
C
C   Compute longitudinal force
C
      IF(ABS(SLIP) .LE. ABS(SSTAR)) THEN
        FX = -CS*SLIP
      ELSE
```

```fortran
      FX1 = U*ABS(FZ)
      FX2 = (U*FZ)**2/(4.D0*ABS(SLIP)*CS)
      FX = -(FX1-FX2)*SIGN(1.0D0,SLIP)
      ENDIF
C
C   Compute lateral force
C
      CALL CUBSPL (ALPHA,FZL,102,0,ARRAY,ERRFLG)
      FY=ARRAY(1)
C
C   Compute self aligning moment
C
      CALL CUBSPL (ALPHA,FZL,105,0,ARRAY,ERRFLG)
      TZL=ARRAY(1)
C
C   Convert to Nmm
C
      TZ = TZL*1000.0
C
C   Copy the calculated values for FX, FY, FZ, TY & TZ to FSAE
C   and TSAE arrays
C
1000  FSAE(1) = FX
      FSAE(2) = FY
      FSAE(3) = FZ
      TSAE(1) = 0.0
      TSAE(2) = 0.0
      TSAE(3) = TZ
      FPROP(1) = 0.0
      FPROP(2) = 0.0
      RETURN
      END
```

D.4 Pacjeka Tyre Model (Monte Carlo Version) Subroutine

```
      SUBROUTINE TIRSUB ( ID, TIME, T0, CPROP, TPROP, MPROP,
     &            PAR, NPAR, STR, NSTR, DFLAG,
     &            IFLAG, FSAE, TSAE, FPROP )
C
C    This program is part of the CUTyre system - M Blundell, Feb 1997
C    This version is based on the Pacjeka tyre model as described
C    in SAE paper 890087. This also referred to as the "Monte Carlo" version.
C
C    The coefficients in the model assume the following units:
C    slip angle: degrees
C    camber angle: degrees
C    slip ratio %
C    Fz (load): kN
C    Fy and Fx: N
C    Tz : Nm
C
C    Note sign changes between Paceka formulation and SAE convention
C
C    If camber is not included set A6,A8,A11,C6,C10,C11,C14,C15 to zero
C
C Inputs:
C
      INTEGER      ID, NPAR, NSTR
      DOUBLE PRECISION TIME, T0
      DOUBLE PRECISION CPROP(*), TPROP(*), MPROP(*), PAR(*)
      CHARACTER*80    STR(*)
      LOGICAL      DFLAG, IFLAG
C
C Outputs:
C
      DOUBLE PRECISION FSAE(*), TSAE(*), FPROP(*)
C
C Local Variables:
C
      DOUBLE PRECISION  SLIP, ALPHA, DEFL, DEFLD
      DOUBLE PRECISION  R2, CZ, CS, CA, CR, DZ, AMASS, WSPIN
C
      DOUBLE PRECISION
     GAMMA,CG,RALPHA,RGAMMA,FXP,FZP,FYP,TZP,SLIPCENT
      DOUBLE PRECISION A0,A1,A2,A3,A4,A5,A6,A7,A8,A9,A10,A111,A112,A13
      DOUBLE PRECISION B0,B1,B2,B3,B4,B5,B6,B7,B8,B9,B10,B11,B12
      DOUBLE PRECISION C0,C1,C2,C3,C4,C5,C6,C7,C8,C9,C10,C11,C12,C13
      DOUBLE PRECISION C14,C15,C16,C17
      DOUBLE PRECISION CFY,DFY,EFY,SHFY,SVFY,PHIFY
      DOUBLE PRECISION CTZ,DTZ,ETZ,BTZ,SHTZ,SVTZ,PHITZ
      DOUBLE PRECISION CFX,DFX,EFX,BFX,SHFX,SVFX,PHIFX
C
      INTEGER      IORD
      DOUBLE PRECISION  ZERO, ONE, SCFACT, DELMAX
      DOUBLE PRECISION  FX, FY, FZ, FX1, FX2, TY, TZ, H, ASTAR, SSTAR
      DOUBLE PRECISION  U, FZDAMP, FZDEFL, WSPNMX, DTOR, RTOD
      LOGICAL      ERFLG
C
      PARAMETER    (ZERO=0.0)
      PARAMETER    (ONE=1.0)
      PARAMETER    (IORD=0)
```

```
      PARAMETER        (WSPNMX=5.0D-1)
      PARAMETER        (DTOR=0.017453292)
      PARAMETER        (RTOD=57.29577951)
C
C     Define Pacejka Coefficients
C
      A0=1.68638
      A1=-46.8451
      A2=1185.46
      A3=1146.06
      A4=4.92921
      A5=0.00547748
      A6=-0.655688
      A7=1.86868
      A8=-0.0280612
      A9=0.0147439
      A10=-0.212575
      A111=-13.4328
      A112=0.428945
      A12=-3.71929
      A13=33.6686
C
      C0=2.41195
      C1=-3.98725
      C2=-2.70372
      C3=0.552334
      C4=-6.22588
      C5=-0.225629
      C6=0.00142515
      C7=-0.0175979
      C8=-0.143857
      C9=-0.822518
      C10=0.0174298
      C11=-0.0244277
      C12=0.0116074
      C13=-0.322245
      C14=0.0210605
      C15=-0.565934
      C16=0.376785
      C17=-2.38039
C
C   EXECUTABLE CODE
C   Extract data from input arrays
C
      SLIP  = CPROP(1)
      DEFL  = CPROP(4)
      DEFLD = CPROP(5)
      WSPIN = CPROP(8)
C
      AMASS = MPROP(1)
C
      R2    = TPROP(2)
      CZ    = TPROP(3)
      CS    = TPROP(4)
      CA    = TPROP(5)
      CR    = TPROP(7)
      DZ    = TPROP(8)
      U     = TPROP(11)
```

```fortran
C
      RALPHA = CPROP(2)
      RGAMMA = CPROP (3)
      CG = TPROP (6)
      ALPHA=RALPHA*RTOD
      GAMMA=RGAMMA*RTOD
C
C   Initialize force values
C
      FX = 0.D0
      FY = 0.D0
      FZ = 0.D0
      TY = 0.D0
      TZ = 0.D0
C
      IF(DEFL .LE. 0.D0) THEN
         GOTO 1000
      ENDIF
C
C   Calculate normal loads due to stiffness (always .LE. zero)
C
      FZDEFL = -DEFL*CZ
C
C   Calculate normal loads due to damping
C
      FZDAMP = - 2.D0*SQRT(AMASS*CZ)*DZ*(DEFLD)
C
C   Calculate total normal force (fz)
C
      FZ   =  MIN (0.0D0, (FZDEFL + FZDAMP) )
C
C   Convert to kN and change sign
C
      FZP = -FZ/1000.0
C
C   Compute longitudinal force
C
      IF(ABS(SLIP) .LE. ABS(SSTAR)) THEN
      FX = -CS*SLIP
      ELSE
       FX1 = U*ABS(FZ)
       FX2 = (U*FZ)**2/(4.D0*ABS(SLIP)*CS)
       FX = -(FX1-FX2)*SIGN(1.0D0,SLIP)
      ENDIF
C
C   Compute lateral force
C
      CFY=1.3
      DFY=A1*FZP**2+A2*FZP
      EFY=A6*FZP+A7
      BFY=((A3*SIN(2*ATAN(FZP/A4)))*(1-A5*ABS(GAMMA)))/(CFY+DFY)
      SHFY=A8*GAMMA+A9*FZP+A10
C     SVFY=A12*FZP+A13+(A112*FZP**2+A111*FZP)*GAMMA
      SVFY=A11*FZP*GAMMA+A12*FZP+A13
      PHIFY=(1-EFY)*(ALPHA+SHFY)+(EFY/BFY)*ATAN(BFY*(ALPHA+SHFY))
      FYP=DFY*SIN(CFY*ATAN(BFY*PHIFY))+SVFY
C
C   Change sign
```

```fortran
C
      FY=-FYP
C
C   Compute self aligning moment
C
      CTZ=2.4
      DTZ=C1*FZP**2+C2*FZP
      ETZ=(C7*FZP**2+C8*FZP+C9)/(1-C10*ABS(GAMMA))
      BTZ=((C3*FZP**2+C4*FZP)*(1-C6*ABS(GAMMA))*EXP(-C5*FZP))/(CTZ+DTZ)
      SHTZ=C11*GAMMA+C12*FZP+C13
      SVTZ=(C14*FZP**2+C15*FZP)*GAMMA+C16*FZP+C17
      PHITZ=(1-ETZ)*(ALPHA+SHTZ)+(ETZ/BTZ)*ATAN(BTZ*(ALPHA+SHTZ))
      TZP=DTZ*SIN(CTZ*ATAN(BTZ*PHITZ))+SVTZ
C
C   Convert to Nmm and change sign
C
      TZ = -TZP*1000.0
C
C   Copy the calculated values for FX, FY, FZ, TY & TZ to FSAE
C    and TSAE arrays
C
1000  FSAE(1) = FX
      FSAE(2) = FY
      FSAE(3) = FZ
C
      TSAE(1) = 0.0
      TSAE(2) = 0.0
      TSAE(3) = TZ
C
      FPROP(1) = 0.0
      FPROP(2) = 0.0
C
      RETURN
      END
```

D.5 Limited Interpolation Tyre Model Subroutine

```fortran
      SUBROUTINE TIRSUB ( ID, TIME, T0, CPROP, TPROP, MPROP,
     &             PAR, NPAR, STR, NSTR, DFLAG,
     &             IFLAG, FSAE, TSAE, FPROP )
C
C     This program is part of the CUTyre system - M Blundell, Feb 1997
C     This version is based on an interpolation approach using measured
C     tyre test data which is include in SPLINE statements. The model is referred to as the
C     limited version based on the limited testing where camber and slip are varied
C     independently.
C     Fx based on Fiala model
C
C     The coefficients in the model asume the following units:
C     slip angle: degrees
C     camber angle: degrees
C     Fz (load): kg
C     Fy and Fx: N
C     Tz : Nm
C
C     Note this subroutine is developed to not accounr for offsets
C     twice. The offsets are include for slip interpolation
C     but for camber the offset at zero camber is subtracted.
C
C Inputs:
C
      INTEGER        ID, NPAR, NSTR
      DOUBLE PRECISION TIME, T0
      DOUBLE PRECISION CPROP(*), TPROP(*), MPROP(*), PAR(*)
      CHARACTER*80    STR(*)
      LOGICAL        DFLAG, IFLAG, ERRFLG
C
C Outputs:
C
      DOUBLE PRECISION FSAE(*), TSAE(*), FPROP(*), ARRAY(3)
C
C Local Variables:
C
      DOUBLE PRECISION  SLIP, ALPHA, DEFL, DEFLD
      DOUBLE PRECISION  R2, CZ, CS, CA, CR, DZ, AMASS, WSPIN
C
      DOUBLE PRECISION  GAMMA,CG,RALPHA,RGAMMA,FZL,TZL,TZLA,TZLG
      DOUBLE PRECISION CFY,DFY,EFY,SHFY,SVFY,PHIFY,TZLG0,TZLG1
      DOUBLE PRECISION CTZ,DTZ,ETZ,BTZ,SHTZ,SVTZ,PHITZ
      DOUBLE PRECISION CFX,DFX,EFX,BFX,SHFX,SVFX,PHIFX
C
      INTEGER        IORD
      DOUBLE PRECISION  ZERO, ONE, SCFACT, DELMAX,FYA,FYG,FYG0,FYG1
      DOUBLE PRECISION  FX, FY, FZ, FX1, FX2, TY, TZ, H, ASTAR, SSTAR
      DOUBLE PRECISION  U, FZDAMP, FZDEFL, WSPNMX, DTOR, RTOD
      LOGICAL        ERFLG
C
      PARAMETER      (ZERO=0.0)
      PARAMETER      (ONE=1.0)
      PARAMETER      (IORD=0)
      PARAMETER      (WSPNMX=5.0D-1)
      PARAMETER      (DTOR=0.017453292)
      PARAMETER      (RTOD=57.29577951)
```

```fortran
C
C
C   EXECUTABLE CODE
C
C
C   Extract data from input arrays
C
      SLIP  = CPROP(1)
      DEFL  = CPROP(4)
      DEFLD = CPROP(5)
      WSPIN = CPROP(8)
C
      AMASS = MPROP(1)
C
      R2    = TPROP(2)
      CZ    = TPROP(3)
      CS    = TPROP(4)
      CA    = TPROP(5)
      CR    = TPROP(7)
      DZ    = TPROP(8)
      U     = TPROP(11)
C
      RALPHA = CPROP(2)
      RGAMMA = CPROP (3)
      CG = TPROP (6)
      ALPHA=RALPHA*RTOD
      GAMMA=RGAMMA*RTOD
C   .
C   Initialize force values
C
      FX = 0.D0
      FY = 0.D0
      FZ = 0.D0
      TY = 0.D0
      TZ = 0.D0
C
      IF(DEFL .LE. 0.D0) THEN
        GOTO 1000
      ENDIF
C
C   Calculate normal loads due to stiffness (always .LE. zero)
C
      FZDEFL = -DEFL*CZ
C
C   Calculate normal loads due to damping
C
      FZDAMP = - 2.D0*SQRT(AMASS*CZ)*DZ*(DEFLD)
C
C   Calculate total normal force (fz)
C
      FZ   =  MIN (0.0D0, (FZDEFL + FZDAMP) )
C
C   Convert to kg and change sign
C
      FZL = -FZ/9.81
C
C   Calculate critical longitudinal slip value
C
```

```fortran
      SSTAR = ABS(U*FZ/(2.D0*CS))
C
C   Compute longitudinal force
C
      IF(ABS(SLIP) .LE. ABS(SSTAR)) THEN
       FX = -CS*SLIP
       ELSE
        FX1 = U*ABS(FZ)
        FX2 = (U*FZ)**2/(4.D0*ABS(SLIP)*CS)
        FX = -(FX1-FX2)*SIGN(1.0D0,SLIP)
       ENDIF
C
C   Compute lateral force
C
      CALL CUBSPL (ALPHA,FZL,100,0,ARRAY,ERRFLG)
      FYA=ARRAY(1)
      CALL CUBSPL (0,FZL,300,0,ARRAY,ERRFLG)
      FYG0=ARRAY(1)
      CALL CUBSPL (GAMMA,FZL,300,0,ARRAY,ERRFLG)
      FYG1=ARRAY(1)
      FYG=FYG1-FYG0
      FY=FYA+FYG
C
C   Compute self aligning moment
C
      CALL CUBSPL (ALPHA,FZL,200,0,ARRAY,ERRFLG)
      TZLA=ARRAY(1)
      CALL CUBSPL (0,FZL,400,0,ARRAY,ERRFLG)
      TZLG0=ARRAY(1)
      CALL CUBSPL (GAMMA,FZL,400,0,ARRAY,ERRFLG)
      TZLG1=ARRAY(1)
      TZLG=TZLG1-TZLG0
      TZL=TZLA+TZLG
C
C   Convert to Nmm
C
      TZ = TZL*1000.0
C
C   Copy the calculated values for FX, FY, FZ, TY & TZ to FSAE
C   and TSAE arrays
C
1000  FSAE(1) = FX
      FSAE(2) = FY
      FSAE(3) = FZ
C
      TSAE(1) = 0.0
      TSAE(2) = 0.0
      TSAE(3) = TZ
C
      FPROP(1) = 0.0
      FPROP(2) = 0.0
C
      RETURN
      END
```

D.6 Limited Interpolation Tyre Model Subroutine (No Camber)

```
      SUBROUTINE TIRSUB ( ID, TIME, T0, CPROP, TPROP, MPROP,
     &             PAR, NPAR, STR, NSTR, DFLAG,
     &             IFLAG, FSAE, TSAE, FPROP )
C
C     This program is part of the CUTyre system - M Blundell, Feb 1997
C     This version is based on an interpolation approach using measured
C     tyre test data which is include in SPLINE statements. The model is referred to as the
C     limited version based on the limited testing where camber and slip are varied
C     independently.
C
C     Note that in this version the effects of camber have been omitted.
C
C     Fx based on Fiala model
C
C     The coefficients in the model asume the following units:
C     slip angle: degrees
C     camber angle: degrees
C     Fz (load): kg
C     Fy and Fx: N
C     Tz : Nm
C
C     Note this subroutine is developed to not account for offsets
C     twice. The offsets are include for slip interpolation
C     but for camber the offset at zero camber is subtracted.
C
C Inputs:
C
      INTEGER       ID, NPAR, NSTR
      DOUBLE PRECISION TIME, T0
      DOUBLE PRECISION CPROP(*), TPROP(*), MPROP(*), PAR(*)
      CHARACTER*80   STR(*)
      LOGICAL        DFLAG, IFLAG, ERRFLG
C
C Outputs:
C
      DOUBLE PRECISION FSAE(*), TSAE(*), FPROP(*), ARRAY(3)
C
C Local Variables:
C
      DOUBLE PRECISION  SLIP, ALPHA, DEFL, DEFLD
      DOUBLE PRECISION  R2, CZ, CS, CA, CR, DZ, AMASS, WSPIN
C
      DOUBLE PRECISION  GAMMA,CG,RALPHA,RGAMMA,FZL,TZL,TZLA,TZLG
      DOUBLE PRECISION  CFY,DFY,EFY,SHFY,SVFY,PHIFY,TZLG0,TZLG1
      DOUBLE PRECISION  CTZ,DTZ,ETZ,BTZ,SHTZ,SVTZ,PHITZ
      DOUBLE PRECISION  CFX,DFX,EFX,BFX,SHFX,SVFX,PHIFX
C
      INTEGER        IORD
      DOUBLE PRECISION  ZERO, ONE, SCFACT, DELMAX,FYA,FYG,FYG0,FYG1
      DOUBLE PRECISION  FX, FY, FZ, FX1, FX2, TY, TZ, H, ASTAR, SSTAR
      DOUBLE PRECISION  U, FZDAMP, FZDEFL, WSPNMX, DTOR, RTOD
      LOGICAL        ERFLG
C
      PARAMETER     (ZERO=0.0)
      PARAMETER     (ONE=1.0)
      PARAMETER     (IORD=0)
```

```fortran
      PARAMETER     (WSPNMX=5.0D-1)
      PARAMETER     (DTOR=0.017453292)
      PARAMETER     (RTOD=57.29577951)
C
C
C   EXECUTABLE CODE
C
C   Extract data from input arrays
C
      SLIP  = CPROP(1)
      DEFL  = CPROP(4)
      DEFLD = CPROP(5)
      WSPIN = CPROP(8)
C
      AMASS = MPROP(1)
C
      R2    = TPROP(2)
      CZ    = TPROP(3)
      CS    = TPROP(4)
      CA    = TPROP(5)
      CR    = TPROP(7)
      DZ    = TPROP(8)
      U     = TPROP(11)
C
      RALPHA = CPROP(2)
      RGAMMA = CPROP (3)
      CG = TPROP (6)
      ALPHA=RALPHA*RTOD
      GAMMA=RGAMMA*RTOD
C
C   Initialize force values
C
      FX = 0.D0
      FY = 0.D0
      FZ = 0.D0
      TY = 0.D0
      TZ = 0.D0
C
      IF(DEFL .LE. 0.D0) THEN
         GOTO 1000
      ENDIF
C
C   Calculate normal loads due to stiffness (always .LE. zero)
C
      FZDEFL = -DEFL*CZ
C
C   Calculate normal loads due to damping
C
      FZDAMP = - 2.D0*SQRT(AMASS*CZ)*DZ*(DEFLD)
C
C   Calculate total normal force (fz)
C
      FZ    = MIN (0.0D0, (FZDEFL + FZDAMP) )
C
C   Convert to kg and change sign
C
      FZL = -FZ/9.81
C
```

```fortran
C    Calculate critical longitudinal slip value
C
     SSTAR = ABS(U*FZ/(2.D0*CS))
C
C    Compute longitudinal force
C
     IF(ABS(SLIP) .LE. ABS(SSTAR)) THEN
       FX = -CS*SLIP
     ELSE
       FX1 = U*ABS(FZ)
       FX2 = (U*FZ)**2/(4.D0*ABS(SLIP)*CS)
       FX = -(FX1-FX2)*SIGN(1.0D0,SLIP)
     ENDIF
C
C    Compute lateral force
C
     CALL CUBSPL (ALPHA,FZL,100,0,ARRAY,ERRFLG)
     FYA=ARRAY(1)
c    CALL CUBSPL (0,FZL,300,0,ARRAY,ERRFLG)
c    FYG0=ARRAY(1)
c    CALL CUBSPL (GAMMA,FZL,300,0,ARRAY,ERRFLG)
c    FYG1=ARRAY(1)
c    FYG=FYG1-FYG0
     FY=FYA
C
C    Compute self aligning moment
C
     CALL CUBSPL (ALPHA,FZL,200,0,ARRAY,ERRFLG)
     TZLA=ARRAY(1)
c    CALL CUBSPL (0,FZL,400,0,ARRAY,ERRFLG)
c    TZLG0=ARRAY(1)
c    CALL CUBSPL (GAMMA,FZL,400,0,ARRAY,ERRFLG)
c    TZLG1=ARRAY(1)
c    TZLG=TZLG1-TZLG0
     TZL=TZLA
C
C    Convert to Nmm
C
     TZ = TZL*1000.0
C
C    Copy the calculated values for FX, FY, FZ, TY & TZ to FSAE
C    and TSAE arrays
C
1000 FSAE(1) = FX
     FSAE(2) = FY
     FSAE(3) = FZ
C
     TSAE(1) = 0.0
     TSAE(2) = 0.0
     TSAE(3) = TZ
C
     FPROP(1) = 0.0
     FPROP(2) = 0.0
C
     RETURN
     END
```

D.7 Pacjeka Tyre Model (Version 3) Subroutine

```
      SUBROUTINE TIRSUB ( ID, TIME, T0, CPROP, TPROP, MPROP,
     &            PAR, NPAR, STR, NSTR, DFLAG,
     &            IFLAG, FSAE, TSAE, FPROP )
C
C    This program is part of the CUTyre system - M Blundell, Feb 1997
C    This version is based on the Pacjeka tyre model (Version 3).
C    Coefficients are for TYRE B
C
C    The coefficients in the model assume the following units:
C    slip angle: radians
C    camber angle: radians
C    slip ratio %
C    Fz (load): N
C    Fy and Fx: N
C    Tz : Nm
C    Note sign changes between Paceka formulation and SAE convention
C    If camber is not included set A5,A10,A13,A14,A15,A16
C    and C6,C10,C13,C16,C17,C18,C19,C20 to zero
C
C Inputs:
C
      INTEGER      ID, NPAR, NSTR
      DOUBLE PRECISION TIME, T0
      DOUBLE PRECISION CPROP(*), TPROP(*), MPROP(*), PAR(*)
      CHARACTER*80    STR(*)
      LOGICAL      DFLAG, IFLAG
C
C Outputs:
C
      DOUBLE PRECISION FSAE(*), TSAE(*), FPROP(*)
C
C Local Variables:
C
      DOUBLE PRECISION  SLIP, ALPHA, DEFL, DEFLD
      DOUBLE PRECISION  R2, CZ, CS, CA, CR, DZ, AMASS, WSPIN
C
C
C
      DOUBLE PRECISION GAMMA,CG,RALPHA,RGAMMA,FXP,FZP,FYP,TZP
      DOUBLE PRECISION A0,A1,A2,A3,A4,A5,A6,A7,A8,A9,A10,A11,A12,A13
      DOUBLE PRECISION A14,A15,A16,A17,SLIPCENT
      DOUBLE PRECISION C0,C1,C2,C3,C4,C5,C6,C7,C8,C9,C10,C11,C12,C13
      DOUBLE PRECISION C14,C15,C16,C17,C18,C19,C20
      DOUBLE PRECISION CFY,DFY,EFY,SHFY,SVFY,PHIFY
      DOUBLE PRECISION CTZ,DTZ,ETZ,BTZ,SHTZ,SVTZ,PHITZ
      DOUBLE PRECISION CFX,DFX,EFX,BFX,SHFX,SVFX,PHIFX,DUMTZ,DUMFY
C
      INTEGER      IORD
      DOUBLE PRECISION  ZERO, ONE, SCFACT, DELMAX
      DOUBLE PRECISION  FX, FY, FZ, FX1, FX2, TY, TZ, H, ASTAR, SSTAR
      DOUBLE PRECISION  U, FZDAMP, FZDEFL, WSPNMX, DTOR, RTOD
      LOGICAL      ERFLG
C
      PARAMETER    (ZERO=0.0)
      PARAMETER    (ONE=1.0)
      PARAMETER    (IORD=0)
```

```fortran
      PARAMETER    (WSPNMX=5.0D-1)
      PARAMETER    (DTOR=0.017453292)
      PARAMETER    (RTOD=57.29577951)
C
C     Define Pacejka Coefficients
C
      A0=.103370E+01
      A1=-.224482E-05
      A2=.132185E+01
      A3=.604035E+05
      A4=.877727E+04
      A5=0.0
      A6=.458114E-04
      A7=.468222
      A8=.381896E-06
      A9=.516209E-02
      A10=0.00
      A11=-.366375E-01
      A12=-.568859E+02
      A13=0.00
      A14=0.00
      A15=0.00
      A16=0.00
      A17=.379913
C
C
      C0=.235000E+01
      C1=.266333E-05
      C2=.249270E-02
      C3=-.159794E-03
      C4=-.254777E-01
      C5=.142145E-03
      C6=0.00
      C7=.197277E-07
      C8=-.359537E-03
      C9=.630223
      C10=0.00
      C11=.120220E-06
      C12=.275062E-02
      C13=0.00
      C14=-.172742E-02
      C15=.544249E+01
      C16=0.00
      C17=0.00
      C18=0.00
      C19=0.00
      C20=0.00
C
C
C     EXECUTABLE CODE
C
C
C     Extract data from input arrays
C
      SLIP  = CPROP(1)
      DEFL  = CPROP(4)
      DEFLD = CPROP(5)
      WSPIN = CPROP(8)
```

```
C
      AMASS = MPROP(1)
C
      R2    = TPROP(2)
      CZ    = TPROP(3)
      CS    = TPROP(4)
      CA    = TPROP(5)
      CR    = TPROP(7)
      DZ    = TPROP(8)
      U     = TPROP(11)
C
C   Convert sign on alpha
C
      RALPHA  = CPROP(2)
      RGAMMA = CPROP (3)
      CG = TPROP (6)
      ALPHA=-RALPHA
      GAMMA=RGAMMA
C
C   Initialize force values
C
      FX = 0.D0
      FY = 0.D0
      FZ = 0.D0
      TY = 0.D0
      TZ = 0.D0
C
      IF(DEFL .LE. 0.D0) THEN
         GOTO 1000
      ENDIF
C
C   Calculate normal loads due to stiffness (always .LE. zero)
C
      FZDEFL = -DEFL*CZ
C
C   Calculate normal loads due to damping
C
      FZDAMP = - 2.D0*SQRT(AMASS*CZ)*DZ*(DEFLD)
C
C   Calculate total normal force (fz)
C
      FZ    =  MIN (0.0D0, (FZDEFL + FZDAMP) )
C
C   Convert to kN and change sign
C
      FZP = -FZ
C
C   Compute longitudinal force
C
C
C    In absence of Pacjeka terms use the fiala Fx model
C
      IF(ABS(SLIP) .LE. ABS(SSTAR)) THEN
         FX = -CS*SLIP
      ELSE
         FX1 = U*ABS(FZ)
         FX2 = (U*FZ)**2/(4.D0*ABS(SLIP)*CS)
         FX = -(FX1-FX2)*SIGN(1.0D0,SLIP)
```

```
      ENDIF
C
C    Compute lateral force
C
      CFY=A0
      SHFY=A8*FZP+A9+A10*GAMMA
      DFY=(A1*FZP+A2)*(1-A15*GAMMA**2)*FZP
      IF(ALPHA+SHFY.LT.0.0)THEN
       DUMFY=-1.0
      ELSE
       DUMFY=1.0
      ENDIF
      EFY=(A6*FZP+A7)*(1-(A16*GAMMA+A17)*DUMFY)
      BFY=((A3*SIN(2*ATAN(FZP/A4)))*(1-A5*ABS(GAMMA)))/(CFY+DFY)
      SVFY=A11*FZP+A12+(A13*FZP**2+A14*FZP)*GAMMA
      PHIFY=(1-EFY)*(ALPHA+SHFY)+(EFY/BFY)*ATAN(BFY*(ALPHA+SHFY))
      FYP=DFY*SIN(CFY*ATAN(BFY*PHIFY))+SVFY
C
C    Change sign
C
      FY=FYP
C
C    Compute self aligning moment
C
      CTZ=C0
      SHTZ=C11*FZP+C12+C13*GAMMA
      DTZ=(C1*FZP**2+C2*FZP)*(1-C18*GAMMA**2)
      IF(ALPHA+SHTZ.LT.0.0)THEN
       DUMTZ=-1.0
      ELSE
       DUMTZ=1.0
      ENDIF
      ETZ=(C7*FZP**2+C8*FZP+C9)*(1-(C19*GAMMA+C20)*DUMTZ)
      ETZ=ETZ/(1-C10*ABS(GAMMA))
      BTZ=((C3*FZP**2+C4*FZP)*(1-C6*ABS(GAMMA))*EXP(-C5*FZP))/(CTZ+DTZ)
      SVTZ=C14*FZP+C15+(C16*FZP**2+C17*FZP)*GAMMA
      PHITZ=(1-ETZ)*(ALPHA+SHTZ)+(ETZ/BTZ)*ATAN(BTZ*(ALPHA+SHTZ))
      TZP=DTZ*SIN(CTZ*ATAN(BTZ*PHITZ))+SVTZ
C
C    Convert to Nmm and change sign   ·
C
      TZ = TZP*1000.0
C
C    Copy the calculated values for FX, FY, FZ, TY & TZ to FSAE
C    and TSAE arrays
C
1000  FSAE(1) = FX
      FSAE(2) = FY
      FSAE(3) = FZ
C
      TSAE(1) = 0.0
      TSAE(2) = 0.0
      TSAE(3) = TZ
      FPROP(1) = 0.0
      FPROP(2) = 0.0
C
      RETURN
      END
```

APPENDIX E

TYRE MODEL PLOTS FROM THE *CUTyre* RIG MODEL
USING DATA FOR TYRE A

INTERPOLATION TYRE MODEL - TYRE A 195/65 R15

Vertical Load Increments - 200kg 400kg 600kg 800kg
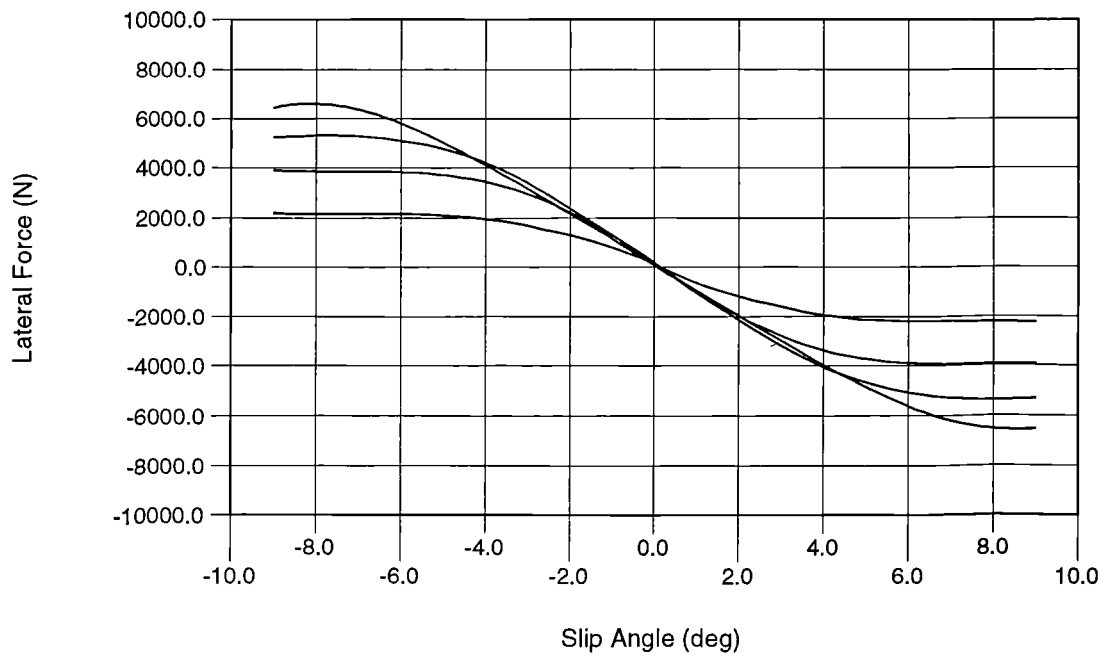
Figure E.1 Interpolation model (TYRE A) - lateral force with slip angle

INTERPOLATION TYRE MODEL - TYRE A 195/65 R15

Vertical Load Increments - 200kg 400kg 600kg 800kg
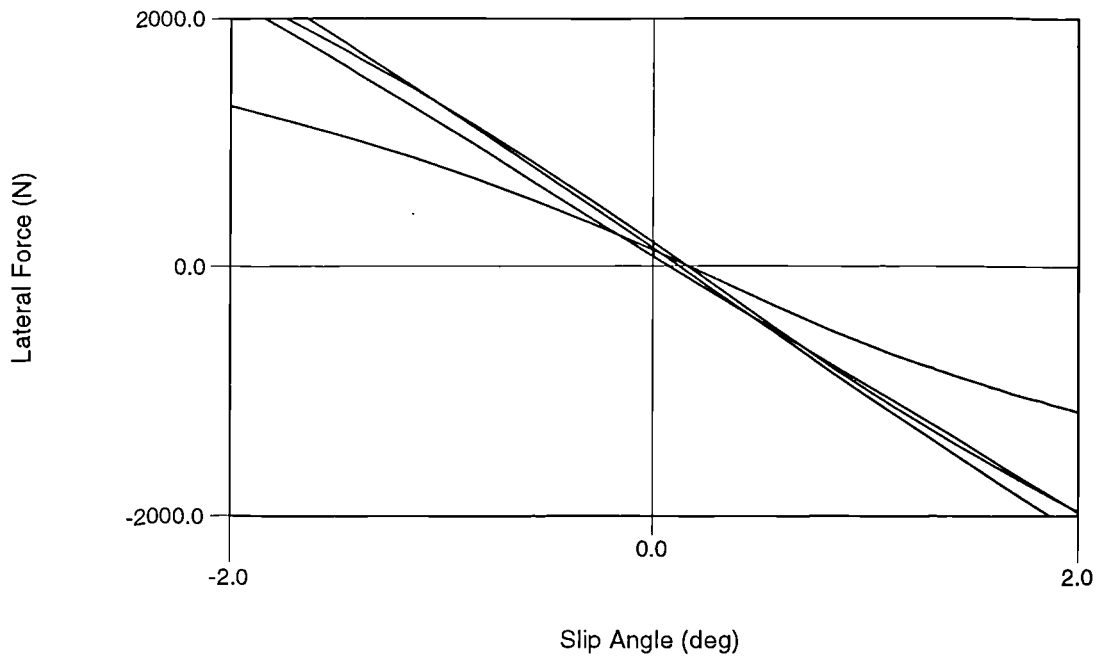
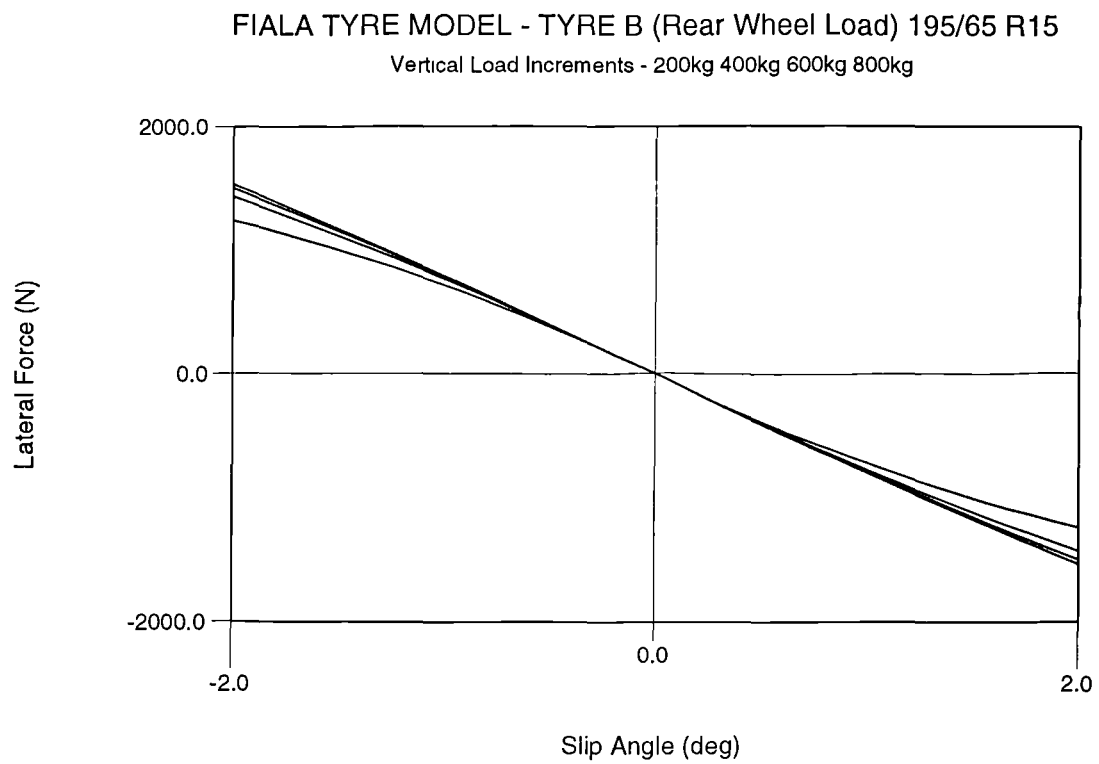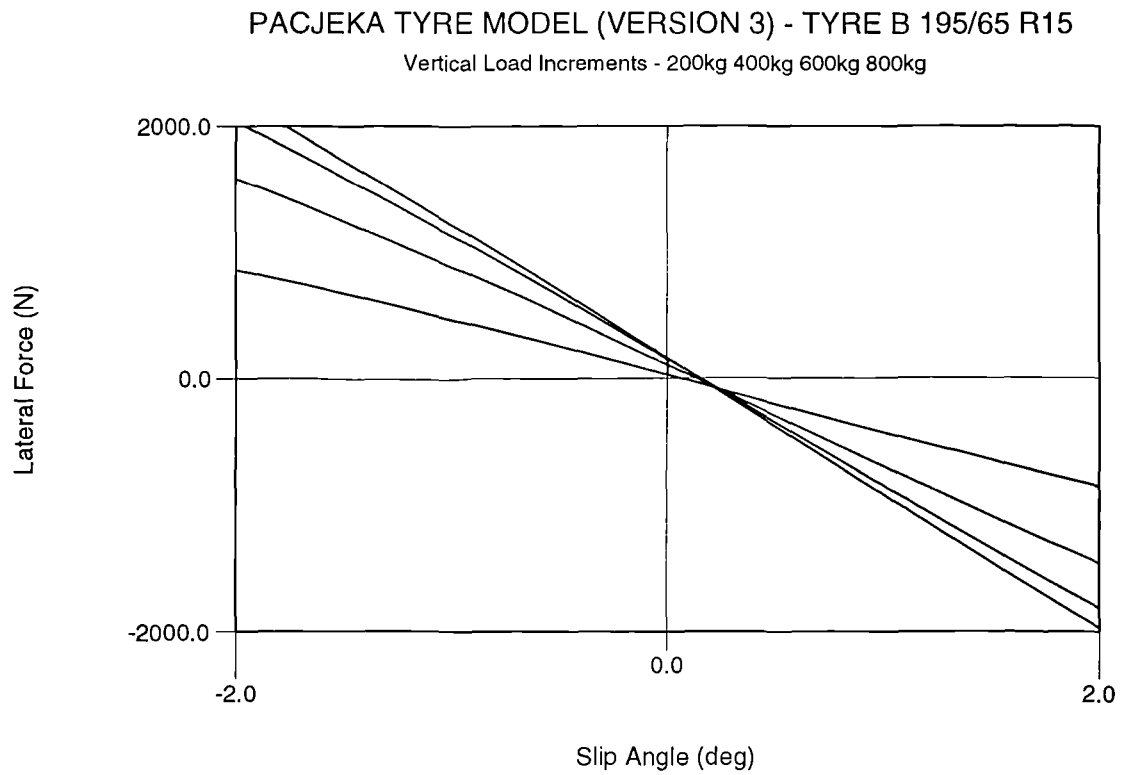Figure E.2 Interpolation model (TYRE A) - lateral force with slip angle at near zero slip

INTERPOLATION TYRE MODEL - TYRE A 195/65 R15

Vertical Load Increments - 200kg 400kg 600kg 800kg
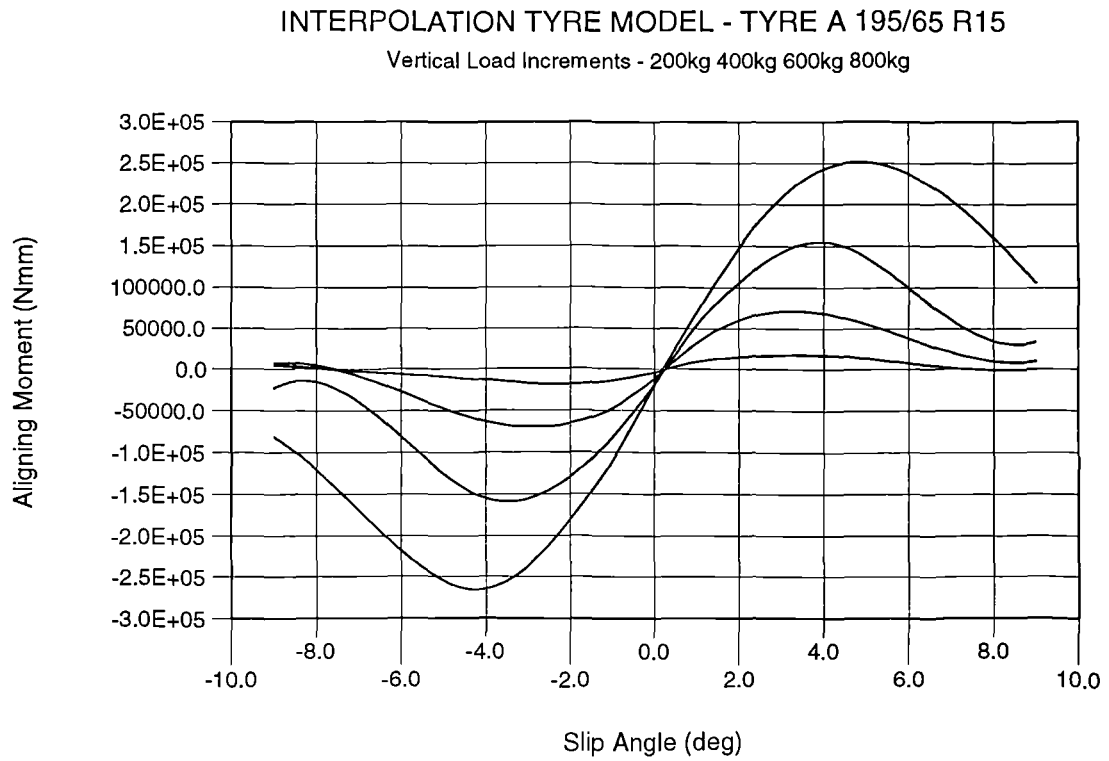
Figure E.3 Interpolation model (TYRE A) - aligning moment with slip angle

INTERPOLATION TYRE MODEL - TYRE A 195/65 R15

Vertical Load Increments - 200kg 400kg 600kg 800kg
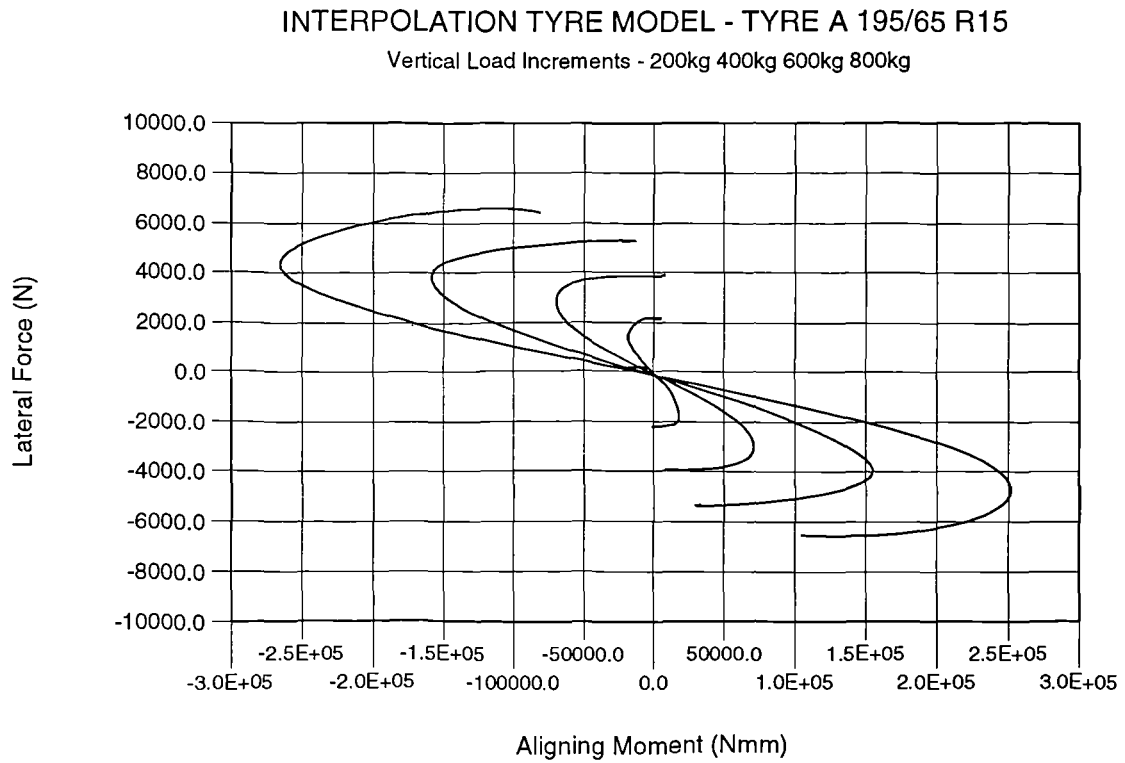
Figure E.4 Interpolation model (TYRE A) - lateral force with aligning moment

INTERPOLATION TYRE MODEL - TYRE A 195/65 R15
Vertical Load Increments - 200kg 400kg 600kg 800kg
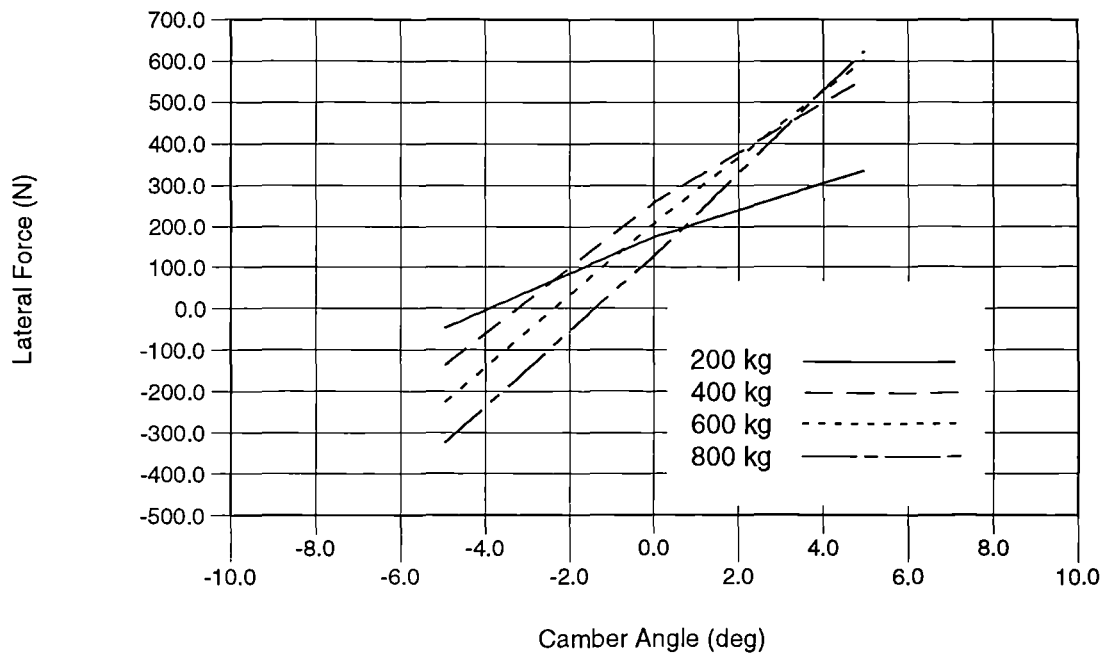
Figure E.5 Interpolation model (TYRE A) - lateral force with camber angle

FIALA TYRE MODEL - TYRE A (Average Wheel Load) 195/65 R15
Vertical Load Increments - 200kg 400kg 600kg 800kg
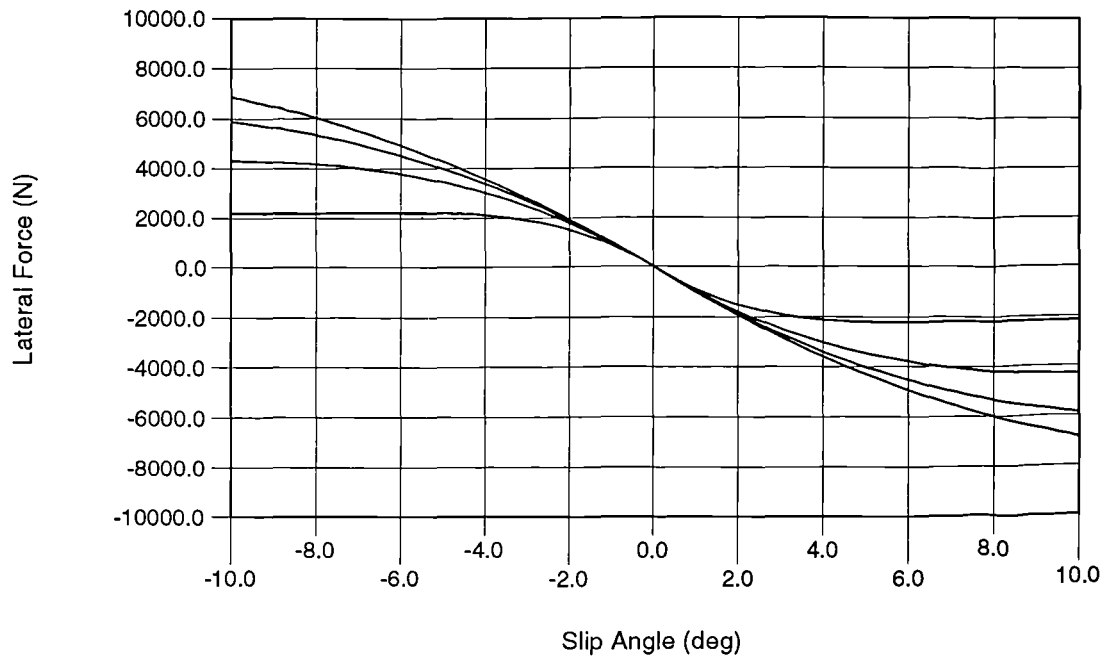
Figure E.6 Fiala model (TYRE A) - lateral force with slip angle

FIALA TYRE MODEL - TYRE A (Average Wheel Load) 195/65 R15

Vertical Load Increments - 200kg 400kg 600kg 800kg
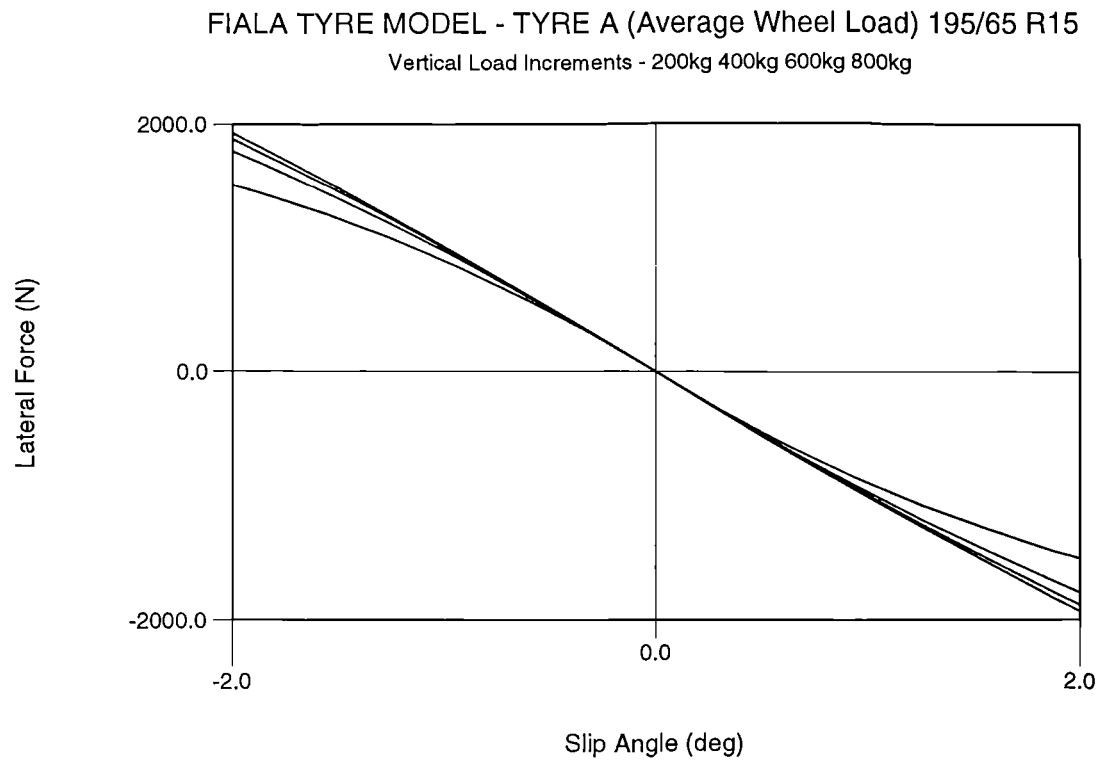
Figure E.7 Fiala model (TYRE A) - lateral force with slip angle at near zero slip

FIALA TYRE MODEL - TYRE A (Average Wheel Load) 195/65 R15

Vertical Load Increments - 200kg 400kg 600kg 800kg
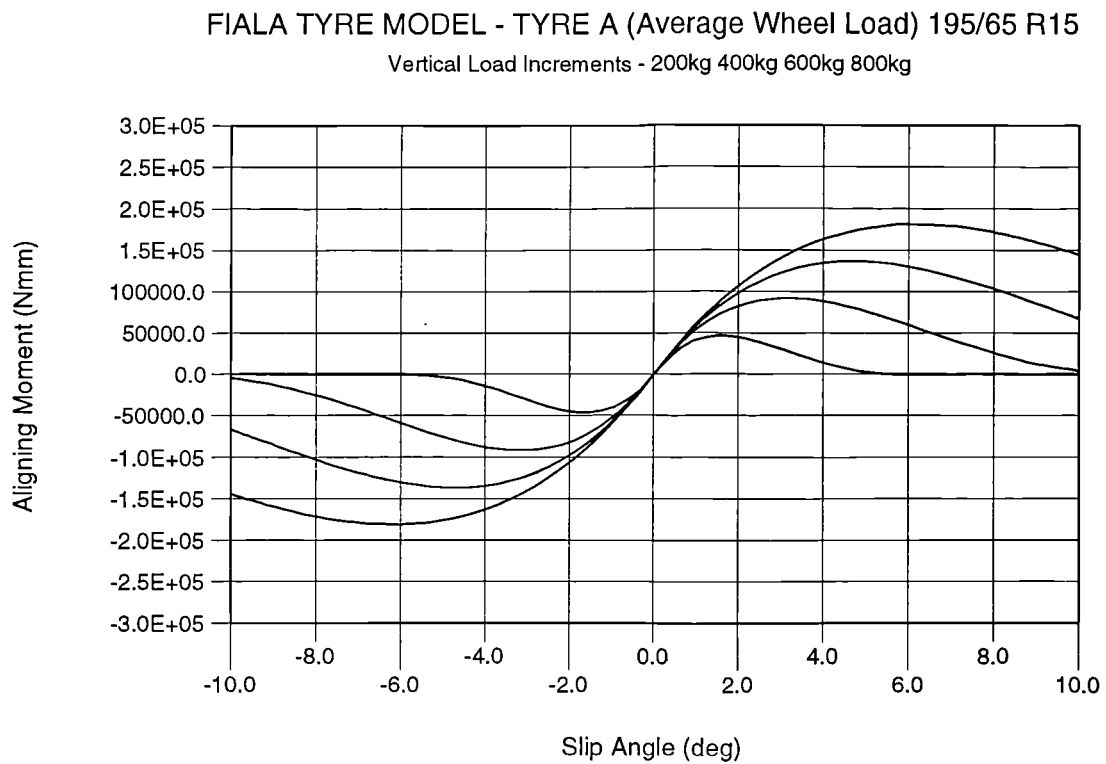
Figure E.8 Fiala model (TYRE A) - aligning moment with slip angle

FIALA TYRE MODEL - TYRE A (Average Wheel Load) 195/65 R15
Vertical Load Increments - 200kg 400kg 600kg 800kg
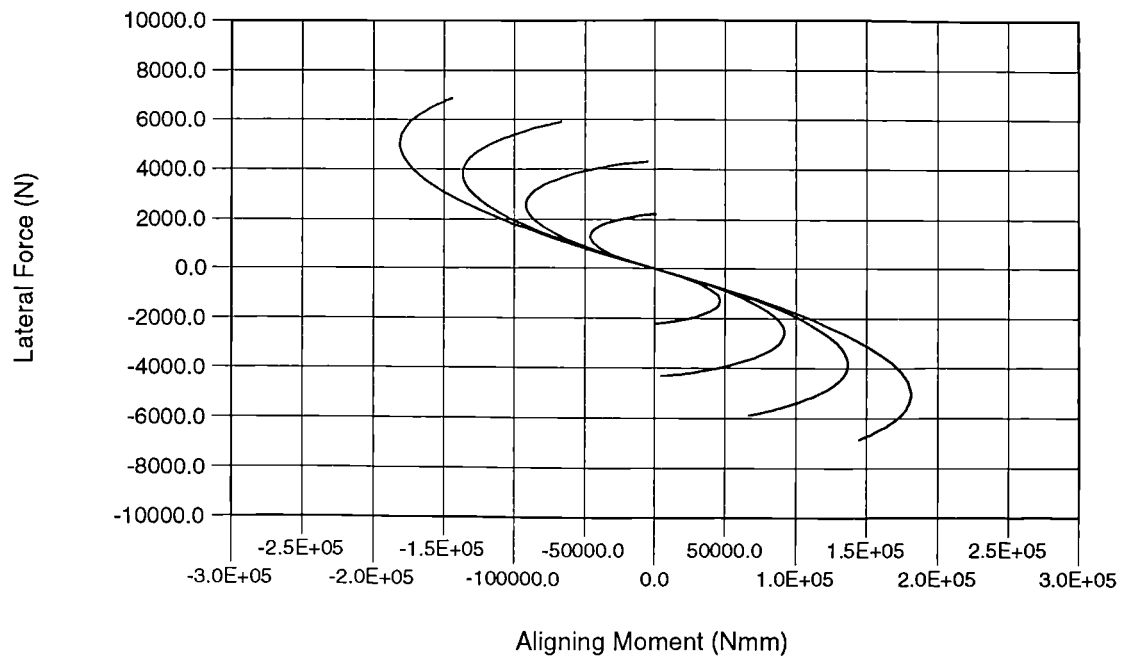
Figure E.9 Fiala model (TYRE A) - lateral force with aligning moment

FIALA TYRE MODEL - TYRE A (Front Wheel Load) 195/65 R15
Vertical Load Increments - 200kg 400kg 600kg 800kg
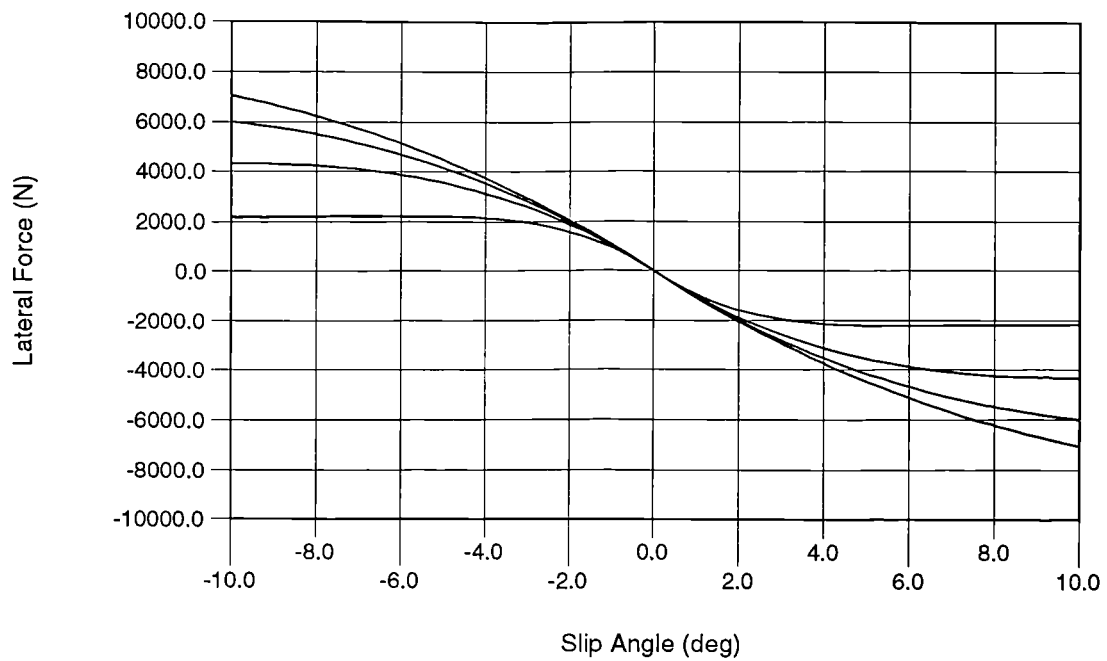
Figure E.10 Fiala model (TYRE A) - lateral force with slip angle

FIALA TYRE MODEL - TYRE A (Front Wheel Load) 195/65 R15

Vertical Load Increments - 200kg 400kg 600kg 800kg
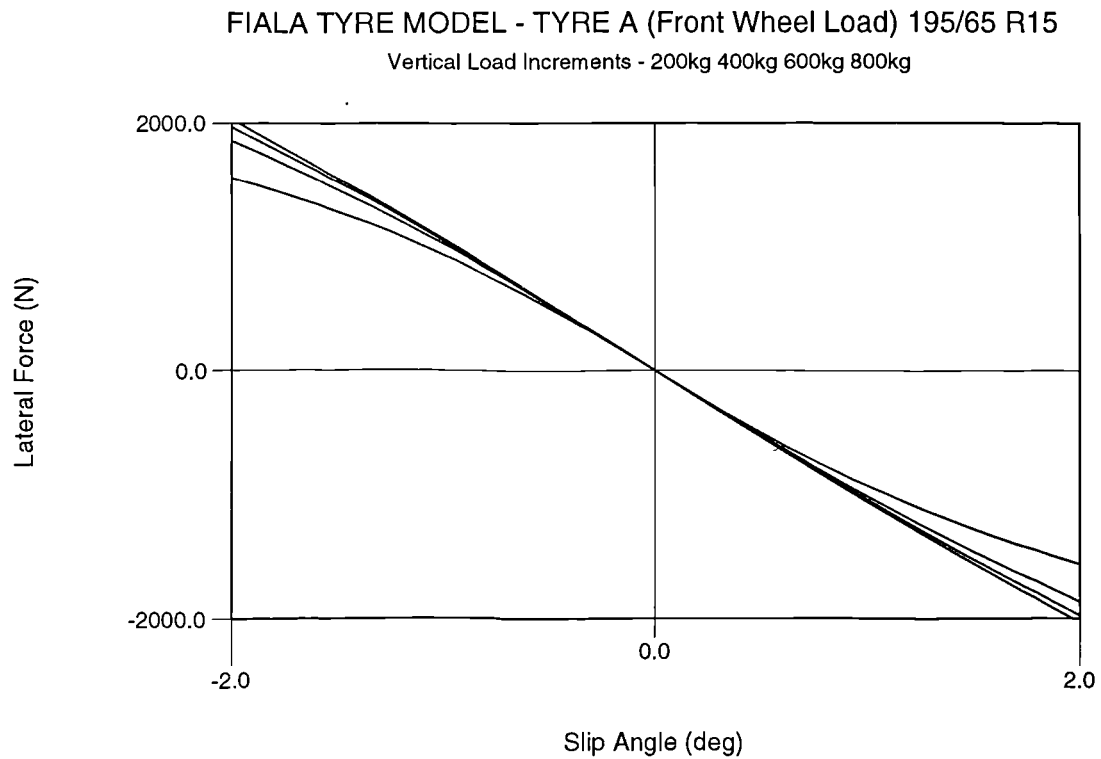
Figure E.11 Fiala model (TYRE A) - lateral force with slip angle at near zero slip

FIALA TYRE MODEL - TYRE A (Front Wheel Load) 195/65 R15

Vertical Load Increments - 200kg 400kg 600kg 800kg
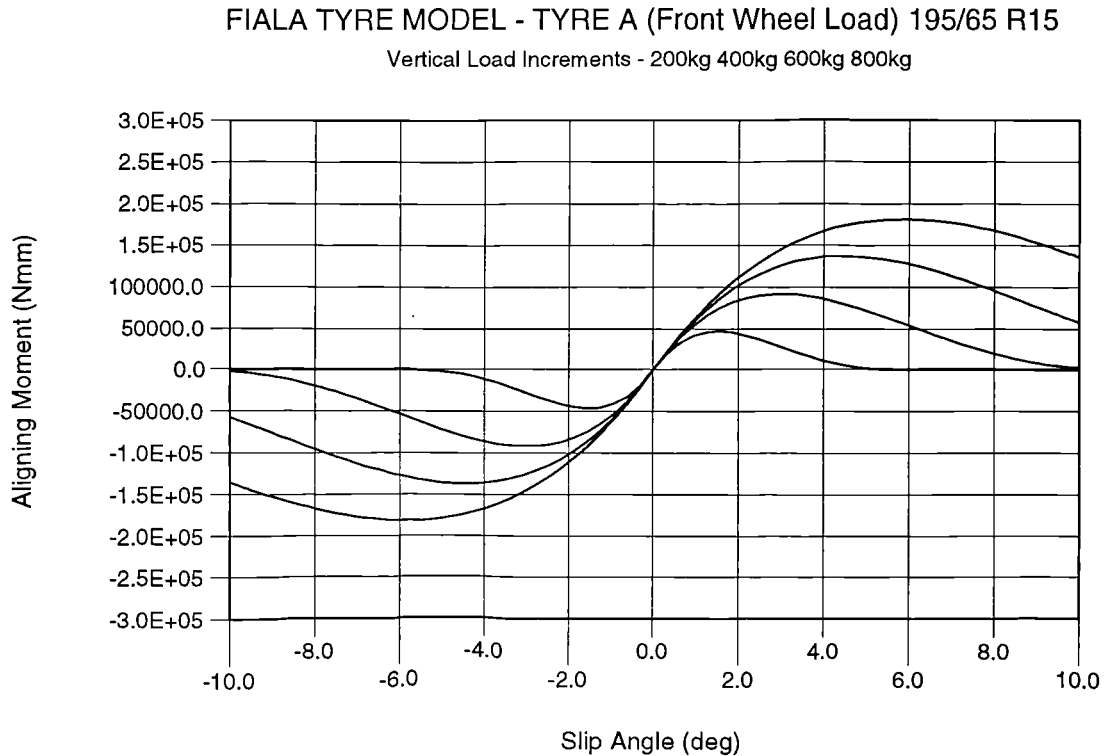
Figure E.12 Fiala model (TYRE A) - aligning moment with slip angle

FIALA TYRE MODEL - TYRE A (Front Wheel Load) 195/65 R15
Vertical Load Increments - 200kg 400kg 600kg 800kg

Aligning Moment (Nmm)
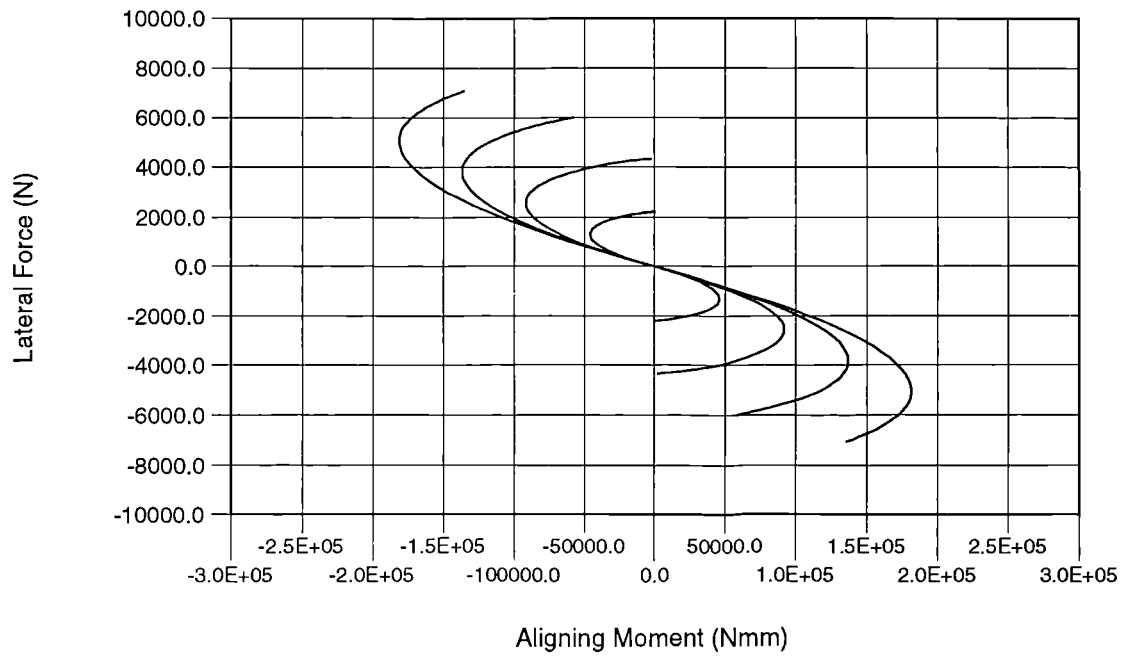
Figure E.13 Fiala model (TYRE A) - lateral force with aligning moment

FIALA TYRE MODEL - TYRE A (Rear Wheel Load) 195/65 R15
Vertical Load Increments - 200kg 400kg 600kg 800kg
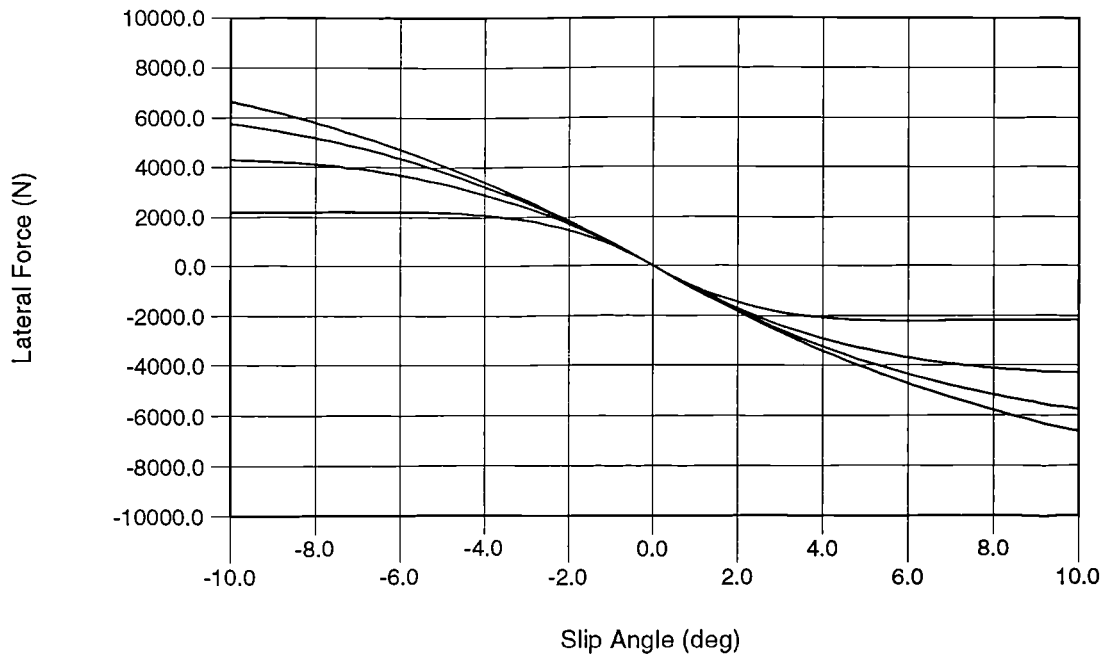
Slip Angle (deg)

Figure E.14 Fiala model (TYRE A) - lateral force with slip angle

FIALA TYRE MODEL - TYRE A (Rear Wheel Load) 195/65 R15

Vertical Load Increments - 200kg 400kg 600kg 800kg
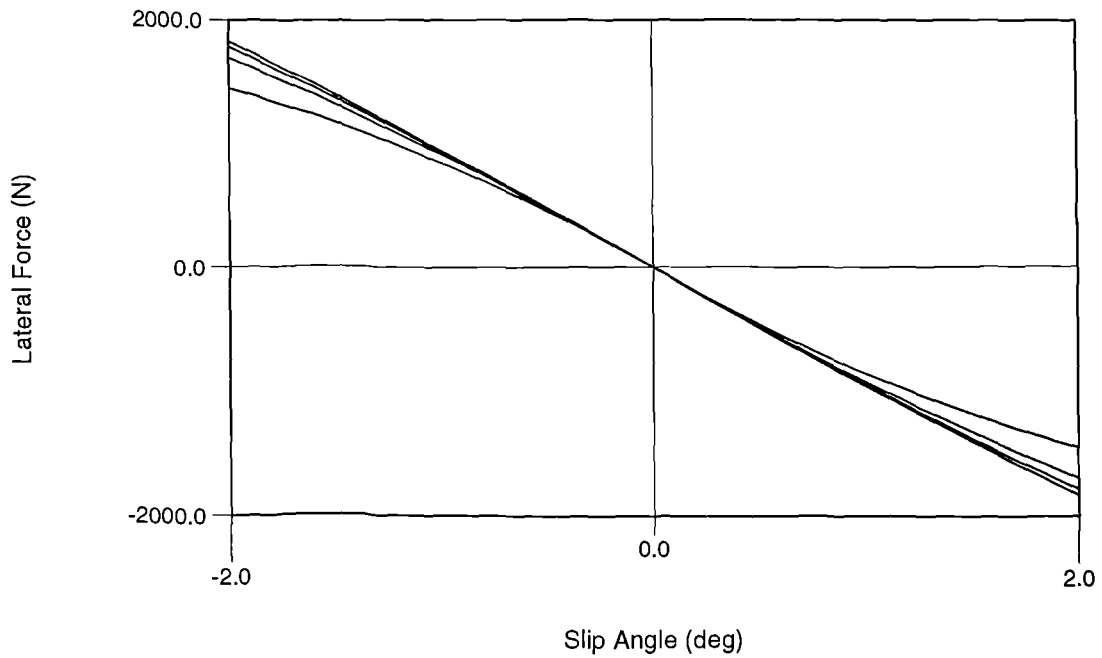
Figure E.15 Fiala model (TYRE A) - lateral force with slip angle at near zero slip

FIALA TYRE MODEL - TYRE A (Rear Wheel Load) 195/65 R15

Vertical Load Increments - 200kg 400kg 600kg 800kg
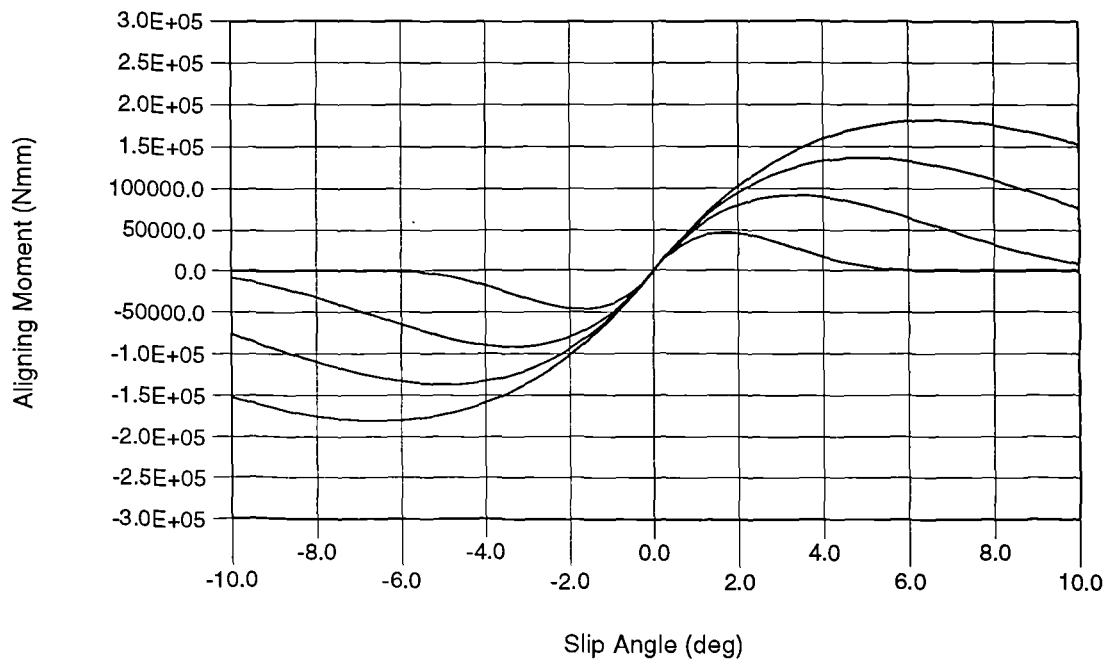
Figure E.16 Fiala model (TYRE A) - aligning moment with slip angle

FIALA TYRE MODEL - TYRE A (Rear Wheel Load) 195/65 R15
Vertical Load Increments - 200kg 400kg 600kg 800kg
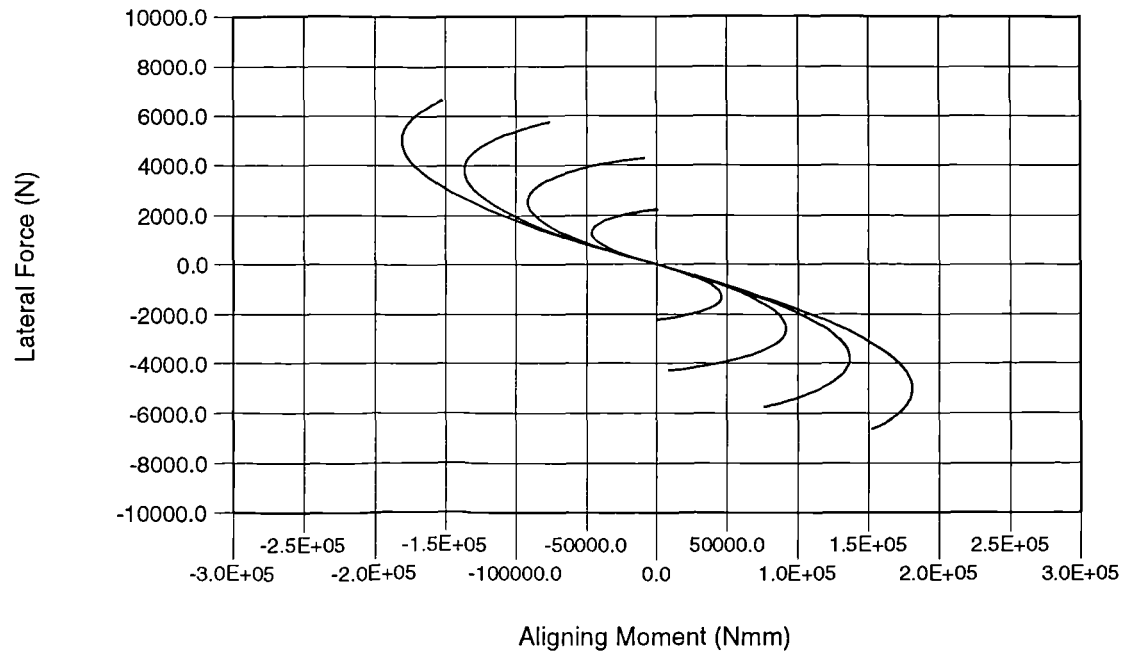
Figure E.17 Fiala model (TYRE A) - lateral force with aligning moment

PACEJKA (Monte Carlo Version) TYRE MODEL - TYRE A 195/65 R15
Vertical Load Increments - 200kg 400kg 600kg 800kg
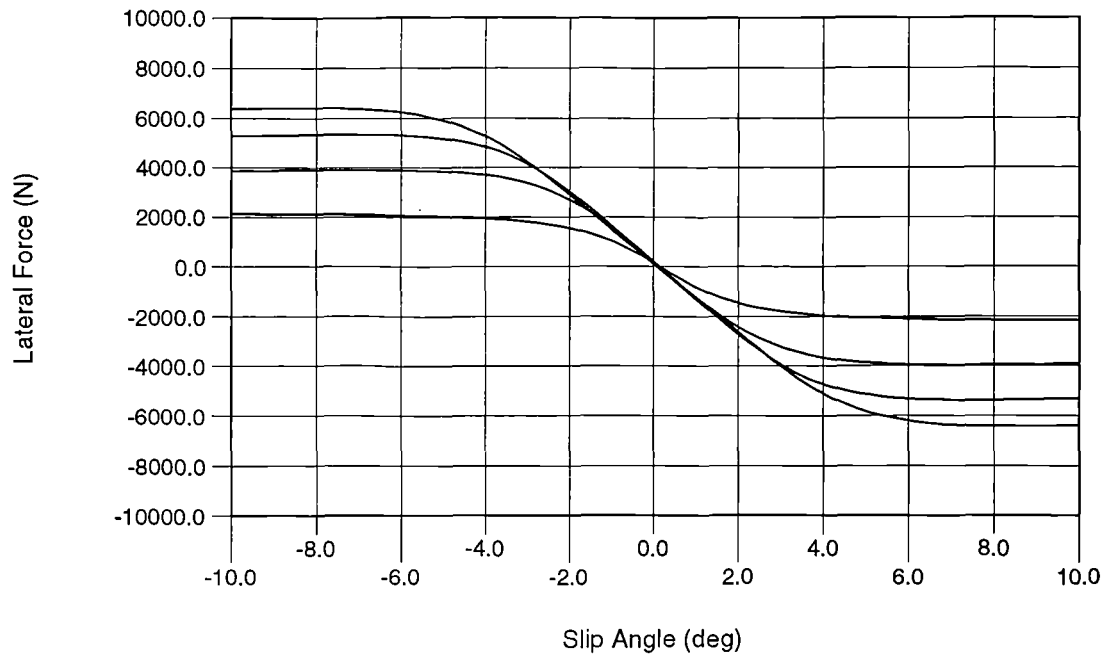
Figure E.18 Pacejka model (TYRE A) - lateral force with slip angle

PACEJKA (Monte Carlo Version) TYRE MODEL - TYRE A 195/65 R15
Vertical Load Increments - 200kg 400kg 600kg 800kg
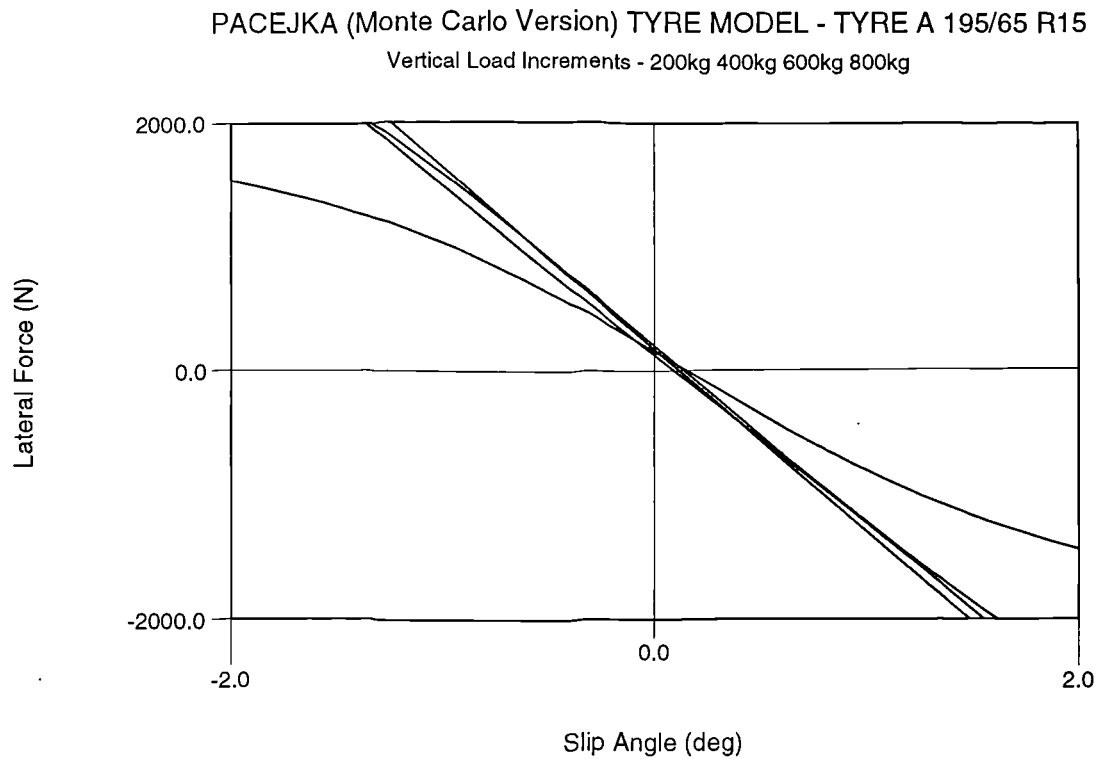
Figure E.19 Pacejka model (TYRE A) - lateral force with slip angle at near zero slip

PACEJKA (Monte Carlo Version) TYRE MODEL - TYRE A 195/65 R15
Vertical Load Increments - 200kg 400kg 600kg 800kg
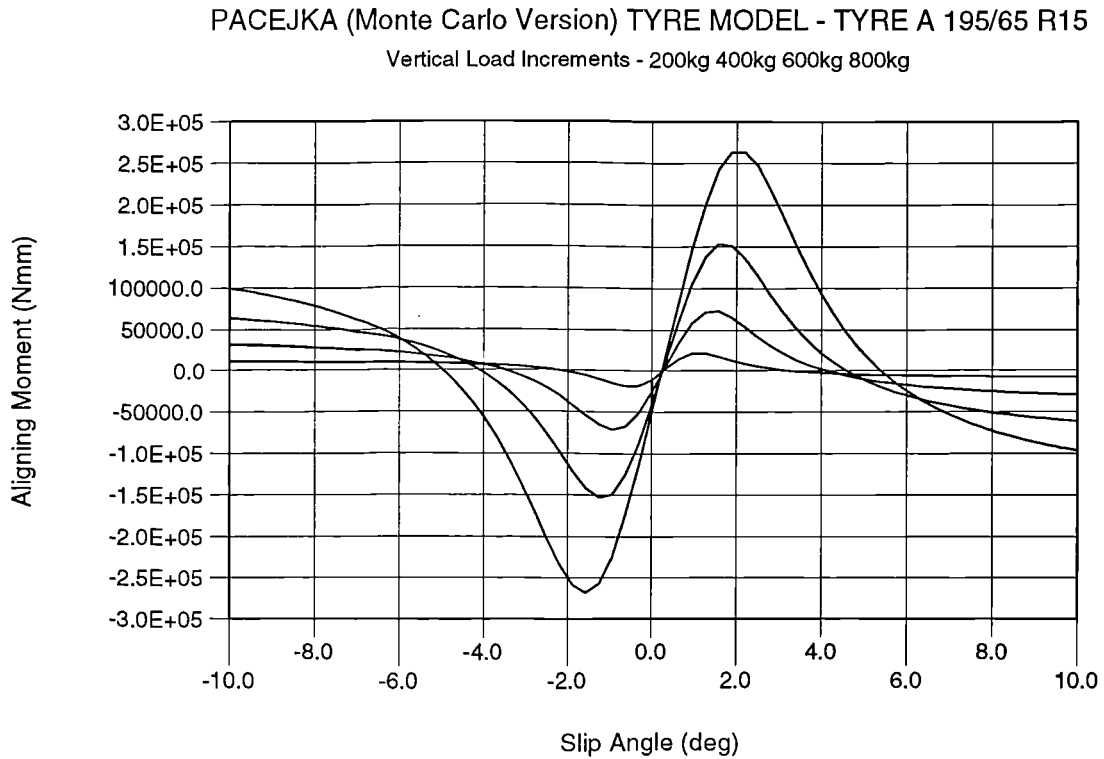
Figure E.20 Pacejka model (TYRE A) - aligning moment with slip angle

PACEJKA (Monte Carlo Version) TYRE MODEL - TYRE A 195/65 R15

Vertical Load Increments - 200kg 400kg 600kg 800kg

Aligning Moment (Nmm)
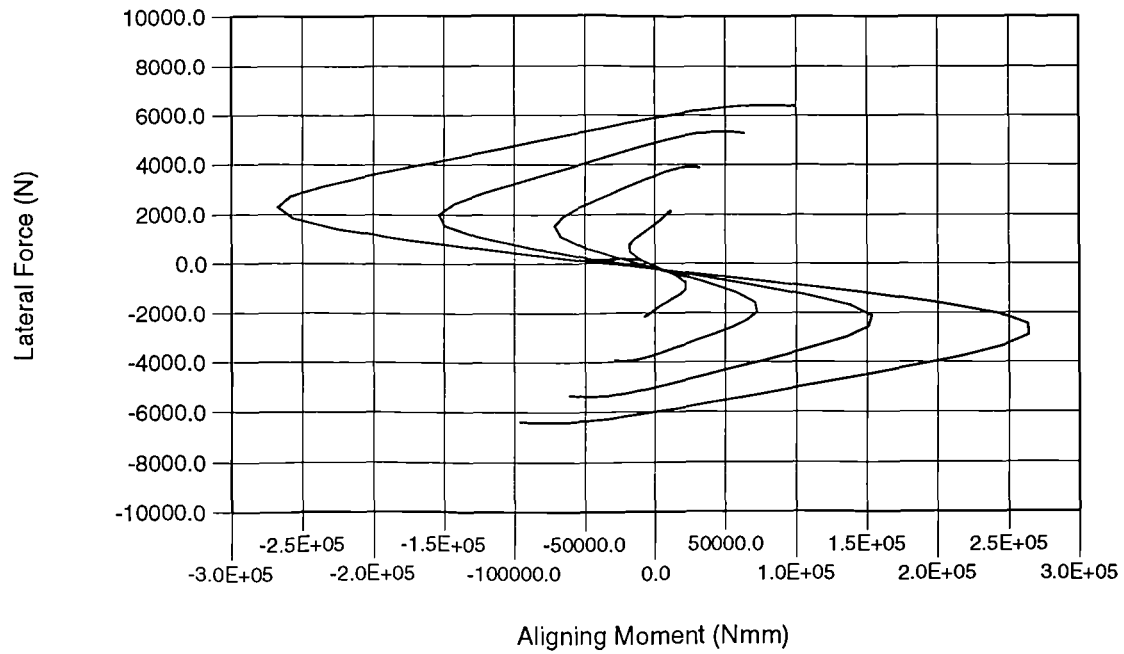
Figure E.21 Pacejka model (TYRE A) - lateral force with aligning moment

PACEJKA (Monte Carlo Version) TYRE MODEL - TYRE A 195/65 R15

Vertical Load Increments - 200kg 400kg 600kg 800kg
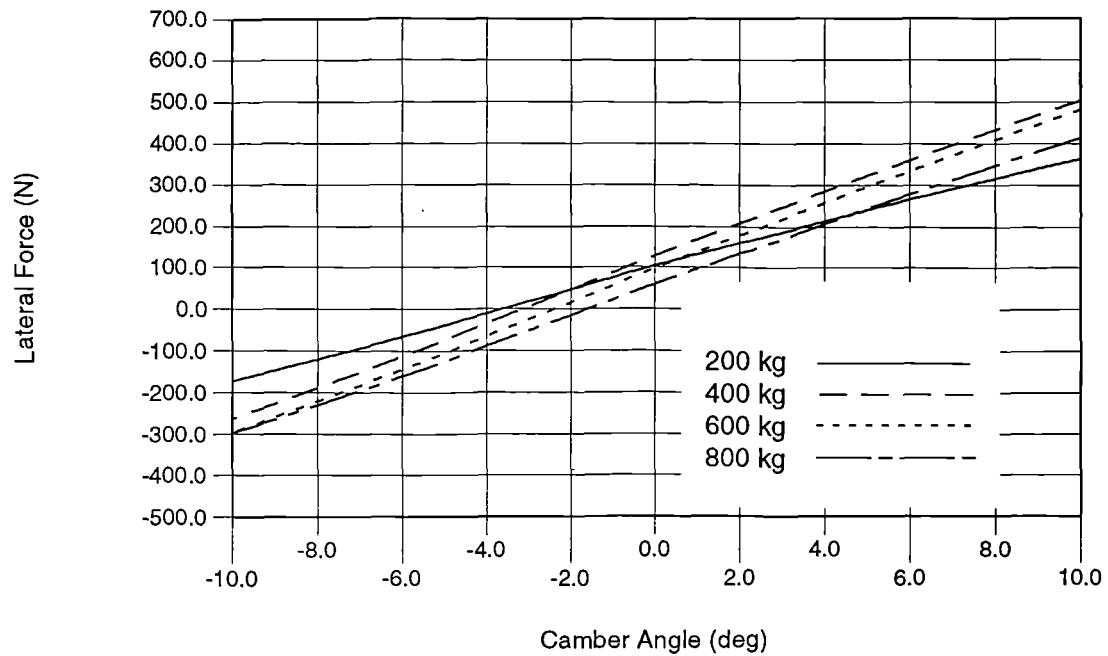
Camber Angle (deg)

Figure E.22 Pacejka model (TYRE A) - lateral force with camber angle

APPENDIX F

TYRE MODEL PLOTS FROM THE *CUTyre* RIG MODEL USING DATA FOR TYRE B

INTERPOLATION TYRE MODEL - TYRE B 195/65 R15

Vertical Load Increments - 200kg 400kg 600kg 800kg

SP TYRES UK LTD.
TEST MACHINE
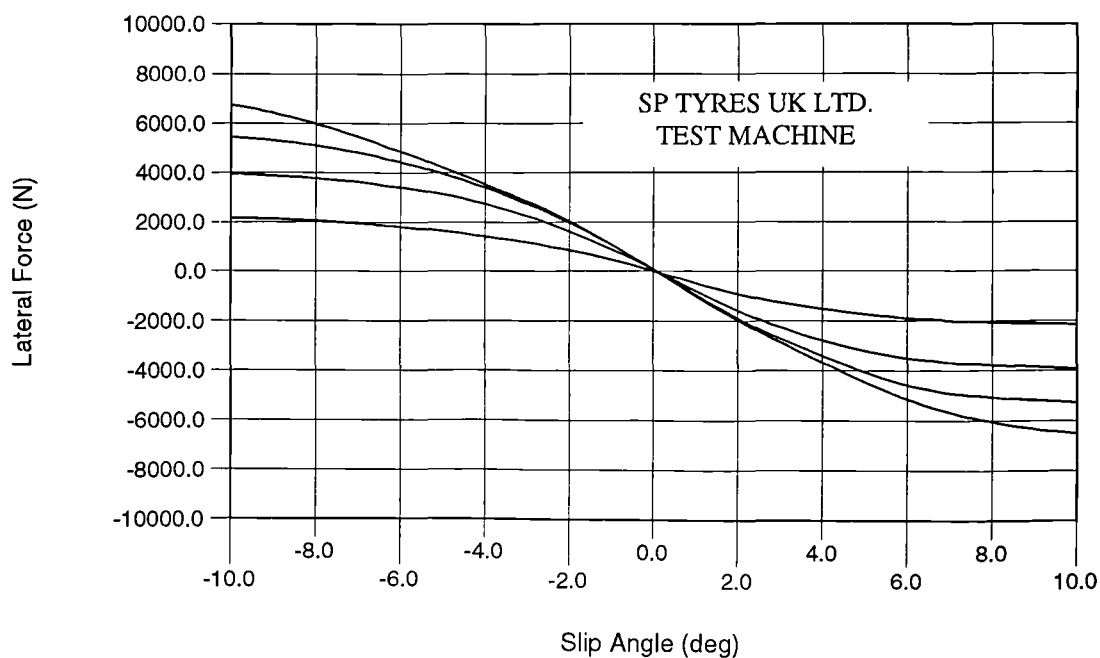
Figure F.1 Interpolation model (TYRE B) - lateral force with slip angle

INTERPOLATION TYRE MODEL - TYRE B 195/65 R15

Vertical Load Increments - 200kg 400kg 600kg 800kg

SP TYRES UK LTD.
TEST MACHINE
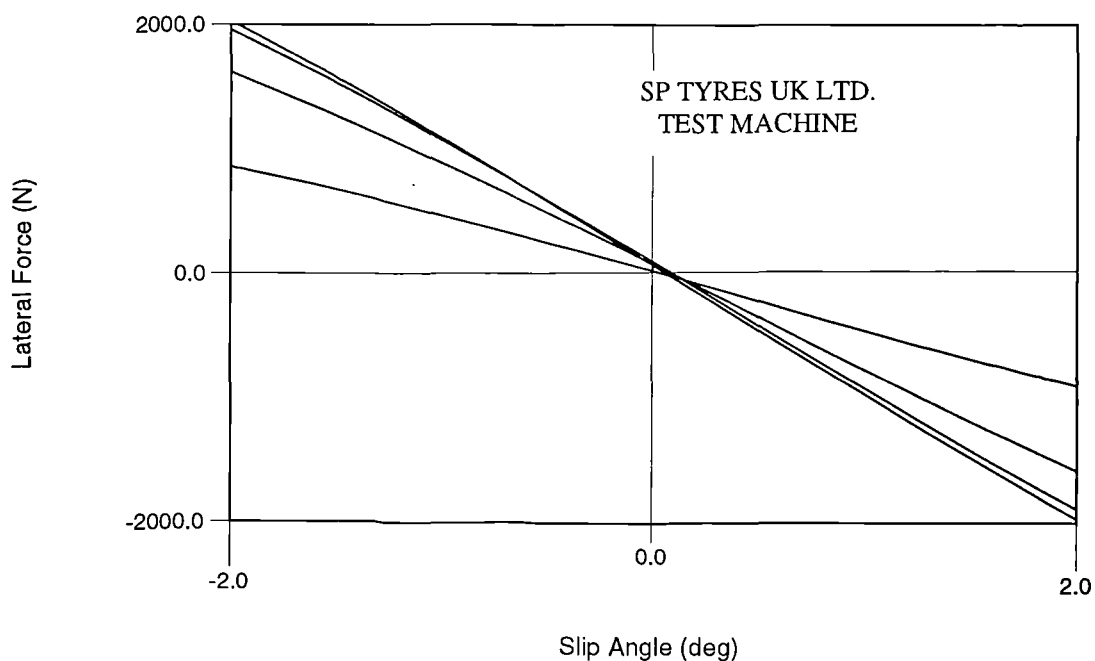
Figure F.2 Interpolation model (TYRE B) - lateral force with slip angle at near zero slip

INTERPOLATION TYRE MODEL - TYRE B 195/65 R15

Vertical Load Increments - 200kg 400kg 600kg 800kg
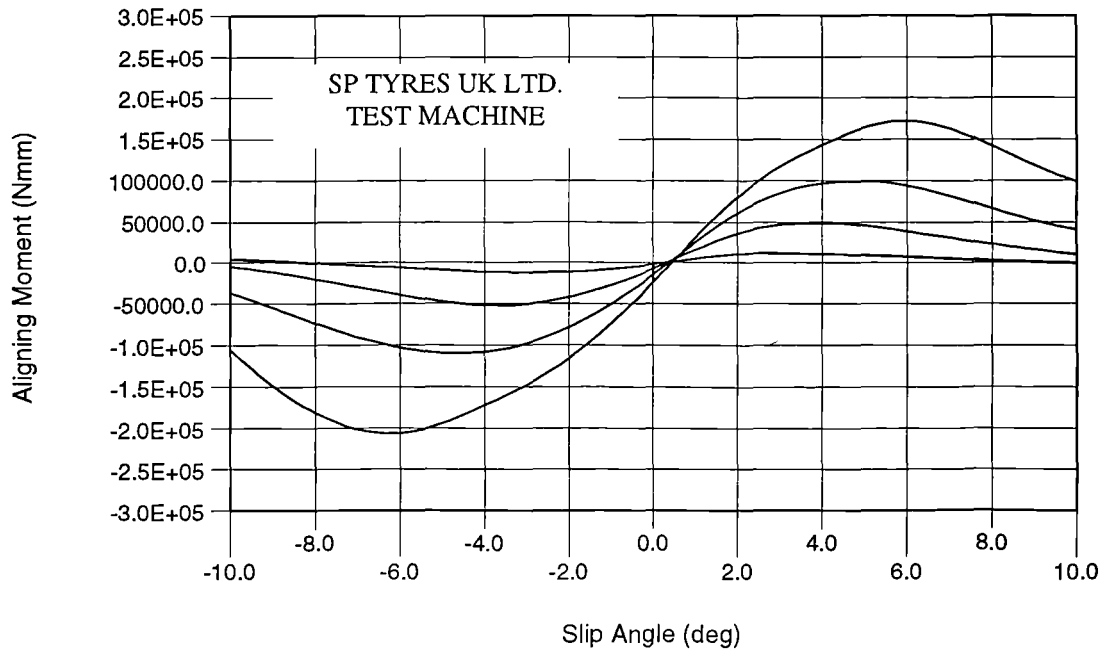
Figure F.3 Interpolation model (TYRE B) - aligning moment with slip angle

INTERPOLATION TYRE MODEL - TYRE B 195/65 R15

Vertical Load Increments - 200kg 400kg 600kg 800kg
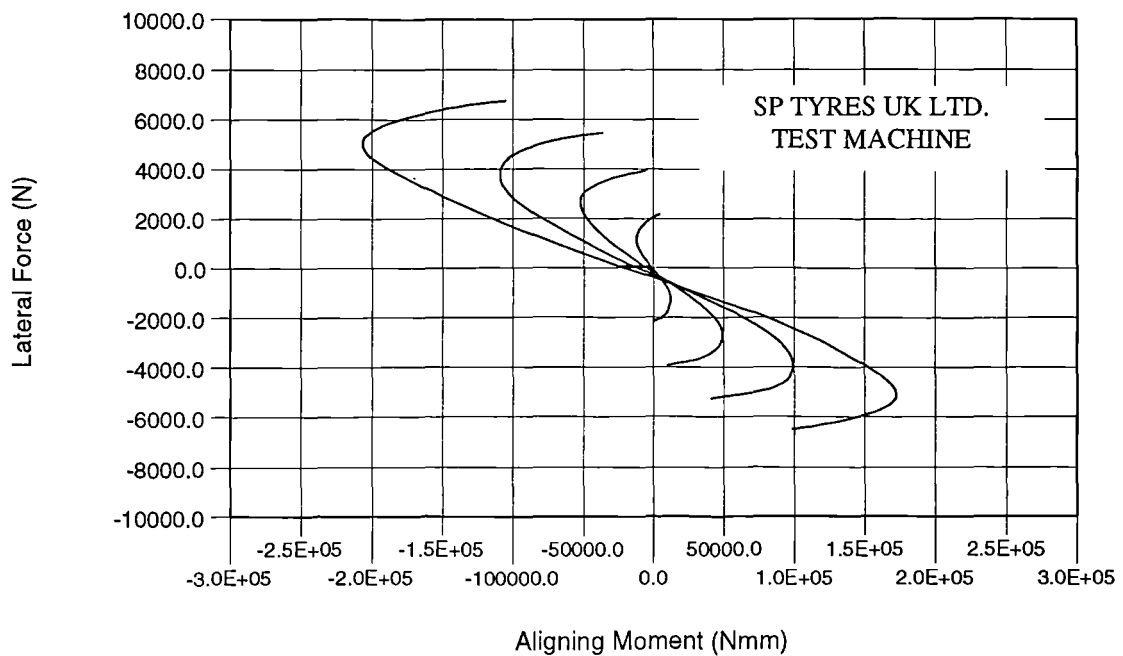
Figure F.4 Interpolation model (TYRE B) - lateral force with aligning moment

INTERPOLATION TYRE MODEL - TYRE B 195/65 R15

Vertical Load Increments - 200kg 400kg 600kg 800kg
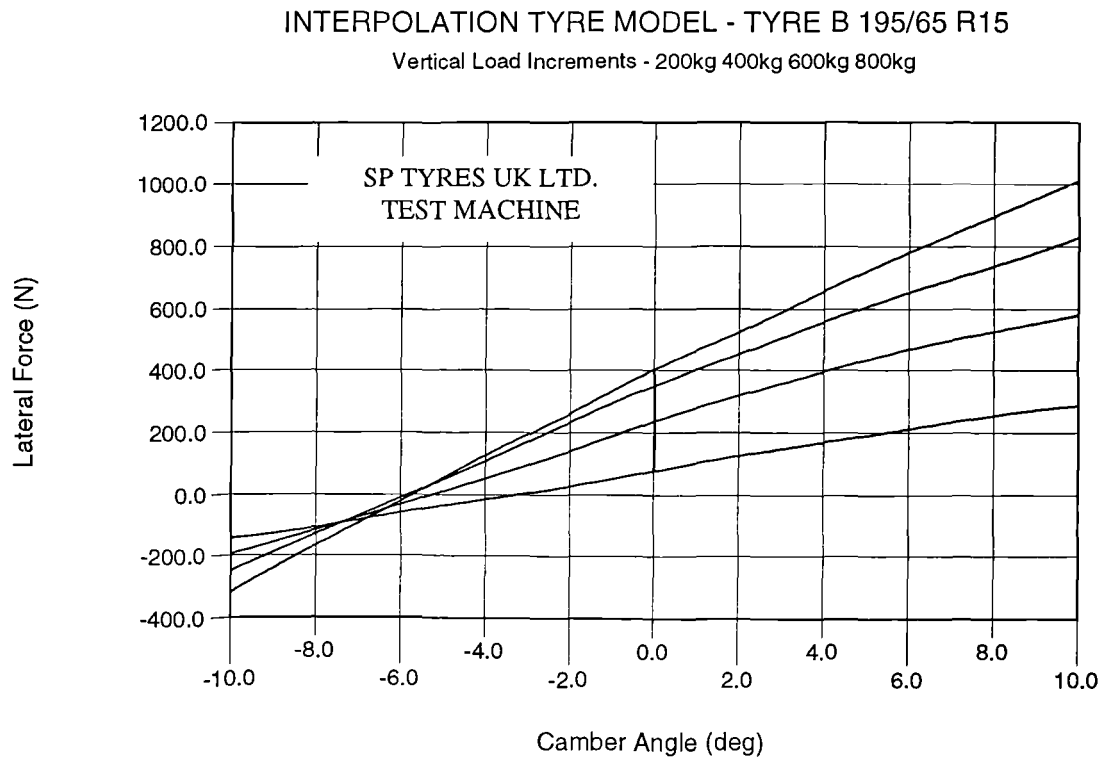
Figure F.5 Interpolation model (TYRE B) - lateral force with camber angle

INTERPOLATION TYRE MODEL - TYRE B 195/65 R15

Vertical Load Increments - 200kg 400kg 600kg
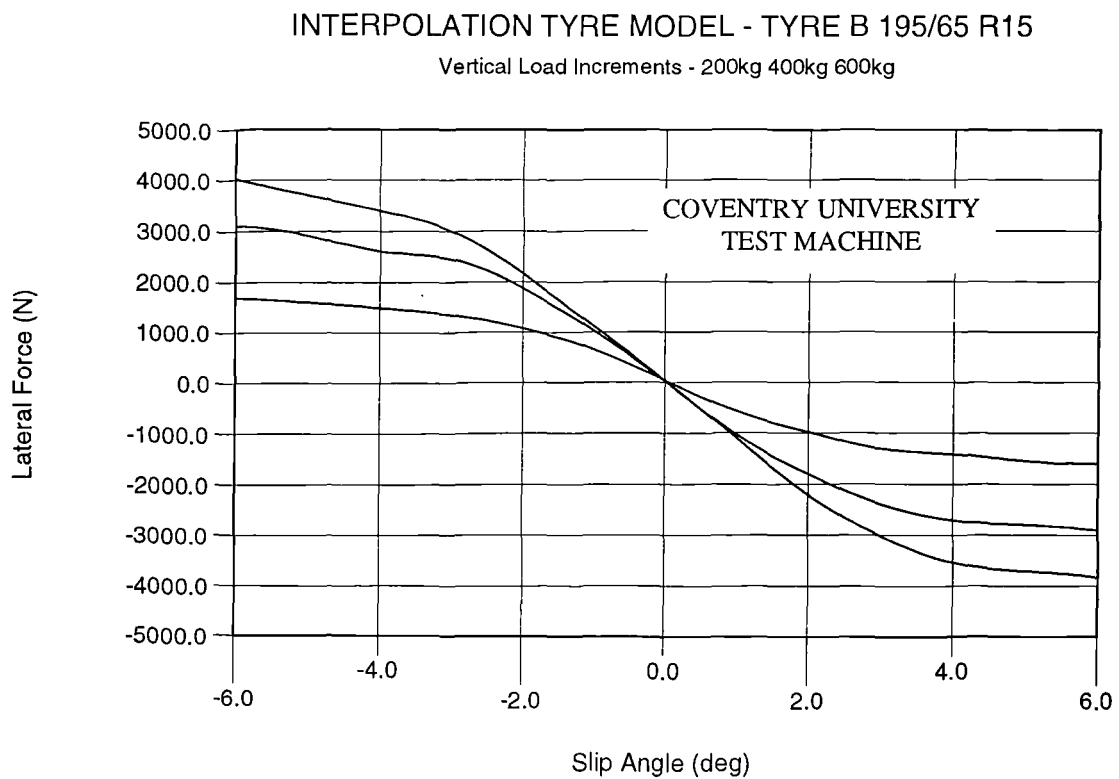
Figure F.6 Interpolation model (TYRE B) - lateral force with slip angle

INTERPOLATION TYRE MODEL - TYRE B 195/65 R15

Vertical Load Increments - 200kg 400kg 600kg
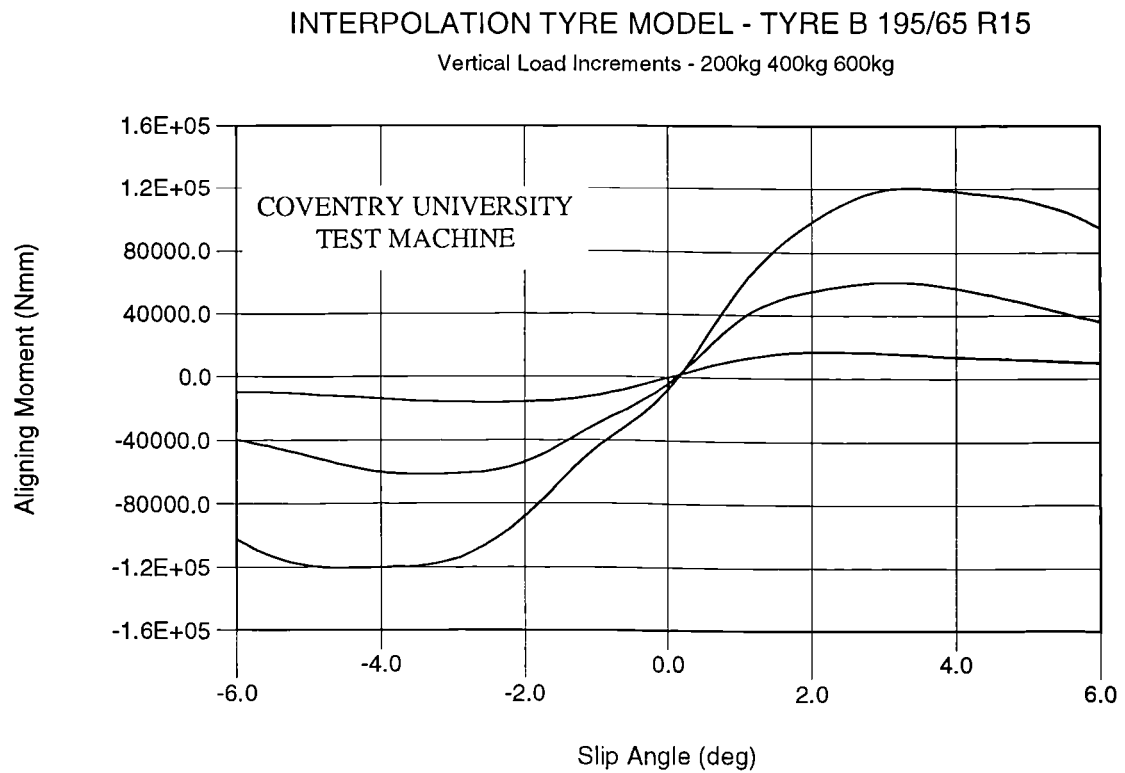
Figure F.7 Interpolation model (TYRE B) - aligning moment with slip angle

INTERPOLATION TYRE MODEL - TYRE B 195/65 R15

Vertical Load Increments - 200kg 400kg 600kg
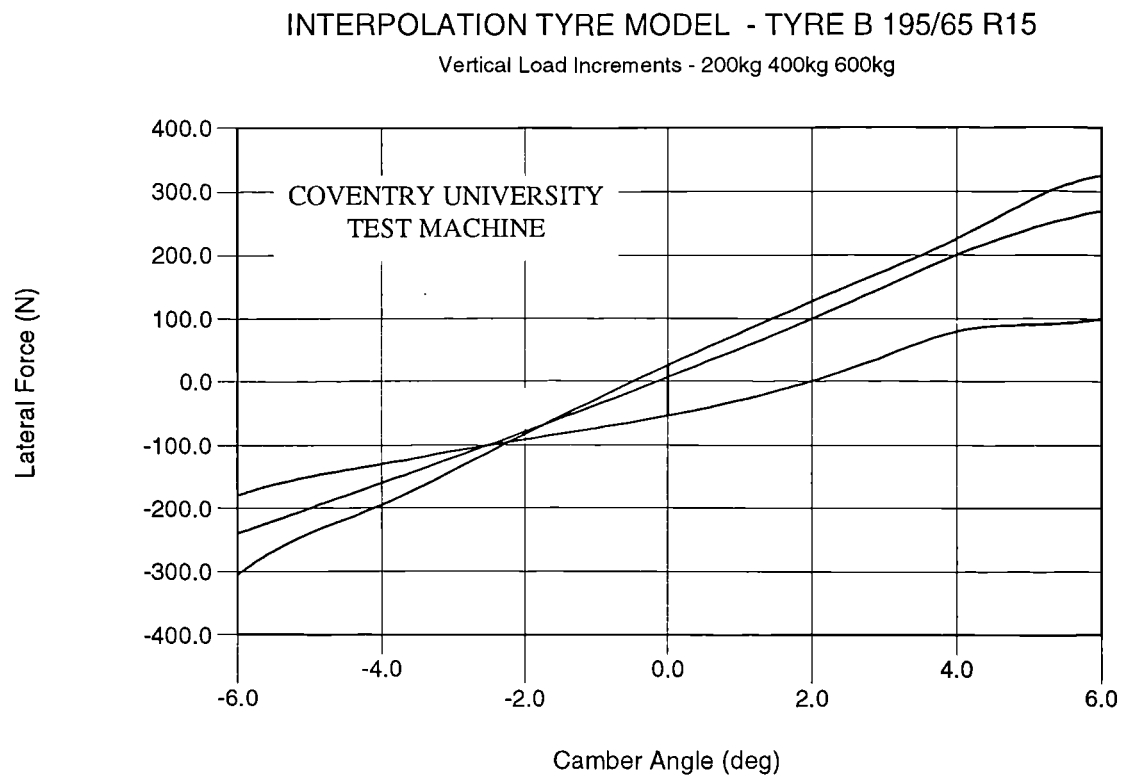
Figure F.8 Interpolation model (TYRE B) - lateral force with camber angle

INTERPOLATION TYRE MODEL - TYRE B 195/65 R15

Vertical Increments - 200kg 400kg 600kg 800kg
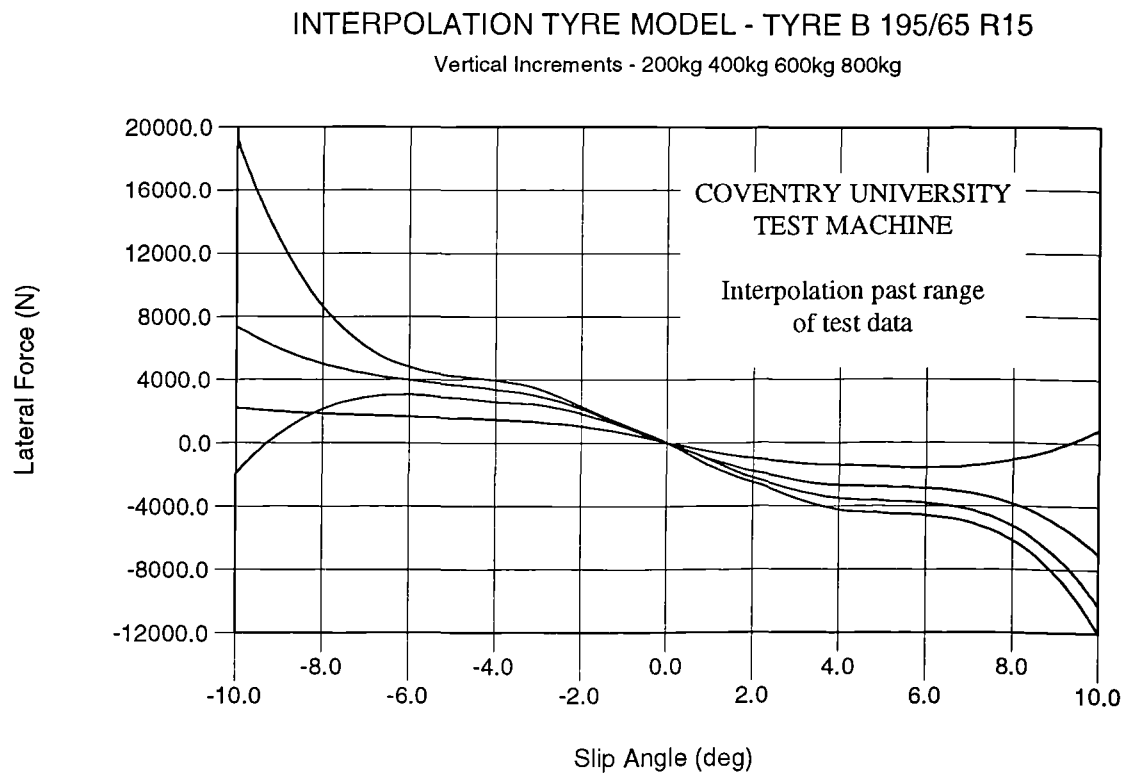
Figure F.9 Interpolation model (TYRE B) - lateral force with slip angle

FIALA TYRE MODEL - TYRE B (Average Wheel Load) 195/65 R15

Vertical Load Increments - 200kg 400kg 600kg 800kg
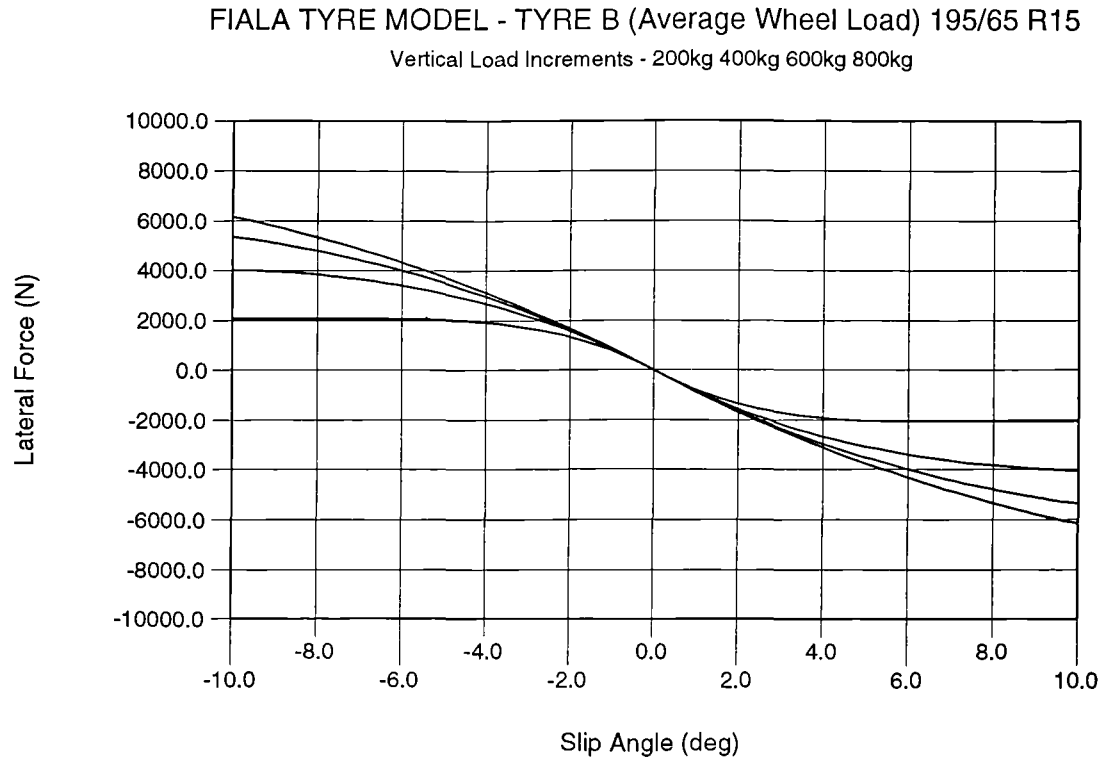
Figure F.10 Fiala model (TYRE B) - lateral force with slip angle

FIALA TYRE MODEL - TYRE B (Average Wheel Load) 195/65 R15

Vertical Load Increments - 200kg 400kg 600kg 800kg
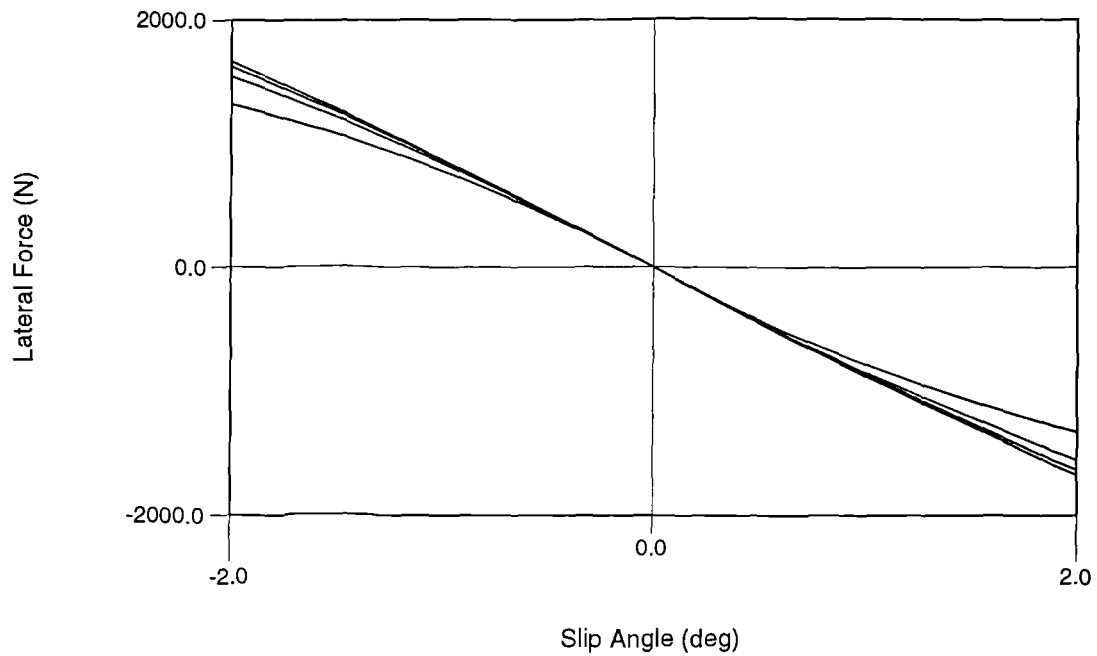
Figure F.11 Fiala model (TYRE B) - lateral force with slip angle at near zero slip

FIALA TYRE MODEL - TYRE B (Average Wheel Load) 195/65 R15

Vertical Load Increments - 200kg 400kg 600kg 800kg
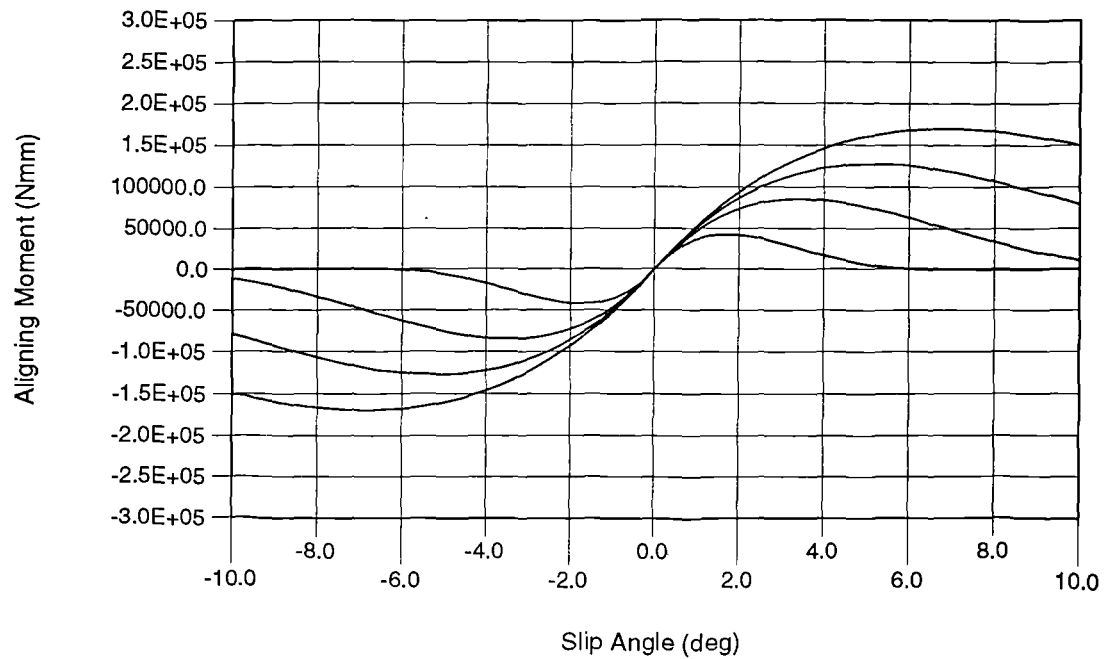
Figure F.12 Fiala model (TYRE B) - aligning moment with slip angle

FIALA TYRE MODEL - TYRE B (Average Wheel Load) 195/65 R15
Vertical Load Increments - 200kg 400kg 600kg 800kg
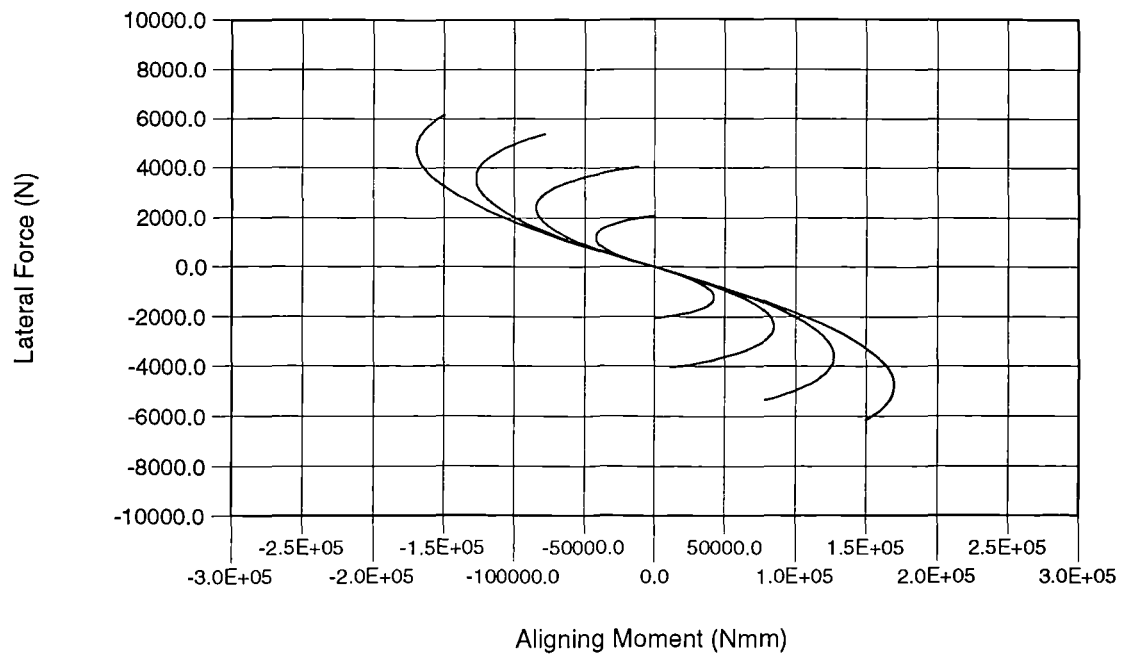
Figure F.13 Fiala model (TYRE B) - lateral force with aligning moment

FIALA TYRE MODEL - TYRE B (Front Wheel Load) 195/65 R15
Vertical Load Increments - 200kg 400kg 600kg 800kg
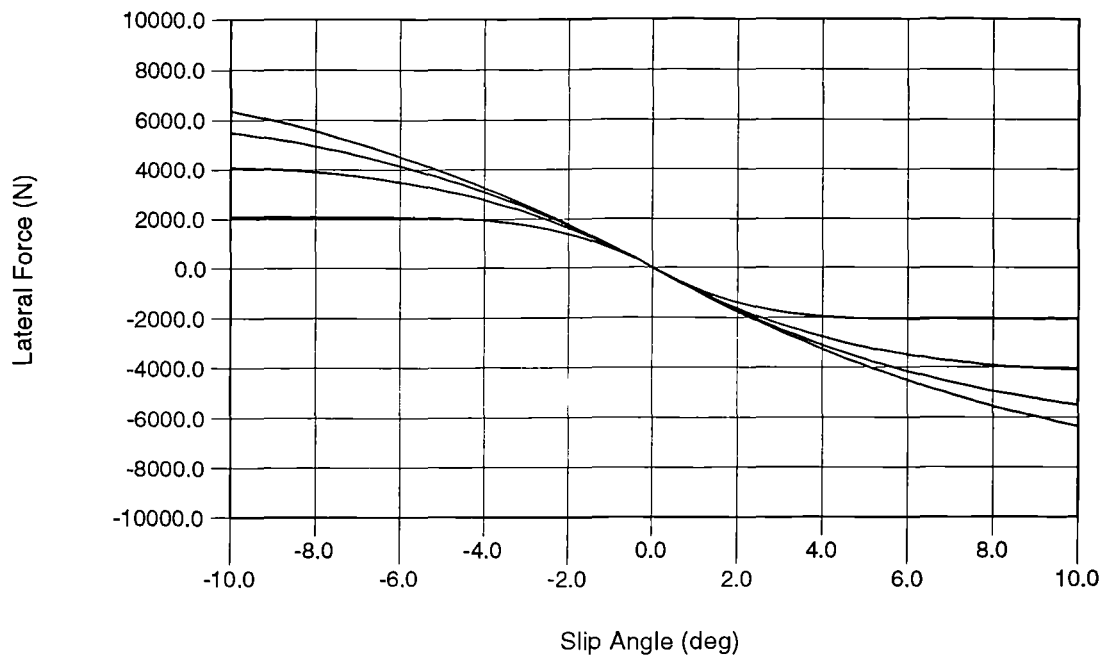
Figure F.14 Fiala model (TYRE B) - lateral force with slip angle

FIALA TYRE MODEL - TYRE B (Front Wheel Load) 195/65 R15
Vertical Load Increments - 200kg 400kg 600kg 800kg
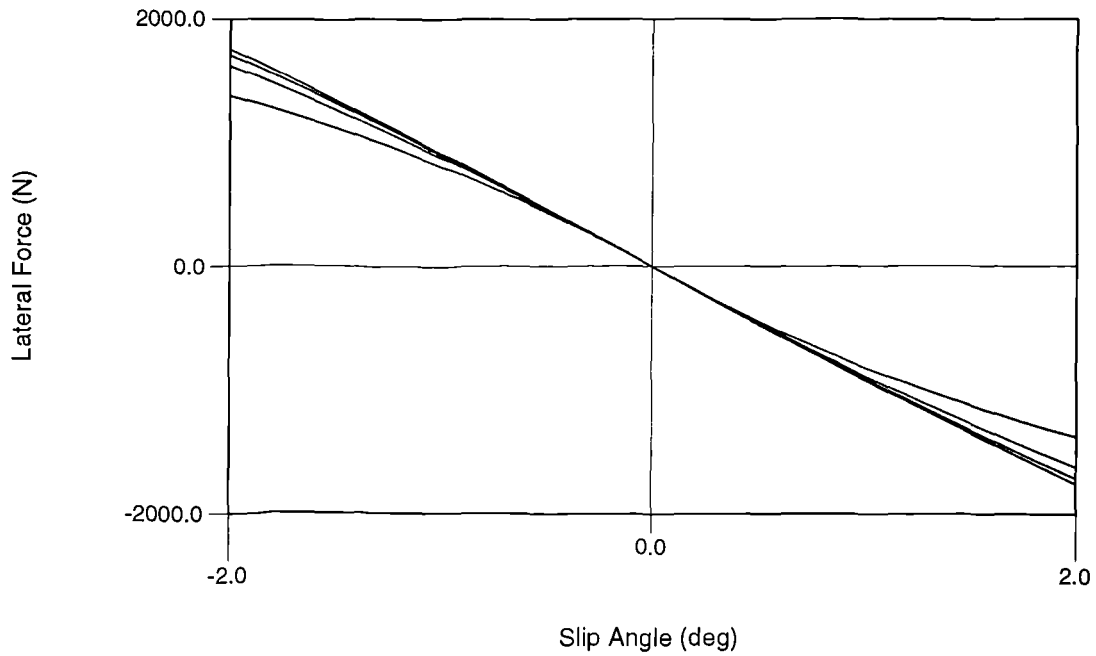
Figure F.15 Fiala model (TYRE B) - lateral force with slip angle at near zero slip

FIALA TYRE MODEL - TYRE B (Front Wheel Load) 195/65 R15
Vertical Load Increments - 200kg 400kg 600kg 800kg
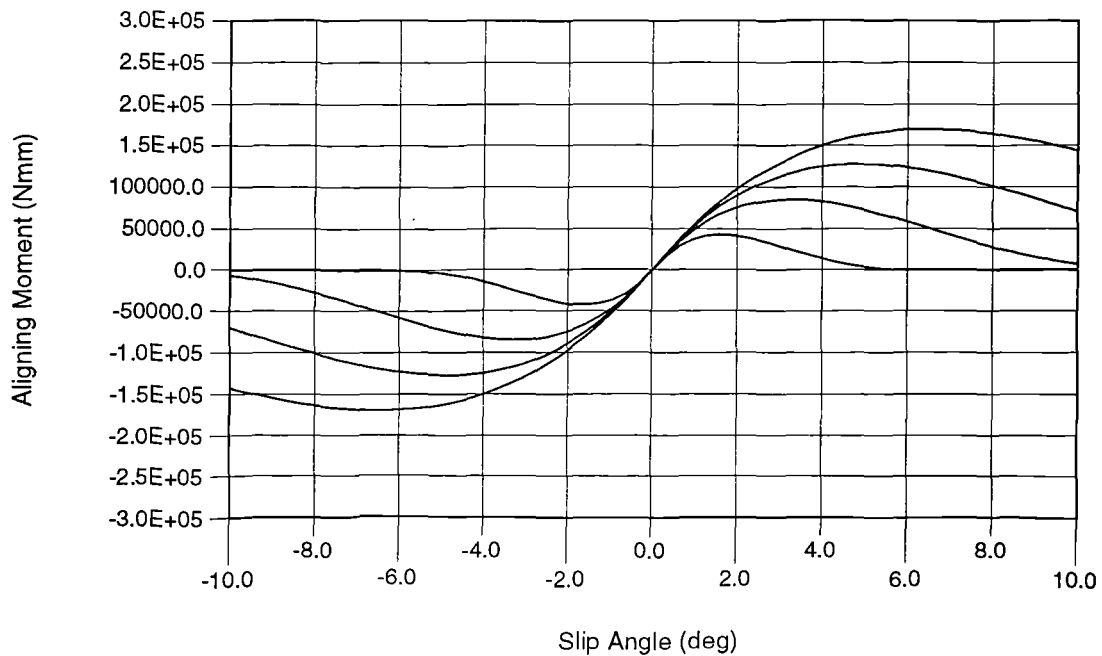
Figure F.16 Fiala model (TYRE B) - aligning moment with slip angle

FIALA TYRE MODEL - TYRE B (Front Wheel Load) 195/65 R15

Vertical Load Increments - 200kg 400kg 600kg 800kg

Lateral Force (N)

Aligning Moment (Nmm)
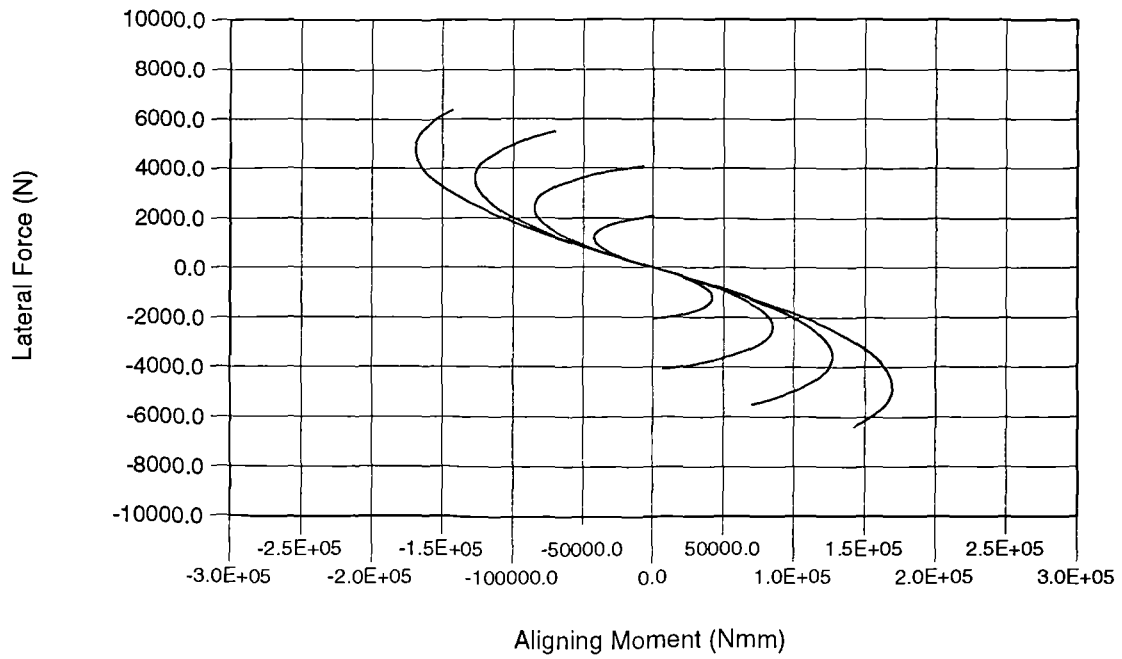
Figure F.17 Fiala model (TYRE B) - lateral force with aligning moment

FIALA TYRE MODEL - TYRE B (Rear Wheel Load) 195/65 R15

Vertical Load Increments - 200kg 400kg 600kg 800kg

Lateral Force (N)
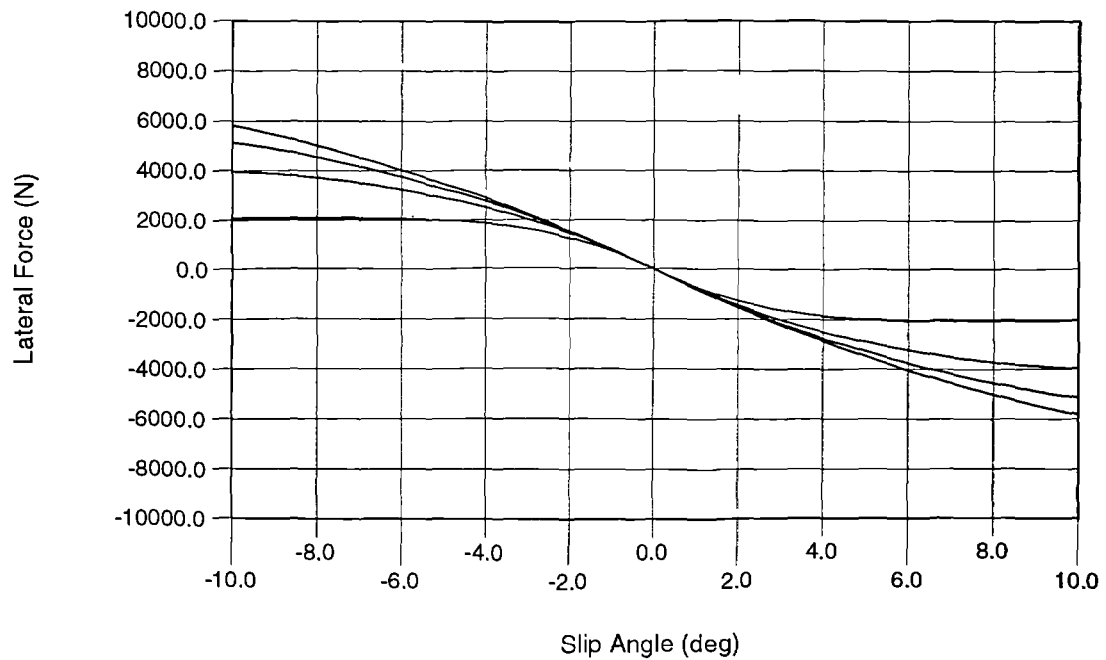
Slip Angle (deg)

Figure F.18 Fiala model (TYRE B) - lateral force with slip angle

FIALA TYRE MODEL - TYRE B (Rear Wheel Load) 195/65 R15
Vertical Load Increments - 200kg 400kg 600kg 800kg

Figure F.19 Fiala model (TYRE B) - lateral force with slip angle at near zero slip

FIALA TYRE MODEL - TYRE B (Rear Wheel Load) 195/65 R15
Vertical Load Increments - 200kg 400kg 600kg 800kg
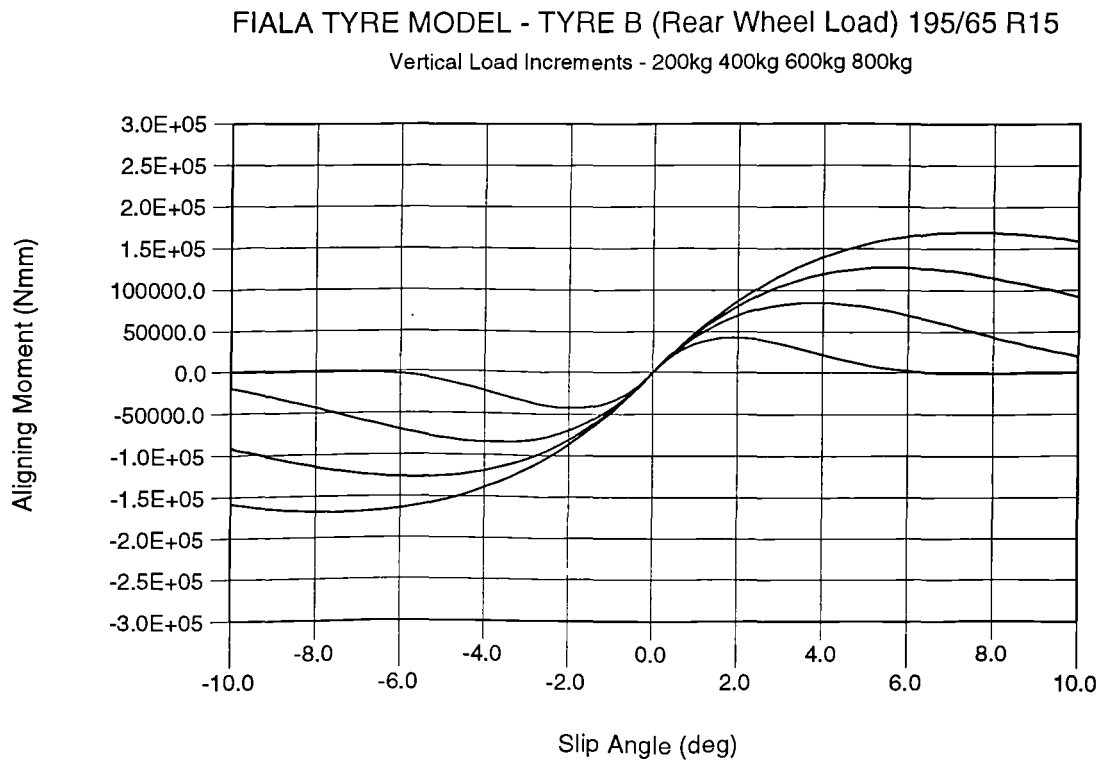
Figure F.20 Fiala model (TYRE B) - aligning moment with slip angle

FIALA TYRE MODEL - TYRE B (Rear Wheel Load) 195/65 R15

Vertical Load Increments - 200kg 400kg 600kg 800kg
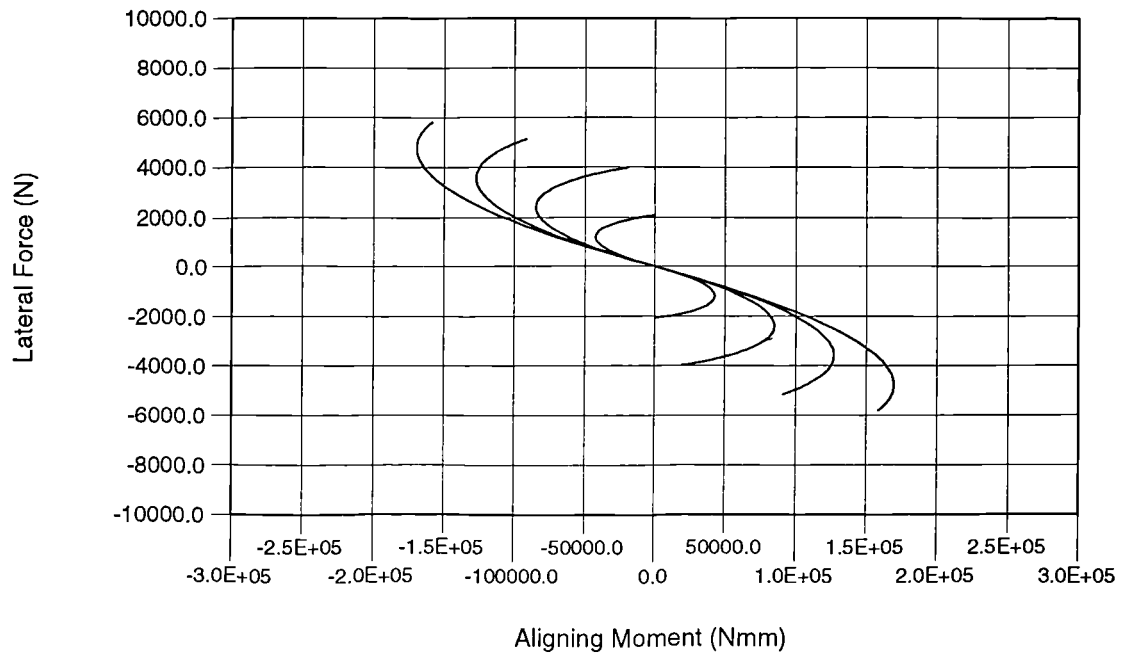
Figure F.21 Fiala model (TYRE B) - lateral force with aligning moment

PACJEKA TYRE MODEL (VERSION 3) - TYRE B 195/65 R15

Vertical Load Increments - 200kg 400kg 600kg 800kg
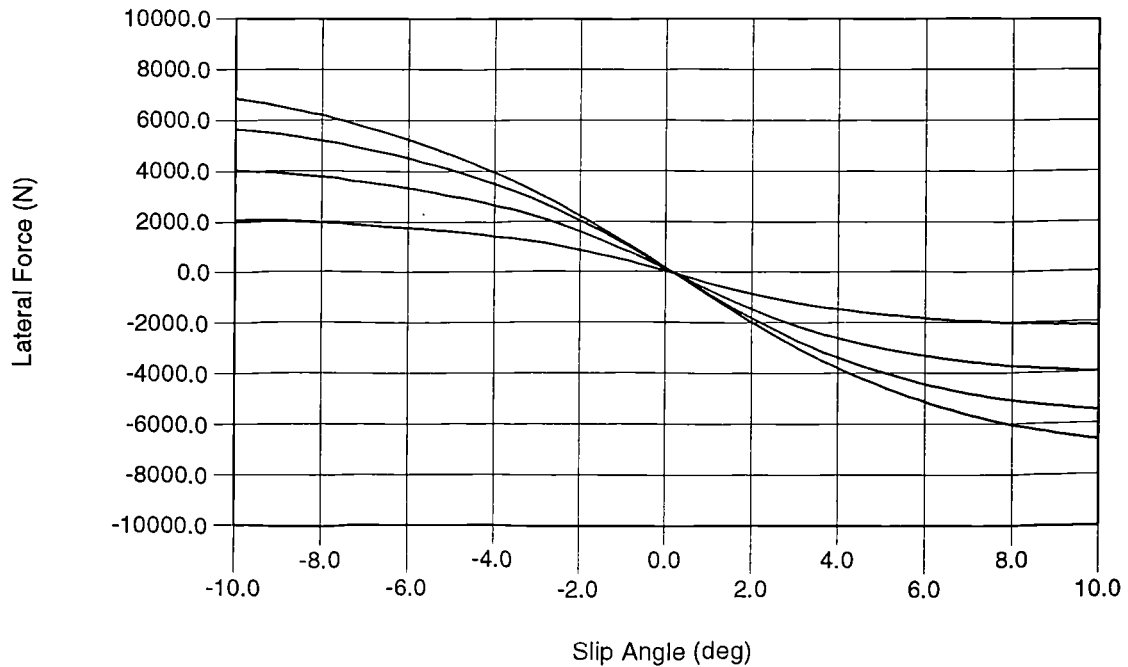
Figure F.22 Pacejka model (TYRE B) - lateral force with slip angle

PACJEKA TYRE MODEL (VERSION 3) - TYRE B 195/65 R15

Vertical Load Increments - 200kg 400kg 600kg 800kg

Figure F.23 Pacejka model (TYRE B) - lateral force with slip angle at near zero slip

PACJEKA TYRE MODEL (VERSION 3) - TYRE B 195/65 R15

Vertical Load Increments - 200kg 400kg 600kg 800kg
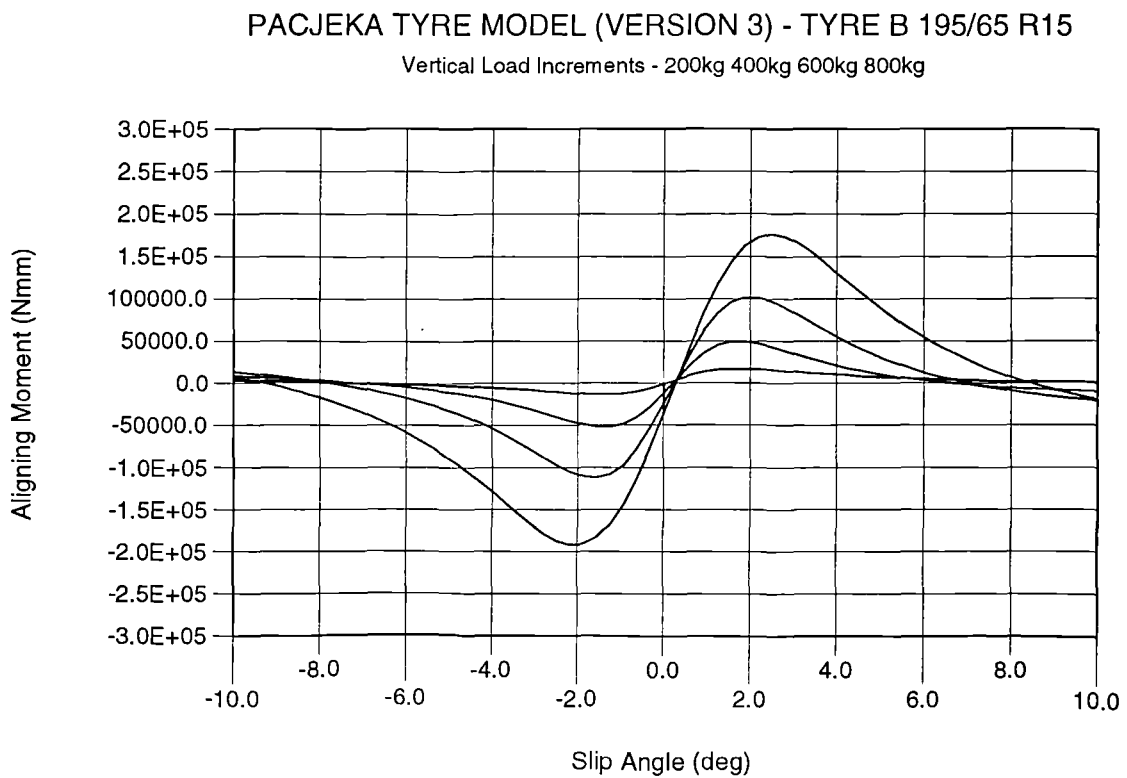
Figure F.24 Pacejka model (TYRE B) - aligning moment with slip angle

PACJEKA TYRE MODEL (VERSION 3) - TYRE B 195/65 R15
Vertical Load Increments - 200kg 400kg 600kg 800kg

Lateral Force (N)

Aligning Moment (Nmm)
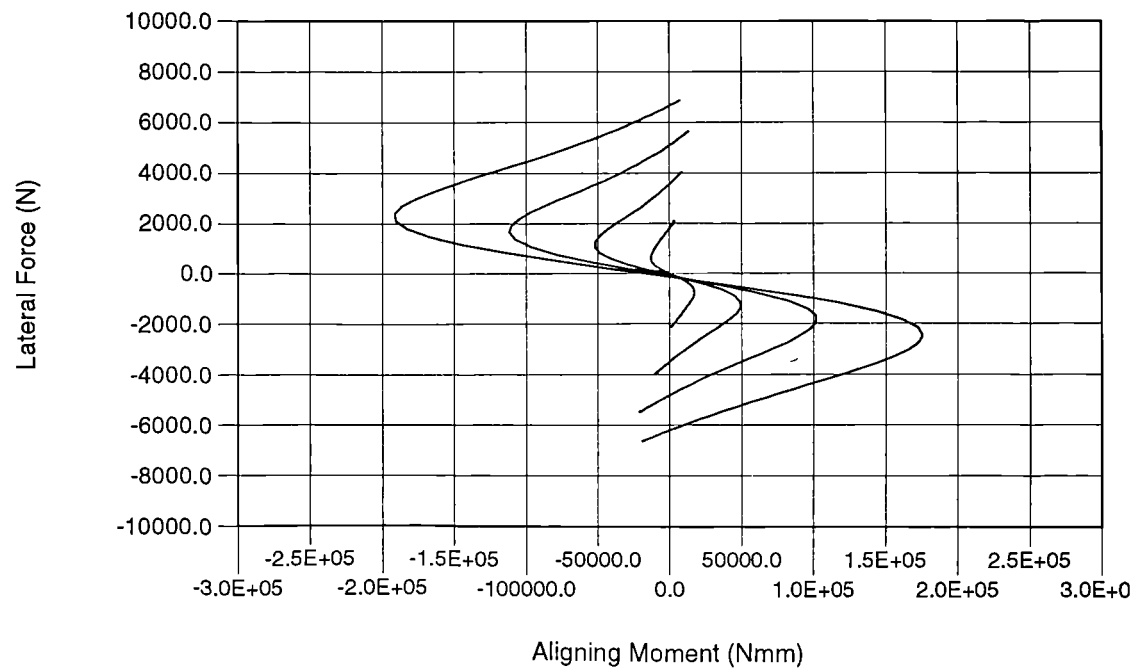
Figure F.25 Pacejka model (TYRE B) - lateral force with aligning moment

APPENDIX G

INVESTIGATION OF LANE CHANGE
MANOEUVRE (INTERPOLATION MODEL - TYRE A)

LUMPED MASS MODEL (TYRE A/INTERPOLATION) - 100 KPH LANE CHANGE
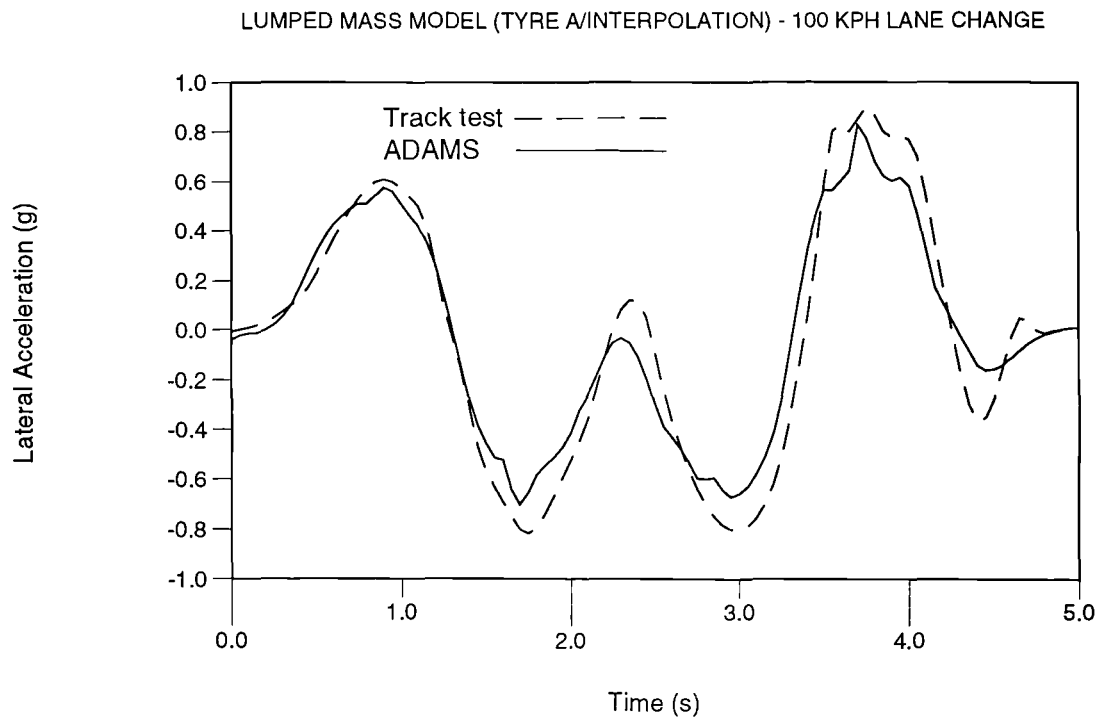
Figure G.1 Lateral acceleration comparison - lumped mass model and test

SWING ARM MODEL (TYRE A/INTERPOLATION) - 100 KPH LANE CHANGE
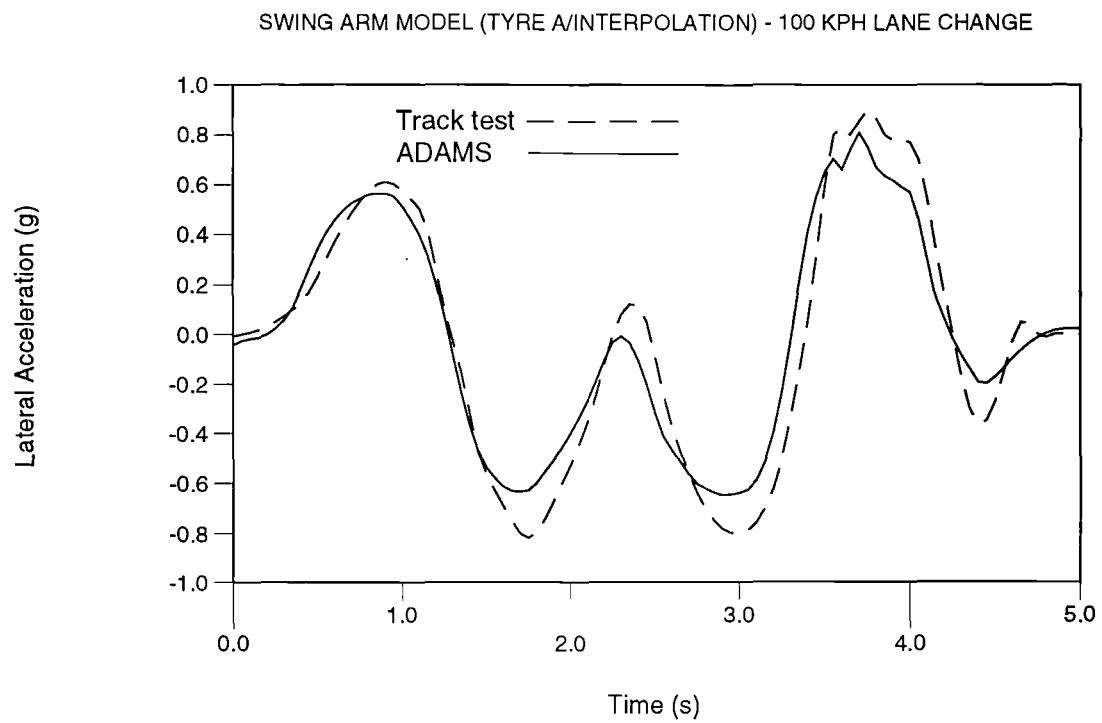
Figure G.2 Lateral acceleration comparison - swing arm model and test

ROLL STIFFNESS MODEL (TYRE A/INTERPOLATION) - 100 KPH LANE CHANGE
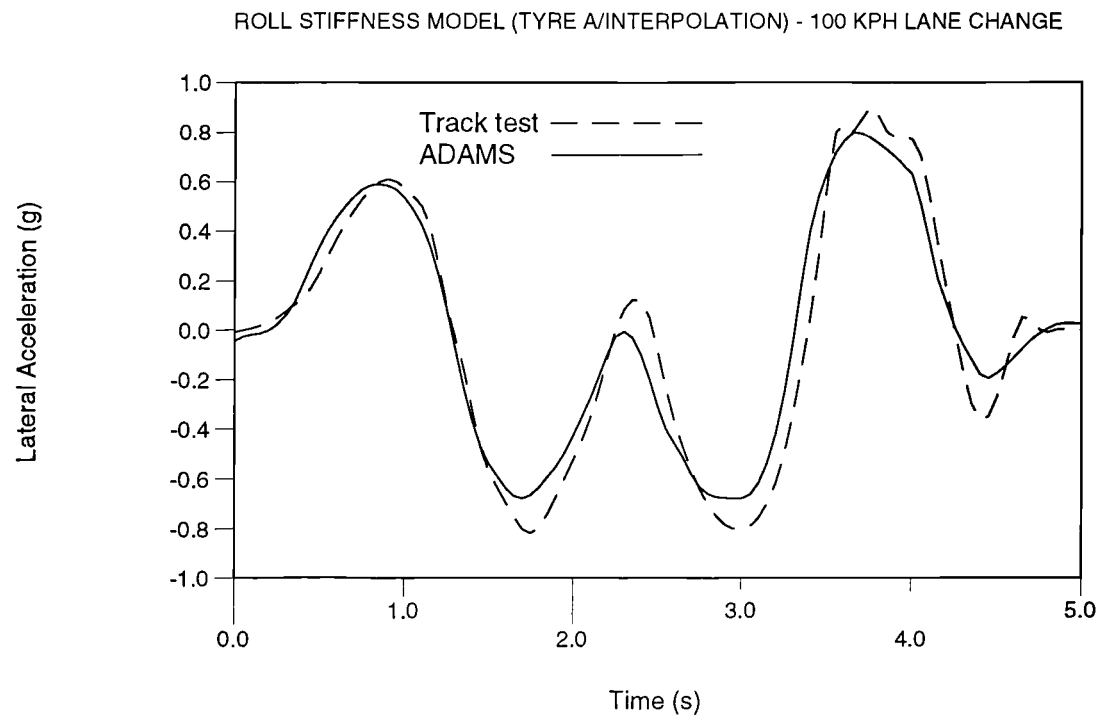
Figure G.3 Lateral acceleration comparison - roll stiffness model and test

LINKAGE MODEL (TYRE A/INTERPOLATION) - 100 KPH LANE CHANGE
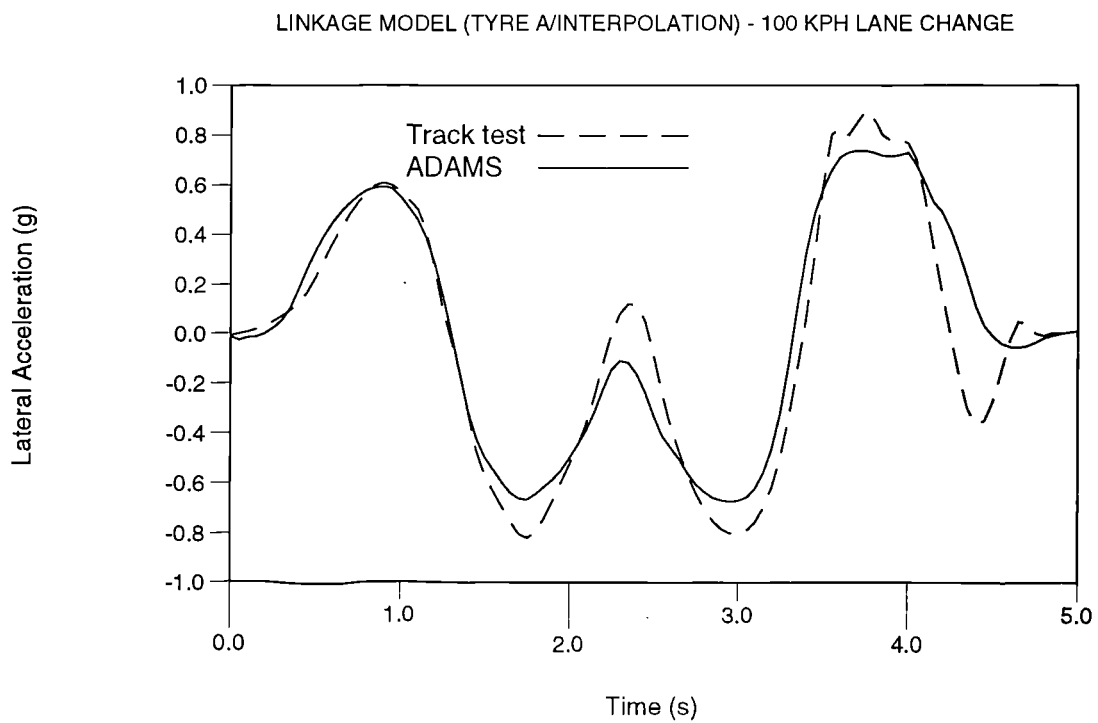
Figure G.4 Lateral acceleration comparison - linkage model and test

LUMPED MASS MODEL (TYRE A/INTERPOLATION) - 100 KPH LANE CHANGE
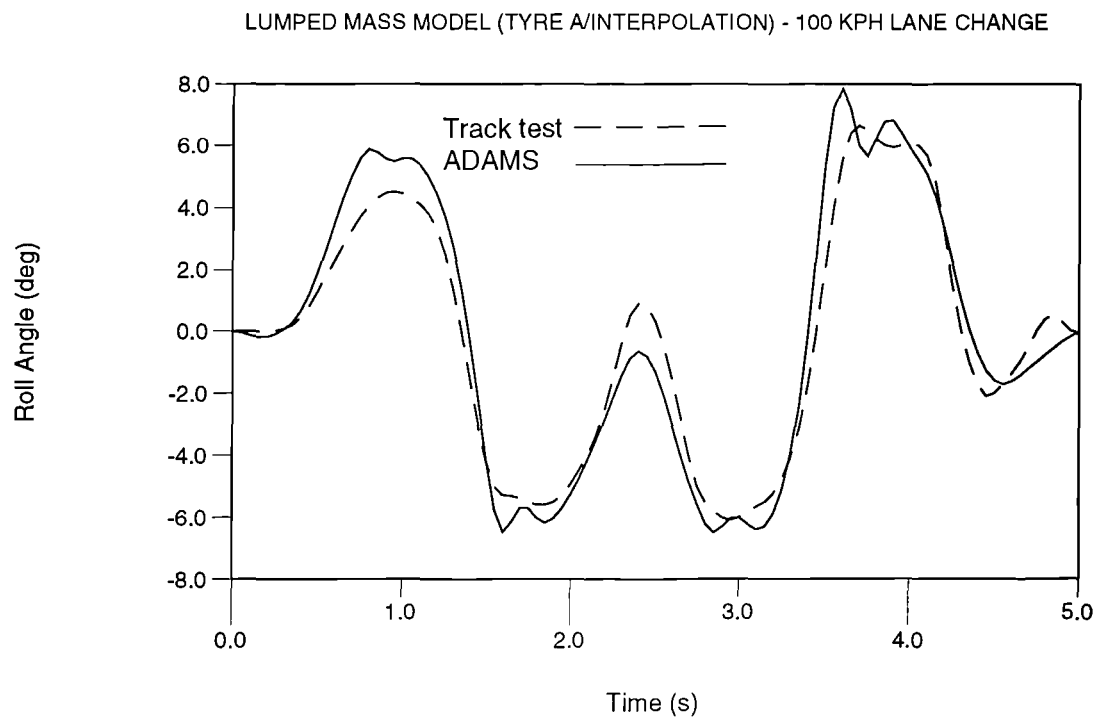
Figure G.5 Roll angle comparison - lumped mass model and test

SWING ARM MODEL (TYRE A/INTERPOLATION) - 100 KPH LANE CHANGE
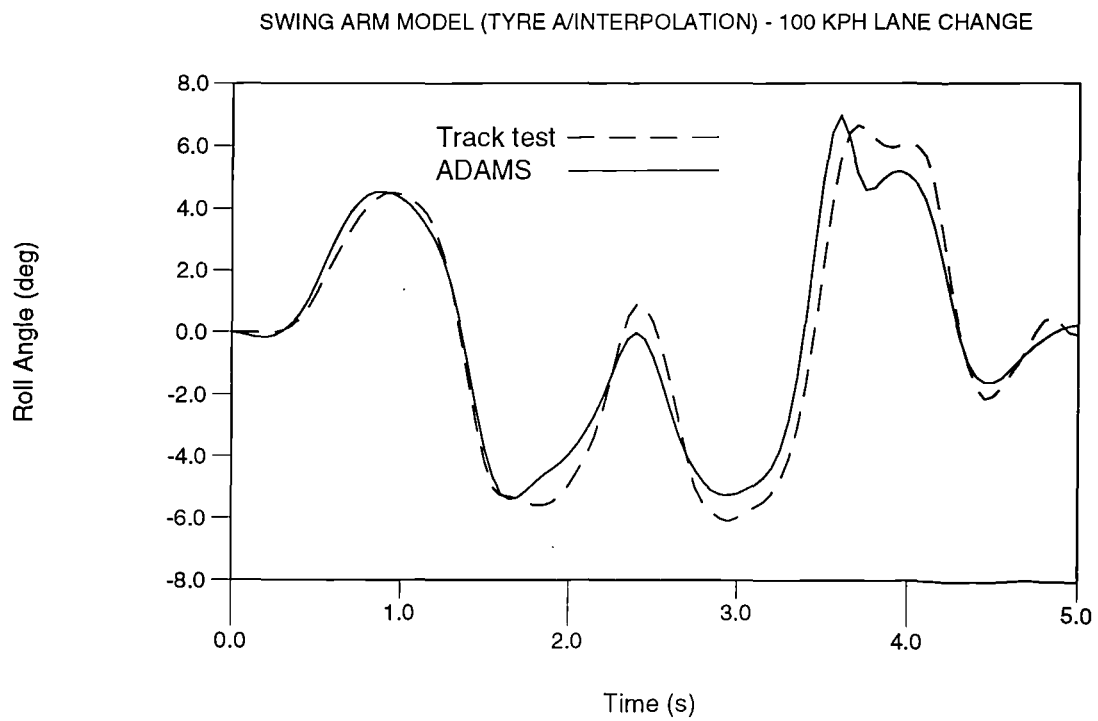
Figure G.6 Roll angle comparison - swing arm model and test

ROLL STIFFNESS MODEL (TYRE A/INTERPOLATION) - 100 KPH LANE CHANGE
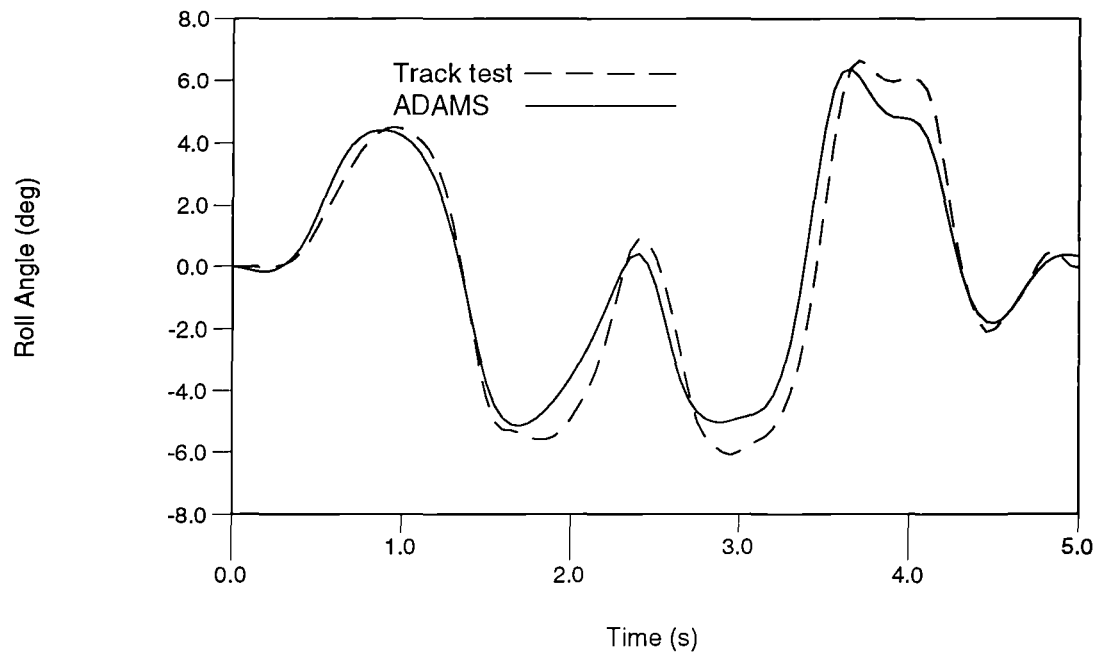
Figure G.7 Roll angle comparison - roll stiffness model and test

LINKAGE MODEL (TYRE A/INTERPOLATION) - 100 KPH LANE CHANGE
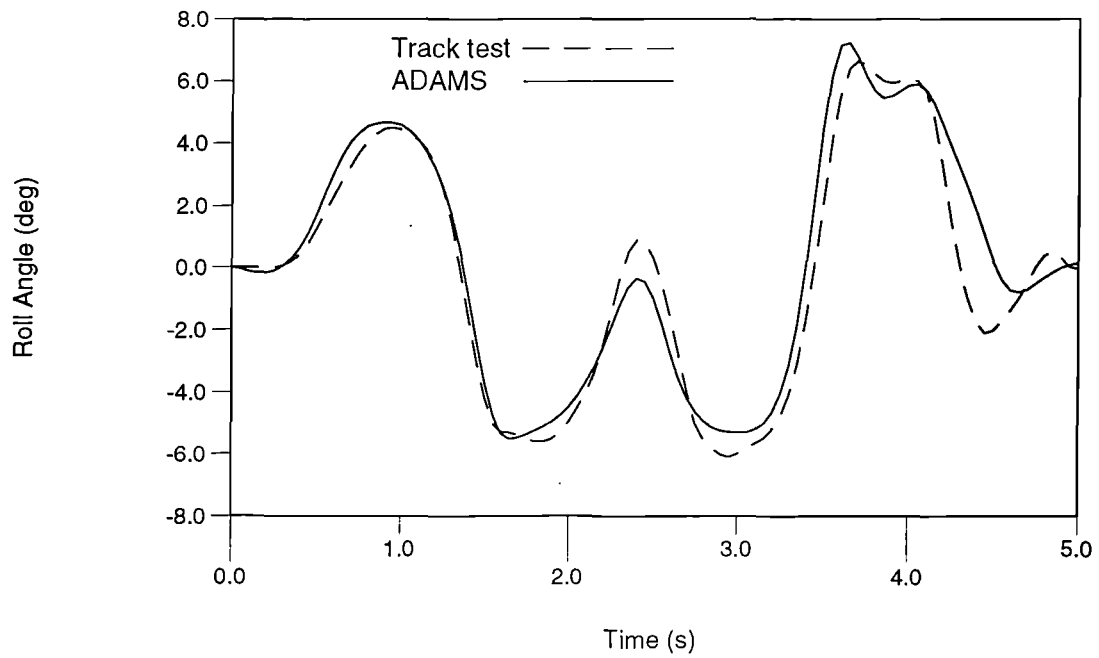
Figure G.8 Roll angle comparison - linkage model and test

LUMPED MASS MODEL (TYRE A/INTERPOLATION) - 100 KPH LANE CHANGE
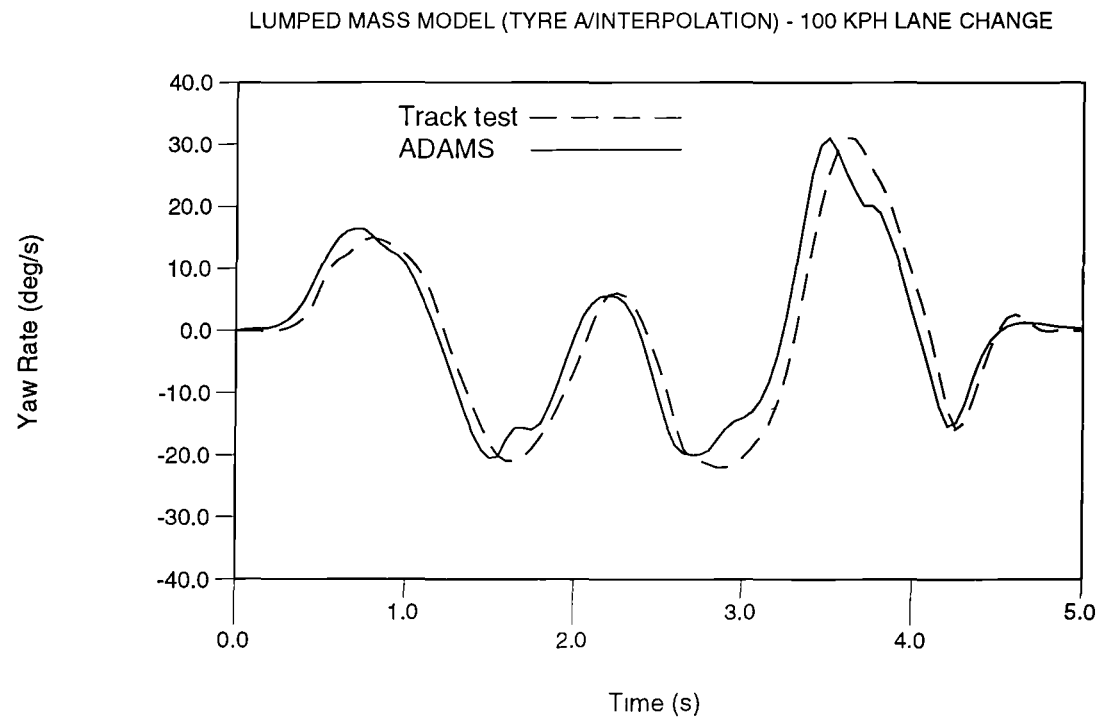
Figure G.9 Yaw rate comparison - lumped mass model and test

SWING ARM MODEL (TYRE A/INTERPOLATION) - 100 KPH LANE CHANGE
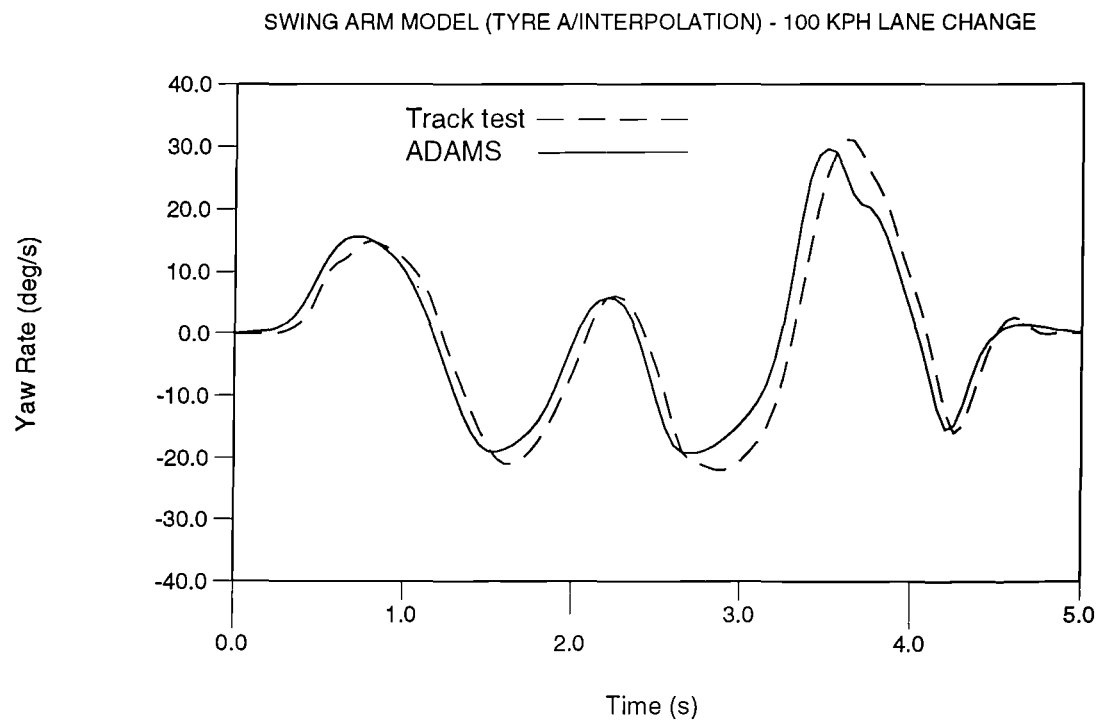
Figure G.10 Yaw rate comparison - swing arm model and test

ROLL STIFFNESS MODEL (TYRE A/INTERPOLATION) - 100 KPH LANE CHANGE
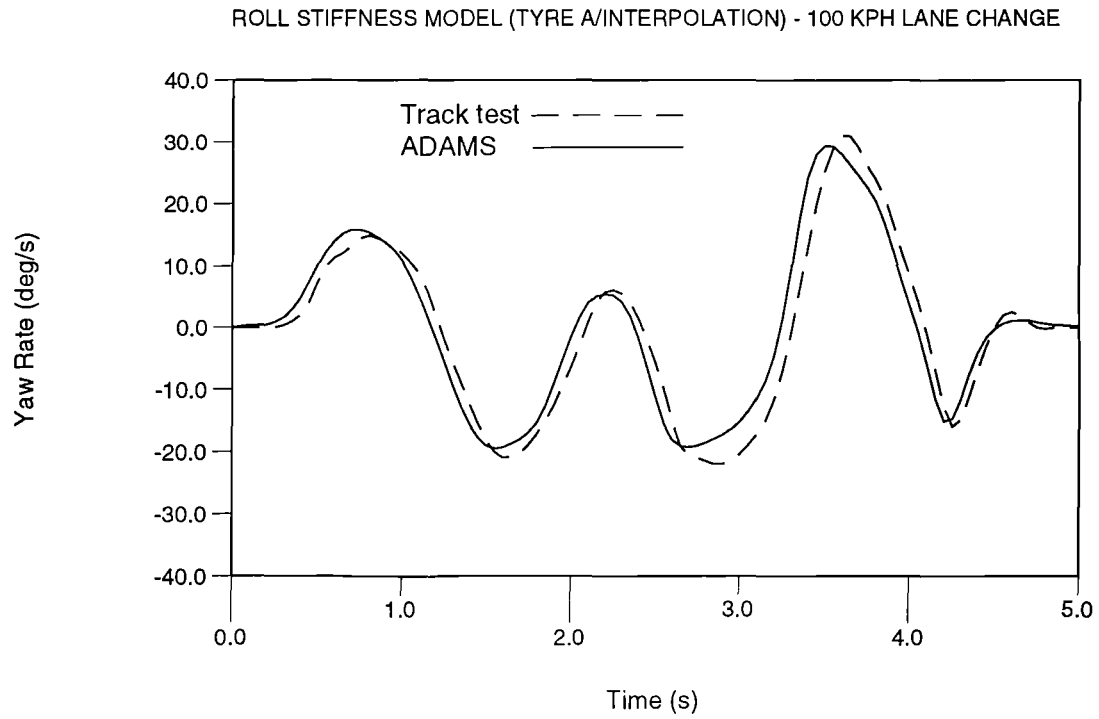
Figure G.11 Yaw rate comparison - roll stiffness model and test

LINKAGE MODEL (TYRE A/INTERPOLATION) - 100 KPH LANE CHANGE
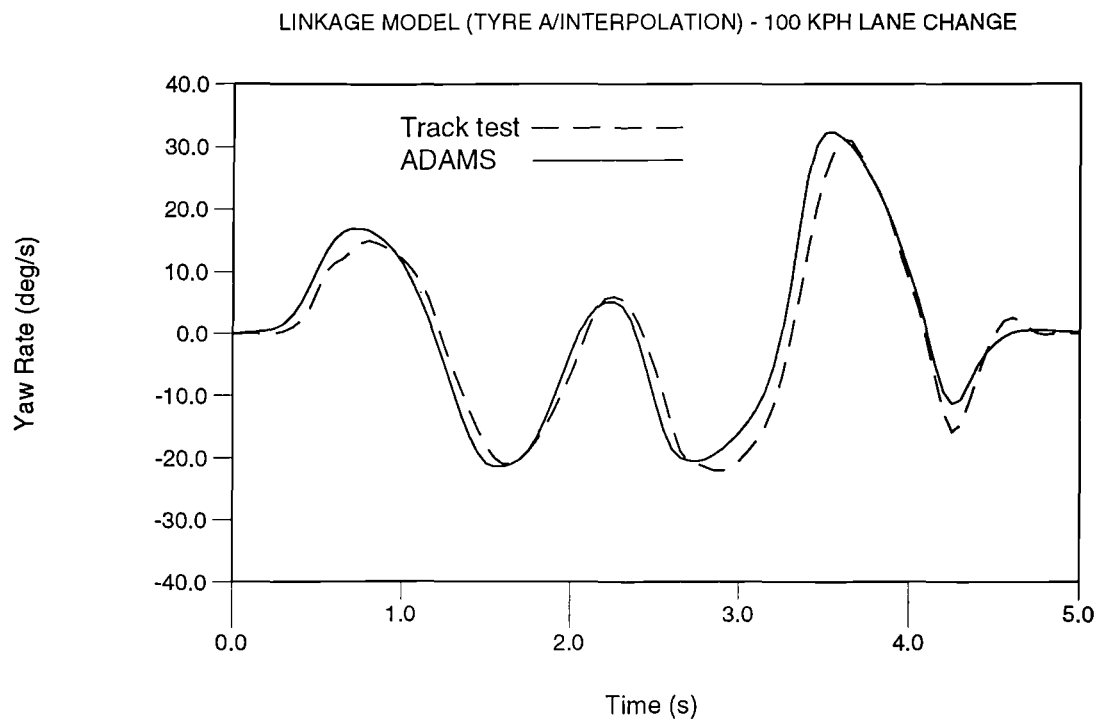
Figure G.12 Yaw rate comparison - linkage model and test
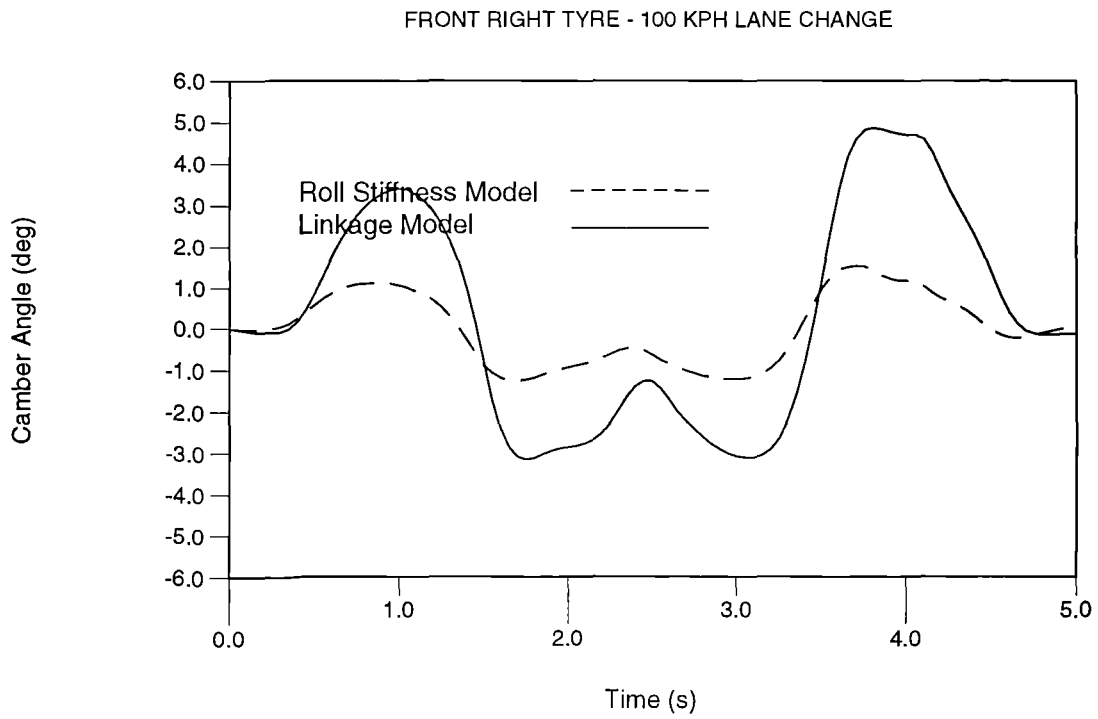
Figure G.13 Camber angle comparison - linkage and roll stiffness models
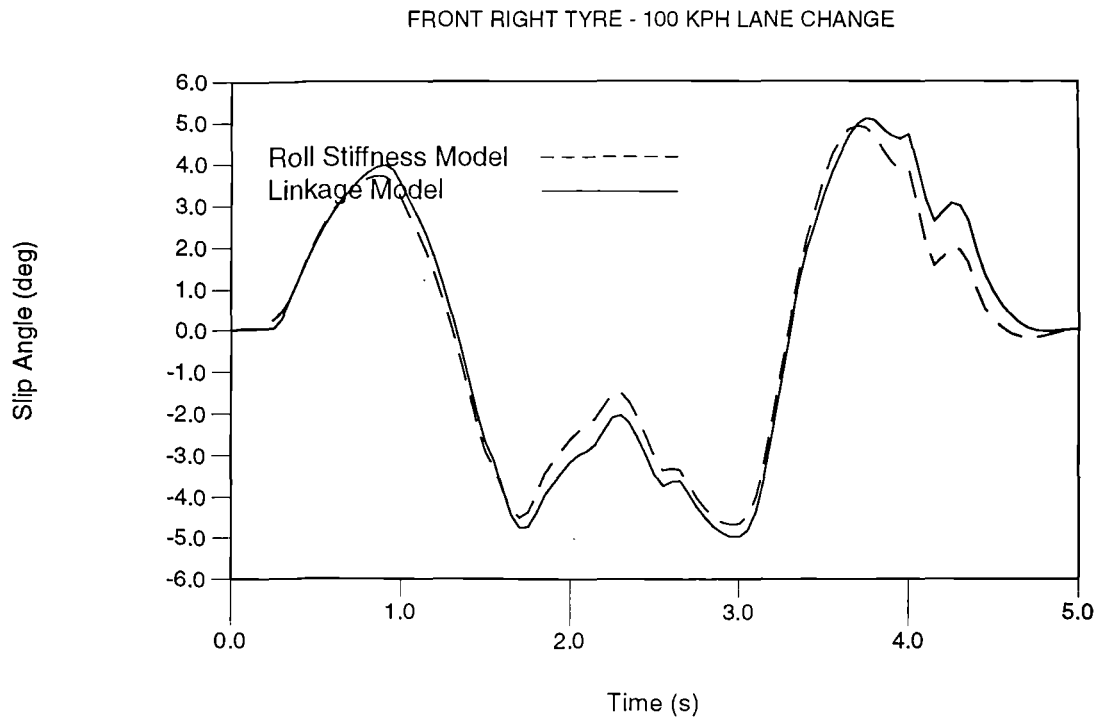
Figure G.14 Slip angle comparison - linkage and roll stiffness models

FRONT RIGHT TYRE - 100 KPH LANE CHANGE
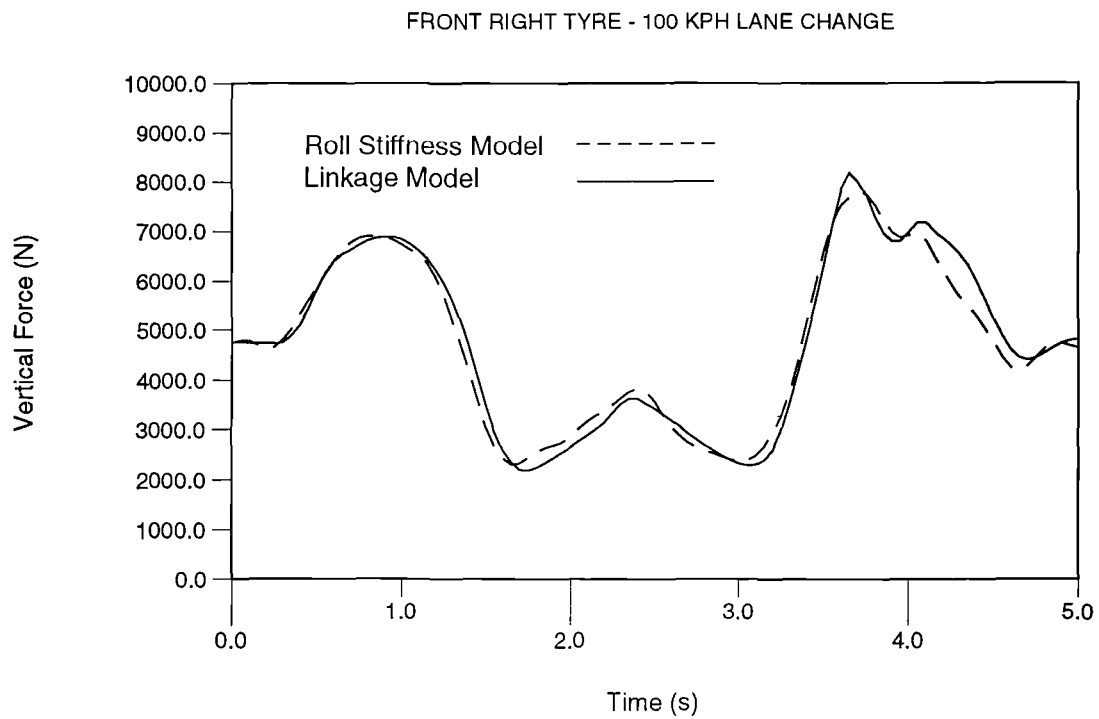
Figure G.15 Vertical tyre force comparison - linkage and roll stiffness models

FRONT LEFT TYRE - 100 KPH LANE CHANGE
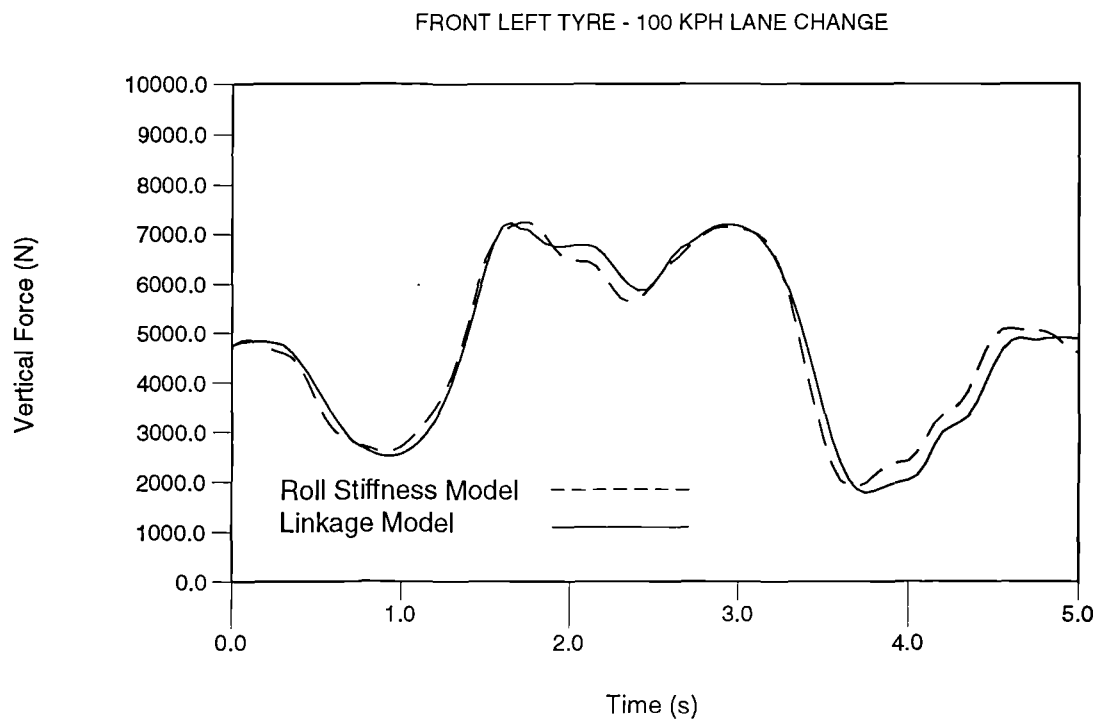
Figure G.16 Vertical tyre force comparison - linkage and roll stiffness models
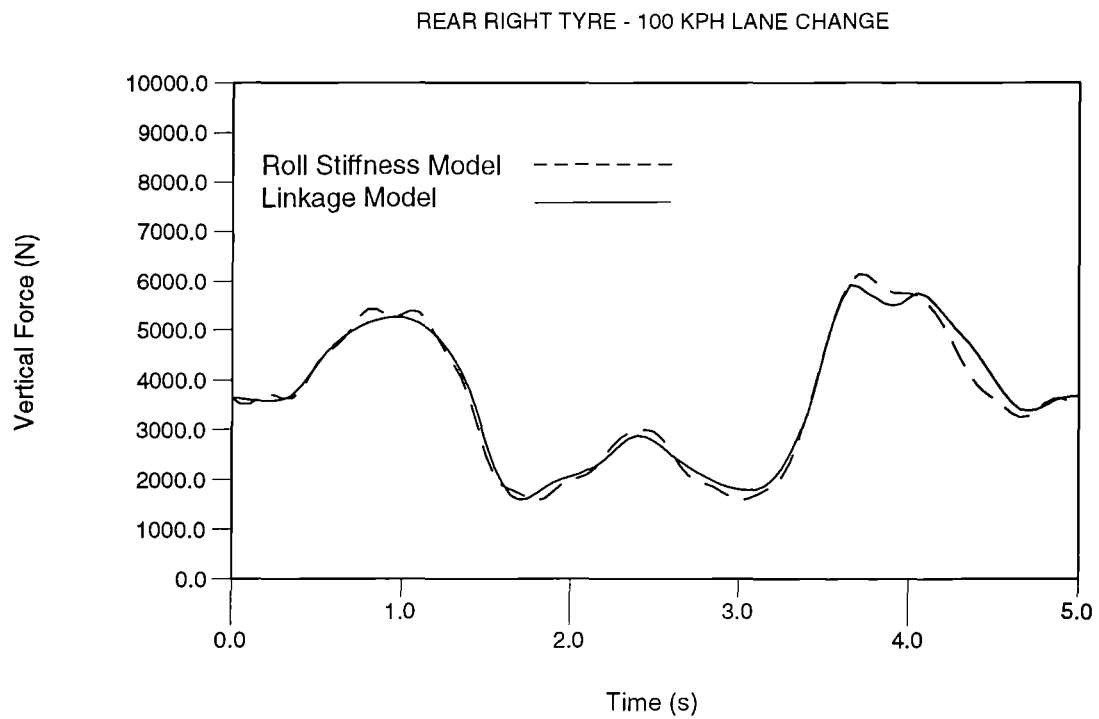
Figure G.17 Vertical tyre force comparison - linkage and roll stiffness models
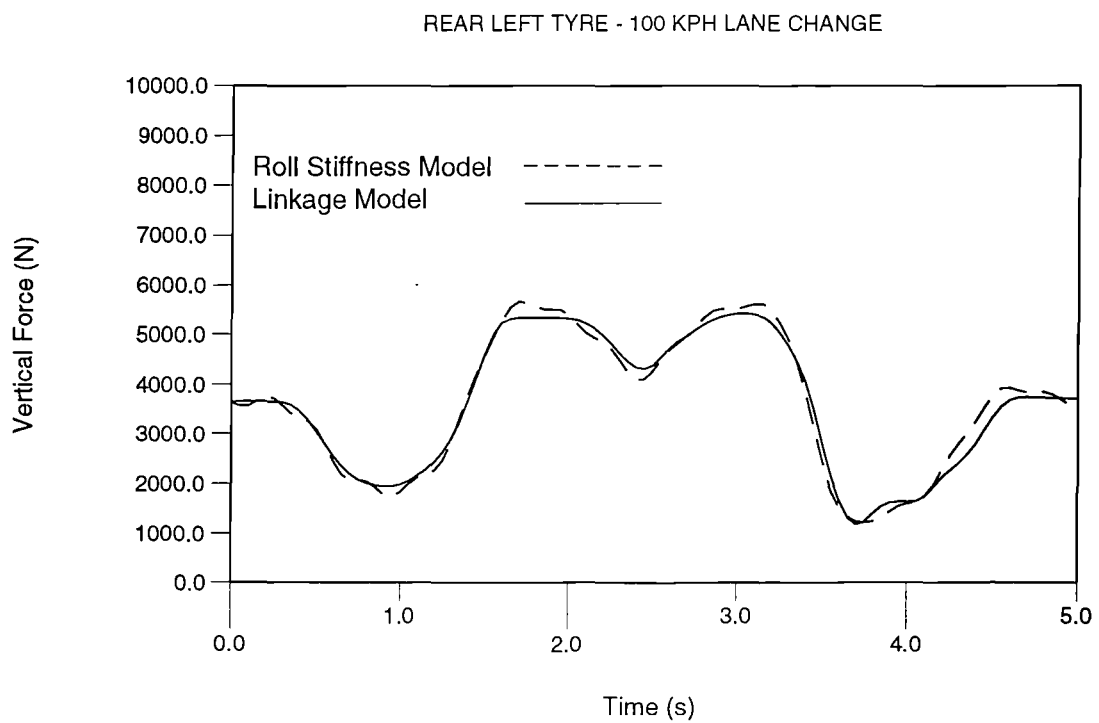
Figure G.18 Vertical tyre force comparison - linkage and roll stiffness models

APPENDIX H

INVESTIGATION OF LANE CHANGE MANOEUVRE SENSITIVITY TO TYRE DATA AND MODELS (LINKAGE MODEL)

LINKAGE MODEL (TYRE A/INTERPOLATION) - 100 KPH LANE CHANGE
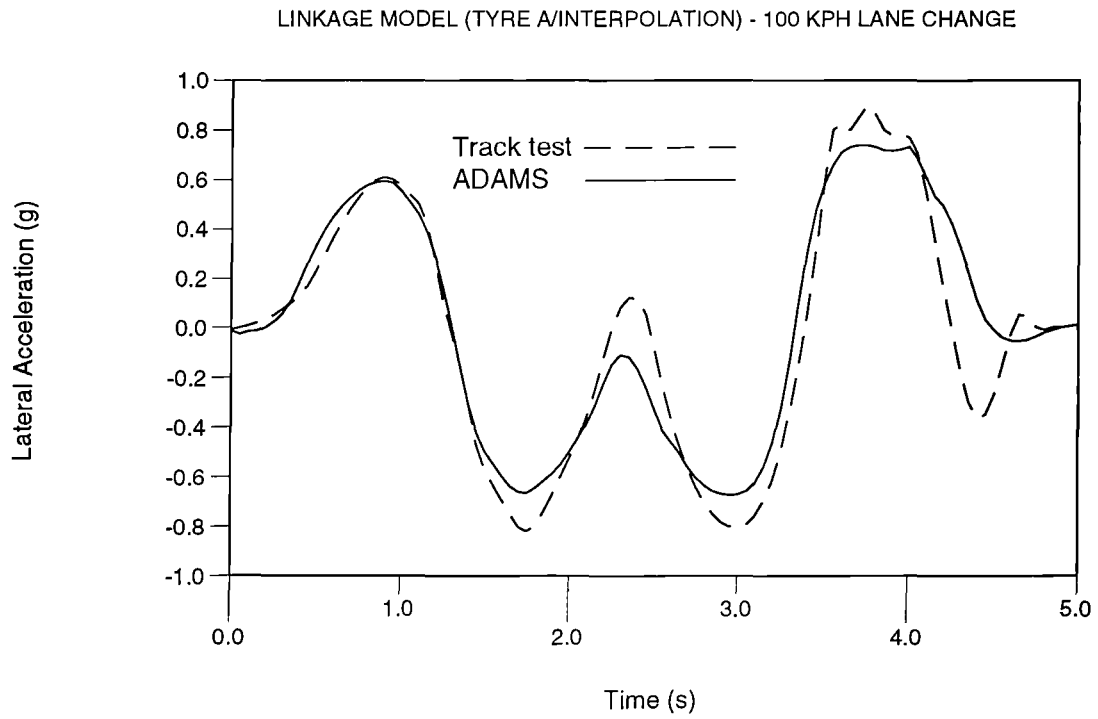
Figure H.1 Lateral acceleration comparison - Interpolation model TYRE A and test

LINKAGE MODEL (TYRE A/INTERPOLATION) - 100 KPH LANE CHANGE
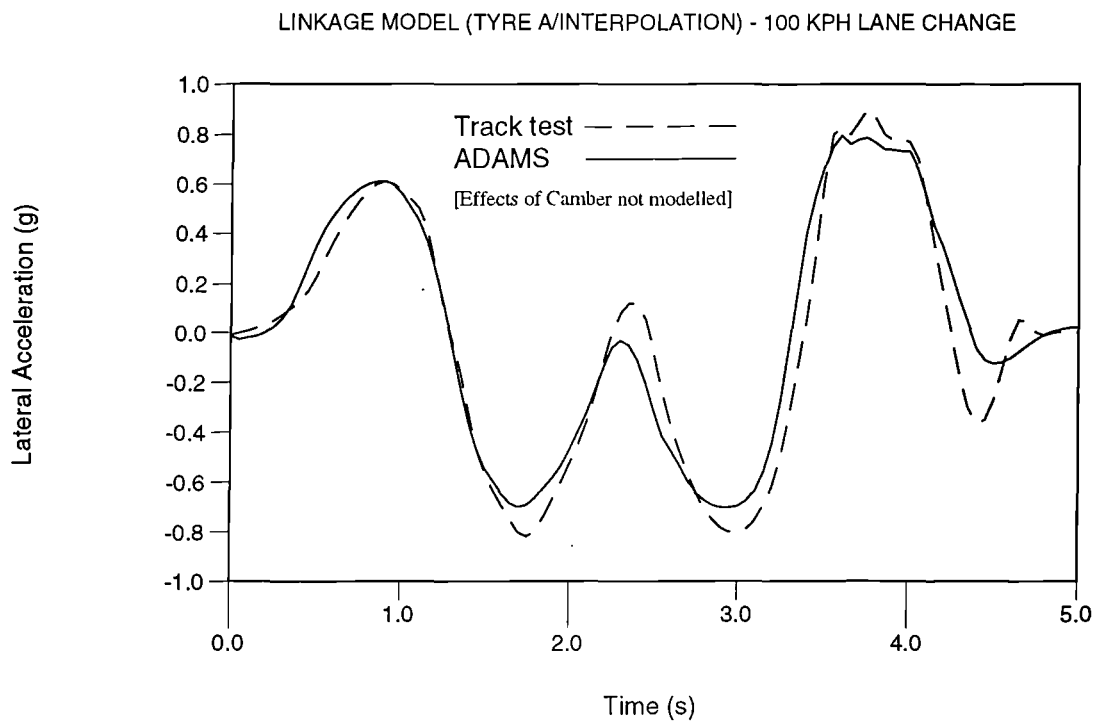
Figure H.2 Lateral acceleration comparison - Interpolation model TYRE A and test

LINKAGE MODEL (TYRE A/PACEJKA) - 100 KPH LANE CHANGE
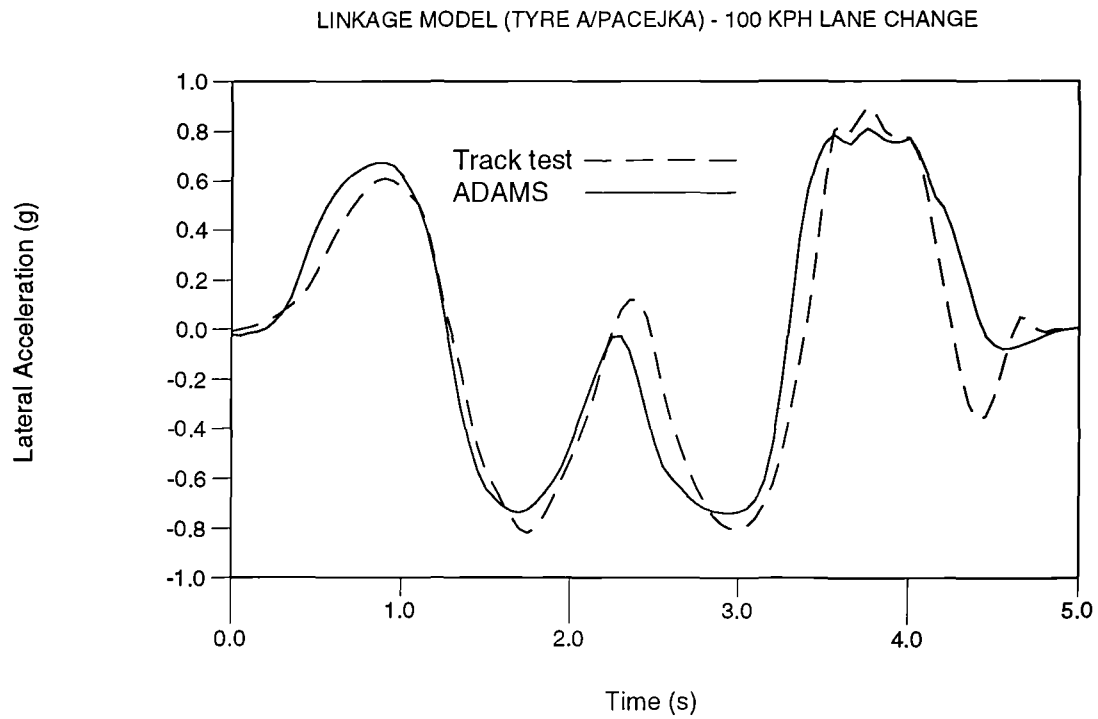
Figure H.3 Lateral acceleration comparison - Pacjeka model TYRE A and test

LINKAGE MODEL (TYRE A/PACEJKA) - 100 KPH LANE CHANGE
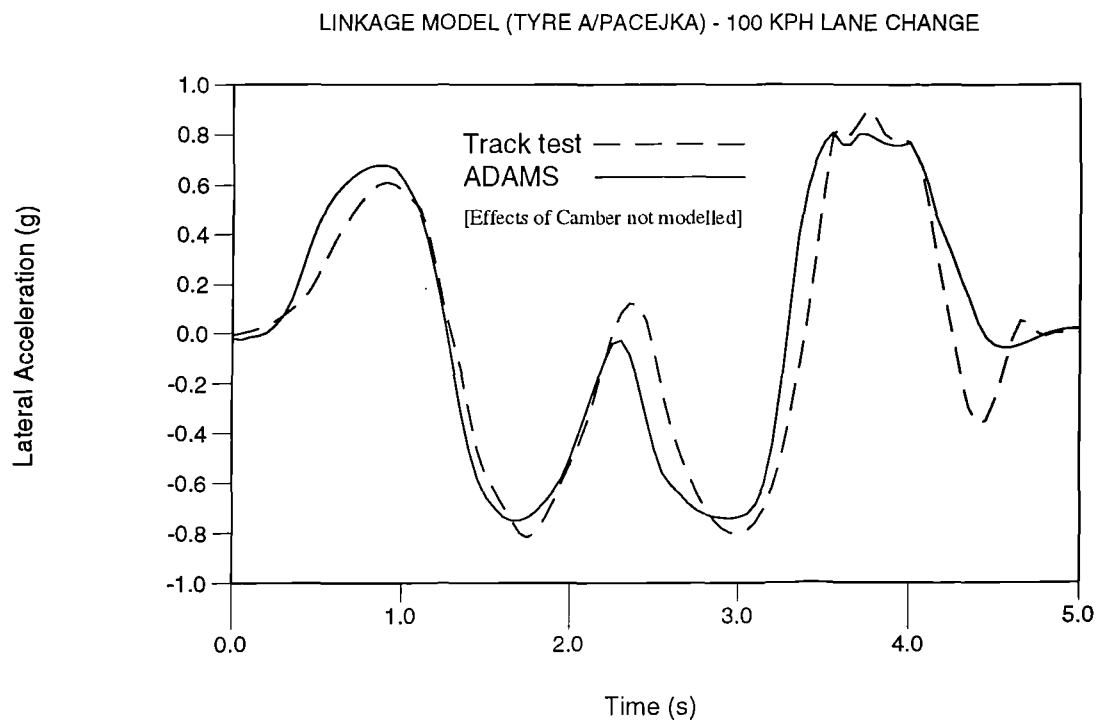
Figure H.4 Lateral acceleration comparison - Pacjeka model TYRE A and test

LINKAGE MODEL (TYRE A/FIALA) - 100 KPH LANE CHANGE
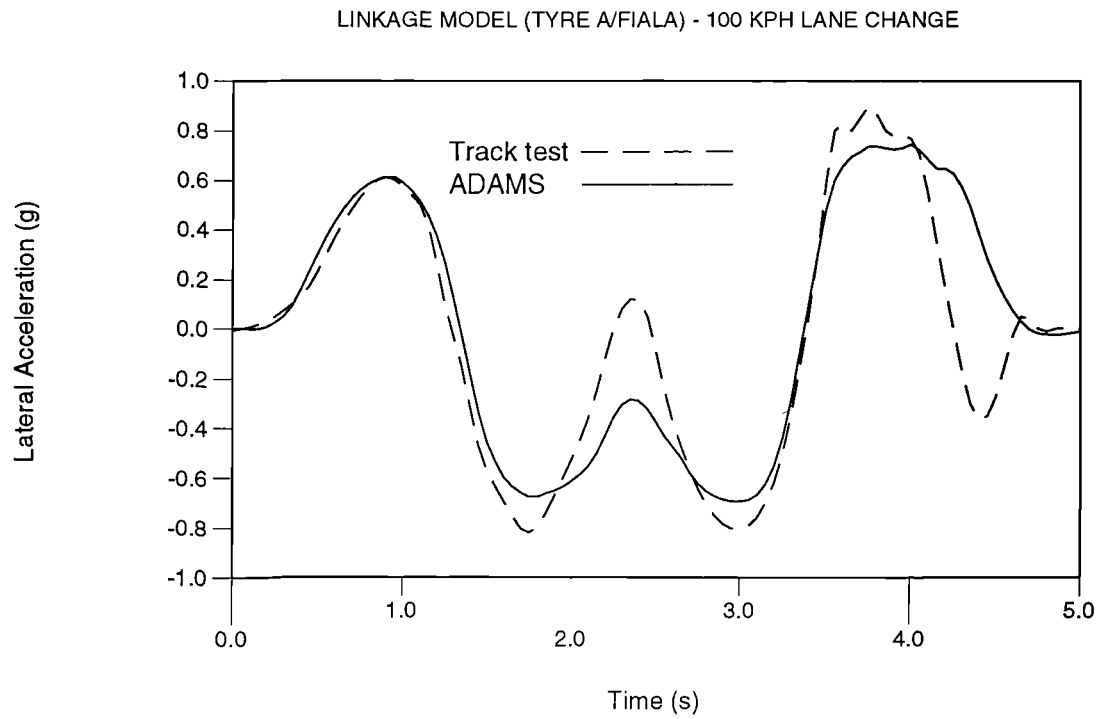
Figure H.5 Lateral acceleration comparison - Fiala model TYRE A and test

LINKAGE MODEL (TYRE A/INTERPOLATION) - 100 KPH LANE CHANGE
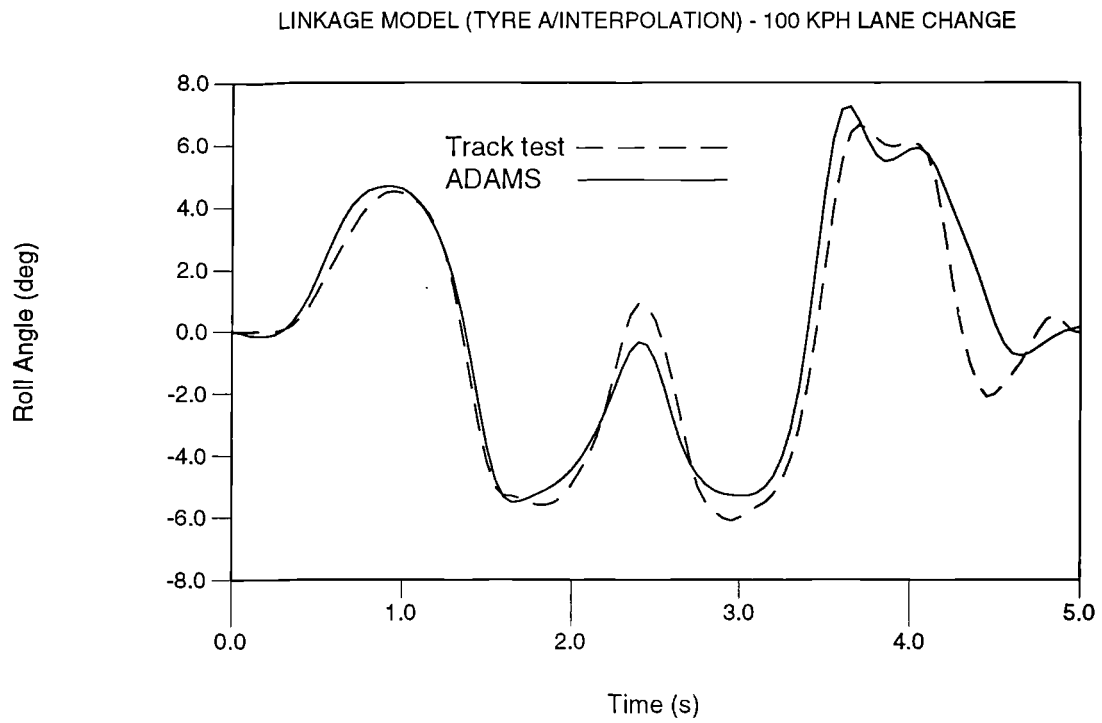
Figure H.6 Roll angle comparison - Interpolation model TYRE A and test

LINKAGE MODEL (TYRE A/INTERPOLATION) - 100 KPH LANE CHANGE
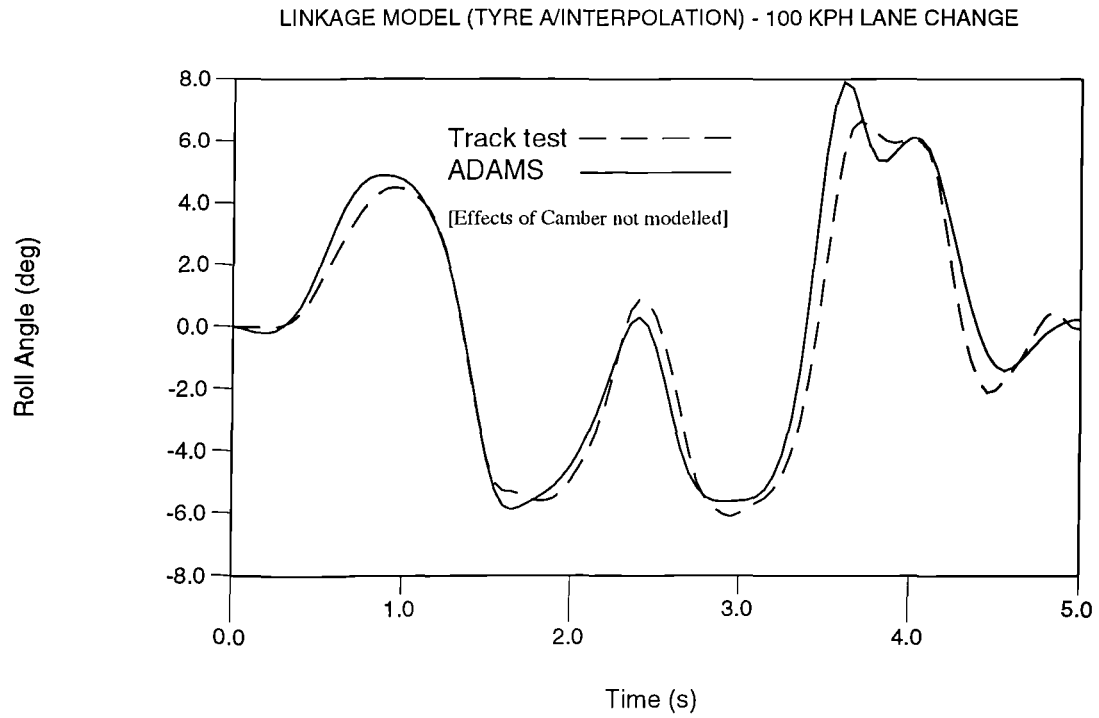
Figure H.7 Roll angle comparison - Interpolation model TYRE A and test

LINKAGE MODEL (TYRE A/PACEJKA) - 100 KPH LANE CHANGE
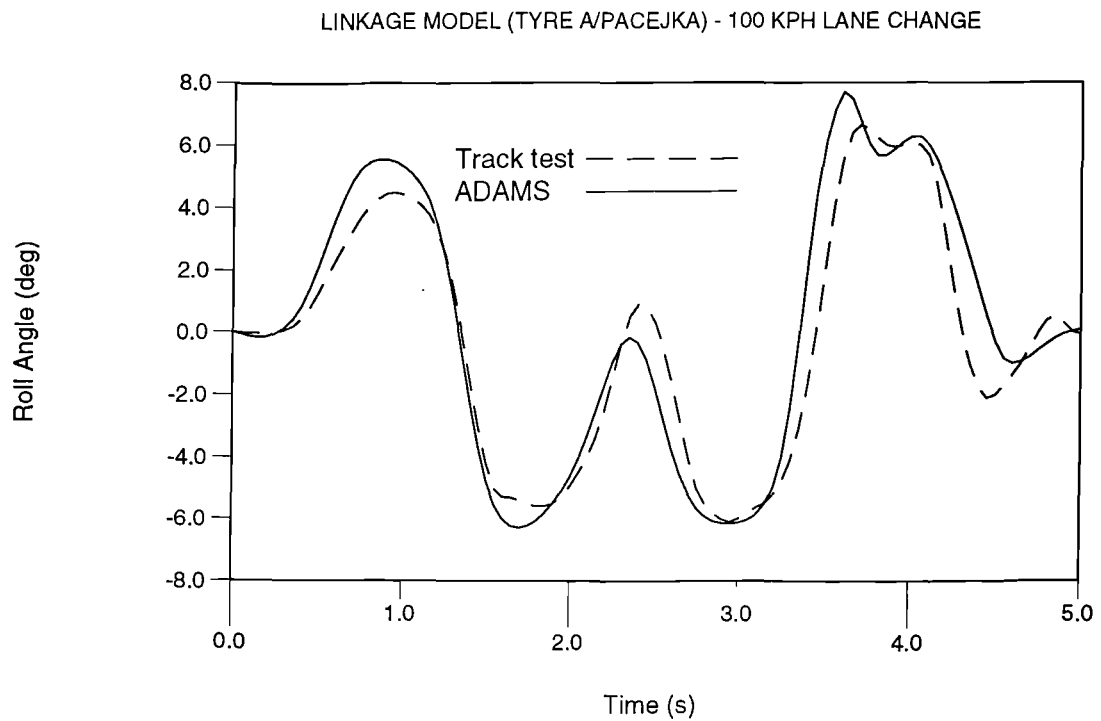
Figure H.8 Roll angle comparison - Pacejka model TYRE A and test

LINKAGE MODEL (TYRE A/PACEJKA) - 100 KPH LANE CHANGE
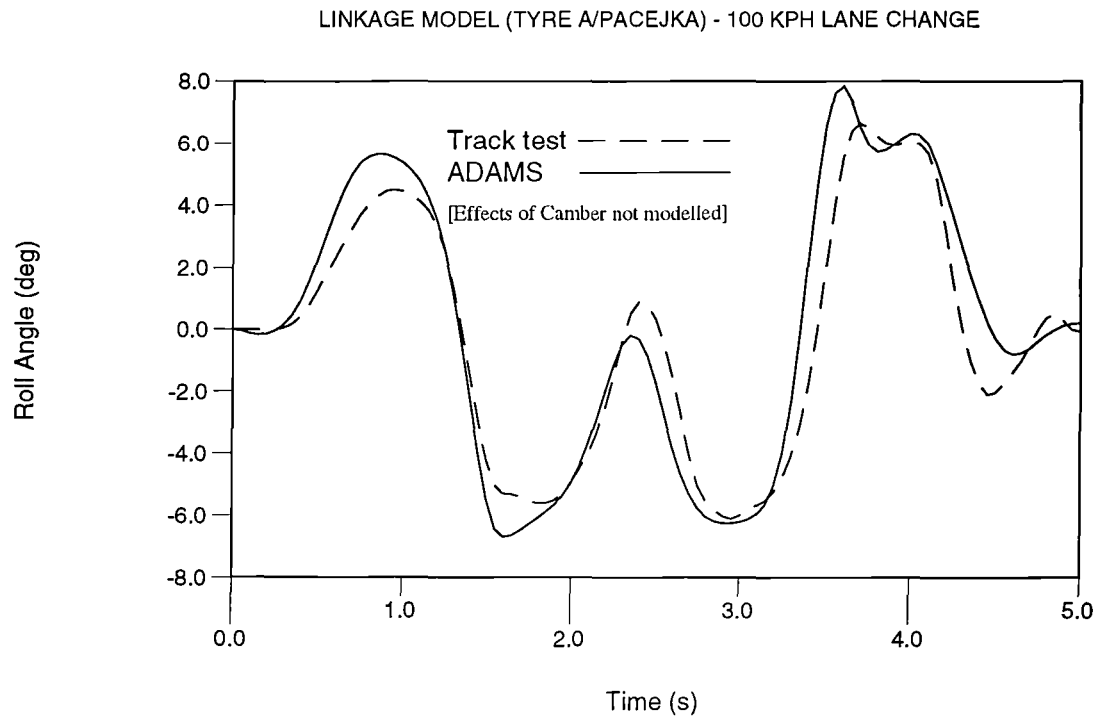
Figure H.9 Roll angle comparison - Pacejka model TYRE A and test

LINKAGE MODEL (TYRE A/FIALA) - 100 KPH LANE CHANGE
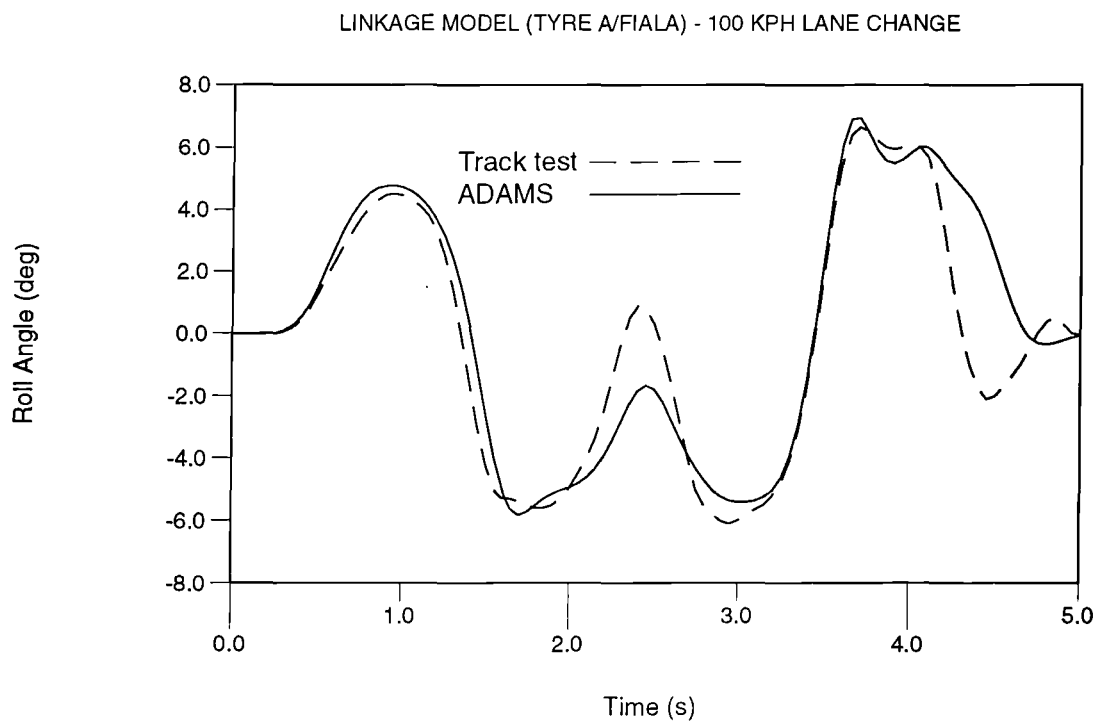
Figure H.10 Roll angle comparison - Fiala model TYRE A and test

LINKAGE MODEL (TYRE A/INTERPOLATION) - 100 KPH LANE CHANGE
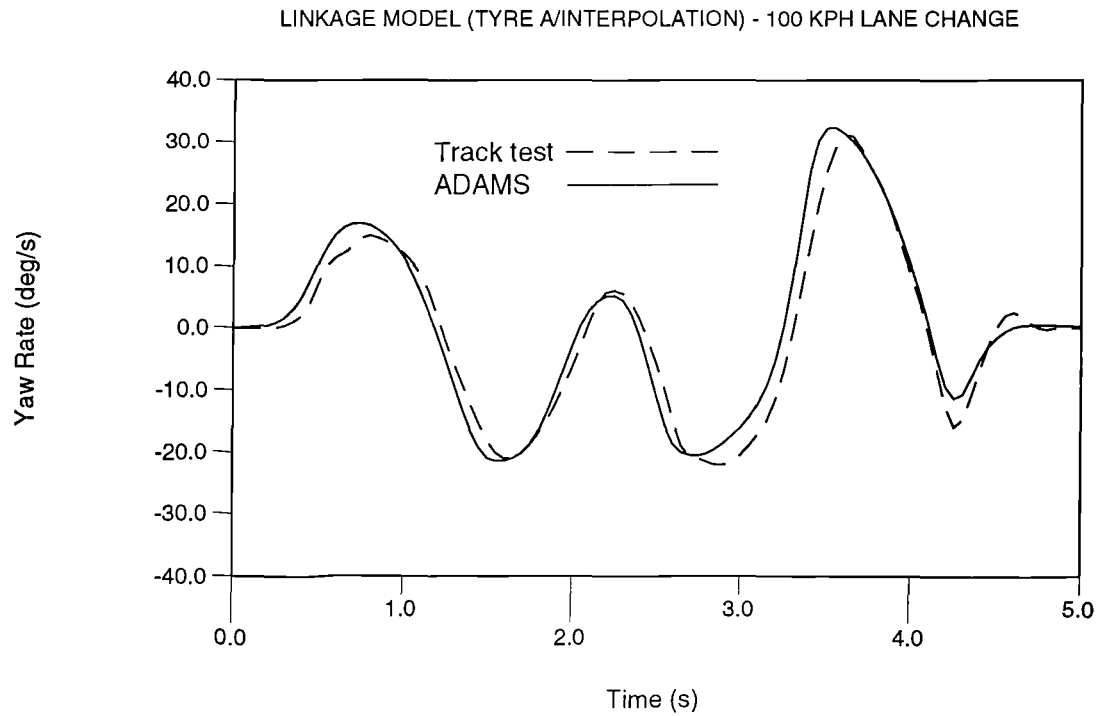
Figure H.11 Yaw rate comparison - Interpolation model TYRE A and test

LINKAGE MODEL (TYRE A/INTERPOLATION) - 100 KPH LANE CHANGE
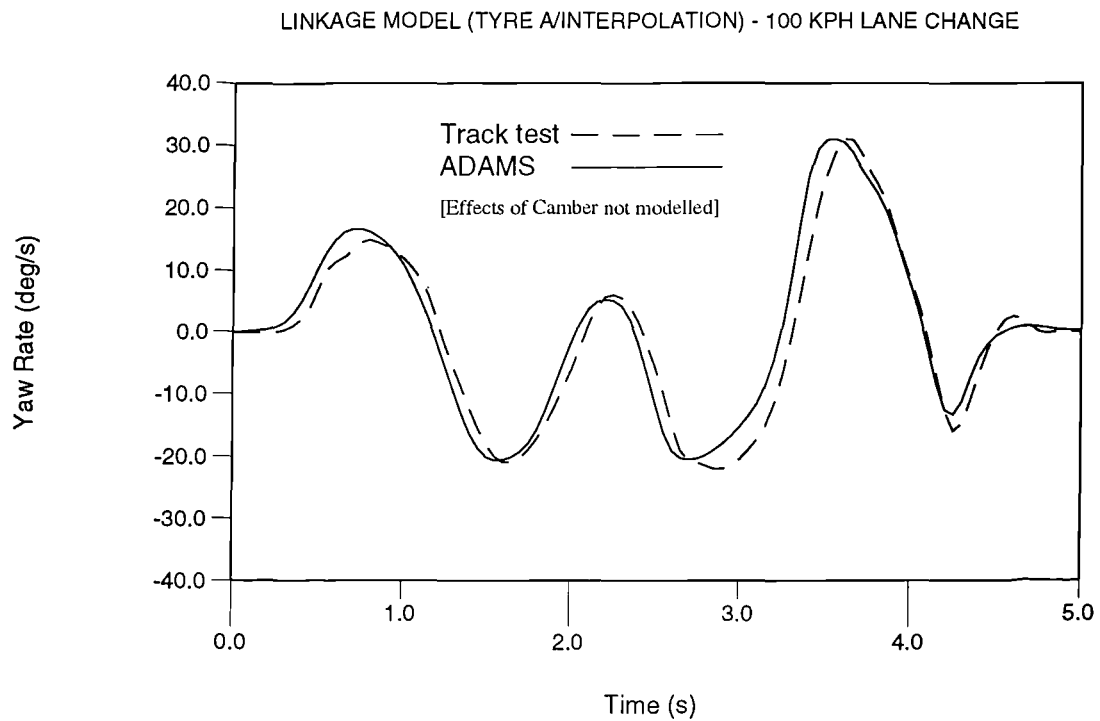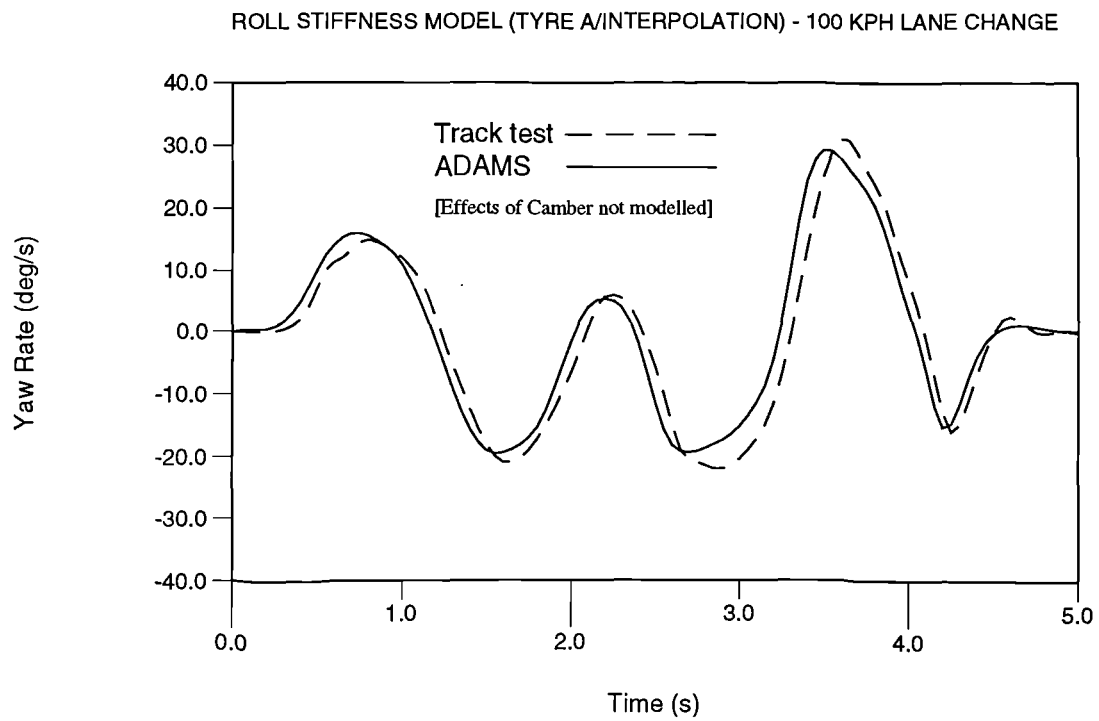

Figure H.12 Yaw rate comparison - Interpolation model TYRE A and test
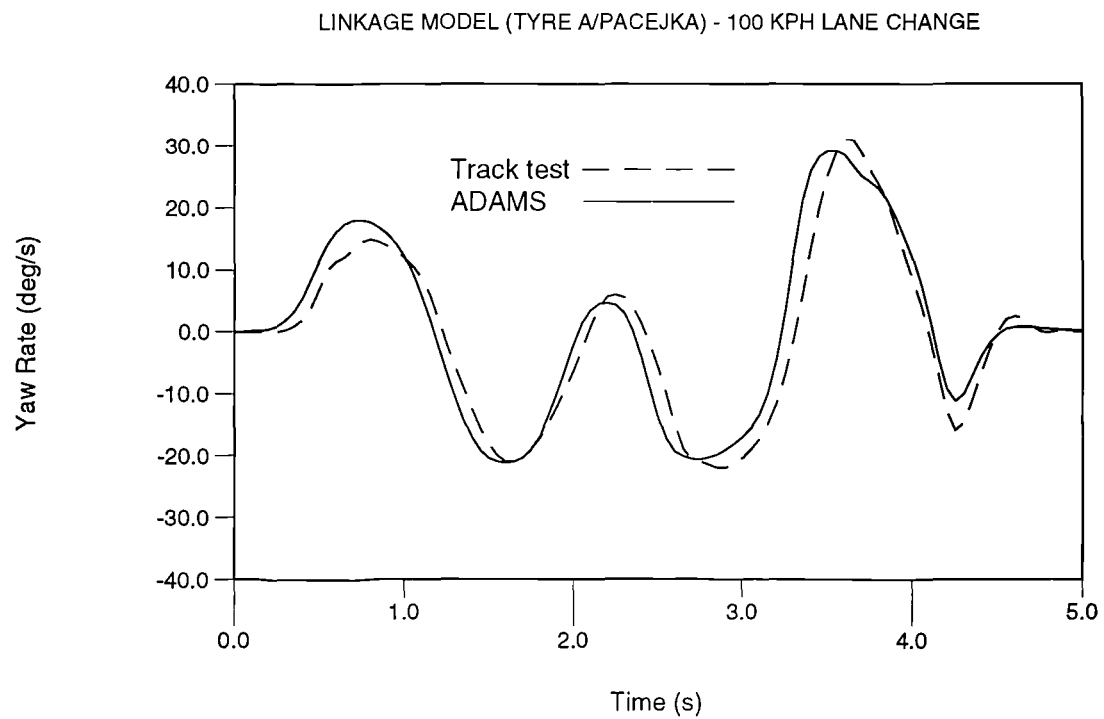
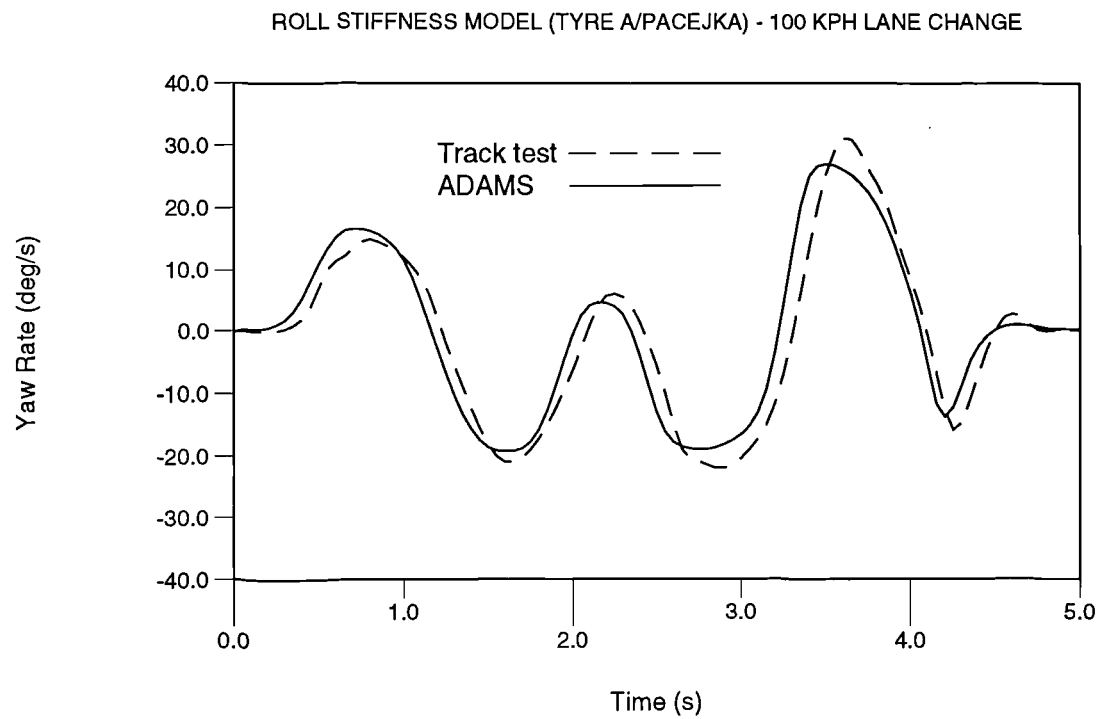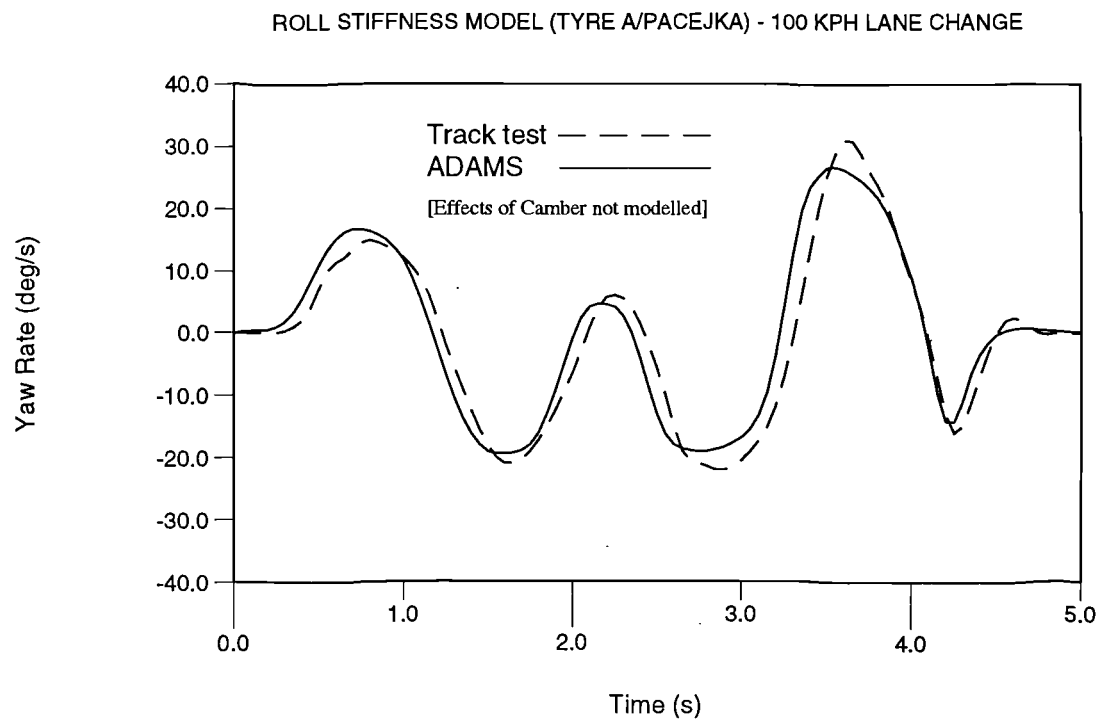Figure H.13 Yaw rate comparison - Pacejka model TYRE A and test

LINKAGE MODEL (TYRE A/PACEJKA) - 100 KPH LANE CHANGE
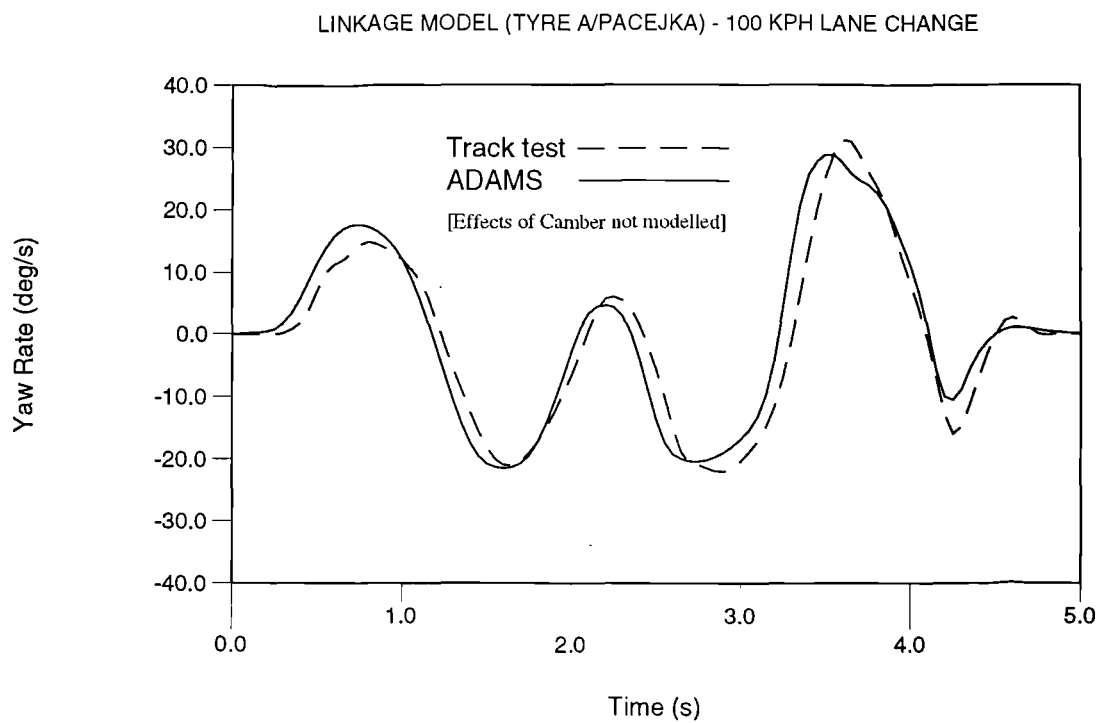
Figure H.14 Yaw rate comparison - Pacejka model TYRE A and test

LINKAGE MODEL (TYRE A/FIALA) - 100 KPH LANE CHANGE
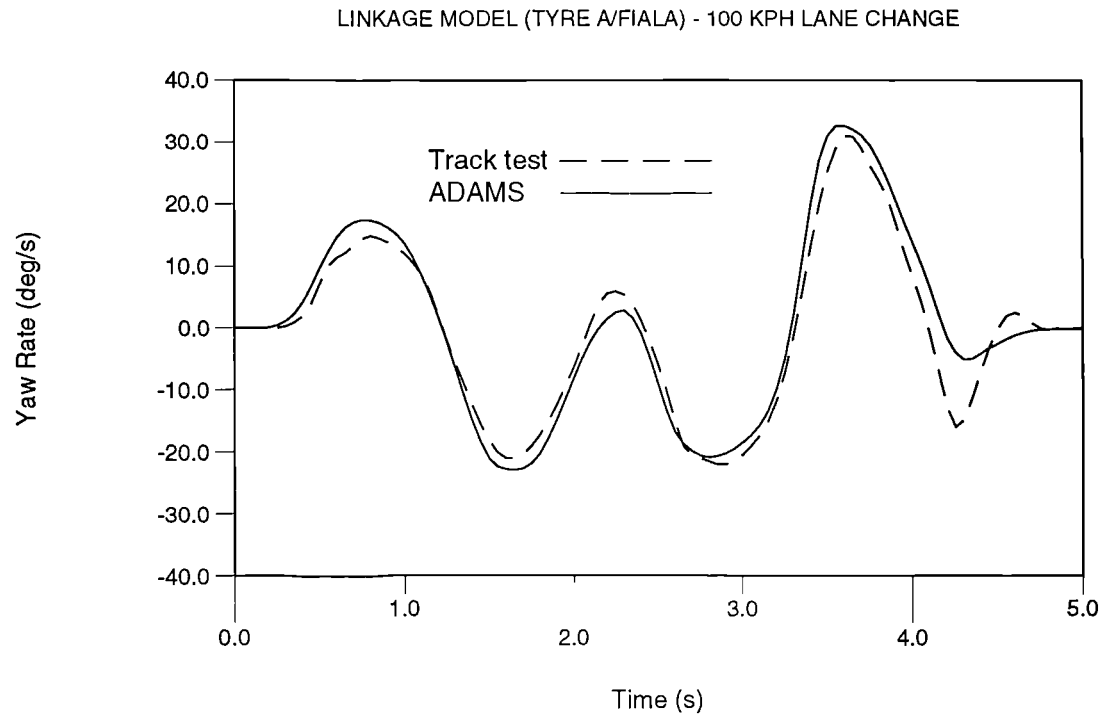
Figure H.15 Yaw rate comparison - Fiala model TYRE A and test

LINKAGE MODEL (TYRE B/INTERPOLATION) - 100 KPH LANE CHANGE
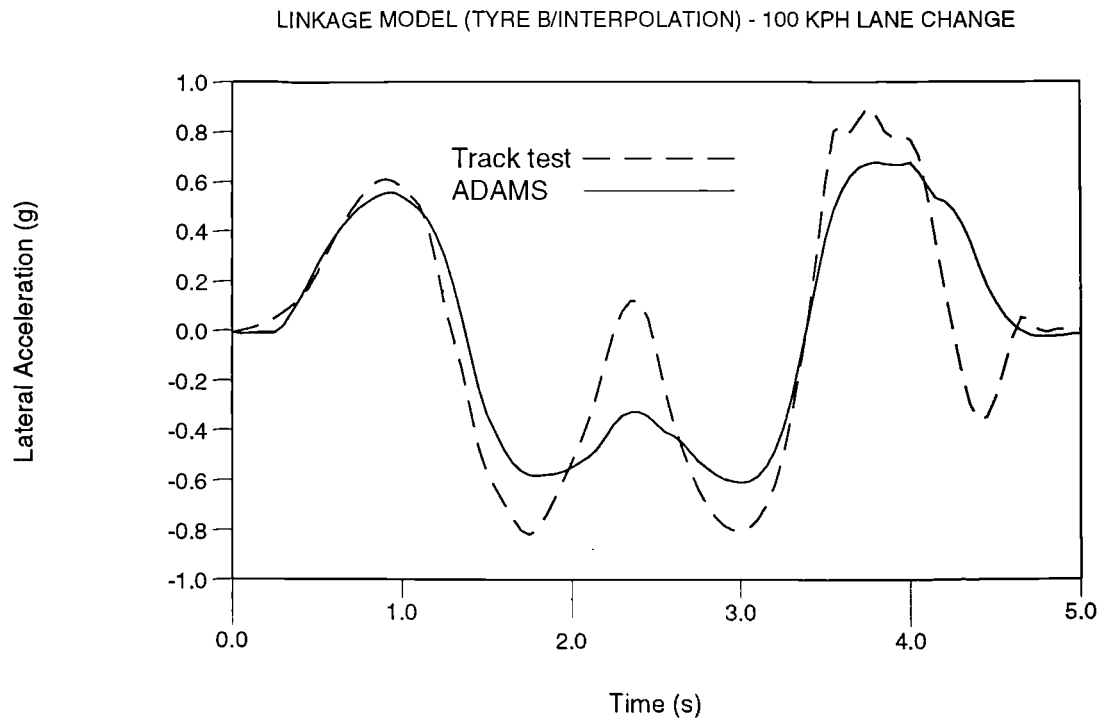
Figure H.16 Lateral acceleration comparison - Interpolation model TYRE B and test

LINKAGE MODEL (TYRE B/INTERPOLATION) - 100 KPH LANE CHANGE
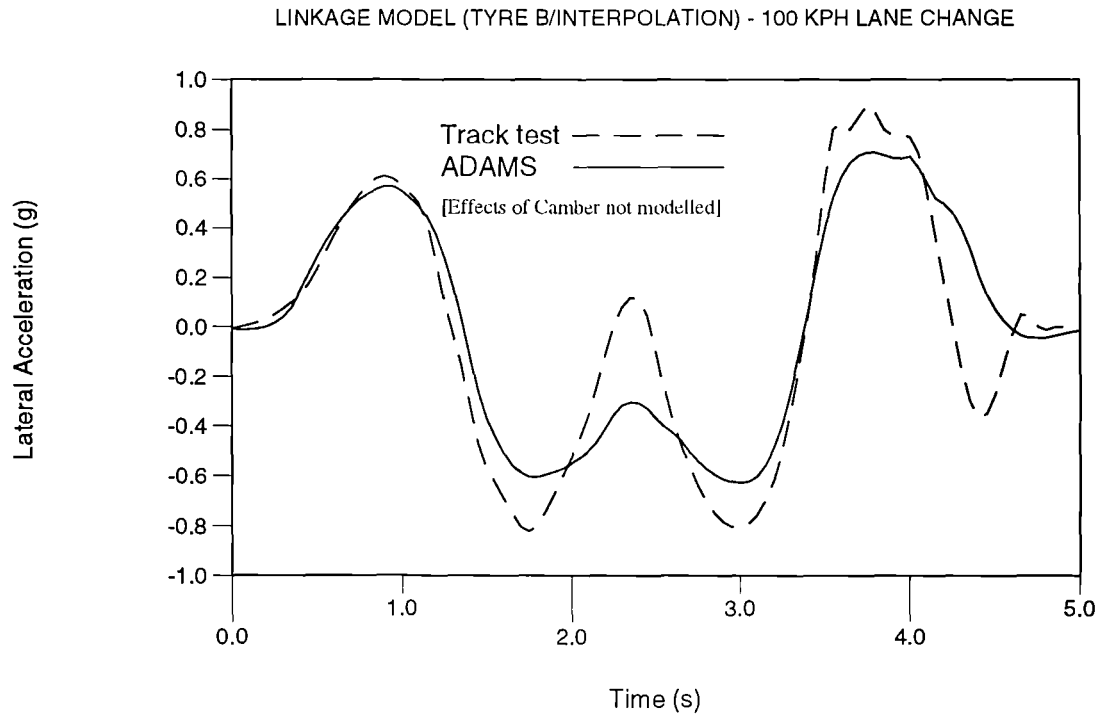
Figure H.17 Lateral acceleration comparison - Interpolation model TYRE B and test

LINKAGE MODEL (TYRE B/PACEJKA) - 100 KPH LANE CHANGE
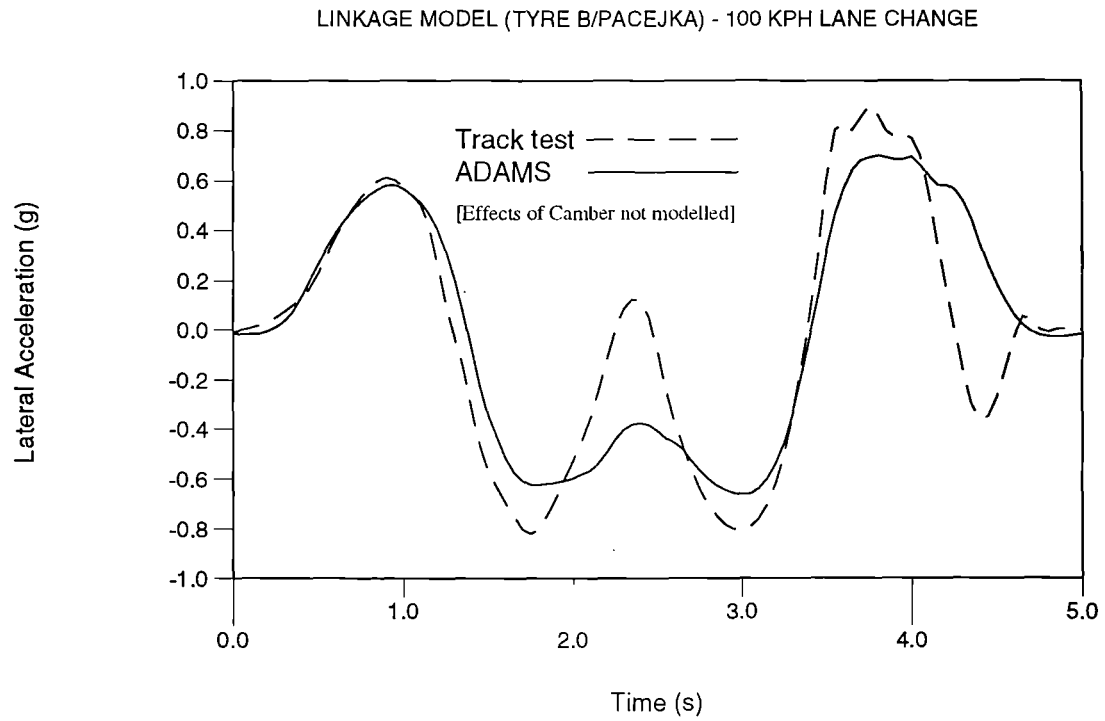
Figure H.18 Lateral acceleration comparison - Pacejka model TYRE B and test

LINKAGE MODEL (TYRE B/FIALA) - 100 KPH LANE CHANGE
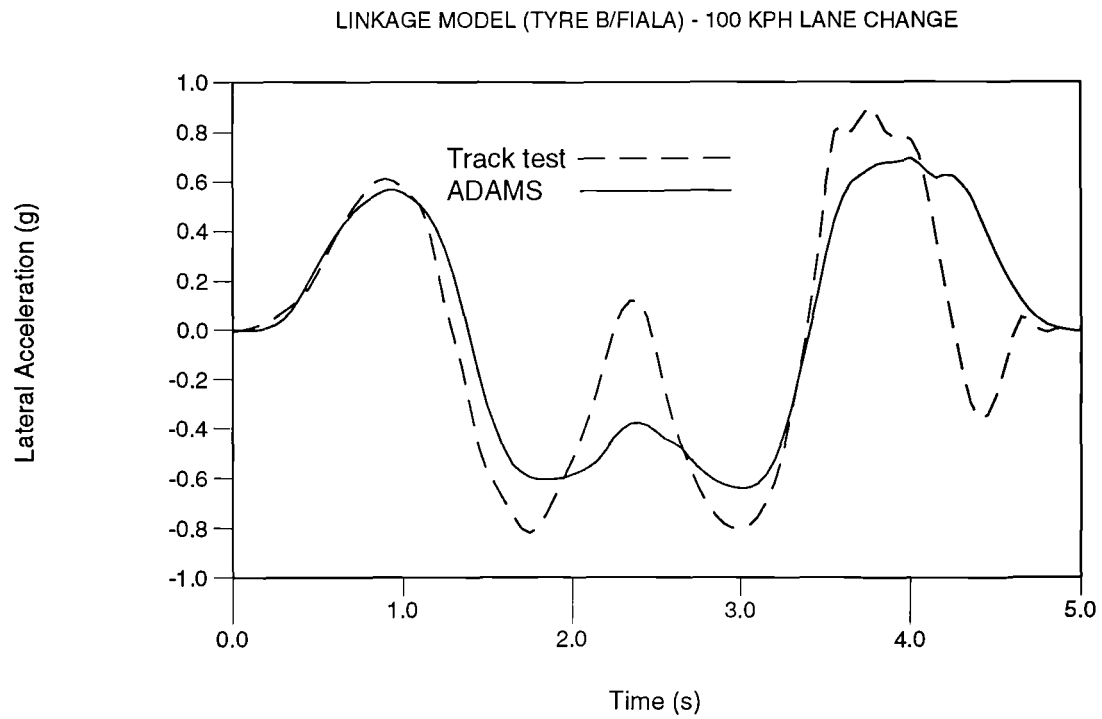
Figure H.19 Lateral acceleration comparison - Fiala model TYRE B and test

LINKAGE MODEL (TYRE B/INTERPOLATION) - 100 KPH LANE CHANGE
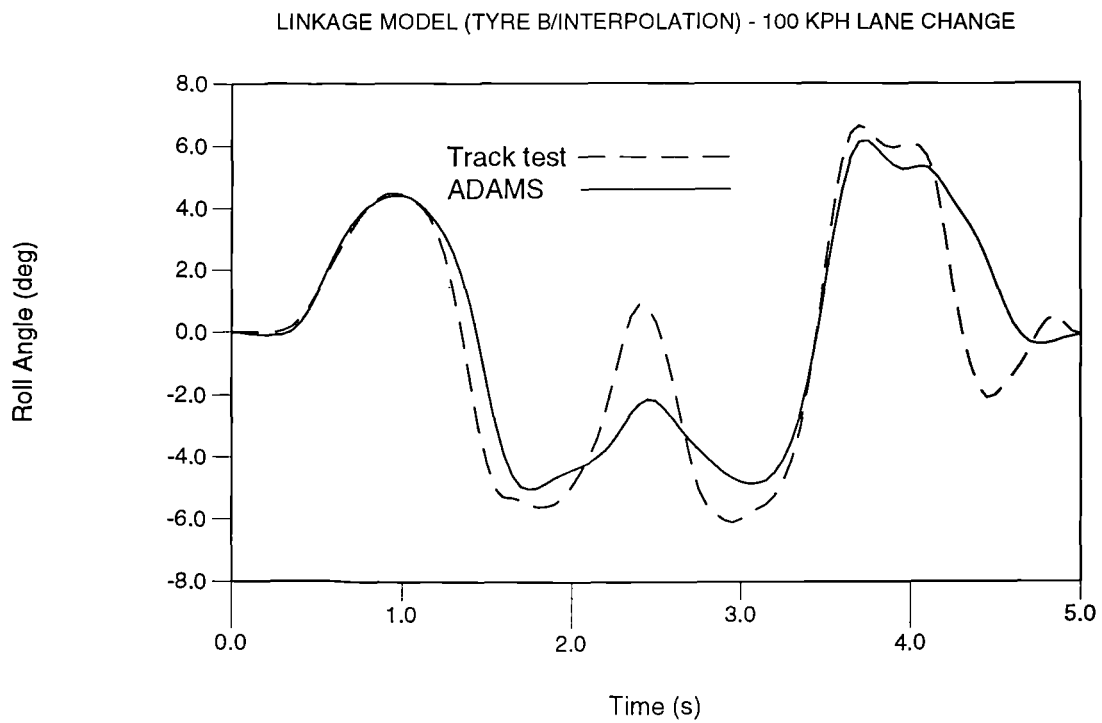
Figure H.20 Roll angle comparison - Interpolation model TYRE B and test

LINKAGE MODEL (TYRE B/INTERPOLATION) - 100 KPH LANE CHANGE
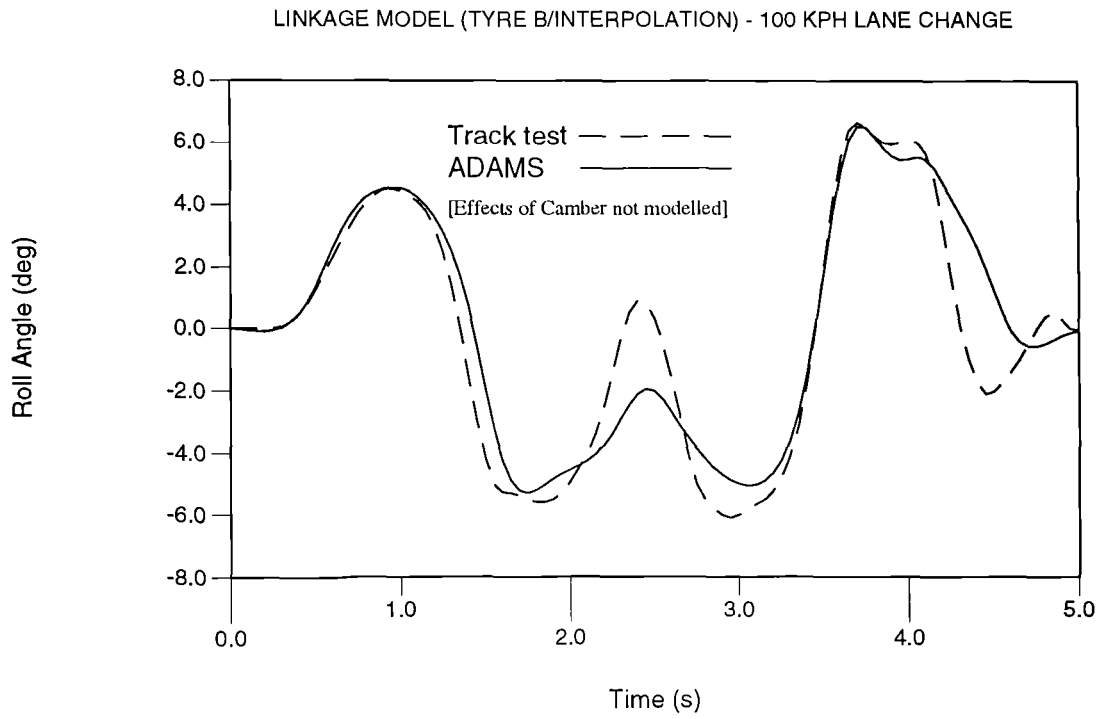
Figure H.21 Roll angle comparison - Interpolation model TYRE B and test

LINKAGE MODEL (TYRE B/PACEJKA) - 100 KPH LANE CHANGE
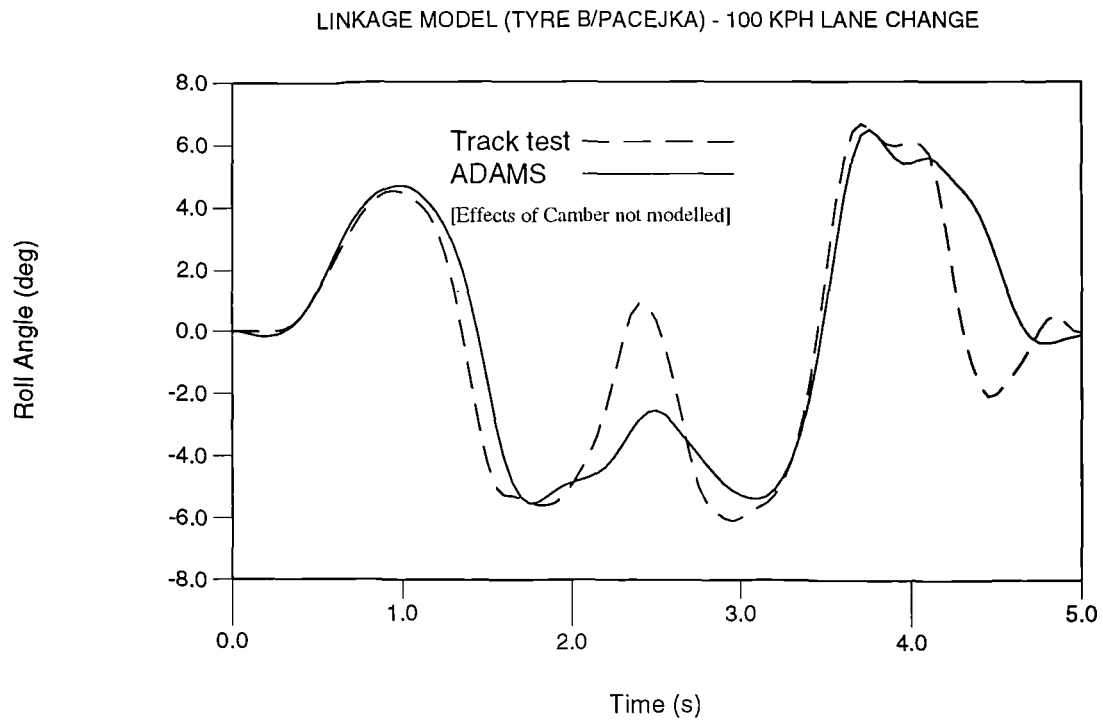
Figure H.22 Roll angle comparison - Pacejka model TYRE B and test

LINKAGE MODEL (TYRE B/FIALA) - 100 KPH LANE CHANGE
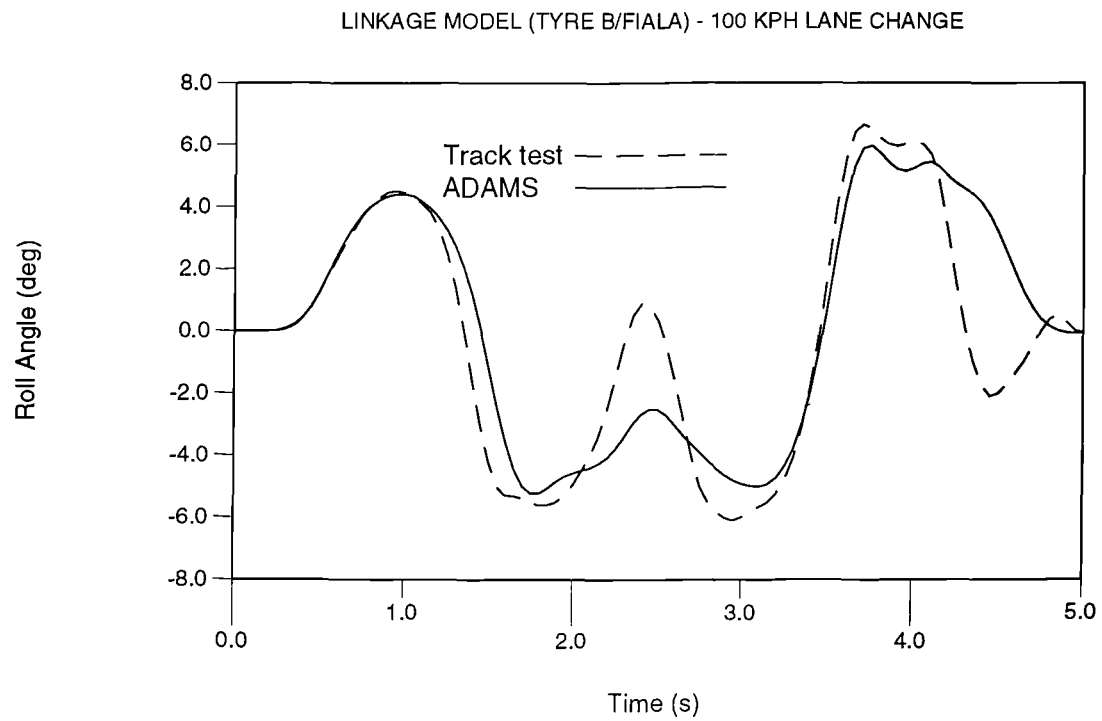
Figure H.23 Roll angle comparison - Fiala model TYRE B and test

LINKAGE MODEL (TYRE B/INTERPOLATION) - 100 KPH LANE CHANGE
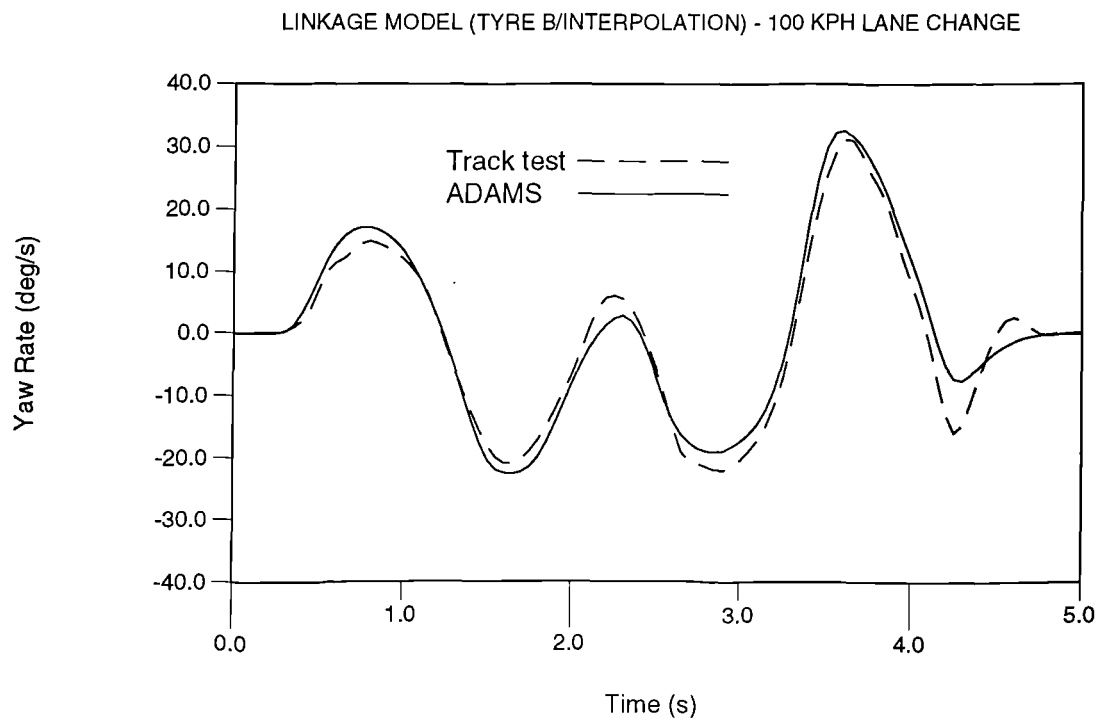
Figure H.24 Yaw rate comparison - Interpolation model TYRE B and test

LINKAGE MODEL (TYRE B/INTERPOLATION) - 100 KPH LANE CHANGE
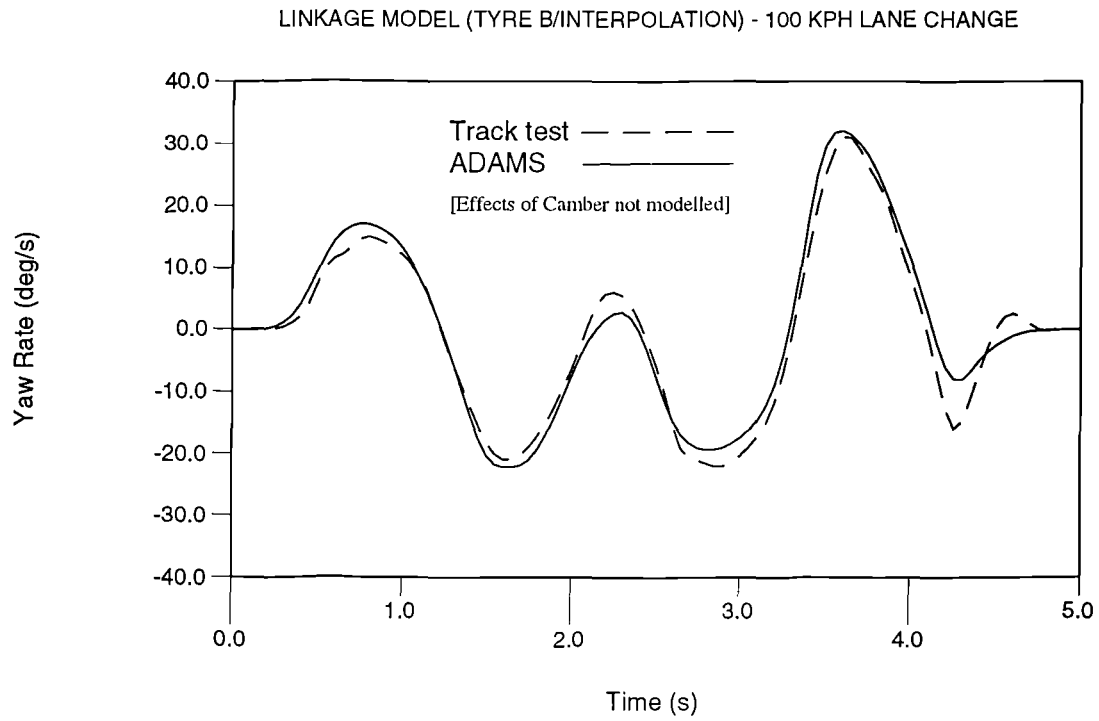
Figure H.25 Yaw rate comparison - Interpolation model TYRE B and test

LINKAGE MODEL (TYRE B/PACEJKA) - 100 KPH LANE CHANGE
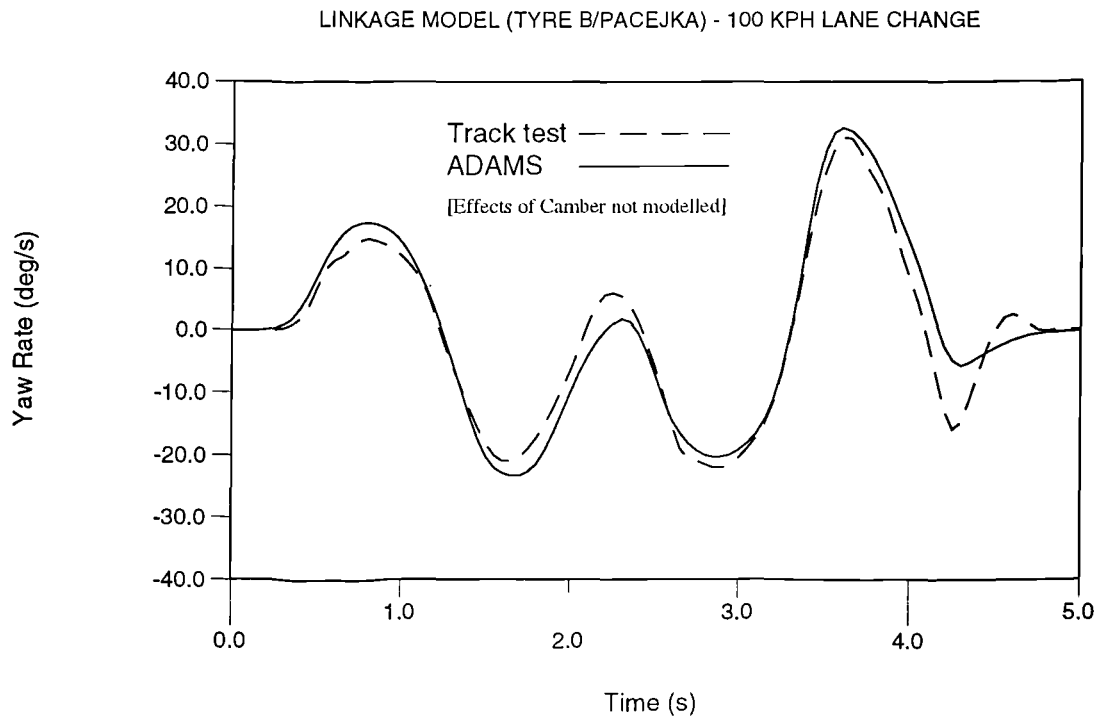
Figure H.26 Yaw rate comparison - Pacejka model TYRE B and test

LINKAGE MODEL (TYRE B/FIALA) - 100 KPH LANE CHANGE
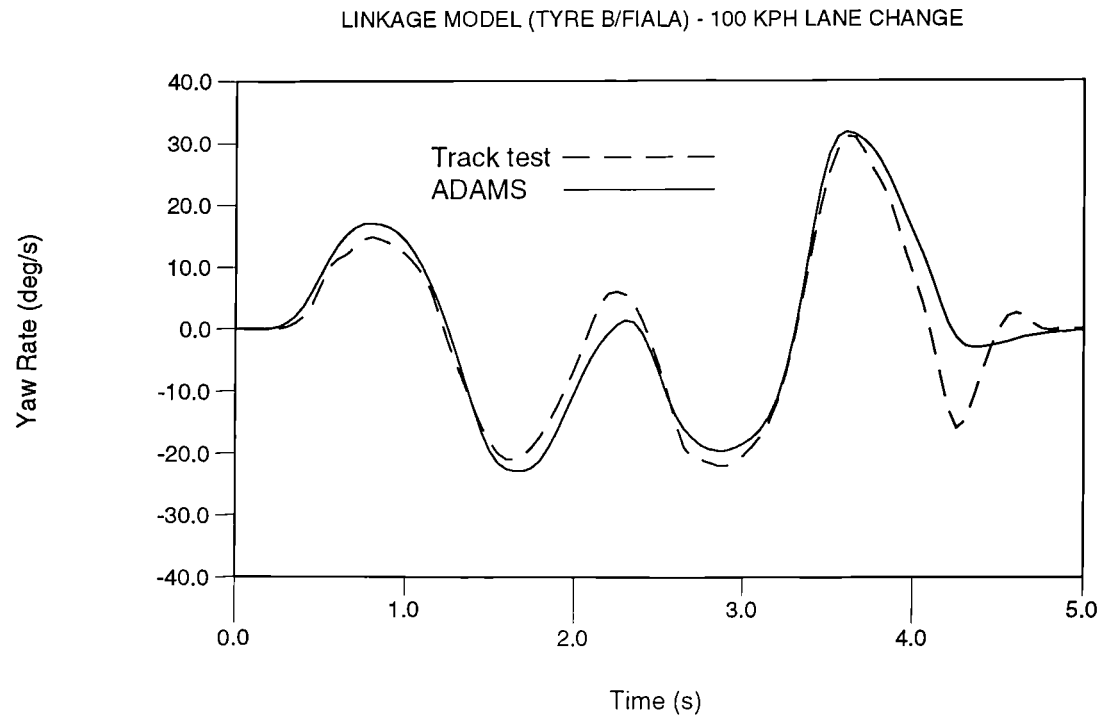
Figure H.27 Yaw rate comparison - Fiala model TYRE B and test

APPENDIX I

INVESTIGATION OF LANE CHANGE MANOEUVRE SENSITIVITY TO TYRE DATA AND MODELS (ROLL STIFFNESS MODEL)

ROLL STIFFNESS MODEL (TYRE A/INTERPOLATION) - 100 KPH LANE CHANGE
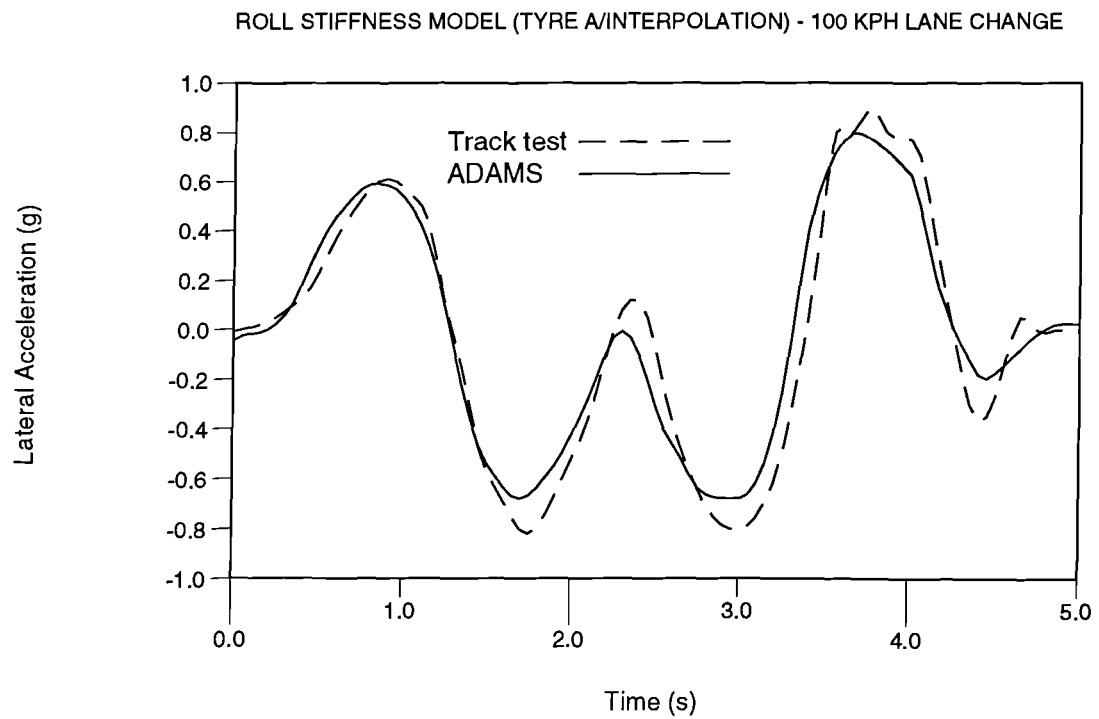
Figure I.1 Lateral acceleration comparison - Interpolation model TYRE A and test

ROLL STIFFNESS MODEL (TYRE A/INTERPOLATION) - 100 KPH LANE CHANGE
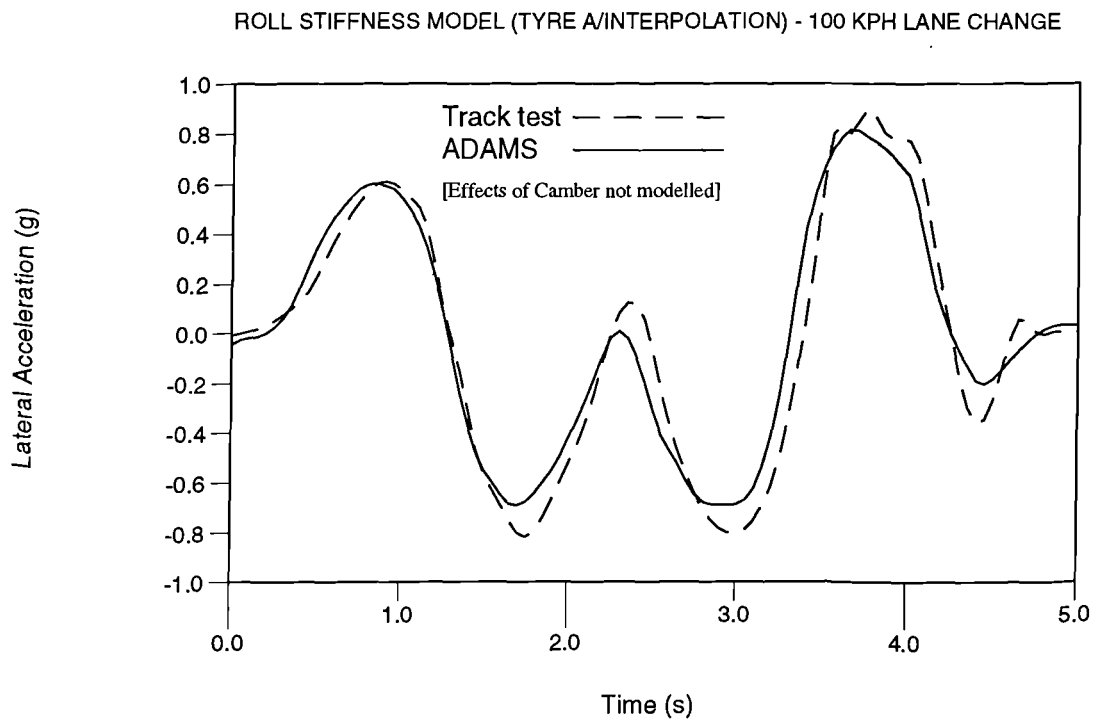
Figure I.2 Lateral acceleration comparison - Interpolation model TYRE A and test

ROLL STIFFNESS MODEL (TYRE A/PACEJKA) - 100 KPH LANE CHANGE
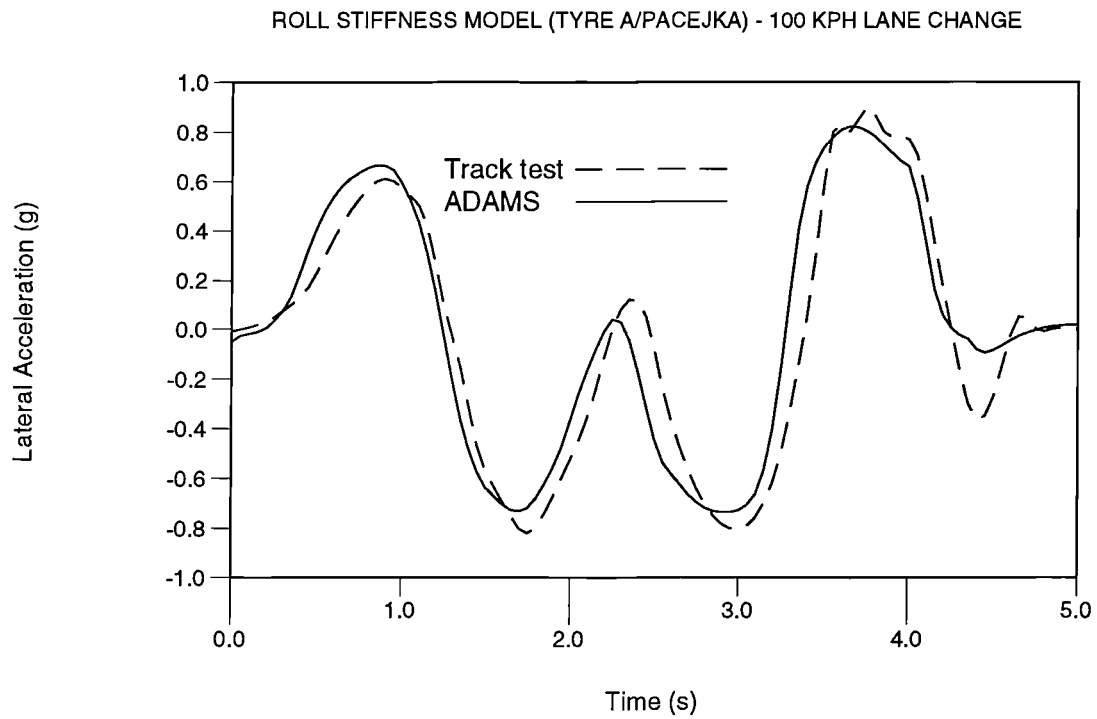
Figure I.3 Lateral acceleration comparison - Pacjeka model TYRE A and test

ROLL STIFFNESS MODEL (TYRE A/PACEJKA) - 100 KPH LANE CHANGE
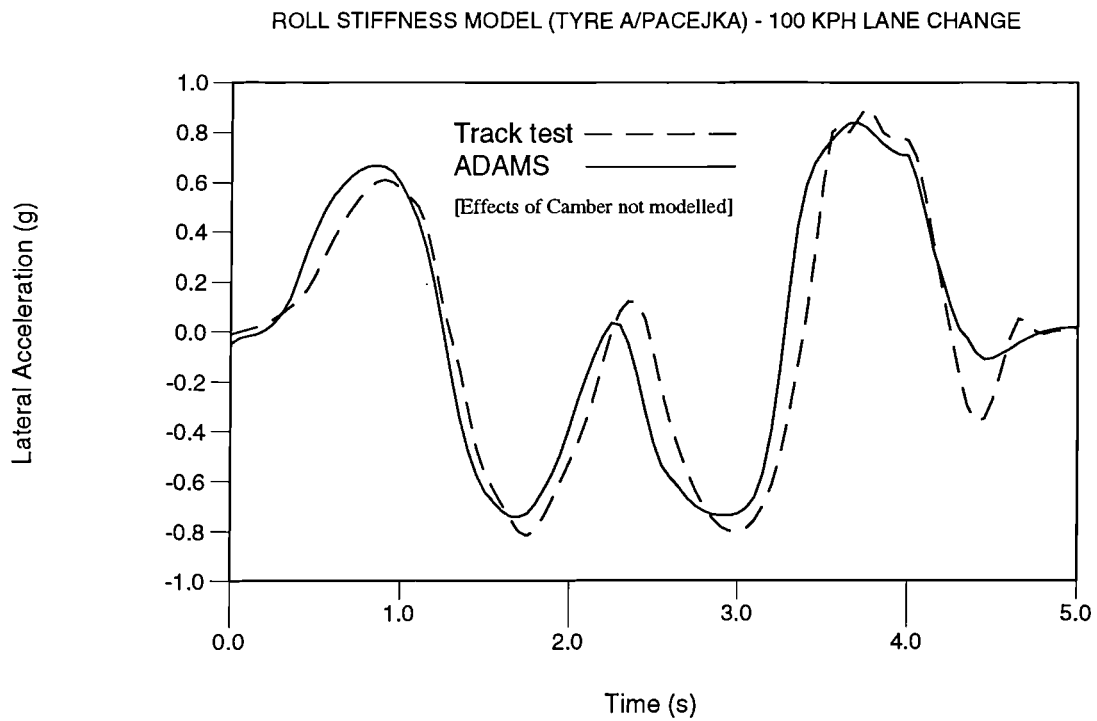
Figure I.4 Lateral acceleration comparison - Pacjeka model TYRE A and test

ROLL STIFFNESS MODEL (TYRE A/FIALA) - 100 KPH LANE CHANGE
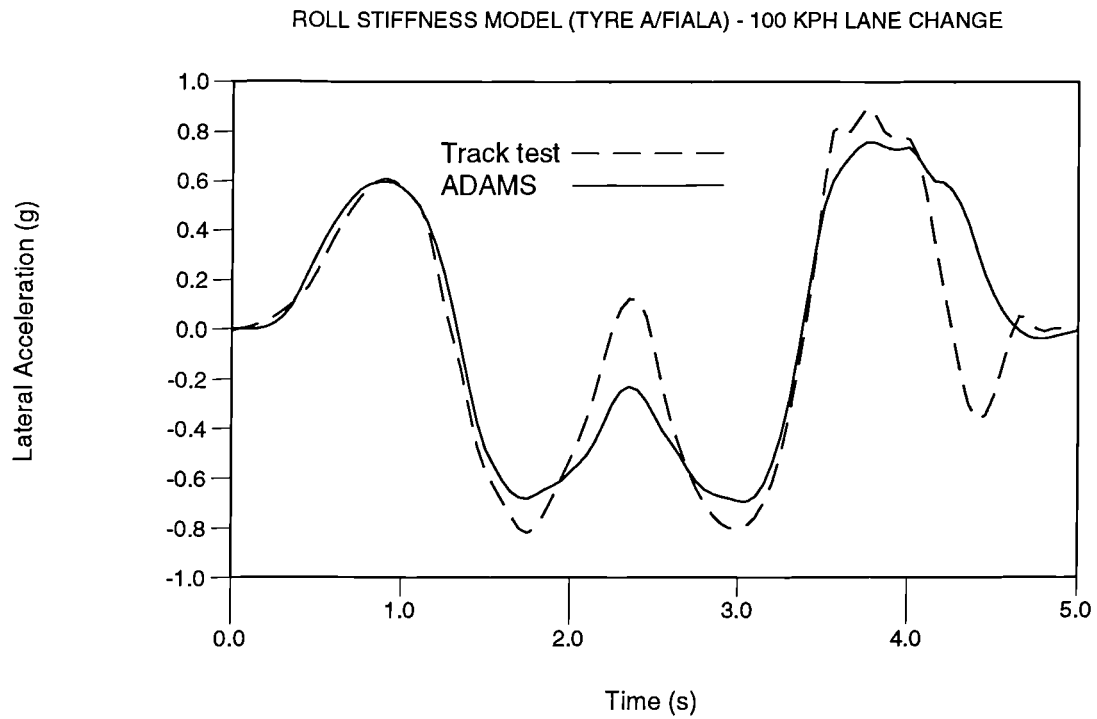
Figure I.5 Lateral acceleration comparison - Fiala model TYRE A and test

ROLL STIFFNESS MODEL (TYRE A/INTERPOLATION) - 100 KPH LANE CHANGE
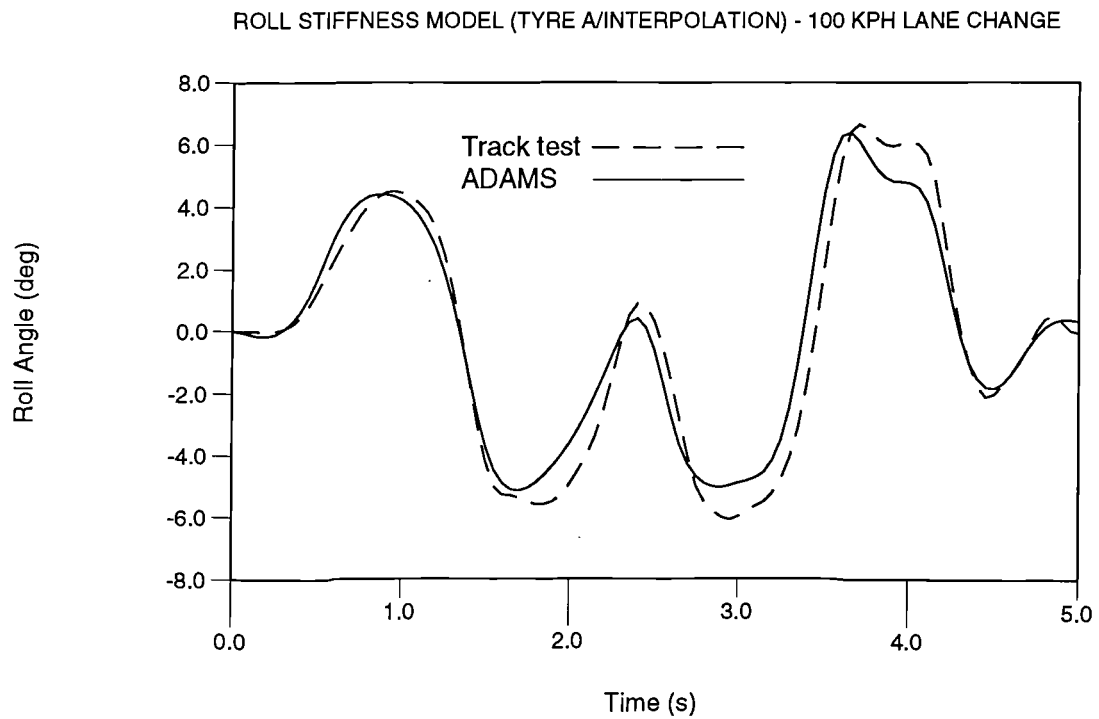
Figure I.6 Roll angle comparison - Interpolation model TYRE A and test

ROLL STIFFNESS MODEL (TYRE A/INTERPOLATION) - 100 KPH LANE CHANGE
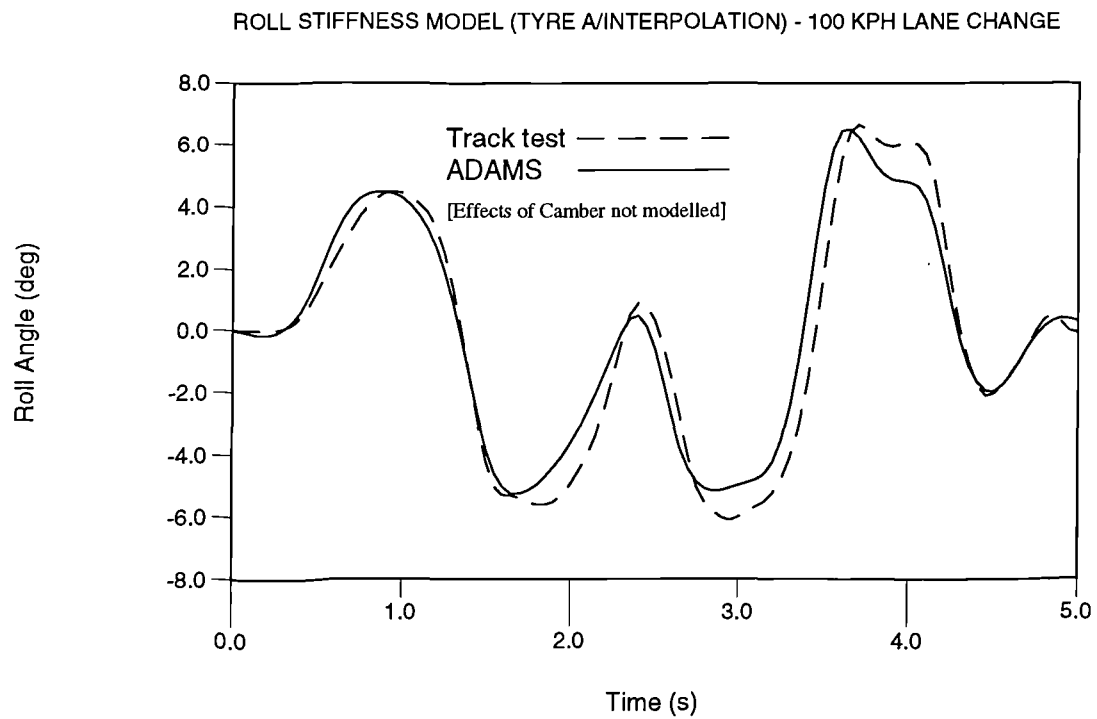
Figure I.7 Roll angle comparison - Interpolation model TYRE A and test

ROLL STIFFNESS MODEL (TYRE A/PACEJKA) - 100 KPH LANE CHANGE
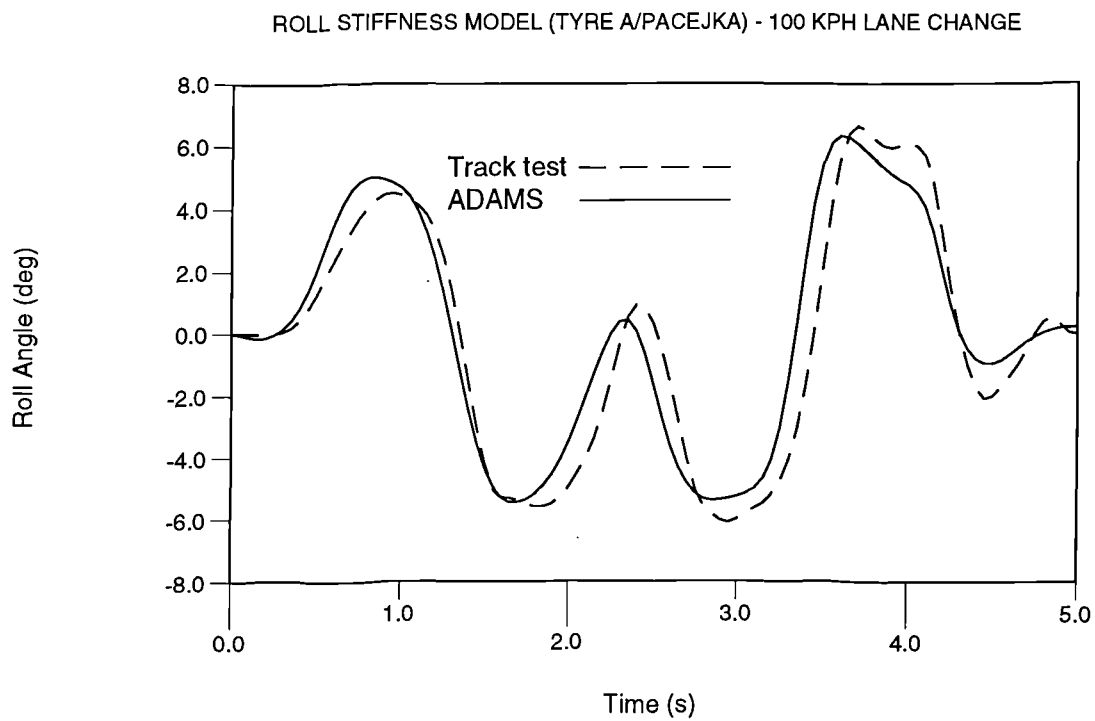
Figure I.8 Roll angle comparison - Pacejka model TYRE A and test

ROLL STIFFNESS MODEL (TYRE A/PACEJKA) - 100 KPH LANE CHANGE
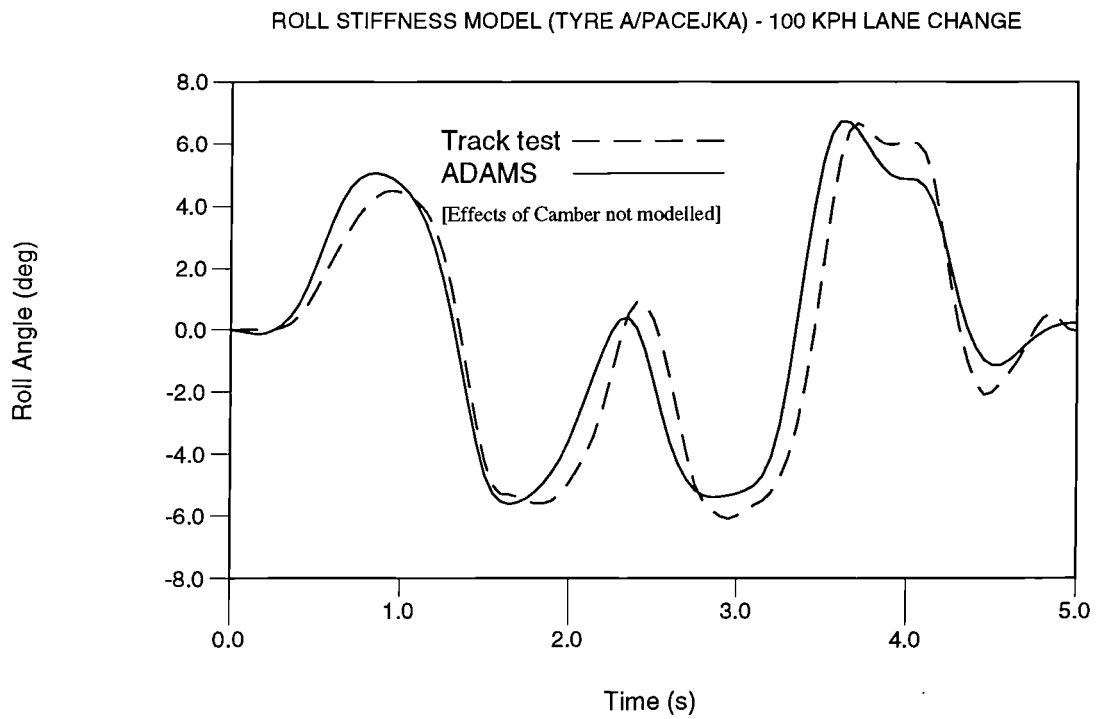
Figure I.9 Roll angle comparison - Pacejka model TYRE A and test

ROLL STIFFNESS MODEL (TYRE A/FIALA) - 100 KPH LANE CHANGE
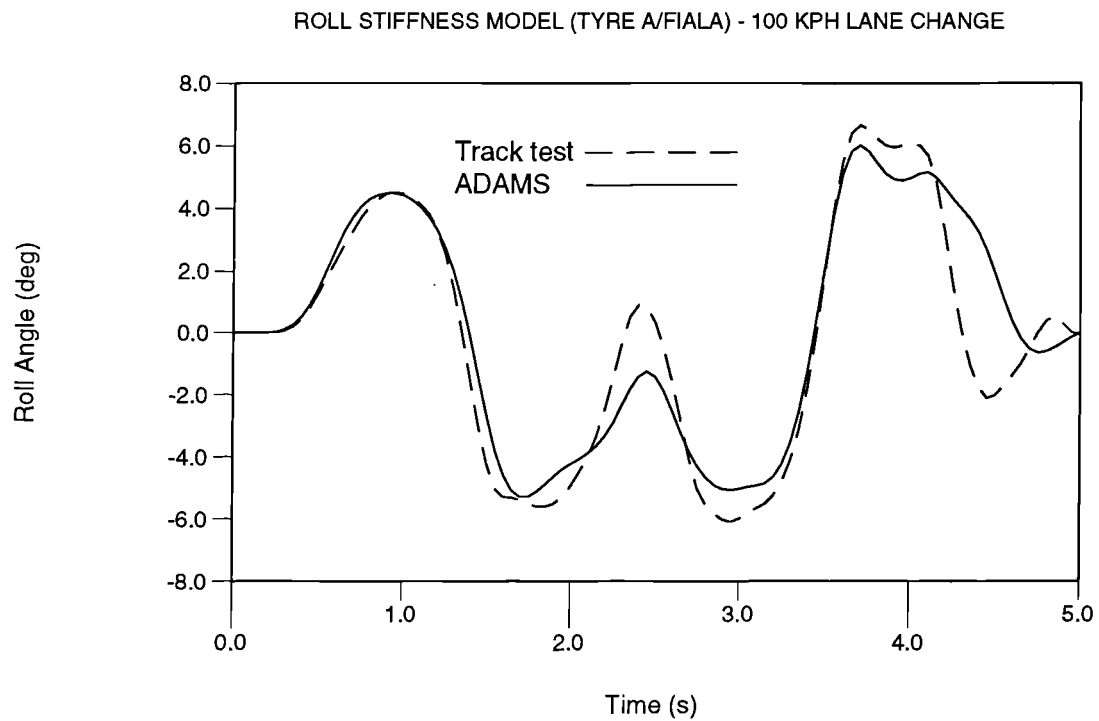
Figure I.10 Roll angle comparison - Fiala model TYRE A and test

ROLL STIFFNESS MODEL (TYRE A/INTERPOLATION) - 100 KPH LANE CHANGE
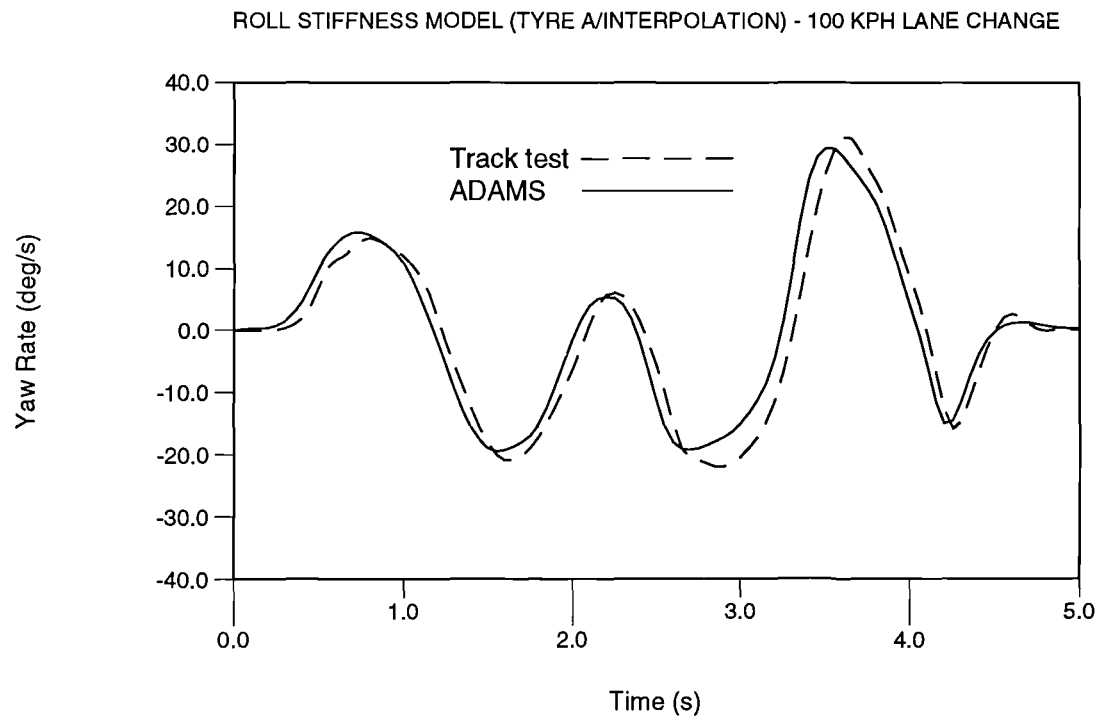
Figure I.11 Yaw rate comparison - Interpolation model TYRE A and test

ROLL STIFFNESS MODEL (TYRE A/INTERPOLATION) - 100 KPH LANE CHANGE

Figure I.12 Yaw rate comparison - Interpolation model TYRE A and test

Figure I.13 Yaw rate comparison - Pacejka model TYRE A and test

Figure I.14 Yaw rate comparison - Pacejka model TYRE A and test

ROLL STIFFNESS MODEL (TYRE A/FIALA) - 100 KPH LANE CHANGE
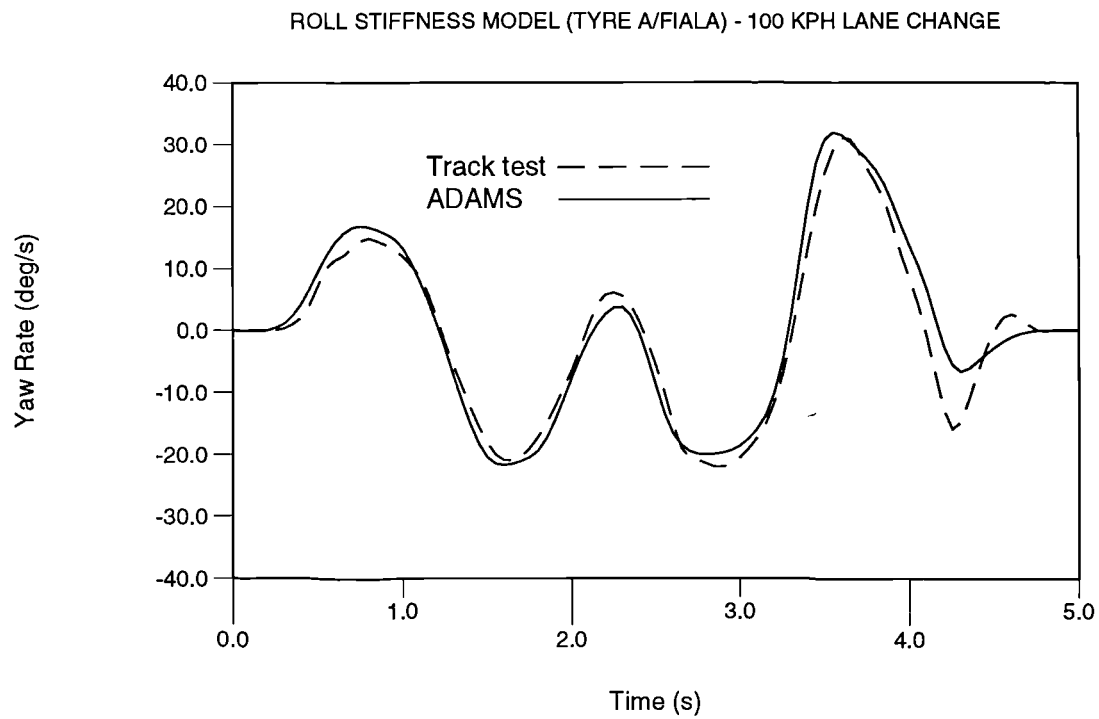
Figure I.15 Yaw rate comparison - Fiala model TYRE A and test

ROLL STIFFNESS MODEL (TYRE B/INTERPOLATION) - 100 KPH LANE CHANGE
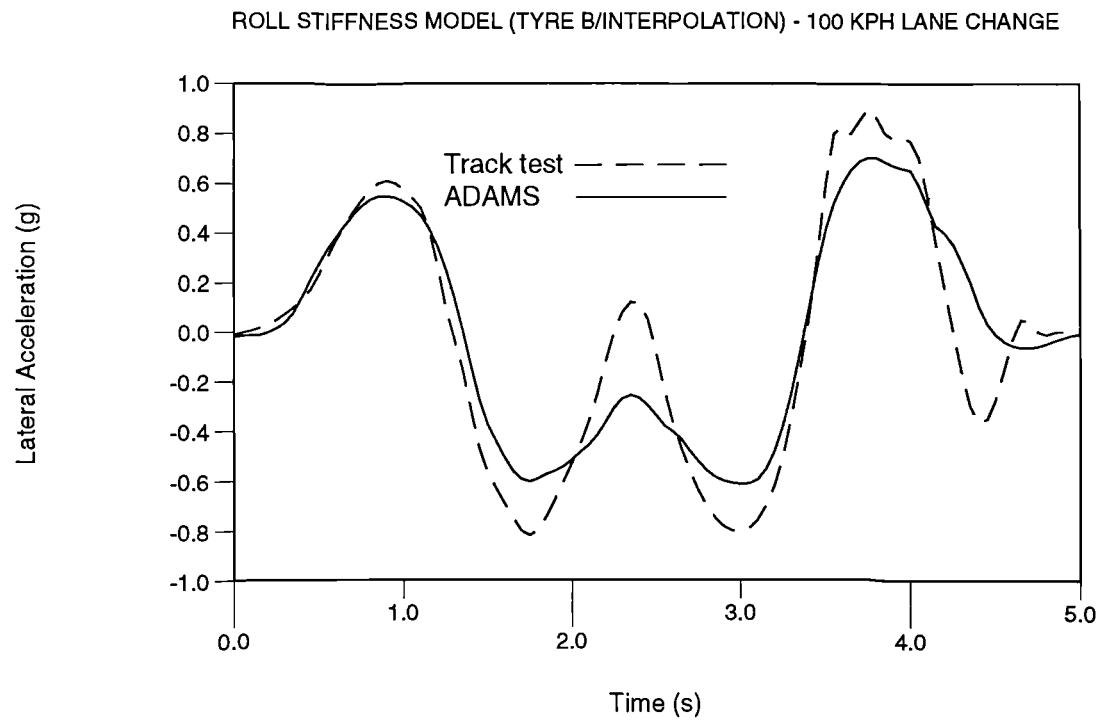
Figure I.16 Lateral acceleration comparison - Interpolation model TYRE B and test

ROLL STIFFNESS MODEL (TYRE B/INTERPOLATION) - 100 KPH LANE CHANGE
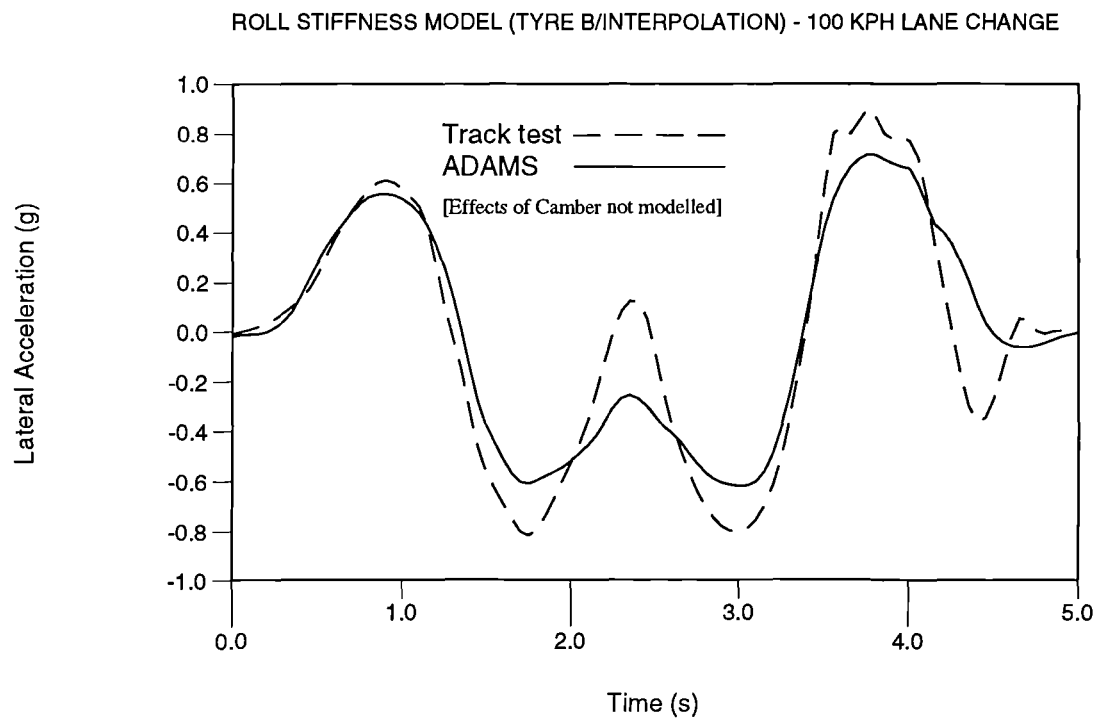
Figure I.17 Lateral acceleration comparison - Interpolation model TYRE B and test

ROLL STIFFNESS MODEL (TYRE B/PACEJKA) - 100 KPH LANE CHANGE
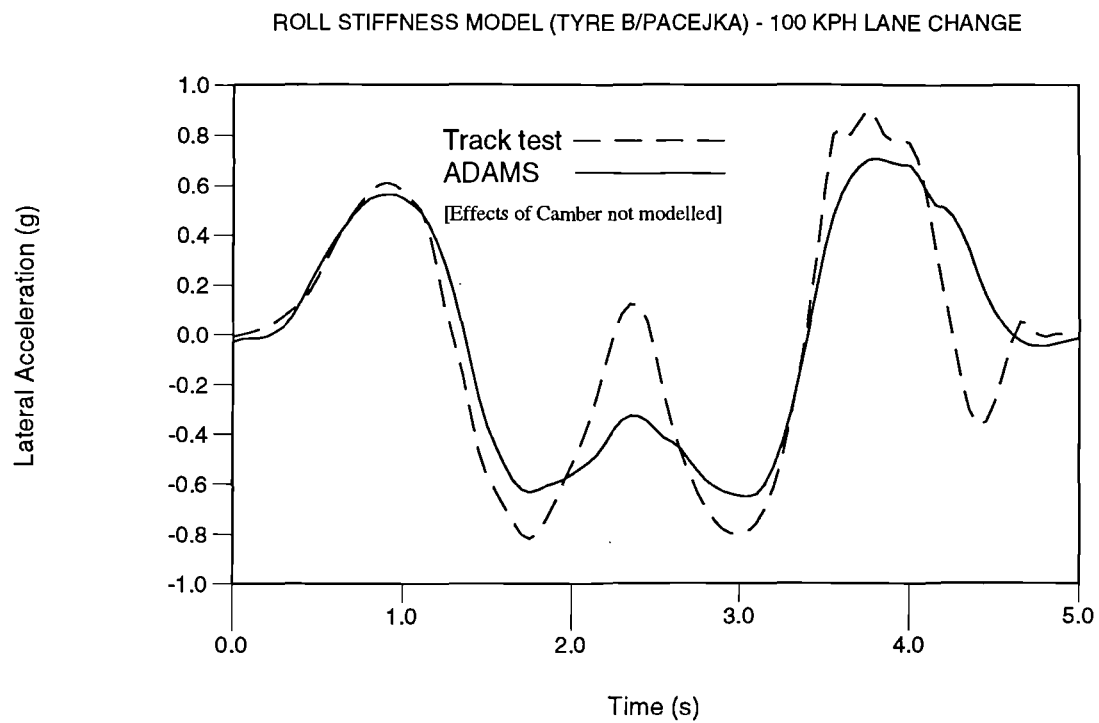
Figure I.18 Lateral acceleration comparison - Pacejka model TYRE B and test

ROLL STIFFNESS MODEL (TYRE B/FIALA) - 100 KPH LANE CHANGE
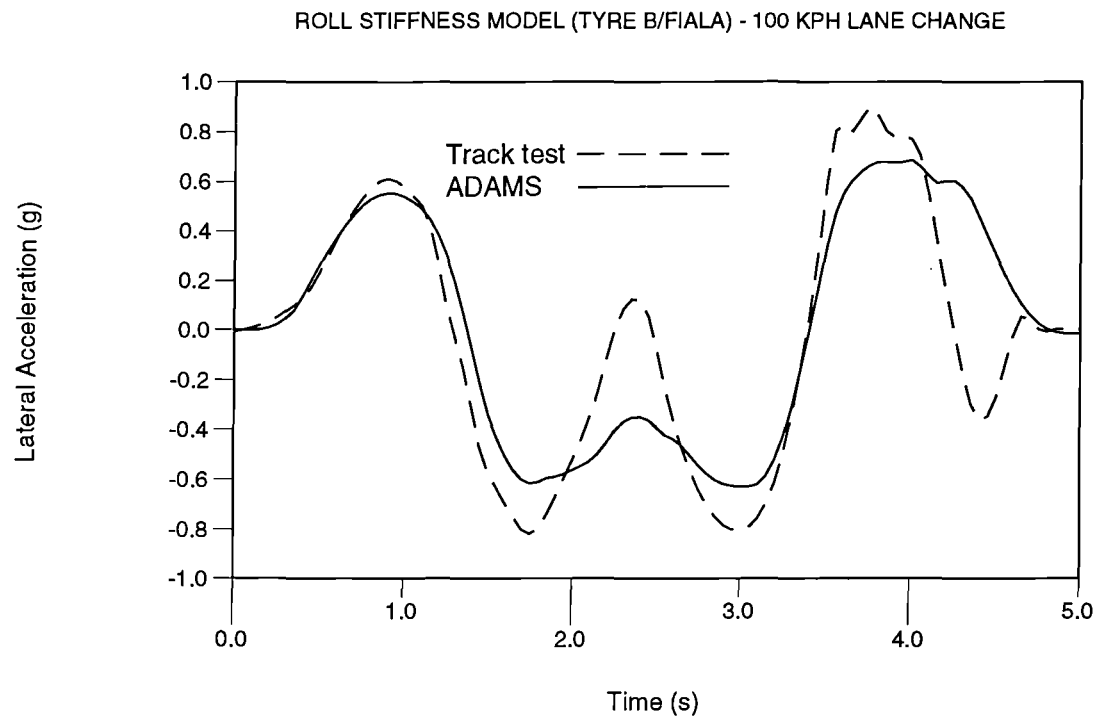
Figure I.19 Lateral acceleration comparison - Fiala model TYRE B and test

LINKAGE MODEL (TYRE B/INTERPOLATION) - 100 KPH LANE CHANGE
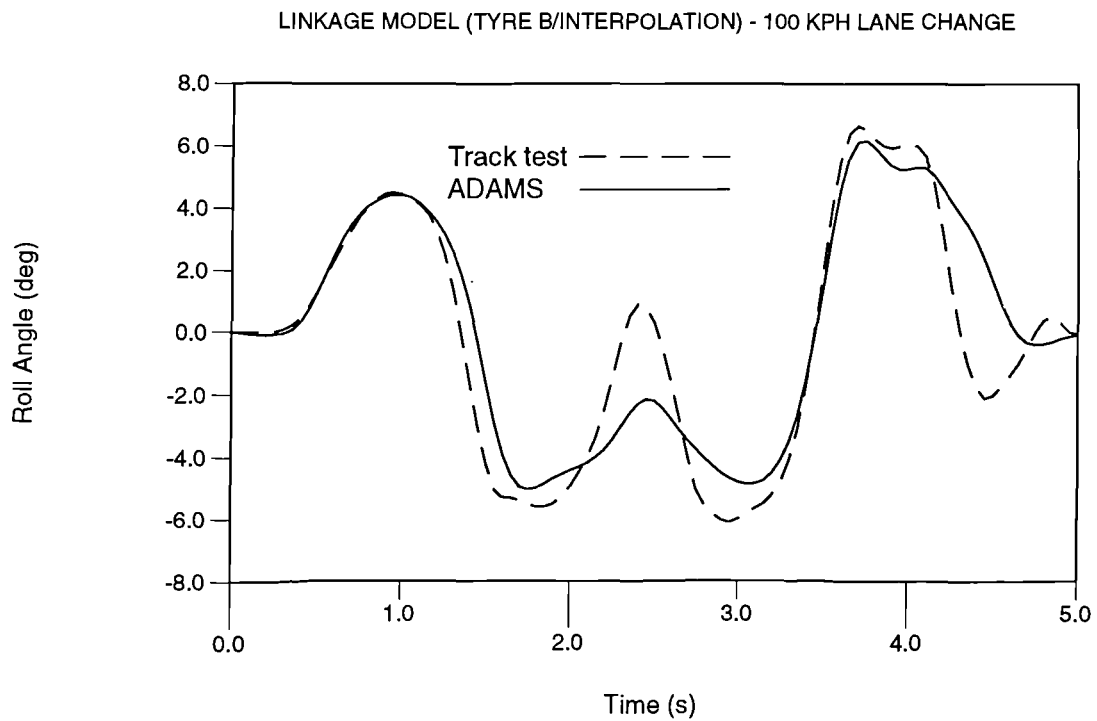
Figure I.20 Roll angle comparison - Interpolation model TYRE B and test

ROLL STIFFNESS MODEL (TYRE B/INTERPOLATION) - 100 KPH LANE CHANGE
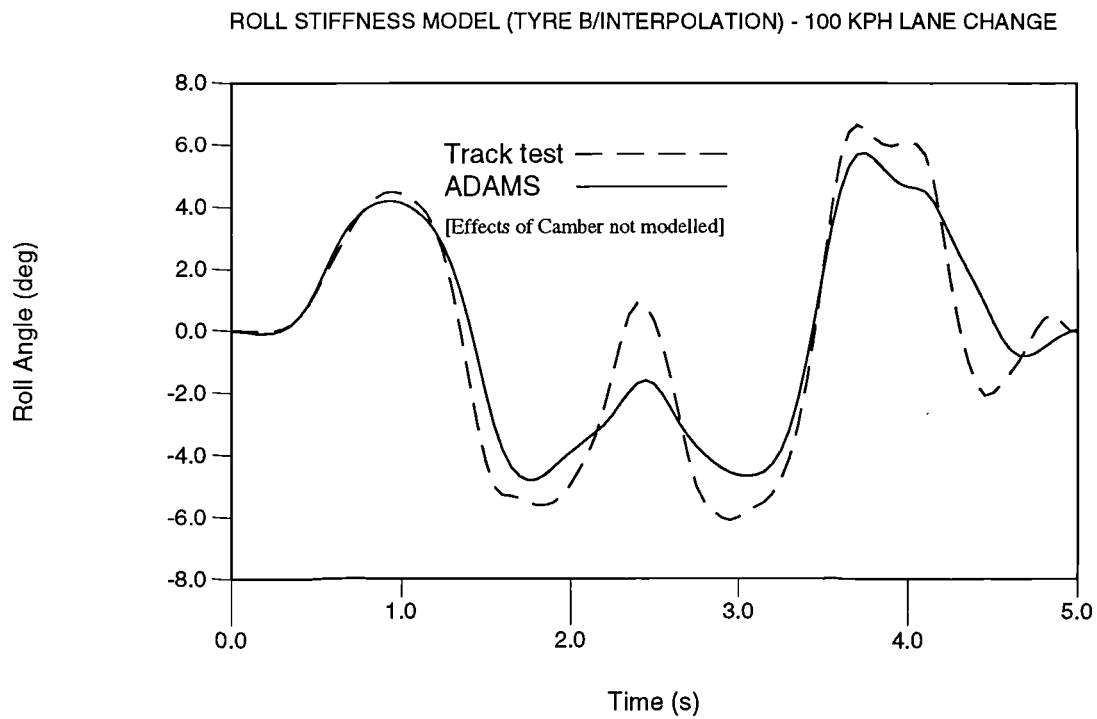
Figure I.21 Roll angle comparison - Interpolation model TYRE B and test

ROLL STIFFNESS MODEL (TYRE B/PACEJKA) - 100 KPH LANE CHANGE
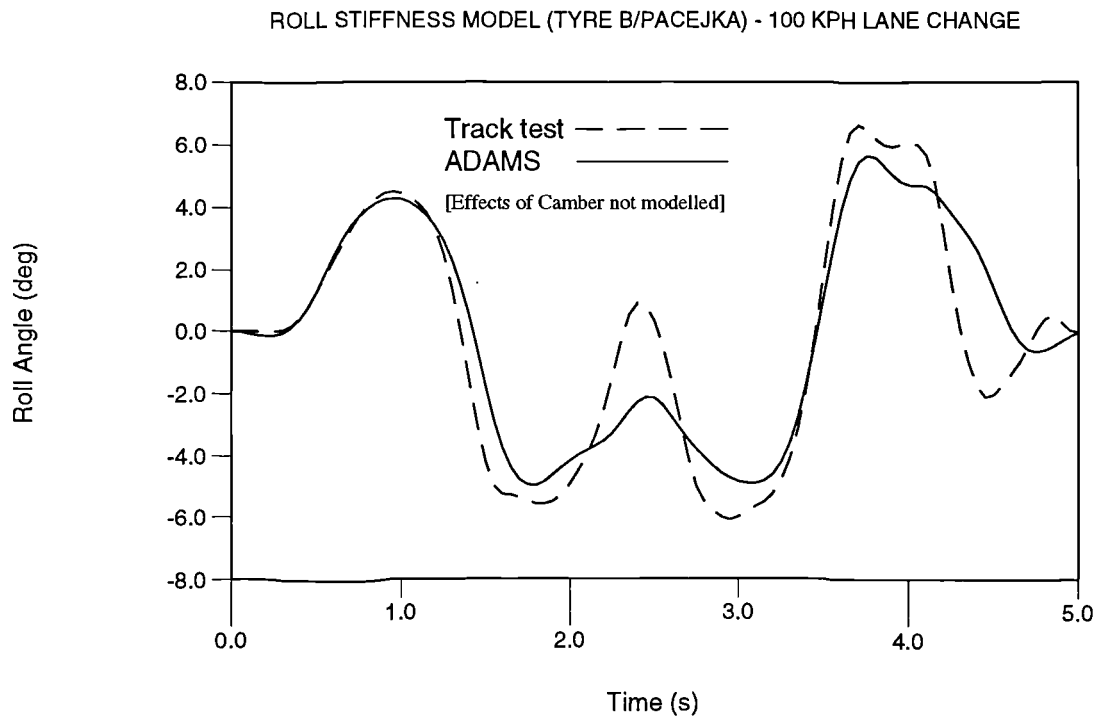
Figure I.22 Roll angle comparison - Pacejka model TYRE B and test

ROLL STIFFNESS MODEL (TYRE B/FIALA) - 100 KPH LANE CHANGE
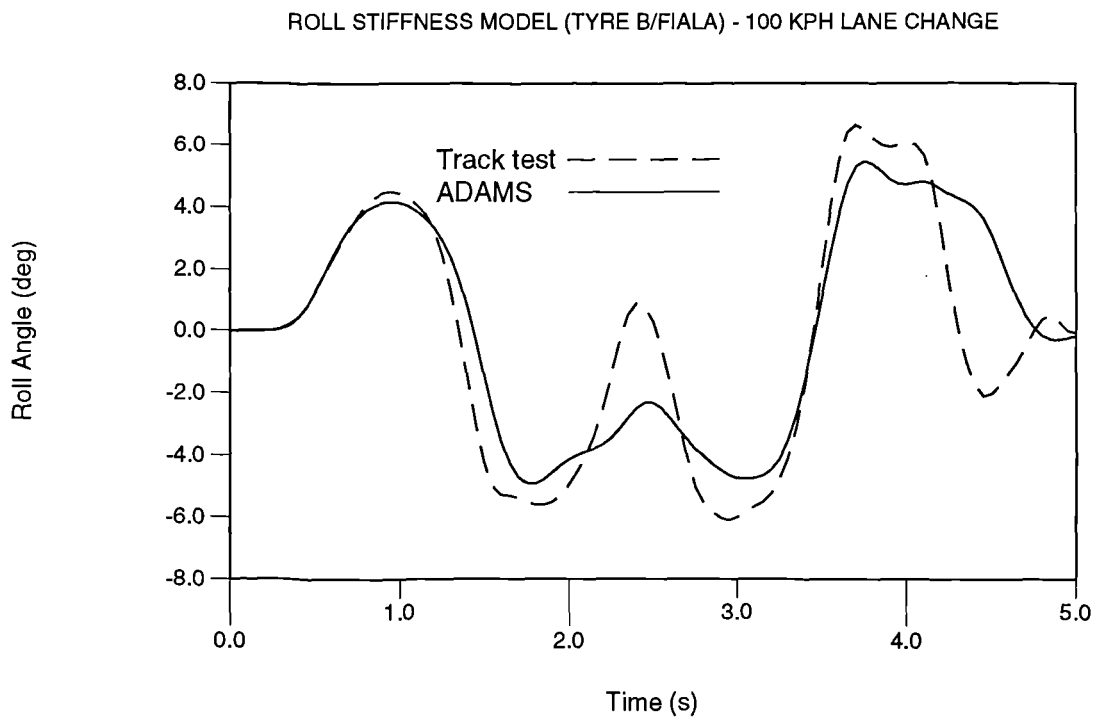
Figure I.23 Roll angle comparison - Fiala model TYRE B and test

ROLL STIFFNESS MODEL (TYRE B/INTERPOLATION) - 100 KPH LANE CHANGE
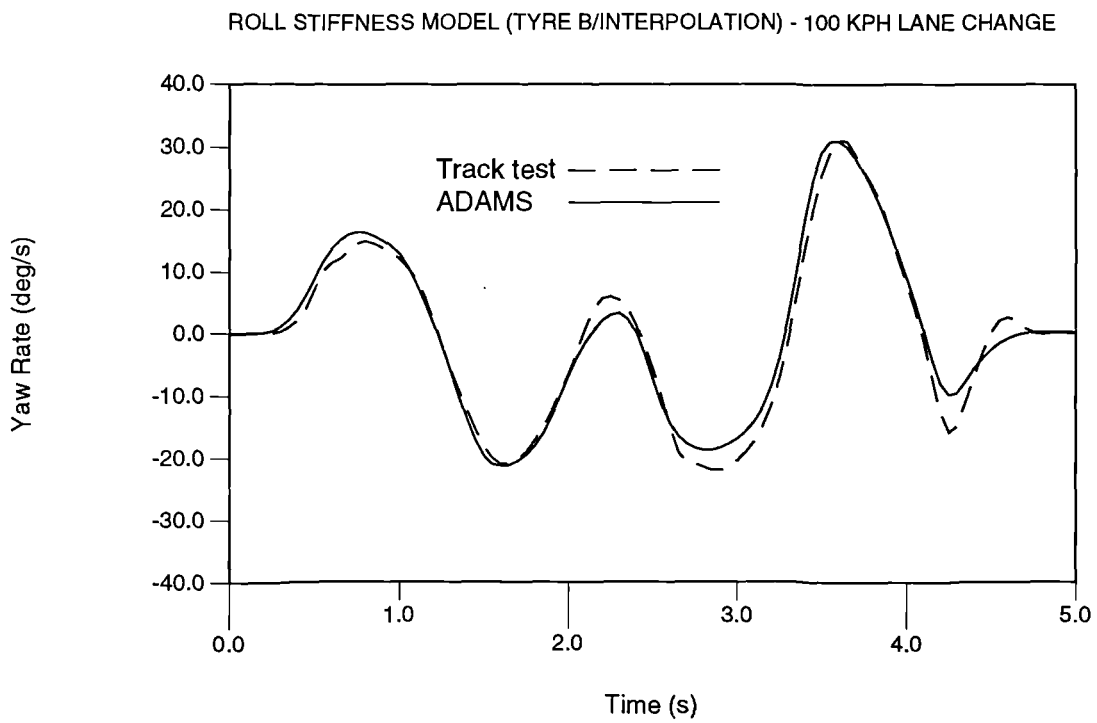
Figure I.24 Yaw rate comparison - Interpolation model TYRE B and test

ROLL STIFFNESS MODEL (TYRE B/INTERPOLATION) - 100 KPH LANE CHANGE
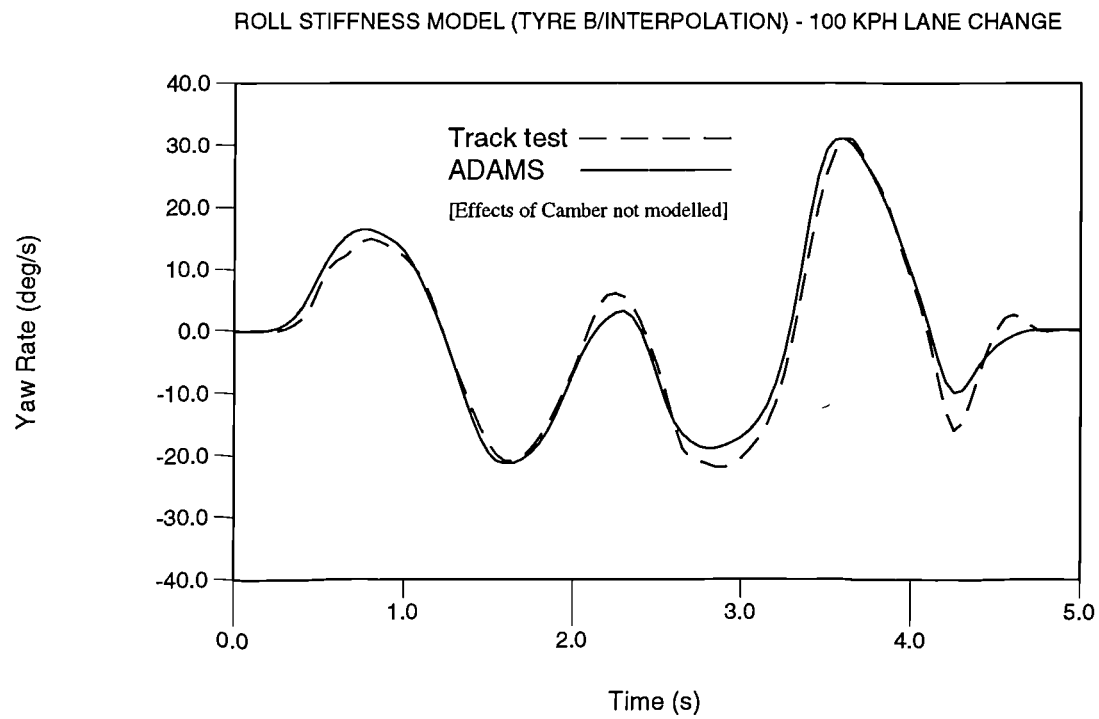
Figure I.25 Yaw rate comparison - Interpolation model TYRE B and test

ROLL STIFFNESS MODEL (TYRE B/PACEJKA) - 100 KPH LANE CHANGE
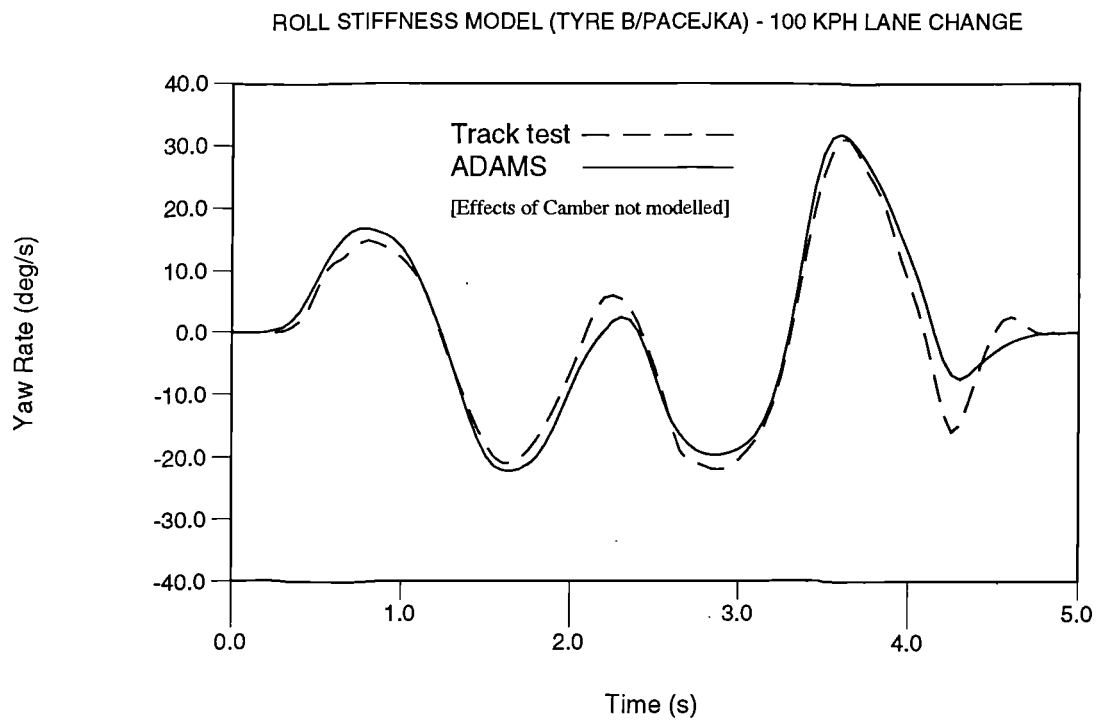
Figure I.26 Yaw rate comparison - Pacejka model TYRE B and test

ROLL STIFFNESS MODEL (TYRE B/FIALA) - 100 KPH LANE CHANGE
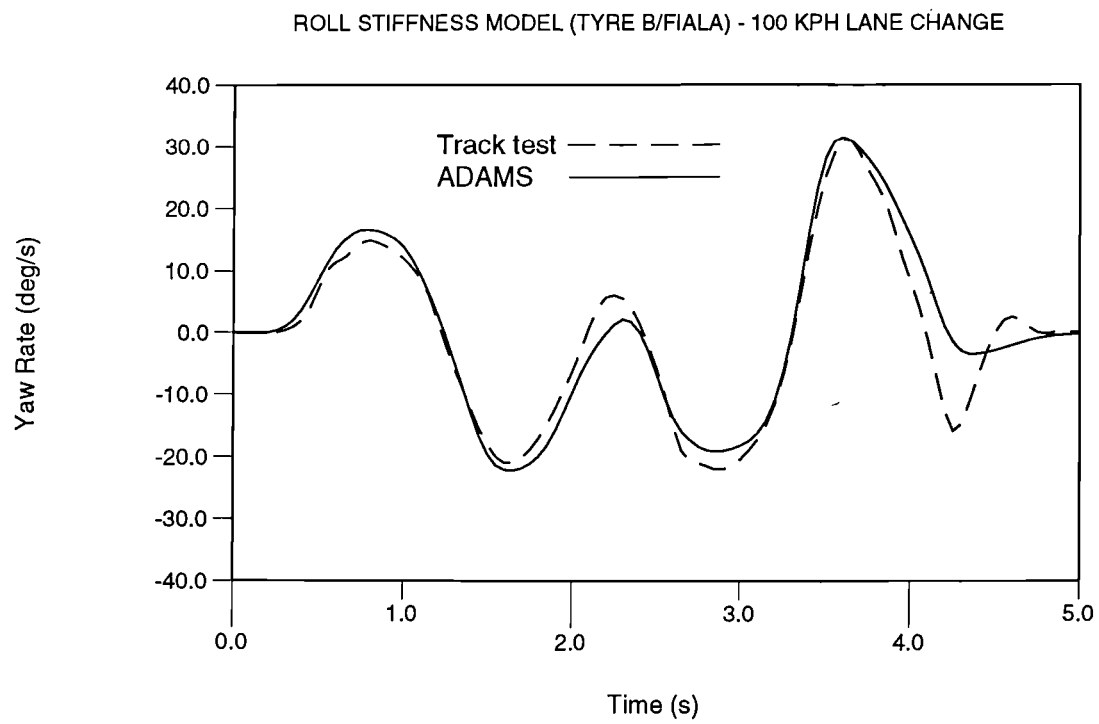
Figure I.27 Yaw rate comparison - Fiala model TYRE B and test

APPENDIX J

SUMMARY OF RESULTS FOR TYRE MODEL VARIATION USING TYRE A AND TYRE B

LINKAGE MODEL (TYRE A) - 100 KPH LANE CHANGE
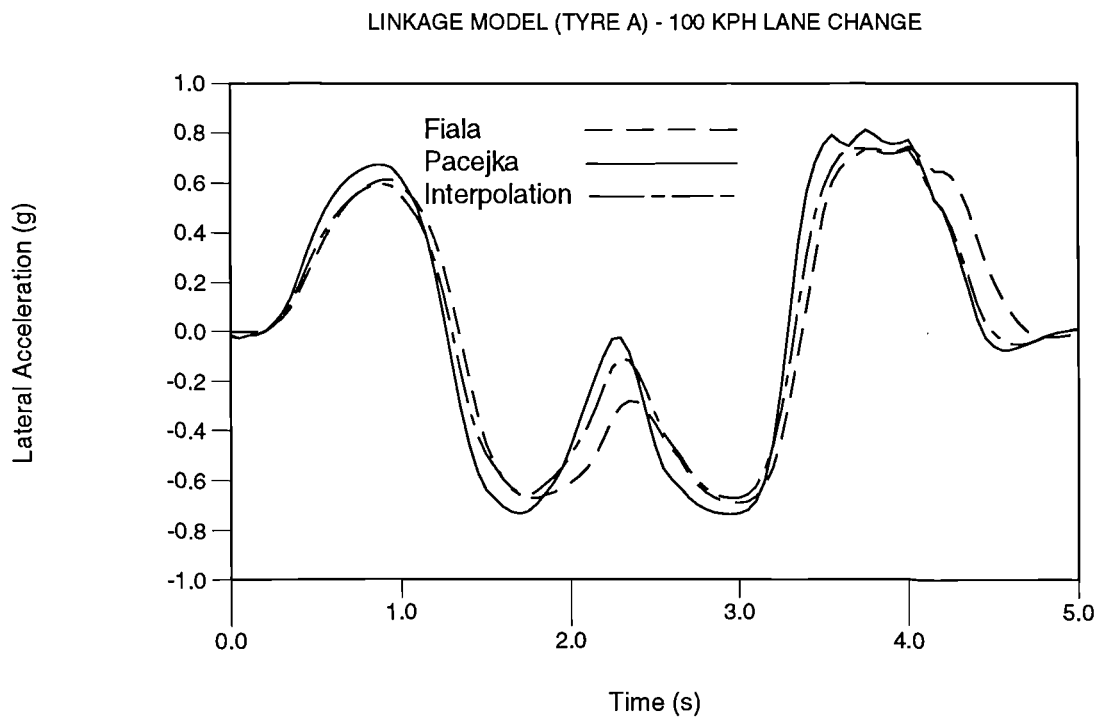
Figure J.1 Lateral acceleration comparison using linkage model and TYRE A

ROLL STIFFNESS MODEL (TYRE A) - 100 KPH LANE CHANGE
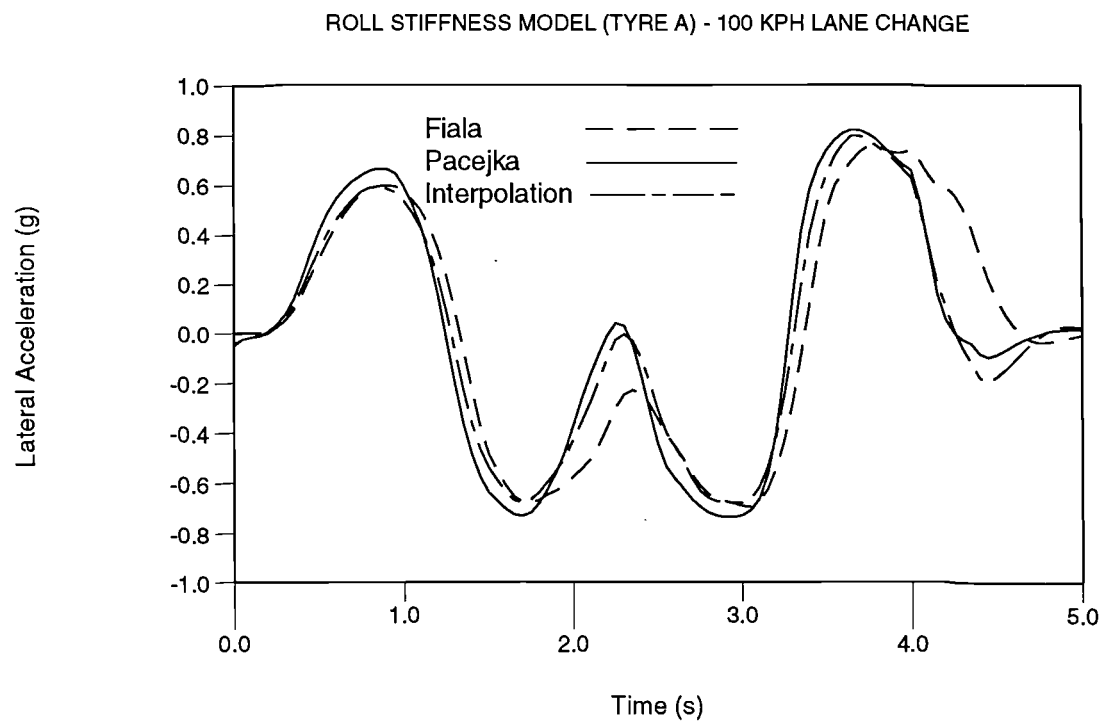
Figure J.2 Lateral acceleration comparison using roll stiffness model and TYRE A

LINKAGE MODEL (TYRE A) - 100 KPH LANE CHANGE
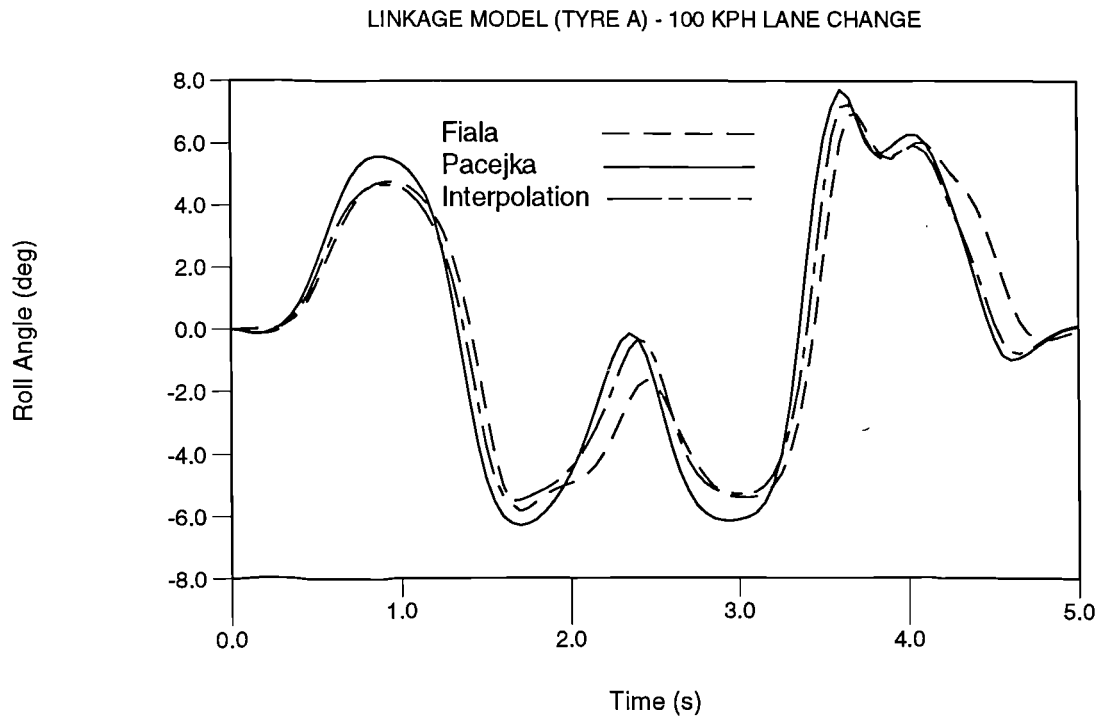
Figure J.3 Roll angle comparison using linkage model and TYRE A

ROLL STIFFNESS MODEL (TYRE A) - 100 KPH LANE CHANGE
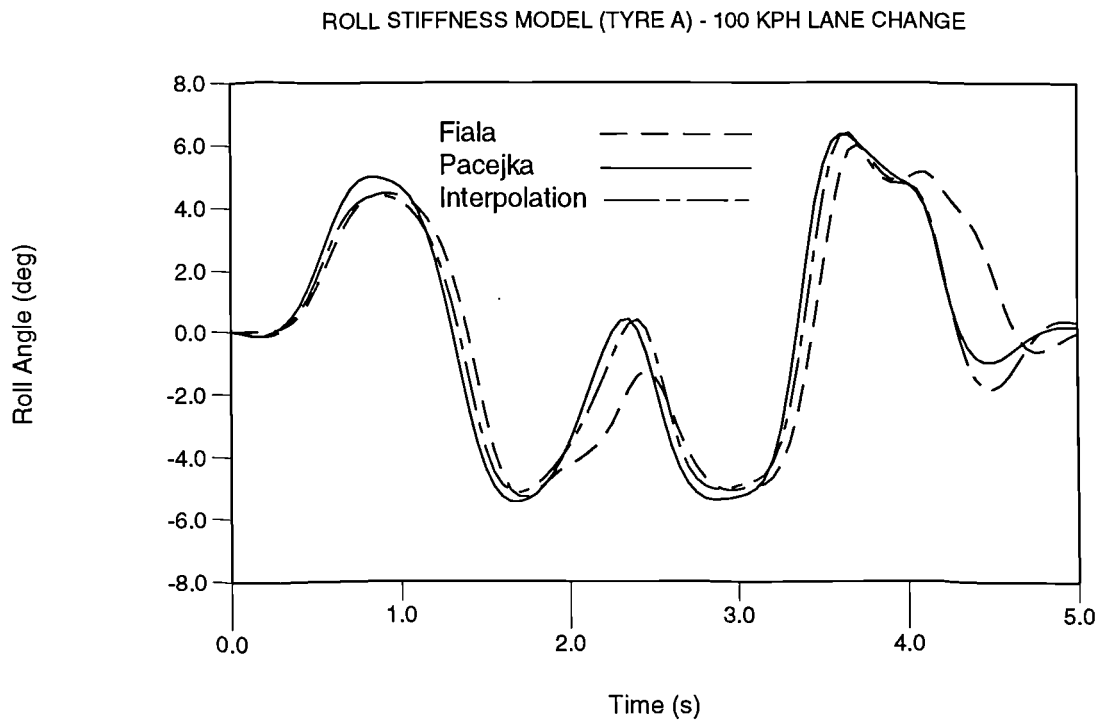
Figure J.4 Roll angle comparison using roll stiffness model and TYRE A

LINKAGE MODEL (TYRE A) - 100 KPH LANE CHANGE

Yaw Rate (deg/s)

Fiala ― ― ― ―
Pacejka ――――――
Interpolation ――― ― ―

40.0
30.0
20.0
10.0
0.0
-10.0
-20.0
-30.0
-40.0

0.0   1.0   2.0   3.0   4.0   5.0

Time (s)
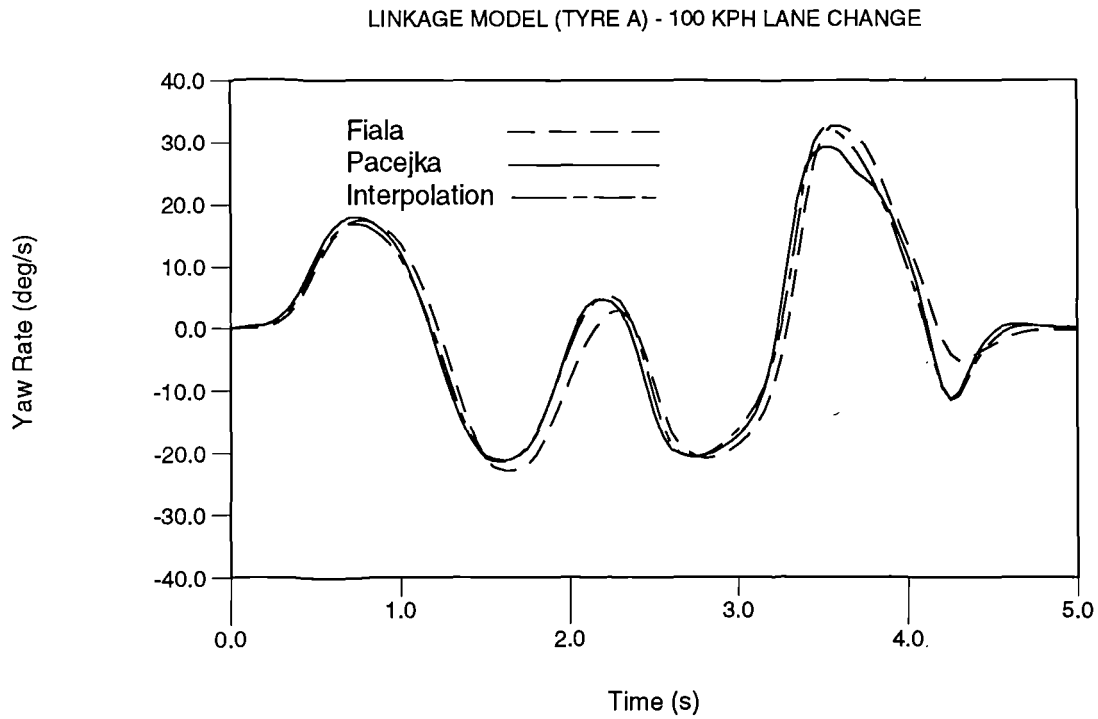
Figure J.5 Yaw rate comparison using linkage model and TYRE A

ROLL STIFFNESS MODEL (TYRE A) - 100 KPH LANE CHANGE

Yaw Rate (deg/s)

Fiala ― ― ― ―
Pacejka ――――――
Interpolation ――― ― ―

40.0
30.0
20.0
10.0
0.0
-10.0
-20.0
-30.0
-40.0

0.0   1.0   2.0   3.0   4.0   5.0

Time (s)
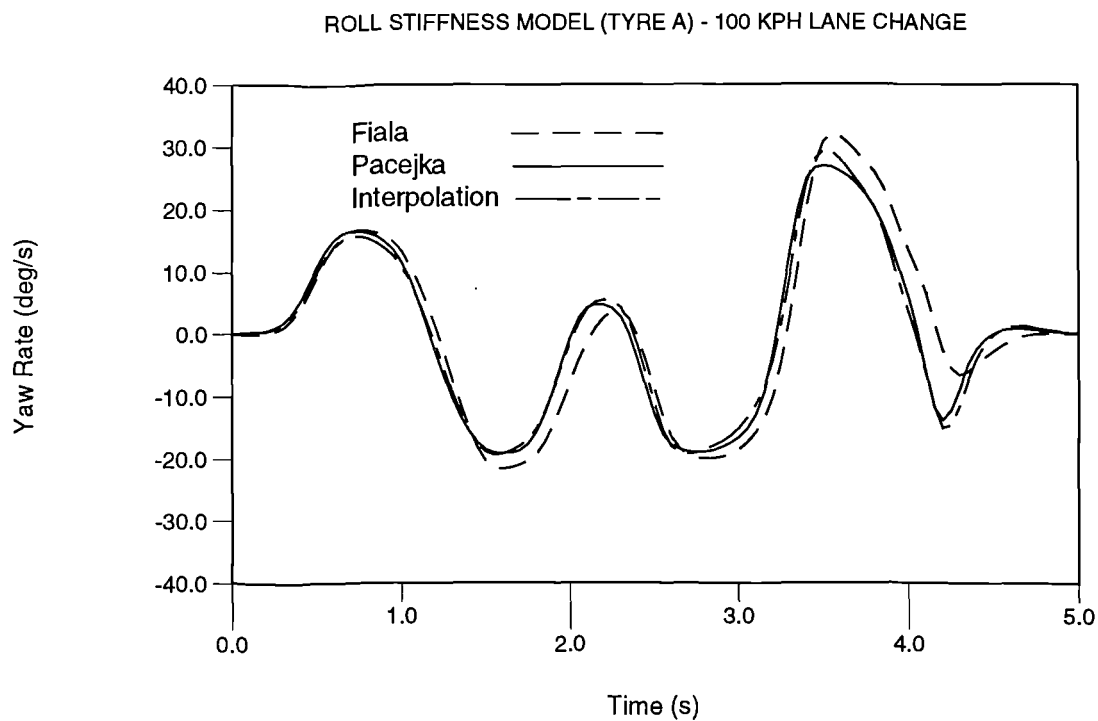
Figure J.6 Yaw rate comparison using roll stiffness model and TYRE A

LINKAGE MODEL (TYRE A) - 100 KPH LANE CHANGE
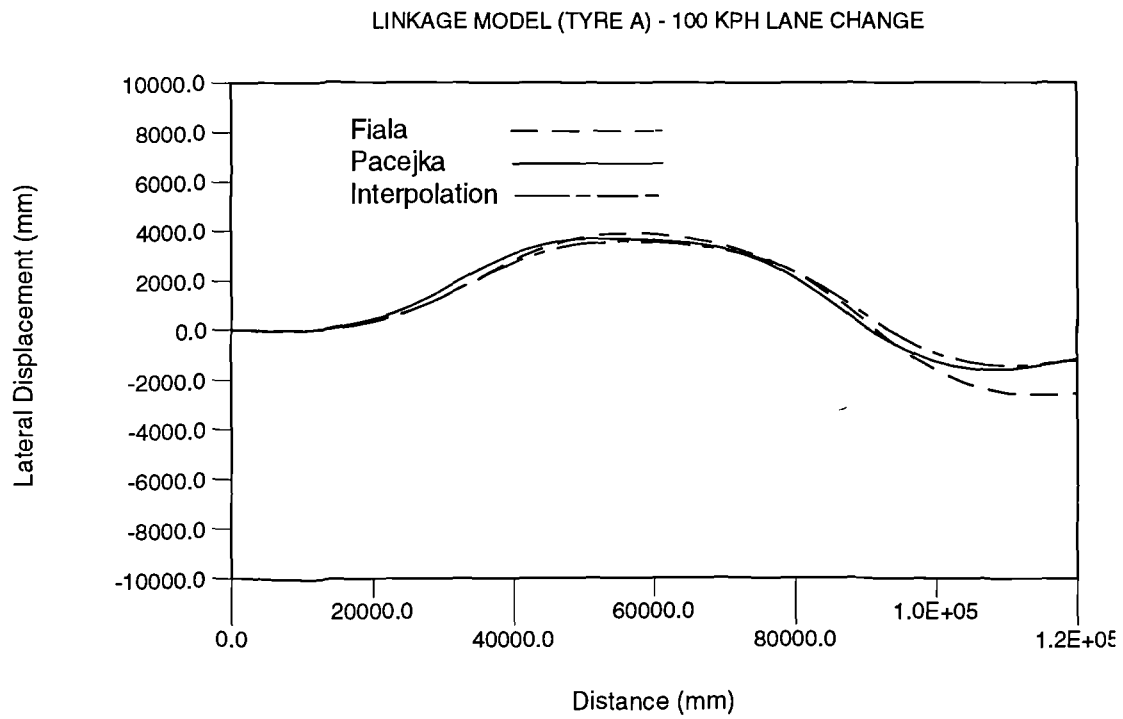
Figure J.7 Trajectory comparison using linkage model and TYRE A

ROLL STIFFNESS MODEL (TYRE A) - 100 KPH LANE CHANGE
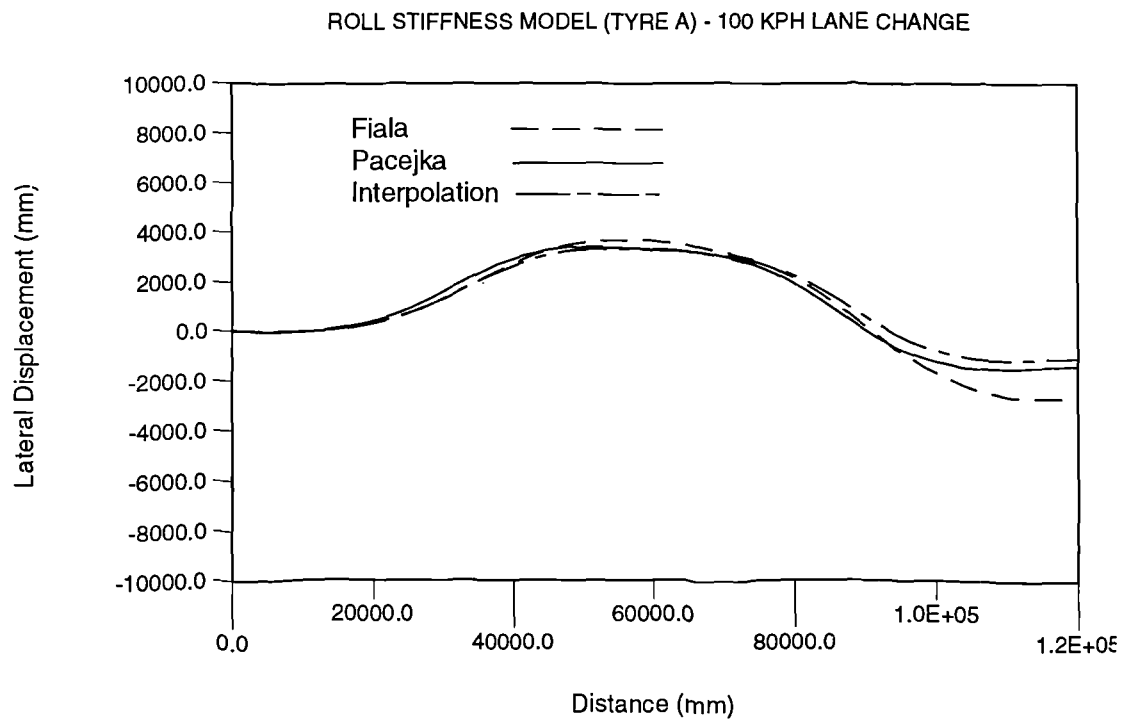
Figure J.8 Trajectory comparison using roll stiffness model and TYRE A

LINKAGE MODEL (TYRE A) - 100 KPH LANE CHANGE
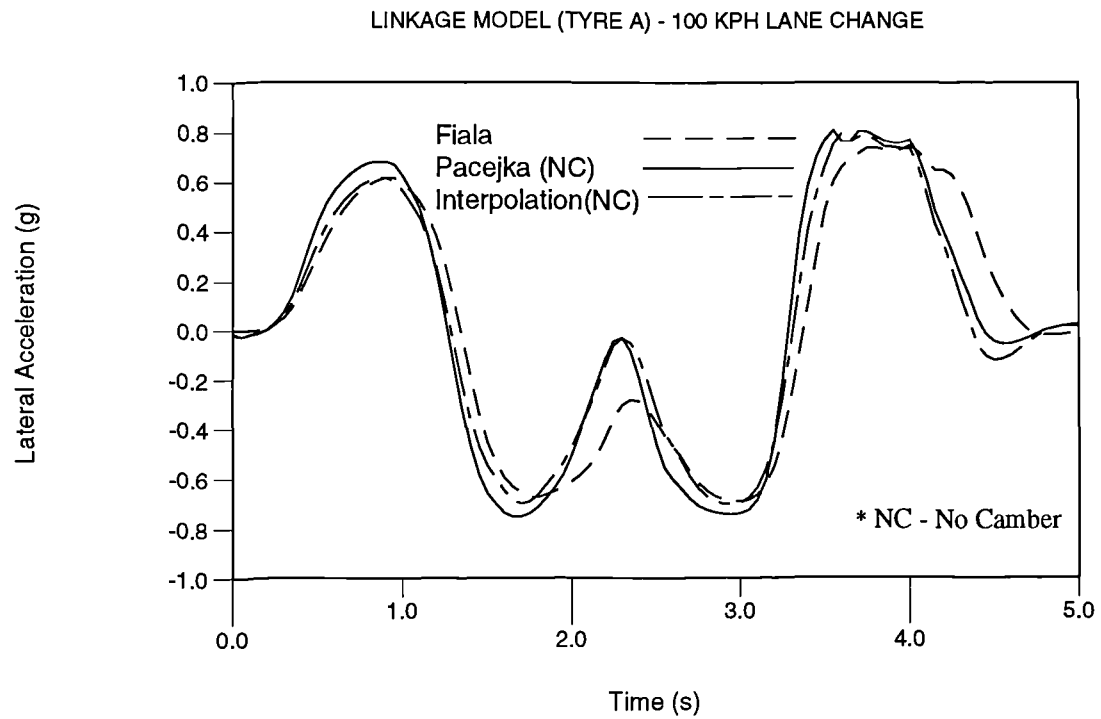
Figure J.9 Lateral acceleration comparison using linkage model and TYRE A

ROLL STIFFNESS MODEL (TYRE A) - 100 KPH LANE CHANGE
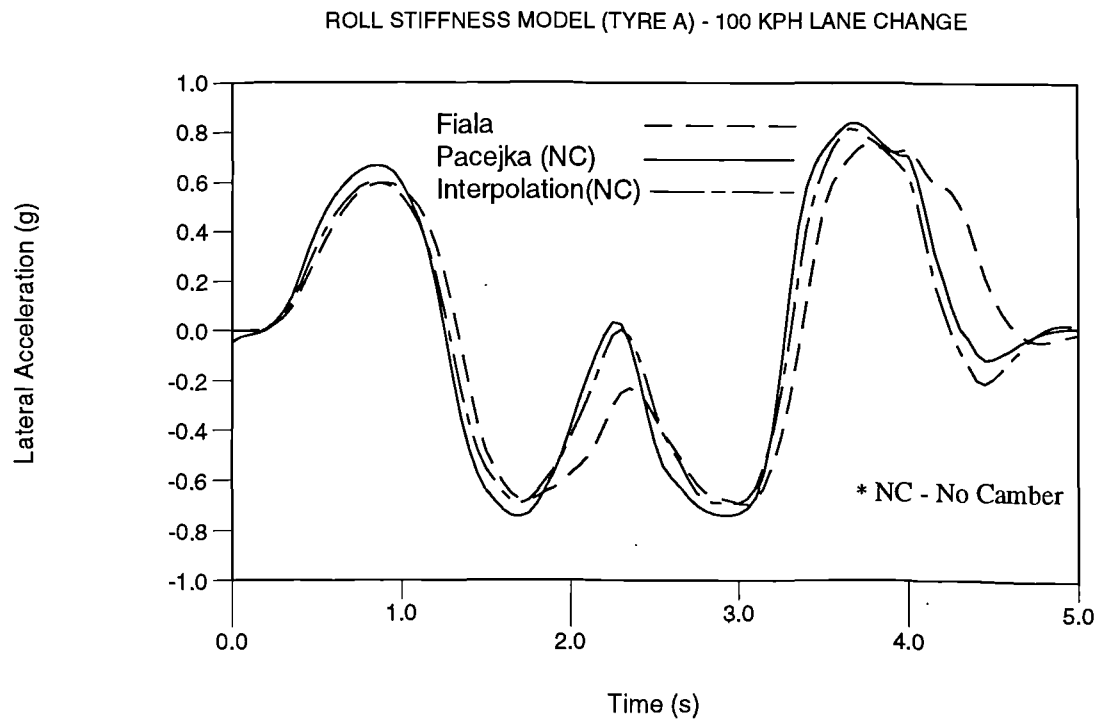
Figure J.10 Lateral acceleration comparison using roll stiffness model and TYRE A

LINKAGE MODEL (TYRE A) - 100 KPH LANE CHANGE
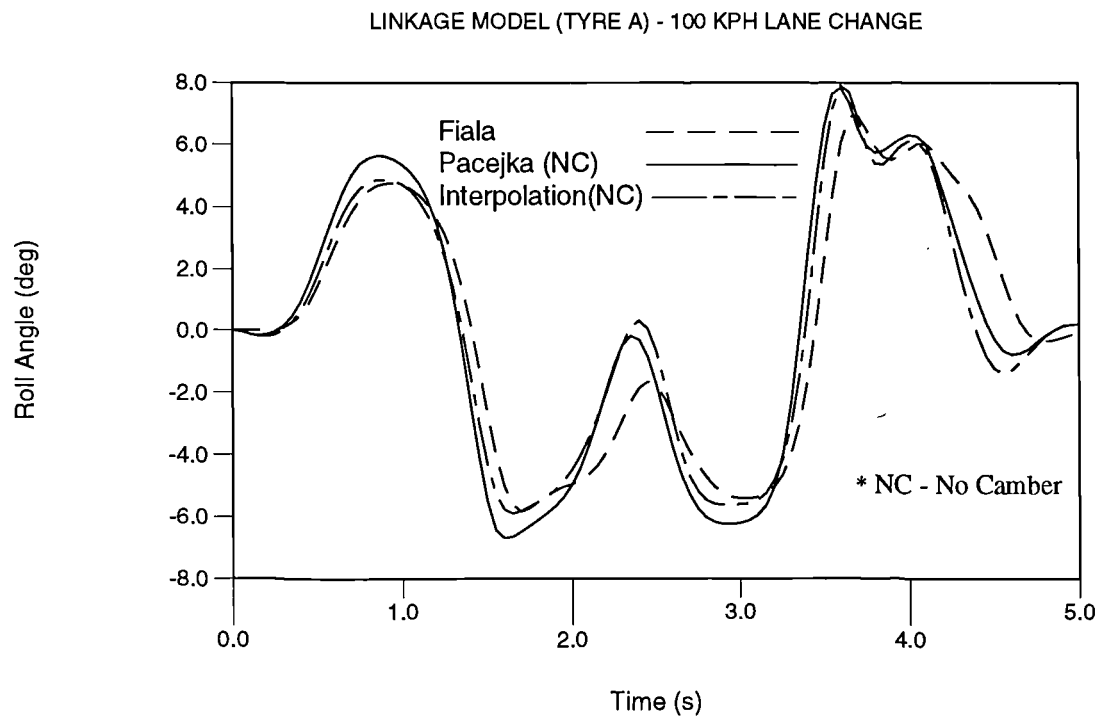
Figure J.11 Roll angle comparison using linkage model and TYRE A

ROLL STIFFNESS MODEL (TYRE A) - 100 KPH LANE CHANGE
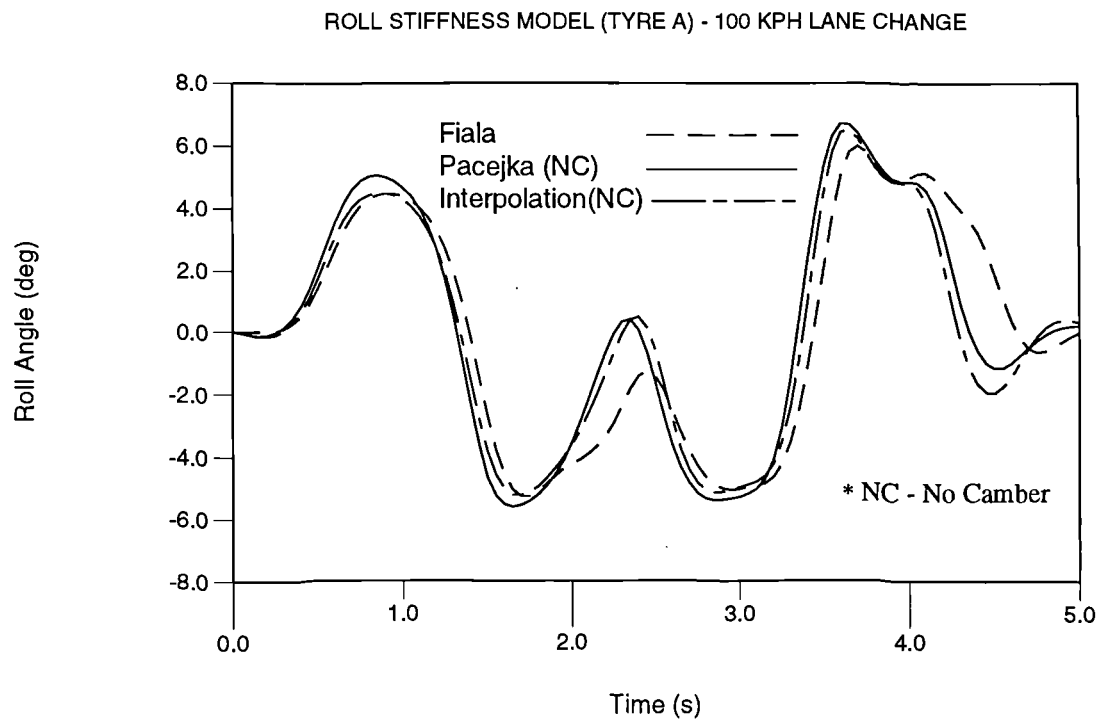
Figure J.12 Roll angle comparison using roll stiffness model and TYRE A

LINKAGE MODEL (TYRE A) - 100 KPH LANE CHANGE
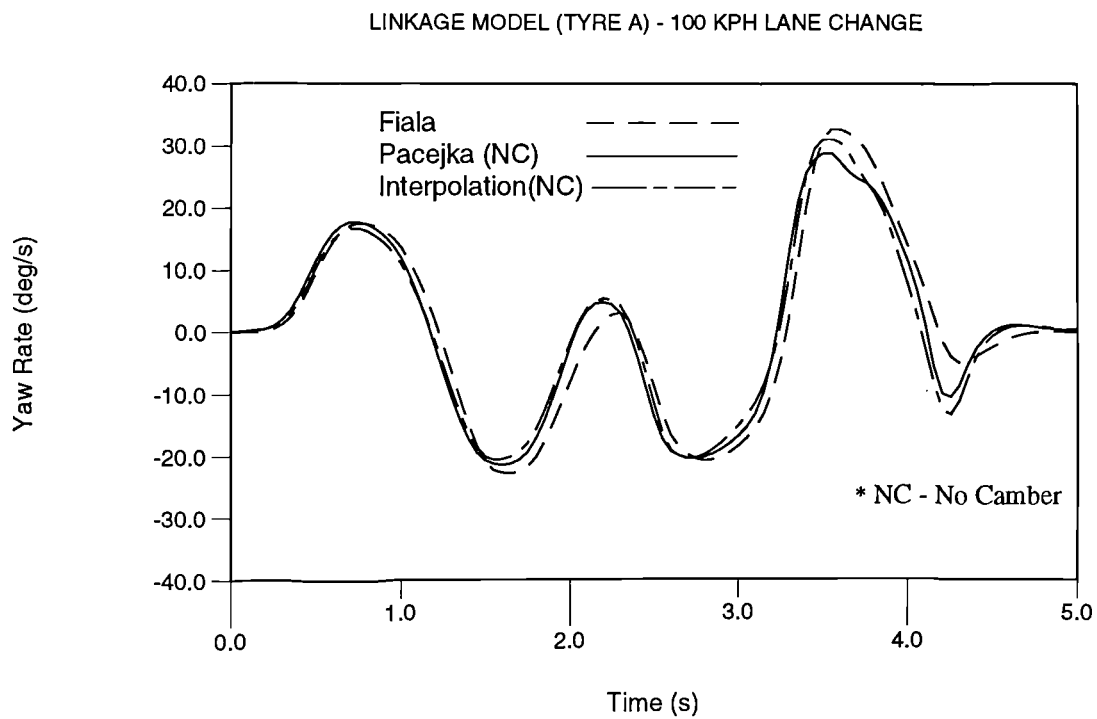
Figure J.13 Yaw rate comparison using linkage model and TYRE A

ROLL STIFFNESS MODEL (TYRE A) - 100 KPH LANE CHANGE
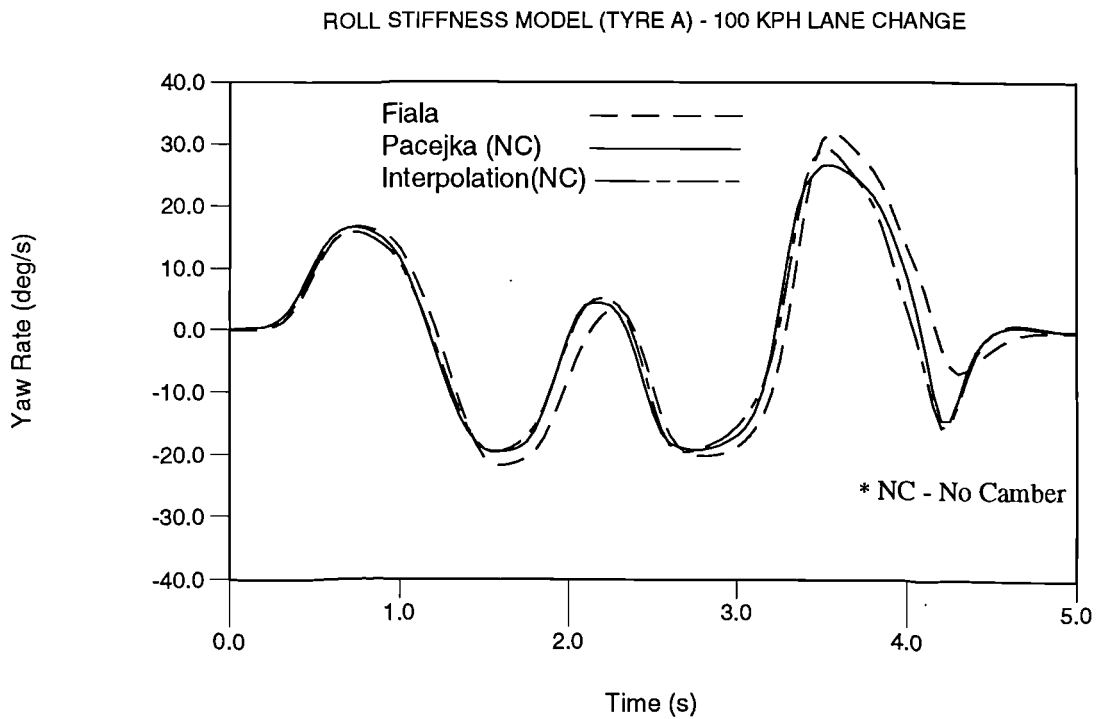
Figure J.14 Yaw rate comparison using roll stiffness model and TYRE A

LINKAGE MODEL (TYRE A) - 100 KPH LANE CHANGE

Fiala — — — —
Pacejka (NC) ————
Interpolation(NC) — — - — -

* NC - No Camber

Distance (mm)
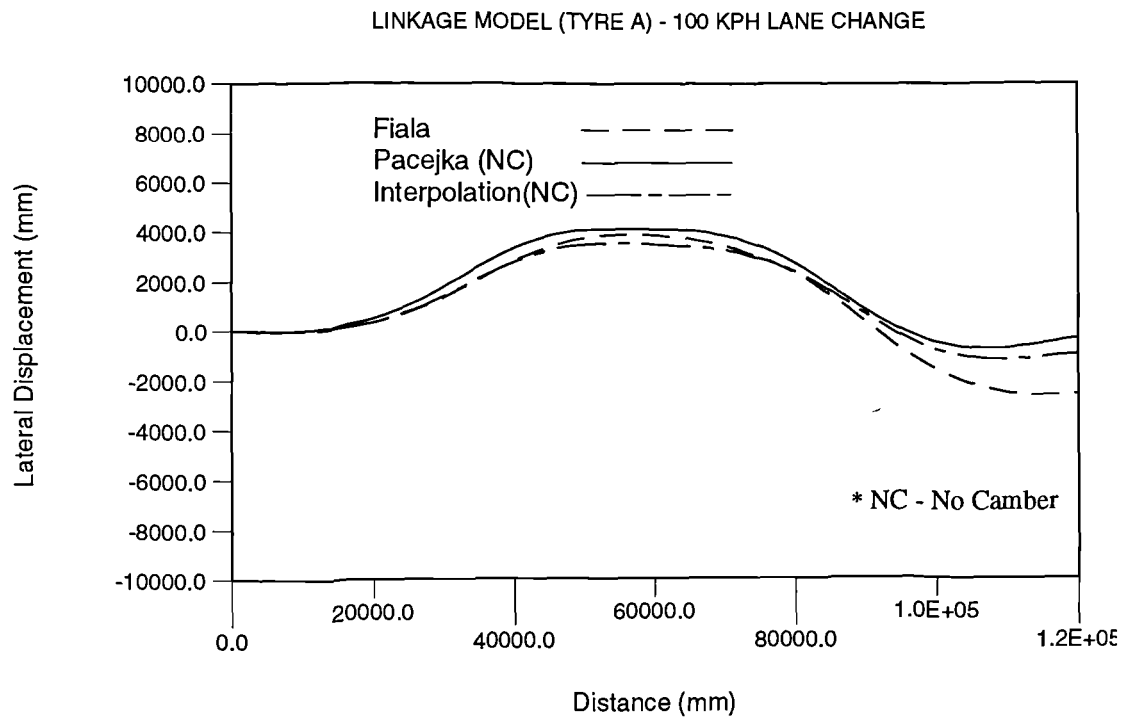
Figure J.15 Trajectory comparison using linkage model and TYRE A

ROLL STIFFNESS MODEL (TYRE A) - 100 KPH LANE CHANGE

Fiala — — — —
Pacejka (NC) ————
Interpolation(NC) — — - — -

* NC - No Camber

Distance (mm)
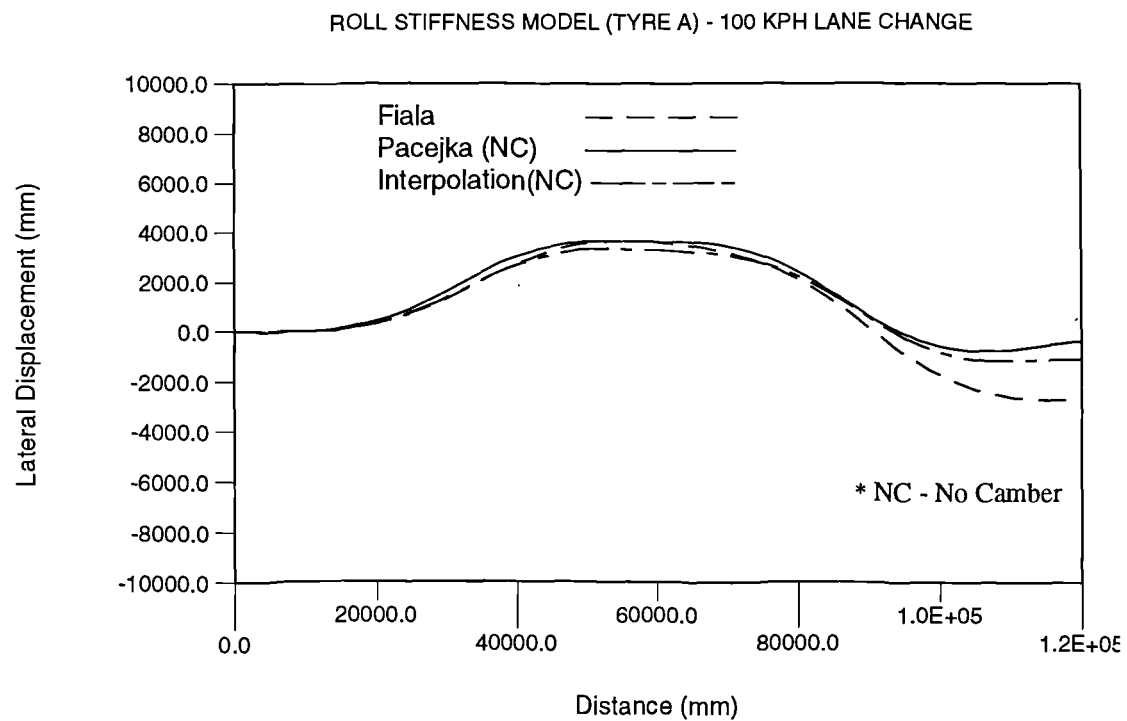
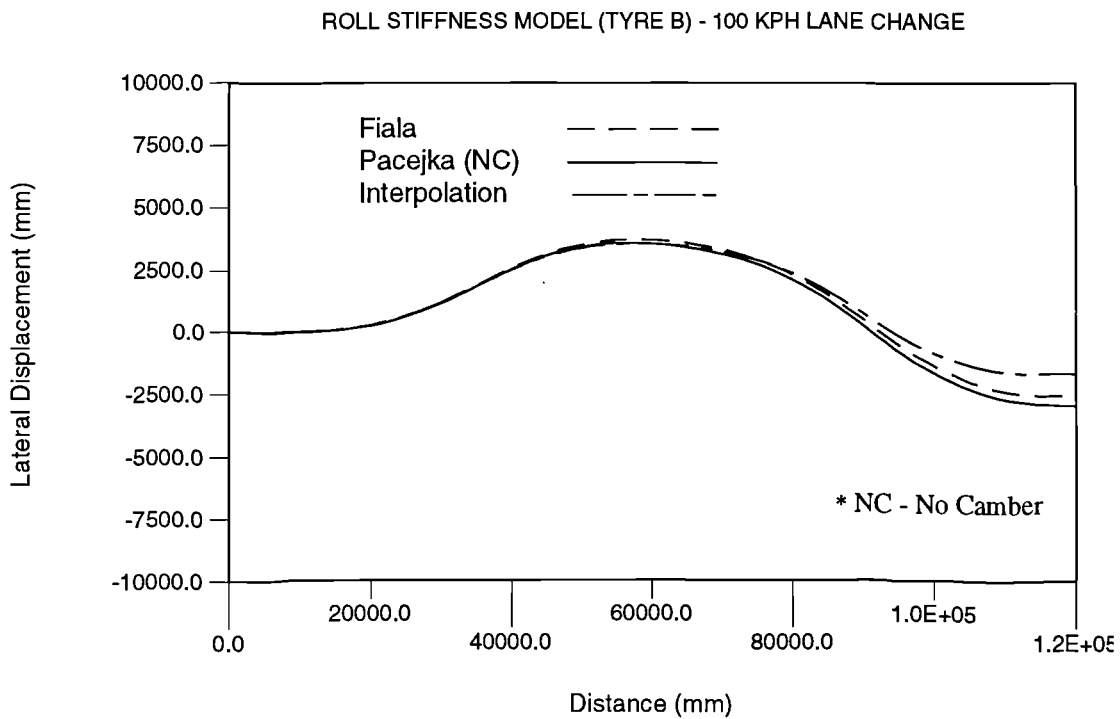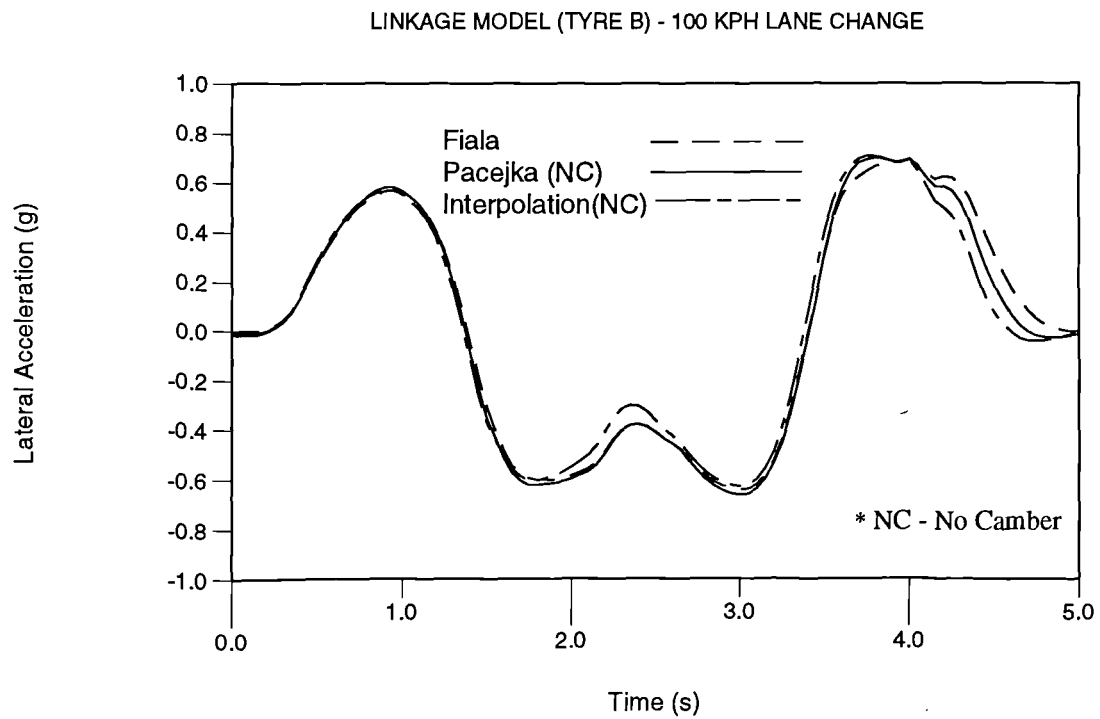Figure J.16 Trajectory comparison using roll stiffness model and TYRE A
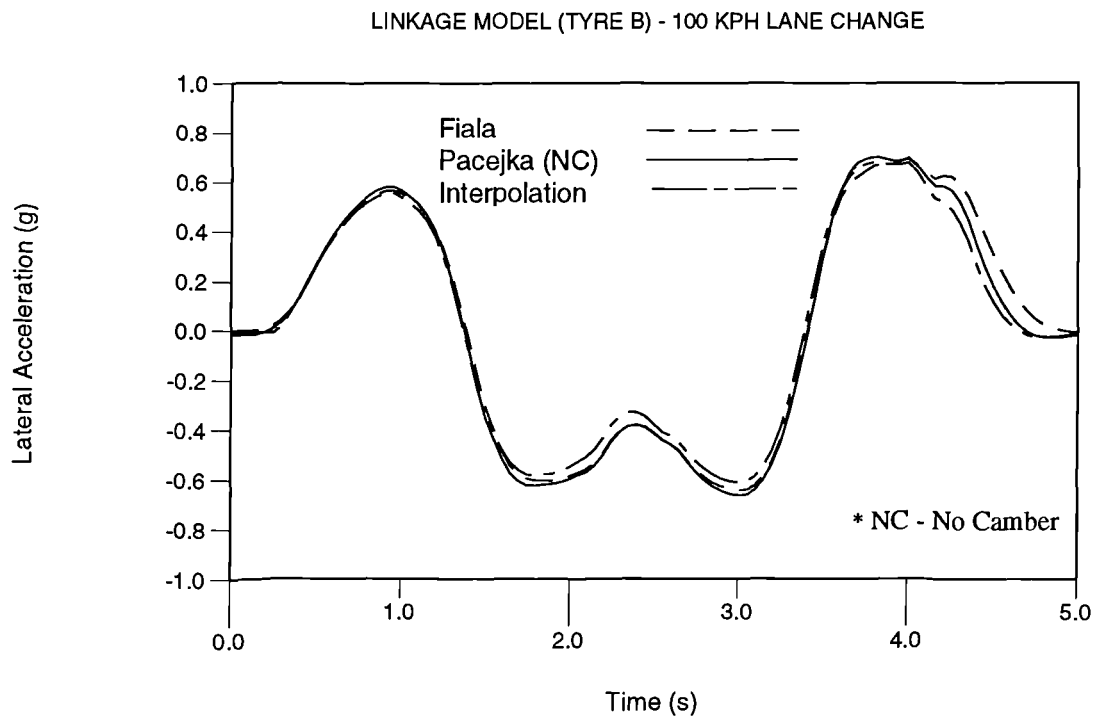
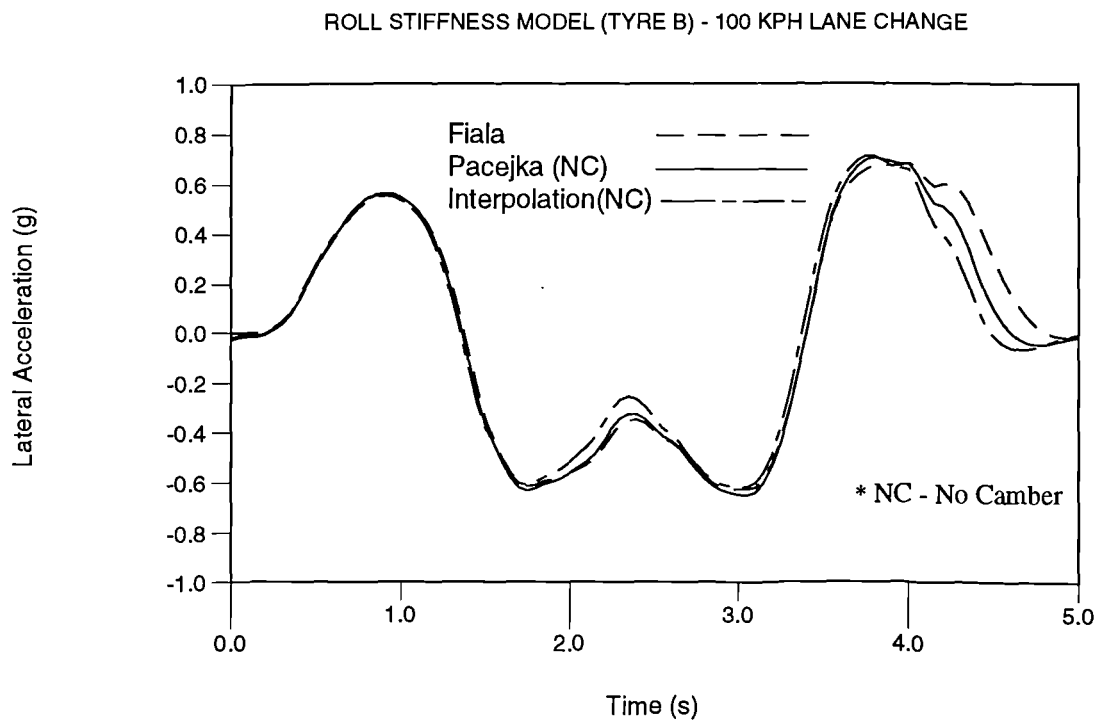Figure J.17 Lateral acceleration comparison using linkage model and TYRE B
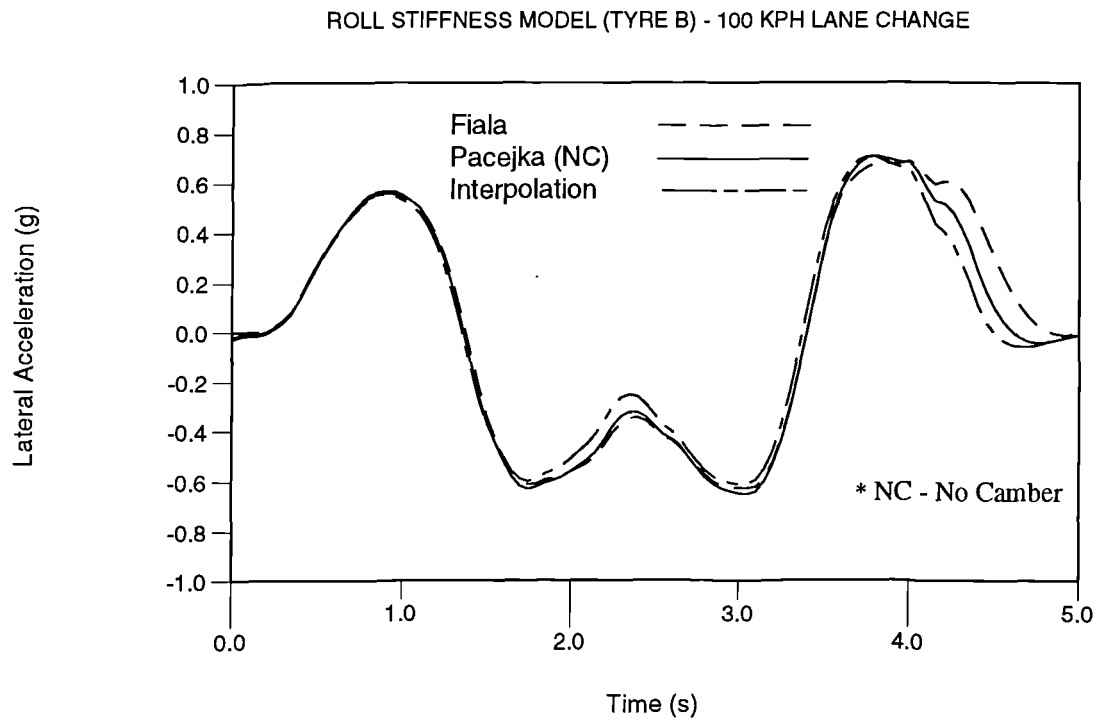
Figure J.18 Lateral acceleration comparison using roll stiffness model and TYRE B
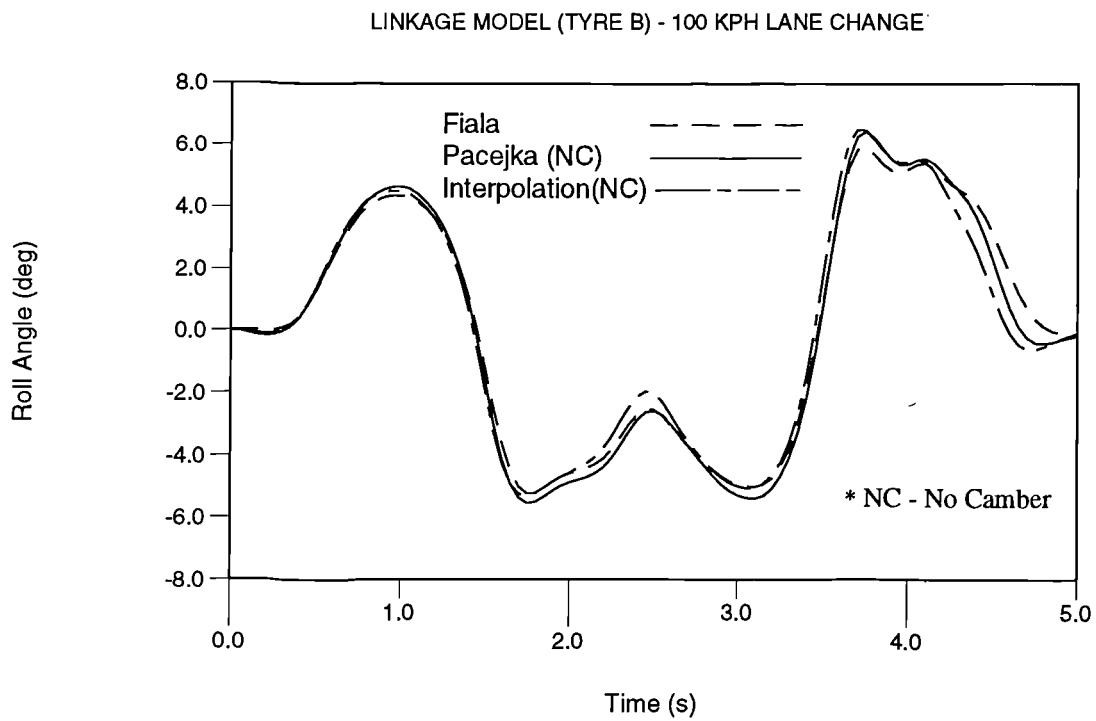
LINKAGE MODEL (TYRE B) - 100 KPH LANE CHANGE
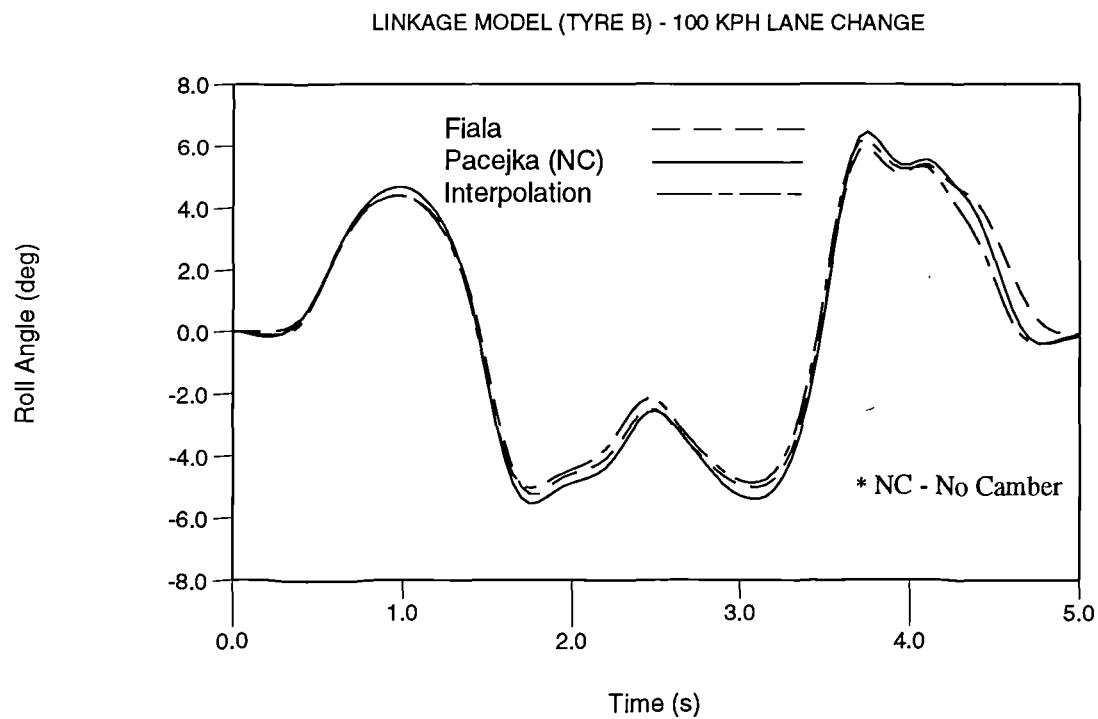
Figure J.19 Roll angle comparison using linkage model and TYRE B

ROLL STIFFNESS MODEL (TYRE B) - 100 KPH LANE CHANGE
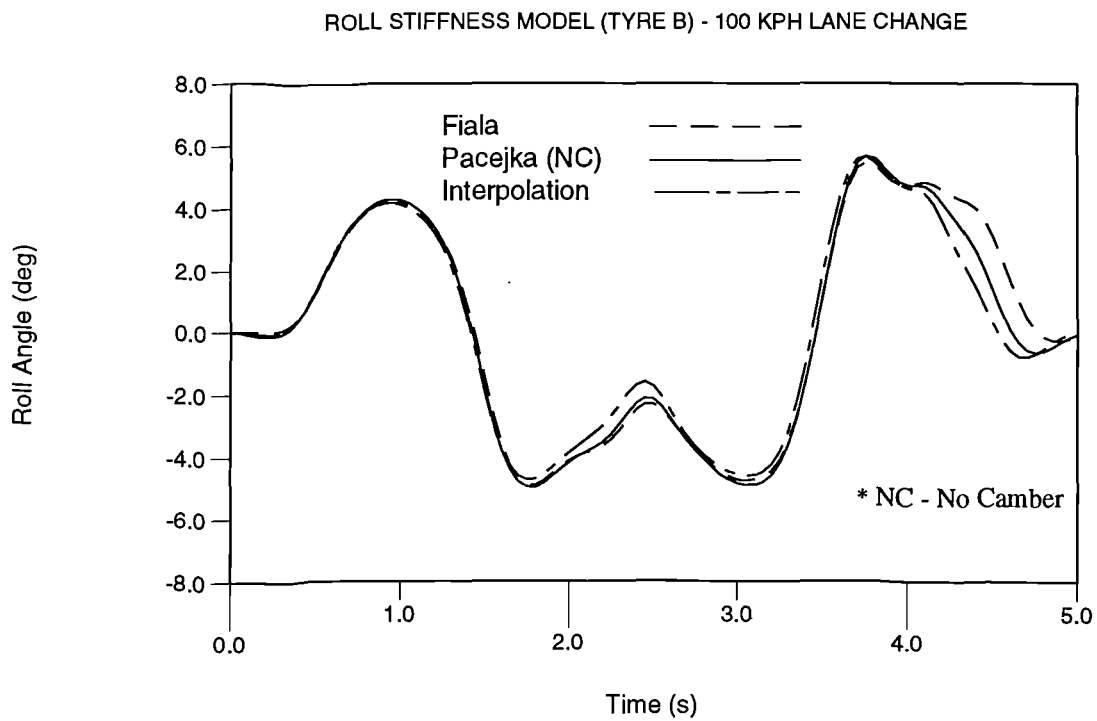
Figure J.20 Roll angle comparison using roll stiffness model and TYRE B

LINKAGE MODEL (TYRE B) - 100 KPH LANE CHANGE
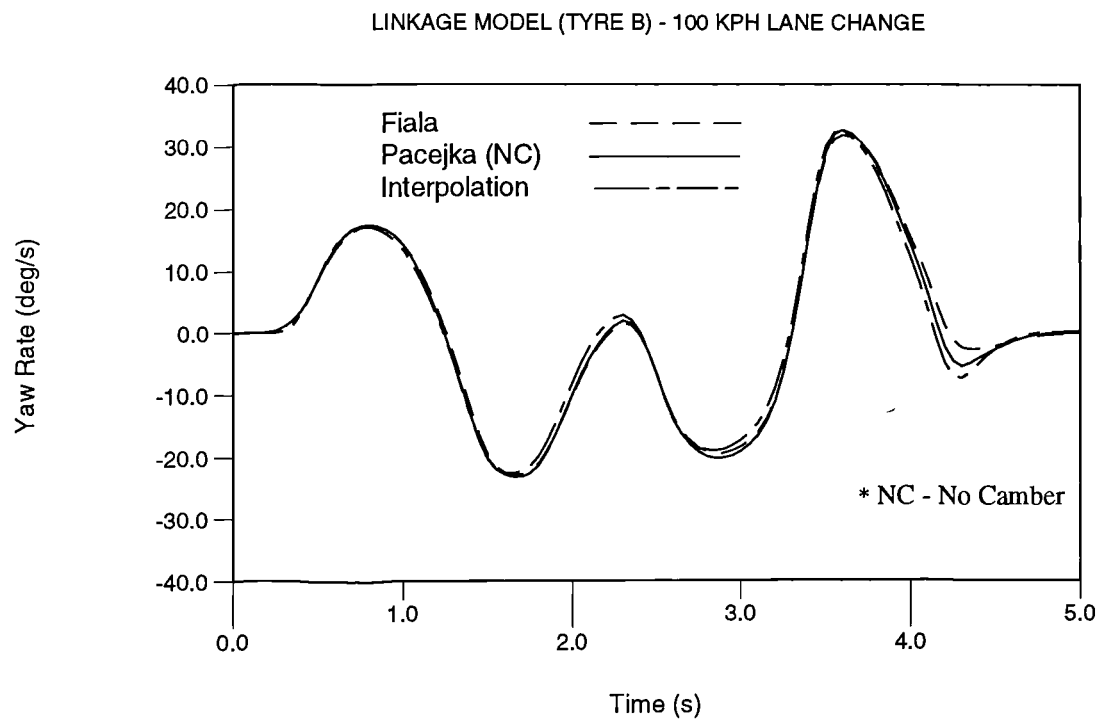
Figure J.21 Yaw rate comparison using linkage model and TYRE B

ROLL STIFFNESS MODEL (TYRE B) - 100 KPH LANE CHANGE
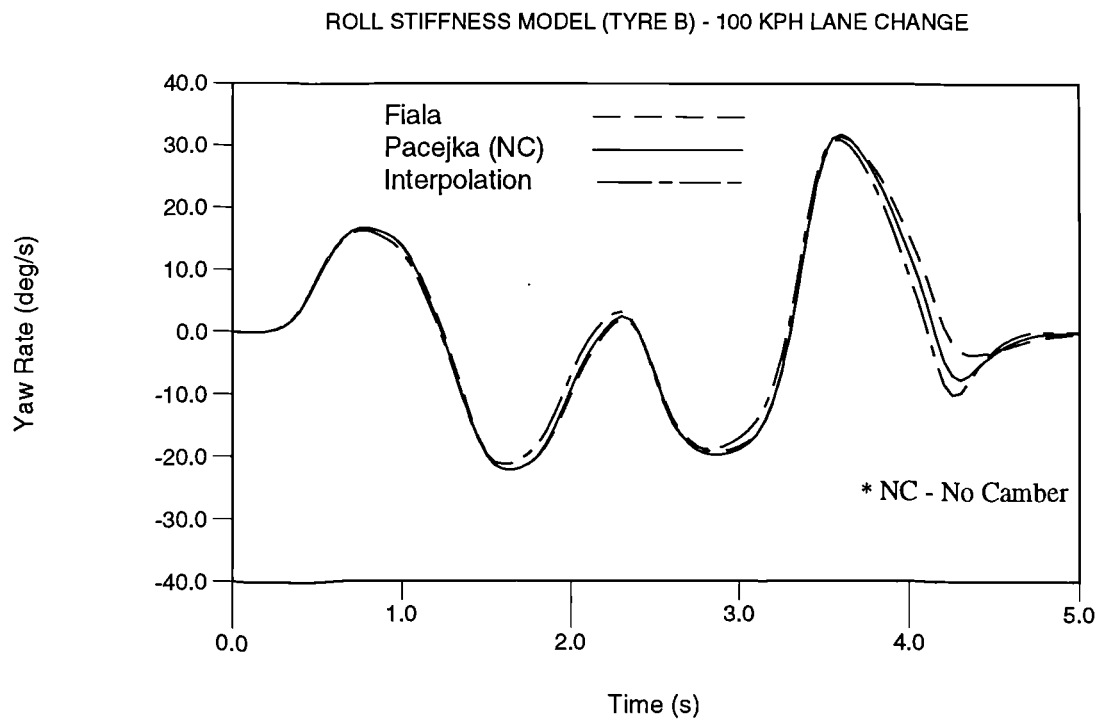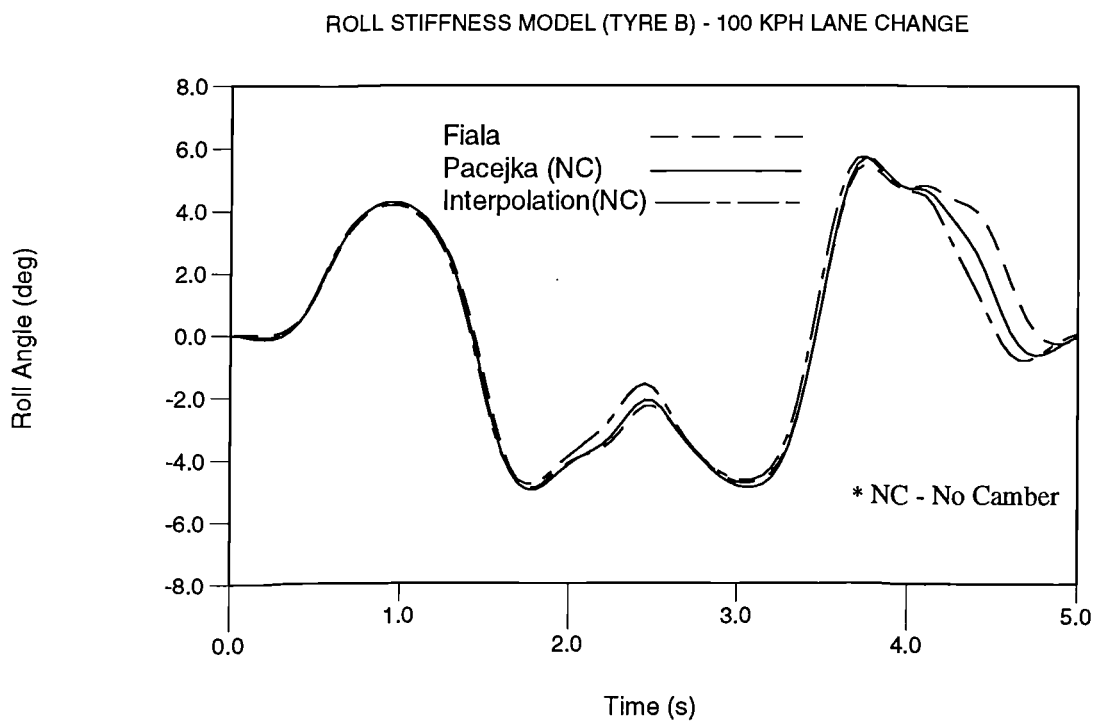

Figure J.22 Yaw rate comparison using roll stiffness model and TYRE B
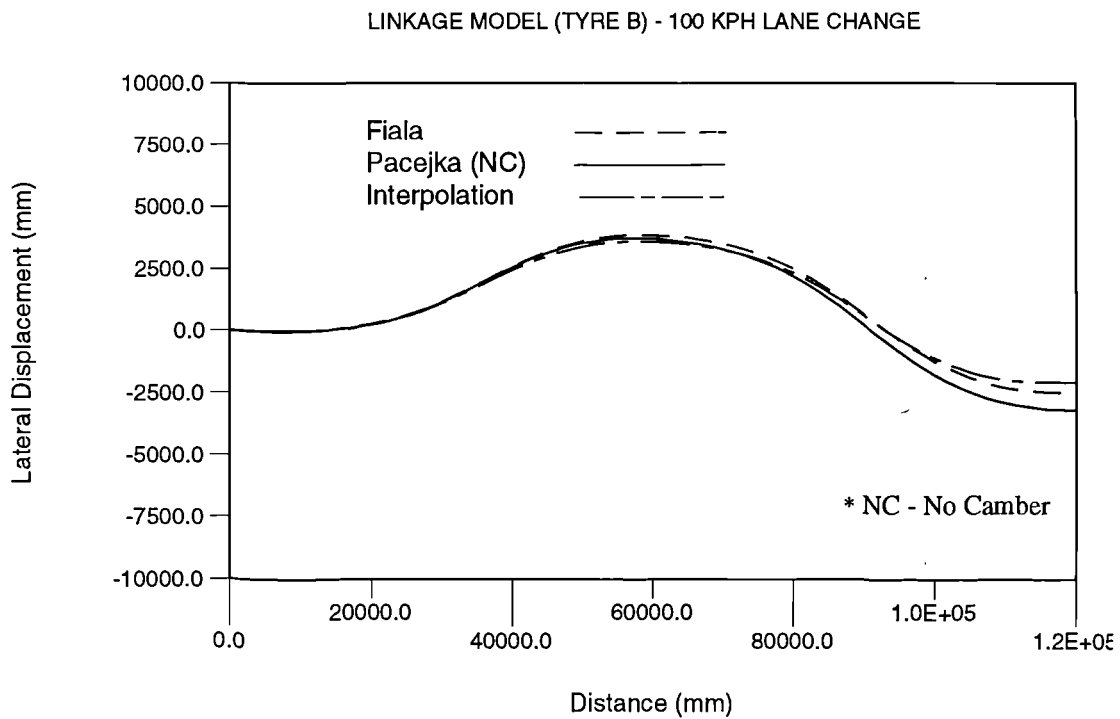
Figure J.23 Trajectory comparison using linkage model and TYRE B

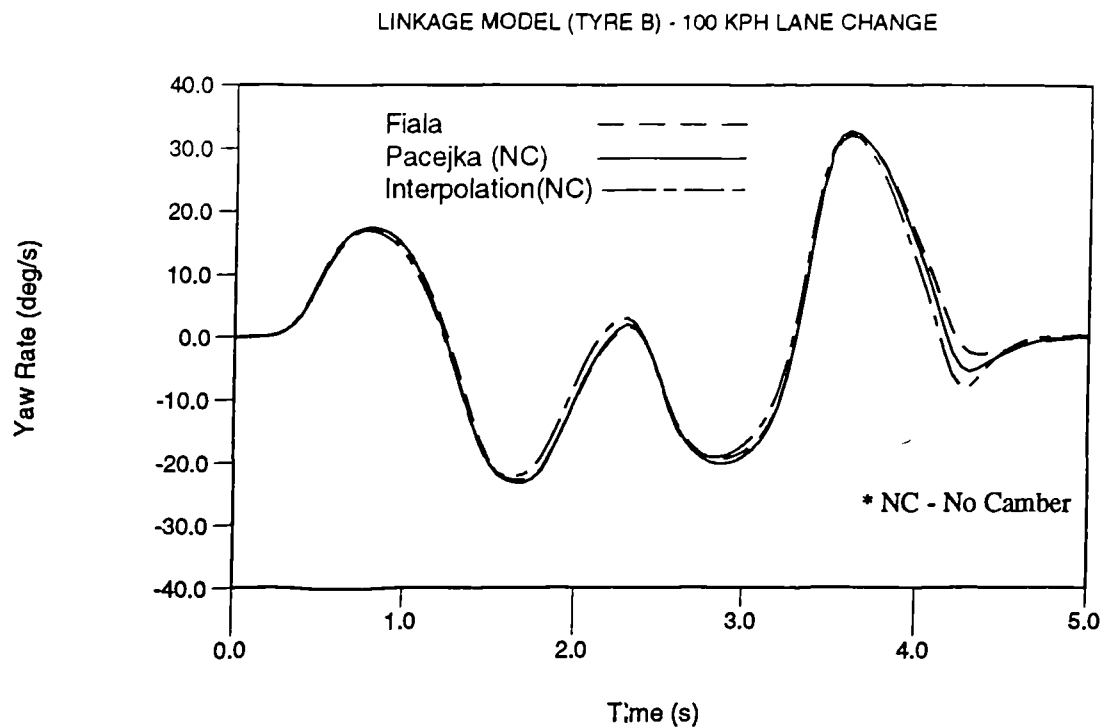Figure J.24 Trajectory comparison using roll stiffness model and TYRE B

LINKAGE MODEL (TYRE B) - 100 KPH LANE CHANGE

Figure J.25 Lateral acceleration comparison using linkage model and TYRE B

ROLL STIFFNESS MODEL (TYRE B) - 100 KPH LANE CHANGE

Figure J.26 Lateral acceleration comparison using roll stiffness model and TYRE B

LINKAGE MODEL (TYRE B) - 100 KPH LANE CHANGE

Figure J.27 Roll angle comparison using linkage model and TYRE B

ROLL STIFFNESS MODEL (TYRE B) - 100 KPH LANE CHANGE

Figure J.28 Roll angle comparison using roll stiffness model and TYRE B

LINKAGE MODEL (TYRE B) - 100 KPH LANE CHANGE

Figure J.29 Yaw rate comparison using linkage model and TYRE B

ROLL STIFFNESS MODEL (TYRE B) - 100 KPH LANE CHANGE
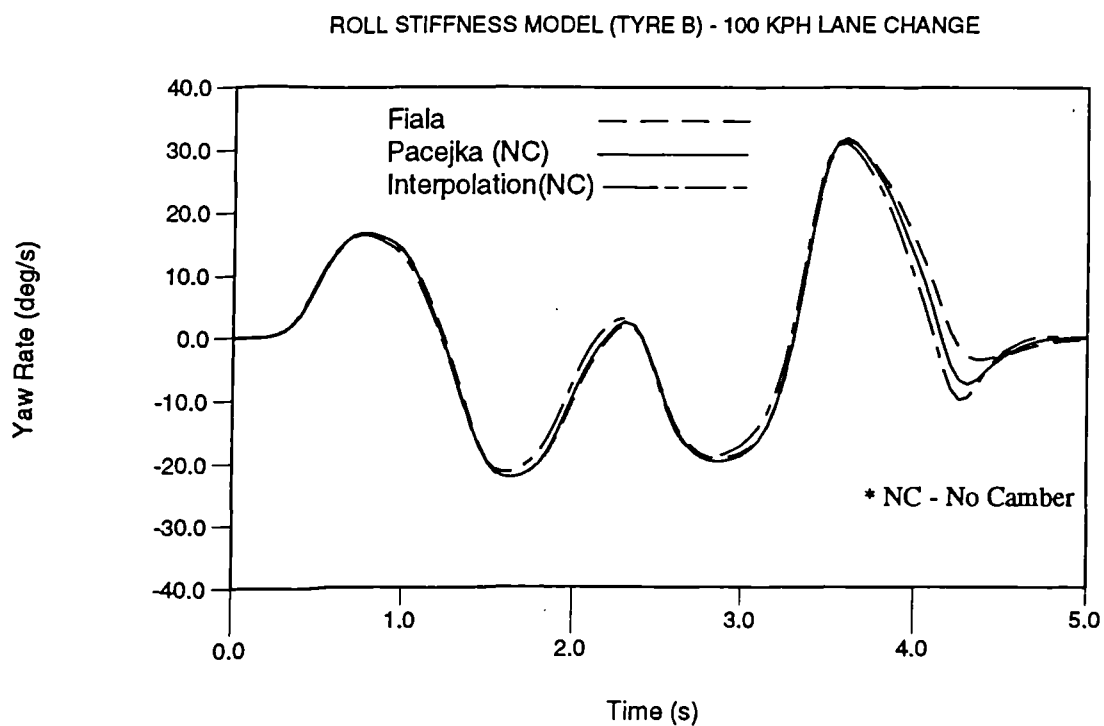
Figure J.30 Yaw rate comparison using roll stiffness model and TYRE B

LINKAGE MODEL (TYRE B) - 100 KPH LANE CHANGE
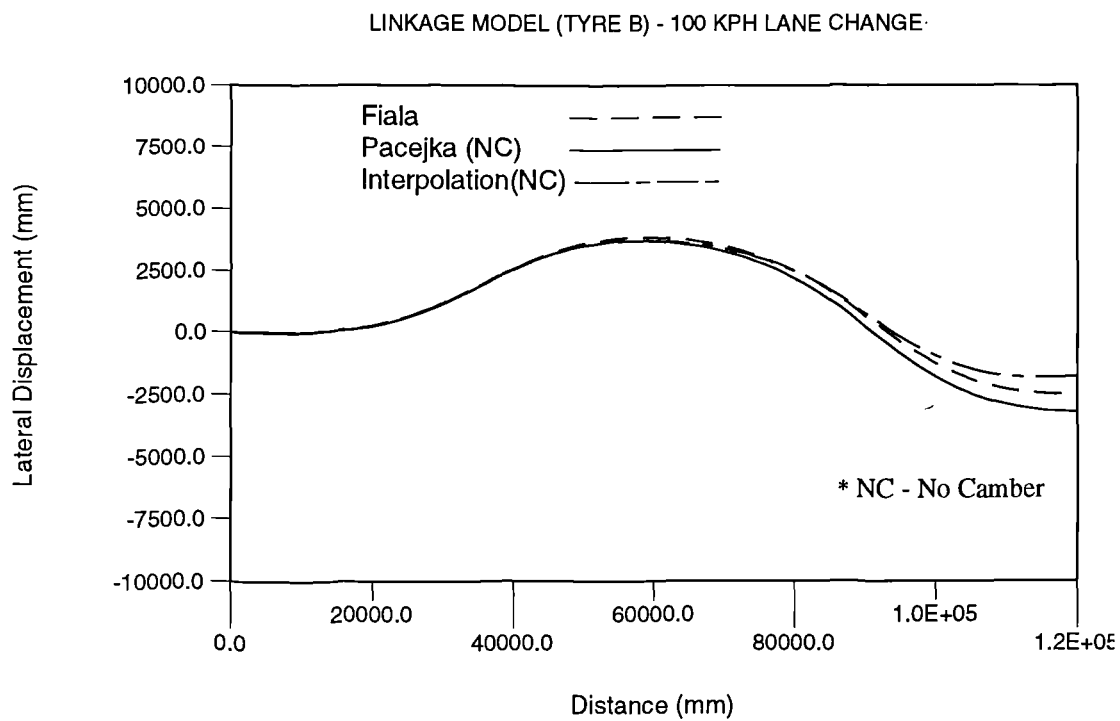
Figure J.31 Trajectory comparison using linkage model and TYRE B
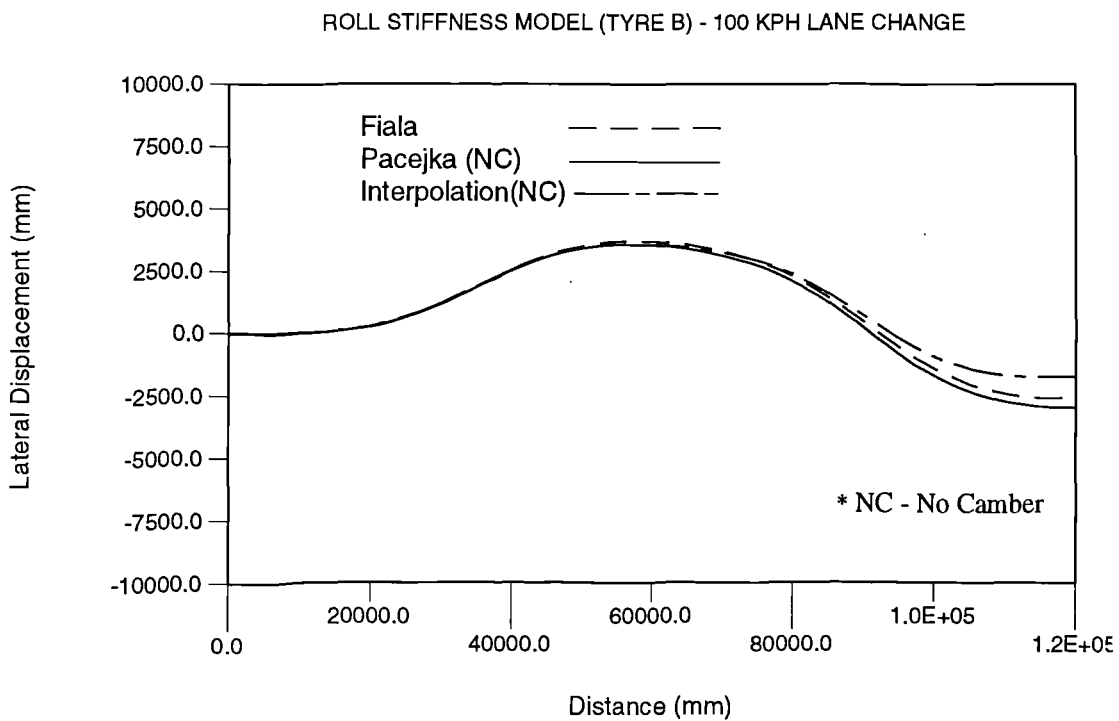
ROLL STIFFNESS MODEL (TYRE B) - 100 KPH LANE CHANGE

Figure J.32 Trajectory comparison using roll stiffness model and TYRE B

APPENDIX K

SENSITIVITY STUDIES BASED ON TYRE B AND THE ROLL STIFFNESS MODEL

ROLL STIFFNESS MODEL - 100 KPH LANE CHANGE

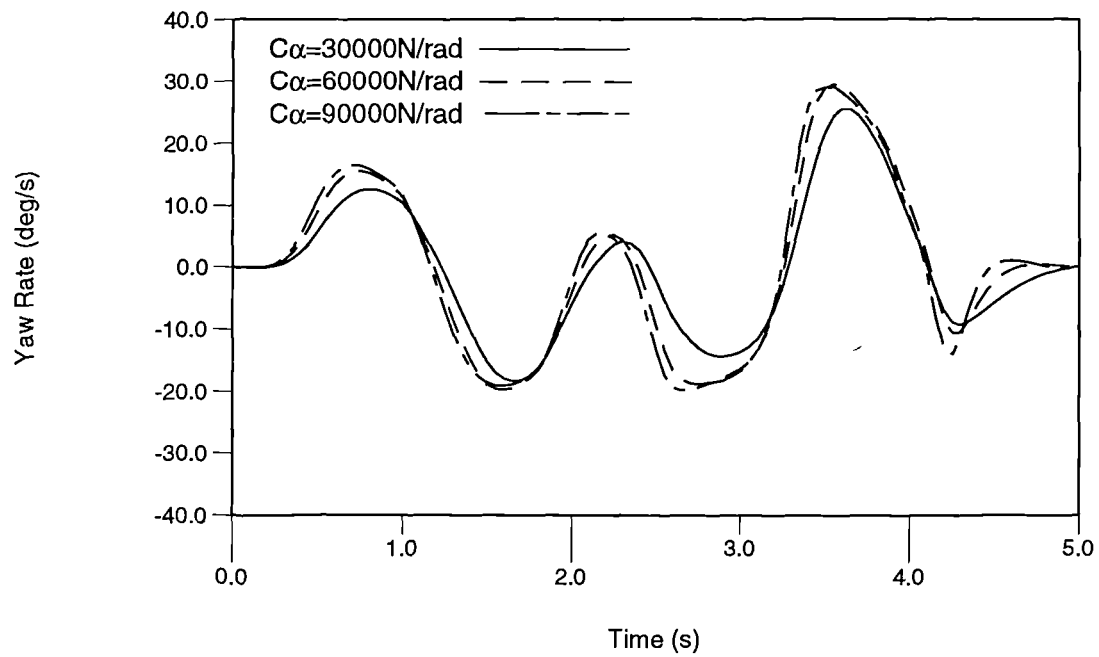CORNERING STIFFNESS COMPARISON - TYRE B

Figure K.1 Yaw rate comparison for varying cornering stiffness

ROLL STIFFNESS MODEL - 100 KPH LANE CHANGE

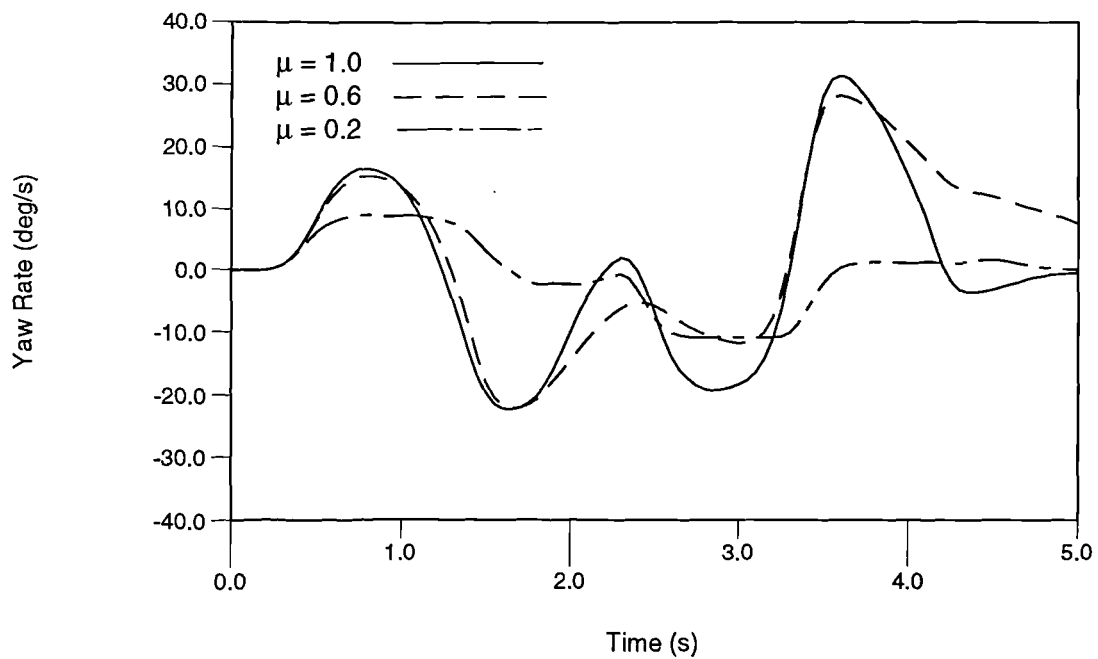FRICTION COEFFICIENT COMPARISON - TYRE B

Figure K.2 Yaw rate comparison for varying friction coefficient

ROLL STIFFNESS MODEL - 100 KPH LANE CHANGE
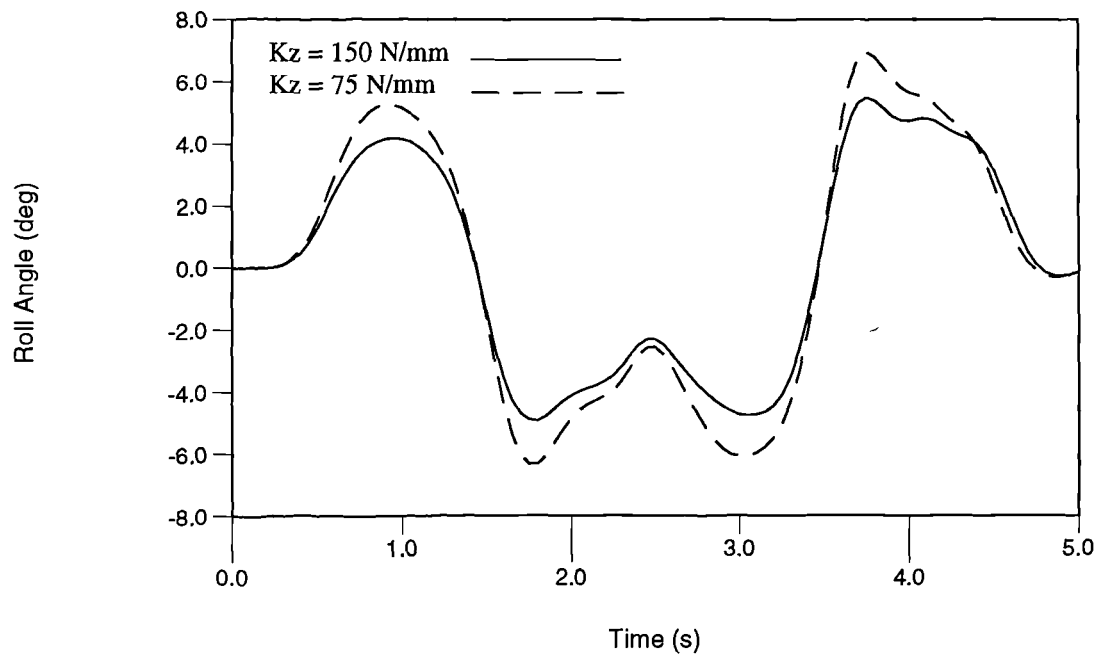## RADIAL STIFFNESS COMPARISON - TYRE B

Figure K.3 Roll angle comparison for varying radial stiffness

ROLL STIFFNESS MODEL - 100 KPH LANE CHANGE
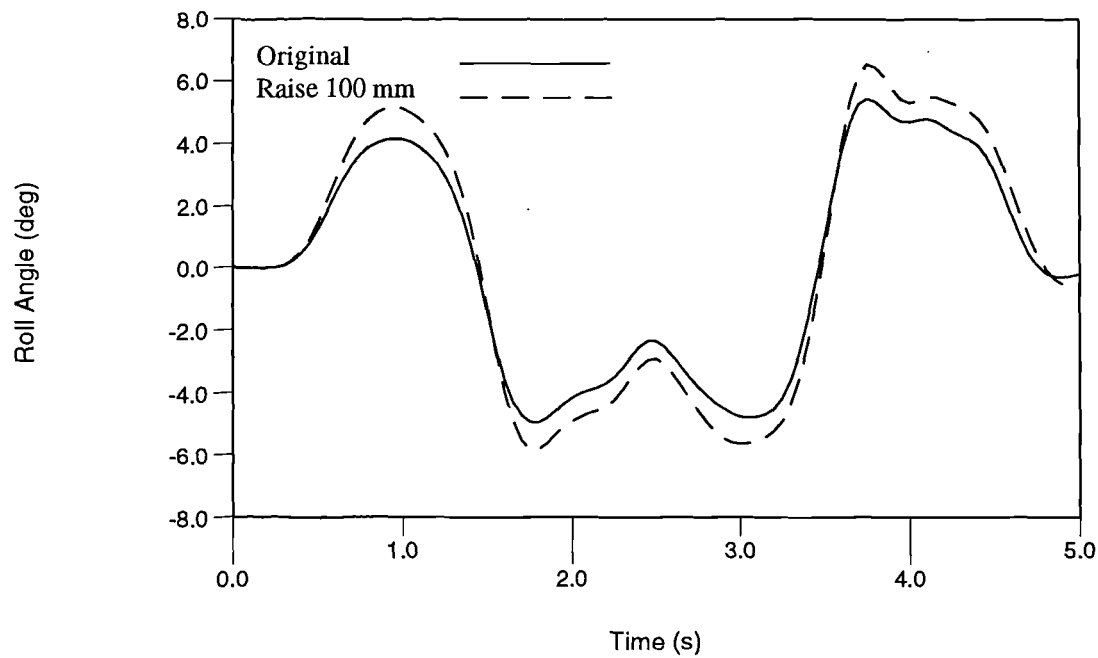## CENTRE OF MASS HEIGHT COMPARISON - TYRE B

Figure K.4 Roll angle comparison for varying mass centre height

ROLL STIFFNESS MODEL - 100 KPH LANE CHANGE
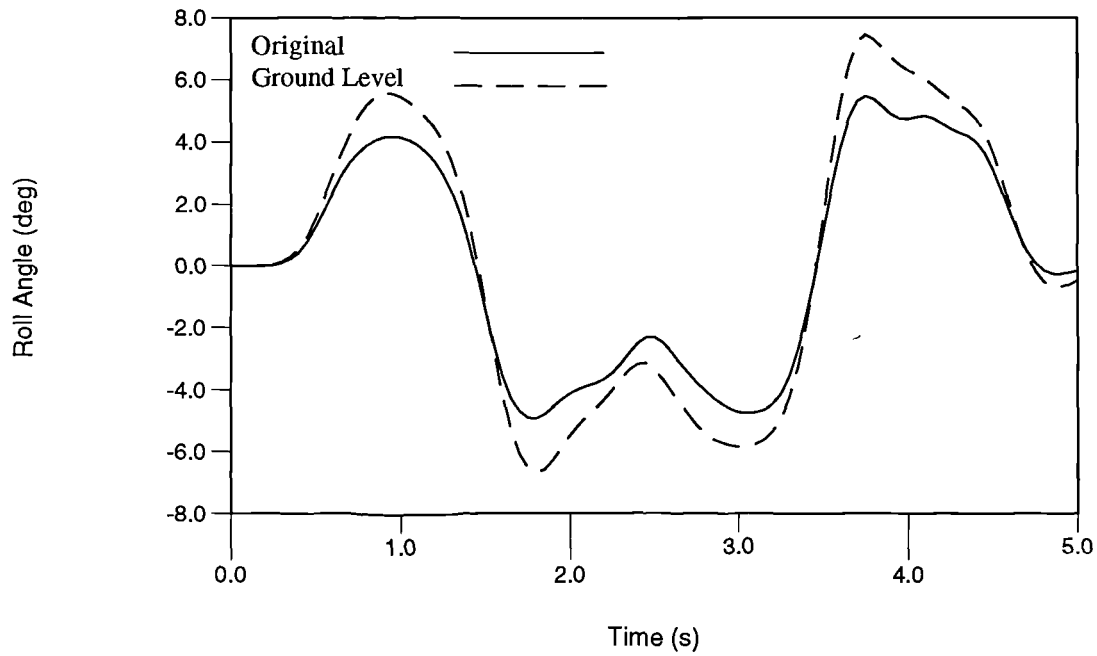### ROLL CENTRE HEIGHT COMPARISON - TYRE B

Figure K.5 Roll angle comparison for varying roll axis position

ROLL STIFFNESS MODEL - 100 KPH LANE CHANGE
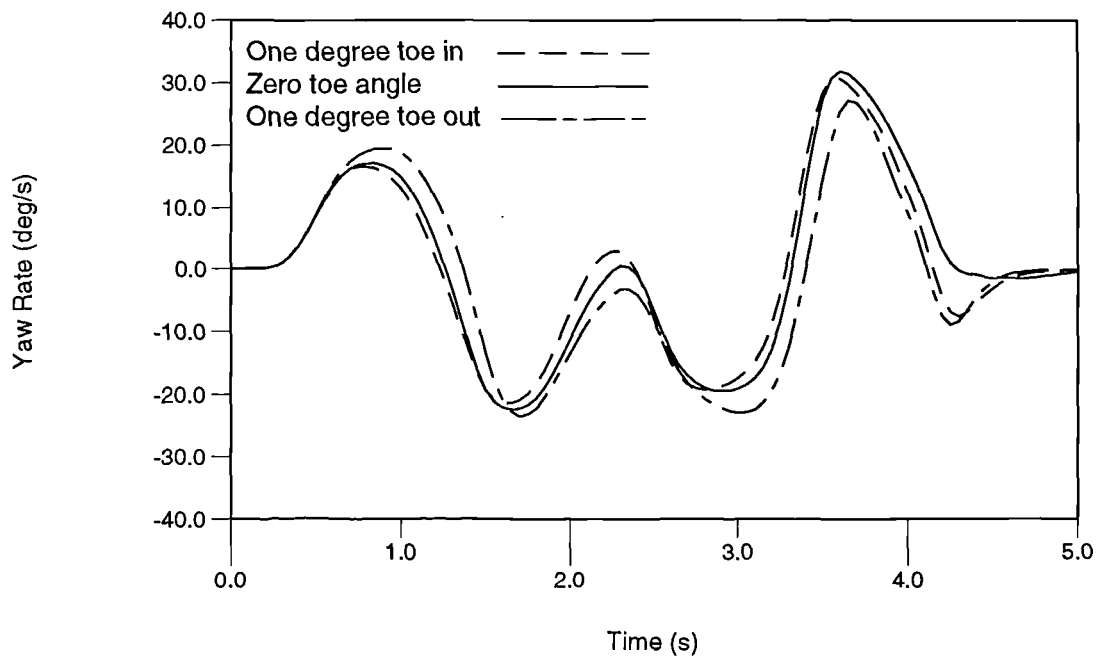### REAR WHEEL TOE ANGLE STUDY

Figure K.6 Yaw rate comparison for rear wheel toe angle study

APPENDIX L

ASSOCIATED PUBLICATIONS

1. **Blundell M.V.** Automatic dynamic analysis of mechanical systems. *Proc. Computer Vision UK Users Group - Summer Conference, Birmingham, June 1990.*

2. **Blundell M.V.** Full vehicle modelling and simulation using the ADAMS software system. *IMechE Paper C427/16/170, Autotech '91, Birmingham, November 1991.*

3. **Manning A.S. and Blundell M.V.** The modelling and simulation of automotive suspension systems. *Proc. Thirteenth IASTED International Conference - Modelling, Identification and Control (MIC '94), ISBN 0-88986-183-8, pp 83-85, Grindelwald, February 1994.*

4. **Blundell M.V.** The use of multibody systems analysis software for an engineering student project. *Proc. Thirteenth IASTED International Conference - Modelling, Identification and Control (MIC '94), ISBN 0-88986-183-8, pp 462-464, Grindelwald, February 1994 .*

5. **Blundell M.V.** Vehicle suspension and handling studies. *Proc. IMechE Seminar S275, Multi-Body System Dynamic Codes for Vehicle Dynamic Applications, London, June 1994.*

6. **Blundell M.V., Phillips B.D.A. and Mackie A.** The modelling and simulation of suspension systems, tyre forces and full vehicle handling performance. *Proc. Tenth International Conference on Systems Engineering (ICSE '94), ISBN 090594234, pp 111-118, Coventry, September 1994.*

7. **Manning A.S. and Blundell M.V.** The modelling requirements of automotive suspension systems for accurate handling simulations. *Proc Fourteenth IASTED International Conference - Modelling, Identification and Control (MIC'95), ISBN 0-88986-212-5, pp 158-160, Innsbruck, February 1995.*

8. **Blundell M.V., Phillips B.D.A. and Mackie A.** A comparison of three full vehicle models for vehicle handling simulation. *Proc. Fourteenth IASTED International Conference - Modelling, Identification and Control (MIC'95), ISBN 0-88986-212-5, pp 155-157, Innsbruck, February 1995.*

9. **Mackie A., Blundell M.V. and Phillips B.D.A.** The modelling and simulation of Anti-Lock Braking systems in ADAMS. *Proc. Fourteenth IASTED International Conference - Modelling, Identification and Control (MIC'95), ISBN 0-88986-212-5, pp 161-163, Innsbruck, February 1995.*

10. **Blundell M.V. and Mackie A**. Mechanical system simulation - a possible tool for product design students. *Proc. of the 2nd National Conference on Product Design Education, PDE95, Coventry, July 1995.*

11. **Blundell M.V.** Prediction of dynamic loads for finite element models. *The Fifth International Conference on Structural Failure, Product Liability and Technical Assurance - SPT-5, Vienna, July 1995.*

12. **Blundell M.V., Phillips B.D.A. and Mackie A.** The modelling and simulation of vehicle handling and braking. *Proc. of the 2nd International Conference on Road Vehicle Automation, ROVA '95, Bolton, September 1995.*

13. **Blundell M.V.** Full vehicle modelling and the requirements for accurate handling simulations. *IMechE Conference, Autotech '95, Birmingham, November 1995.*

14. **Manning A.S. and Blundell M.V.** A range of full vehicle models for transient handling simulations. *Proc Fifteenth IASTED International Conference - Modelling, Identification and Control (MIC'96), ISBN 0-88986-193-5, pp 194-196, Innsbruck, February 1996.*

15. **Dunn W.H. and Blundell M.V.** Simulation as a tool to predict vehicle handling. *Proc 29th ISATA Conference - Simulation, Diagnosis, and Virtual Reality Applications in the Automotive Industry, ISBN 0-947719-80-6, pp 129-136, Florence, June 1996.*

16. **Mackie A.R., Blundell M.V. and Dunn W.H.** Simulation as a tool to predict anti-lock braking performance. *Proc 29th ISATA Conference - Simulation, Diagnosis, and Virtual Reality Applications in the Automotive Industry, ISBN 0-947719-80-6, pp 69-75, Florence, June 1996.*

17. **Blundell M.V.** Full vehicle modelling and the requirements for accurate handling simulations. *IMechE book publication "Automotive Refinement" (1 86058 021 1), C498/7/005/95, pp. 77-91, July 1996.*

18. **Blundell M.V., Phillips B.D.A. and Mackie A.** The role of multibody systems analysis in vehicle design. *Journal of Engineering Design, Vol. 7, No. 4, pp. 377-396, December 1996.*

19. **Blundell M.V.** Prediction of dynamic loads for finite element models. *ISTL Special Publication 3, Failures and the Law, (Structural Failure, Product Liability and Technical Insurance 5), E & FN SPON (An Imprint of Chapman & Hall), ISBN 0-419-22080-1, pp 523-531, 1996.*

20. **Blundell M.V., Dunn W.H. and Manning A.S.** The development of suspension models for vehicle handling simulation. *Proc. of the IASTED/ISMM International Conference - Modelling and Simulation, ISBN 0-88986-221-4, pp 247-249, Pittsburgh, May 1997.*

21. **Blundell M.V., Dunn W.H. and Manning A.S.** The interpretation of tyre models for vehicle handling simulation. *Proc. of the IASTED/ISMM International Conference - Modelling and Simulation, ISBN 0-88986-221-4, pp 250-253, Pittsburgh, May 1997.*

22. **Blundell M.V., Phillips B.D.A. and Mackie A.** The modelling and simulation of vehicle handling and braking. *Road Vehicle Automation II, edited by C. Nwagboso, Wiley, ISBN 0-471-96726-2, pp 133-14, 1997.*

23. **Blundell M.V.** The modelling and simulation of a vehicle lane change manoeuvre. *3rd International Conference on Road Vehicle Automation, ROVA '97, Salamanca, September 1997.*